

Systems Design Study of the Pioneer Venus Spacecraft

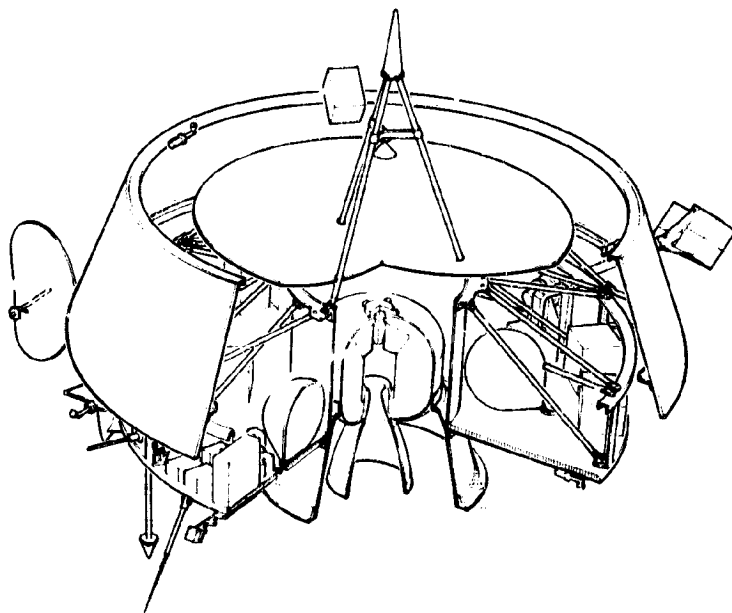
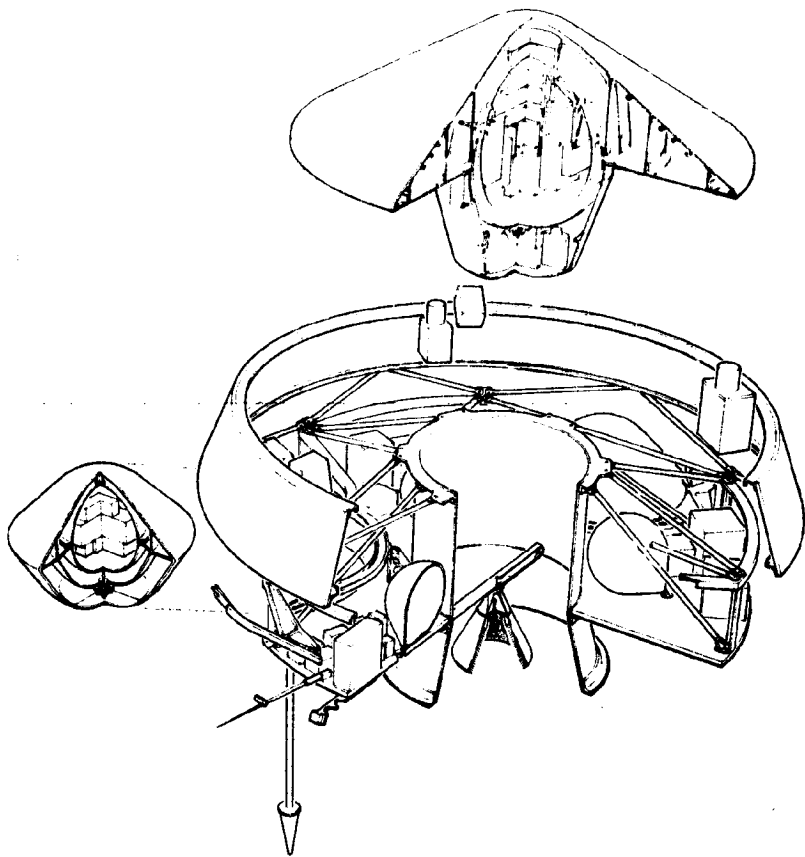
Final Study Report

(NASA-CR-137527) SYSTEMS DESIGN STUDY OF THE PIONEER VENUS SPACECRAFT. VOLUME 1: TECHNICAL ANALYSIS AND TRADEOFFS, SECTIONS R-12 (PART 4) Final Study (TRW Systems Group) 511 p HC 426.75 CSCT 228 63/31 47384

N74-32507

Unclass

47384



LIST OF VOLUMES

VOLUME I. TECHNICAL ANALYSES AND TRADEOFFS

SECTIONS 1-4 (PART 1 OF 4)

1. Introduction
2. Summary
3. Science Analysis and Evaluation
4. Mission Analysis and Design

VOLUME I. TECHNICAL ANALYSES AND TRADEOFFS

SECTIONS 5-6 (PART 2 OF 4)

5. System Configuration Concepts and Tradeoffs
6. Spacecraft System Definition

VOLUME I. TECHNICAL ANALYSES AND TRADEOFFS

SECTION 7 (PART 3 OF 4)

7. Probe Subsystem Definition

VOLUME I. TECHNICAL ANALYSES AND TRADEOFFS

SECTIONS 8-12 (PART 4 OF 4)

8. Probe Bus and Orbiter Subsystem Definition and Tradeoffs
9. NASA/ESRO Orbiter Interface
10. Mission Operations and Flight Support
11. Launch Vehicle-Related Cost Reductions
12. Long Lead Items and Critical Areas

VOLUME I APPENDICES

SECTIONS 3-6 (PART 1 OF 3)

VOLUME I APPENDICES

SECTION 7 (PART 2 OF 3)

VOLUME I APPENDICES

SECTIONS 8-11 (PART 3 OF 3)

VOLUME II. PRELIMINARY PROGRAM DEVELOPMENT PLAN

VOLUME III. SPECIFICATIONS

C.R. 137507

NASA
TRW Document No. 2291 6008 RU 00

Systems Design Study of the Pioneer Venus Spacecraft

Final Study Report

Volume I. Technical Analyses and Tradeoffs Sections 8-12 (Part 4 of 4)

29 July 1973

Contract No. NAS2 7249

Prepared for

AMES RESEARCH CENTER
NATIONAL AERONAUTICS AND SPACE ADMINISTRATION

TRW
SYSTEMS GROUP

MARTIN MARIETTA

CONTENTS

	Page
8. PROBE BUS AND ORBITER SUBSYSTEM DEFINITION AND TRADEOFFS	8.1-1
8.1 Electrical Power Subsystem	8.1-1
8.1.1 Introduction and Summary	8.1-1
8.1.2 Power Subsystem Tradeoffs, Version III Science Payload	8.1-5
8.1.2.1 Power Subsystem Configuration Tradeoffs Version III Science Payload	8.1-6
8.1.2.2 Secondary Power Conditioning Tradeoffs, Version III Science Payload	8.1-12
8.1.2.3 Conical Versus Cylindrical Array Tradeoff, Version III Science Payloads	8.1-15
8.1.3 Orbiter Power Subsystem Tradeoffs, Version III Science Payload	8.1-17
8.1.3.1 Orbiter Battery Tradeoff, Version III Science Payload	8.1-17
8.1.3.2 Sunlit Periapsis Pass Array Sizing Tradeoffs	8.1-20
8.1.4 Recommended Thor/Delta Orbiter Subsystem Design, Version III Science Payload	8.1-21
8.1.4.1 Configuration	8.1-21
8.1.4.2 Power Control Unit	8.1-23
8.1.4.3 Equipment Converter	8.1-25
8.1.4.4 Solar Array	8.1-25
8.1.4.5 Battery	8.1-29
8.1.5 Atlas/Centaur Orbiter Subsystem, Version III Science Payload	8.1-31
8.1.5.1 Configuration	8.1-31
8.1.5.2 Inverter and Central Transformer Rectifier Filter (CTRF)	8.1-32
8.1.5.3 Solar Array	8.1-33
8.1.5.4 Battery	8.1-34
8.1.6 Orbiter Options, Version III Science Payload	8.1-34
8.1.7 Probe Bus	8.1-35
8.1.7.1 Recommended Thor/Delta Probe Bus System	8.1-36

CONTENTS (Continued)

	Page	
8.1.7.2	Recommended Atlas/Centaur Probe Bus Subsystem, Version III Science Payload	8.1-40
8.1.7.3	Power Interface With Probes (Umbilical)	8.1-42
8.2	Communications Subsystem	8.2-1
8.2.1	Introduction and Summary	8.2-1
8.2.2	Requirements	8.2-2
8.2.3	Tradeoffs	8.2-5
8.2.3.1	High-Gain Antennas - Orbiter	8.2-5
8.2.3.2	Medium-Gain Antenna	8.2-17
8.2.3.3	Low Gain (Omni) Antennas	8.2-19
8.2.3.4	Solid State Versus TWTA Power Amplifiers	8.2-22
8.2.3.5	Lightweight Versus Standard Weight Transponders	3.2-29
8.2.3.6	Ranging Versus Combination S- and X-band	8.2-31
8.2.4	Preferred Subsystem Description	8.2-45
8.2.4.1	Probe Bus	8.2-46
8.2.4.2	Preferred Orbiter	8.2-59
8.2.5	Recommended Communications Subsystem	8.2-78
8.2.5.1	Probe Bus (1977 Probe Mission Launch)	8.2-78
8.2.5.2	Orbiter	8.2-85
8.2.6	Orbiter Options	8.2-95
8.2.6.1	Despun Reflector	8.2-95
8.2.6.2	35-Watt/Fanbeam Fanscan Option	8.2-97
8.2.6.3	12-Watt Fanbeam/Fanscan Option	8.2-99
8.3	Data Handling Subsystem	8.3-1
8.3.1	Introduction and Summary	8.3-1
8.3.2	Requirements Analyses	8.3-2
8.3.2.1	Probe Bus Requirements Analysis	8.3-2
8.3.2.2	Probe Bus Requirements Analyses (Version IV Science Payload)	8.3-5
8.3.2.3	Orbiter Requirements Analysis (Version III Science Payload)	8.3-6
8.3.2.4	Orbiter Requirements Analysis (Version IV Science Payload)	8.3-10

CONTENTS (Continued)

	Page
8.3.3 Tradeoff Studies	8.3-13
8.3.3.1 Off-the-Shelf Telemetry Equipment	8.3-14
8.3.3.2 Low Weight, Advanced Technology Alternate	8.3-14
8.3.3.3 Centralized Processing	8.3-17
8.3.3.4 Memory Alternative	8.3-18
8.3.3.5 Science Interfaces	8.3-19
8.3.4 Data Handling Subsystem for Version III Science Payload	8.3-20
8.3.4.1 Probe Bus Data Handling Subsystem Description (Version III Science Payload)	8.3-20
8.3.4.2 Orbiter Data Handling Subsystem Description (Version III Science Payload)	8.3-24
8.3.5 Preferred Data Handling Subsystem for Atlas/Centaur Spacecraft (Version IV Science)	8.3-28
8.3.5.1 Preferred Earth-Pointing Atlas/Centaur Version IV Science Probe Bus Data Handling Subsystem	8.3-28
8.3.5.2 Preferred Atlas/Centaur Orbiter, Version IV Science, Data Handling Subsystem	8.3-31
8.4 Command Subsystem	8.4-1
8.4.1 Introduction and Summary	8.4-1
8.4.2 Requirements Versus Capabilities	8.4-1
8.4.2.1 Commands	8.4-1
8.4.2.2 Ordnance Firing Circuits	8.4-5
8.4.2.3 Thruster Firing Counters	8.4-6
8.4.3 Tradeoff Studies	8.4-6
8.4.3.1 Command Memory	8.4-6
8.4.3.2 Ordnance Firing Circuit Augmentation	8.4-7
8.4.4 Preferred Subsystem Design	8.4-8
8.4.4.1 Digital Decoder Unit	8.4-8
8.4.4.2 Command Distribution Unit	8.4-10
8.5 Attitude Determination and Control Subsystem (ADCS)	8.5-1
8.5.1 Introduction and Summary	8.5-1

CONTENTS (Continued)

		Page
8.5.2	Functions and Requirements, 1977 Probe Mission, Version III Science Payload and Both Thor/Delta and Atlas/Centaur Option	8.5-4
8.5.3	Functions and Requirements	8.5-8
8.5.4	ADCS Concept Selection Tradeoffs	8.5-9
8.5.4.1	Thruster Control Tradeoffs (All Configurations)	8.5-10
8.5.4.2	Attitude Determination Tradeoffs (All Configurations)	8.5-10
8.5.4.3	Antenna Despin Control Tradeoffs	8.5-19
8.5.4.4	Probe Deployment and Retargeting Maneuver Tradeoffs (1977 Probe Missions, Atlas/Centaur and Thor/Delta)	8.5-22
8.5.4.5	Orbiter Maneuver Tradeoffs (All Configurations, Version III Science Payload)	8.5-23
8.5.5	ADCS Concept Selection Tradeoffs	8.5-24
8.5.6	Preferred ADCS Design Description	8.5-30
8.5.6.1	ADCS Design for the Preferred Probe Bus Configuration	8.5-31
8.5.6.2	ADCS Design for the Fanbeam, Fanscan Orbiter Configuration	8.5-34
8.5.6.3	ADCS Designs for the Optional Orbiter Configurations	8.5-34
8.5.6.4	Functional Block Diagram	8.5-35
8.5.6.5	Sun Sensor Assembly	8.5-38
8.5.6.6	Control Electronics Assembly (CEA)	8.5-39
8.5.6.7	Despin Drive Assembly	8.5-42
8.5.6.8	Despin Electronics Assembly	8.5-45
8.5.7	Descriptions of ADCS Designs for the Preferred Atlas/Centaur Configurations for the Version IV Science Payload	8.5-47
8.5.8	Attitude Determination and Control Performance, Version III Science Payload	8.5-48
8.5.8.1	Probe Mission (1977 Launch)	8.5-48
8.5.8.2	Orbiter Mission	8.5-62
8.5.9	Attitude Determination and Control Performance, Version IV Science Payload, 1978 Probe Mission Launch	8.5-73
8.5.9.1	1978 Probe Mission	8.5-73
8.5.9.2	Orbiter Mission	8.5-77

CONTENTS (Continued)

		Page
8.5.10	ADCS/Science Interface	8.5-83
8.5.10.1	Radar Altimeter and Ram Experiment Gimballing Requirements	8.5-83
8.5.10.2	Gimbal Actuator Design Example	8.5-86
8.5.10.3	Refracted Ray Tracking During Occultation Experiments	8.5-87
8.5.10.4	Dual Frequency Occultation ADCS Interface	8.5-88
8.6	Propulsion	8.6-1
8.6.1	Reaction Control System	8.6-1
8.6.1.1	RCS Requirements	8.6-1
8.6.1.2	RCS Tradeoff Studies	8.6-4
8.6.1.3	Preferred Atlas/Centaur RCS Description	8.6-12
8.6.1.4	Preferred Thor/Delta RCS Description	8.6-17
8.6.2	Orbit Insertion Motor	8.6-17
8.6.2.1	Requirements	8.6-17
8.6.2.2	Tradeoffs	8.6-18
8.6.2.3	Preferred Atlas/Centaur Subsystem	8.6-24
8.6.2.4	Preferred Thor/Delta Subsystem	8.6-26
8.7	Thermal Control	8.7-1
8.7.1	Introduction	8.7-1
8.7.2	Preferred Atlas/Centaur Configurations	8.7-2
8.7.2.1	Probe Bus Spacecraft	8.7-2
8.7.2.2	Orbiter Spacecraft	8.7-6
8.7.3	Thor/Delta Configurations	8.7-14
8.7.3.1	Probe Bus Spacecraft	8.7-14
8.7.3.2	Orbiter Spacecraft	8.7-20
8.7.4	Optional Spacecraft Configurations	8.7-24
8.7.4.1	Probe Bus Spacecraft	8.7-24
8.7.4.2	Orbiter Spacecraft	8.7-24
8.7.5	Tradeoffs	8.7-26
8.7.5.1	Methods of Accommodating Power Variations	8.7-26
8.7.5.2	Influence of Large Probe on Thermal Control System Design	8.7-28
8.7.5.3	Transmitter Heat Distribution System	8.7-31

CONTENTS (Continued)

	Page
8.8 Structure and Mechanisms	8.8-1
8.8.1 Structural Subsystem	8.8-1
8.8.1.1 Design Requirements	8.8-1
8.8.1.2 Structural Description	8.8-1
8.8.2 Structural and Dynamic Analyses	8.8-5
8.8.2.1 Structural Analysis	8.8-5
8.8.2.2 Dynamic Analysis	8.8-7
8.8.3 Mechanisms	8.8-9
8.8.3.1 Large Probe Release Mechanism	8.8-9
8.8.3.2 Small Probe Retention and Release Mechanism	8.8-11
8.8.3.3 Probe Electrical Disconnects	8.8-14
8.8.3.4 Magnetometer Boom	8.8-14
8.8.3.5 Nutation Damper	8.8-18
8.8.4 Probe Separation Analysis	8.8-23
8.8.4.1 Large Probe-Atlas/Centaur and Thor/Delta	8.8-23
8.8.4.2 Small Probe Separation Analysis, Atlas/Centaur and Thor/Delta	8.8-26
9. NASA/ESRO ORBITER INTERFACE	9-1
10. MISSION OPERATIONS AND FLIGHT SUPPORT	10-1
10.1 Introduction	10-1
10.1.1 Orbiter Mission Operations	10-1
10.1.2 Probe Mission Operations	10-2
10.1.3 Commonality of Configurations	10-3
10.2 ΔV Maneuver Procedures	10-4
10.2.1 First Midcourse	10-4
10.2.2 Second and Third Midcourse	10-7
10.2.3 Maneuver Options	10-8
10.3 Attitude Determination Procedures	10-11
10.3.1 Introduction	10-11
10.3.2 Open-Loop Attitude Accuracy	10-12
10.3.3 Precession Calibration	10-13
10.3.4 Earth Aspect Measurement	10-13
10.4 Attitude Corrections	10-15
10.5 Ground Station Support Requirement	10-17
10.5.1 DSN Support	10-17
10.5.2 Interference with Other Missions	10-18

CONTENTS (Continued)

	Page
10.5.3 Support Software Modifications	10-19
10.6 Probe Deployment Sequences	10-21
10.6.1 Probe Target Selection and Release Strategy	10-21
10.6.2 Probe Release Timeline	10-22
10.7 Bus and Probe Entry DSN Coverage	10-26
10.8 Orbit Operations	10-30
10.8.1 Venus Orbit Insertion (VOI)	10-30
10.8.2 Precession to VOI Attitude	10-30
10.8.3 Stabilization Spin	10-33
10.8.4 VOI Solid Rocket Motor Ignition Command Control	10-34
10.8.5 Periapsis Maintenance	10-34
10.8.6 Attitude Corrections	10-36
10.8.7 Orbiter Science Operations and Options	10-37
10.8.7.1 Introduction	10-37
10.8.7.2 Use of the Data Storage Unit and the Command Memory	10-38
10.8.7.3 Occultation Experiment Operation	10-41
10.8.7.4 Experiment Platform Updating	10-42
10.8.7.5 Ultraviolet Spectrometer Dayglow Maneuver	10-43
11. Launch Vehicle-Related Cost Reductions	11-1
11.1 Introduction	11-1
11.2 Qualitative Effects of Weight/Volume Relief	11-1
11.3 Cost/Weight Allocation	11-2
11.3.1 Optimum use of Increased Capability	11-2
11.3.2 Cost/Weight Sensitivity—Thor/Delta	11-5
11.3.3 Cost/Weight Sensitivity—Atlas/Centaur	11-7
11.4 Hardware Impact	11-8
11.4.1 Increased Utilization of Existing Designs	11-8
11.4.2 Increased Design Commonality	11-10
11.4.3 Design Simplification	11-12
11.5 Other Launch Vehicle-Related Factors	11-13
11.6 Thor/Delta-Atlas/Centaur Cost Tradeoffs	11-14
11.7 Recommended Mission System	11-16
12. Long Lead Items and Critical Areas	12-1
12.1 Long Lead	12-1
12.2 Critical Areas	12-1

ILLUSTRATIONS

		Page
8.1-1	Preferred Orbiter and Probe Bus Power Subsystem Summary Atlas Centaur/Version IV Science	8.1-3
8.1-2	Pioneer Venus Power Profile, Recommended Thor/Delta Orbiter	8.1-4
8.1-3	Pioneer Venus Power Profile, Atlas/Centaur Orbiter	8.1-4
8.1-4	Pioneer Venus Power Profile, Recommended Thor/Delta Probe Bus	8.1-5
8.1-5	Pioneer Venus Power Profile, Atlas/Centaur Probe Bus	8.1-5
8.1-6	Orbiter Power Tradeoff Studies (Sizing Based on Thor/Delta Version III Science Payload)	8.1-7
8.1-7	Version III Science Power Subsystem Cost/Weight Data	8.1-9
8.1-8	Configuration 14: Pioneers 10 and 11 Type Subsystem	8.1-9
8.1-9	Configuration 6: Regulated Bus	8.1-10
8.1-10	Configuration 15: Pioneers 10 and 11 Type Subsystem (Nickel-Cadmium Battery)	8.1-10
8.1-11	Probe Bus Power Tradeoff Studies (Sizing Based on Version III Science Payload Thor/Delta)	8.1-12
8.1-12	Candidate Power Conditioning Designs, Version III Science Payload	8.1-14
8.1-13	Orbiter Array Power Versus Sun Angle, 225.7-Watt Recommended Thor/Delta	8.1-16
8.1-14	Orbiter Payload Eclipse Loads and Profile	8.1-18
8.1-15	Orbiter Periapsis Pass Situation, Version III Science Payload	8.1-21
8.1-16	Recommended Thor/Delta Orbiter Subsystem Block Diagram (28 VDC \pm 2 Percent Regulated Bus)	8.1-22
8.1-17	Thor/Delta Orbiter Power Control Unit, Version III Science Payload	8.1-23
8.1-18	Thor/Delta Orbiter Equipment Converter, Version III Science Payload	8.1-26
8.1-19	Solar Flare Radiation Environment	8.1-27

ILLUSTRATIONS (Continued)

		Page
8.1-20	Solar Cell and Coverglass Selection	8.1-30
8.1-21	Thor/Delta Orbiter Solar Array	8.1-31
8.1-22	Atlas/Centaur Power Subsystem, Version III Science Payload	8.1-32
8.1-23	Atlas/Centaur Inverter Assembly Block Diagram, Version III Science Payload	8.1-32
8.1-24	Atlas/Centaur Typical Parallel Redundant CTRF	8.1-33
8.1-25	Atlas/Centaur Orbiter Central Transformer Rectifier Filter	8.1-34
8.1-26	Atlas/Centaur Orbiter Solar Array Summary, Version III Science Payload	8.1-34
8.1-27	Recommended Thor/Delta Probe Bus Configuration (28 VDC \pm 2 Percent Regulated Bus)	8.1-37
8.1-28	Recommended Probe Bus Power Control Unit, Thor/Delta and Atlas/Centaur Missions, Version III Science Payload	8.1-37
8.1-29	Thor/Delta Probe Bus Array, Version III Science Payload	8.1-39
8.1-30	Thor/Delta Probe Bus Battery Sizing, Version III Science Payload	8.1-39
8.1-31	Atlas/Centaur Probe Bus Power Subsystem Block Diagram, Version III Science Payload	8.1-40
8.1-32	Atlas/Centaur Probe Bus Central Transformer Rectifier Filter, Version III Science Payload	8.1-41
8.1-33	Atlas/Centaur Probe Bus Solar Array Version III Science Payload	8.1-41
8.1-34	Atlas/Centaur Probe Bus Battery Sizing, Version III Science Payload	8.1-42
8.1-35	Probe Bus Power Interface Version III Science Payload	8.1-42
8.2-1	Preferred Atlas/Centaur Communication Subsystem Description	8.2-3
8.2-2	Orbiter High-Gain Antenna Tradeoff Characteristics	8.2-6
8.2-3	Antenna Pattern with Defocussing	8.2-7
8.2-4	Candidate Orbiter Despun High-Gain Antenna Tradeoff Configurations	8.2-9

ILLUSTRATIONS (Continued)

		Page
8.2-5	Candidate Orbiter Reduced EIRP Antenna Tradeoff Characteristics	8.2-13
8.2-6	Rotary Joints (Noncontacting Inner and Outer Conductors)	8.2-15
8.2-7	Candidate Medium-Gain Antenna Configuration	8.2-17
8.2-8	Horn Gain vs. Pattern Angle	8.2-18
8.2-9	Candidate Probe Bus and Orbiter Low-Gain (Omni) Antenna	8.2-20
8.2-10	Allowable Spacecraft Spin Speed (f) Versus Antenna Distance from Spin Axis (r) and Receiver Loop Bandwidth ($2B_L$)	8.2-21
8.2-11	Power Amplifier Combining Techniques	8.2-28
8.2-12	Combination S-Band and X-Band Antenna Designs	8.2-34
8.2-13	X-Band Occultation Experiment Antenna	8.2-35
8.2-14	X-Band Transmitter Block Diagram	8.2-41
8.2-15	Range Acquisition Time versus Range (Preferred Thor/Delta Orbiter)	8.2-43
8.2-16	X-Band Margin versus Range (Preferred Thor/Delta Orbiter)	8.2-45
8.2-17	Atlas/Centaur Probe Bus Communications Subsystem Block Diagram	8.2-47
8.2-18	Probe Bus Telemetry Rate Profile	8.2-49
8.2-19	Baseline Probe Bus Spacecraft Antennas	8.2-53
8.2-20	Probe Bus Model Tests	8.2-54
8.2-21	Baseline Probe Spacecraft Diplexer and RF Switch	8.2-54
8.2-22	Pioneer 10 and 11 Receiver	8.2-56
8.2-23	Pioneer 10 and 11 Transmitter	8.2-57
8.2-24	Two 6-Watt Solid State Power Amplifier Designs	8.2-58
8.2-25	Atlas/Centaur Orbiter Communications Subsystem Block Diagram	8.2-60
8.2-26	Orbiter Telemetry Rate Profile	8.2-61
8.2-27	Spacecraft Occultation Positioning	8.2-64
8.2-28	Occultation Defocusing Loss versus Defocusing Angle (S-band and X-band)	8.2-64

ILLUSTRATIONS (Continued)

	Page	
8.2-29	Mariner V Occultation Data	8.2-66
8.2-30	Baseline Orbiter Spacecraft Antennas	8.2-69
8.2-31	Typical Philco Receiver	8.2-72
8.2-32	TRW Lightweight Receiver	8.2-73
8.2-33	Transmitter Drivers	8.2-74
8.2-34	Digital Conscan Signal Processor	8.2-77
8.2-35	Thor/Delta Communications Subsystem	8.2-79
8.2-36	Bus Telemetry Rate History	8.2-81
8.2-37	Thor/Delta Probe Spacecraft Medium-Gain Antenna	8.2-84
8.2-38	Orbiter Communication Subsystem Block Diagram	8.2-86
8.2-39	Orbiter Telemetry Rate History	8.2-88
8.2-40	Recommended Thor/Delta Orbiter Spacecraft Antennas	8.2-92
8.2-41	Communications Subsystem Block Diagram	8.2-96
8.2-42	Linear Polarization Low-Gain (Omni) Coverage with Conscan	8.2-96
8.2-43	Orbiter Telemetry Rate Profile	8.2-99
8.3-1	Preferred Data Handling Subsystem	8.3-3
8.3-2	Orbiter Sun and Earth Occultation Profiles	8.3-8
8.3-3	Orbiter Version III Science Payload Instrument Data Acquisition Profiles	8.3-9
8.3-4	Orbiter Version IV Science Payload Data Rate Profile	8.3-12
8.3-5	Alternate Data and Command Subsystem	8.3-16
8.3-6	Digital Telemetry Unit (DTU)	8.3-21
8.3-7	Basic Telemetry Format for Version III Science Payload	8.3-22
8.3-8	Telemetry Formats for Probe Bus Version III Science Payload	8.3-23
8.3-9	DTU/Probe Interface	8.3-24
8.3-10	Orbiter Formats	8.3-25
8.3-11	DSN Usage	8.3-26
8.3-12	DSN Usage for Fanbeam Orbiter	8.3-26

ILLUSTRATIONS (Continued)

		Page
8.3-13	Data Storage Configuration	8.3-27
8.3-14	Memory Module Block Diagram	8.3-27
8.3-15	Probe Bus Entry Format (1024 bits/s)	8.3-30
8.3-16	Storage Configuration	8.3-31
8.3-17	Orbiter Data Storage Timeline	8.3-33
8.3-18	Orbiter Formats	8.3-34
8.4-1	Command Subsystem	8.4-3
8.4-2	Command Subsystem Interface Diagram	8.4-9
8.4-3	Pioneer Digital Decoder Unit	8.4-9
8.4-4	Ordnance Firing System	8.4-11
8.4-5	Command Processor	8.4-14
8.4-6	CDU Functional Block Diagram	8.4-15
8.4-7	CDU/Probe Interface	8.4-16
8.5-1	Attitude Determination and Control	8.5-3
8.5-2	Maneuver Sensitivities to Spacecraft Attitude Errors	8.5-6
8.5-3	Maximum Allowable Attitude Errors	8.5-7
8.5-4	Maximum Attitude Errors Allowed by Ram Experiments	8.5-9
8.5-5	Attitude Determination and Control by Antenna Pattern Searching	8.5-13
8.5-6	Conscan/Fanscan Attitude Determination and Control	8.5-14
8.5-7	Doppler Measurement of Earth Aspect Angle	8.5-15
8.5-8	Star Mapper Design Requirements	8.5-17
8.5-9	Effect of Sun-Spacecraft-Earth Geometry on Attitude Determination Accuracy	8.5-20
8.5-10	Probe Deployment and Retargeting Maneuver Tradeoffs	8.5-22
8.5-11	Probe Deployment and Retargeting Maneuver Tradeoffs	8.5-25
8.5-12	Probe Deployment and Retargeting Maneuver Tradeoffs	8.5-27
8.5-13	Periapsis Maintenance Maneuver Tradeoffs	8.5-28
8.5-14	Selected Platform Drive Assembly Design	8.5-29

ILLUSTRATIONS (Continued)

		Page
8.5-15	Attitude Determination and Control Subsystem for the Preferred Probe Bus Configurations	8.5-32
8.5-16	Attitude Determination and Control Subsystem Configuration for the Fanbeam, Fanscan Orbiters	8.5-34
8.5-17	Attitude Determination and Control Subsystem Configuration for the Earth-Pointing Orbiters	8.5-35
8.5-18	Attitude Determination and Control Subsystem Configuration for the Orbiters with Despun Antenna Reflector	8.5-36
8.5-19	ADCS Functional Block Diagram	8.5-37
8.5-20	Sun Sensor Assembly Summary Description	8.5-39
8.5-21	Sun Sensor Signal Processing Electronics	8.5-40
8.5-22	Control Electronics Assembly Summary Description	8.5-40
8.5-23	Despin Drive Assembly Summary Description	8.5-42
8.5-24	Despin Drive Electronics Block Diagram	8.5-45
8.5-25	Despin Electronics Assembly Summary Description	8.5-46
8.5-26	Platform Drive Assembly Summary Description	8.5-48
8.5-27	Pictorial Representation of Spin Axis Attitude Errors During Separation from Third Stage	8.5-50
8.5-28	Stereographic Projection Method for Plane Representation of Three-Dimensional Angular Geometry	8.5-51
8.5-29	Stereographic Projection Showing Sun-Earth-Spacecraft Geometry During Probe Bus Cruise	8.5-32
8.5-30	Solar Pressure Drift Rate Versus Time, Probe Bus Cruise Phase	8.5-53
8.5-31	Probe Deployment and Retargeting Attitude Determination Accuracies	8.5-59
8.5-32	Stereographic Projection Showing Locations of the Spin Axis, Sun, and Earth During Probe Release and Probe Bus Retargeting Maneuvers	8.5-59
8.5-33	Small Probe Trajectories Relative to Probe Bus Coordinate System	8.5-60
8.5-34	Small Probe Release Geometry	8.5-60

ILLUSTRATIONS (Continued)

		Page
8.5-35	Forces Inducing Traverse Rates During Small Probe Release	3.5-61
8.5-36	Small Probe Tipoff Errors for a Preloaded Release System	8.5-61
8.5-37	Stereographic Projection Showing Sun-Earth-Spacecraft Geometry During Orbiter Cruise	8.5-64
8.5-38	Solar Pressure Drift Rate Versus Time Orbiter Cruise Phase	8.5-65
8.5-39	Attitude Determination Accuracy During Orbiter Cruise	8.5-66
8.5-40	Stereographic Projection Showing Sun-Earth-Spacecraft Geometry in Orbit	8.5-69
8.5-41	Attitude Drift Produced by Environmental Disturbance Torques in Orbit	8.5-70
8.5-42	Attitude Determination Accuracy in Orbit	8.5-71
8.5-43	Stereographic Projection Showing Angular Geometry During Probe Bus Cruise and Probe Deployment and Retargeting Maneuvers	8.5-74
8.5-44	Precession Rates During 1978 Probe Bus Cruise	8.5-74
8.5-45	Precession Rates Due to Solar Pressure and Earth Tracking	8.5-79
8.5-46	Doppler Attitude Determination Accuracies	8.5-80
8.5-47	Venus Orbit Insertion and Orbit Phase Geometry	8.5-81
8.5-48	Attitude Drift Rates in Orbit Due to Solar Pressure and Earth Motion	8.5-82
8.5-49	Radar Altimeter and Ram Experiment Gimbal Angles for Tracking, Spin Axis Normal to Venus Orbit Plane	8.5-84
8.5-50	Radar Altimeter Gimbal Angles for Tracking, Earth-Pointing Configurations	8.5-85
8.5-51	Ram Experiment Gimbal Angles for Tracking, Earth-Pointing Configurations	8.5-86
8.5-52	Gimbal Actuator Design Example for Altimeter and Ram Platform	8.5-86
8.5-53	Earth Occultation Experiment Tracking Requirements	8.5-88
8.6-1	Preferred Atlas/Centaur Reaction Control Subsystem and Orbit Insertion Motor	8.6-3

ILLUSTRATIONS (Continued)

		Page
8. 6-2	Required Number and Location of Thrusters Tradeoff	8. 6-5
8. 6-3	Maximum Allowable Precession Thruster Radius Arm to Meet 0. 017 Radian (1 Degree) Precession Limit at 0. 125 Second Pulsewidth as a Function of Thrust Level and Spacecraft Moment of Inertia	8. 6-6
8. 6-4	RCS Propellant Tradeoffs	8. 6-7
8. 6-5	Blowdown Versus Regulated Pressurization Tradeoff	8. 6-8
8. 6-6	Bladder Versus Spin Forces	8. 6-9
8. 6-7	Atlas/Centaur Propellant Position at End of Life with +X Axis Thrusters Firing	8. 6-12
8. 6-8	Residual Propellant Necessary to Prevent Propellant Unporting in Atlas/Centaur Conospheroid Tanks	8. 6-12
8. 6-9	Preferred Atlas/Centaur RCS	8. 6-12
8. 6-10	Atlas/Centaur RCS Piping Diagram	8. 6-14
8. 6-11	Other Features of the Preferred Atlas/Centaur RCS	8. 6-19
8. 6-12	Preferred Thor/Delta RCS	8. 6-20
8. 7-1	Preferred Atlas/Centaur Probe Bus Spacecraft Thermal Control System Description	8. 7-3
8. 7-2	Preferred Atlas/Centaur Probe Bus Spacecraft Thermal Performance	8. 7-4
8. 7-3	Preferred Atlas/Centaur Probe Bus Spacecraft Thermal Environment	8. 7-7
8. 7-4	Preferred Atlas/Centaur Probe Bus Spacecraft Thermal Analysis	8. 7-8
8. 7-5	Preferred Atlas/Centaur Orbiter Spacecraft Thermal Control System Description	8. 7-9
8. 7-6	Preferred Atlas/Centaur Orbiter Spacecraft Thermal Performance	8. 7-10
8. 7-7	Preferred Atlas/Centaur Orbiter Thermal Environment	8. 7-13
8. 7-8	Preferred Atlas/Centaur Orbiter Spacecraft Thermal Model	8. 7-15
8. 7-9	Thor/Delta Bus Spacecraft Thermal Control System Description	8. 7-17
8. 7-10	Thor/Delta Bus Spacecraft Thermal Performance	8. 7-18

ILLUSTRATIONS (Continued)

		Page
8. 7-11	Thor/Delta Probe Bus Spacecraft Thermal Environment	8. 7-19
8. 7-12	Thor/Delta Orbiter Spacecraft Thermal Control Description	8. 7-21
8. 7-13	Thor/Delta Orbiter Spacecraft Thermal Performance	8. 7-22
8. 7-14	Recommended Thor/Delta Orbiter Spacecraft Thermal Environment	8. 7-23
8. 7-15	Optional Despin Reflector Orbiter Spacecraft Thermal Control System Description	8. 7-25
8. 7-16	Optional Orbiter Despun Reflector Spacecraft Thermal Performance	8. 7-26
8. 8-1	Structure and Mechanisms Subsystem Summary	8. 8-3
8. 8-2	Computer Printout, Pioneer Venus Probe Bus	8. 8-5
8. 8-3	Probe/Bus Mechanical Interfaces	8. 8-10
8. 8-4	Small Probe Retention and Release Mechanism	8. 8-13
8. 8-5	Existing Boom Design Recommended for Magnetometer Deployment	8. 8-17
8. 8-6	Nutation Damper Configuration for Thor/Delta Probe Bus ($\omega_n/\Omega = 0.80$)	8. 8-19
8. 8-7	Thor/Delta Probe Bus Nutation Damper Theoretical Performance	8. 8-21
8. 8-8	Thor/Delta Probe Bus Damper Theoretical Performance for Various Spin Rates	8. 8-21
8. 8-9	Thor/Delta Orbiter Theoretical Damper Performance for Various Spin Rates	8. 8-21
8. 8-10	Atlas/Centaur Theoretical Damper Performance for Various Spin Rates	8. 8-21
8. 8-11	Atlas/Centaur Nutation Damper Theoretical Performance for Various Spin Rates	8. 8-21
8. 8-12	Small Probe Trajectories Relative to Bus (Thor/Delta Configuration)	8. 8-29
8. 8-13	Small Probe Tipoff Errors for a Preloaded Release System	8. 8-31
9-1	ESRO Hardware Participation	9-2
9-2	NASA/ESRO Participation Options	9-3
10-1	Functional Elements for Midcourse Maneuvers	10-4
10-2	Probe Mission First Midcourse	10-5

ILLUSTRATIONS (Continued)

	Page
10-3	Effects of First Midcourse Pointing Error on Second Midcourse Requirements 10-8
10-4	Spin Coupling Effects for Worst Case ΔV 10-10
10-5	Geometry Effect on Attitude Determination Accuracy 10-11
10-6	Conscan Concept 10-13
10-7	Doppler Modulation Earth Aspect Attitude Determination 10-14
10-8	Doppler Attitude Measurement Accuracy 10-14
10-9	Doppler Shift Earth Aspect Attitude Determination 10-14
10-10	Doppler Shift for Orbit Insertion 10-15
10-11	Precession Rates Due to Solar Pressure and Earth Tracking 10-16
10-12	Bit Rate Capability Profile for Probe Mission 10-18
10-13	Bit Rate Capability Profile for Orbiter Mission 10-18
10-14	Interplanetary Mission Overlap 10-18
10-15	Example of Crt Telemetry Display 10-20
10-16	Probe Entry Locations for Simultaneous or Sequential Release 10-21
10-17	Propulsion Events Timeline 10-23
10-18	Probe Deployment Timeline 10-24
10-19	Stereographic Projection Showing Angular Geometry During Probe Bus Cruise and Probe 10-26
10-20	Tracking Station Coverage for 1978 Probe Mission 10-27
10-21	Probe and Bus Entry Transmission Profile 10-28
10-22	Probe and Bus Data Recovery Sequential Entry 10-29
10-23a	Orbiter Mission Trajectory Characteristics 10-31
10-23b	Venus Orbit Insertion and Orbit Phase Geometry 10-31
10-24	Venus Orbiter Insertion Sequence 10-32
10-25	Orbit Period Error as a Function of Pointing Error 10-32
10-26	Periapsis Maintenance Altitude Variation Effects 10-35
10-27	Periapsis Altitude Maintenance 10-35
10-28	Attitude Drift Rates in Orbit Due to Solar Pressure and Earth Motion 10-37

ILLUSTRATIONS (Continued)

		Page
10-29	Orbiter Version IV Science Payload Data Rate Profile	10-38
10-30	Orbiter Version III Science Payload Occultation Profiles	10-41
10-31	Experiment Platform Gimballing	10-43
10-32	Planet Aspect to Probe Bus Spin Axis	10-44
10-33	Stereographic Projection of Relative Location of Earth, Venus, Sun, and the Ultraviolet Field of View for the Dayglow Experiment	10-45
11-1	Atlas/Centaur Cost/Weight Allocation, Total Capability Increase: 386 kg (851 lb)	11-4
11-2	Thor/Delta Cost/Weight Tradeoffs	11-6
11-3	Atlas/Centaur Cost/Weight Tradeoffs	11-7
11-4	Use of Existing Designs Lowers Development Cost	11-10
11-5	Despin Commonality Lowers Development Cost	11-12
12-1	Schedule Summary	12-1
12-2	Critical Activities	12-2

ACRONYMS AND ABBREVIATIONS

A	ampere analog
abA	abampere
AC	alternating current
A/C	Atlas/Centaur
ADA	avalanche diode amplifier
ADCS	attitude determination and control subsystem
ADPE	automatic data processing equipment
AEHS	advanced entry heating simulator
AEO	aureole/extinction detector
AEDC	Arnold Engineering Development Corporation
AF	audio frequency
AGC	automatic gain control
AgCd	silver-cadmium
AgO	silver oxide
AgZn	silver zinc
ALU	authorized limited usage
AM	amplitude modulation
a. m.	ante meridian
AMP	amplifier
APM	assistant project manager
ARC	Ames Research Center
ARO	after receipt of order
ASK	amplitude shift key
at. wt	atomic weight
ATM	atmosphere
ATRS	attenuated total refractance spectrometer
AU	astronomical unit
AWG	American wire gauge
AWGN	additive white gaussian noise
B	bilevel
B	bus (probe bus)
BED	bus entry degradation

ACRONYMS AND ABBREVIATIONS (CONTINUED)

BER	bit error rate
BLIMP	boundary layer integral matrix procedure
BPIS	bus-probe interface simulator
BPL	bandpass limiter
BPN	boron potassium nitrate
bps	bits per second
BTU	British thermal unit
C	Canberra tracking station - NASA DSN
CADM	configuration administration and data management
C&CO	calibration and checkout
CCU	central control unit
CDU	command distribution unit
CEA	control electronics assembly
CFA	crossed field amplifier
cg	centigram
c.g.	center of gravity
CIA	counting/integration assembly
CKAFS	Cape Kennedy Air Force Station
cm	centimeter
c.m.	center of mass
C/M	current monitor
CMD	command
CMO	configuration management office
C-MOS	complementary metal oxide silicon
CMS	configuration management system
const	constant construction
COSMOS	complementary metal oxide silicon
c.p.	center of pressure
CPSA	cloud particle size analyzer
CPSS	cloud particle size spectrometer

ACRONYMS AND ABBREVIATIONS (CONTINUED)

CPU	central processing unit
CRT	cathode ray tube
CSU	Colorado State University
CTRF	central transformer rectifier filter
D	digital
DACS	data and command subsystem
DCE	despin control electronics
DDA	despin drive assembly
DDE	despin drive electronics
DDU	digital decoder unit
DDULBI	doubly differenced very long baseline interferometry
DEA	despin electronics assembly
DEHP	di-2-ethylhexyl phthalate
DFG	data format generator
DGB	disk gap band
DHC	data handling and command
DIO	direct input/output
DIOC	direct input/output channel
DIP	dual in-line package
DISS REG	dissipative regulator
DLA	declination of the launch azimuth
DLBI	doubly differenced very long baseline interferometry
DMA	despin mechanical assembly
DOF	degree of freedom
DR	design review
DSCS II	Defense System Communications Satellite II
DSIF	Deep Space Instrumentation Facility
DSL	duration and steering logic
DSN	NASA Deep Space Network
DSP	Defense Support Program
DSU	digital storage unit
DTC	design to cost
DTM	decelerator test model

ACRONYMS AND ABBREVIATIONS (CONTINUED)

DTP	descent timer/programmer
DTU	digital telemetry unit
DVU	design verification unit
E	encounter entry
EDA	electronically despun antenna
EGSE	electrical ground support equipment
EIRP	effective isotropic radiated power
EMC	electromagnetic compatibility
EMI	electromagnetic interference
EO	engineering order
EOF	end of frame
EOM	end of mission
EP	earth pointer
ESA	elastomeric silicone ablator
ESLE	equivalent station error level
ESRO	European Space Research Organization
ETM	electrical test model
ETR	Eastern Test Range
EXP	experiment
FFT	fast Fourier transform
FIPP	fabrication/inspection process procedure
FMEA	failure mode and effects analysis
FOV	field of view
FP	fixed price frame pulse (telemetry)
FS	federal stock
FSK	frequency shift keying
FTA	fixed time of arrival

ACRONYMS AND ABBREVIATIONS (CONTINUED)

G	Goldstone Tracking Station - NASA DSN gravitational acceleration
g	gravity
G&A	general and administrative
GCC	ground control console
GFE	government furnished equipment
GHE	ground handling equipment
GMT	Greenwich mean time
GSE	ground support equipment
GSFC	Goddard Space Flight Center
H	Haystack Tracking Station - NASA DSN
HFFB	Ames Hypersonic Free Flight Ballistic Range
HPBW	half-power beamwidth
htr	heater
HTT	heat transfer tunnel
I	current
IA	inverter assembly
IC	integrated circuit
ICD	interface control document
IEEE	Institute of Electrical and Electronics Engineering
IFC	interface control document
IFJ	in-flight jumper
IMP	interplanetary monitoring platform
I/O	input/output
IOP	input/output processor
IR	infrared
IRAD	independent research and development
IRIS	infrared interferometer spectrometer
IST	integrated system test
I&T	integration and test
I-V	current-voltage

ACRONYMS AND ABBREVIATIONS (CONTINUED)

JPL	Jet Propulsion Laboratory
KSC	Kennedy Space Center
L	launch
LD/AD	launch date/arrival date
LP	large probe
LPM	lines per minute
LPTTL	low power transistor-transistor logic
MSI	medium scale integration
LRC	Langley Research Center
M	Madrid tracking station - NASA DSN
MAG	magnetometer
max	maximum
MEOP	maximum expected operating pressure
MFSK	M'ary frequency shift keying
MGSE	mechanical ground support equipment
MH	mechanical handling
MIC	microwave integrated circuit
min	minimum
MJS	Mariner Jupiter-Saturn
MMBPS	multimission bipropellant propulsion subsystem
MMC	Martin Marietta Corporation
MN	Mach number
mod	modulation
MOI	moment of inertia
MOS LSI	metal over silicone large scale integration
MP	maximum power
MSFC	Marshall Space Flight Center
MPSK	M'ary phase shift keying
MSI	medium scale integration
MUX	multiplexer
MVM	Mariner Venus-Mars

ACRONYMS AND ABBREVIATIONS (CONTINUED)

NAD	Naval Ammunition Depot, Crane, Indiana
N/A	not available
NiCd	nickel cadmium
NM/IM	neutral mass spectrometer and ion mass spectrometer
NRZ	non-return to zero
NVOP	normal to Venus orbital plane
OEM	other equipment manufacturers
OGO	Orbiting Geophysical Observatory
OIM	orbit insertion motor
P	power
PAM	pulse amplitude modulation
PC	printed circuit
PCM	pulse code modulation
PCM- PSK-PM	pulse code modulation-phase shift keying- phase modulation
PCU	power control unit
PDA	platform drive assembly
PDM	pulse duration modulation
PI	principal investigator proposed instrument
PJU	Pioneer Jupiter-Uranus
PLL	phase-locked loop
PM	phase modulation
p. m.	post meridian
P-MOS	positive channel metal oxide silicon
PMP	parts, materials, processes
PMS	probe mission spacecraft
PMT	photomultiplier tube
PPM	parts per million pulse position modulation
PR	process requirements
PROM	programmable read-only memory
PSE	program storage and execution assembly

ACRONYMS AND ABBREVIATIONS (CONTINUED)

PSIA	pounds per square inch absolute
PSK	phase shift key
PSU	Pioneer Saturn-Uranus
PTE	probe test equipment
QOI	quality operation instructions
QTM	qualification test model
RCS	reaction control subsystem
REF	reference
RF	radio frequency
RHCP	right hand circularly polarized
RHS	reflecting heat shield
RMP-B	Reentry Measurements Program, Phase B
RMS	root mean square
RMU	remote multiplexer unit
ROM	read only memory rough order of magnitude
RSS	root sum square
RT	retargeting
RTU	remote terminal unit
S	separation
SBASI	single bridgewire Apollo standard initiator
SCP	stored command programmer
SCR	silicon controlled rectifier
SCT	spin control thrusters
SEA	shunt electronics assembly
SFOF	Space Flight Operations Facility
SGLS	space ground link subsystem
SHIV	shock induced vorticity
SLR	shock layer radiometer
SLRC	shock layer radiometer calibration

ACRONYMS AND ABBREVIATIONS (CONTINUED)

SMAA	semimajor axis
SMIA	semiminor axis
SNR	signal to noise ratio
SP	small probe
SPC	sensor and power control
SPSG	spin sector generator
SR	shunt radiator
SRM	solid rocket motor
SSG	Science Steering Group
SSI	small scale integration
STM	structural test model
STM/TTM	structural test model/thermal test model
STS	system test set
sync	synchronous
TBD	to be determined
TCC	test conductor's console
T/D	Thor/Delta
TDC	telemetry data console
TEMP	temperature
TS	test set
TTL MSI	transistor-transistor logic medium scale integration
TLM	telemetry
TOF	time of flight
TRF	tuned radio frequency
TTM	thermal test model
T/V	thermo vacuum
TWT	travelling wave tube
TWTA	travelling wave tube amplifier
UHF	ultrahigh frequency
UV	ultraviolet

ACRONYMS AND ABBREVIATIONS (CONTINUED)

VAC	volts alternating current
VCM	vacuum condensable matter
VCO	voltage controlled oscillator
VDC	volts direct current
VLBI	very long baseline interferometry
VOI	Venus orbit insertion
VOP	Venus orbital plane
VSI	Viking standard initiator
VTA	variable time of arrival
XDS	Xerox Data Systems

8. Probe Bus and Orbiter Subsystem Definition and Tradeoffs

8. PROBE BUS AND ORBITER SUBSYSTEM DEFINITION AND TRADEOFFS

8.1 ELECTRICAL POWER SUBSYSTEM

8.1.1 Introduction and Summary A/C IV A/C IV

The electrical power subsystem consists of the solar array, power controls, power conditioning, and battery plus the associated command and telemetry provisions. Design of this subsystem was guided by the desirability of using common hardware for the orbiter and the probe bus to the maximum extent feasible. For the Atlas/Centaur version, emphasis was on low cost and low development risk, unconstrained by weight or volume considerations.

Figure 8.1-1 presents all the essential data on the preferred power subsystem designs for the orbiter and probe bus. This preferred design was selected primarily on the basis of low total cost, achieved by making extensive use of Pioneers 10 and 11 hardware. Design features include the following (letters indicate the relevant parts of Figure 8.1-1):

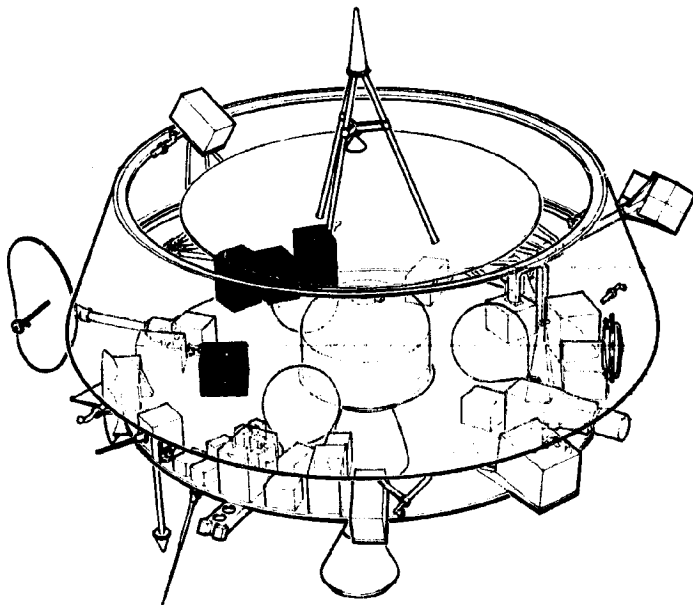
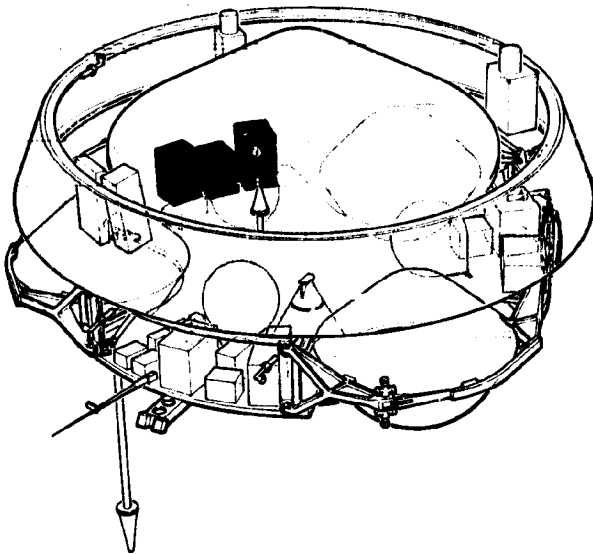
- A power control unit controls the shunt, charge, and discharge regulators to provide ± 2 percent regulation of the 28-volt bus. (See Figure 8.1-1B).
- The CTRF (central transformer rectifier filter) receives a 61-volt AC input from the inverter and provides secondary voltage outputs for most subsystem loads. Both the inverter and the CTRF are Pioneers 10 and 11 designs. (See Figure 8.1-1B).
- The orbiter uses a low-cost and risk nickel-cadmium battery. The probe bus uses a silver-zinc battery with a nonredundant discharge regulator, because battery power is required during launch and probe checkout only and the weight and cost savings are significant. (See Figure 8.1-1B).
- The battery chargers are consequently different for the probe bus and orbiter; the charger for the probe bus is designed to float the battery as was done for the silver-zinc battery of Pioneers 6 through 9. The orbiter charger supplies a maximum of 2 amperes during Venus orbit eclipse seasons, and is in a trickle charge mode during cruise. (See Figure 8.1-1C).
- The CTRF for the probe bus uses Pioneers 10 and 11 slices without modification; the orbiter needs only minimal modifications for the DSU and DTU power regulators. (See Figure 8.1-1D).

- The inverter is a Pioneers 10 and 11 design modified to accept the 28-volt input. The two inverters normally share the load, but either is capable of handling the full CTRF load if necessary. (See Figure 8.1-1E).
- The nickel-cadmium battery for the orbiter uses cells that were flight-proven on the DSP. The 60 percent maximum depth of discharge is conservative, considering that only 125 charge/discharge cycles are needed and only a few of which are at the maximum depth. (See Figure 8.1-1F).
- The probe bus battery uses cells identical in design to those used in the large and small probes, reducing development and test costs. (See Figure 8.1-1F).
- The 0.39 radian (22.5-degree) cone angle solar arrays provide nearly constant power over sun aspect angles from 0 to 1.57 radians (0 to 90 degrees). Load requirements are met or exceeded under all conditions, including maximum array degradation. (See Figures 8.1-1F through 8.1-1I).
- The Pioneers 10 and 11 shunt driver is used unchanged for the probe bus; for the orbiter, two additional shunt power transistor strings in separate packages are added. The supplemental transistor strings are identical to those used in the Pioneers 10 and 11 PCU. (See Figure 8.1-1J).
- The orbiter power profile during periapsis passage shows that the battery shares the load with the radar altimeter turned on, providing a total of 9 watt-hours. This does not result in a depth of discharge beyond the 60 percent occurring during eclipse operation. (See Figure 8.1-1K).

Tradeoff studies and initial subsystem definition were based on the orbiter Version III science payload with a Thor/Delta booster. This was the most stringent design because of weight limitations. The probe bus subsystem was derived from the orbiter to maintain maximum commonality. The low cost Atlas/Centaur versions were derived from the Thor/Delta orbiter and probe bus subsystems, without the weight constraints.

Details of the effects on these designs of the Version IV science payload are given in Appendices 8.1D and 8.1E, which supplement Figure 8.1-1. Appendix 8.1-F contains detailed power budgets.

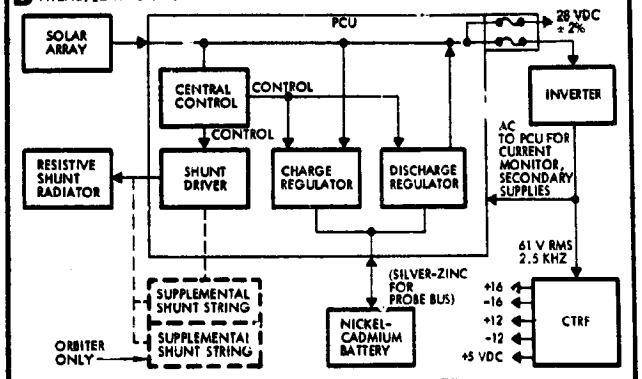
The complete power profiles for the four Version III science payload missions analyzed (Thor/Delta orbiter and probe bus, and Atlas/Centaur orbiter and probe bus) are shown in Figures 8.1-2 through 8.1-5.



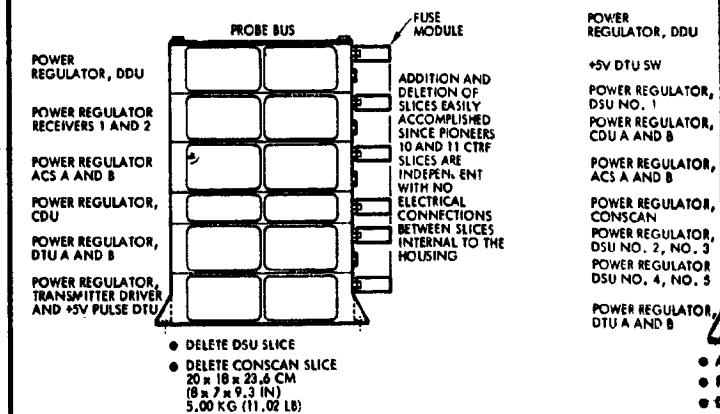
A REQUIREMENTS

	ORBITER	PROBE BUS
MISSION DURATION (DAYS)	425	114
TIME PERIOD (YEAR)	1978	1978
ORIENTATION OF SPIN AXIS	EARTH POINTING	EARTH POINTING
MAGNETIC CLEANLINESS, (NANO TESLA)	< 0.5	----
LAUNCH POWER (WATTS)	56.1	52.6
CRUISE POWER (WATTS)	68.3	59.6
ORBITAL OPERATION/ENCOUNTER (WATTS)	181.8	88.3
VOLTAGES TO USERS		
SUBSYSTEMS VDC	+28, +16, +12, +5	+28, +16, +12, +5
COMMUNICATIONS VDC	28 ± 5 PERCENT	28 ± 5 PERCENT
SCIENCE VOLTAGE INPUT	NOT SPECIFIED	
BATTERY USAGE	LAUNCH AND VENUS ORBIT ECLIPSE	LAUNCH AND PEAK LOADS

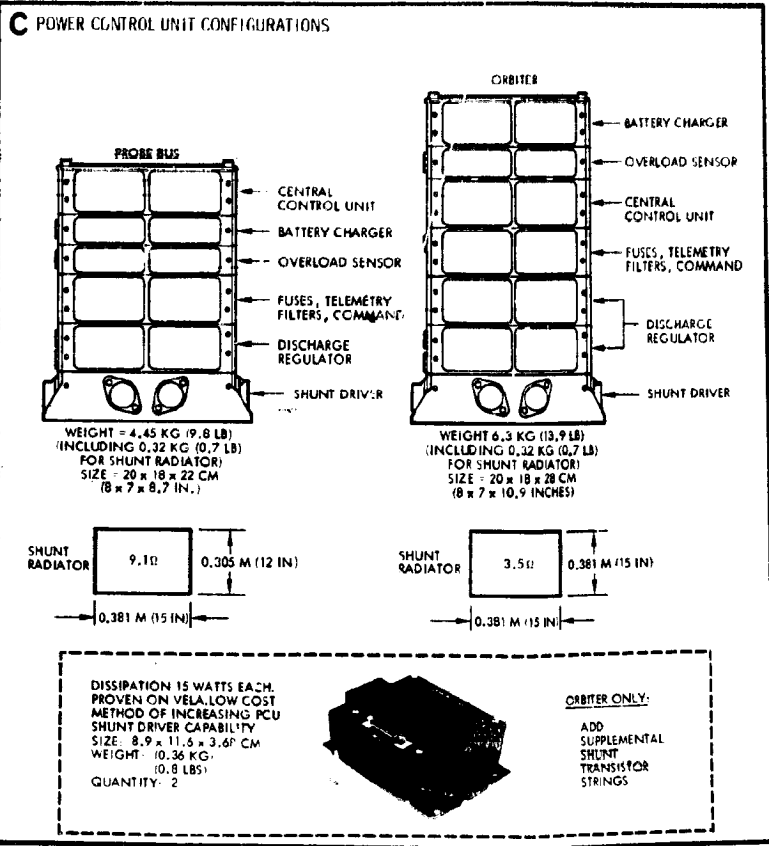
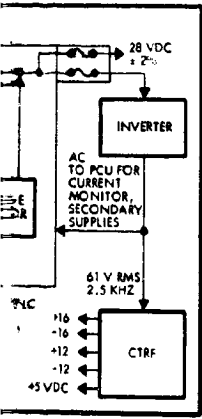
B ATLAS/CENTAUR POWER SUBSYSTEM BLOCK DIAGRAM



D CENTRAL TRANSFORMER RECTIFIER FILTER

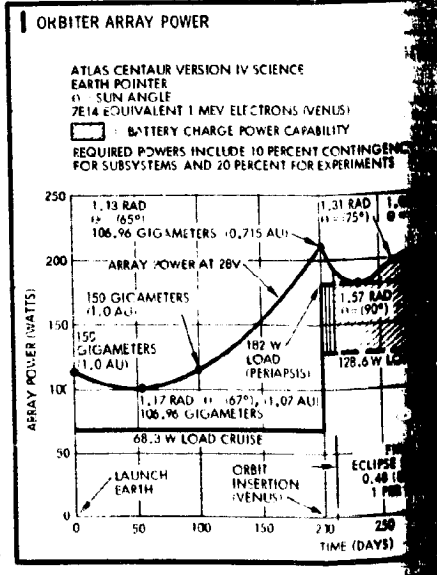
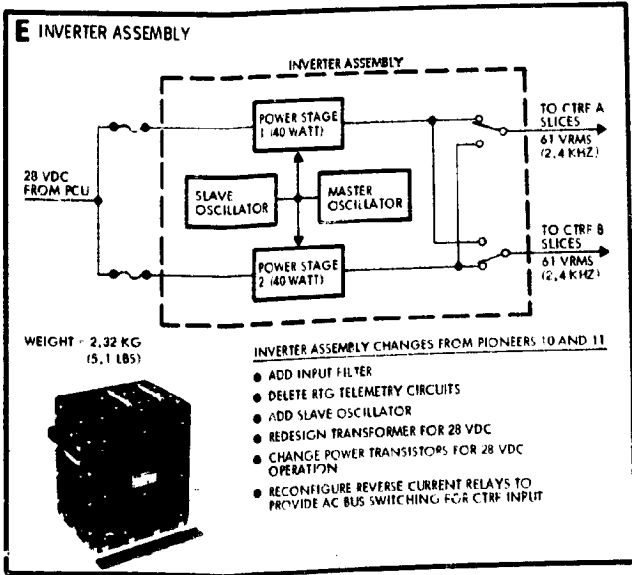
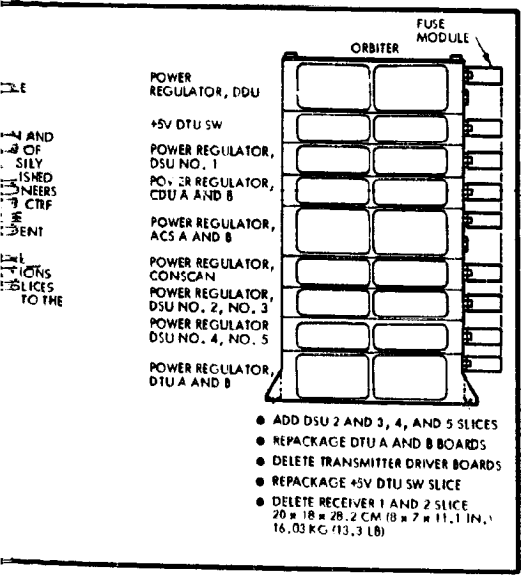
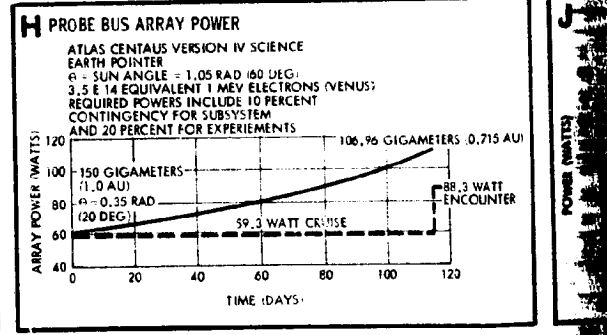


PROBE BUS	
114	1978
EARTH POINTING	
52.6	
59.6	
88.3	
+5	+28, +16, +12, +5
	28 ± 5 PERCENT
LAUNCH AND PEAK LOADS	



F BATTERY DESIGN

ORBITER		TYPE
TYPE	NICEL-CADMIUM	TYPE
1.42-HOUR ECLIPSE	62 PERCENT	CELL SIZE
CELL SIZE	18 A-HR (DSP 61)	CELL QUANTITY
CELL QUANTITY	16	CAPACITY
*CAPACITY	346 W-HR (145600) (100%)	DEPTH OF DISCHARGE
BATTERY WEIGHT	13.1 KG (28.8 LB)	WEIGHT



FOLDOUT FRAME

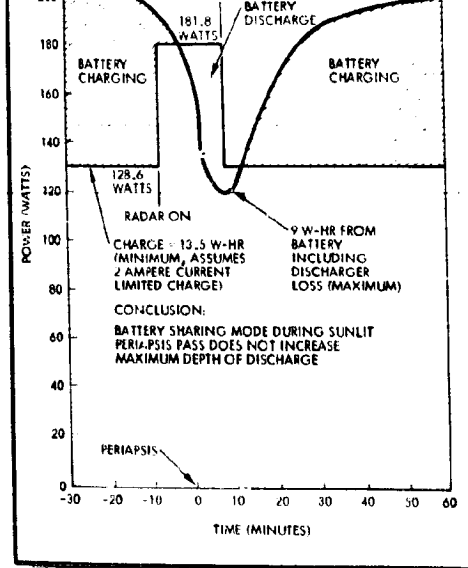
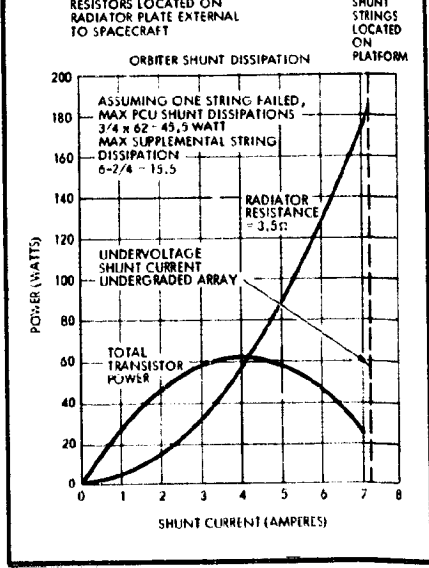
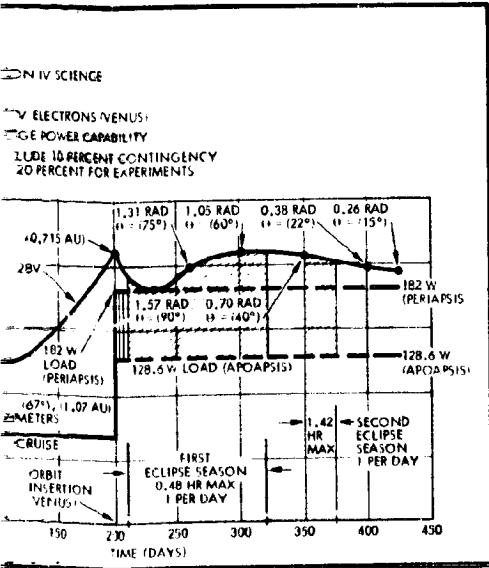
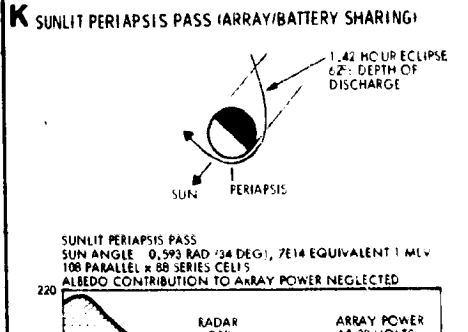
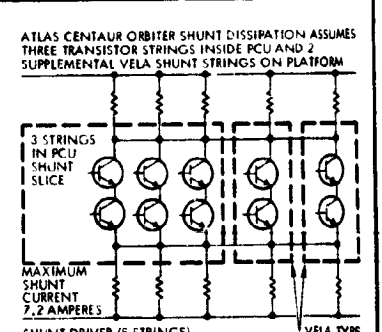
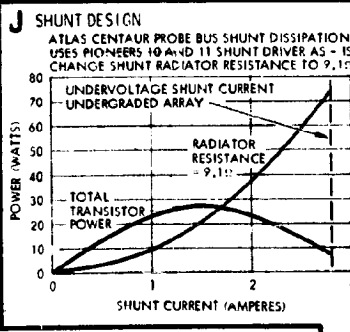
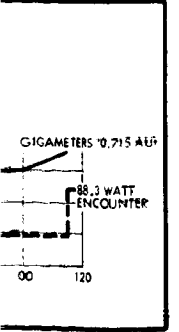
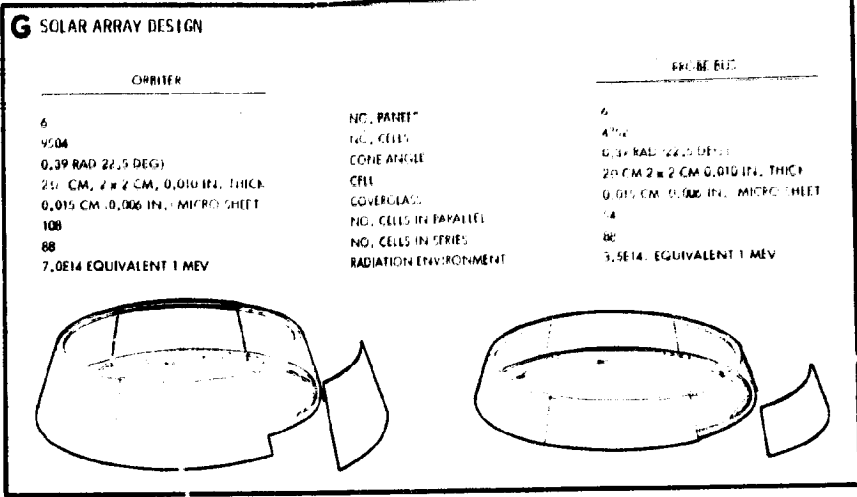
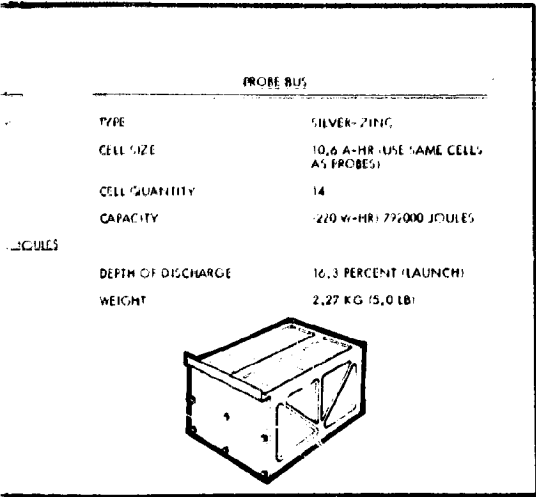


Figure 8.1-1. Preferred Orbiter and Probe Bus Power Subsystem Summary Atlas Centaur/Version IV Science

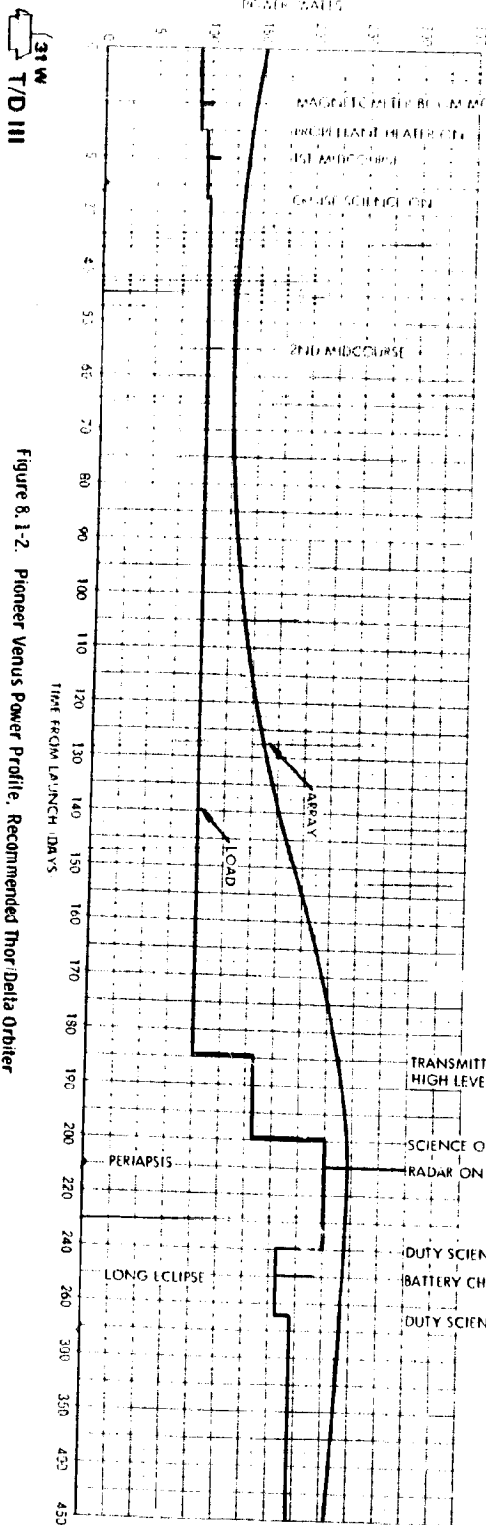


Figure 8.1-2. Pioneer Venus Power Profile, Recommended Thor/Delta Orbiter

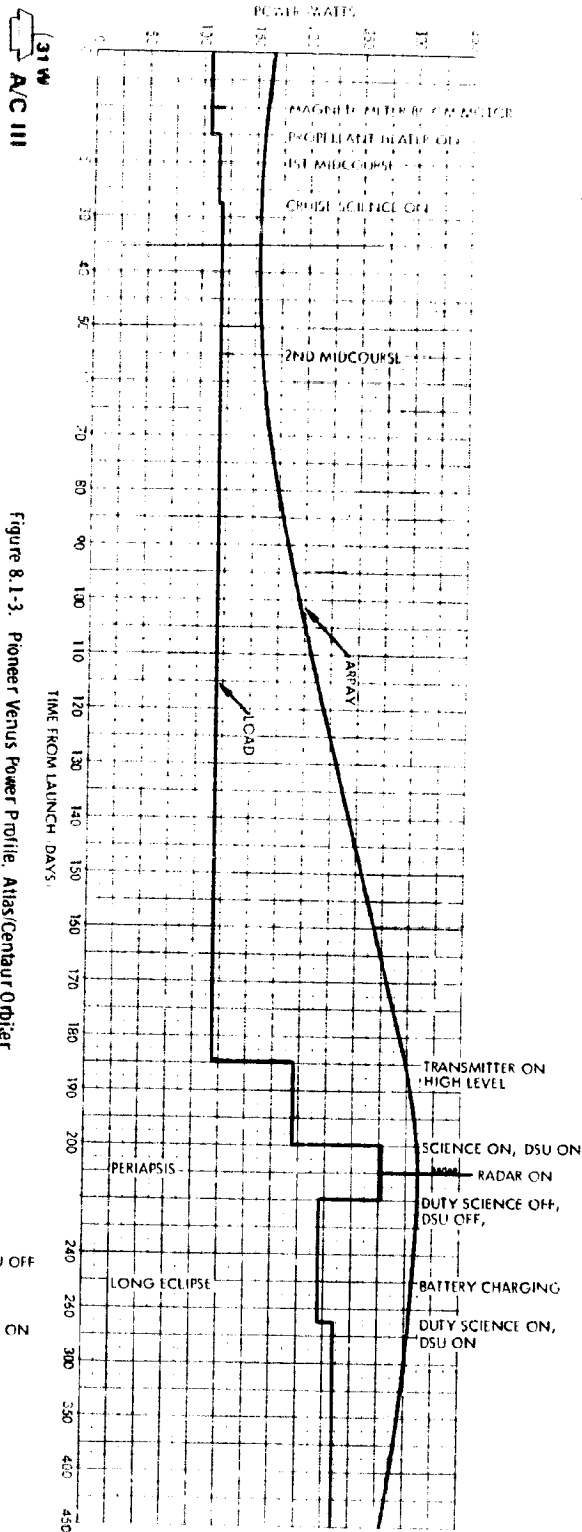


Figure 8.1-3. Pioneer Venus Power Profile, Atlas/Centaur Orbiter

ENC.

T/D III

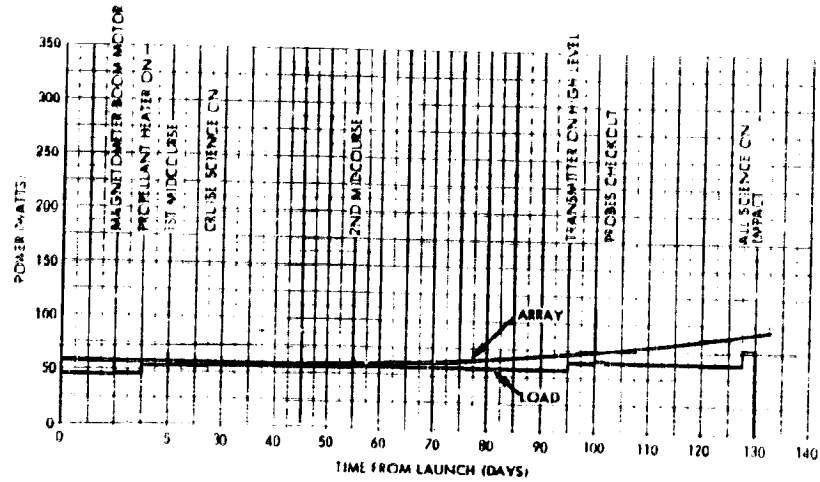


Figure 8.1-4. Pioneer Venus Power Profile, Recommended Thor/Delta Probe Bus

A/C III

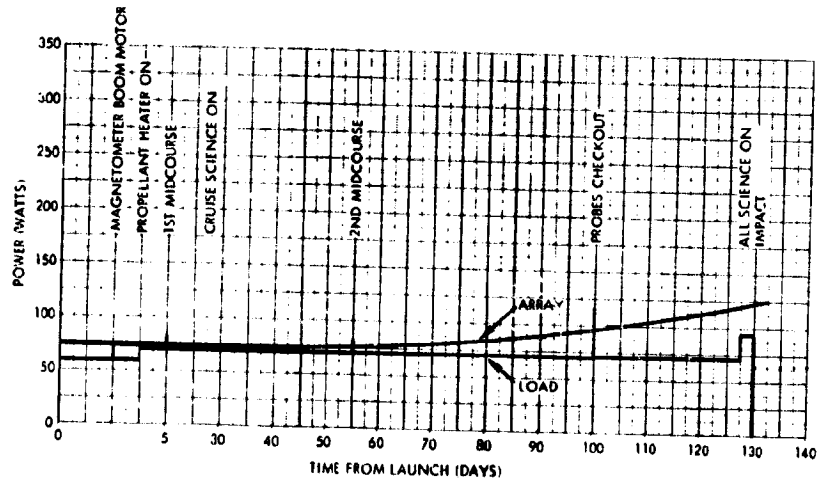


Figure 8.1-5. Pioneer Venus Power Profile, Atlas/Centaur Probe Bus

Section 8.1-2 presents the results of tradeoff studies leading to definition of the selected Thor/Delta subsystem. Sections 8.1-3 through 8.1-6 present details of the orbiter designs and design studies for the Version III science payload. Section 8.1.7 discusses the changes in these designs required for the probe bus, Version III science payload.

8.1.2 Power Subsystem Tradeoffs, Version III Science Payload

Two major tradeoff studies were made to establish the recommended Version III science payload subsystem configuration and solar array designs. The results apply to the orbiter and probe bus. The requirements serving as a basis for tradeoff studies are summarized in Table 8.1-1.

ALL VERSION III
SCIENCE PAYLOAD

Table 8.1-1. Subsystem Design Requirements, Version III Science Payload

REQUIREMENT	ORBITER		PROBE BUS	
	THOR/ DELTA	ATLAS/ CENTAUR	THOR/ DELTA	ATLAS/ CENTAUR
MISSION DURATION, DAYS	425	425	133	133
TIME PERIOD, YEARS	1978-79	1978-79	1977	1977
ORIENTATION OF SPIN AXIS	TO EARTH LINE		EARTH POINTING	
MAGNETIC CLEANLINESS,	<5 nT	<5 nT	<5 nT	<5 nT
LAUNCH POWER, WATTS	90.6	107.2	45.7	59.3
CRUISE POWER, WATTS	100.7/157.9 ¹	118.4/194.7 ²	56.4/64.3 ³	70.5
ORBITAL OPERATION/ ENCOUNTER POWER, WATTS	225.7	276.6	78.2	93.5
VOLTAGE TO USERS				
SUBSYSTEMS, VDC	±16, ±12, +5	±16, ±12, +5	±16, ±12, +5	±16 ±12, +5
COMMUNICATIONS, VDC	28 ± 2%	28 ± 5%	28 ± 5%	28 ± 2%-16, ±12
SCIENCE VOLTAGE INPUT	NOT SPECIFIED			
BATTERY USAGE	LAUNCH AND VENUS ORBIT ECLIPSE		LAUNCH AND PEAK LOADS (SHORT DURATION)	

¹DUAL POWER LEVELS INDICATE TRANSMITTER POWER OUTPUT SWITCHING FROM 16 TO 31 WATTS

²TRANSMITTER POWER SWITCH FROM 8.8 TO 35 WATTS

³TRANSMITTER POWER SWITCH FROM 3 TO 6 WATTS

8.1.2.1 Power Subsystem Configuration Tradeoff, Version III Science Payload

Fifteen different subsystem configurations were evaluated in arriving at the recommended Thor/Delta design as shown in Figure 8.1-6. The orbiter configuration was used as the basis for the tradeoff since it requires more power and is more complex than the probe bus. The probe bus subsystem was then derived from the orbiter to obtain the desired commonality with minimum redesign.

Orbiter Tradeoff Configurations

Configurations 1 through 4, 8, and 13 use series buck, buckboost, or shunt/boost regulators to limit array voltage to 33 VDC or regulate the bus voltage to 28 VDC ± 2 percent. Systems using 22-33 VDC are equipped with an off-the-shelf 22-cell nickel-cadmium battery, a DC/DC

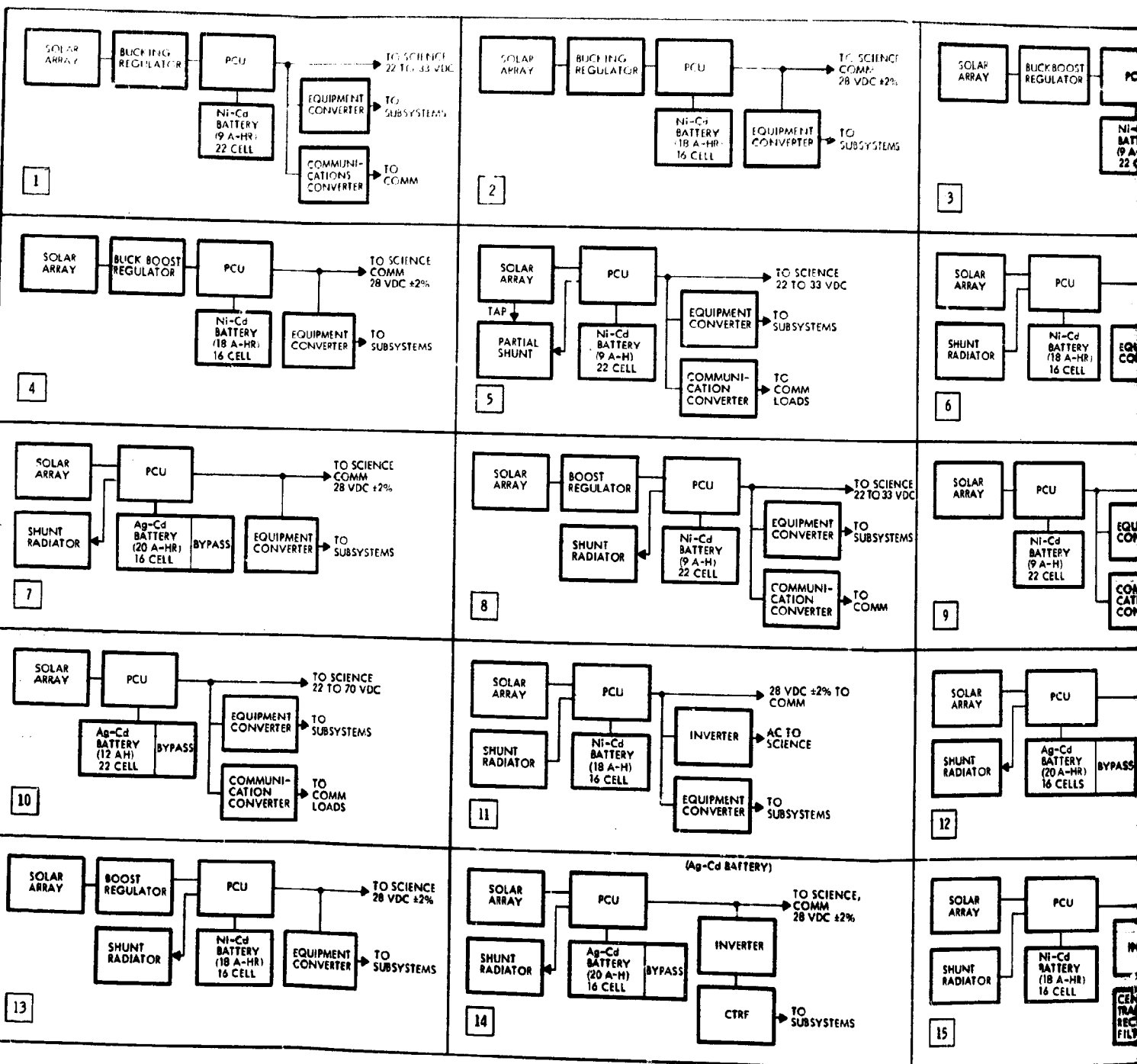


Figure 8. 1-6. Orbiter Power Trade Version III Science

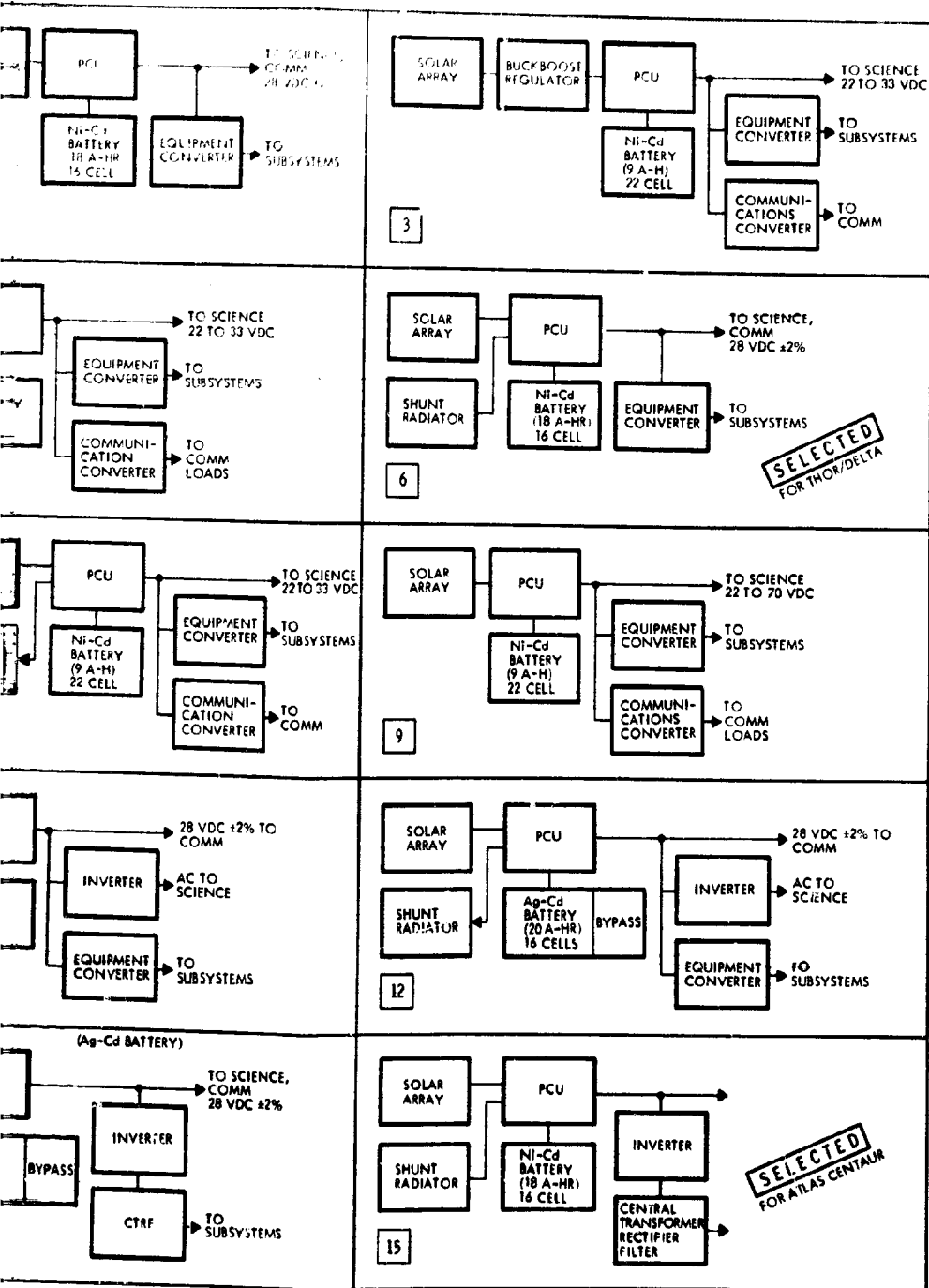


Figure 8.1-6. Orbiter Power Tradeoff Studies (Sizing Based on Thor/Delta Version III Science Payload)

converter which provides secondary voltage to the subsystems and a converter which supplies 28 VDC ± 5 percent to the communication loads. The battery is discharged directly to the bus. The 28 VDC ± 2 percent systems use a 16-cell battery which discharges to the bus through a boost regulator. A DC/DC converter provides subsystem secondary voltages and the communication loads operate directly from the bus.

Configurations 5, 6, 11 and 15 use a shunted array to limit the bus voltage to 33 VDC or regulate the bus voltage to 28 VDC ± 2 percent. Configurations 5 and 6 employ nickel cadmium batteries and secondary power conditioning as above. Configuration 11 employs an AC bus to the science instruments, while 15 uses the Pioneers 10 and 11 inverter/central transformer rectifier filter (CTRF) to supply the subsystems with secondary voltages.

Shunt array control provides minimum array size because of high efficiency at end of life when shunt current is minimum. This method of controlling the bus voltage is identical to that used on Pioneers 10 and 11. The shunt driver in the power control unit drives either a shunt element assembly (electronic) or a shunt radiator (resistive) to dissipate a portion of array power in excess of load requirements. The remainder is dissipated in the array as heat due to operating point control on the array I-V curve (constant voltage).

Configuration 7 is a silver-cadmium battery version of configuration 6. Similarly, 12 and 14 are silver-cadmium versions of 11 and 15, respectively.

All of the above configurations employ some type of array regulation which reduces the bus impedance, and results in minimum voltage transients on the bus during load changes or pulse load activation.

The remaining configurations (9 and 10) have no array voltage controls and the loads operate directly from the high impedance array. Bus voltage ranges from 22 to 70 VDC with the upper limit established by the array operating point at eclipse exit with a low temperature array. Configuration 9 uses a nickel-cadmium battery and Configuration 10 a silver-cadmium. Secondary power conditioning consists of two DC/DC converters for the subsystems and communication loads. The batteries are discharged directly to the bus.

Detailed cost and weight data for each major component of the candidate subsystems is presented in Appendix 8.1-A.

Orbiter Tradeoff Results

The weight and cost of each subsystem is shown in Figure 8.1-7. The cost data allows for sufficient quantities of hardware for both the probe bus and orbiter missions. Recurring and nonrecurring costs are included.

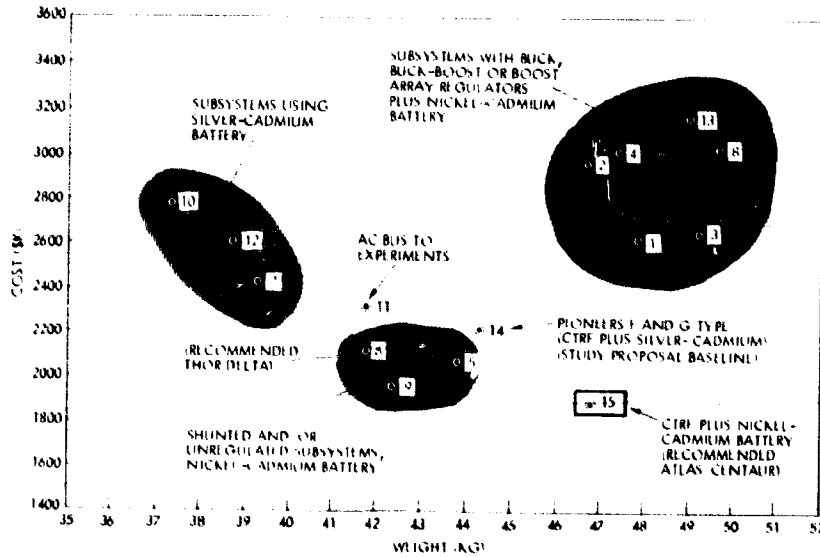


Figure 8.1-7. Version III Science Power Subsystem Cost/Weight Data

Configuration 14, the study proposal baseline subsystem, is a modified Pioneers 10 and 11 type subsystem with a CTRF, silver-cadmium battery, and inverter to convert the 28 VDC bus to a square wave AC input for the CTRF. This configuration (Figure 8.1-8), is too heavy for the Thor/Delta

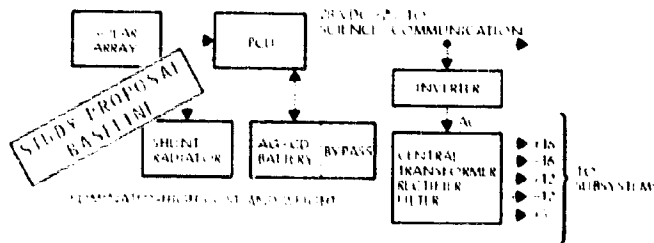


Figure 8.1-8. Configuration 14 Pioneers 10 and 11 Type Subsystem

mission because it provides isolated secondary voltages for each user to meet the stringent magnetic cleanliness requirements of Pioneers 10 and 11 (currents in platform eliminated).

Configuration 6, Figure 8.1-9, has a shunt connected across the array terminals which controls the bus upper voltage limit. The battery

is discharged through a regulator to maintain the bus voltage above the lower limit. A nickel-cadmium battery provides high reliability and long cycle life with high depth of discharge. Science and communication loads

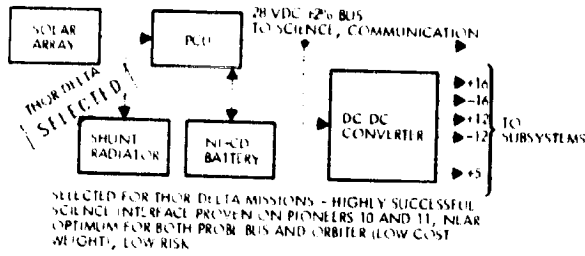


Figure 8.1-9. Configuration 6: Regulated Bus

operate directly from the regulated bus. A DC/DC converter provides separate isolated windings for high current loads to minimize magnetic field generation due to ground loops. This is the selected Thor/Delta orbiter configuration.

Three other systems, characterized by low cost and weight were considered for the Thor/Delta missions. Configuration 11, which supplies an AC bus to the science instruments, was eliminated because the nonstandard science power interface was judged to be high risk. Configuration 5, based on Intelsat III hardware, was suitable for the orbiter, but required extensive PCU modifications for the probe bus. Configuration 9, which supplied a completely unregulated bus of 22 to 70 VDC to the science loads, was eliminated because of high risk and it was too heavy for the probe version. (Configurations 7, 10, and 12 which were lightest in weight were eliminated because of high cost).

The Atlas/Centaur subsystem was selected for low cost and high reliability, unconstrained by weight or volume considerations. This allowed extensive use of existing hardware, eliminating many development risks.

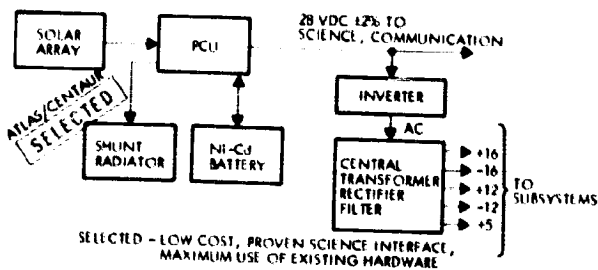


Figure 8.1-10. Configuration 15: Pioneers 10 and 11 Type Subsystem (Nickel-Cadmium Battery)

Configuration 15, Figure 8.1-10, was selected for low cost Atlas/Centaur versions. Derived from Configuration 14, it substitutes a nickel-cadmium battery, resulting in substantial cost savings, primarily due to the deletion of the cell bypass circuits and simple charge control.

Probe Bus Tradeoff Configurations and Tradeoff Results

Configurations 6 and 15, selected from the orbiter trade study, were then configured for the probe bus mission and further weight/tradeoffs performed. Four probe bus subsystems based on the lowest cost and weight orbiter configurations were defined (Figure 8.1-11). These are distinguished by the voltage characteristics of the main DC bus (i.e., regulated, voltage-limited and unregulated). In Configuration 1, the PCU includes a battery discharge regulator to maintain the bus at 28 volts \pm 2 percent. In Configuration 2 the battery discharges directly to the main bus. In Configuration 3, the shunt voltage limiter function is deleted and bus voltage is determined only by solar array and battery voltage characteristics. Configuration 4 is similar to Configuration 1, but uses an inverter/CTRF to generate secondary voltages.

In each configuration a silver-zinc battery is used due to the limited discharge requirements for the probe bus. The selection of 14 series cells in Configuration 1 permits battery charging from the main bus since the battery full charge voltage is less than 28 volts. In Configurations 2 and 3, more series cells are used to raise the bus voltage on discharge, but this requires a voltage greater than 28 volts for charging from the equipment converter. In each case a simple ground command controlled charging capability may be included to provide operational flexibility in contingency modes should power demands exceed the solar array capability. In normal operation, the battery is used only during the first several days of the mission to support eclipse loads and peak power requirements.

Configurations 1 and 2 are nearly equal in cost and weight. Configuration 3 is highest in cost and weight, and was eliminated. Configuration 4 is lowest in cost, but heavier than 1 and 2.

Configuration 1, the probe bus version of orbiter Configuration 6, was selected for the Thor/Delta missions. It provides maximum commonality between the orbiter and probe bus subsystems. Configuration 4, the probe bus version of orbiter Configuration 15, was selected for the Atlas/Centaur missions. The lowest cost configuration, it also provides maximum commonality between orbiter and probe bus subsystems, including the use of proven, off-the-shelf hardware.

SUBSYSTEM CONFIGURATION	ITEM	WEIGHT (KG)	\$ (A)
① <p>REGULATED BUS 28 VDC +2%</p> <p>THOR/DELTA [SELECTED]</p>	ARRAY	6.83	125
	PCU	4.46	230
	BATTERY	1.6	75
	CONVERTER	2.3	247
	TOTAL	15.19	677
② <p>VOLTAGE LIMITED - 28 VDC +2% -18%</p>	ARRAY	6.83	125
	PCU	3.10	200
	BATTERY	1.83	75
	CONVERTER	3.1	298
	TOTAL	14.86	698
③ <p>UNREGULATED BUS</p>	ARRAY	6.83	125
	PCU	1.82	160
	BATTERY	2.34	75
	CONVERTER	6.6	508
	TOTAL	17.09	868
④ <p>ATLAS/CENTAUR [SELECTED]</p>	ARRAY	6.83	125
	PCU	4.46	230
	BATTERY	1.6	75
	CTR/INVERTER	5.8	55
	TOTAL	18.7KG	485K

Figure 8.1-11. Probe Bus Power Tradeoff Studies (Sizing Based on Version III Science Payload Thor/Delta)

8.1.2.2 Secondary Power Conditioning Tradeoffs, Version III Science Payload

Requirements

Secondary loads comprise a mixture of active redundant, standby redundant, and internally redundant configurations. All are required for the orbiter. The major power users require 5-volt regulated power and resulting high currents. Each load is internally grounded and return current flow in the spacecraft structure is prevented by separate transformer windings where resultant magnetic fields could degrade performance of the magnetometer. Secondary voltage generation and distribution provide

protection against any component or wiring failure through the use of redundancy, current limiting, and fault isolation for each load. The secondary load requirements are summarized in Table 8.1-2.

Table 8.1-2. Secondary Load Requirements, Version III Science Payload

VOLTAGE	EQUIPMENT	MAXIMUM POWER (WATTS)	AVERAGE POWER (WATTS)
+5 ± 5%	CDU ACTIVE CHANNEL	1.83	1.34
	CDU STANDBY CHANNEL	0.50	0.50
	DSU, THREE ACTIVE CHANNELS*	4.50	4.50
	DTU, ACTIVE CHANNEL	2.99	2.83
	DTU, STANDBY CHANNEL	0.28	0.27
	DDU, TWO ACTIVE CHANNELS	0.04	0.04
	CEA, INTERNAL REDUNDANCY	3.00	3.00
	CONSCAN, NONREDUNDANT*	1.00	0.8
+12 ± 5%	DTU, TWO ACTIVE CHANNELS	0.22	0.22
+12 ± 1.5%	CEA, INTERNAL REDUNDANCY	0.12	0.12
+12 ± 3%	CONSCAN, NONREDUNDANT*	0.35	0.25
-12 ± 5%	DTU, TWO ACTIVE CHANNELS	0.14	0.12
-12 ± 1.5%	CEA, INTERNAL REDUNDANCY	0.07	0.07
-12 ± 3%	CONSCAN, NONREDUNDANT*	0.35	0.26
+16 ± 5%	DDU, TWO ACTIVE CHANNELS	0.14	0.12
-16 ± 5%	DTU, TWO ACTIVE CHANNELS	0.30	0.30
	DDU, TWO ACTIVE CHANNELS	0.14	0.14

* ORBITER ONLY

Experiments and command receivers require regulated multiple secondary voltages. These units (which will be powered from the main bus) will provide their own power conditioning.

Tradeoff Designs

Candidate power conditioning designs are shown in Figure 8.1-12. The tradeoff study is based upon the interface with science instruments, communication loads and user subsystem power requirements.

Science Power. Configuration 1 distributes regulated square wave AC power to transformer-rectifiers in each experiment, which centralizes the experiment power conditioning inversion functions. This saves weight

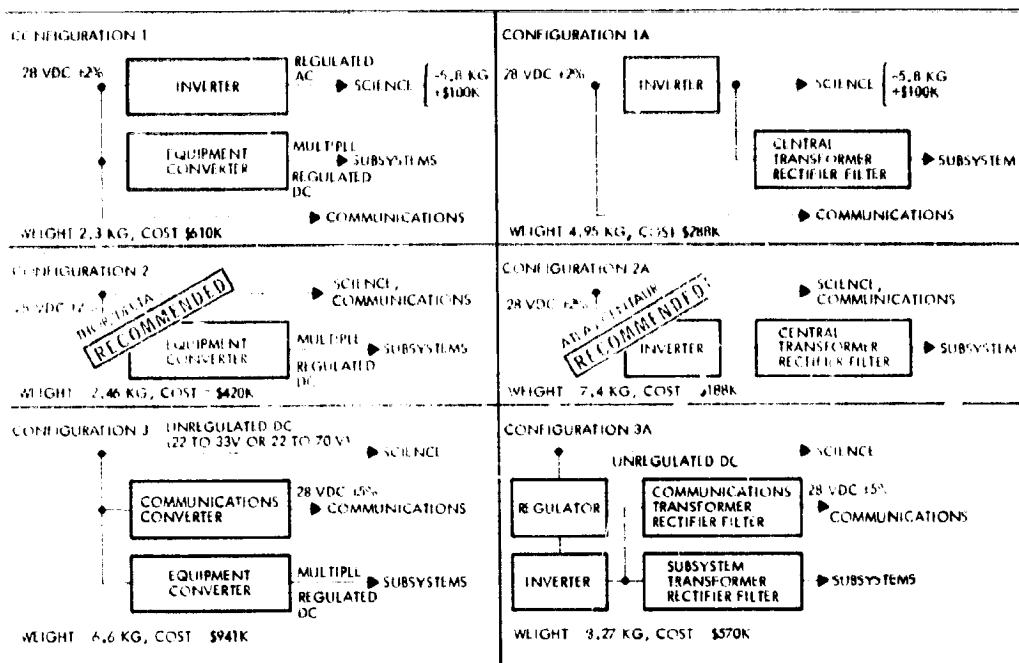


Figure 8.1-12. Candidate Power Conditioning Designs, Version III Science Payload

in comparison to Configurations 2 and 3 which use DC/DC converters in each experiment. The major disadvantages of the square wave AC interface is the difficulty in specifying transient characteristics of the power bus early enough to minimize program risk in experiment design and integration, and the lack of accurate AC power measurement instrumentation. Also, the AC interface requires control of load power factor and waveform rise time to limit radiated EMI. In Configuration 3, the experiment converters require additional parts to regulate the wider bus voltage variations.

Communications Power. Configuration 3 requires a separate DC/DC conversion function to supply regulated 28 volts to the S-band amplifiers. In Configurations 1 and 2, this function is provided by the bus regulation control directly.

Subsystems Power. Configurations 1, 2 and 3 use a central DC/DC converter to supply the regulated DC voltages required by the spacecraft subsystems. In Configurations 1A, 2A and 3A, a central transformer-rectifier filter (CTRF) fed from an inverter performs this function.

Although heavier, the inverter/CTRF approach utilizes modified Pioneers 10 and 11 equipment to minimize development cost and risk, facilitating interfaces with other elements of the subsystem, such as the Pioneers 10 and 11 inverter.

Tradeoff Results

The power conditioning weights and costs, listed for each configuration, were used for subsystem level weight/cost tradeoffs. Configuration 2, the selected Thor/Delta subsystem, is simple and lightweight. Configuration 2A, selected for Atlas/Centaur missions, is the most cost-effective approach. It combines minimum development cost and risk, through the use of Pioneers 10 and 11 designs and hardware.

8.1.2.3 Conical Versus Cylindrical Array Tradeoff, Version III Science Payloads

For the Version III science payloads, the recommended orbiter spin axis is perpendicular to the earth line, while the recommended probe bus spin axis orientation is earth pointing. However, during orbiter ΔV and periapsis maintenance maneuvers, the angle between the sun and spin axis may be as small as 0.35 to 0.52 radian (20 to 30 degrees). The probe bus spin orientation varies between 0.17 and 0.555 radian (10 and 32 degrees) from the sun line normally, with angles as large as 1.487 radians (85 degrees) possible during probe release maneuvers. A comparison of conical and cylindrical arrays was made because of this wide variation in sun angles present during both missions.

Figure 8.1-13 shows the relative power output capability as a function of angle for conical and cylindrical arrays sized to produce approximately equal power at 1.658 radians (95 degrees) sun angle. The conical array power output is relatively flat for sun angles from 0 to 1.66 radians (0 to 95 degrees), while the cylindrical array power approximates a cosine function and requires battery discharge to support the required load with small sun angles. The cone permits performance of ΔV , periapsis maintenance, and probe release maneuvers in a leisurely fashion independent of battery capacity limitations. Large probe thermal control is achieved through orientation of the bus to the desired sun angle. Earth pointing and spin axis perpendicular options are retained without significant impact on design.

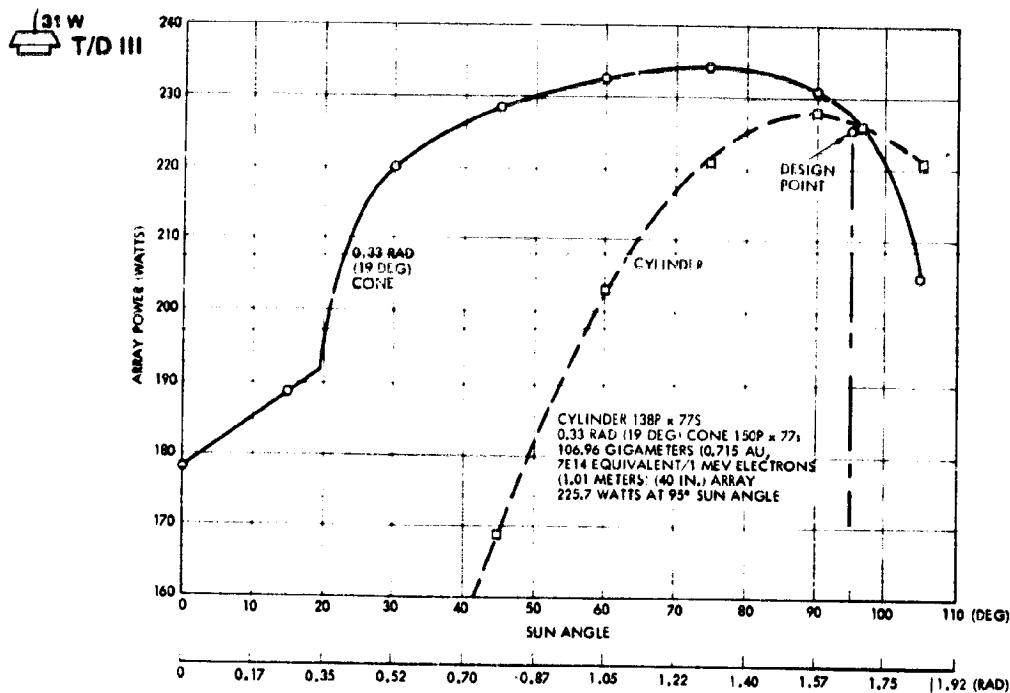


Figure 8.1-3. Orbiter Array Power Versus Sun Angle, 225.7-Watt Recommended Thor/Delta

Table 8.1-3 contains quantitative comparison data for the cone and cylinder. Note that weight and cost deltas are quite low. TRW has extensive design, manufacturing, and flight experience with conical arrays used on the DSP. This flight-proven technology is a resource directly applicable to the Pioneer Venus conical array design. Consideration of the operational advantages, flight-proven design, and modest weight and cost increases led to the selection of the conical array for Pioneer Venus.

The Thor/Delta orbiter array is sized to provide battery independent operation near Venus when oriented with the spin axis perpendicular to the earth line. The minimum sun angle near Venus is 0.52 radian (30 degrees) for periapsis maintenance. The array power decreases for sun angles near 0.52 radian (30 degrees). Load reduction is permissible during periapsis maintenance which is performed at apoapsis (radar off).

The probe bus array for the 1977 launch is sized to preclude battery discharge for all possible sun angles from 0 to 1.65 radians (0 to 95 degrees) at earth and Venus. The minimum cone angle which satisfies this requirement is 0.33 radian (19 degrees). (See Appendix 8.1E).

(31 W)

T/D III Table 8.1-3. Thor/Delta Orbiter and Probe Bus Comparison of Conical and Cylindrical Arrays for Version III Science Payload

SIZING CONDITIONS: 106.96 GIGAMETERS (0.715 AU), SUN ANGLE 1.66 RAD (95 DEG), P_{LOAD} 225.7 WATTS
2 x 2 CM CELLS, 7 x 10¹⁴ EQUIVALENT 1 MeV ELECTRONS (ORBITER), 2 OHM-CM CELLS

1. ORBITER					
CONFIGURATION	106.96 GIGAMETERS (0.715 AU) POWER (WATT)	NUMBER OF PARALLEL CELLS	NUMBER OF SERIES CELLS	TOTAL CELLS	WEIGHT (KG (LB))
0.33 RAD (19 DEG) CONE	227	150	77	11 550	14.8 (32.6)
CYLINDER	226	138	77	10 626	13.6 (30.0)
				ΔCELLS = 924 ΔW =	1.2 (2.6)
		COST OF 924 CELLS	=	13.85 K	
		COST OF TOOLING + LAYUP	=	5.0 K	
		ΔCOST \$		18.85 K	
2. PROBE BUS USES 4960 CELLS; CELLS CONE VERSUS CYLINDER = 402 CELLS					
P _{LOAD} = 56.4W CRUISE		COST OF 402 CELLS	=	6.05 K	
78.2W ENCOUNTER		COST OF TOOLING + LAYUP	=	2.5 K	
		ΔCOST \$		8.55 K	
		TOTAL COST \$		27.4 K	

A cone angle of 0.33 radian (19 degrees) (common to both the orbiter and probe) was selected to minimize array substrate tooling costs while meeting the power requirements of both missions over the required sun angles.

8.1.3 Orbiter Power Subsystem Tradeoffs, Version III Science Payload

(31 W)

A/C III

(31 W)

T/D III

Two study areas concerned solely with the orbiter are the orbiter battery and the sunlit periapsis pass array sizing.

8.1.3.1 Orbiter Battery Tradeoff, Version III Science Payload

The orbiter battery supplies power to the loads during launch, solar eclipses at Venus and whenever load requirements exceed array capability. The battery is sized by the eclipse loads and profile shown in Figure 8.1-14. There are two eclipse seasons; a long season of short eclipses (0.48 hour maximum), and a short season of long eclipses (1.42 hour

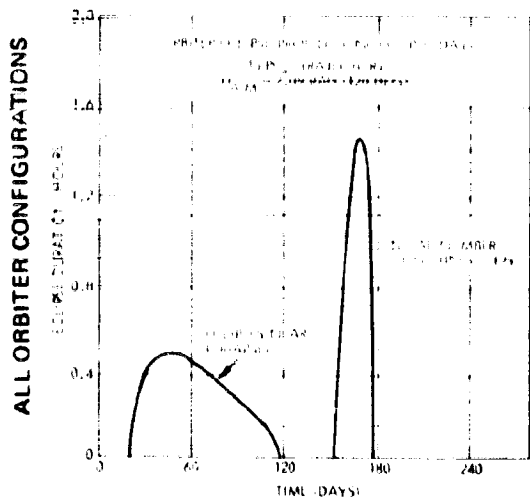


Figure 8.1-14. Orbiter Payload Eclipse Loads and Profile

maximum). There is only one eclipse during each 24-hour orbit. Between eclipse seasons the spacecraft is in 100 percent sunlight and battery discharge is not required. The total number of eclipses is 125.

The cycle life and wet stand capability of three types of rechargeable battery cells are compared in Table 8.1-4. Cycle life data for silver-cadmium, silver-zinc (secondary), and nickel-cadmium cells are in Appendix 8.1B.

Table 8.1-4. Orbiter Battery Selection Summary, Version III Science Payload

	NI-CD	AG-CD WITH BYPASS	AG-ZN (SECONDARY)
CYCLE LIFE	PREDICTABLE	TEST DATA SCATTERED	TEST DATA SCATTERED
TIME DEPENDENT CAPACITY LOSS (425 DAYS)	APPROXIMATELY 10%	20 TO 50%	HIGHER THAN AG-CD
RECOMMENDED MAXIMUM DEPTH OF DISCHARGE	80%	60% (WITH BYPASS)	30%
TEMPERATURE RANGE	5 TO 35°C	5 TO 25°C	5 TO 25°C
STATUS	FLIGHT PROVEN CELLS	FLIGHT PROVEN DESIGN (PIONEERS 10 AND 11)	NOT PROVEN IN PLANETARY CYCLIC DISCHARGE OPERATION
RISK	LOW	MODERATE	HIGH
MAGNETIC PROPERTIES	APPROXIMATELY 3000 AT 30.5 CM (5 AMP, DISCHARGING)	17 AT 30.5 CM (OPEN CIRCUIT)	COMPARABLE TO AG-CD
CONFIGURATION	16 24 A-HR CELLS	16 30 A-HR CELLS	12 60 A-HR CELLS
WEIGHT	17.5 KG (38.6 LB)	13.9 KG (30.7 LB)	11.6 KG (25.6 LB)
COST	\$300 K	\$585K	--

Silver-Zinc

Data for silver-zinc cells show a cycle life of 100 to 200 days for 24-hour cycles at 25°C and depths of discharge ranging from 20 to 60 percent. Under the most favorable circumstances a silver-zinc secondary battery would probably complete this mission. The cycle life data is widely scattered, indicating an apparent lack of understanding and control

of the causes of wide variability in silver-zinc cell performance. This unpredictability leads to reduced depths of discharge resulting in higher weight. Another factor is the paucity of flight experience for silver-zinc batteries operated in charge/discharge cycling regimes. Silver-zinc cells, applied to the orbiter mission, would result in a design of unacceptably high risk and they were rejected.

Silver-Cadmium

Silver-cadmium cells have a theoretical energy density considerably greater than that for nickel-cadmium cells and are magnetically clean. However, a number of factors act to reduce the usable energy density for the orbiter mission. These include time dependent capacity loss, tendency toward leakage and cell shorting. Appendix 8.1B shows data for capacity loss as a function of time. For this analysis a capacity loss of 20 percent was assumed (float charge method used) and an additional 20 percent was allowed for capacity loss due to cycling. The maximum depth of discharge allowable is approximately 60 percent.

Silver-cadmium cells have substantial flight experience, but there have been notable in-flight failures due mainly to high temperature susceptibility and inability to accept high charge rates. Cycling data presented in Appendix 8.1B shows scattered performance similar to silver-zinc cells, although the cycle life is somewhat better.

Because overcharge current is highly sensitive to applied voltage limit in these cells, and because the I-V characteristic of each cell is different, the cell voltage dispersion tends to become larger with operating time. For this reason individual cell overcharge limiting was used. Additionally, the 60-percent depth of discharge was made possible by using cell bypass circuits which protect against cell reversal. This is the technique employed on Pioneers 10 and 11. The requirement for cell bypass protection results in substantially higher battery costs. The cost data shown in Table 8.1-4 also includes allowance for a life test which is necessary because of the lack of data for silver-cadmium batteries used in planetary missions having long cruise times followed by charge-discharge cycling.

Nickel-Cadmium

The relaxed magnetic cleanliness requirements of Pioneer Venus vis a vis Pioneers 10 and 11 made nickel-cadmium batteries a viable

31W

A/C III candidate. A discussion of the magnetic field impact on magnetometer boom length is provided in Section 3.2.2. Nickel-cadmium batteries are characterized by superior cycle life at high depths of discharge, simple charge control, low cost, and extensive flight experience. Most recently, a single nickel-cadmium battery was successfully employed during the 9 months of orbital operation on the Mariner Mars '71 mission (70 percent maximum depth of discharge, 126 cycles). Manufacturer process controls and materials usage have improved to the point performance predictability is far superior to silver-cadmium and silver-zinc cells. Appendix 8.1B shows that cycle life even at 80 percent depth of discharge is considerably in excess of the orbiter mission requirement of 125 charge/discharge cycles. Conservative cycle life rating together with careful cell matching procedures eliminates the need for cell bypass circuits. The battery reliability is calculated to be 0.998 for 425 days.

31W

T/D III

While battery cell open circuit failure would cause loss of power during eclipse, the likelihood of such a failure is virtually nil. Battery redundancy (two batteries in parallel) would increase orbiter weight by approximately 18.2 kilograms and would cost \$75K including charge control and cabling. Cell bypass circuits would add 3.63 kilograms and \$198K to the weight and cost of the orbiter battery.

The cost of the nickel-cadmium battery is approximately one-half that of the silver-cadmium battery. It is 3.6 kilograms heavier. The low risk, low cost nickel-cadmium battery is the recommended Thor/Delta and Atlas/Centaur orbiter design.

8.1.3.2 Sunlit Periapsis Pass Array Sizing Tradeoffs (31W T/D III

Approximately 0.65 hour after the 1.42-hour eclipse, the spacecraft will pass close to Venus on the sunlit side. The added light intensity due to planetary albedo causes array heating which reduces the array voltage. Figure 8.1-15 depicts the periapsis pass situation. It should be noted that this condition exists for only a few orbits during the mission. The Thor/Delta array has been sized to provide 226 watts at 28 volts at a temperature of 50°C and sun angle of 1.657 radians (95 degrees).

The increased array temperature reduces the power available at 28 VDC. The shaded area above the array power versus time curve

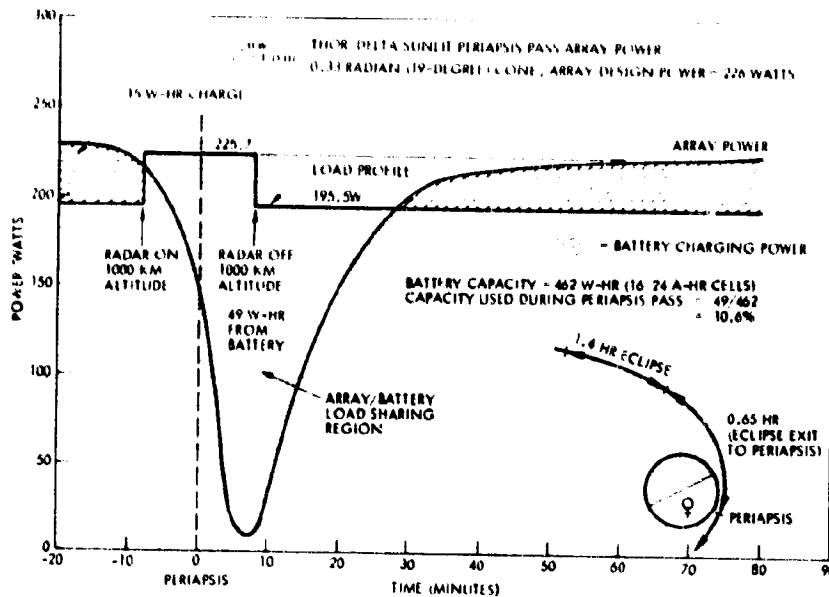


Figure 8.1-15. Orbiter Periapsis Pass Situation, Version III Science Payload

shows that the array capability falls below the load requirements for a short period. The battery is discharged to support the load. The total battery energy used is 49 W-hr or only 10 percent of the battery capacity. During the time after the 1.42-hour eclipse and before periapsis, the battery is charged with 15 W-hr. The Section 8.1.4.5 shows that the battery depth of discharge is 66 percent during the 1.42-hour eclipse. Hence, using the battery to supplement the array results in a maximum depth of discharge of 73.5 percent.

Increasing the number of series cells on the array would preclude battery discharge at high array temperatures, but this would add weight and cost. Since the battery is easily capable of supplementing the array during the periapsis hot pass condition and discharge is required only during a few orbits. Battery discharge during the hot pass is the selected approach.

8.1.4 Recommended Thor/Delta Orbiter Subsystem Design, Version III Science Payload

8.1.4.1 Configuration

The Thor/Delta power subsystem was selected for low weight with reasonably low cost. A detailed block diagram of the Thor/Delta orbiter

power subsystem is shown in Figure 8.1-16. The recommended subsystem uses a highly successful bus voltage control method proven on Pioneers 10 and 11. Appendix 8.1C provides a description of the various operating modes. The power control unit contains a central control unit (CCU) which senses the bus voltage to enable the shunt when the array power exceeds load power. A shunt driver acts as a variable load to control shunt radiator current and dissipation. The charge regulator is enabled whenever array power exceeds load power. When the bus voltage decreases slightly due to load demand exceeding array capability, the discharge regulator is enabled and the battery supports the bus. The CCU logic precludes shunting and discharging simultaneously. Commands and telemetry are processed in the PCU. The nickel-cadmium battery provides a highly reliable energy source for eclipse power. The DC/DC converter provides secondary voltages to the subsystems.

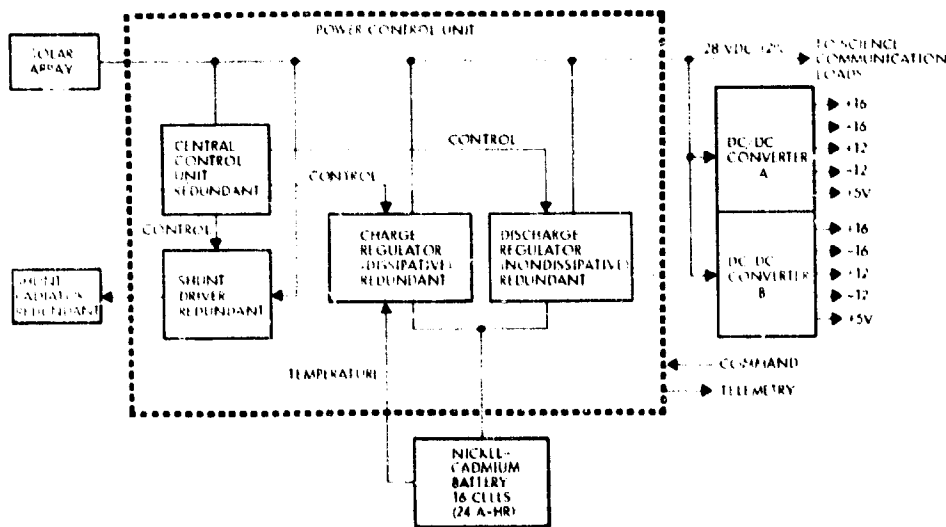


Figure 8.1-16. Recommended Thor/Delta Orbiter Subsystem Block Diagram (28 VDC \pm 2 Percent Regulated Bus)

Redundancy has been incorporated in critical areas to preclude single point failures. The central control unit employs two of three majority voting circuitry. The shunt driver is quad redundant to prevent loss of shunt control due to open or short failure modes in the power amplifiers. The charge and discharge regulators are redundant to prevent loss of the battery. The DC/DC converter supplies redundant secondary voltages to redundant user subsystems. Each secondary output is current-limited to

prevent fault propagation. The shunt power capability has been sized to allow for single failures in the strip resistors (open-circuited resistive element) of the shunt radiator. Possible faults in the solar array are isolated by blocking diodes in the array harness.

8.1.4.2 Power Control Unit

The power control unit for the Thor/Delta orbiter (Figure 8.1-17) uses existing Pioneers 10 and 11 designs wherever possible to minimize costs. The central control unit, shunt driver, and overload sensor off-the-shelf Pioneers 10 and 11 designs. Because of the change from RTG's (radioisotope thermoelectric generators) to a solar array and the use of a nickel-cadmium battery in a cycling mode new designs are required for the battery charger, bus filter, and discharge regulator slices. Telemetry and command circuitry will be minimally modified Pioneers 10 and 11 designs.

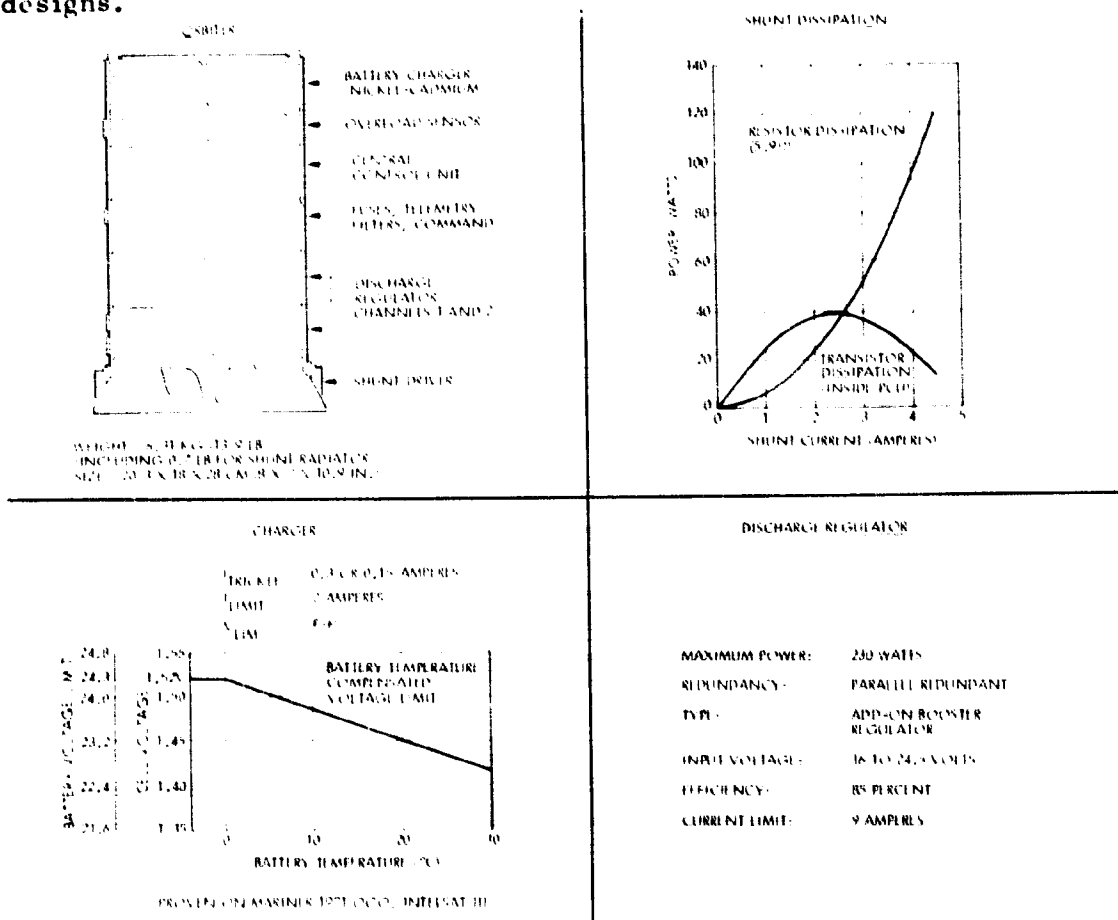


Figure 8.1-17. Thor/Delta Orbiter Power Control Unit, Version III Science Payload

The shunt dissipation as a function of shunt current is also shown in Figure 8.1-17. Peak PCU dissipation within the equipment compartment due to the shunt driver losses is 40 watts. The shunt radiator is simply a resistive load (5.9 ohms) and its dissipation varies as the square of the current. A maximum shunt current of 4.5 amperes is possible at Venus if the array degradation and load are minimum. The peak current capability of the shunt driver with one power transistor inoperative is 4.5 amperes. Therefore, the shunt driver capability is adequate even for failure mode conditions. A discussion of shunt sizing is in Appendix 8.1D.

The shunt radiator maximum dissipation is 119 watts. The location and size of the shunt radiator has been selected to accommodate a temperature range of -156.5 to $+121.5^{\circ}\text{C}$ (-250 to $+250^{\circ}\text{F}$). The shunt radiator size is 38 by 32 by 3.3 cm (15 by 12 by 1.3 inches).

The nickel-cadmium battery charger is located in the PCU. The charge control method selected has been flight-proven on OGO, Intelsat III, and Mariner Mars '71. The battery voltage is limited as a function of temperature by a series dissipative regulator to prevent battery thermal runaway. The maximum charge current is limited to 2 amperes with switch to trickle charge when the voltage limit is reached. The 0.15-ampere trickle charge rate can be selected by ground command to limit battery dissipation during cruise. During the orbital phase of the mission the 0.3-ampere trickle charge rate can be used to increase the battery state of charge.

Battery charging power is derived from turning off science instruments which only desire data near periapsis. This provides a minimum of 22 hours battery charging capability during orbits with a maximum eclipse.

The PCU contains a redundant discharge regulator (nondissipative switching type) which boosts the 16- to 24-volt battery to 28 VDC. The discharger efficiency is greater than 85 percent at 230 watts load. Redundancy is provided to preclude single part failures. Six pounds have been allocated for the redundant discharge regulator. The discharger dissipation of 35 watts for maximum load conditions requires a good thermal path to the spacecraft platform through the shunt slice.

8.1.4.3 Equipment Converter

Parallel redundant DC/DC converters in a single package are used (Figure 8.1-18). Each converter input is fused to protect the main DC bus against converter faults. Output power switching is by command to select converter channels for internally redundant loads (DSU, switched 5 volts for DTU, CEA) and to provide complete fault isolation for each load fed from a common output. Only compatible loads requiring low currents are supplied from common outputs to assure noninterference and eliminate magnetic fields generated by return currents in the structure which could affect the magnetometer.

Each converter channel supplies 11 isolated, regulated outputs. All secondary power grounds are located in the load equipment. The dissipative type output regulators provide excellent dynamic response to load variations and also provide current limiting in the event of overload to protect the converter. Overvoltage protection is provided for each output. Each channel is capable of supporting the total secondary load. The loads are approximately equally divided between channels during normal operation to maximize converter efficiency.

This approach was selected for the recommended Thor/Delta subsystem because of weight savings achieved by combining transformers into one multiple-secondary power transformer per channel.

8.1.4.4 Solar Array

The Thor/Delta orbiter array was sized to provide at least 225.7 watts at Venus with a 1.657-radian (95-degree) sun angle. There are many interrelated factors which affect the size of the solar array. The temperatures predicted for a 0.33-radian (19-degree) cone angle vary with solar aspect angle and distance from the sun, and range from -4 to 71°C, while the light intensity varies from 0.87 to 1.96 times the mean intensity at earth.

The most efficient combination of series and parallel cells was determined by an iterative computer analysis considering the required range of solar intensity and temperature after radiation degradation. The different sun angle requirements for the orbiter and probe lead to different numbers of cells in series as well as parallel for the two missions.

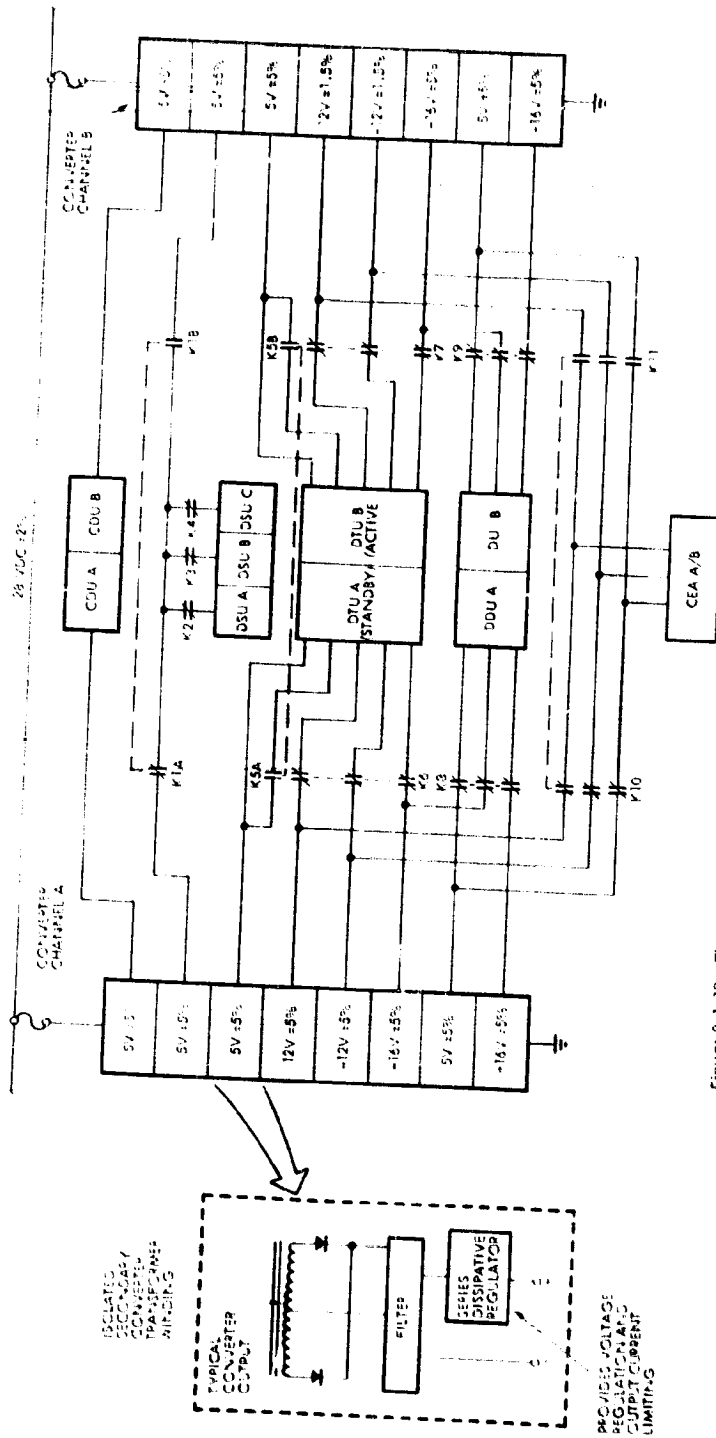


Figure 8.1-18. Thor/Delta Or jitter Equipment Converter, Version III Science Payload

The cell characteristics were determined from measured properties of JPL cells at high intensity adjusted for the configuration and thickness best suited to these missions (Reference 1).

Radiation Environment

The dominant factor in radiation degradation for the Pioneer Venus solar array is solar flare protons. Passage through the earth's trapped radiation belts has a negligible effect.

The radiation factors used are based upon NASA predictions for the time period of interest, and over 20 percent of the orbiter array is required to make up for anticipated radiation losses.

The radiation model used throughout the analysis was based upon NASA's predictions for the cycle peak of the 21st solar cycle. Three NASA

documents (References 2, 3, and 4) were reviewed describing space environment criteria guidelines for use in space vehicle development for the time period between 1977 and 1982. All agree with the curved line shown in Figure 8.1-19. An independent JPL analysis (Reference 5) intended for the 20th solar cycle is shown as a straight line.

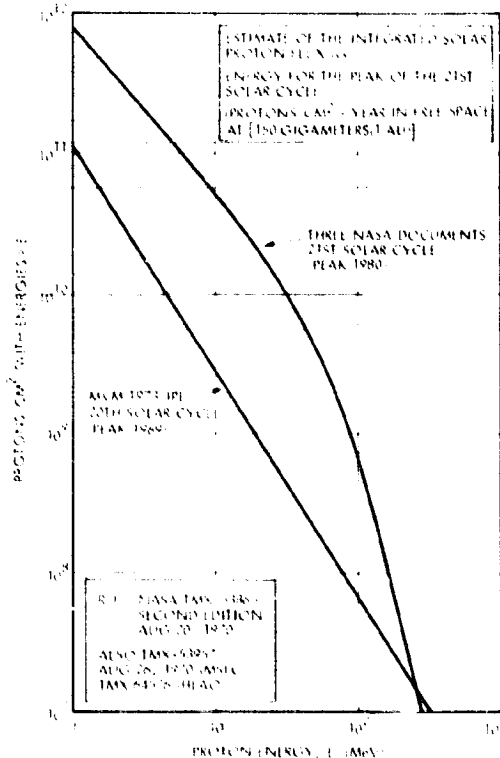


Figure 8.1-19. Solar Flare Radiation Environment

There is more than an order of magnitude difference between the observed peak of the 20th solar cycle and the predicted peak for the 21st cycle. The data for the 21st cycle is based upon the cycle 19 (1959) peak which was the worst event in 188 years of measured data. Cycle 20 (1968-1969)

data shows that it was a typical medium peak. Basing the solar array degradation on cycle 21 data results in a conservative array design which increases array weight and cost.

A less conservative approach might be to use the maximum predicted point for the 20th cycle. JPL is currently using the low point (1975) of this cycle for the Mariner Venus Mercury mission. Assuming use of the predicted 20th cycle would reduce the size and cost of the solar array.

It was assumed that the 425-day orbiter mission would incur 425/365 times the annual 150 gigameters (1 AU) fluence, adjusted for $1/r^2$ during its mission to Venus in 1978-1979. Solar flares are discrete events, and there may be two to four in a year with random spacing. For approximately 60 days the orbiter will be over 150 gigameters (1 AU) from the sun and the proton fluence used was 60/365 times the annual 150 gigameters (1 AU) fluence. The proton fluence was converted to equivalent 1 MeV electrons as shown in Table 8.1-5.

Table 8.1-5. 21st Cycle Used for Thor/Delta Array Design, 20th versus 21st Solar Cycles (Peak)

	20TH	21ST
PEAK YEAR	1969	1980
60 DAYS, EARTH	2.7×10^{12} (1 MEV)	5.8×10^{13} (1MEV)
DEGRADATION	0	5.3 PERCENT
365 DAYS, VENUS	3.2×10^{13} (1 MEV)	7×10^{14} (1 MEV)
DEGRADATION	2.6 PERCENT	22.5 PERCENT

Solar Cell and Coverglass Selection

The cost of solar cells decreases with thickness due to breakage of thinner cells. Added material cost above about 10 mils is negligible, but thicker cells have somewhat higher power output. After a moderately heavy radiation dose, however, the output of cells is independent of thickness.

Similar conditions hold for fused silica covers, except that material cost is a higher fraction of total cost, with 20-mil fused silica covers least expensive. Microsheet is generally used only in 6-mil thickness, which is considerably cheaper than fused silica. For the intended mission, microsheet darkening will not be significant.

In order to make a selection (Figure 8.1-20), it was assumed that 5000 cells of 10 Ω cm base resistivity 10 mils thick, with 6-mil micro-sheet at 150 gigameters (1 AU) from the sun, 28°C and 1 year of radiation were used. This formed an arbitrary baseline for comparison, considering cost, weight, and number of cells, holding output power constant. Cost includes installation on the substrate.

The 10 Ω -cm cells were slightly preferred over 2 Ω -cm, but since reliable data was not available on 10 Ω -cm cells at high intensity and the cost difference was small, the 2 Ω -cm cell was selected. With 12- or 20-mil fused silica covers the cost is slightly less, but the weight is increased by a pound or two, which imposes an even higher penalty and negates the cost improvement.

Array Temperature

The solar array temperature varies as a function of solar distance and distance from Venus near periapsis. Appendix 8.1E shows the array temperature data upon which the design is based. Temperature variation as a function of solar distance, cone angle and sun angle was included in the array sizing calculations.

Array Sizing Summary

The sizing factors are presented in Table 8.1-6.

The array consists of six equal-sized panels arranged to form a cone with a 0.33 radian (19-degree) half angle. The packing factor is 0.84 percent. The strings are comprised of modules containing 3 parallel by 6 series 2 x 2 cm cells. The selected Thor/Delta array configuration is shown in Figure 8.1-21.

8.1.4.5 Battery

The recommended Thor/Delta orbiter has a load of 182.6 watts during the maximum eclipse time of 1.42 hours. This is a total energy of 181.5 x 1.42 = 258 W-hr (303 W-hr including discharger loss).

Sixteen 24-A-hr cells provide 462 w-hr assuming an average discharge voltage of 19.2 volts (1.2 volts/cell). Each cell weighs 0.91 kilogram (2 pounds) which results in a total battery weight of 17.5 kilograms

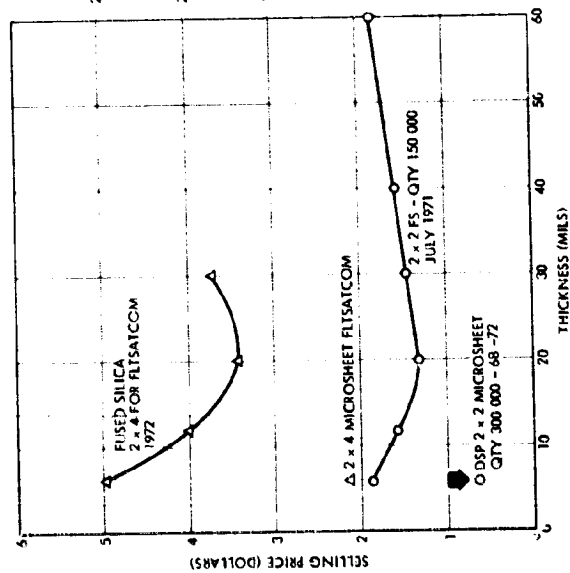
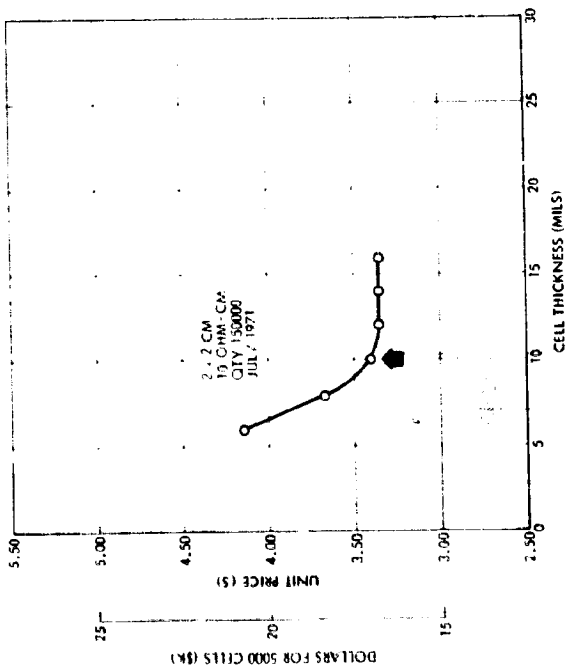
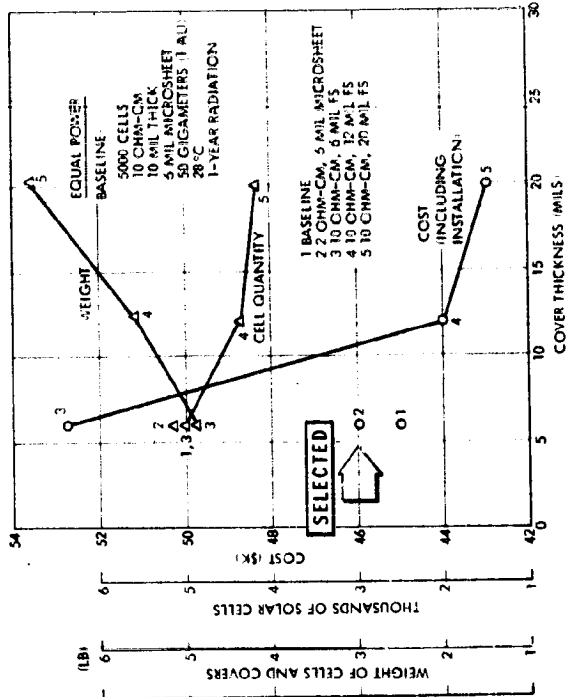
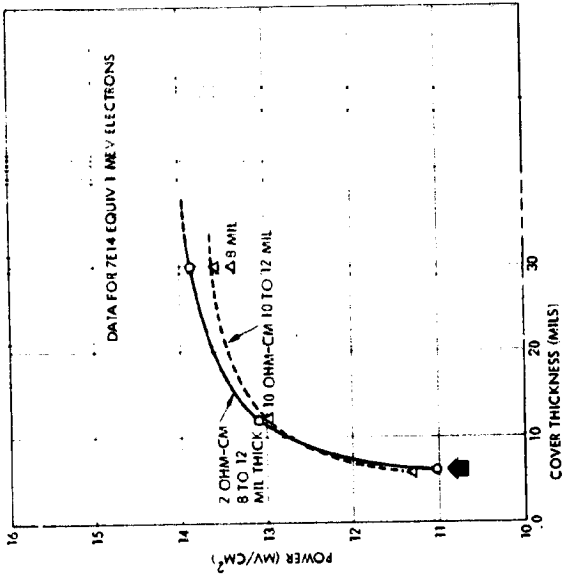
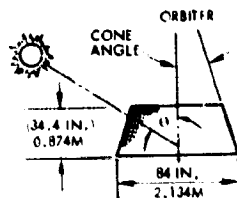


Figure 8.1-20. Solar Cell and Coverglass Selection

(31W) T/D III Table 8.1-6. Thor/Delta Orbiter Solar Array Sizing Factors

1. TEMPERATURE (°C)		4. RADIATION:			
	MAXIMUM	MINIMUM	1 MeV μ CM ²	DEG	
EARTH	17	5	60 DAYS AT EARTH	5.8×10^{13}	5.3
120,02 GIGAMETERS (1.07 AU)	7	-22	137 DAYS AT 128,66 GIGAMETERS (1.186 AU)	1.7×10^{14}	12.6
VEHICLES	71	40	1 YEAR AT VENUS	7×10^{14}	22.9
2. OTHER DEGRADATION FACTORS USED		5. CONSTRUCTION:			
INSTALLATION AND MISMATCH		4 PERCENT	ARRAY BACK-WIRED SIMILAR TO PIONEERS 6 THROUGH 9 TO MINIMIZE MAGNETIC FIELDS		
ULTRAVIOLET, COVER AND ADHESIVE		3 PERCENT	ARRAY COMPRISED OF 3 CELL BY 6 CELL MODULES OF PROVEN DESIGN (PIONEERS 6 THROUGH 9, DSP, PSCS-II)		
ALL OTHER FACTORS		1 PERCENT			
3. CELL CHARACTERISTICS:		6. COVER DESCRIPTION:			
2 x 2 CM x 0.025 (0.010 IN.) THICK		2 x 2 CM x 0.15 CM (0.006 IN.) THICK			
N P SILICON, SiO COATING		CORNING 0211 MICROSHEET			
20 CM BASE RESISTIVITY		410 NANOMETER FILTER			
173 mA AT 470 mV, 28°C, 150 GIGAMETERS (1 AU)		R63489 ADHESIVE			

(31W) T/D III



ORBITER	
AREA	5.3M ² (57.17 FT ²)
NO. OF CELLS	11550
NO. OF SERIES	77
NO. OF PARALLEL	150
NO. OF PANELS	6
CONE ANGLE	0.33 RAD (19 DEG)
DESIGN POWER	225.7 WATTS

Figure 8.1-21. Thor/Delta Orbiter Solar Array

(38.6 pounds) including case, terminals, wiring, and connectors. The depth of discharge is 66 percent during the maximum eclipse.

8.1.5 Atlas/Centaur Orbiter Subsystem, Version III Science Payload

(31W) A/C III

8.1.5.1 Configuration

The Atlas/Centaur power subsystem block diagram is shown in Figure 8.1-22. The method of controlling the bus voltage to 28 VDC \pm 2 percent within the PCU is identical to that of Section 8.1.3.1. The major difference involves use of the more cost-effective Pioneer 10 and 11 CTRF and inverter in place of the DC/DC converter. The battery, solar array, and shunt radiator design approach is identical to the Thor/Delta version.

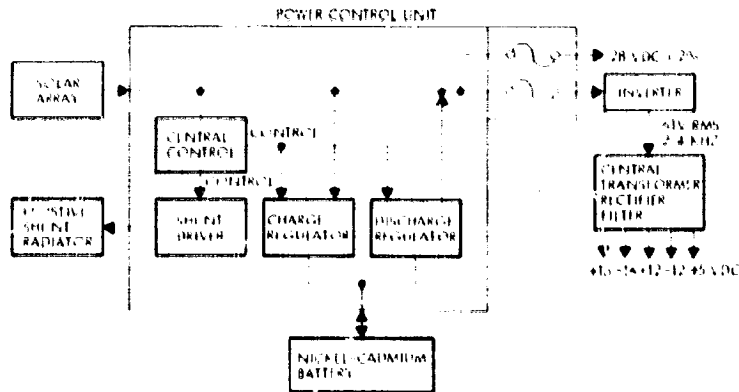


Figure 8.1-22. Atlas Centaur Power Subsystem, Version III Science Payload

Redundancy and fault isolation have been included to eliminate single point failure modes. The inverter and CTRF are parallel redundant. For details of the PCU design and operation see Section 8.1.3.2.

8.1.5.2 Inverter and Central Transformer Rectifier Filter (CTRF)

The inverter (Figure 8.1-23) is a modified Pioneers 10 and 11 assembly. Two 2.4 kHz inverters each having a maximum power capability of 46 watts are operated in parallel. Fault isolation at the inputs is provided by fusing. Relays are used to cross-strap the AC bus input to the CTRF power regulators.

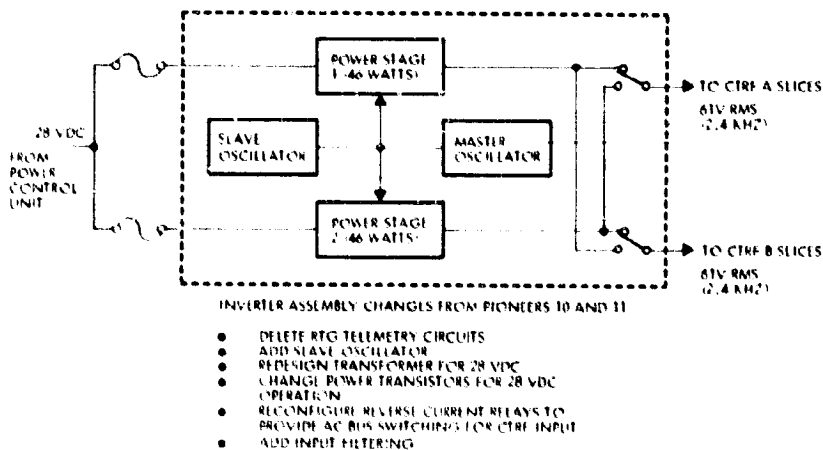


Figure 8.1-23. Atlas Centaur Inverter Assembly Block Diagram, Version III Science Payload

Deletion of the Pioneers 10 and 11 RTG telemetry circuit board permits installation of a redundant oscillator board. The main power switching transistors and transformer are modified for 2nd VDC input. Characteristics of the inverter output waveform are identical to the Pioneers 10 and 11 AC bus to minimize CTRF redesign. The inverter size is 11.4 x 15.2 x 17.8 centimeters (4.5 x 6 x 7 inches) and the weight is 2.32 kilograms (5.1 pounds).

The CTRF provides redundant, multiple secondary output voltages to each subsystem load which is redundant. A typical CTRF slice block diagram is shown in Figure 8.1-24. The Pioneers 10 and 11 CTRF is used with only minor modifications: the DTU A and B circuit boards are repackaged into a base slice replacing the transmitter driver slice, a slice is added for DSU 2 and 3, and the +5-volt switched CTU circuit board is repackaged.

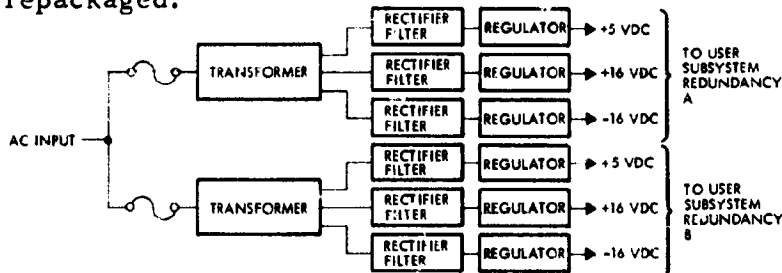


Figure 8.1-24. Atlas/Centaur Typical Parallel Redundant CTRF

Series dissipative regulators provide current limiting and over-voltage protection at each output. The common AC bus input is protected against low impedance faults in the TRF by fuses. The total power output is approximately 20 watts. All slices are flight-proven designs. Figure 8.1-25 shows the orbiter CTRF weight and size.

The inverter/CTRF overall efficiency is 60 percent.

8.1.5.3 Solar Array

The Atlas/Centaur orbiter solar array, Figure 8.1-26, was sized to supply 276.6 watts at Venus with a 1.66-radian (95-degree) sun angle. Sizing factors used are identical to those of Section 8.1.3.4. The same solar cells and coverglass thickness are used as for the Thor/Delta version. The major difference in array sizing is due to the spacecraft diameter increase to 2.62 meters (103 inches).

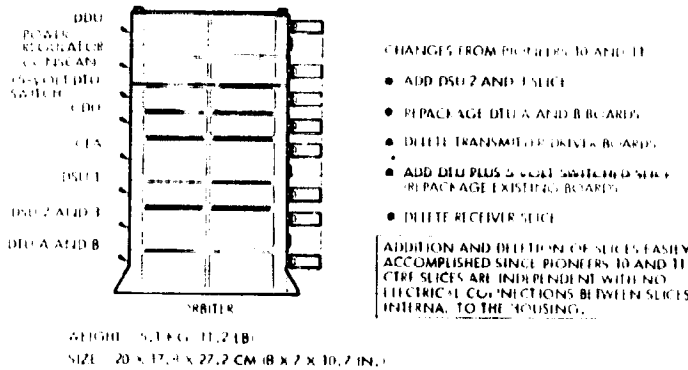


Figure 8.1.25. Atlas/Centaur Orbiter Central Transformer Rectifier Filter

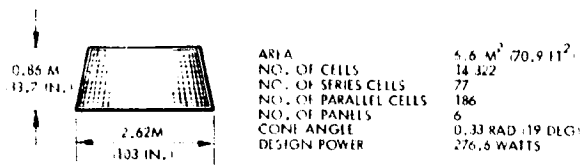


Figure 8.1.26. Atlas/Centaur Orbiter Solar Array Summary, Version III Science Payload

The array temperatures were assumed to be the same as for the Thor/Delta orbiter. This assumption is conservative since the Atlas/Centaur array is shorter, providing a larger radiating area at the top of the spacecraft.

8.1.5.4 Battery

The Atlas/Centaur orbiter has a load of 219.4 watts during the maximum eclipse time of 1.42 hours. This is a total energy of 219.4 x 1.42 = 312 watt-hr. The discharger efficiency is 85 percent so the battery must supply 366 watt-hr. An 18-cell, 24 A-hr battery supplies this load at a depth of discharge of 70 percent. The battery weight is estimated at 19.6 kilograms including wiring, case, terminals, and connectors.

8.1.6 Orbiter Options, Version III Science Payload

Solar array and battery sizing are main areas of difference between the recommended Thor/Delta and Atlas/Centaur power subsystems, and those in the optional missions. Power control unit design variations are minimal. The array design power varies from 156.2 watts for Thor/Delta earth-pointer to 276.6 watts for the Atlas/Centaur. The range of battery sizing power requirements is from 111.9 to 219.4 watts during the 1.42-hour eclipse.

T/D III Table 8.1-7 summarizes the solar array size and weight for the Version III science payload recommended and optional configurations. A/C III These sizes and weights are based upon the load power requirements of T/D III Section 8.1.2.

Table 8.1-7. Orbiter Solar Array Sizing Summary, Version III Science Payload

SIZING CONDITIONS: 7×10^{14} M_eV EQUIVALENT ELECTRONS CM⁻², 0.327 RAD (19 DEG) CONE ANGLE, SIZED TO PROVIDE REQUIRED POWER AT 1.657 RAD (95 DEG) SUN ANGLE

CONFIGURATION	POWER AVAILABLE ON AT VENUS (WATTS)	NUMBER OF PARALLEL CELLS	NUMBER OF SERIES CELLS	TOTAL CELLS	AREA INCLUDING PACKING FACTOR (M ²)	ARRAY DIAMETER AT BASE (M (IN.))	ARRAY HEIGHT (M (IN.))
ATLAS/CENTAUR 31-WATT FANBEAM/FANSCAN	276.6	186	77	14,322	6.58 (70.87)	2.62 (103)	0.856 (33.7)
RECOMMENDED THOR DELTA FANBEAM/FANSCAN	223.7	150	77	11,550	5.31 (57.17)	2.13 (84)	0.874 (34.4)
ATLAS/CENTAUR ORBITER 12-WATT	173.4	114	77	8,778	4.03 (43.4)	2.62 (103)	0.50 (19.8)
THOR/DELTA 12-WATT	156.2	108	77	8,316	3.82 (41.16)	2.13 (84)	0.60 (23.64)
THOR DELTA EARTH POINTER	156.2	108	87	9,396	4.36 (46.5)	2.13 (84)	0.686 (27.0)
ATLAS/CENTAUR DESPUN	184.4	126	77	9,702	4.46 (48.02)	2.62 (103)	0.56 (21.96)
THOR DELTA DESPUN	166.3	114	77	8,778	4.04 (43.4)	2.13 (84)	0.64 (25.1)

AT 28 VDC

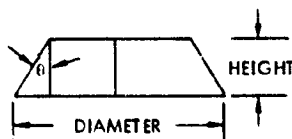


Table 8.1-8 summarizes the battery weight and cell size for the Version III science payload recommended and optional missions. The maximum eclipse depth of discharge is less than 80 percent for all versions.

The secondary power conditioning requirements are invariant except for versions which require additional secondary voltages for the despun reflector motor and electronics. This results in a net increase in weight of 1.8 kilograms for the CTRF or 0.45 kilograms for the DC/DC converter.





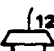

8.1.7 Probe Bus

ALL VERSION III SCIENCE PAYLOAD

The probe bus power subsystem configurations recommended in Figure 8.1-11 for the Thor/Delta and Atlas/Centaur missions are

discussed in the following sections. Descriptions of the units comprising the subsystem are presented where they differ significantly from the orbiter versions. The probe bus design is based on the requirements presented in Table 8.1-2.

Table 8.1-8. Orbiter Battery Sizing Summary, Version III Science Payload

	CONFIGURATION	1.42 HOUR ECLIPSE LOAD (WATTS)	ECLIPSE ENERGY INCLUDING 15% DISCHARGER LOSS (W-HR)	BATTERY CELL QUANTITY SIZE (A-HR) AND WEIGHT (KG)	BATTERY CAPACITY (W-HR)	DEPTH OF DISCHARGE (%)
 A/C III	ATLAS/CENTAUR 31-WATT FANBEAM/FANSCAN	219.4	366	18 CELLS 24 A-HR 19.6 KG	520	70
 T/D III	RECOMMENDED THOR/DELTA FANBEAM/FANSCAN	181.5	303	16 CELLS 24 17.5	462	66
 12W A/C III	ATLAS/CENTAUR 12-WATT AND EARTH POINTER	116.2	194	16 CELLS 18 13.1	346	56
 12W T/D III	THOR/DELTA 12-WATT AND EARTH POINTER	111.9	186	16 CELLS 18 13.1	346	54
 31W A/C III	ATLAS/CENTAUR DESPUN	127.2	212	16 CELLS 18 13.1	346	61
 31W T/D III	THOR/DELTA DESPUN	122	204	16 CELLS 18 13.1	346	59

8.1.7.1 Recommended Thor/Delta Probe Bus System



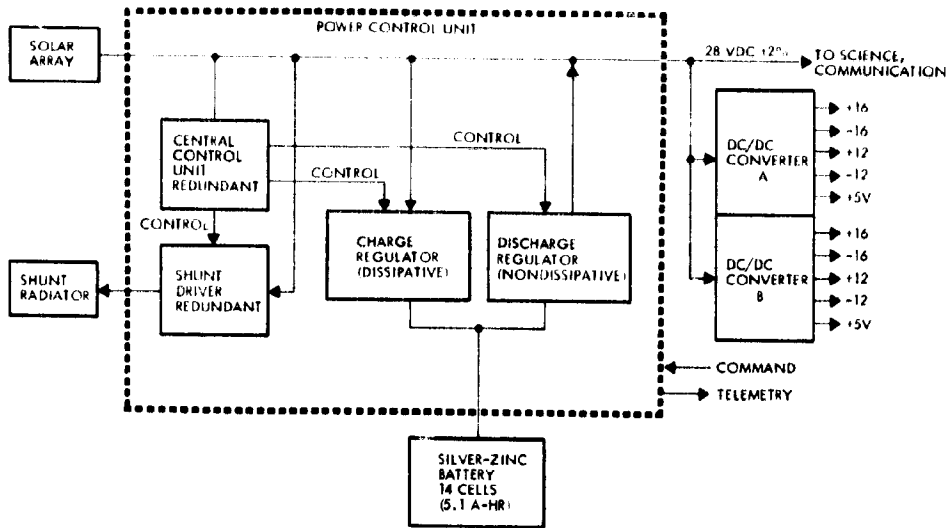
A block diagram of the Thor/Delta probe bus power subsystem is shown in Figure 8.1-27. The commonality with the orbiter subsystem (Figure 8.1-16) is apparent.

Power Control Unit

The power control unit is identical to that of the orbiter with the following exceptions:

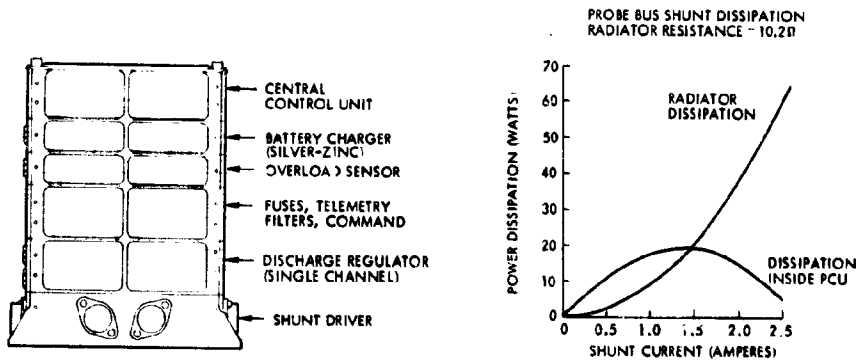
- The charge regulator is nonredundant and has been changed to be compatible with silver-zinc battery charging
- One channel of the discharge regulator is deleted since the bus battery is only required during launch and for peak loads.

The power control unit is shown in Figure 8.1-28. The weight and size are less than the orbiter PCU because of deletions of redundant functions.

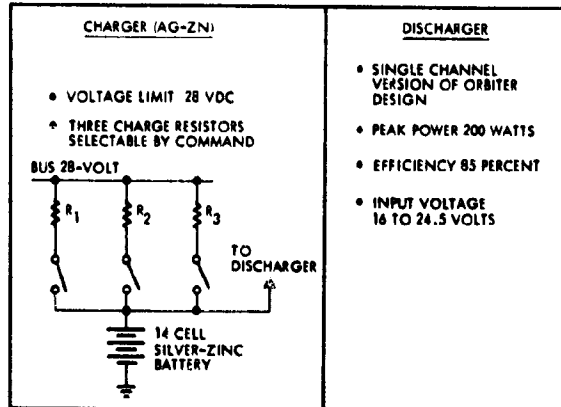


T/D III

Figure 8.1-27. Recommended Thor/Delta Probe Bus Configuration (28 VDC ± 2 Percent Regulated Bus)



WEIGHT = 4.45 KG (9.8 LB)
 (INCLUDING 0.3 KG (0.7 LB) FOR
 SHUNT RADIATOR)
 SIZE = 20 x 17.8 x 22.2 CM (8 x 7 x 8.7 IN.)



A/C III

T/D III

Figure 8.1-28. Recommended Probe Bus Power Control Unit, Thor/Delta and Atlas/Centaur Missions, Version III Science Payload

The resistance of the shunt radiator is increased to 10.2 ohms which decreases the shunt current and reduces the peak shunt driver dissipation to 20 watts. This eases PCU thermal interface with the remainder of the spacecraft.

The battery charger is a simple, low-cost design which provides three current-limiting resistors for control of charge current. The battery voltage is limited to 28 VDC by the shunt regulator. Selection of current-limiting resistors during charging is by ground command with telemetry monitoring of battery current, temperature and voltage provided. This method of charging is used primarily after launch when depth of discharge is deepest. Although returning the battery to full charge is not possible, sufficient state of charge is maintained for pulse load support, probe checkout and possible contingency mode operation.

Power Conditioning

The DC/DC converter is identical to that of the orbiter (see Section 8.1.4.3). Redundancy is provided by dual windings and regulators for each voltage output to redundant loads.

Solar Array

The Thor/Delta probe bus array was sized to supply 56.4 watts near earth and 78.2 watts at Venus. The sun angle for the earth-pointing probe bus is normally 0.17 to 0.56 radian (10 to 32 degrees). During probe release maneuvers the sun angle may be as high as 1.48 radians (85 degrees). Therefore, the array was sized to meet the load requirements over a large range of sun angles from earth to Venus. The array sizing factors are as shown in Section 8.1.6.

The radiation environment differs from the orbiter because of the decreased mission time. The probe mission was sized for 0.5 times the annual fluence with a $1/r^2$ relationship as a function of AU* assumed. The array characteristics are summarized in Figure 8.1-29.

* One AU is 1.5×10^{11} meters

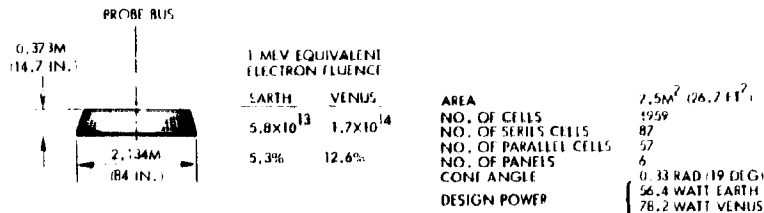


Figure 8.1-29. Thor/Delta Probe Bus Array, Version III Science Payload

Battery

The probe bus battery supplies power during launch and possibly for one eclipse while in a 185-kilometer parking orbit near earth. The battery supplies power for probe checkout approximately 104 days after launch. The battery sizing calculations are shown in Figure 8.1-30. During launch and earth-orbit eclipse the depth of discharge is 46.6 per cent. After insertion into the trans-Venus trajectory the battery is recharged by ground command.

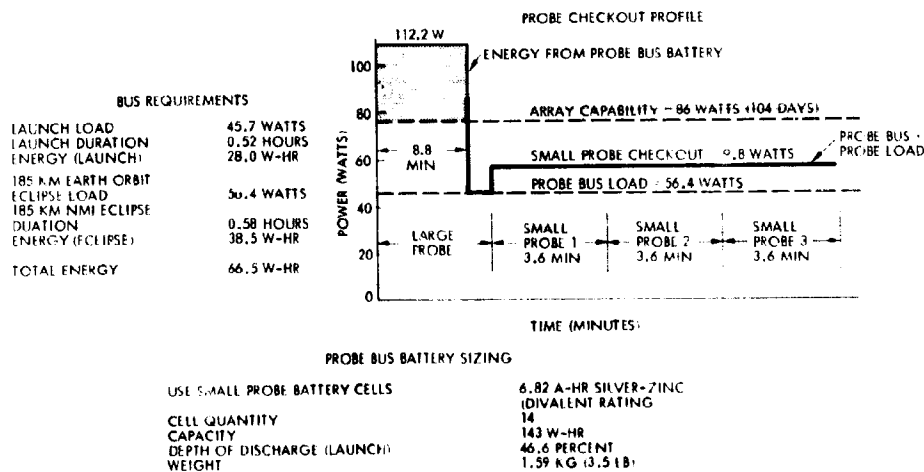


Figure 8.1-30. Thor/Delta Probe Bus Battery Sizing, Version III Science Payload

During large probe checkout the solar array and bus battery operate in a sharing mode to supply power. Bus science loads are turned off to maximize array power available to the probe and minimize battery discharge. The array capability is 86 watts at 104 days from launch. The bus load is 56.4 watts which provides 29.6 watts for four minutes of the probe checkout prior to probe transmitter turn-on. The total energy required from the bus battery is 70 W-hr.

8.1.7.2 Recommended Atlas/Centaur Probe Bus Subsystem, Version III Science Payload

A block diagram of the Atlas/Centaur probe bus power subsystem is shown in Figure 8.1-31. Commonality with the orbiter power subsystem (Figure 8.1-22) is provided. The major difference between the orbiter and bus subsystems is the PCU charge and discharge control for the silver-zinc battery and use of the inverter/CTRF for generation of secondary voltages.

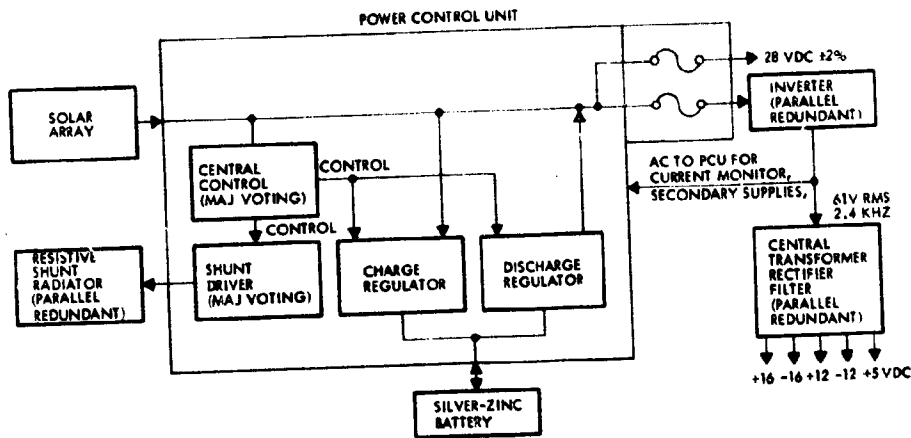


Figure 8.1-31. Atlas/Centaur Probe Bus Power Subsystem Block Diagram.
Version III Science Payload

Power Control Unit

The power control unit design is identical to the Thor/Delta bus version except that AC power from the inverter is used to generate internal secondary voltages for PCU operational amplifiers and current monitors. The descriptive data presented in Figure 8.1-28 apply to the Atlas/Centaur bus PCU.

Inverter and Central Transformer Rectifier Filter (CTRF)

The inverter design is identical to that of Section 8.1.5.2. The CTRF is modified as shown in Figure 8.1-32. Changes from the orbiter include deletion of the conscan and DSU slices and the retention of the receiver and transmitter driver slices. The remaining slices are common with the orbiter and bus. Redundancy is provided for each output.

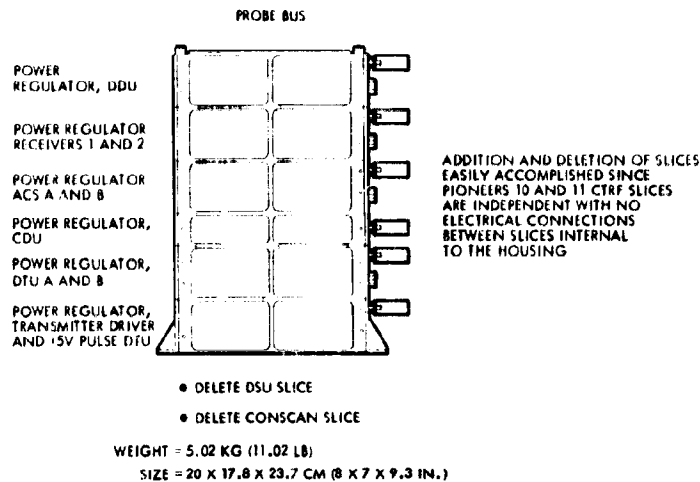


Figure 8.1-32. Atlas/Centaur Probe Bus Central Transformer Rectifier Filter, Version III Science Payload

Solar Array

The Atlas/Centaur probe bus solar array is sized to supply 70.5 watts near earth and 93.5 watts at Venus. The design sun angles and radiation environment are presented in Section 8.1.7.1. Other sizing factors are discussed in Section 8.1.5.1. The array characteristics are summarized in Figure 8.1-33.

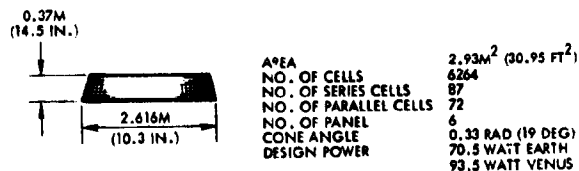


Figure 8.1-33. Atlas/Centaur Probe Bus Solar Array Version III Science Payload

Battery

The Atlas/Centaur bus load during launch exceeds that of the Thor/Delta version by about 14 watts. Calculations of launch and power and probe checkout load sharing profile is shown in Figure 8.1-34. The silver-zinc battery for the Atlas/Centaur small probe uses cells rated at 10.6 A-hr. For commonality these cells have been selected for the probe bus. Depth of discharge during the launch and earth orbit eclipse is 16.3 percent. The battery is charged after insertion into the trans-Venus

A/C III trajectory by ground command. Operation during probe checkout is similar to that described for the Thor/Delta version in Section 8.1.7.1.

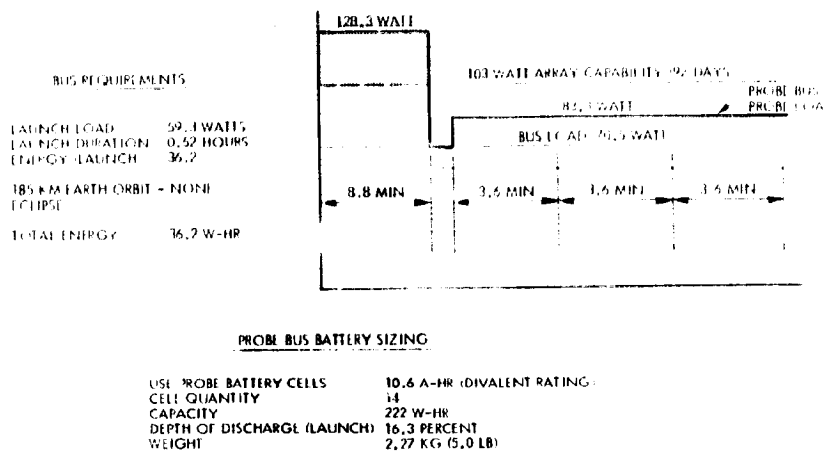


Figure 8.1-34. Atlas/Centaur Probe Bus Battery Sizing, Version: III Science Payload

A/C III 8.1.7.3 Power Interface with Probes (Umbilical)

A/C IV T/D III The power interface with the probes consists of power switching and fault isolation in the probe bus power control unit. The block diagram Figure 8.1-35, shows the bus/probe power interface. The bus PCU provides fusing for each of the four probes and a power on/off relay which permits probe checkout by ground command. Bilevel telemetry status points indicate the on/off position of the probe power control relays. The fuse module is mounted external to the PCU for easy access.

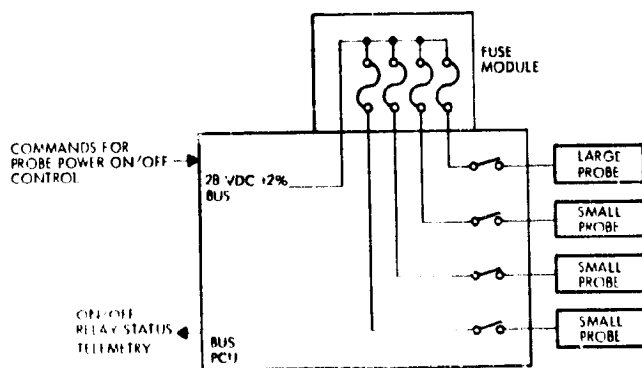


Figure 8.1-35. Probe Bus Power Interface
Version III Science Payload

REFERENCES

1. JPL Technical Memo 33-473, "Measured Performance of Silicon Solar Cell Assemblies Designed for Use at High Solar Intensities," 15 March 1971.
2. "Space Environment Criteria Guidelines for Use in Space Vehicle Development," (1969 Revision), NASA TMX53957, 17 October 1969.
3. "Natural Environment Criteria for the NASA High Energy Astronomy Observatory (HEAO)," NASA TMX 64516, 25 March 1971.
4. "Space Environment Criteria Guidelines for Use in Space Vehicle Development, Second Edition, NASA TMX 53865, 20 August 1970.
5. "MVM '73 Solar Proton Environment," John R. Thomas, Boeing Scientific Research Laboratories, Seattle, Washington.

8.2 Communications

8.2 COMMUNICATIONS SUBSYSTEM

8.2.1 Introduction and Summary

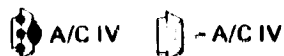




Figure 8.2-1 summarizes the basic data on the communications subsystem that has been defined for the Version IV science configuration of the probe bus and orbiter, assuming Atlas/Centaur launches for both.

As the table indicates, nearly all of the components are derived from other programs and are flight-proven, off-the-shelf designs with very low development cost and risk. The weight margin available with the Atlas/Centaur launch vehicle makes it possible to choose components primarily on the basis of development cost and risk, without the necessity for new designs with maximum use of advanced lightweight technology. The only component identified as new is the 6-watt power amplifier; in this case, two existing units have been identified that may be suitable, but require some modification and a flight qualification program. As will be discussed in detail in later subsections, some of the existing units are not only existing designs, but physically existing residual units from the Pioneers 10 and 11 program that can be used without modification.

Points of particular interest are:

- The communications subsystem allows for adequate link margins and bit rates under all conditions, including spacecraft attitudes and attitude maneuvers that are required for thermal reasons, probe deployment, entry flight path angle, science instrument pointing, and orbit insertion. This has been achieved without constraining mission or subsystem performance or placing severe requirements on other subsystems.
- The 64-meter ground stations are required for only brief periods during the probe mission, intermittently over a 9-day period during probe release and retargeting, and again for about 3 hours at the time of probe and bus entry.
- The entire orbiter mission can be handled by the 26-meter stations except for the second flip maneuver and orbit insertion. If shorter readout times are desired before and after periapsis passage, the 64-meter stations can be used to increase the data rate for these readout periods, at a minimum bit rate of 1024 bits/s.

-  A/C IV ● The occultation experiment requires only repositioning of the spacecraft spin axis.

 - A/C IV

- Provision is made for a 64-bit/s readout rate for the orbiter, even though the mission could be accomplished with a 32-bit/s maximum telemetry rate at a slight saving in antenna cost. The 64-bit/s capability is provided to reduce the amount of ground station personnel and equipment tied up in reading out the stored data. At 32-bit/s readout rate, nearly 24-hour coverage would be needed at the three 26-meter stations, while at the 64 bit/s rate only two stations are needed. Over the mission lifetime, this amounts to a considerable saving in program costs.
- The occultation experiment makes use of the two aft-mounted horn antennas, which are pointed toward earth during the first 35 days in Venus orbit. Horn antenna beamwidths allow for offsetting the spin axis 0.21 radian (12 degrees) from the earth-pointing direction while still maintaining communications up to the point of occultation; the offset is necessary to provide for near-maximum antenna gain at the point of maximum defocusing by the Venusian atmosphere.
- After 35 days in Venus orbit, the spacecraft is reversed to point the high-gain antenna at the earth, providing maximum data rate capability (64 bit/s with the 26-meter stations) up to the end of the mission. The occultation experiments will have been completed before this reorientation.

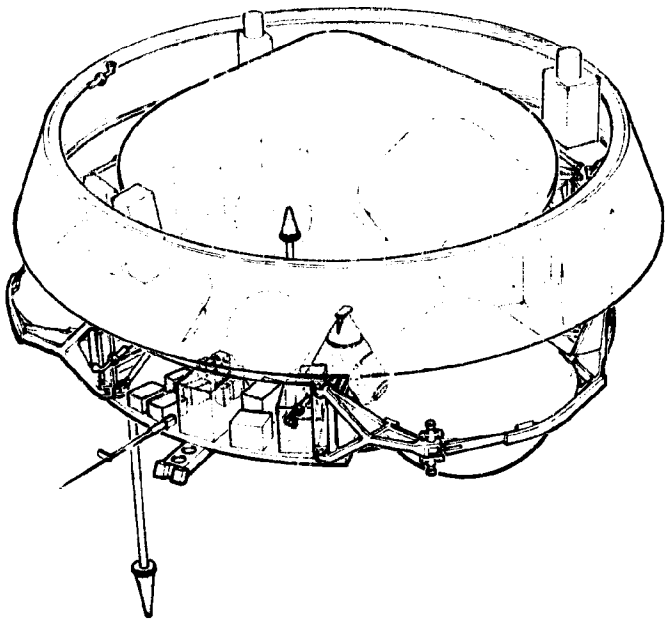
8.2.2 Requirements

ALL CONFIGURATIONS

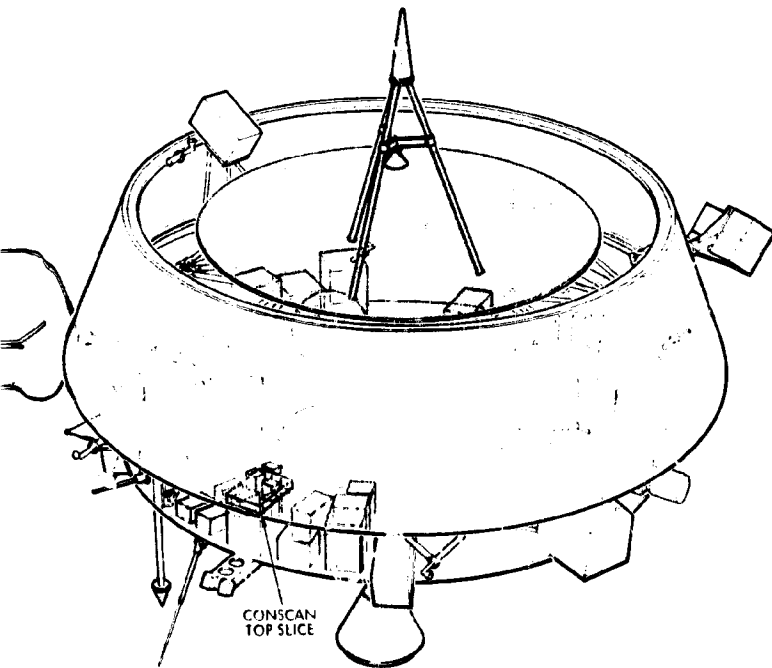
Table 8.2-1 lists the communications subsystem requirements used to derive subsystem designs based on the various spacecraft configurations considered throughout the study. These requirements were either given by the study guidelines, derived from interface requirements with other spacecraft subsystems and science experiments, or were imposed and/or interpreted from operational constraints on the mission and existing spacecraft hardware.

Notice that two requirements, bit rate and X-band occultation, were affected by the Version IV update of the science payload. Prior to this update, various interpretations of the desire for orbiter real-time versus nonreal-time science data led to variations in the real-time data rate from 8 to 128 bits/s. This in turn led to different combinations of transmitter power and antenna gain for the various spacecraft configurations and also in the same configuration.

PROBE BUS



ORBITER



SUBSYSTEM FEATURES

- FLIGHT-PROVEN COMPONENTS, MINIMUM DEVELOPMENT COST
- ACCOMMODATES ALL ATTITUDE CHANGE REQUIREMENTS
- NO SINGLE-POINT FAILURE MODES
- SWITCHABLE DUAL MODULATION INDEX ON ORBITER TO ACCOMMODATE CARRIER AND OCCULTATION REQUIREMENTS
- MINIMUM USE OF 64-METER GROUND TRACKING STATIONS
- OCCULTATION EXPERIMENT DOES NOT REQUIRE PRECESSION OR GIMBALS
- ALL SOLID STATE DESIGN

COMPONENT SUMMARY

	NUMBER USED	WEIGHT (KG)	POWER (WATTS)	DERIVATION	NOTES
FORWARD OMNI*	1	0.14	-	PIONEERS 10 AND 11	
AFT OMNI*	1	0.41	-	DSP	
AFT HORN	1	1.7	-	PIONEERS 10 AND 11	
DISH ANTENNA**	1	6.0	-	PIONEERS 10 AND 11 DSCS-II	FEED REFLECTOR
DIPLEXER	2	0.95	-	PIONEERS 10 AND 11	
COAXIAL SWITCH	5 (6)**	0.3	-	PIONEERS 10 AND 11	
RECEIVER	2	2.45	2	PIONEERS 10 AND 11	(WIKING ORBITER)
TRANSMITTER DRIVER	2	0.64	1.5	PIONEERS 10 AND 11	(WIKING ORBITER)
POWER AMPLIFIER	2	0.3	19	NEW	EXISTING BUT NOT FLIGHT-QUALIFIED
CONSCAN SIGNAL PROCESSOR**	1	0.76	1.2	PIONEERS 10 AND 11	
X-BAND HORN**	1	GFE	GFE		
X-BAND TRANSMITTER**	1	GFE	GFE		

* FORWARD AND AFT OMNIS ARE REVERSED ON ORBITER SPACECRAFT
 ** ORBITER ONLY

A PROBE BUS (ATLAS)

FORWARD OMNI

AFT OMNI

AFT OMNI (DSP)

C ORBITER

1.5 (5-DISK) (20)

AFT (PIONEERS)

AFT (PIONEERS)

FORWARD

ORBITER

ORBITER

OUT FRAME

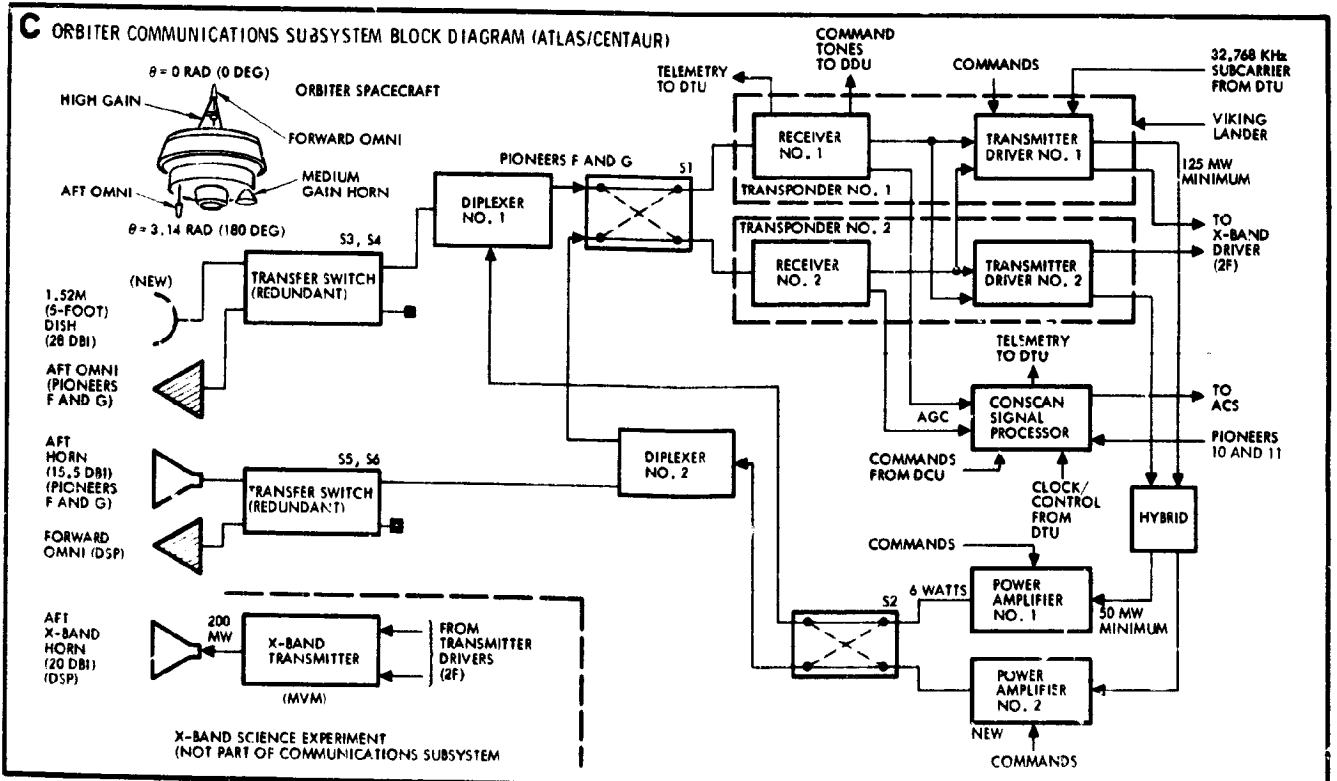
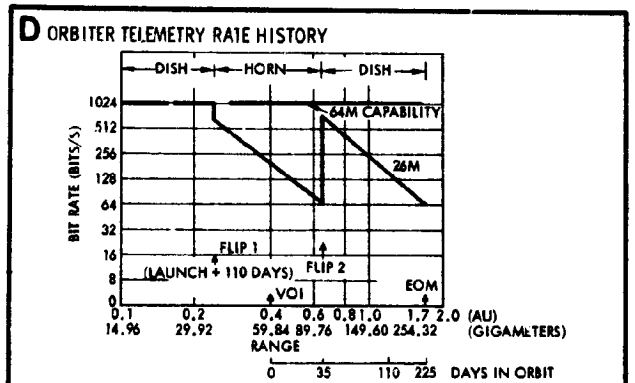
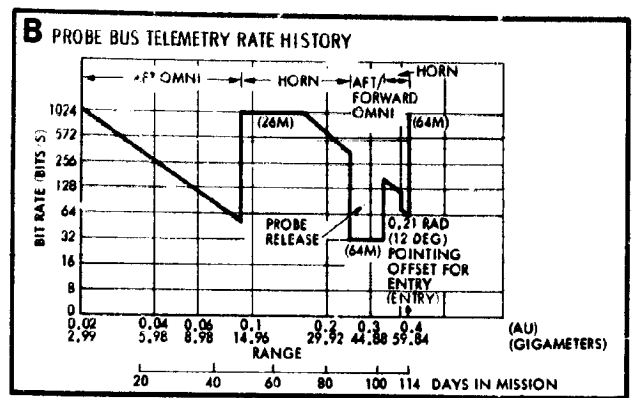
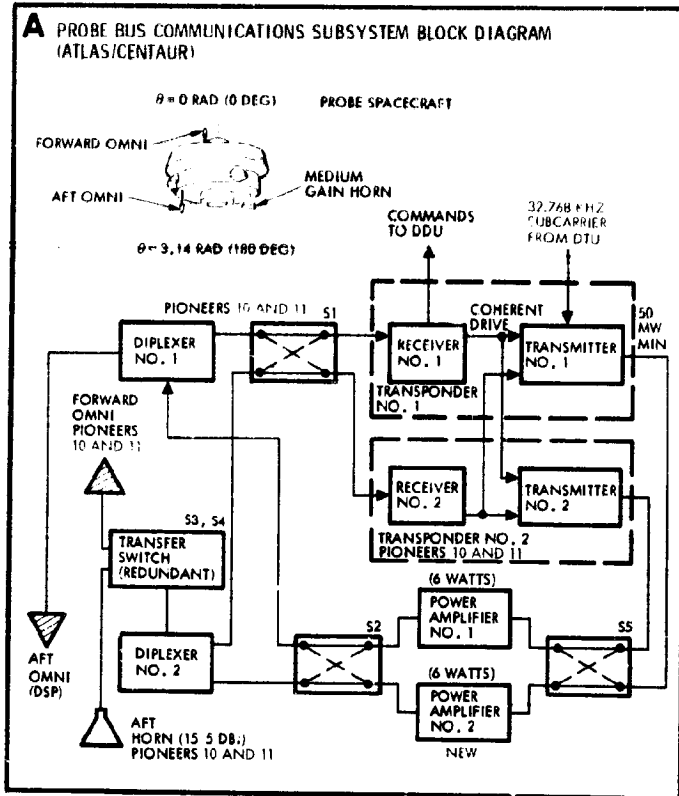


Figure 8.2-1. Preferred Atlas/Centaur Communication Subsystem Description

FRAME

Table 8.2-1. Communications Subsystem Requirements

- LOW COST (MAXIMUM USE OF EXISTING HARDWARE, COMMONALITY BETWEEN BUS/ORBITER/PROBES)
 - THOR/DELTA: LIGHTWEIGHT
 - ATLAS/CENTAUR: LOWEST COST WITHOUT REGARD TO WEIGHT
- OMNI DIRECTIONAL COVERAGE FOR SPACECRAFT MANEUVERS AND ORBIT INSERTION
- PROVIDE TELEMETRY, TRACKING, AND COMMAND FUNCTIONS TO 64.33 GIGAMETERS (BUS) AND 254.32 GIGAMETERS (ORBITER) (0.43 AU (BUS) AND 1.7 AU (ORBITER))
 - TELEMETRY: (PCM/PSK/PM)

	BIT RATES (BITS/S)			
	BUS		ORBITER	
	ENTRY	CRUISE	IN-ORBIT	CRUISE
PPE- 13 APRIL 1973	512	16	8-128	16
POST- 13 APRIL 1973	1024	16	≥ 64	16
ERROR RATE:	≤ 10 ⁻³ FRAME DELETION RATE			
 - TRACKING: COHERENT (TWO-WAY) DOPPLER TRACKING (NO RANGING)
 - COMMAND: PCM/FSK/PM (1 BIT/S)
BIT ERROR RATE: 10⁻⁵
- DSN COMPATIBLE:
 - UPLINK FREQUENCY: 2115 ±5 MHZ
 - DOWNLINK FREQUENCY: 2295 ±5 MHZ S-BAND
~8400 X-BAND (VERSION IV SCIENCE PAYLOAD)
 - TURNAROUND RATIO: 240/221 S-BAND
880/221 X-BAND
 - 26-METER NETWORK: ROUTINE TRACKING
 - 64-METER NETWORK: CRITICAL MANEUVERS AND OCCASIONAL HIGH DATA RATE READOUTS
- S-BAND OCCULTATION EXPERIMENT
X-BAND OCCULTATION EXPERIMENT
- ENVIRONMENT: 160.0 TO 104.71 GIGAMETERS (1.07 TO 0.7 AU)
MAGNETICS: FACTOR OF 5 LESS SEVERE THAN PIONEERS 10 AND 11
- DOPPLER RATES: BUS - 35 HZ/S AT ENTRY
ORBITER - 45 HZ/S AT PERIAPSIS
- MISSION DURATION: BUS - ~114 DAYS
ORBITER - ~425 DAYS (225 DAYS IN ORBIT)
- ACQUISITION THRESHOLD (LOOP SNR = 6 DB): -148 DBM, OMNI AT END OF MISSION WITH 26-METER COMMAND

Preferred subsystem designs for both the Thor/Delta and Atlas/Centaur launch vehicles were chosen. The Version IV science payload directive specified the Atlas/Centaur vehicle, increased the science data, and added an X-band occultation experiment. The Atlas/Centaur recommended subsystem design was then changed and updated to the final preferred version. It is described in Section 8.2.4, along

with the recommended Thor/Delta design which does not reflect the new (Version IV) science requirements. The various options that were considered in this study as a result of the varying science requirements are presented in Section 8.2.5.

8.2.3 Tradeoffs ALL CONFIGURATIONS

The following tradeoffs present cost, weight, power, and risk comparisons for various antennas, transponders, and power amplifiers that were considered in arriving at the many spacecraft configurations examined during the study. Based on these and other spacecraft and DSN tradeoffs, final preferred Atlas/Centaur and recommended Thor/Delta spacecraft and subsystem configurations were chosen. (These are presented in Section 8.2.4.)

8.2.3.1 High-Gain Antennas - Orbiter ALL ORBITER CONFIGURATIONS

The high-gain antenna for the orbiter spacecraft was required to be compatible with each candidate spacecraft configuration in size, weight, mass properties, and pointing mode, i.e., spinning and pointing along the spacecraft spin axis (earth-pointers), despun and pointing perpendicular to the spin axis (despun antennas), or spinning and pointing perpendicular to the spin axis (fanbeam antennas). Performance requirements for the antennas were established by system EIRP and radiation pattern coverage requirements during transit, orbit insertion, and orbit phases of the mission.

Tradeoff studies were made of antenna designs capable of meeting the following basic communication system RF performance requirements.

- Earth-pointer with conscan and system EIRP greater than 62 dBm.
- Despun antenna with system EIRP greater than 62 dBm.
- Fanbeam antenna with system EIRP greater than 55 dBm.

Since weight, primary power, and costs were critical tradeoff parameters, subsystem tradeoff studies were made to establish parameter characteristics which, when combined with other interfacing system parameters, could lead to the selection of an optimum system.

The antenna weights and gains (as a function of aperture size), shown in Figure 8.2-2, were used in system level tradeoffs that included power amplifiers and solar arrays. The antenna designs selected for these tradeoffs represented proven designs requiring minimum development (minimum cost and risk). From system level tradeoffs, the nominal subsystem performance and design requirements were established for further tradeoffs involving cost and detailed designs.

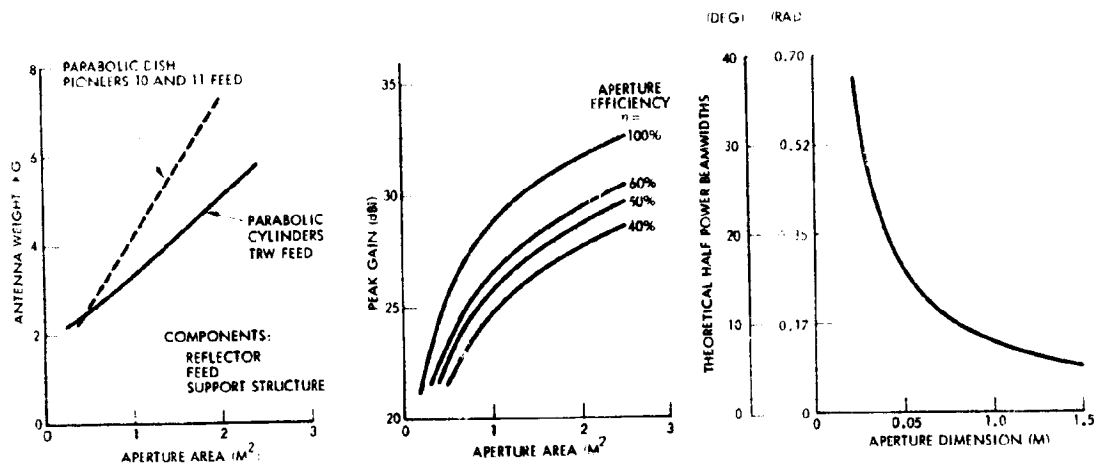


Figure 8.2-2. Orbiter High-Gain Antenna Tradeoff Characteristics

As indicated by the curves, antenna weight is a function of the design concept and aperture area, while antenna gain is a function of the efficiency and aperture area. Beamwidths are also a function of aperture gain at coverage angles of interest, beamwidths were not critical tradeoff parameters. From the detailed design and cost tradeoffs, preferred antenna configurations for each spacecraft pointing mode were selected. The antenna designs were not directly affected by the type of launch vehicle, Thor/Delta versus Atlas/Centaur.

Candidate earth-pointing antenna designs were all parabolic antenna configurations of different diameters and feed designs because peak gain requirements exceeded 28 dBi with 6-watt transmitters as a baseline. The orbiter configurations were all spin stabilized; therefore, the high-gain antenna requirements included an offset beam and a first pattern null position greater than 0.17 radian (10 degrees) off the spin axis for conscan attitude determination and acquisition.

Design tradeoff studies consisted of feed defocusing, as shown in Figure 8.2-3, to establish an optimum dish diameter and feed location which provide the required gain for telemetry coverage at the end of the mission and the best pattern performance for conscan: a 1 dB conscan crossover and acquisition beyond 0.17 radian (10 degrees) off of the spin axis. Already developed high-gain antenna designs such as those used on the 1973 MVM and 1975 Viking program were considered, but these designs required modifications to provide the conscan capability. Other configurations included the use of the Pioneers 10 and 11 high-gain antenna feed in various diameter dishes. Since use of an existing feed represented a low-cost approach, new feed designs were not seriously considered. Feed movement mechanisms were considered, but this represented significantly higher cost for only 1 dB gain improvement.

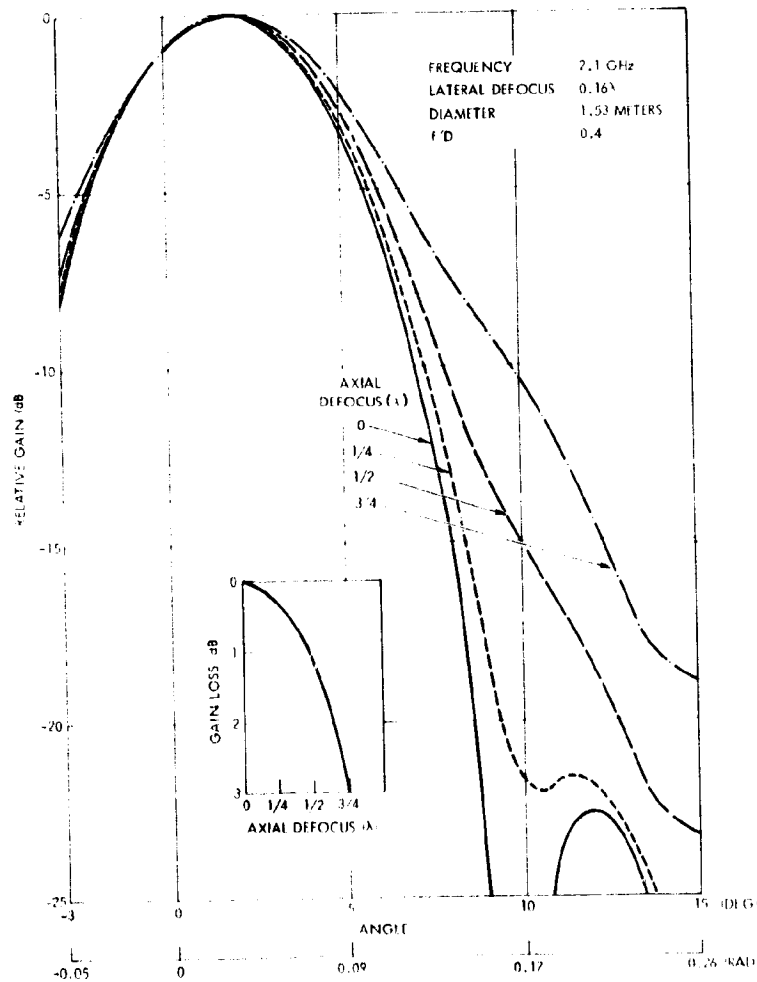


Figure 8.2-3. Antenna Pattern With Defocussing

The results of the design and cost tradeoffs indicated that the preferred earth pointing high-gain antenna configuration is a 1.53-meter dish, similar in construction to designs flown on the DSCS-II spacecraft, of aluminum honeycomb construction with fiberglass facesheets and vacuum deposited aluminum reflecting surface, with the Pioneers 10 and 11 high-gain antenna feed. The cost of parabolic reflectors that are from 2 to 3 meters in diameter such as those used on the MVM 1973, Viking 1975, and the selected Pioneer Venus earth pointing orbiter are essentially the same. If reflector tooling or residual reflectors are available from the MVM or Viking programs, the only development costs will be those for incorporating the conscan capability. Based upon Pioneers 10 and 11 experience, the development effort should be minimal. The selected earth pointing design is a simple, lightweight, lowest cost design which meets system requirements and is based upon flight-qualified design concepts.

The candidate despun orbiter high-gain antennas shown in Figure 8.2-4 represented preferred configurations derived from subtrades within the same class of similar design configurations. Aperture size, gain, weight, despun mechanical assembly/despun electronics assembly (DMA/DEA) configuration, omni antenna impact, and cost were subtrade parameters for mechanically despun antennas; gain, weight, despun technique, and development status were primary subtrade parameters for electronically despun antennas. Antenna gain, primary power, weight, and program costs were determined from the combination of antenna, power amplifier, and solar array sizes required to meet a minimum system EIRP of 62 dBm. Relative program costs included nonredundant and redundant costs for two flight systems. Reliability is based upon standby electronic assemblies for mechanically despun antennas and a redundant driver amplifier for the electronically despun antenna.

Redundancy and spares were not included in the cost and weight tradeoffs, since each type of system (earth pointer, mechanically or electronically despun antennas) requires a unique redundancy and component spares scheme. Cost and weight does include essential system-associated equipment such as rotary couplers, caging equipment, special test equipment, and forward omni antenna. Also shown for the despun parabolic cylinder antenna are cost and weights associated with the use of the Helios

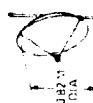
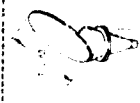



CHARACTERISTICS CONCEPTS	ANTENNA GAIN AT 2.3 GHz (DBI)	REQUIRED TRANSMITTER POWER (WATTS)	REQUIRED PRIMARY POWER (WATTS)			RELATIVE WEIGHT PENALTY (KG)			RELIABILITY	MAJOR SYSTEM COMPONENTS	RELATIVE PROGRAM COSTS (5000)	DEVELOPMENT STATUS
			DMA/DEA	AMPLIFIER POWER	TOTAL	DMA/DEA	ANTENNAS	POWER AMP ARRAY				
 DESPUN PARABOLIC ANTENNA	22.5	12	12	44	56	8.7	3.0	4.6	16.3 (35.8)	0.983	841	DUAL CHANNEL ROTARY COUPLER IS A NEW DESIGN. MINOR MODIFICATIONS TO ANTENNA, DMA, DEA, AND POWER AMPLIFIERS REQUIRED.
 DESPUN FLAT PLATE REFLECTOR	21	18	8	70	78	4.9	8.1	8.0	21.0 (46.1)	0.9860	1029	ANTENNA SIZE AND GAIN LIMITED BY AXIAL LOAD HANDLING CAPABILITY OF LVA. CAGING IS REQUIRED. ANTENNA IS A NEW DESIGN BASED ON PROVEN CONCEPTS. DMA/DEA MAJOR MODIFICATIONS REQUIRED.
 DESPUN PARABOLIC CYLINDER REFLECTOR	22.5	12	12	44	56	8.1	2.2	4.6	14.9 (32.8)	0.9860	873	QUALIFIED HELIOS ANTENNA MAY BE USED AS IS, OR A NEW DESIGN BASED UPON PROVEN CONCEPTS MAY BE USED. MINOR MODIFICATIONS TO DMA, DEA, AND POWER AMPLIFIERS REQUIRED.
 PARABOLIC ANTENNA ON A DESPUN PLATFORM	22.5	12	12	44	55	17.9	3.0	4.2	70.1 (43.2)	0.9860	857	PENALTY ASSOCIATED WITH AUXILIARY CDU AND REMOTE MULTIPLEXER IS NOT INCLUDED. AFT OMNI COVERAGE IS A PROBLEM. MINOR MODIFICATIONS TO ANTENNA, DMA, DEA, AND POWER AMPLIFIERS REQUIRED.
 ELECTRONICALLY DESPUN ARRAY	22	23	10	72	82	1.2	5.3	8.9	15.4 (33.8)	0.9651	1088	NEW CONCEPT REPRESENTS DEVELOPMENT RISK WITH GREATEST PERFORMANCE AND COST UNCERTAINTY

Figure 8.2-4. Candidate Orbiter Despun High-Gain Antenna Tradeoff Configurations

antenna. Detailed weight and cost estimates used in the tradeoff study are shown in Tables 8.2-2 and 8.2-3. For comparison, the earth-pointing antenna subsystem characteristics are included in the detailed evaluation.

As each major subsystem component such as the antenna, the DMA, and power amplifier was being evaluated, it was clear that the greatest design and cost uncertainties were associated with unqualified design concepts. The electronically despun antenna system performance characteristics were attractive; however, costs were high and performance predictions were thought to be optimistic in view of producing a space-qualified design. Performance degradation due to manufacturing tolerances and environmental exposures are critical to the design, and are the areas of greatest performance uncertainty and/or cost uncertainty for assurance of qualification. The requirement for additional power amplifiers for omnidirectional antennas or the increased design complexity required to incorporate an omni mode into the despun array were significant factors against the electronically despun antenna.

Since the largest weight and cost item in the mechanically despun antenna system is the DMA/DEA, candidate mechanically despun antennas were designed for use with flight-qualified DMA's. These were the Skynet DMA, the Atmospheric Explorer DMA, the Helios DMA, and the DSCS-II DMA. Each DMA/DEA considered requires modifications for low spin rate operations; however, other problems such as caging requirements, magnetic cleanliness, weight, pipers for position information, slip rings, redundancy, and diameter of despun shaft were considered in the selection of the antenna configuration for each DMA and in the cost of the DMA/DEA. DMA subtrades have indicated that the Helios DMA may be the only existing unit suitable for use with Pioneer Venus mission mechanically despun antennas.

Because of the development status of the Helios DMA/DEA and the possibility of using the qualified Helios antenna interchangeably, the preferred despun antenna for the Thor/Delta Version III science payload and Atlas/Centaur Version III science payload is the despun parabolic cylinder reflector. TRW's design would use the qualified Helios DMA/DEA with minor modifications for low spin rate operations, and a shortened Pioneer 6 through 9 Franklin array as the feed for the despun reflector.

Table 8.2-2. Candidate Orbiter High-Gain Antenna System Detailed Weights

SYSTEM COMPONENTS	ANTENNA EARTH-POINTING 87-CM DISH (KG)	DESPUN 82-CM DISH (KG)	DESPUN 140-CM FLAT PLATE REFLECTOR (SKYNET TYPE) (KG)	DESPUN 110-CM PARABOLIC CYLINDER REFLECTOR (KG)		DESPUN PLATFORM WITH 82-CM DISH (KG)	ELECTRONICALLY DESPUN ANTENNA (TEXAS INSTRUMENTS) (KG)
				TRW	HELIOS		
(1) REFLECTOR AND SUPPORT STRUCTURE	1.95	1.90	5.50	1.60	2.32	1.90	1.86
(2) FEED AND FEED INSTALLATION	0.59	0.59	1.23	0.45	1.14	0.59	2.95
(3) DMA AND PLATFORM OR ROTARY COUPLER INSTALLATION		6.83	1.68	5.50	6.50	6.83	
(4) DEA (NONREDUNDANT)		1.59	2.73	1.59	1.59	1.59	1.23
(5) ROTARY COUPLER PLATFORM		0.32	0.45			4.50	
(6) OMNI INSTALLATION	0.27	0.45	1.36	0.14	0.14	0.45	0.45
(7) POWER AMPLIFIERS - HYBRIDS	0.45	0.45	2.18	0.45	0.45	0.45	2.27
(8) CONSCAN PROCESSOR	0.36						
(9) SOLAR CELLS	2.80	4.20	5.82	4.20	4.20	4.20	6.26
DMA/DEA TOTAL (3)(4)(5)(8)	0.36	8.74	4.86	8.09	8.09	12.92	1.23
ANTENNA TOTAL (1)(2)(6)	2.81	2.94	8.09	2.19	3.60	2.94	5.26
POWER AMPLIFIER TOTAL (7)(9)	3.25	4.65	8.00	4.65	4.65	4.65	8.91
SYSTEM TOTAL	6.42	16.33	20.95	14.93	16.34	20.51	15.40

Table 8.2-3. Candidate Orbiter High-Gain Antenna System Detailed Costs

CONFIGURATION ITEM	MECHANICALLY DESPUN ASSEMBLIES										ELECTRONICALLY DESPUN ANTENNAS							
	FIXED PARABOLOID EARTH-POINTING		SKYNET DESPUN REFLECTOR				HELIOS				PROGRAM DESPUN PLATFORM		SYNCHRONOUS METEOROLOGICAL SATELLITE (PHILCO-FORD)		TEXAS INSTRUMENT	RADIOTECH SYSTEMS INC.		
	NONRE-CURRING EXPENSE (\$K)	RECURRING EXPENSE (\$K)	NONRE-CURRING EXPENSE (\$K)	RECURRING EXPENSE (\$K)	DESPUN REFLECTOR (MBB)	DESPUN REFLECTOR (TRW)	NONRE-CURRING EXPENSE (\$K)	RECURRING EXPENSE (\$K)	DESPUN ANTENNA	DESPUN PLATFORM	NONRE-CURRING EXPENSE (\$K)	RECURRING EXPENSE (\$K)	NONRE-CURRING EXPENSE (\$K)	RECURRING EXPENSE (\$K)	NONRE-CURRING EXPENSE (\$K)	RECURRING EXPENSE (\$K)	NONRE-CURRING EXPENSE (\$K)	RECURRING EXPENSE (\$K)
ANTENNA	20	25	60	31	30	64	50	20	25	20	25	20	25	20	25	100	70	NO QUOTE
DESPUN MECHANICAL (DMA)	---	---	50	50	125	125	50	100	125	125	100	100	100	100	100	---	---	---
DESPUN ELECTRICAL (DEA) (NON-REDUNDANT)	---	---	100	75	50	50	50	50	50	50	50	100	68	39	22	---	---	---
▲ ELECTRICAL POWER (ESTIMATED)	---	---	---	---	---	---	---	---	---	---	---	---	---	---	---	---	---	---
▲ EGSE AND SUBSYSTEM ENGINEERING (EQA)	---	---	---	---	---	---	---	---	---	---	---	---	---	---	---	---	---	---
POWER AMPLIFIER (PGA) (REDUNDANT)	---	---	---	---	---	---	---	---	---	---	---	---	---	---	---	---	---	---
ROTARY JOINT	---	---	---	---	---	---	---	---	---	---	---	---	---	---	---	---	---	---
CAGING	---	---	---	---	---	---	---	---	---	---	---	---	---	---	---	---	---	---
FORWARD OMNI	4	8	100	15	---	---	---	4	8	4	8	4	8	4	8	---	---	---
PROGRAM COSTS	24	216	383	646	181	660	215	658	292	600	247	610	304	775	514	---	---	---
TOTAL	240	1029	841	873	892	857 ¹⁾	779	1	857 ¹⁾	779	1	857 ¹⁾	779	1	857 ¹⁾	1029	1029	1029

NOTES: ALL RECURRING COSTS (EXCEPT PROGRAM COSTS) ARE ON UNIT BASIS.

¹⁾ DOES NOT INCLUDE COSTS ASSOCIATED WITH REMOTE MULTIPLEXER, AUXILIARY CDU, AND PLATFORM ASSEMBLY

Candidate orbiter antenna designs for the reduced EIRP spacecraft configuration were the flight-qualified Pioneers 6 through 9 fanbeam antenna and a reduced EIRP electronically despun antenna, as shown in Figure 8.2-5. Tradeoff parameters include the system impact of required power amplifiers, solar array sizes, and omni antennas. Program costs include nonredundant and redundant costs for two systems.

CONCEPT	CHARACTERISTIC	EIRP AT 2.3 GHz (DBM)	REQUIRED TRANSMITTER POWER (WATTS)	REQUIRED PRIMARY POWER (WATTS)	RELATIVE WEIGHT PENALTY (KG)		PROGRAM COSTS (\$ '000)	DEVELOPMENT STATUS	
					ANTENNAS	POWER AMPS AND SOLAR ARRAY			
 PIONEER A-E FRANKLIN ARRAY		55.00	31.0	136.0	1.44	11.1	12.54	439	ANTENNAS ARE SPACE-QUALIFIED PIONEERS 6 THROUGH 9 FRANKLIN ARRAY AND PIONEERS 10 AND 11 OMNI. POWER AMPLIFIERS ARE PARALLELED 20-WATT UNITS
 ELECTRONICALLY DESPUN ARRAY		1 RING: 55.75	13.0	83.0	4.73	8.55	13.28	1044	<ul style="list-style-type: none"> NEW CONCEPT REQUIRES ADDITIONAL OMNI ANTENNA WITH 10-WATT POWER AMPLIFIERS ASSUMED PIONEERS 10 AND 11 OMNI AND PARALLELED RADIATION, INC. 6-WATT POWER AMPLIFIERS
		2 RINGS: 59.12	13.0		5.25		13.80		
		3 RINGS: 61.95	13.0		5.77		14.32		
		OMNI ANT: 44.0	10.0						

Figure 8.2-5. Candidate Orbiter Reduced EIRP Antenna Tradeoff Characteristics

As indicated from Figures 8.2-4 and 8.2-5, the cost saving is minimal for the reduced EIRP electronically despun antenna, since EIRP reduction is accomplished only by reducing the number of array elements. The only cost saving is in material costs for array elements and power dividers, which may be eliminated. A reduction in the number of active columns in the array would not reduce costs significantly, since there would be no reduction in the number of components required for the complete array design. A reduction in the array diameter was considered; however, the expected reduction in EIRP was excessive and/or spin amplitude and phase ripple were considered to be major problems if the array diameter or the number of columns in the circular array were reduced. The requirement for additional power amplifiers for an omnidirectional antenna was also an unattractive feature of the electronically despun antenna.

ALL ORBITER CONFIGURATIONS

Four fanbeam configurations: the Atlas/Centaur and Thor/Delta Version III science payload (12-watt) and the Atlas/Centaur and Thor/Delta Version III science payload (31-watt) were considered for use with the flight-qualified Pioneers 6 through 9 Franklin array. The low power versions are compatible, at the longer ranges, only with the 64-meter DSN stations. The 31-watt version is, however, compatible with the 26-meter DSN stations (Version III science payload requirements) and uses identical power amplifiers with the large probe, resulting in procurement savings. A fanscan (uplink) and omni antenna would replace the two omni antennas of the existing Pioneer antenna package. This is the lowest cost of all the antennas considered. Since minimum conductor spacing in the existing design is on the order of 0.2 centimeter, the design is capable of handling RF power levels greater than 100 watts.

Rotary Joints

Rotary joints were investigated for mechanically despun antenna configurations which could have required both an S- and X-band capability. If the spacecraft antenna configuration has a rotary joint requirement, the use of a single-channel S-band, noncontacting coaxial type design could be the recommended approach. The single-channel design which uses frequency up-conversion equipment on the despun side of the rotary coupler represents the lowest risk, lowest cost rotary joint approach. If the bandwidth of the single-channel design can be made broad enough to accommodate both S- and X-band without significantly increasing the design complexity and cost, then this design would be preferred for handling both S- and X-band. Unless the despun motor assembly has slip rings to provide power and commands to a switch, a minimum of two S-band channels are required to feed a forward omni antenna and the despun high-gain antenna. Shown in Figure 8.2-6 are the characteristics and status of 1, 2, and 3 channel coaxial rotary joints. The results of the rotary joint survey indicates that, although single and multiple channel S-band rotary joints have been developed by a number of companies, i.e., SAGE, Philco-Ford, and TRW, none of these to our knowledge have been flown. Circular waveguide designs were flown on the Intelsat III and the Skynet spacecraft, but these designs would be undesirable because of the excessive size and weight of an equivalent S-band system. Until multiple-channel

coaxial rotary coupler designs are qualified, they represent high design risk equipment with associated development cost uncertainties.



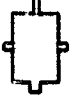

 (SAGE) SINGLE CHANNEL (S-BAND)	 (SAGE) DUAL CHANNEL (S-BAND AND X-BAND)	 (SAGE) SINGLE CHANNEL (S-BAND AND X-BAND)	 (PRECO FORD) THREE CHANNEL (DUAL S-BAND AND X-BAND)
TYPE: COAXIAL FREQUENCY: 2.0 TO 2.4 GHz CONNECTORS: INPUT: SMA OUTPUT: 0.36 CM COAX SIZE: LENGTH: 10 CM DIAMETER: 4.5 CM WEIGHT: 0.22 KG DESIGN STATUS: SIMILAR ITEM DEVELOPED BUT NOT FLOWN DEVELOPMENT COSTS: \$40,000 DESIGN RISK: LOWEST	TYPE: TRIAXIAL FREQUENCY: S-BAND: 2.0 TO 2.4 GHz X-BAND: 8.35 TO 8.50 GHz CONNECTORS: INPUT: SMA OUTPUT: S-BAND: SMA X-BAND: 0.36 CM COAX SIZE: LENGTH: 11.5 CM DIAMETER: 6.3 CM WEIGHT: 0.35 KG DESIGN STATUS: UNDEVELOPED DEVELOPMENT COSTS: \$66,500 DESIGN RISK: HIGHEST	TYPE: COAXIAL (BROAD-BAND) FREQUENCY: S-BAND: 2.0 TO 2.4 GHz X-BAND: 8.35 TO 8.50 GHz CONNECTORS: INPUT: SMA OUTPUT: 0.36 CM COAX SIZE: LENGTH: 10 CM DIAMETER: 4.5 CM WEIGHT: 0.22 KG DESIGN STATUS: UNDEVELOPED DEVELOPMENT COSTS: \$10,000 DESIGN RISK: HIGH	TYPE: QUADRANTAL FREQUENCY: S-BAND: 2.0 TO 2.4 GHz X-BAND: 8.35 TO 8.50 GHz CONNECTORS: INPUT: SMA OR INCL OUTPUT: SMA OR INCL SIZE: TBD WEIGHT: TBD DESIGN STATUS: UNDEVELOPED DEVELOPMENT COSTS: TBD DESIGN RISK: MAY BE LOW SINCE A 3-CHANNEL X-BAND UNIT HAS BEEN DEVELOPED BUT NOT FLOWN.

Figure 8.2-6. Rotary Joints (Noncontacting Inner and Outer Conductors)

S-band Electronically Despun Antennas

Electronically despun antennas (EDA) were investigated for possible applications as the orbiter despun high-gain antenna. Shown in Table 8.2-4 are characteristics of three S-band systems which represented designs which had progressed beyond the analytical phase of antenna development. The antenna designs by Texas Instruments and Radiation Systems were the only ones which were sized for the Venus mission frequency of 2300 MHz.

The Texas Instruments (TI) EDA system was selected for further tradeoffs because it has the highest gain and lightest weight, and cost estimates were available. The basic difference between the TI concept and the others is the use of TI power amplifiers between the inherent lossy beam steering circuits and the antenna array. In this configuration the power amplifiers are switched on and off at the DC power supply level

ALL ORBITER CONFIGURATIONS

Table 8.2-4. S-Band Electronically Despuned Antennas
(Transmit Only Capability)

PARAMETER	ANTENNA		
	SYNCHRONOUS METEOROLOGICAL SATELLITE (SMS) PHILCO FORD	TEXAS INSTRUMENT (TI) STUDY FOR AMES	RADIATION SYSTEMS INC. (RSI) DEVELOPMENT FOR GODDARD
TRANSMITTER FREQUENCY (GHZ)	1700* (RECEIVE ON 2030)	2300	2300
RF SWITCHING	YES	NO	YES
GAIN (PEAK, DB)	18.7	22	16 (19 PREDICTED)
3-DB BEAMWIDTH [RAD (DEG)]			
AZIMUTH	0.19 (~11.0)	0.19 (10.5)	0.17 (10)
ELEVATION	0.29 (16.6)	0.28 (16.3)	0.31 (18)
EFFECTIVE POWER AMPLIFIER OUTPUT (WATT)	20* (30)	13	(50-WATT TRANSMITTER REQUIRED) (CAN ONLY HANDLE 20)
LOSSES (DB)	1.7	0.4	1.2
EIRP (PEAK, DBM)	60* (62)	62.3	62
WEIGHT (KGM)	12.55*	7.79	28.05 (11.3 PROPOSED)
	(INCLUDES POWER AMPLIFIERS, RECEIVE PHASE SHIFTERS AND COMBINER/SW)	(INCLUDES POWER AMPLIFIERS AND BEAM STEERING CONTROL UNITS)	(INCLUDES BEAM STEERING CONTROL UNITS)
SIZE:			
DIAMETER (CM)	142.0*	76.1	91.4
HEIGHT (CM)	53.4*	58.4	38.1
DEVELOPMENT STATUS	DEVELOPED (TO BE FLOWN IN 1974?)	UNDEVELOPED	PROTOTYPE (NO FURTHER DEVELOPMENT SINCE 1970)
COST:			
DEVELOPMENT (\$K)	PHILCO-FORD DECLINED TO QUOTE	510	
RECURRING (3 UNITS) (\$K)		570	

*MODIFICATION REQUIRED FOR PIONEER VENUS TO PROVIDE 128 BITS/S AT 1.7 AU (EIRP OF 62 DBM)

eliminating the need for RF switching, a major advantage. With this arrangement, where beam steering circuit losses are absorbed at low RF power levels, lower power final amplifiers can be used to obtain the required EIRP. This results in lower prime power requirements with associated cost and weight savings.

The TI design has a unique disadvantage. Since low power (1-watt) modular amplifiers are used in the array, a separate higher power amplifier (~6 watts) is still required to transmit with the omni antennas during third midcourse and orbit insertion, if a downlink is desired at those times.

8.2.3.2 Medium-Gain Antenna

Medium-gain antenna configurations, shown in Figure 8.2-7, were considered for use on the Thor/Delta and Atlas/Centaur-launched probe bus and orbiter spacecraft. These configurations represent existing flight-qualified or breadboard antennas which were considered for use on the earth-pointing and spin axis normal-to-the-ecliptic spacecraft missions. The dish and horn antennas provide a beam along the axis of the antenna while the Franklin array and the bicone array each provide fan-beam normal to the array axis.



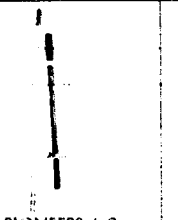

ANTENNAS				
CHARACTERISTICS	DSP 0.6M DISH	PIONEERS 10 AND 11 MEDIUM GAIN HORN	PIONEERS 6-9 FRANKLIN ARRAY	BICONE ARRAY
ANTENNA GAIN (dBi)	20.0	15.5	8	8
HALF POWER BEAMWIDTH, RAD (DEG)	0.24(13.5)	0.49(28)	0.17 X 6.28 (10 X 360)	0.17 X 6.28 (10 X 360)
POLARIZATION	RHCP	RHCP	LINEAR	LINEAR
WEIGHT, KG (LB)	0.9 (2)	1.67 (3.7)	0.45 (1)	2.3 (5)
DEVELOPMENT STATUS	SPACE QUALIFIED	SPACE QUALIFIED	SHORTENED PIONEERS 6 THROUGH 9 WITH OMNI'S REMOVED	NEW DESIGN
PROGRAM COSTS (\$K)	30	20	70	100
REMARKS	ENTRY AND TRANSIT APPLICATION	ENTRY AND TRANSIT APPLICATION	TRANSIT APPLICATION ONLY	TRANSIT APPLICATION ONLY

Figure 8.2-7 Candidate Medium Gain Antenna Configuration

Both types of antennas are required for the spin axis normal-to-the-ecliptic probe bus mission, where higher gain along the spacecraft axis is required during probe entry and coverage normal to the spin axis is required during transit. Since the baseline probe bus is earth-pointing, the medium-gain antenna candidate narrowed to a tradeoff between the dish and the horn. Both candidates are flight-qualified designs; available hardware includes engineering models and a flight horn antenna. The

ALL CONFIGURATIONS

horn was selected over the dish for the probe bus because of: 1) the wider beamwidth needed for the 1978 bus entry and 2) lower program costs for three units (including cost savings for available Pioneers 10 and 11 hardware).

Medium-gain antennas were considered for the orbiter spacecraft for a number of different applications:

- As a backup antenna for the despun high-gain antenna
- As a primary communication antenna
- As a conscan antenna for attitude determination
- As an S-band occultation antenna.

For the earth-pointing missions, the primary candidates are the dish and the horn. The dish is preferred over the horn on configurations which require higher gains and where weight is critical. The major advantage of the horn is its coverage gain; where maximum gain over a broad [<0.35 radian (<20 degrees)] coverage angle is required, the horn would be preferred over the dish. Various horn designs were evaluated to establish an optimum design for the baseline spacecraft configurations. As

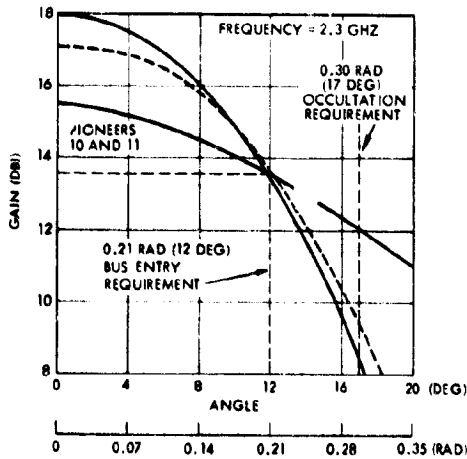


Figure 8.2-8. Horn Gain vs. Pattern Angle

shown in Figure 8.2-8, a tradeoff between the gain and pattern coverage for new design optimum conical horns and the existing Pioneer 10 and 11 corrugated horns shows the corrugated horn best for both the probe bus and the orbiter. The use of an existing qualified design and commonality between bus and orbiter is the lowest cost medium-gain antenna approach for the earth-pointing spacecraft configurations.

The fanbeam antenna is required for the spacecraft mission which has its spin axis normal to the earth line. The preferred fanbeam antenna is the flight-qualified Pioneers 6 through 9 design. The Pioneers 6 through 9 antenna is a lightweight antenna which provides antenna gains efficiently up to approximately 12 dBi with an addition or reduction in the number of elements in the array. Modifications to the existing design to reduce the

number of array elements or to remove integral omni antennas are considered minor modifications. Removal of the existing omni antennas would significantly reduce the design complexity and manufacturing costs. The existing design utilizes concentric coaxial transmission lines to service the Franklin array and two omni antennas. This same concept can be used to service a high-gain 11 dBi array, a shortened array for fanscan, and an omni antenna. To minimize the feed system complexity, miniature coaxial cables would be used to feed the fanscan and omni antenna. Program costs shown in Figure 8.2-7 are for the shortened array with omni antennas removed. Utilization of the full array to obtain the 11-dBi gain measured on Pioneers 6 through 9 units would not significantly increase costs.

8.2.3.3 Low Gain (Omni) Antennas

Omni antenna configurations considered for use on the bus and orbiter are shown in Figure 8.2-9. The horn, which is used as a pattern fill in antenna, and the other candidate antenna configurations are existing flight-proven designs which provide the two basic types of broad radiation pattern coverage obtainable from spacecraft omni antenna elements. Each omni antenna provides approximately half the spherical radiation pattern coverage required for the orbiter and probe missions. The required near-spherical coverage and gain is achievable with combinations of two or more of the candidate antenna configurations. Primary tradeoff considerations were: 1) coverage and gain during critical phases of the missions, 2) weight, and 3) program costs, which included the cost of three units with cost savings for available hardware (engineering models of some configurations are available). Also considered in the tradeoff was polarization compatibility with other spacecraft antennas for minimum DSN operational impact and equipment commonality between the orbiter and probe spacecraft.

Except for the reduced EIRP orbiter spacecraft configuration, the two conical log spiral antennas were the selected omni antennas for all probe bus and orbiters because of their good overlap, proven design, performance, and low cost. With a log conical spiral on the forward and aft ends of the spacecraft, near spherical coverage is obtained. Pattern

ALL CONFIGURATIONS

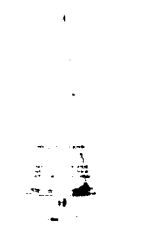






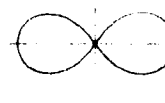
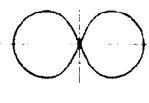

ANTENNAS					
CHARACTERISTICS	CONICAL LOG SPIRAL	CONICAL LOG SPIRAL	SLOT ARRAY	LINDENBLAD	HORN
RADIATION PATTERNS					
PEAK GAIN (dBi)	2.0	4.0	0.0	0.0	7.5
POLARIZATION	RHCP	RHCP	LINEAR	RHCP	RHCP
WEIGHT. KG (LB)	0.4 (0.9)	0.14 (0.3)	0.1 (0.2)	0.1 (0.2)	0.45 (1.0)
DEVELOPMENT STATUS	FLOWN ON DSP	FLOWN ON PIONEERS 10 AND 11	FLOWN ON PIONEERS 6 THROUGH 9	FLOWN ON PARTICLES AND FIELD (APOLLO PROGRAM)	FLOWN ON PIONEERS 10 AND 11
RELATIVE PROGRAM COSTS (\$K)	24	20	30	18	18

Figure 8.2-9. Candidate Probe Bus and Orbiter Low-Gain (Omni) Antenna

interference between antennas is minimized by connecting each antenna to different transmitters and receivers. For the reduced EIRP spacecraft configuration, the slot array and horn were selected to provide near spherical coverage except for a pattern null along the forward axis of the spacecraft. The slot array was selected because of its linear polarization, which is orthogonal to the linear polarization of the fanbeam antenna. With orthogonal polarizations, maximum isolation is obtained between the omni antenna and fanbeam antennas. The aft horn was selected to complement the slot array and provide aft coverage for entry. The spinning circularly polarized horn provides full aft coverage to a linearly polarized ground antenna.

Antenna Spin Doppler Considerations

For spinning spacecraft, the location of antennas with respect to spin-doppler effects must be considered. The sinusoidal doppler rate (\dot{D}) as seen by a tracking station depends on spacecraft spin frequency (ω , rad/s), location of antenna from spin axis (r , meters), communication angle (θ , degrees) off the spin axis; and the carrier frequency (F , Hz);

$$\dot{D} = \frac{\omega^2 r F \sin \theta}{c} \text{ Hz/s}$$

where c is the speed of light in m/s. The tracking loop bandwidth ($2 B_L$, Hz) required is approximately

$$(2 B_L)^2 \approx 2\pi\dot{D}/\Delta\phi, \text{ Hz}$$

where $\Delta\phi$ is the allowed loop static phase error in radians. The loop static phase error is a function of receiver signal-to-noise ratio in $2 B_L$. These relationships are plotted as a family of curves in Figure 8.2-10, showing the allowable spacecraft spin speed as a function of antenna distance from spin axis, tracking loop threshold bandwidth, and received signal-to-noise ratio in that bandwidth. A worst-case communication angle of 1.57 radian (90 degrees) and an allowable static phase error of 0.4 radian is assumed.

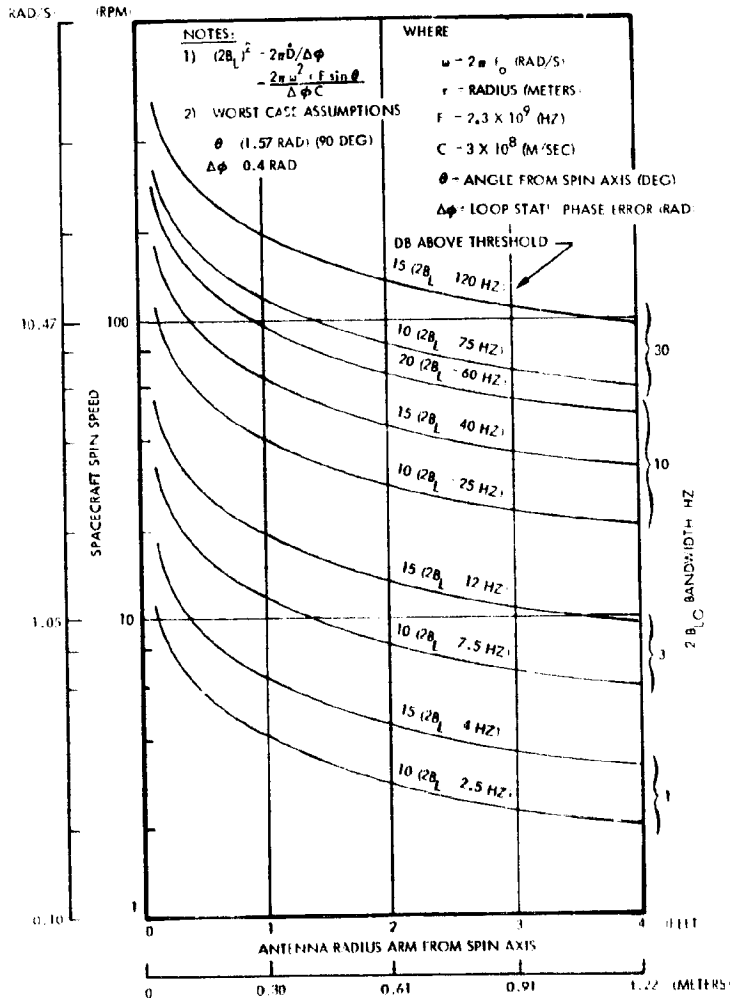


Figure 8.2-10. Allowable Spacecraft Spin Speed (f) Versus Antenna Distance From Spin Axis (r) and Receiver Loop Bandwidth (2B_L)

The results show that, for the preferred nominal cruise spin speed of about 0.52 rad/s (5 rpm), there is no problem with 10 Hz $2 B_L$ bandwidth tracking. However, for high spin rates like 6.28 rad/s (60 rpm), for special mission events like bus entry or orbit insertion, either a 30 Hz loop bandwidth or an antenna mounted near the spin axis must be used. For the preferred Atlas/Centaur orbiter configuration, the Pioneers 10 and 11 forward omni is mounted on the axis and there is no doppler problem for orbit insertion. However, if we desired, for doppler tracking attitude control reasons, to mount the omni at the edge of the 1.52-meter (5-foot dish), there is enough margin to perform the insertion tracking at 6.28 rad/s (60 rpm) with a 30 Hz loop. The margin is provided by using a 0.54 radian modulation index (i.e. more power in the carrier).

8.2.3.4 Solid State Versus TWTA Power Amplifiers

The tradeoff studies of the various S-band power amplifiers required for the different missions, launch vehicles, and options covered both solid-state amplifiers and traveling wave tube amplifiers (TWTA's) at RF power levels from 3 to 36 watts. Each particular requirement was reviewed and potentially usable hardware was considered for size, weight, cost, efficiency, development risk, and availability. The power amplifiers sized for the various orbiter and probe bus options are:

- 3/6-watt amplifier (dual mode)
- 3/12-watt amplifier (dual mode)
- 8-watt amplifier
- 9/36-watt amplifier (dual mode)
- 16/36-watt amplifier (dual mode).

In addition to these there are large and small probe options with output powers in this range. The tradeoffs have considered the commonality of requirements and its potential effect in reducing unit costs.

Survey of S-band Power Amplifiers

A survey was made of available solid-state and TWTA's (including power supply and control circuitry) with emphasis on lightweight characteristics for the Thor/Delta application and minimum cost and development risk for the Atlas/Centaur configuration.

The source of space-qualified TWT's for S-band is principally limited to two companies, i.e., Watkins Johnson and Hughes Aircraft Company (HAC). An analysis of previous program cost histories clearly indicates that both new TWT development and the integration of tubes with power supplies (particularly when supplied by different vendors) are risky and costly endeavors. It was therefore decided to restrict our attention to qualified TWTA units now under development for similar space applications, or a combination of an existing TWT and a power supply requiring only minor modifications. These survey criteria greatly reduced the number of candidates for consideration and highlighted the fact that the TWTA market (and TWT's also) is essentially divided by frequency, with Watkins Johnson controlling the S-band market and HAC controlling the X-band market. Although HAC was a leader in the development of TWT's for space communications, the S-band development work done by Watkins Johnson has clearly made it the leading supplier of space-qualified S-band TWTA's. The notable exception is the dual mode TWTA used on Mariner, where the 10/20-watt tube is provided by HAC and the power supply by Watkins Johnson. A recent change in this program has replaced the HAC 10/20-watt TWT with a more efficient 16/36-watt tube from Watkins Johnson.

A summary of the characteristics for the TWTA's considered for Pioneer Venus is given in Table 8.2-5. Three designs are clearly much lighter and more efficient than all the others, i.e., the 8-watt 1171-1 series flown on Pioneers 10 and 11, the 10/20-watt 1171-3 series qualified for the Helios program, and the 16/36-watt unit being supplied to MVM 1973. Since these units cover the power range of interest, they are the leading contenders for the TWTA application.

The results of the solid-state amplifier survey are also given in Table 8.2-6 for comparison purposes. Although only four suppliers are listed, it is anticipated that firm bids will be received from a number of other sources with space hardware experience. Note on Table 8.2-6 that even the lightest TWTA on the list (Pioneers 10 and 11, 1171-1) is much heavier than the heaviest solid-state unit, and that cost considerations also make the solid-state amplifier attractive.

Table 8.2-5. Survey of S-Band Power Amplifiers

MANUFACTURER	PROGRAM	STATUS	WEIGHT (KG (LB))	DC POWER (WATT)	RF POWER (WATT)	COMMENTS
RADIATION INC	TECHNOLOGY PROGRAM GSFC	DELIVERED	0.14 (0.3)*	18	6	MUST MODIFY DESIGN (NEW POWER TRANSISTORS) TO REDUCE JUNCTION TEMPERATURE
TRW	MODEL 35	ENGINEERING MODEL	0.36 (0.8)	15	4	30 DB GAIN
WATKINS JOHNSON	PIONEERS 10 AND 11	FLIGHT	1.8 (4)	28	8	WATKINS JOHNSON 1171-1
WATKINS JOHNSON	ERTS	FLIGHT	4.1 (9)	85	20	WATKINS JOHNSON 1176
WATKINS JOHNSON	APOLLO - CCS	FLIGHT	6.4 (14)	95	15	
WATKINS JOHNSON	NASA HUNTSVILLE	LAB/TEST	5.4 (12)	132	50	DELIVERED FOUR UNITS
WATKINS JOHNSON	RCA	FLIGHT	3.9 (8.5)	85	20	CLASSIFIED PROGRAM
WATKINS JOHNSON	VIKING LANDER	QUALIFIED AUGUST 1973	4.4 (9.6)	86	20	WATKINS JOHNSON 1185
WATKINS JOHNSON/HAC	MARINER	FLIGHT	4.5 (10)	40, 80	10/20	
WATKINS JOHNSON	MVM 73	DEVELOPMENT	4.5 (10)	52/104	16/31	NEW TUBE, MODIFIED MARINER P.S.
WATKINS JOHNSON	PROPOSED	DEVELOPMENT	2.3 (5)	55/110	16/31	NEW TUBE, MODIFIED HELIOS P.S.
WATKINS JOHNSON	HELIOS	QUAL	2.2 (4.8)	45, 70	10/20	WATKINS JOHNSON 1171-3
MSC	COMMERCIAL OFF SHELF	MUST QUALIFY	0.14 (0.3)*	15	6	CUSTOMER MAY HAVE QUALIFIED
MSC	COMMERCIAL OFF SHELF	MUST QUALIFY	0.3 (0.6)*	44	12	CUSTOMER MAY HAVE QUALIFIED
MSC	COMMERCIAL OFF SHELF	MUST QUALIFY	0.3 (0.6)*	80	20	CUSTOMER MAY HAVE QUALIFIED
PHILCO FORD	PROPOSED		0.45 (1) 0.9 (2) 1.5 (3.3)	27 40 105	5 10 20	5-WATT UNIT QUALIFIED ON ATS
MOTOROLA	PROPOSED		0.63 (1.4) NA NA	25 50 100	5 10 20	

* LOW-GAIN VERSION

Table 8.2-6. Solid-State versus TWTA Tradeoffs for 6 Watts

	TWTA		SOLID STATE		
	PIONEERS 10&11	HELIOS	MSC	RADIATION INC.	TRW
RF POWER (WATT)	8	10/20	6	6	6
WEIGHT, KG (LB)	1.8 (4)	2.2 (4.8)	0.2 (0.5)*	0.2 (0.5)*	0.2 (0.5)*
EFFICIENCY (%)	28	22/29	32	33	33
RELIABILITY (BITS)	3382	4000 (EST)	1115 (EST)	1115 (EST)	1115 (EST)
STATUS	FLIGHT PROVEN	QUALIFIED	COMMERCIAL	LIMITED QUALIFICATION	QUAL 3.5 W IN 1973
RF POWER ADJUSTMENT	NONE	DUAL LEVEL TWT	VOLTAGE	VOLTAGE	VOLTAGE
UNIT COST (6 EACH) (\$K)	72**	80**	NA	23	20
MODIFICATIONS REQUIRED	NONE	INCREASED SPACECRAFT PRIME POWER	REPACKAGED FOR SPACE USE	REDESIGN TO REDUCE JUNCTION TEMPERATURE INCREASE GAIN	REDESIGN TO 6 WATTS

* HIGH-GAIN VERSION
** VENDOR COST LEVEL

Solid State Versus TWTA Tradeoffs for 6 Watts

1) TWTA's. While there are many TWT's available for S-band use, there are few lightweight TWTA's (including the power supply). At the 8-watt level, the most efficient and lightweight unit available is the

Pioneers 10 and 11 unit. For higher power, the dual mode TWTA developed for Helios is the lightest weight unit available. The cost of both units is similar. Table 8.2-6 shows that the weight and cost of the TWTA is considerably greater than the solid state units shown.

2) Solid State Power Amplifiers. A cost analysis leads to the conclusion that it is cheaper to qualify solid state units than to use the qualified TWTA's presently available. In addition to the three sources of solid state units given in Table 8.2-6, Motorola, Philco-Ford, and Teledyne are capable of providing the required units; however, at present the three sources shown are preferred because of existing and ongoing programs. Due to the anticipated number of sources available, it is not necessary to limit the selection at this time. Since all available sources presently use Microwave Semiconductor's (MSC) transistors, it might seem obvious that the MSC power amplifier should be chosen; but the company's limited experience with space-qualified hardware will require them to be critically reviewed. Based on ongoing efforts both MSC and TRW are expected to have qualified solid state power amplifiers in time for use on Pioneer Venus. Radiation, Inc. has done limited qualification testing on a low-gain amplifier for NASA/GSFC, but the unit must be redesigned to increase its gain and to reduce junction temperatures; no efforts are presently being expended toward this.

Solid State Versus TWTA Tradeoff for 36-Watt. There is a requirement for 36-watt nominal (31 watts minimum) for some configurations. Slightly modified TWTA's have been compared to solid state units for this application.

1) TWTA's. As mentioned earlier, the high efficiency S-band TWTA market is dominated by Watkins Johnson. Although HAC has experimental tubes at 50 watts, the most logical choice for this power level is the TWT being supplied to MVM 1973. Watkins Johnson is under contract now to replace the existing 10/20-watt tube with a 14/31-watt (minimum) tube with much greater efficiency. Unfortunately, the power supply used on Mariner is heavy, resulting in a TWTA weight of approximately 4.5 kilograms (10 pounds). For Pioneer Venus the best choice would appear to be to use the new MVM 1973 TWT with a modified Helios power supply. These modifications would be slight, limited to a few component parts.

ALL CONFIGURATIONS

2) Solid-State Power Amplifiers. The requirement for a single 36-watt unit (31 watts minimum) cannot be satisfied with existing hardware. Microwave Semiconductors has a 90,000 series unit which can provide an output power of 30 watts. The low advertised efficiency (22 percent) of the unit makes it unattractive.

If new transistors from the 4000 series are substituted, the solid state unit becomes more competitive. A TRW proposed design shows an efficiency of 28 percent at about 20 watts. For purposes of this study, it is proposed that two nominal 20-watt amplifiers be paralleled to provide the 36 watts. This approach is less costly since only one design is required for both the orbiter and the large and small probes. A preliminary cost estimate shows a saving of approximately \$200,000 if a parallel approach is chosen over a new 36-watt solid state design.

3) Tradeoffs. Table 8.2-7 summarizes pertinent data for the MVM 1973 TWTA and a solid state approach using parallel 20-watt units. Note that the TWTA is more efficient, but heavier and more costly. The present baseline uses the MVM 1973 TWTA for the Thor/Delta orbiter because its greater efficiency is compatible with the solar array capability of the Thor/Delta design. On the Atlas/Centaur Version III orbiter, where more solar cell output is available, the parallel 20-watt solid state units are baselined because of reduced cost.

Table 8.2-7. Solid-State versus TWTA Tradeoffs for 36 Watts

	TWTA MVM73/HELIOS	SOLID STATE (4005 TRANSISTORS) (PARALLEL 20-WATT UNITS)	COMMENTS
RF POWER (WATTS)	16.36 (NOM) 14.31 (MIN)	9.36 (NOM) 7.8/31 (MIN)	
DC POWER (WATTS)	55.106	68.136	
EFFICIENCY (%)	29.34	14.28	ASSUMES ONE 20-WATT ON - ONE OFF
WEIGHT, KG (LB)	2.7 (6)	1.0 (2.2)	SS INCLUDES TWO HYBRIDS
RELIABILITY (BITS)	4000 (EST)	6450 (EST)	
STATUS	TWT TO BE QUALIFIED P.S. IS MODIFIED VERSION OF QUALIFIED UNIT	COMMERCIAL - MUST QUALIFY	
RF POWER ADJUSTMENT	DUAL LEVEL TWT	TURN OFF ONE 20-WATT UNIT	
UNIT COST (\$K)	187 (2 FLIGHT + SPARE + QUAL REQUIRED)	86 (4 FLIGHT + SPARE + QUAL REQUIRED)	ASSUMES COMMONALITY WITH LARGE AND SMALL PROBES
MODIFICATIONS REQUIRED	CHANGE P.S. VOLTAGE AND CURRENT	REPACKAGE FOR SPACE - CHANGE TRANSISTOR TYPE	

Power Amplifier Combining Techniques

We limited the number of power amplifiers that must be developed and qualified by continuously considering commonality of design requirements between the bus, orbiter, and probes. A further effort was made to reduce the new designs by using modular combining techniques.

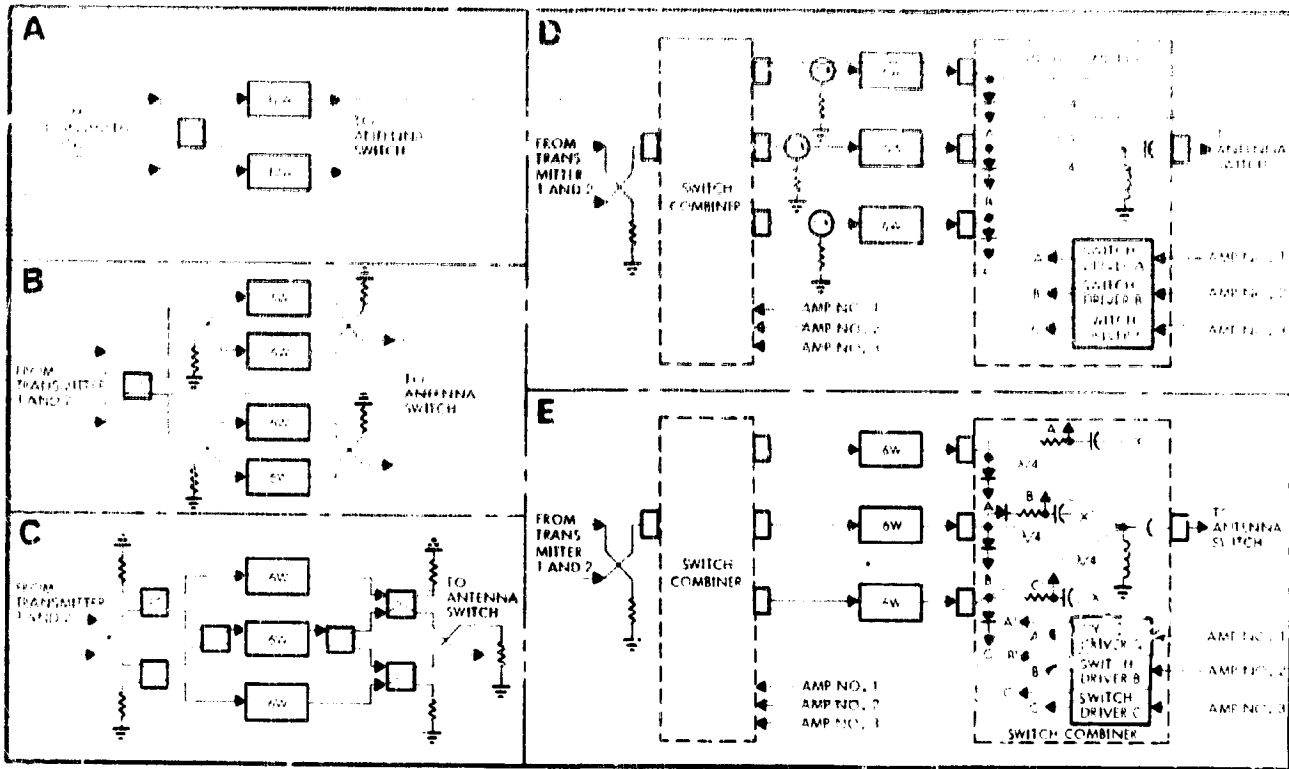
Figure 8.2-11 shows four techniques which allow the use of one basic 6-watt design to serve the dual purpose of providing 10 to 11 watts for the orbiter and 6 watts for the probe (nonredundant). Four methods of doing this are shown in Figure 8.2-11B, C, D, and E, along with a list of characteristics. A 12-watt amplifier is also included for comparison in Figure 8.2-11A.

The method shown in Figure 8.2-11B utilizes redundant parallel 6-watt power amplifiers combined with hybrids to provide approximately 11 watts of output power.

The method shown in Figure 8.2-11C allows the generation of the required 11 watts using only three power amplifiers for a redundant three-for-two system using five additional transfer switches. This approach is heavy, as space-qualified relays weigh 0.3 kilogram (0.6 pound) each.

The method shown in Figure 8.2-11D utilizes diode switched quarter wave transmission lines to provide three-for-two redundancy without the use of transfer relays. An alternate version of this approach, shown in Figure 8.2-11E, uses a diode-switched Wilkinson hybrid combiner. They differ in that the Wilkinson approach does not require isolators to reduce interaction between amplifiers. Although this approach has been used on communication transponders where numerous power levels must be accomplished, its complexity (including telemetry and command interfaces) does not make it attractive for the Pioneer Venus application. After reviewing all the data in Figure 8.2-11, the method in Figure 8.2-11B has been chosen. When firm cost estimates are available from each of the vendors, and the baseline transmitters powers have been selected, the number of power amplifier designs will again be considered.

Although not illustrated, the same techniques can be used to provide 36 watts nominal from a 20-watt design. The exact values in the summary table will change, but the relative values are still useful in making the tradeoff decision.



	MODIFY & TO 10 WATTS (A)	HYBRIDS (B)	SWITCHES (C)	TRANSMISSION LINES (D)	SWITCHED AMPLIFIERS (E)
COMPLEXITY	SIMPLE DESIGN	SIMPLE ASSEMBLY	SIMPLE ASSEMBLY	MORE COMPLEX	MOST COMPLEX
WEIGHT (COMPARATIVE TO C-180)	1.1 (2.4)	1.5 (3.2)	2.8 (6.3)	1.5 (3.2)	1.2 (2.7)
COMPACTNESS	WOULD CREATE A SECOND POWER AMPLIFIER DESIGN NOT NEEDED FOR BUS	SINGLE 6-WATT DESIGN REQUIRED	SINGLE 6-WATT DESIGN REQUIRED	REQUIRES NEW DEVELOPMENT FOR SWITCHING COMBINER NOT NEEDED FOR BUS	REQUIRES NEW DEVELOPMENT FOR SWITCHING COMBINER NOT NEEDED FOR BUS
RELIABILITY (10,000 HRS)	0.9926	0.9962	0.9928	0.9945	0.9923
SWITCHING TIME REQUIRED ASSUMING THAT THE SWITCHING AMPLIFIERS WILL LAST	ADD ONE POWER STAGE AND TWO MICROSECOND HYBRID DEVELOPMENT	USE OFF-THE-SHELF COMPONENTS, MUST QUALIFY	USE OFF-THE-SHELF COMPONENTS, MUST QUALIFY	DESIGNS EXIST AT 250 AMP, 1000 AMP, AND 100 AMP. MULTIPLE DESIGNS ARE REQUIRED TO PERFORM DESIGN	DESIGNS EXIST AT 250 AMP, AND 100 AMP. MULTIPLE DESIGNS ARE REQUIRED TO PERFORM DESIGN
WEIGHT OF ONE POWER AMPLIFIER SYSTEM	23	47	90	43	24

Figure 8.2-11. Power Amplifier Combining Techniques

8.2.3.5 Lightweight Versus Standard Weight Transponders

The survey of transponders has shown that only three companies are actively engaged in the manufacture of coherent DSN-compatible (240/221 turnaround) transponders, i.e., Philco-Ford, Motorola, and TRW. Available and developmental hardware can be further segregated into lightweight and standard designs. A summary of candidate hardware is given in Table 8.2-8.

Table 8.2-8. DSN Compatible Transponders

MANUFACTURER	PROGRAM	STATUS	WEIGHT (KG (LB))	DC POWER (WATTS)	RF POWER (WATTS)	COST** (\$K)	MODIFICATIONS REQUIRED
ATLAS/CENTAUR ORBITER							
LIGHTWEIGHT TRANSPONDERS							
PHILCO FORD	VIKING LANDER	IN QUAL	1.7 (3.8)	7.0	0.125	150-200	CONSCAN AGC*** OUTPUT DIFFERENT INHIBIT CONTROL MODULATION CIRCUIT INTERFACE FACTORS
TRW	COMPANY- FUNDED	ENGINEERING MODEL	1.5 (3.4)	7.5	0.125	153	COHERENCE RATIO REDUCE LOOP BANDWIDTH MODULATION CIRCUIT
MOTOROLA	COMPANY- FUNDED	ENGINEERING	1.6 (3.5)	7.0	0.125	---	EARLY DEVELOPMENT
MOTOROLA	COMPANY- FUNDED	DEVELOPMENT	2.4 (5.3)	7.0	0.125	---	WILL SELL MID-1973
ATLAS/CENTAUR PROBE BUS							
STANDARD TRANSPONDERS							
TRW	PIONEERS 10 & 11	FLIGHT	3.1 (6.8)	3.5	0.06	194	NONE
TRW	P&F	FLIGHT	4.3 (9.5)	15.2	0.7	80*	REDUCE LOOP BANDWIDTH IMPROVE NOISE FIGURE
MOTOROLA	ERTS	FLIGHT	5 (11)	28	1.0	65*	REDUCE LOOP BANDWIDTH IMPROVE NOISE FIGURE
MOTOROLA	MARINER	FLIGHT	8.2 (18)	27	0.2	110	POWER SUPPLY

* INCLUDES MODIFICATION COSTS
 ** VENDOR COST LEVEL
 *** AUTOMATIC GAIN CONTROL

Lightweight Transponders

Thor/Delta-launched payloads require the use of lightweight hardware. Only one company presently is supplying lightweight transponders, i.e., Philco-Ford. For deep-space applications, the Viking Lander presently being qualified meets the Pioneer Venus requirements with certain modifications. Motorola is in the early development of a 1.6-kilogram (3.5-pound) unit, but expects to sell a somewhat heavier design [2.4 kilograms (5.3 pounds)] by mid-1973. TRW is continuing the development of a microminiature transponder with the goal of developing a DSN

compatible unit by late 1973. A Defense Support Program (DSP) design is presently being tested.

Although it is expected that all three suppliers will be able to supply DSN compatible units to the Pioneer Venus schedule, the Viking Lander unit has been selected for the Thor/Delta probe bus and orbiter configurations and for the Atlas/Centaur orbiters. The stability of the auxiliary oscillator must be improved, or as an alternate, the Pioneers 10 and 11 oscillator could be included in the package. These modifications are considered minor and should have minimal cost impact on the Viking Lander design.

Standard Transponders

The Atlas/Centaur-launched payloads are not severely weight limited, and heavier transponders can be considered where there is a cost or development risk reduction. Only TRW and Motorola have provided standard weight DSN-compatible hardware in recent years. The Motorola ERTS equipment is not designed for deep space and would require both an increased threshold sensitivity and a reduced loop noise bandwidth to be usable. The Motorola Mariner equipment is adaptable with only minor changes, but is extremely heavy and is being phased out as the lightweight designs become available.

A TRW transponder, supplied to the NASA Particles and Fields Program, is designed for near-space applications and would require modifications to increase the sensitivity and reduce the loop noise bandwidth.

The Pioneers 10 and 11 hardware is usable as is and requires no modification. Moreover, residual units are available as spares, prototypes, and qualification items which afford a significant program cost savings if assigned to Pioneer Venus. Based on the availability of the Pioneers 10 and 11 residuals, the present baseline system will use the Pioneers 10 and 11 receiver, transmitter driver, and a 6-watt solid-state amplifier for the Atlas/Centaur probe bus. The Atlas/Centaur orbiter will use the modified Viking Lander hardware.

8.2.3.6 Ranging Versus Combination S- and X-band

Tradeoffs were made between adding either a ranging or a combination S- and X-band capability to the spacecraft. Corresponding capabilities; ease of spacecraft implementation; power, weight, and cost factors were compared. Neither ranging nor X-band is required for spacecraft tracking and the preferred configurations do not include either capability explicitly.

The section first presents a summary of the tradeoff, then the detailed antenna and transponder tradeoffs, and finally the ranging and S-band performance capabilities, assuming they were to be implemented in the spacecraft. This section does not deal with the X-band occultation parameters and capabilities. The preferred S- and X-band occultation implementation is described in Section 8.2.4.1.

Table 8.2-9 summarizes the advantages and disadvantages of adding either a ranging capability or an X-band downlink (880/221 coherency ratio with the S-band uplink) to the spacecraft. Weight, power, and cost penalties are also shown for the Atlas/Centaur and Thor/Delta Version III science payloads.

Table 8.2-9. Ranging vs. Combination S- and X-Band Tradeoff Summary (Spacecraft Spin Axis Perpendicular to Earth Line)

	RANGING		X-BAND
	VIKING TRANSPONDER	PIONEERS 10 AND 11 TRANSPONDER	
FEATURES	<ul style="list-style-type: none"> • NO MODIFICATIONS • DEGRADED DOWN-LINK TELEMETRY 	<ul style="list-style-type: none"> • EXTENSIVE MODIFICATIONS • DEGRADED DOWN-LINK TELEMETRY 	<ul style="list-style-type: none"> • REQUIRES X-BAND TRANSMITTER AND ANTENNA • NO S-BAND DEGRADATION • ADDITIONAL EXPERIMENT CAPABILITY (X-BAND OCCULTATION)
POWER PENALTY	NONE	0.5 WATTS	63 WATTS (20-WATT TWTA)
WEIGHT PENALTY	NONE	2.4 KG (5.3 LB)	4.6 KG (10.1 LB)
PROGRAM COST	NONE	\$320 K (2 FLIGHT, 1 SPARE)	\$130 K - ANTENNA \$666 K - TRANSMITTER (DRIVER + TWTA) (1 FLIGHT, 1 SPARE)

*MOST LIGHTWEIGHT CANDIDATE TRANSPONDERS BEING DEVELOPED PROVIDE A RANGING CAPABILITY AND ONLY A SMALL COST SAVINGS MIGHT BE REALIZED BY PROCURING A TRANSPONDER WITHOUT A RANGING REQUIREMENT.

One of the reasons for adding either a ranging or an X-band capability to the spacecraft is to improve trajectory and orbit tracking accuracy. One of the largest errors in doppler tracking is introduced by the frequency shifting effects of interplanetary charged particles. These effects can effectively be calibrated out by the use of either ranging or a combination of two widely separated frequencies, e.g., S- and X-band. Mission analysis (Task 4132-08) has shown that neither is required to accomplish the basic mission objectives. However, if desired, an improvement in tracking by calibrating out the effects of charged particles is possible to the following accuracies (see JPL Technical Report 32-1526, Volume XI, page 42):

	<u>Charged Particle Calibration Range Error (1σ)</u>
Combination S- and X-band downlink	0.5 m
Ranging (differenced range versus integrated doppler, DRVID)	1.0 m

Table 8.2-10 shows that the ranging capability exists on the orbiter baseline and costs little to implement. The telemetry degradation depends on the chosen telemetry and ranging modulation indices and could range from a fraction of a dB to many dB's. However, since for almost the entire mission ranging would be performed with the 64-meter DSN with about 10 dB greater sensitivity, G/T, the normal cruise telemetry rate would be sustained while ranging. The Pioneers 10 and 11 transponder circuitry does not have the necessary wideband response for ranging and would require extensive modifications.

X-band, on the other hand, even though more expensive to implement, has the added attraction of providing an additional experiment, X-band occultation. For weight, power, and cost comparisons, a TRW X-band transmitter driver and a 20-watt Hughes TWTA were used. The MVM 1973 200-mW transmitter by Motorola is included in the following tradeoffs. For Thor/Delta an 8- to 10-watt TWTA would be preferred to save on DC power. However, some development would be required for a 10-watt tube. The X-band antenna used in Table 8.2-10 is an 11-dB X-band version of the Franklin fanbeam array, about 0.36 meter (14 inches) long, and corresponds to spacecraft configurations perpendicular to the

earth line. For an earth-pointing configuration a 20-watt TWTA would not be required (a 200-mW driver would be sufficient), as an aft horn (probe bus and orbiter) and a forward 1.5 meter antenna (orbiter) would be used. The X-band costs would therefore be somewhat lower than those shown in Table 8.2-9.

Combination S/X-band Antenna Designs

Each candidate spacecraft antenna subsystem design was evaluated for the possible addition of an X-band capability. The antenna configurations described below represent the best candidate designs compatible with earth-pointing and spin-axis-perpendicular orbiter spacecraft configurations. Figure 8.2-12 shows various S/X-band antenna designs.

Earth-Pointing Antenna Configurations. X-band antennas for the probe bus and aft end of the orbiter can be a simple horn and do not have a significant impact on the design. X-band antennas on the forward end of the orbiter, where higher gain is needed, do have an impact. For this case, the X-band antenna was to have maximum gain and was to be compatible with forward looking S-band dish antennas. The S-band feed was laterally defocused for conscan and, to minimize costs, no feed movement mechanism was added. Three approaches to the S- and X-band antenna system which used the S-band dish for TT&C and conscan are shown in Figure 8.2-12. These are the dish with a dual frequency S- and X-band feed, the dish with separate S- and X-band feeds, and the dish with a separate X-band horn antenna. The preferred design for these orbiters was the S-band dish with separate S- and X-band feeds. This design was selected because of its lighter weight, minimum development, and maximum X-band gain without any defocussing penalty.

The occultation experiment, per the Version IV science payload, is conducted from the aft end of the baseline Atlas/Centaur earth-pointing orbiter mission. Because of the revised mission requirements and more emphasis on X-band coverage gain, lower gain antennas with broader beamwidths imply horn designs for simplicity and lowest cost. The medium-gain antenna tradeoffs of Section 8.2.3.2 showed the Pioneers 10 and 11 horn to be the preferred S-band antenna based upon being a qualified design, with optimum coverage gain and minimum costs. The


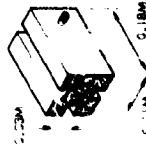

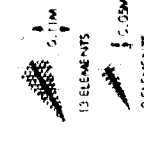

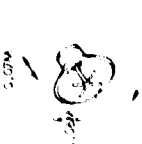
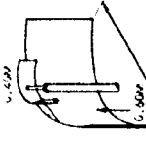
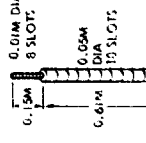
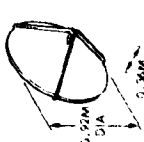
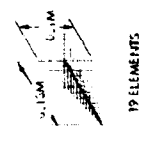
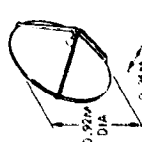
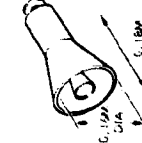
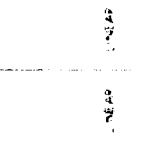
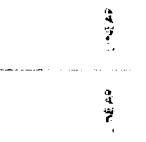
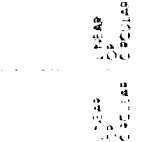
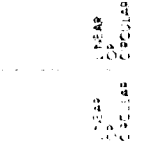
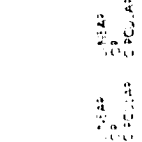
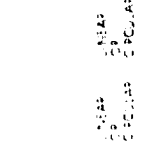
EARTH POINTING SPACECRAFT ANTENNA WITH 5-BAND CONSCAN				MECHANICALLY DESPIN ANTENNA			
5-BAND AND 7-BAND ANTENNA CONFIGURATION	FEED DESIGN	ON AXIS GAIN (INCLUDES TOB CONSCAN LOSS)		3 DB BEAMWIDTH		POLARIZATION	
		5-BAND	7-BAND	5-BAND	7-BAND	5-BAND	7-BAND
 <p>0.92 METER DISH WITH DUAL 5-BAND AND 7-BAND EDGE WAVE QUARTER WAVE FEED</p>	 <p>0.18M HORN 0.18M DIA</p>	>23 DB	>31 DB	0.16 RAD (9.0 DEG)	0.08 RAD (4.7 DEG)	LINEAR	LINEAR
 <p>0.92 METER DISH WITH SEPARATE LOG PERIODIC CROSS-DIPOLE 5-BAND AND 7-BAND FEEDS</p>	 <p>0.18M HORN 13 ELEMENTS 0.05M DIA</p>	>23 DB	>35 DB	0.16 RAD (9.0 DEG)	0.08 RAD (4.7 DEG)	LINEAR CIRCULAR	LINEAR CIRCULAR
 <p>0.92 METER DISH WITH PICNICKS 10 AND 11 HORN FEED</p>	 <p>0.18M HORN 0.18M DIA</p>	>24 DB	>28 DB	0.16 RAD (9.0 DEG)	0.16 RAD (9.0 DEG)	CIRCULAR	CIRCULAR
 <p>0.92 METER DISH WITH HELICAL DESPIN REFLECTOR FOR 5-BAND AND 7-BAND</p>	 <p>0.18M HORN 0.18M DIA</p>	>27.5 DB	>31 DB	0.16 RAD (9.0 DEG)	0.08 RAD (4.7 DEG)	LINEAR	LINEAR
 <p>0.92 METER DISH WITH LOG PERIODIC CROSS-DIPOLE FEED</p>	 <p>0.18M HORN 19 ELEMENTS 0.11M DIA</p>	>24 DB	>35 DB	0.16 RAD (9.0 DEG)	0.08 RAD (4.7 DEG)	LINEAR CIRCULAR	LINEAR CIRCULAR
 <p>0.92 METER DISH WITH DUAL 5-BAND AND X-BAND HORN FEED</p>	 <p>0.18M HORN 0.18M DIA</p>	>24 DB	>28 DB	0.16 RAD (9.0 DEG)	0.16 RAD (9.0 DEG)	CIRCULAR	CIRCULAR
 <p>0.61M DIA 0.61M DIA 0.61M DIA 15 SLOTS COLINEAR SLOT DIPOLE ARRAY</p>	 <p>0.18M HORN 0.18M DIA</p>	>27.5 DB	>31 DB	0.16 RAD (9.0 DEG)	0.08 RAD (4.7 DEG)	LINEAR	LINEAR
 <p>0.17M DIA 0.17M DIA 0.17M DIA 10 DEGS 0.17 RAD 2.5 DEG</p>	 <p>0.18M HORN 0.18M DIA</p>	>24 DB	>35 DB	0.16 RAD (9.0 DEG)	0.08 RAD (4.7 DEG)	LINEAR CIRCULAR	LINEAR CIRCULAR
 <p>0.17M DIA 0.17M DIA 0.17M DIA 10 DEGS 0.17 RAD 2.5 DEG</p>	 <p>0.18M HORN 0.18M DIA</p>	>24 DB	>28 DB	0.16 RAD (9.0 DEG)	0.16 RAD (9.0 DEG)	CIRCULAR	CIRCULAR

Figure 8.2-12. Combination 5-Band and X-Band Antenna Designs

same maximum coverage gain requirements are applicable to the X-band antenna; therefore, an existing X-band medium gain horn design would be the preferred X-band antenna because of minimum costs. New designs or scaled S-band horns were considered, but new development represents a significant cost increase. The preferred X-band horn for the aft looking orbiter is the existing qualified DSCS-II earth coverage receive horn. Figure 8.2-13 describes the existing design and radiation pattern at 8.4 GHz.

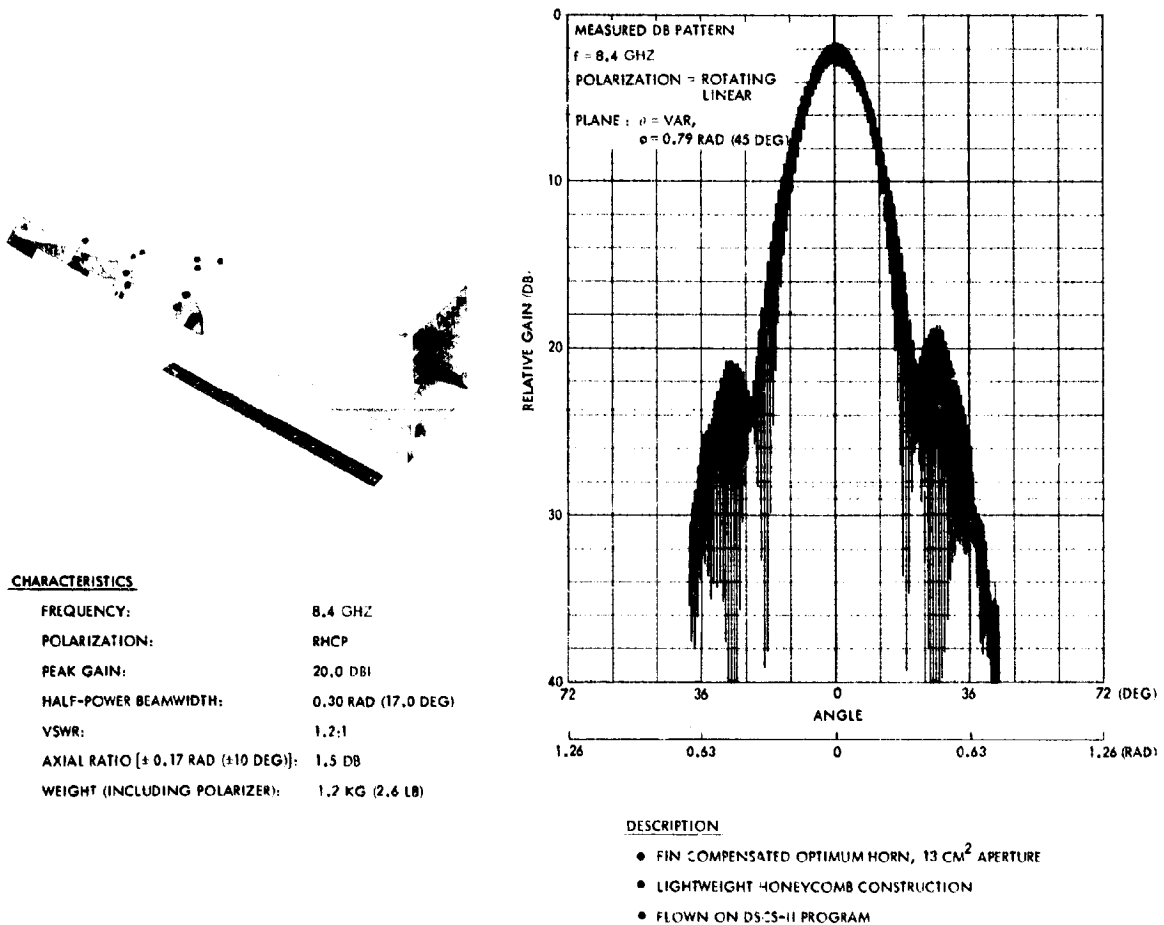


Figure 8.2-13. X-Band Occultation Experiment Antenna

Mechanically Despun Antenna Configurations. The primary design problem in adding an X-band capability to the mechanically despun antenna (DMA) system is that an added despun channel must be accommodated by either the feed system in the despun reflector approach or in the rotary coupler/DMA system in the despun antenna approach (see Figure 5.8-12).

Separate channels are required for the omni antenna, the S-band high-gain antenna, and the X-band antenna. The despun antenna approach using a dual frequency S- and X-band feed is the simplest antenna design; however, this concept requires a three-channel rotary coupler or a DMA with slip rings for switching and frequency multipliers. A rotary coupler increases the system complexity and cost. A multiple coaxial feed system similar to the Pioneers 6 through 9 antenna can be used for the despun reflector approach. Since the dual reflector system has been flown on the ATS-III program, this approach has been shown to be feasible. The dual reflector system is the preferred S- and X-band approach for the MDA for the Atlas/Centaur and Thor/Delta Version III science payload configurations.

Fanbeam Antenna Configurations. The candidate fanbeam X-band antenna configurations considered were the same ones considered for the S-band fanbeam antenna: collinear arrays and biconical horn apertures. Because of size, weight, and cost advantages, the proven Pioneers 6 through 9 Franklin array design, scaled for X-band, is the preferred approach. Fanbeam antennas having gains much greater than 12 dBi are not considered to be cost effective because the relative size and feed system inefficiency increases significantly for small increases in gain. With three S-band antennas located on the forward side of the spacecraft, the X-band antenna would be separately fed and located on the aft side of the spacecraft to minimize the complexity of the S-band antenna stack. The scaled X-band array [about 0.36 meter (14 inches) long] would provide the same performance as the S-band antenna.

X-Band Transmitter

As part of this study, various methods were considered for generating RF power at X-band (8400 MHz). For the earth-pointing and mechanically despun options, 200 mW is sufficient and the MVM 1973 unit is a logical choice. For the fanbeam antenna options (11 dB gain), 6 watts is required for real-time tracking out to 254.32 gigameters (1.7 AU).

With a power requirement of 6 watts the system needs a TWTA. A solid-state design which is an extension of a TRW IR&D development of a 200 mW design has been considered for tradeoff purposes, and it appears reasonable to consider a solid-state design up to a 1.5-watt requirement.

A 6-watt requirement is not considered possible at this time with solid-state devices at reasonable efficiency. Bulk effect amplifiers such as the avalanche diode amplifier (ADA) can produce the required power in a laboratory environment, but at very low efficiency (<5 percent). ADA's operating in the TRAPAT mode have shown greater efficiency (40 percent) using gallium arsenide diodes, but these units must be considered laboratory curiosities at this time. It is also possible to use a crossed field amplifier (CFA) for these powers for efficiencies of 30 to 40 percent, but these amplifiers (linear field) are still developmental items.

For higher powers and increased efficiency, the TWTA must still be considered the most promising, if not the only, candidate. As mentioned previously, Hughes Aircraft Company (HAC) supplies most of the X-band TWTA's. Watkins Johnson built the IDCSP amplifier at 2-1/2-watt output, but this unit must be considered obsolete. HAC has built TWTA's for ATS-F and DSCS-II and has provided TWT's from 1 to 20 watts to numerous spacecraft programs. The DSCS-II TWTA is the latest built by HAC for TRW. The HAC Model 1202H is a space-qualified TWTA utilizing the 265 TWT. It produces an output power of 22 watts for a maximum input power of 98 watts. Other TWT's, such as the 219H developed by NASA/Langley or the 240H developed for TACSAT and Skynet II, could also be utilized in this amplifier. However, the TWTA is relatively heavy, 4.3 kilograms (9.5 pounds), and somewhat inefficient (\cong 20 percent).

NASA has sponsored programs at both HAC and Watkins Johnson to develop high efficiency X-band TWT's at the 20-watt level for the TOPS program. The Watkins Johnson tube was the WJ3703. Since Watkins Johnson has no contract on TOPS, they are continuing on company funds to complete the development by the end of 1973. They expect the tube to be 45 percent efficient and weigh 1 to 1-1/2 pounds. A Helios type power supply would be 80 to 85 percent efficient and weigh 1.36 to 1.81 kilograms (3 to 4 pounds).

The HAC tube developed for NASA was the 285H. HAC has indicated that the 285H has been tested to a JPL specification. This tube shows a nominal efficiency of 46 percent and a minimum efficiency of 44 percent.

ALL CONFIGURATIONS

To provide the required 6 watts at 8400 MHz, two options are considered most attractive. The first would be to use the TRW or MVM 1973 unit as a driver and mate the HAC 285H with a lightweight power supply (comparable to the Watkins Johnson Helios unit) to provide 20 watts (16 watts minimum after filtering) of output. This is a relatively low risk approach requiring only power supply modification and repackaging. For Atlas/Centaur, where the extra prime power is available, this approach would be acceptable. On the Thor/Delta, where prime power is very important, the TWT would be scaled down in power to 8 watts nominal. HAC has indicated that this should add about \$50,000 to their program.

Table 8.2-10 summarizes the pertinent characteristics for a 1-1/2-watt solid-state transmitter and an 8- and 16-watt TWTA using a solid-state driver.

Table 8.2-10. Transmitter Tradeoffs (High Power Outputs)

	SOLID STATE ⁽¹⁾	DRIVER PLUS TWTA ⁽²⁾	
		ATLAS/CENTAUR ORBITER	THOR DELTA ORBITER
INPUT FREQUENCY (MHZ)	95.625 (10F)	95.625 (10F)	95.625 (10F)
DRIVE POWER REQUIRED (DBM)	0 ± 1 DB	0 ± 1 DB	0 ± 1 DB
INPUT POWER (WATTS)	24	63	37
OUTPUT POWER (WATTS)	1.5 ⁽³⁾	16 ⁽⁴⁾	8 ⁽⁴⁾
MODULATION	NONE	NONE	NONE
WEIGHT (KG (LB))	1.1 (2.5)	4.3 (9.5) ⁽⁵⁾	3.9 (8.5) ⁽⁵⁾
DEVELOPMENT STATUS			
DRIVER	REDESIGN OF EXISTING UNIT ⁽⁶⁾		SEE APPENDIX 8D
TWTA		HAC TWT #285H HAS QUALIFIED TO JPL SPECIFICATION. POWER SUPPLY IS NEW LIGHTWEIGHT PACKAGE.	HAC TWT #285H MUST BE MODIFIED. POWER SUPPLY IS NEW LIGHTWEIGHT PACKAGE.
MODIFICATIONS REQUIRED	INCREASE S-BAND DRIVER POWER - MORE EFFICIENT MULTIPLIER	DRIVER AS DESCRIBED IN APPENDIX 8D - TWT AS IS - REPACKAGE POWER SUPPLY	DRIVER AS DESCRIBED IN APPENDIX 8D. SCALE TWT. REPACKAGE POWER SUPPLY.
COST PER UNIT			
SOLID STATE DRIVER, \$K ⁽⁶⁾	120	75	75
TWTA, \$K	---	250	283

⁽¹⁾ ALLOWS OPERATION TO 0.9 AU

⁽²⁾ ALLOWS OPERATION TO END OF MISSION - 254.32 GIGAMETERS (1.7 AU)

⁽³⁾ ALLOWS 1 DB FOR ISO FILTER, LIFE AND TEMPERATURE

⁽⁴⁾ ALLOWS 1 DB FOR FILTER AND LINE LOSS

⁽⁵⁾ EXISTING POWER SUPPLY FOR DSCS II WOULD ADD 20.91 METER (2 LB)

⁽⁶⁾ TABLE BASED ON REDESIGN OF TRW S-BAND TRANSMITTER

Low Power Output (Solid-State)

The DSN requires an X-band signal which is coherently related to the received S-band signal by a ratio of 880/221. Several methods of achieving this ratio were considered; all were constrained by the coherent drive signals available from the S-band receiver used in the baseline system, since only one receiver is used to drive both the S-band and the X-band transmitters. Three different approaches were studied in providing the X-band transmitter:

- If a new design is considered, it requires the development of a X11 multiplier, since 11 is a prime number in the 880 coherence term. High-order multipliers tend to have stability problems and may present severe filtering problems. Luckily, two approaches based on existing designs were found which removed the necessity for a new design. A completely new design was also not considered cost effective, since only one flight unit and a spare would probably be required.
- A second approach utilizes an existing unit produced by Motorola for the MVM 1973 program. Interface changes are necessary to allow its use with either the Viking Lander, Pioneers 10 and 11, or TRW microminiature receivers and transmitter drivers. No interface changes would be required if used with the Motorola receiver and driver. A list of pertinent characteristics for the Motorola MVM 1973 unit are given in Table 8.2-11. Figure 8.2-14 includes a block diagram of this X-band transmitter.
- A third approach utilizes a simple modification of a TRW S-band transmitter. A block diagram of the proposed transmitter as modified is given in Figure 8.2-14. By using a mixer to provide a coherent signal at 220 f, the requirement for a times 11 is removed. Only slight retuning of the power amplifiers (from 240 to 220 f) is required to allow their use as a driver for a balanced varactor quadrupler. The additional multiplier and an isofilter are packaged in one additional module in the modified transmitter. A list of pertinent characteristics for the TRW and Motorola X-band transmitters is given in Table 8.2-11.

No X-band transmitter has been selected at this time since it appears clear that either approach discussed will provide a usable system. A modification of the Philco-Ford S-band transmitter similar to that proposed for the TRW unit may also be attractive. TRW would propose to make a source selection for the X-band transmitter after firm cost proposals are received.

Ranging and X-band Performance

Ranging is a method for estimating the earth-spacecraft distance by measuring the delay of a signal transmitted to the spacecraft and transponded back to earth. This is normally accomplished with square-wave-modulated carrier signals which are coded in certain ways to resolve ambiguities in the range measurement. There are presently two types of planetary ranging codes used by the DSN, the so-called "Tau" and "Mu" codes which are described in some detail in the Telecommunications System Design Handbook (JPL Technical Memorandum 33-571). The major difference between the two systems is the time required to acquire the ranging code with probability 0.99. These times are given by JPL IOM 3300-73-70):

$$T_{ACQ} = \begin{cases} 1850 \frac{N_o}{P_R} & \text{for Tau ranging} \\ 75 \frac{N_o}{P_R} & \text{for Mu ranging} \end{cases} \quad (1)$$

where enough code components are chosen for a given range ambiguity, here 5000 kilometers. N_o is the receiver noise spectral density in watts/Hz, P_R is the ranging signal power in watts, and T_{ACQ} is in seconds.

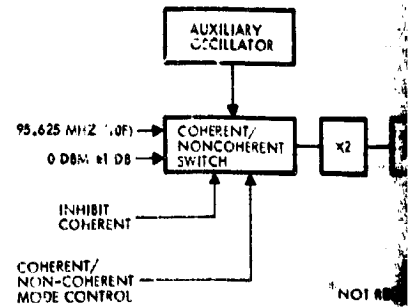
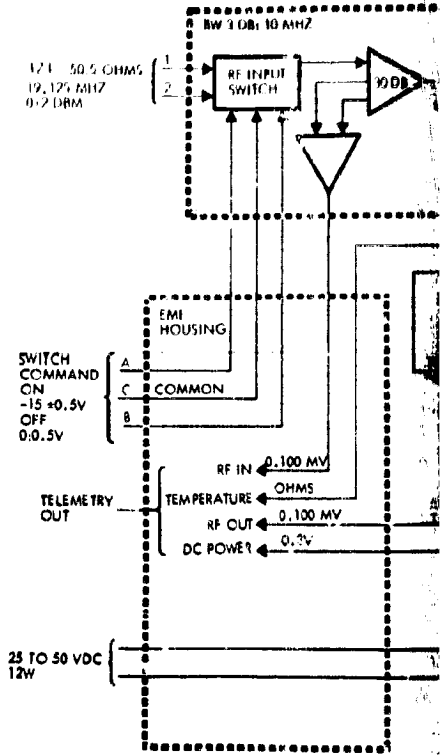
Recommended Thor/Delta Configuration (See Section 8.2.4.2).

Table 8.2-12 shows an uplink ranging design control table for the orbiter at the end of the mission. The ranging code is phase-modulated onto the uplink carrier, demodulated in the spacecraft ranging channel, limited, and remodulated onto the downlink carrier. Some budget parameters for the ranging channel were taken from the MVM 1973 Telecommunications Link Performance document (JPL 615-11, Revision A). The final parameter, ranging suppression, is the amount of ranging signal power in the squarewave plus noise output of a unit amplifier limiter.

The uplink assumes a 64-meter station with a 20-kW transmitter. Higher outputs, up to 400 kW, are available and could be used to reduce acquisition time. Table 8.2-13 shows the corresponding downlink design control table for ranging. The data subcarrier and ranging are phase

Table 8.2-11. X-Band Transmitter Tradeoffs

	MOTOROLA MVM 1973	TRW
INPUT FREQUENCY (MHZ)	19.125 (2f)	95.625 (10f)
DRIVE POWER REQUIRED	0 DBM +2 DB	0 DBM +1 DB
INPUT POWER (WATTS)	12 W	10 W
OUTPUT FREQUENCY (MHZ)	8415 (860f)	8415 (880f)
OUTPUT POWER (WATTS)	0.2 MINIMUM	0.2 MINIMUM
MODULATION	LINEAR PM (NOT REQUIRED)	NOT REQUIRED
SIZE (IN.)	2 x 6.9 x 8	1.52 x 4.52 x 4.53
WEIGHT KG (LB)	1.8 (4)	0.9 (2)
EMI (DB)		
HARMONICS OF 19.125 MHZ	-30	-40
SPURIOUS	-50	-60
POTENTIAL INTERFERENCE (221f)	POWER AMPLIFIER AT 176f	POWER AMPLIFIER AT 220f
DEVELOPMENT STATUS	QUALIFIED	MODIFICATION OF TRANSMITTER TO BE QUALIFIED FOR DSP
COST (\$K)	250	150
	1 FLIGHT	1 FLIGHT
	1 SPARE (JPL TYPE PROGRAM)	1 SPARE
RECEIVER MODIFICATIONS REQUIRED		
MOTOROLA (MICROMIN)	N/A	ADD X5 TO TRANSMITTER
MOTOROLA (STANDARD)	NONE	ADD X5 TO TRANSMITTER
PHILCO FORD (MICROMIN)	ADD BUFFER AMPLIFIER TO RECEIVER AND PROVIDE VCO OUTPUT AT 2f	ADD BUFFER AMPLIFIER TO RECEIVER AND PROVIDE VCO OUTPUT AT 2f. ADD X5 TO TRANSMITTER
TRW (MICROMIN)	ADD BUFFER AMPLIFIER TO RECEIVER AND PROVIDE VCO AT 2f	NONE
TRW (PIONEERS 10 AND 11)	ADD BUFFER AMPLIFIER TO RECEIVER AND PROVIDE VCO OUTPUT AT 2f.	ADD BUFFER AMPLIFIER TO RECEIVER AND PROVIDE VCO OUTPUT AT 2f. ADD X5 TO TRANSMITTER



FOLDOUT FRAME

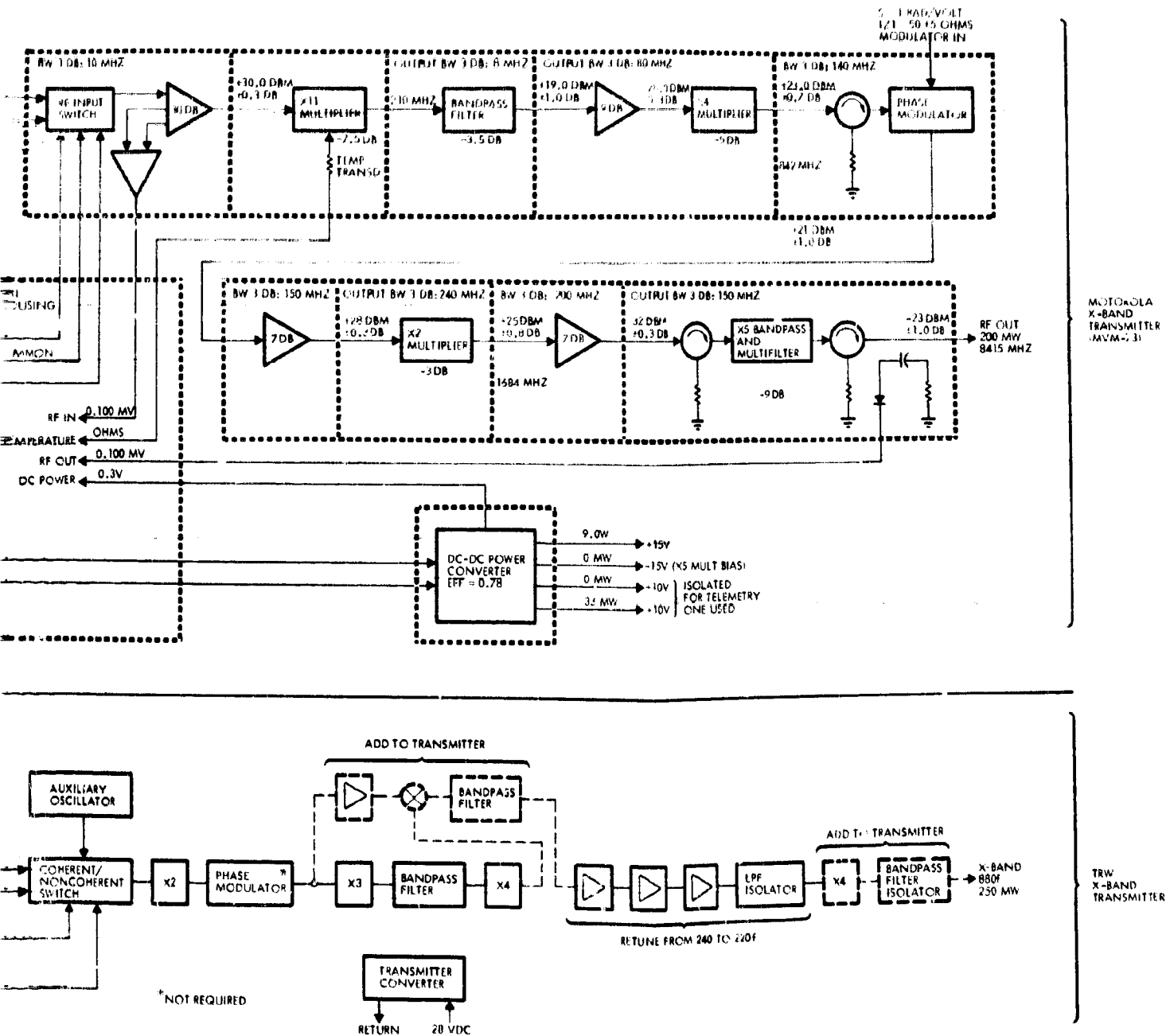


Figure 8.2-14. X-Band Transmitter Block Diagrams

Table 8.2-13.

Table 8.2-12. Uplink Ranging, Recommended Thor/Delta Orbiter

NO.	PARAMETER	NOMINAL	ADVERSE	NOTES
1	FREQUENCY (MHZ)	2115	-	-
2	RANGE [GIGAMETER (AU)]	254.32 (1.7)	-	-
3	TRANSMITTER POWER (DBM)	73.0	0	20 KW
4	TRANSMITTER ANTENNA GAIN (DB)	60.6	0.7	64 METER
5	SPACE LOSS (DB)	-267.1	-	-
6	RECEIVER ANTENNA GAIN (DB)	3.5	0.3	UPLINK FANSCAN
7	POINTING LOSS (DB)	-0.6	0.2	0.017 RAD (-1 DEG) POINTING ERROR
8	POLARIZATION LOSS (DB)	-0.1	0.1	0.17 RAD (10 DEG) OFFSET LINEAR
9	RECEIVER CIRCUIT LOSS (DB)	-1.3	0.2	-
10	TOTAL RECEIVED POWER (DBM) (3+4+5+6+7+8+9)	-132.0	-	-
11	RECEIVER NOISE SPECTRAL DENSITY (DBM/HZ)	-169.0	1.0	$T_{SYS} = 15.9$ RAD (910 DEG) K; NF = 6 DB
12	P_T/N_O (DB-HZ) (10-11)	37.0	1.3	RSS TOLERANCE
<u>CARRIER TRACKING PERFORMANCE</u>				
13	CARRIER MODULATION LOSS (DB)	-11.5	0.7	1.3 RAD
14	THRESHOLD LOOP BANDWIDTH (DB-HZ)	13.0	1.0	20 HZ LOOP
15	LOOP SNR (DB) (12+13-14)	12.5	-	-
16	REQUIRED LOOP SNR + LIMITER LOSS (DB)	6.3	-	LIM LOSS = -0.3 DB
17	PERFORMANCE MARGIN (DB) (15-16)	6.2	1.8	RSS TOLERANCE
<u>RANGING CHANNEL PERFORMANCE</u>				
18	RANGING MODULATION LOSS (DB)	-0.3	0.1	1.3 RAD
19	RANGING BANDWIDTH (DB-HZ)	61.8	0.8	1.5 MHZ
20	SNR AT LIMITER INPUT (DB) (12+18-19)	-25.1	1.5	RSS TOLERANCE
21	RANGING SUPPRESSION (DB)	-21.1	-	615-11 (JPL)

NO.	
1	FREQUENCY (MHZ)
2	RANGE [GIGAMETER (AU)]
3	TRANSMITTER POWER (DBM)
4	TRANSMITTER ANTENNA GAIN (DB)
5	SPACE LOSS (DB)
6	POINTING LOSS (DB)
7	POLARIZATION LOSS (DB)
8	SPACE LOSS (DB)
9	RECEIVER ANTENNA GAIN (DB)
10	TOTAL RECEIVED POWER (DBM)
11	RECEIVER NOISE SPECTRAL DENSITY (DBM/HZ)
12	P_T/N_O (DB-HZ)
<u>CARRIER TRACKING PERFORMANCE</u>	
13	CARRIER MODULATION LOSS (DB)
14	THRESHOLD LOOP BANDWIDTH (DB-HZ)
15	LOOP SNR (DB)
16	REQUIRED LOOP SNR + LIMITER LOSS (DB)
17	PERFORMANCE MARGIN (DB)
<u>DATA CHANNEL PERFORMANCE</u>	
18	DATA MODULATION LOSS (DB)
19	DATA BIT RATE (KBPS)
20	RECEIVER LOSS (DB)
21	E_b/N_O (DB) (12+18-19)
22	REQUIRED E_b/N_O (DB)
23	PERFORMANCE MARGIN (DB)
<u>RANGING CHANNEL PERFORMANCE</u>	
24	RANGING MODULATION LOSS (DB)
25	TOTAL RANGING MODULATION LOSS (DB)
26	P_R/N_O (DB-HZ)

Table 8.2-13. Downlink Ranging, Recommended Thor/Delta Orbiter

NO.	PARAMETER	NOMINAL	ADVERSE	NOTES
1	FREQUENCY (MHZ)	2300	-	-
2	RANGE [GIGAMETER (AU)]	254.32 (1.7)	-	-
3	TRANSMITTER POWER (DBM)	45.2	0.3	33-WATT NOMINAL (31-WATT ADVERSE)
4	TRANSMITTER CIRCUIT LOSS (DB)	-0.5	0.1	-
5	TRANSMITTER ANTENNA GAIN (DB)	11.0	0.3	FANBEAM
6	POINTING LOSS (DB)	-0.3	0.2	-
7	POLARIZATION LOSS (DB)	-0.1	0.0	0.17 RAD (10 DEG) OFFSET LINEAR
8	SPACE LOSS (DB)	-267.8	-	-
9	RECEIVER ANTENNA GAIN (DB)	61.6	0.4	64 METER (0.1 DB LOSS AT 0.35 RAD (20 DEG) ELEVATION)
10	TOTAL RECEIVED POWER (DBM) (3+4+5+6+7+8+9)	-150.9	-	-
11	RECEIVER NOISE SPECTRAL DENSITY (DBM/HZ)	-184.0	0.6	0.51 RAD (29 DEG) K; 0.35 RAD (20 DEG) ELEVATION
12	P_T/N_O (DB-HZ) (10-11)	33.1	0.8	RSS TOLERANCE
<u>CARRIER TRACKING PERFORMANCE</u>				
13	CARRIER MODULATION LOSS (DB)	-8.8	2.5	$\theta_D = 1.15$; $\theta_R = 0.46$ RAD
14	THRESHOLD LOOP BANDWIDTH (DB-HZ)	10.0	0.4	10 HZ LOOP
15	LOOP SNR (DB) (12+13-14)	14.3	-	-
16	REQUIRED LOOP SNR (DB)	10.0	-	-
17	PERFORMANCE MARGIN (DB) (15-16)	4.3	2.7	RSS TOLERANCE
<u>DATA CHANNEL PERFORMANCE</u>				
18	DATA MODULATION LOSS (DB)	-8.6	0.8	$\theta_D = 1.15$ RAD; $\theta_R = 0.46$ RAD
19	DATA BIT RATE (DB-BITS/S)	24.1	-	256
20	RECEIVER LOSS (DB)	-2.7	0.5	-
21	E_b/N_O (DB) (12+18-19+20)	4.5	-	-
22	REQUIRED E_b/N_O (DB)	3.0	-	10^{-3} DELETION RATE
23	PERFORMANCE MARGIN (DB) (21-22)	1.5	1.3	RSS TOLERANCE
<u>RANGING CHANNEL PERFORMANCE</u>				
24	RANGING MODULATION LOSS (DB)	-14.7	3.1	$\theta_D = 1.15$ RAD; $\theta_R = 0.46$ RAD
25	TOTAL RANGING LOSS (DB) (21 UL + 24)	-41.8	1.5	-
26	P_R/N_O (DB-HZ) (12+25)	-8.7	3.4	RSS TOLERANCE

FOLDOUT FRAME

modulated on the downlink carrier at 1.15 and 0.46 radian, respectively. In the ranging channel the total loss is the sum of the modulation loss and the uplink ranging suppression. Figure 8.2-15 shows acquisition times versus spacecraft range for each ranging code for the 64-meter DSS. The Mark I ranging for the 26-meter subnet could provide ranging to 2 million kilometers (0.012 AU) early in the mission, but would be replaced by the 64-meter DSN for the remainder of the mission.

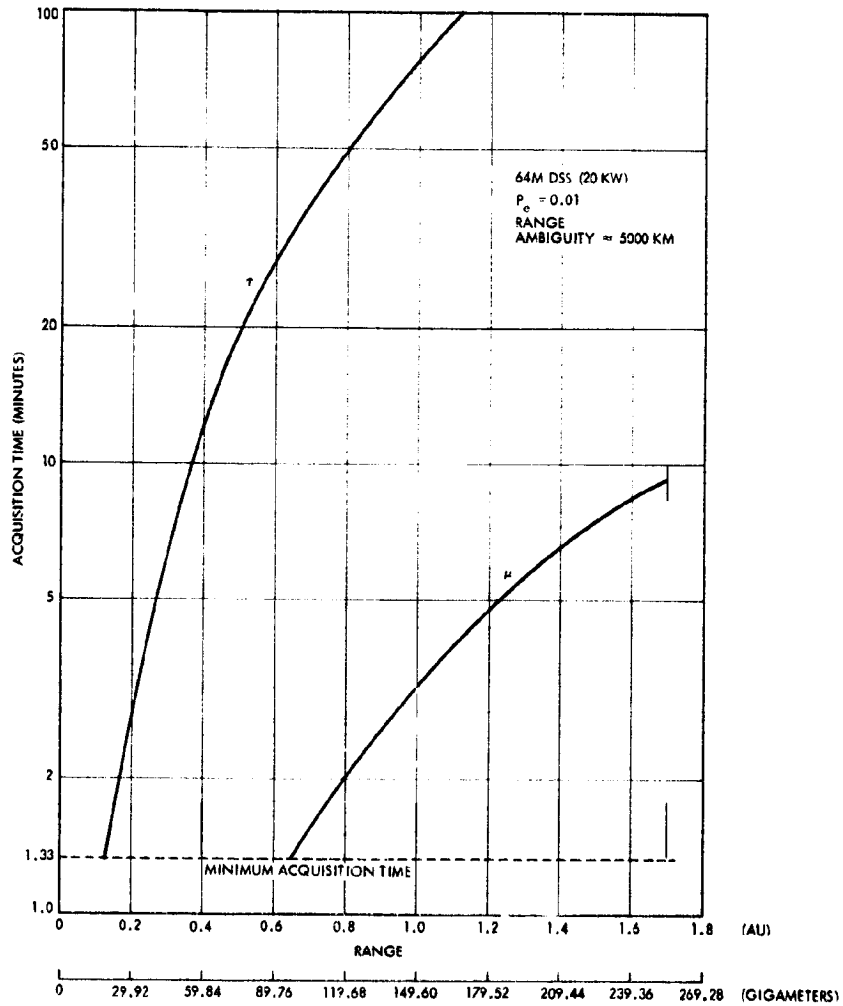


Figure 8.2-15. Range Acquisition Time versus Range (Preferred Thor/Delta Orbiter)

An X-band design control table for the orbiter at the end-of-mission is shown in Table 8.2-14. Assuming a separate X-band fanbeam antenna with a 11 dB of gain, a spacecraft transmitter power greater than 6 watts

Table 8.2-14. X-Band Downlink

NO.	PARAMETER	NOMINAL	ADVERSE	NOTES
1	FREQUENCY (MHZ)	8400	-	-
2	RANGE GIGAMETER (AU)	254.32 (1.7)	-	END-OF-MISSION
3	TRANSMITTER POWER (DBM)	43.0	0.5	20-WATT TWTA
4	TRANSMITTER CIRCUIT LOSS (DB)	-1.0	0.2	-
5	TRANSMITTER ANTENNA GAIN (DB)	11.0	0.3	FANBEAM
6	POINTING LOSS (DB)	-0.3	0.2	-
7	ATMOSPHERIC LOSS (DB)	-0.2	0.4	0.52 RAD (30 DEG) ELEVATION NOMINAL [0.17 RAD (10 DEG) ADVERSE]
8	SPACE LOSS (DB)	-279.0	0.0	-
9	RECEIVER ANTENNA GAIN (DB)	71.6	0.3	0.4 METER, 0.52 RAD (30 DEG) ELEVATION; 30 MPH WIND
10	TOTAL RECEIVED POWER (DBM) (3+4+5+6+7+8+9)	-154.9	-	-
11	RECEIVER NOISE SPECTRAL DENSITY (DBM, HZ)	-182.7	2.3	0.52 RAD (30 DEG) ELEVATION, 39°K NOMINAL, 66°K ADVERSE
12	$P_f N_o$ (DB-HZ) (10-11)	27.8	2.4	RSS TOLERANCE
<u>CARRIER TRACKING PERFORMANCE</u>				
13	CARRIER MODULATION LOSS (DB)	0.0	0.0	NO MODULATION
14	THRESHOLD LOOP BANDWIDTH (DB-HZ)	10.0	0.4	10 HZ LOOP
15	LOOP SNR (DB) (12+13-14)	17.8	-	-
16	REQUIRED LOOP SNR (DB)	10.0	-	-
17	PERFORMANCE MARGIN (DB) (15-16)	7.8	2.5	RSS TOLERANCE

is needed for the carrier margin to exceed the adverse tolerance. If 20 watts of output power is assumed, the X-band system can operate out to 1.7 AU with the carrier margin about 5 dB in excess of the tolerance. A plot of excess margin versus range is given in Figure 8.2-16. One to two watts is the approximate state-of-the-art in solid-state X-band amplifiers; therefore, a TWTA is required. A 10-watt TWTA would be sufficient to 254.32 gigameters (1.7 AU) with about 2 dB margin, but a 20-watt off-the-shelf TWTA is chosen as baseline on the basis of cost (no development cost). Note that the plot of margin versus range in Figure 8.2-16 is for a 20-watt TWTA.

Preferred Atlas/Centaur Configuration

Prior to the Version IV update of the science payload definition, the recommended Thor/Delta and the preferred Atlas/Centaur subsystems were essentially the same and were based on a spacecraft configuration whose spin axis was perpendicular to the earth line. Version IV changed the Atlas/Centaur spacecraft configuration to earth-pointing (spin axis parallel to the earth line).

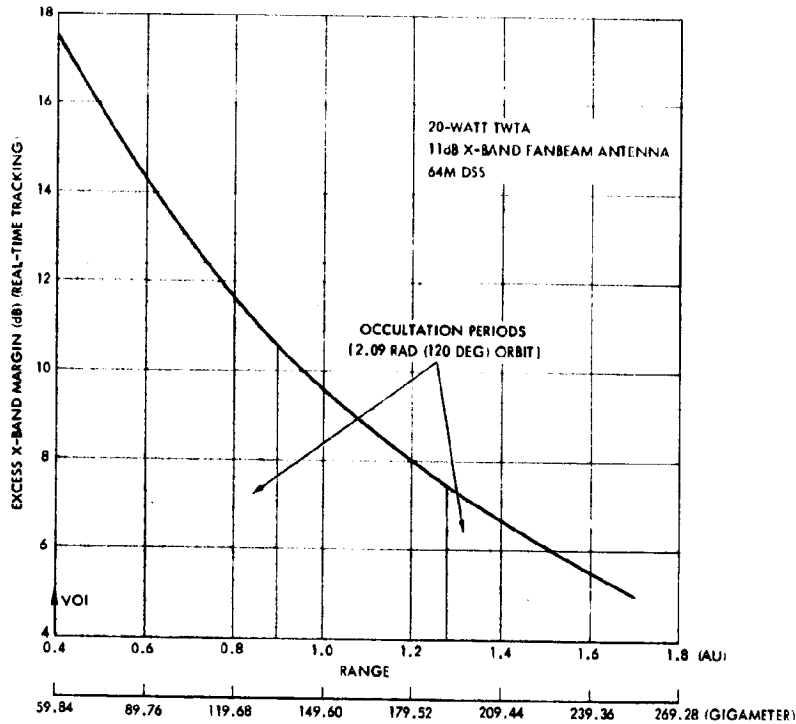


Figure 8.2-16. X-Band Margin versus Range (Preferred Thor/Delta Orbiter)

Tables 8.2-15 and -16 present the ranging design control tables at end-of-mission with the 64-meter network. The acquisition times are not plotted, since the calculated numbers using Equation (1) above are below the 80-second minimum quoted in JPL IOM 3300-73-70. The signal-to-noise ratios are much higher, since the antenna gains are higher than for the recommended Thor/Delta configuration.

The X-band transmitter output power can be reduced (also reducing cost) over the Thor/Delta version for real time tracking to 254.32 gigameters (1.7 AU). The 200 mW MVM 1973 unit would be sufficient with a 1.52-meter (5-foot) X-band dish (utilizing a dual S- and X-band feed design) since greater than 35 dBi gain is available. The margins would exceed those shown in Figure 8.2-16 for a 20-watt TWTA and an 11 dB fanbeam antenna.

8.2.4 Preferred Subsystem Description  

This section describes the preferred Atlas/Centaur communication subsystems based on the Version IV science payload and the 1978 probe mission launch.

Both the probe bus and the orbiter are based on the preferred spacecraft configuration — earth pointing. The main communication modes are therefore designed around antennas pointing along the spacecraft spin axis.

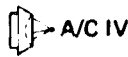
8.2.4.1 Probe Bus A/C IV

The block diagram for the probe bus, Figure 8.2-17, shows a redundant set of transponders and a redundant set of 6-watt solid-state power amplifiers connected through switches and diplexers to an aft omni, forward omni, and aft-pointing horn. Maximum reliability and minimum cost is reflected in this configuration in that all equipment except the power amplifiers has been flight-proven. Similar 6-watt amplifiers of slightly less efficiency have been designed and built by Microwave Semiconductors Corporation (MSC) and qualified and space flown by Teledyne.

The transponders selected for the baseline are residual Pioneers 10 and 11 units (two flight spares and two prototypes which will be upgraded). The forward omni, switches, diplexers, and aft medium-gain horn are also identical to Pioneers 10 and 11 hardware and the aft omni is a Defense Support Program (DSP) unit. The Pioneer horn was chosen to provide the minimum 13 dBi gain requirement at 0.21 radian (12 degrees) off-axis pointing. This angle for bus entry is required by the science instruments for the new 1978 baseline bus targeting. The gain of the horn [13.5 dBi at 0.21 radian (12 degrees)] and the 6-watt transmitter provide an entry EIRP of 49.9 dBm (including 0.1 dB polarization loss), sufficient to provide 1024 bits/s with the 64-meter station.

The 6-watt solid-state power amplifier was chosen over residual Pioneers 10 and 11 TWTA's on the basis of cost. Knowing that there are only enough residual TWTA's for the bus, 6-watt solid-state units would have to be procured for the orbiter (or vice versa). Preliminary estimates show that it would be less expensive to procure two extra 6-watt units for the bus (and have commonality with the orbiter for integration, test, and spares) than it would be to refurbish the TWTA's to provide two flight units plus a spare as a minimum. On the other hand, on the basis of cost, the Pioneers 10 and 11 residual receivers and transmitter drivers were chosen over the procurement of extra transponders for the orbiter

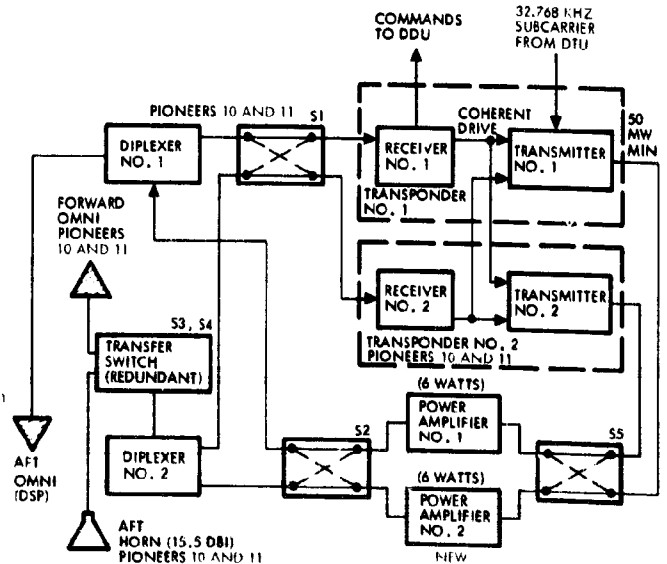
Table 8.2-15. Uplink Ranging, Preferred Atlas/Centaur Orbiter



NO.	PARAMETER	NOMINAL	ADVERSE	NOTES
1	FREQUENCY (MHZ)	2115	-	-
2	RANGE (GIGAMETER (AU))	254.32 (1.7)	-	-
3	TRANSMITTER POWER (DBM)	73	0	20 KW
4	TRANSMITTER ANTENNA GAIN (DB)	60.6	0.7	64 METER
5	SPACE LOSS (DB)	-267.1	0	254.32 GIGAMETERS (1.7 AU)
6	RECEIVER ANTENNA GAIN (DB)	27.5	0.5	1.52 METER DISH
7	POINTING LOSS (DB)	-2.3	0.2	CONSCAN (1 DB) + (1 DEG) POINTING ERROR
8	POLARIZATION LOSS (DB)	-0.2	0.1	-
9	RECEIVER CIRCUIT LOSS (DB)	-1.9	0.2	-
10	TOTAL RECEIVED POWER (DBM) (3+4+5+6+7+8+9)	-110.4	-	-
11	RECEIVER NOISE SPECTRAL DENSITY (DBM/HZ)	-169.0	1.0	$T_{SYS} = 910^{\circ}K$; NF = 6 DB
12	P_r/N_o (DB-HZ) (10-11)	58.6	1.4	RSS TOLERANCE
<u>CARRIER TRACKING PERFORMANCE</u>				
13	CARRIER MODULATION LOSS (DB)	-11.5	0.7	1.3 RAD
14	THRESHOLD LOOP BANDWIDTH	13.0	1.0	20 HZ LOOP
15	LOOP SNR (DB) (13+14)	34.1	-	-
16	REQUIRED LOOP SNR + LIMITER LOSS (DB)	6.3	0	LIM LOSS = -0.3 DB
17	PERFORMANCE MARGIN (DB) (15-16)	27.8	1.8	RSS TOLERANCE
<u>RANGING CHANNEL PERFORMANCE</u>				
18	RANGING MODULATION LOSS (DB)	-0.3	0.1	1.3 RAD
19	RANGING BANDWIDTH (DB-HZ)	61.8	0.8	1.5 MHZ
20	SNR AT LIMITER INPUT (DB) (12+18-19)	-3.5	1.6	RSS TOLERANCE
21	RANGING SUPPRESSION (DB)	-6.0	1.6	-



Figure 8.2-17. Atlas Centaur Probe Bus Communications Subsystem Block Diagram



NOTES

TER

GIGAMETERS (1.7 AU)

METER DISH

CAN (1 DB) + (1 DEG) POINTING ERROR

$T = 910^{\circ}K$; $NF = 6$ DB

TOLERANCE

AD

LOOP

LOSS = -0.3 DB

TOLERANCE

AD

AHZ

TOLERANCE



Table 8.2-16. Downlink Ranging, Preferred Atlas/Centaur Orbiter

NO.	PARAMETER	NOMINAL	ADVERSE	NOTES
1	FREQUENCY (MHZ)	2300	-	-
2	RANGE (GIGAMETERS (AU))	254.32 (1.7)	-	END-OF-MISSION
3	TRANSMITTER POWER (DBM)	37.8	0.	6 WATTS NOMINAL
4	TRANSMITTER CIRCUIT LOSS (DB)	-1.4	0.1	-
5	TRANSMITTER ANTENNA GAIN (DB)	28.0	0.5	1.52 METER (5 FT) DISH
6	POINTING LOSS (DB)	-2.8	0.3	CONSCAN LOSS PLUS 1 PERCENT ATTITUDE ERROR
7	POLARIZATION LOSS (DB)	-0.1	0.1	-
8	SPACE LOSS (DB)	-267.8	0	254.32 GIGAMETERS (1.7 AU)
9	RECEIVER ANTENNA GAIN (DB)	61.6	0.4	64 METER (0.1 DB LOSS AT 20 DEG ELEVATION)
10	TOTAL RECEIVED POWER (DBM) (3+4+5+6+7+8+9)	-144.7	0.8	RSS TOLERANCES
11	RECEIVER NOISE SPECTRAL DENSITY (DBM/HZ)	-184.0	0.6	29 ^o K AT 20 DEG ELEVATION
12	P_T/N_O (DB-HZ) (10-11)	39.3	1.0	RSS TOLERANCES
<u>CARRIER TRACKING PERFORMANCE</u>				
13	CARRIER MODULATION LOSS (DB)	-6.7	1.8	$\sigma_D = 1.05 \pm 10\%$ RAD; $\sigma_R = 0.37 \pm 10\%$ RAD
14	THRESHOLD LOOP BANDWIDTH (DB-HZ)	10.0	0.4	10 HZ LOOP
15	LOOP SNR (DB) (12+13-14)	22.6	2.1	RSS TOLERANCES
16	REQUIRED LOOP SNR (DB)	10.0	0	RECOMMENDED 810-5
17	PERFORMANCE MARGIN (DB) (15-16)	12.6	2.1	RSS TOLERANCES
<u>DATA CHANNEL PERFORMANCE</u>				
18	DATA MODULATION LOSS (DB)	-1.8	0.7	$\sigma_D = 1.05 \pm 10\%$ RAD; $\sigma_R = 0.37 \pm 10\%$ RAD
19	DATA BIT RATE (DB-BITS/S)	30.1	0	1024 BITS/S
20	RECEIVER LOSS (DB)	-1.3	0.5	ESTIMATED FROM NASA/ARC DATA
21	E_B/N_O (DB) (12+18-19+20)	6.1	1.3	RSS TOLERANCES
22	REQUIRED E_B/N_O (DB)	3.6	0	10 ⁻³ FRAME DETECTION
23	PERFORMANCE MARGIN (DB) (21-22)	2.5	1.3	RSS TOLERANCES
<u>RANGING CHANNEL PERFORMANCE</u>				
24	RANGING MODULATION LOSS (DB)	-14.9	2.7	$\sigma_D = 1.05 \pm 10\%$ RAD; $\sigma_R = 0.37 \pm 10\%$ RAD
25	TOTAL RANGING LOSS (DB) (21 UL + 24)	-20.9	3.1	RSS TOLERANCES
26	P_R/N_O (DB-HZ) (12 + 25)	18.4	3.3	RSS TOLERANCES

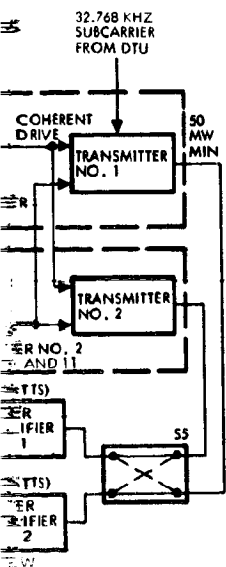


Table 8.2-17. Probe Release (64-Meter)

NO.	PARAMETER	NOMINAL	ADVERSE	NOTES
1	FREQUENCY (MHZ)	2300	0	
2	RANGE [GIGAMETERS (AU)]	50.86 (0.34)	-	E-11 DAYS (LAST RETARGET)
3	TRANSMITTER POWER (DBM)	37.8	0.4	6 WATTS NOMINAL
4	TRANSMITTER CIRCUIT LOSS (DB)	-1.3	0.1	
5	TRANSMITTER ANTENNA GAIN (DB)	-1.0	1.0	OMNI COVERAGE
6	POINTING LOSS (DB)	0	-	
7	POLARIZATION LOSS (DB)	-0.2	0.1	
8	SPACE LOSS (DB)	-253.8	-	50.86 GIGAMETERS (0.34 AU)
9	RECEIVER ANTENNA GAIN (DB)	61.6	0.4	64-METER [0.1 DB LOSS AT 0.35 RAD (20 DEG) ELEVATION]
10	TOTAL RECEIVED POWER (DBM) (3+4+5+6+7+8+9)	-156.9	1.2	
11	RECEIVER NOISE SPECTRAL DENSITY (DBM/HZ)	-184.0	1.0	29°K AT 20 DEG ELEVATION [0.26 RAD (15 DEG) ELEVATION ADVERSE]
12	P_T/N_O (DB-HZ) (10-11)	27.1	1.5	
<u>CARRIER TRACKING PERFORMANCE</u>				
13	CARRIER MODULATION LOSS (DB)	-4.1	1.1	$0.9 \pm 10\%$ RAD
14	THRESHOLD LOOP BANDWIDTH (DB-HZ)	10.0	0.4	$2 B_{LO} = 10 \text{ HZ} \pm 10\%$
15	LOOP SNR (DB) (12+13-14)	13.0	1.9	RSS TOLERANCES
16	REQUIRED LOOP SNR (DB)	10.0	0	RECOMMENDED 810-5
17	PERFORMANCE MARGIN (DB) (15-16)	3.0	1.9	RSS TOLERANCES
<u>DATA CHANNEL PERFORMANCE</u>				
18	DATA MODULATION LOSS (DB)	-2.1	0.7	$0.9 \pm 10\%$ RAD
19	DATA BIT RATE (DB-BITS/S)	15.0	-	32 BITS/S
20	RECEIVER LOSS (DB)	-4.1	0.5	ESTIMATED FROM NASA/ARC DATA
21	E_b/N_O (DB) (12+18-19+20)	5.9	1.7	RSS TOLERANCES
22	REQUIRED E_b/N_O (DB)	2.5	0	10^{-3} FRAME DELETION RATE
23	PERFORMANCE MARGIN (DB) (21-22)	3.4	1.7	RSS TOLERANCES

Table 8.2-18.

NO.	PARAMETER
1	FREQUENCY (MHZ)
2	RANGE [GIGAMETERS (AU)]
3	TRANSMITTER POWER (DBM)
4	TRANSMITTER CIRCUIT LOSS (DB)
5	TRANSMITTER ANTENNA GAIN (DB)
6	POINTING LOSS (DB)
7	POLARIZATION LOSS (DB)
8	SPACE LOSS (DB)
9	RECEIVER ANTENNA GAIN (DB)
10	TOTAL RECEIVED POWER (DBM) (3+4+5+6+7+8+9)
11	RECEIVER NOISE SPECTRAL DENSITY (DBM/HZ)
12	P_T/N_O (DB-HZ) (10-11)
<u>CARRIER TRACKING PERFORMANCE</u>	
13	CARRIER MODULATION LOSS (DB)
14	THRESHOLD LOOP BANDWIDTH (DB-HZ)
15	LOOP SNR (DB) (12+13-14)
16	REQUIRED LOOP SNR (DB)
17	PERFORMANCE MARGIN (DB) (15-16)
<u>DATA CHANNEL PERFORMANCE</u>	
18	DATA MODULATION LOSS (DB)
19	DATA BIT RATE (DB-BITS/S)
20	RECEIVER LOSS (DB)
21	E_b/N_O (DB) (12+18-19+20)
22	REQUIRED E_b/N_O (DB)
23	PERFORMANCE MARGIN (DB) (21-22)

Table 8.2-18. Bus Pre-Entry (26-Meter)

PARAMETER	NOMINAL	ADVERSE	NOTE
FREQUENCY (MHZ)	2300	-	
RANGE (GIGAMETERS (AU))	64.33 (0.43)	-	17 DECEMBER 1978 ENTRY
TRANSMITTER POWER (DBM)	37.8	0.4	6 WATTS NOMINAL
TRANSMITTER CIRCUIT LOSS (DB)	-1.3	0.2	
TRANSMITTER ANTENNA GAIN (DB)	15.5	0.3	PEAK GAIN
SPACE LOSS (DB)	-2.0	0.5	0.21 RAD (12 DEG) NOMINAL, 0.23 RAD (13 DEG) ADVERSE
POINTING LOSS (DB)	-0.1	0.1	
RECEIVER ANTENNA GAIN (DB)	-255.8	0	64.33 GIGAMETERS (0.43 AU)
RECEIVED POWER (DBM) (3+4+5+6+7+8+9)	152.6	0.9	26-METER
RECEIVER NOISE SPECTRAL DENSITY (DBM/HZ)	-181.9	0.9	RSS TOLERANCES
RECEIVED SIGNAL (10-11)	29.3	1.3	47°K AT 0.26 RAD (15 DEG) ELEVATION [0.17 RAD (10 DEG) ELEVATION ADVERSE]
CARRIER TRACKING PERFORMANCE			
CARRIER MODULATION LOSS (DB)	-4.1	1.1	0.9 ± 10% RAD
THRESHOLD LOOP BANDWIDTH (DB-HZ)	10.3	0.5	28 _{LO} = 10.8 ± 10% RAD
LOOP SNR (DB) (12+13-14)	14.9	1.8	RSS TOLERANCES
REQUIRED LOOP SNR (DB)	10.0	0.0	RECOMMENDED 810-5
PERFORMANCE MARGIN (DB) (15-16)	4.9	1.8	RSS TOLERANCES
DATA CHANNEL PERFORMANCE			
DATA MODULATION LOSS (DB)	-2.1	0.6	0.9 ± 10% RAD
DATA BIT RATE (DB-BITS/S)	18.1	0	64 BITS/S
RECEIVER LOSS + DOPPLER LOSS (0.1 DB)	-4.8	0.5	FROM NASA/ARC DATA
REQUIRED LOOP SNR (DB) (12+13-14)	4.2	1.5	RSS TOLERANCES
REQUIRED LOOP SNR (DB)	2.7	0	10 ⁻³ FRAME DELETION RATE
PERFORMANCE MARGIN (DB) (21-22)	1.6	1.5	RSS TOLERANCES

Table 8.2-19. Bus Entry

NO.	PARAMETER	NOMINAL	ADVERSE
1	FREQUENCY (MHZ)	2300	
2	RANGE [GIGAMETERS (AU)]	64.33 (0.43)	
3	TRANSMITTER POWER (DBM)	37.8	
4	TRANSMITTER CIRCUIT LOSS (DB)	-1.3	
5	TRANSMITTER ANTENNA GAIN (DB)	15.5	
6	POINTING LOSS (DB)	-2.0	
7	POLARIZATION LOSS (DB)	-0.1	
8	SPACE LOSS (DB)	-255.8	
9	RECEIVER ANTENNA GAIN (DB)	61.6	
10	TOTAL RECEIVED POWER (DBM) (3+4+5+6+7+8+9)	144.3	
11	RECEIVER NOISE SPECTRAL DENSITY (DBM/HZ)	-184.0	
12	P_r/N_o (DB-HZ) (10-11)	39.7	
<u>CARRIER TRACKING PERFORMANCE</u>			
13	CARRIER MODULATION LOSS (DB)	-4.1	
14	THRESHOLD LOOP BANDWIDTH (DB-HZ)	10.0	
15	LOOP SNR (DB) (12+13-14)	25.6	
16	REQUIRED LOOP SNR (DB)	10.0	
17	PERFORMANCE MARGIN (DB) (15-16)	15.6	
<u>DATA CHANNEL PERFORMANCE</u>			
18	DATA MODULATION LOSS (DB)	-2.1	
19	DATA BIT RATE (DB-BITS/S)	30.1	
20	RECEIVER LOSS + DOPPLER LOSS (0.1 DB)	-1.4	
21	E_b/N_o (DB) (12+18-19+20)	6.1	
22	REQUIRED E_b/N_o (DB)	3.6	
23	PERFORMANCE MARGIN (DB) (21-22)	2.5	

10-11-78

Table 8.2-19. Bus Entry (64-Meter)

PARAMETER	NOMINAL	ADVERSE	NOTES
FREQUENCY (MHZ)	2300	-	
RANGE (GIGAMETERS (AU))	64.33 (0.43)	-	17 DECEMBER 1978 ENTRY
TRANSMITTER POWER (DBM)	37.8	0.4	6 WATTS NOMINAL
TRANSMITTER CIRCUIT LOSS (DB)	-1.3	0.2	
TRANSMITTER ANTENNA GAIN (DB)	15.5	0.3	PEAK GAIN
POINTING LOSS (DB)	-2.0	0.5	0.21 RAD (12 DEG) NOMINAL, 0.23 RAD (13 DEG) ADVERSE
POLARIZATION LOSS (DB)	-0.1	0.1	
SPACE LOSS (DB)	-255.8	-	64.33 GIGAMETERS (0.43 AU)
RECEIVER ANTENNA GAIN (DB)	61.6	0.4	64-METER (0.1 DB LOSS AT 0.26 RAD (20 DEG) ELEVATION)
TOTAL RECEIVED POWER (DBM) (3+4+5+6+7+8+9)	144.3	0.8	RSS TOLERANCES
RECEIVER NOISE SPECTRAL DENSITY (DBM/HZ)	-184.0	1.0	29°K AT 0.35 RAD (20 DEG) ELEVATION [0.26 RAD (15 DEG) ELEVATION ADVERSE]
P_r/N_o (DB-HZ) (10-11)	39.7	1.3	RSS TOLERANCES
<u>CARRIER TRACKING PERFORMANCE</u>			
CARRIER MODULATION LOSS (DB)	-4.1	1.1	0.9 RAD ± 10%
THRESHOLD LOOP BANDWIDTH (DB-HZ)	10.0	0.4	$2 B_{LO} = 10$ HZ
LOOP SNR (DB) (12+13-14)	25.6	1.7	RSS TOLERANCES
REQUIRED LOOP SNR (DB)	10.0	0	RECOMMENDED 810-5
PERFORMANCE MARGIN (DB) (15-16)	15.6	1.7	RSS TOLERANCES
<u>DATA CHANNEL PERFORMANCE</u>			
DATA MODULATION LOSS (DB)	-2.1	0.7	0.9 RAD ± 10%
DATA BIT RATE (DB-BITS/S)	30.1	-	1024 BITS/S
RECEIVER LOSS + DOPPLER LOSS (0.1 DB)	-1.4	0.6	FROM NASA/ARC AT 17 DB SNR
E_b/N_o (DB) (12+18-19+20)	6.1	1.6	
REQUIRED E_b/N_o (DB)	3.6	0	10^{-3} FRAME DELETION RATE
PERFORMANCE MARGIN (DB) (21-22)	2.5	1.6	RSS TOLERANCES

FOLDOUT FRAME

since the refurbishment cost will be much less than extra new transponder costs.

Telemetry Mission Profile

Figure 8.2-18 shows the telemetry rate profile during the mission. Tables 8.2-17, -18, and -19 show telemetry design control tables for probe release (64-meter), bus pre-entry (26-meter), and bus entry (64-meter). Table 8.2-20 shows an uplink carrier-tracking link budget

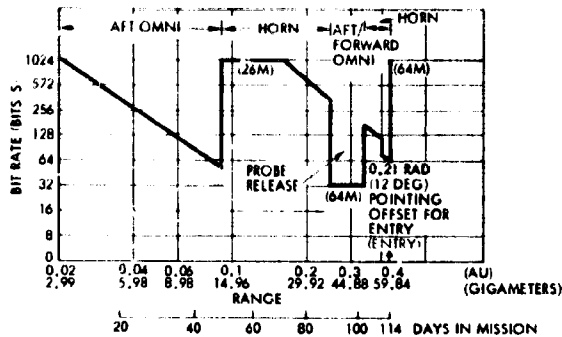


Figure 8.2-18. Probe Bus Telemetry Rate Profile

for a 26-meter station. See Appendix 8.2B for a discussion of the receiver losses used in the telemetry design control tables. For the first 50 days after launch the bus attitude is not earth-pointing, and 26-meter cruise communications are handled by the aft omni.

During this time the two omni antennas are independently connected to the two receivers and two transmitters. The forward omni is not nominally required, but is provided as an attitude control failure backup. For the rest of the mission, except for probe release, earth-pointing is maintained and the medium-gain horn is used. Switch S3 or S4 is activated to connect the horn to a receiver and transmitter as the forward omni is disconnected. Switch S4 is included to prevent a single point bus entry mission failure if switch S3 failed in the forward omni position.

Just prior to entry the bus pointing is offset 0.21 radian (12 degrees) in order to meet the angle-of-attack requirements for ram experiments. This angle represents about a 2 dB drop in antenna gain, but the EIRP is still sufficient to support 64 bits/s with the 26-meter station prior to entry and 1024 bits/s with the 64-meter for the last hour before entry. During probe release and bus retargeting the 64-meter station is needed when the aft omni is used at the required release and retargeting attitudes. Return to earth-pointing after each maneuver can be accomplished, if desired, thereby returning tracking capability to the 26-meter network.

Table 8.2-20. Bus Entry (For Two-Way Tracking,
No Command Modulation)

NO.	PARAMETER	NOMINAL	ADVERSE	NOTES
1	FREQUENCY (MHZ)	2115	-	UPLINK
2	RANGE GIGAMETERS (AU)	64.33 (0.43)	-	AT ENTRY
3	TRANSMITTER POWER (DBM)	73.0	0	20 kW
4	TRANSMITTER ANTENNA GAIN (DB)	51.8	0.9	26-METER DSS
5	SPACE LOSS	-255.1	-	64.33 GIGAMETERS (0.43 AU)
6	RECEIVER ANTENNA GAIN (DB)	14.5	0.3	PEAK GAIN
7	POINTING LOSS (DB)	-1.7	0.3	0.21 RAD (12 DEG) OFFSET PEAK GAIN 0.23 RAD (13 DEG) ADVERSE
8	POLARIZATION LOSS (DB)	-0.2	0.1	
9	RECEIVER CIRCUIT LOSS (DB)	-1.5	0.1	
10	TOTAL RECEIVED POWER (DBM) (3+4+5+6+7+8+9)	-119.2	1.0	RSS
11	RECEIVER NOISE SPECTRAL DENSITY (DBM, HZ)	-169	1.0	T _{SYS} 910°K, NF 6 DB
12	P _T N _O (DB-HZ) (10-11)	49.8	1.4	RSS
<u>CARRIER TRACKING PERFORMANCE</u>				
13	CARRIER MODULATION LOSS (DB)	0	0	
14	THRESHOLD LOOP BANDWIDTH (DB-HZ)	13.0	1.0	2 B _{LO} 20 HZ AT 6 DB SNR
15	LOOP SNR (DB) (12+13-14)	36.8	-	
16	REQUIRED LOOP SNR + LIMITER LOSS (DB)	6.3	0	LIMITER LOSS 0.3 DB
17	PERFORMANCE MARGIN (DB) (15-16)	30.5	1.8	RSS TOLERANCES
<u>COMMAND CHANNEL PERFORMANCE</u>				
18	DATA MODULATION LOSS (DB)	-	-	} NO COMMAND MODULATION
19	DATA BIT RATE (DB-BIT/S)	-	-	
20	RECEIVER LOSS (DB)	-	-	
21	E _b N _O (DB) (12+18-19+20)	-	-	
22	REQUIRED E _b N _O (DB)	-	-	
23	PERFORMANCE MARGIN	-	-	

A single modulation index, 0.9 radian, is used throughout the bus mission with the Pioneers 10 and 11 transmitters. A second modulation index could be implemented if 2 to 3 dB more margin were required during probe release, but the existing Pioneers 10 and 11 transmitter would have to be modified to accommodate two modulation indices.

Note that all three probe bus antennas are located off-axis. This is advantageous for attitude control, as the offset location provides spacecraft pointing information through doppler spin modulation. For this reason a conical scan antenna capability, conscan, is not required on the probe bus mission. For details, see Section 8.5, Attitude Determination and Control.

DSN Configuration During Probe and Bus Entry

It is desirable, from the standpoint of the number of available receivers at the two 64-meter tracking stations at entry, to have the bus tracked in a two-way mode by the 26-meter stations. Two constraints prohibit the 26-meter stations from tracking the bus all the way through bus entry: the two-way doppler rate and the entry high data rate requirement (1024 bits/s). The buildup of the two-way doppler rate from 2 hours before bus entry (~ 0 Hz/s) to entry (~ 60 Hz/s) limits the Block III receiver tracking capability to about one-half to 1 hour before entry (10 to 25 Hz/s) (see JPL Technical Report 32-1526, Vol. XIII, page 23, and also Vol. X, page 168). Also, the 26-meter station can support no more than 64 bits/s at entry. For both these reasons the bus entry is delayed as much as possible without losing communication during the dual Goldstone/Canberra overlap period. The preferred probe and bus entry sequence is as follows:

Large probe and small probe 1 entry:	~70 minutes
Guard space:	~20 minutes
Small probe 2 and small probe 3 entry:	~65 minutes
Guard space:	~25 minutes
Bus Entry	~180 minutes after large probe entry

The 0.26-radian (15-degree) Goldstone/Canberra overlap period is 200 minutes (3 hours, 20 minutes), sufficient to cover the above sequence. This sequence allows two receivers per probe per station (e.g., one Block III and one Block IV) with predetection recording possible on a fifth receiver (Block III) operated open-loop at each station. Approximately 1 hour before bus entry at least one Block IV receiver at either Goldstone or Canberra would have to be switched from one of small probes 2 and 3 to track the bus during the last hour of bus entry. The 64-meter station is required to give the 1024 bits/s capability and the Block IV receiver is required to track (in a programmed oscillator mode) the bus two-way doppler (see Appendix 8.2B). The recommended approach is to switch to the bus one Block IV receiver at Goldstone from small probe 2 and one Block IV receiver at Canberra from small probe 3.

This still leaves a total of three receivers each for probes 2 and 3 during the last half of their entry, four receivers being available for the first half of the entry (high altitude), which is more critical in terms of search, lockup, and doppler. For a detailed diagram of the entry configuration in terms of bus, probes, stations, and receivers, see Section 10.7 of Mission Operations and Flight Support.

Antennas. The baseline antennas for the bus spacecraft are existing, flight-proven designs. The results of antenna tradeoff studies have shown that the selected equipment represents the lowest cost, lowest risk approach in meeting communications requirements for the preferred probe bus configuration.

The bus antennas consist of three separate antennas, providing omnidirectional TT&C coverage during transit and probe entry phases of the mission, as shown in Figure 8.2-19. Two flight-qualified conical log spiral antennas on opposite ends of the spacecraft provide low-gain spherical omnidirectional coverage. There is no interferometer region because the antennas are connected to separate transmitters and receivers. A corrugated conical horn, Pioneers 10 and 11, located on the aft end of the spacecraft provides higher gain for higher bit rate communications during probe entry. For compatibility and minimum DSN operational effect, all the probe bus spacecraft antennas are right-hand circularly polarized. Model tests to verify omni antenna coverage and gain performance have shown that the effects of the large probe and spacecraft structure upon omni antenna pattern performance are negligible. Shown in Figure 8.2-20 are full-scale spacecraft mockups used in the tests and a measured pattern for the combined forward and aft omnis; existing engineering model antennas were used in the tests. While the tests performed with the model did not establish an optimum location for the antennas, they did indicate that adjusting antenna height accomplishes a certain amount of pattern reshaping to fill in low-gain areas. Pattern ripple shown on the measured patterns is primarily due to test range reflections, which will be reduced in future testing.

The use of existing qualified hardware is the lowest cost approach to selecting duplexers and RF switches for the probe and orbiter spacecraft

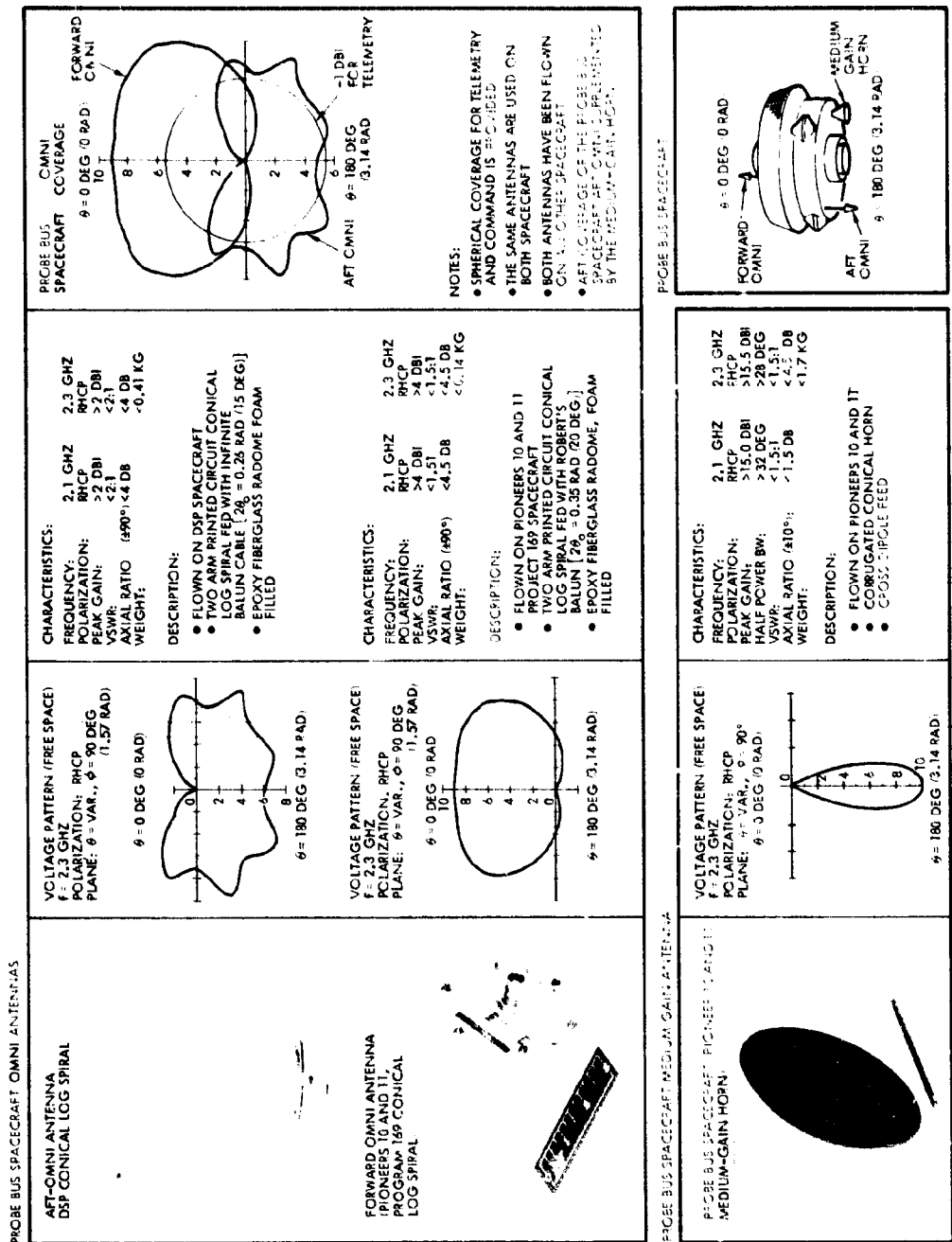
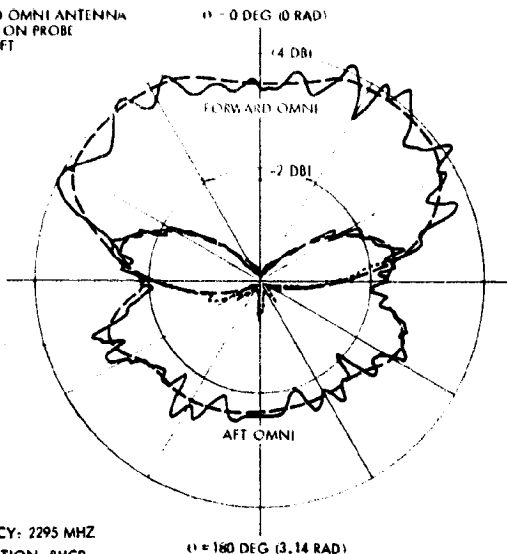


Figure 8.2-19. Baseline Probe Bus Spacecraft Antennas

MEASURED OMNI ANTENNA PATTERNS ON PROBE SPACECRAFT



FREQUENCY: 2295 MHZ
 POLARIZATION: RHCP
 PLANE: ϕ VARIABLE $\theta = 90$ DEG (1.57 RAD)

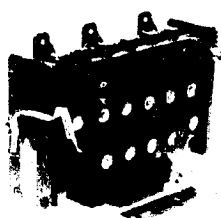


FORWARD OMNI ON SPACECRAFT MOCKUP



AFT OMNI ON SPACECRAFT MOCKUP

Figure 8.2-20. Probe Bus Model Tests



DIPLEXER (PIONEERS 10 AND 11 TYPE I)



RF TRANSFER SWITCH (PIONEERS 10 AND 11)

PERFORMANCE CHARACTERISTICS:

	<u>RECEIVE</u>	<u>TRANSMIT</u>
PASSBAND FREQUENCY	2115 ± 5 MHZ	2295 ± 5 MHZ
PASSBAND INSERTION LOSS	<0.75 DB	<0.3 DB
PASSBAND VSWR	<1.5:1	<1.5:1
OUT-OF-BAND REJECTION	>60 DB	>60 DB
ISOLATION	>85 DB	>85 DB
POWER HANDLING		>12 W CW
WEIGHT	<0.95 KG	
FREQUENCY	2110 TO 2120 MHZ	2290 TO 2300 MHZ
VSWR	<1.2:1	<1.2:1
POWER SWITCHING CAPABILITY		> 9 W CW
INSERTION LOSS	<0.2 DB	<0.2 DB
ISOLATION		> 60 DB
WEIGHT		< 0.3 KG

Figure 8.2-21. Baseline Probe Spacecraft Diplexer and RF Switch

system. The Pioneer 10 and 11 Type II diplexer and RF switch (see Figure 8.2-21) were usable as is for the probe missions and therefore were the selected designs.

Transponder. Section 8.2.3.5 summarized the characteristics of available lightweight and standard weight transponders. It was noted that

only three companies are presently engaged in the manufacture of DSN compatible S-band transponders. The use of hardware available from all three vendors will be considered in following sections for all applications except the Atlas/Centaur probe bus. For the Atlas/Centaur probe bus the residual units from the Pioneers 10 and 11 program are recommended. A brief summary of the characteristics of this transponder follows.

1) Pioneers 10 and 11 Receiver. The Pioneers 10 and 11 receiver differs somewhat in design from both the TRW and Philco-Ford lightweight designs, since it utilizes triple down-conversion. Because the design was accomplished with discrete components, the weight is considerably heavier [2.45 versus 1.36 kilograms (5.4 versus 3 pounds)] and larger in size. The present design is usable for the bus without modification. Although not required for the probe bus, a conscan output for use with an existing conscan signal processor to provide spacecraft pointing information is available from this unit. A brief list of the receiver characteristics is given in Table 8.2-21. A block diagram of the receiver is shown in Figure 8.2-22.

2) Pioneers 10 and 11 Transmitter Driver. The transmitter driver from Pioneers 10 and 11 is capable of generating a phase-modulated S-band signal of 50 to 80 mW. It has an internal oscillator used to provide a stable frequency output when the receiver is not phase-locked to an uplink signal. It has provisions for accepting RF inputs from either of two receivers for coherent operation. The transmitter driver is phase-modulated by a squarewave frequency of 32 kHz.

The transmitter driver consists of two circuit boards. The oscillator board contains a voltage regulator, TCXO, with switch circuit, buffer, amplifier, and a X3 multiplier. The driver module contains the phase-modulator with modulation limiter, buffer amplifier, RF limiter, intermediate power amplifier, X2 multiplier, power amplifier, X10 multiplier, and bandpass filter. The unit weighs 3.0 kilograms (1.4 pounds) and requires 1.5 watts.

A list of pertinent characteristics for the transmitter driver are given in Table 8.2-22. A block diagram is shown in Figure 8.2-23.

Table 8.2-21. Pioneer 10 and 11 S-Band Receiver Performance

RECEIVING FREQUENCY RANGE (FACTORY PRESET)	2110-2120 MHz
NOISE FIGURE (MAXIMUM)	6 DB
INPUT VSWR (MAXIMUM)	1.3:1
ACQUISITION THRESHOLD (LOOP SNR = 6.0 DB)	-148 DBM
LOOP NOISE BANDWIDTH AT THRESHOLD	20 Hz
TRACKING CHARACTERISTICS	
-100 DBM SIGNAL	±30 KHz AT A RATE OF ±150 Hz/S WITH A PHASE ERROR OF ±0.6 RAD
-130 DBM SIGNAL	±200 KHz AT A RATE OF ±30 Hz/S WITH A PHASE ERROR OF ±0.7 RAD
-143 DBM SIGNAL	±12 KHz AT A RATE OF ±20 Hz/S WITH A PHASE ERROR OF ±0.6 RAD
THRESHOLD SENSITIVITY	-149 DBM (1.5 DB (6 DB SNR IN A 20 Hz LOOP BANDWIDTH)
DYNAMIC RANGE	
COMMAND CHANNEL	-147.7 TO -63 DBM (COMMAND OUTPUT NOISE -12.3 DB - Hz AT -146.2 DBM)
COHERENT DRIVE TO TRANSMITTER	
FREQUENCY	12.221 TIMES RECEIVED FREQUENCY
LEVEL	-5 DBM TO -2 DBM
IMPEDANCE	50 Ω
DISABLED LEVEL	-68 DBM
FSK SUBCARRIER OUTPUT	
-63 DBM SIGNAL	9.4 ± 1.5 V PEAK TO PEAK
-146.2 DBM SIGNAL	10.6 ± 1.7 V PEAK TO PEAK
SOURCE Z	30 KΩ
LOAD Z	37 KΩ
FREQUENCIES	128 Hz "0"; 204.8 Hz "1"
AUTOMATIC GAIN CONTROL CONSCAN OUTPUT	
AC COMPONENT	(100 MV ± 13%), DB
SNR	-4 DB - Hz (-135 DBM 2% AM)
SOURCE Z	10 KΩ
LOAD Z	165 KΩ
AUTOMATIC GAIN CONTROL CLOSED LOOP BANDWIDTH (3 DB)	1.9 Hz
VCO FREQUENCY STABILITY	5 PARTS IN 10 ⁶ 10 HR (±30 TO ±90°)
PHASE STABILITY (COHERENT OUTPUT - S-BAND)	0.047 RAD (2.8 DEG RMS), 0.147 RAD (8.4 DEG PEAK)
WEIGHT	2.44 KG (5.4 LB)
POWER REQUIRED	2 WATTS

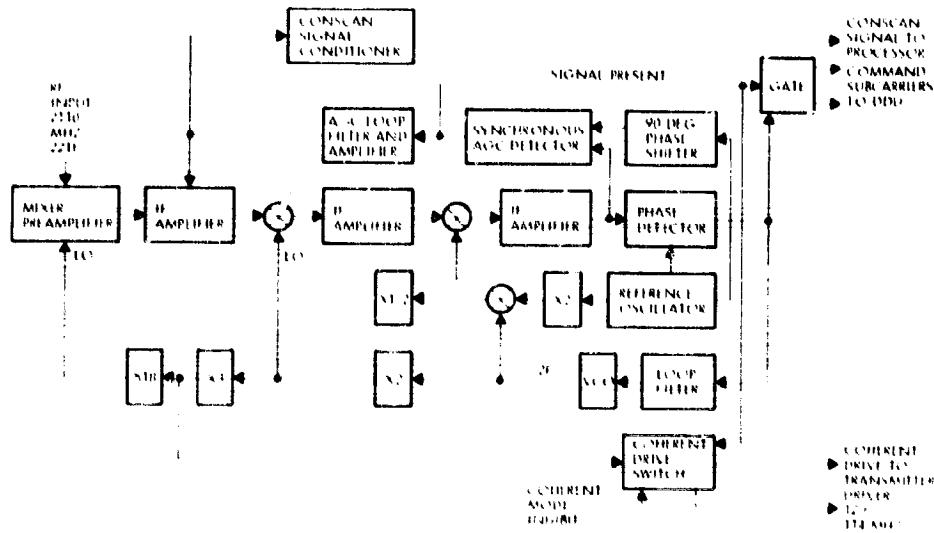


Figure 8.2-22. Pioneer 10 and 11 Receiver

Table 8. 2-22.

Pioneer 10 and 11 Transmitter Driver Performance

FREQUENCY OF OPERATION	
INPUT	114.6 MHz (12.1)
OUTPUT	2290 TO 2300 MHz
DRIVE LEVEL REQUIRED	-5 DBM TO +2 DBM
INPUT IMPEDANCE	50 Ω
INPUT VSWR	1.5:1
MODULATION	
TYPE	CONSTANT PHASE
SENSITIVITY	1.1 RAD INDEX
STABILITY	+0.1 RAD
OUTPUT POWER (MINIMUM)	50 MW
SPURIOUS LEVELS	40 DB
FREQUENCY STABILITY, AUXILIARY OSCILLATOR	
SHORT TERM (0.25 SEC)	3×10^{-11}
LONG TERM	4×10^{-6} 10 HR
INPUT VOLTAGE	-16 ± 0.5 V
INPUT POWER	1.5 WATTS
ENVIRONMENTAL	
TEMPERATURE	-18 TO 49°C
VIBRATION	32 G 40 HZ
SHOCK	400 G 2 KHZ

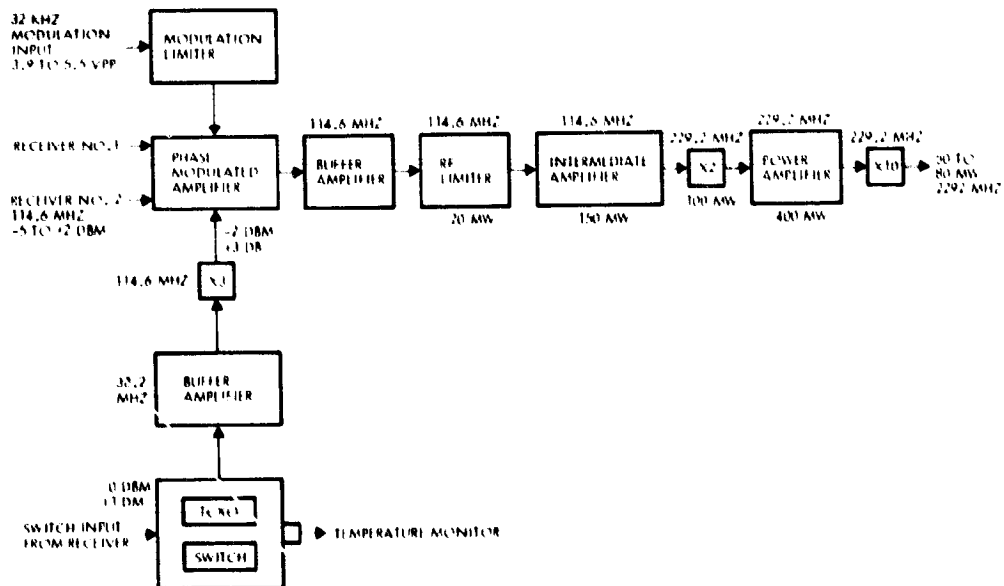


Figure 8.2-23. Pioneer 10 and 11 Transmitter

Power Amplifier. A 6-watt solid-state power amplifier has been chosen.

In an initial attempt to minimize costs, a preliminary decision was made to use TWTA's (8-watt output) from the Pioneers 10 and 11 residuals. After considering the costs of refurbishing and retesting, and the program costs of carrying two different types of amplifiers, it was found less costly to buy additional 6-watt solid-state amplifiers than to use the residual 8-watt TWTA's (6-watt solid-state units must be procured for the orbiter). Details of a 6-watt solid-state versus TWTA tradeoffs have previously been covered in Section 8.2.3.4.

The choice of a solid-state power amplifier in lieu of existing TWTA designs is possible due to the improved performance available from S-band power transistors. Figure 8.2-24 shows two block diagrams for power amplifiers. The first is the preferred approach, as it uses a new family of high-gain, high efficiency transistors from Microwave Semiconductors Corporation. Since no power supply is necessary to work from the regulated 28-watt bus, the overall efficiency is equal to or superior to existing TWTA's, such as the Pioneers 10 and 11 unit.

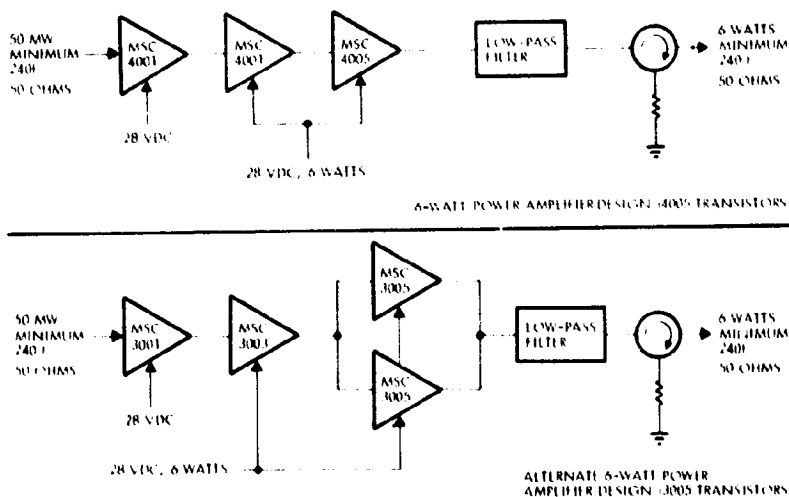


Figure 8.2-24. Two 6-Watt Solid State Power Amplifier Designs

Since the 4000 series transistors have not been flight proven, it might be considered wise to use the 3000 series instead. A look at the block diagram of this alternate approach will show that an additional transistor is required. By the time Pioneer Venus is in the development cycle, TRW believes the 4000 series will be qualified and available for high reliability space applications.

As mentioned in the previous power combining tradeoff charts, the present 6-watt amplifiers can be combined to provide 10 to 11 watts (12 watts nominal), as required for the Atlas/Centaur orbiter options.

Table 8.2-23 lists some pertinent characteristics for the 6-watt solid-state and Pioneers 10 and 11 TWTA power amplifier.

Table 8.2-23. Power Amplifiers

PARAMETER	SOLID STATE	TWTA
FREQUENCY RANGE	2295 MHz ± 5 MHz	2295 MHz ± 5 MHz
POWER OUTPUT	6 WATTS	8 WATTS
DRIVE POWER REQUIRED	50 MW	4 MW
INPUT VSWR	1.4:1	1.4:1
LOAD VSWR	1.5:1	1.5:1
INPUT VOLTAGE	28 V ± 2%	28 V ± 2%
INPUT POWER	19 WATTS	28 WATTS
SPOURIOUS OUTPUTS	30 DB EACH	5 DB (TOTAL SUM)
WEIGHT, KG (LB) (HIGH-GAIN VERSION)	0.3 (0.6)	1.8 (4)
OUTPUT POWER MONITOR	REQUIRED	AVAILABLE

Subsystem Weight and Power Summary. The preferred Atlas/Centaur probe bus communication subsystem weight and power are summarized in Table 8.2-24.

Table 8.2-24. Communications Subsystem Weight and Power Summary

ITEM	QUANTITY	TOTAL WEIGHT KG (LB)	DC POWER (WATTS)
RECEIVER	2	4.9 (10.8)	4.0
TRANSMITTER DRIVER	2	1.3 (2.8)	1.5
POWER AMPLIFIER	2	0.6 (1.2)	22.0
DIPLER	2	1.9 (4.3)	
SWITCHES	5	1.4 (3.0)	
FORWARD OMNI	1	0.1 (0.3)	
AFT OMNI	1	0.4 (0.9)	
AFT HORN	1	1.5 (3.3)	
RE COAX AND CONNECTOR	A R	1.1 (2.5)	
TOTAL		13.2 (29.1)	27.5

8.2.4.2 Preferred Orbiter

The block diagram for the orbiter, Figure 8.2-25, shows a redundant set of transponders, conscan signal processor, and a redundant set

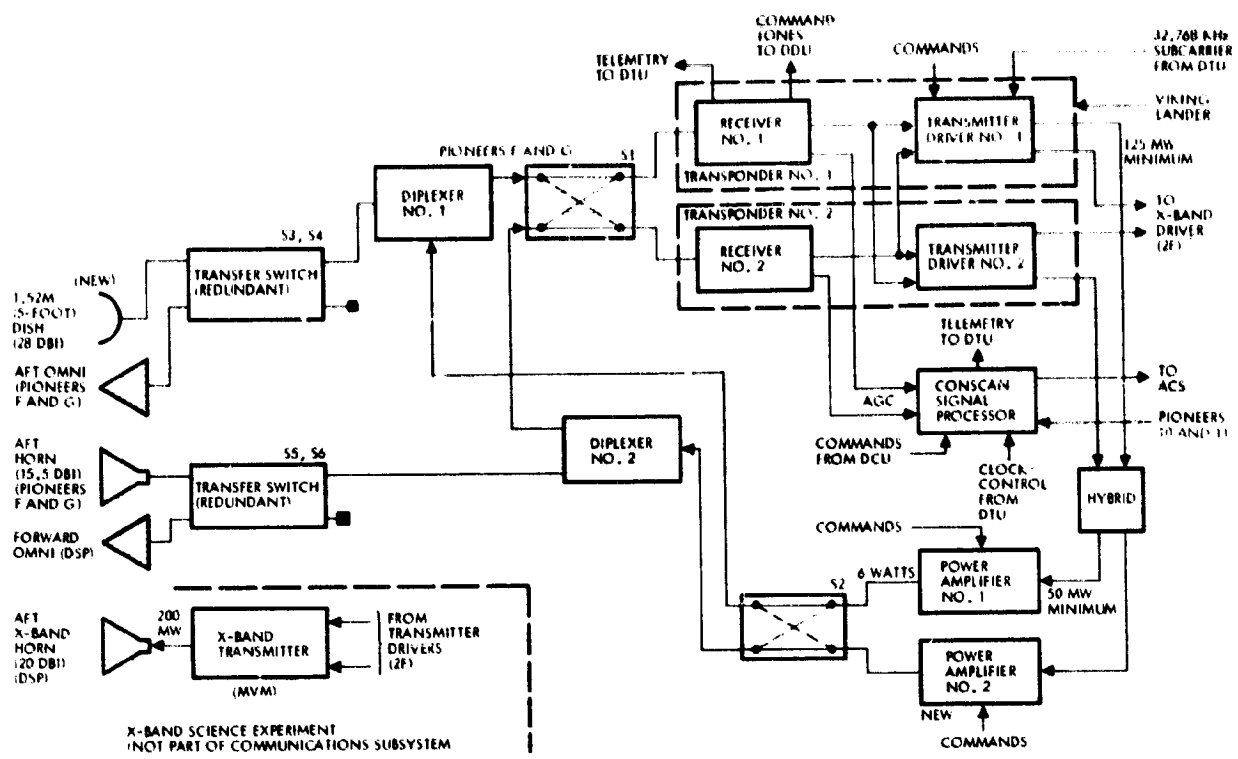


Figure 8.2-25 Atlas-Centaur Orbiter Communications Subsystem Block Diagram

of 6-watt solid-state power amplifiers connected through switches, hybrid-couplers, and diplexers to aft and forward omnis, an aft-pointing horn, and a forward-pointing dish. An X-band science occultation experiment, consisting of a 200-mW transmitter and an aft-pointing horn, is also shown in the diagram. (For the study it was considered not to be part of the communications subsystem.) The X-band interface with the S-band transmitters and its occultation capabilities will be covered later in this section.

The transponders selected for the baseline are Viking Lander units with minor modifications (e.g., the addition of conscan output, coherent inhibit, and possibly an X-band drive). A conscan signal processor is used on the orbiter for attitude control when the high-gain dish is pointed at earth. Conscan is required because offset-omni doppler modulation cannot be used after the first 37 days in Venus orbit when the spacecraft is flipped to point nose to earth. The 6-watt omni downlink does not have sufficient EIRP for tracking, even with the 64-meter station, past that time.

The power amplifiers are 6-watt solid-state devices, the same as those used on the bus. The forward and aft omni are also the same as those used on the bus but reversed, i.e., the bus forward omni is the same as the orbiter aft omni (Pioneers 10 and 11). The aft horn is the same as on the bus (Pioneers 10 and 11), but the 5-foot dish is new. The feed for the dish is the Pioneers 10 and 11 high-gain feed and is permanently offset for conscan capability and also slightly defocused to extend the conscan acquisition range to about 0.17 radian (10 degrees).

The EIRP of the orbiter in the high-gain antenna mode is 61.5 dBm, assuming 0.017 radian (1 degree) attitude pointing error and 1.1 dB polarization loss. This is sufficient for a 64 bits/s downlink at 254.32 gigameters (1.7 AU) with a modulation index of 1.05 radian and a 26-meter tracking station. This permits readout of an entire orbit of stored data in approximately 10 hours. A slightly lower EIRP could have been chosen, at a slightly reduced spacecraft cost, to provide only a 32 bits/s capability, but this would have required full 24-hour coverage by a 26-meter network consisting of three stations. The 10-hour readout capability requires only two stations and the cost savings in ground operations is anticipated to be more than the increased spacecraft cost, thus reducing total program cost.

A further increase in EIRP (and hence data rate) for an anticipated one-station readout capability was ruled out on the basis of our preferred store-and-dump capability; this requires two data dumps per orbit, one of which is required near periapsis. Since periapsis passes are variable with respect to ground station coverage, two stations would be required anyway at one time or another. For further discussion of this, see Section 8.3, Data Handling.

Telemetry Mission Profile

Figure 8.2-26 shows the telemetry rate profile during the cruise and orbit phases of the mission. Tables 8.2-25, 8.2-26, and 8.2-27 are telemetry design control tables for orbit insertion, the second flit

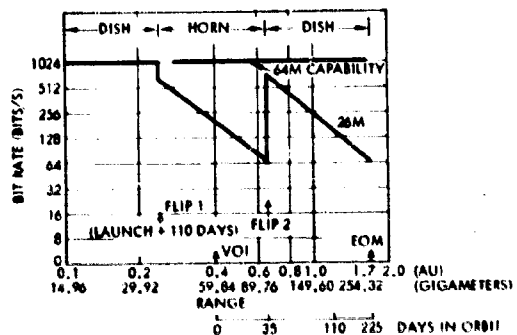


Figure 8.2-26 Orbiter Telemetry Rate Profile

maneuver, and the end-of-mission, respectively. Table 8.2-27 shows the uplink command design control table at end-of-mission. From launch to the first flip maneuver (110 days) the high-gain dish is pointed at earth and provides 1024 bits/s, the limit of the digital telemetry unit (DTU) as modified for Pioneer Venus. After the first flip the aft horn is pointed at earth and provides bit rates from 512 to 64 bits/s until the second flip maneuver 35 days after orbit insertion.

Both flip maneuvers are required for sun heating (thermal) considerations and are not constrained by the communications subsystem. For the remainder of the mission the high-gain dish is pointed at earth and provides bit rates also from 512 to 64 bits/s. Whenever a 64-meter station is used in the mission, a bit rate of 1024 bits/s can be supported reducing the readout time for a full orbit of stored data to less than an hour. For a discussion of orbiter doppler effects, which do not impair the mission but may cause short (10 to 15 minutes) periods of ground loss-of-lock tracking at some periapsis passes, see Appendix 8.2D.

S-Band and X-band Occultation

Tables 8.2-28 and 8.2-29 show the received power shortly after orbit insertion with the 64-meter station for the preferred S-band and X-band spacecraft configuration. For ease of implementation and minimum cost, occultation capability is provided for the first 35 days only, when the aft end of the spacecraft is pointed to earth. The S- and X-band horns are aligned with the spin axis of the spacecraft, providing maximum gain in that direction. The horn beamwidths are sufficient to allow prepositioning of the spacecraft spin axis off the earth line to the desired refraction angle (α) prior to entry before the start of occultation. Real time S-band communications is maintained at 128 bits/s prior to occultation but shortly after refraction (and attendant defocusing) begins [(about 0.05 radian (3 degrees) and 15 dB loss, see Figure 8.2-27)] carrier tracking is lost. Digital recording and processing must be used to further extract the carrier from the increasingly refracted and defocused ray.

Figure 8.2-28 is a plot of defocusing loss versus refraction angle taken from data prepared by Dr. Gunnar Fjeldbo and included in a letter

Table 8.2-25. Orbit Insertion Design Control Table

NO.	PARAMETER	NOMINAL	ADVERSE	NOTES
1	FREQUENCY (MHZ)	2300	0	
2	RANGE (GIGAMETERS (AU))	59.8 (0.4)	0	ORBIT INSERTION
3	TRANSMITTER POWER (DBM)	37.8	0.4	6 WATTS NOMINAL
4	TRANSMITTER CIRCUIT LOSS (DB)	-1.5	0.1	
5	TRANSMITTER ANTENNA GAIN (DB)	2.0	0.3	FORWARD OMNI AT 1.05 RAD (60 DEG)
6	POINTING LOSS (DB)	0	0	
7	POLARIZATION LOSS (DB)	-0.2	0.1	
8	SPACE LOSS	-255.2	0	59.8 GIGAMETERS (0.4 AU)
9	RECEIVER ANTENNA GAIN (DB)	61.6	0.4	64-M DSS (0.1 DB LOSS AT 0.35 RAD (20 DEG) ELEVATION)
10	TOTAL RECEIVED POWER (DBM)(3+4+5+6+7+8+9)	-154.5	-	
11	RECEIVER NOISE SPECTRAL DENSITY (DMB/HZ)	-184.0	0.6	$T_{SYS} = 29^{\circ}K$; 0.35 RAD (20 DEG) ELEVATION
12	P_T/N_O (DB-HZ) (10-11)	29.5	1.0	RSS
<u>CARRIER TRACKING PERFORMANCE</u>				
13	CARRIER MODULATION LOSS (DB)	-6.1	1.7	$\theta = 1.05 \text{ RAD} \pm 10\%$
14	THRESHOLD LOOP BANDWIDTH (DB-HZ)	10.0	0.4	$2 B_{LO} = 10 \text{ HZ}$
15	LOOP SNR (DB) (12+13-14)	13.4	-	
16	REQUIRED LOOP SNR (DB)	10.0	0	
17	PERFORMANCE MARGIN (DB) (15-16)	3.4	2.0	RSS TOLERANCES
<u>DATA CHANNEL PERFORMANCE</u>				
18	DATA MODULATION LOSS (DB)	-1.2	0.6	$\theta = 1.05 \text{ RAD} \pm 10\%$
19	DATA BIT RATE (DB-BITS/S)	18.1	0	64 BITS/S
20	RECEIVER LOSS (DB)	-4.8	0.5	ESTIMATED
21	DOPPLER LOSS (DB)	0	0	INSERTION BEHIND PLANET
22	E_b/N_o (DB) (12+13-19+20+21)	5.4	-	
23	REQUIRED E_b/N_o (DB)	2.7	0	10^{-3} DELETION RATE
24	PERFORMANCE MARGIN (DB) (22-23)	2.7	1.3	RSS TOLERANCES

Table 8.2-26.

NO.	PARAMETER
1	FREQUENCY (MHZ)
2	RANGE (GIGAMETERS (AU))
3	TRANSMITTER POWER (DBM)
4	TRANSMITTER CIRCUIT LOSS (DB)
5	TRANSMITTER ANTENNA GAIN (DB)
6	POINTING LOSS (DB)
7	POLARIZATION LOSS (DB)
8	SPACE LOSS (DB)
9	RECEIVER ANTENNA GAIN (DB)
10	TOTAL RECEIVED POWER (DBM)
11	RECEIVER NOISE SPECTRAL DENSITY (DMB/HZ)
12	P_T/N_O (DB-HZ) (10-11)
<u>CARRIER TRACKING PERFORMANCE</u>	
13	CARRIER MODULATION LOSS (DB)
14	THRESHOLD LOOP BANDWIDTH (DB-HZ)
15	LOOP SNR (DB) (12+13-14)
16	REQUIRED LOOP SNR (DB)
17	PERFORMANCE MARGIN (DB) (15-16)
<u>DATA CHANNEL PERFORMANCE</u>	
18	DATA MODULATION LOSS (DB)
19	DATA BIT RATE (DB-BITS/S)
20	RECEIVER LOSS (DB)
21	E_b/N_o (DB) (12+13-19+20)
22	REQUIRED E_b/N_o (DB)
23	PERFORMANCE MARGIN (DB) (22-23)

OUT FRAME

Table 8.2-26. Flip No. 2 Maneuver (On Omni Antennas)
Design Control Table

PARAMETER	NOMINAL	ADVERSE	NOTES
FREQUENCY (MHZ)	2300	-	
RANGE [GIGAMETERS (AU)]	97.24 (0.65)	-	35 DAYS AFTER ORBIT INSERTION
TRANSMITTER POWER (DBM)	37.8	0.4	6 WATTS NOMINAL, 5.5 WATTS MINIMUM
TRANSMITTER CIRCUIT LOSS (DB)	-1.5	0.3	
TRANSMITTER ANTENNA GAIN (DB)	-1.0	1.0	OMNI COVERAGE
POINTING LOSS (DB)	0	-	
POLARIZATION LOSS (DB)	-0.2	0.1	
SPACE LOSS (DB)	-259.4	-	
RECEIVER ANTENNA GAIN (DB)	61.7	0.4	64-METER
TOTAL RECEIVED POWER (DBM)(3+4+5+6+7+8+9)	-162.6	1.2	RSS TOLERANCES
RECEIVER NOISE SPECTRAL DENSITY (DBM/HZ)	-184.6	0.6	T = 25°K AT 0.79 RAD (45 DEG) ELEVATION (0.35 RAD (20 DEG) ELEVATION ADVERSE)
P_r/N_0 (DB-HZ) (10-11)	22.0	1.3	RSS TOLERANCES
<u>CARRIER TRACKING PERFORMANCE</u>			
CARRIER MODULATION LOSS (DB)	-1.3	0.4	0.54 RAD ±10%
THRESHOLD LOOP BANDWIDTH (DB-HZ)	10.0	0.4	2 B _{LO} = 10 HZ
LOOP SNR (DB) (12+13-14)	10.7	-	
REQUIRED LOOP SNR (DB)	9.0	-	
PERFORMANCE MARGIN (DB) (15-16)	1.7	1.5	RSS TOLERANCES
<u>DATA CHANNEL PERFORMANCE</u>			
DATA MODULATION LOSS (DB)	-5.8	0.9	0.54 RAD ±10%
DATA BIT RATE (DB-BITS/S)	9.0	-	8 BITS/S
RECEIVER LOSS (DB)	-3.2	0.5	ESTIMATED FROM PIONEER 9 DATA AND NEW SDA AND SSA
E_b/N_0 (DB) (12+18-19+20)	4.0	-	
REQUIRED E_b/N_0 (DB)	2.3	-	10 ⁻³ FRAME DELETION RATE
PERFORMANCE MARGIN (DB) (21-22)	1.7	1.7	RSS TOLERANCES

Table 8.2-27. End-of-Mission

NO.	PARAMETER	NOMINAL
1	FREQUENCY (MHZ)	2300
2	RANGE [GIGAMETERS (AU)]	254.32 (1.7)
3	TRANSMITTER POWER (DBM)	37.8
4	TRANSMITTER CIRCUIT LOSS (DB)	-1.5
5	TRANSMITTER ANTENNA GAIN (DB)	28.0
6	POINTING LOSS (DB)	-2.0
7	POLARIZATION LOSS (DB)	-0.2
8	SPACE LOSS (DB)	-267.0
9	RECEIVER ANTENNA GAIN (DB)	53.3
10	TOTAL RECEIVED POWER (DBM)(3+4+5+6+7+8+9)	-153.0
11	RECEIVER NOISE SPECTRAL DENSITY (DBM/HZ)	-181.7
12	P_r/N_0 (DB-HZ) (10-11)	20.0
<u>CARRIER TRACKING PERFORMANCE</u>		
13	CARRIER MODULATION LOSS (DB)	-1.3
14	THRESHOLD LOOP BANDWIDTH (DB-HZ)	10.0
15	LOOP SNR (DB) (12+13-14)	12.0
16	REQUIRED LOOP SNR (DB)	10.0
17	PERFORMANCE MARGIN (DB) (15-16)	2.0
<u>DATA CHANNEL PERFORMANCE</u>		
18	DATA MODULATION LOSS (DB)	-1.3
19	DATA BIT RATE (DB-BITS/S)	10.0
20	RECEIVER LOSS (DB)	-4.0
21	E_b/N_0 (DB) (12+18-19+20)	4.0
22	REQUIRED E_b/N_0 (DB)	2.3
23	PERFORMANCE MARGIN (DB) (21-22)	1.7

OLLOUT FRAME

Table 8.2-27. End-of-Mission Design Control Table

NO.	PARAMETER	NOMINAL	ADVERSE	NOTES
1	FREQUENCY (MHZ)	2300	-	
2	RANGE [GIGAMETERS (AU)]	254.32 (1.7)	-	END OF MISSION
3	TRANSMITTER POWER (DBM)	37.8	0.4	6 WATTS NOMINAL
4	TRANSMITTER CIRCUIT LOSS (DB)	-1.4	0.1	
5	TRANSMITTER ANTENNA GAIN (DB)	28.0	0.5	1.52-METER (5-FOOT) DISH
6	POINTING LOSS (DB)	-2.8	0.3	CONSCAN LOSS PLUS 0.017 RAD (1 DEG) ATTITUDE ERROR
7	POLARIZATION LOSS (DB)	-0.1	0.1	
8	SPACE LOSS (DB)	-267.8	0	254.32 GIGAMETERS (1.7 AU)
9	RECEIVER ANTENNA GAIN (DB)	53.3	0.6	26 METERS
10	TOTAL RECEIVED POWER (DBM)(3+4+5+6+7+8+9)	-153.0	0.9	RSS TOLERANCES
11	RECEIVER NOISE SPECTRAL DENSITY (DBM/HZ)	-181.9	0.9	47°K AT 0.26 RAD (15 DEG) ELEVATION 0.17 RAD (10 DEG) ELEVATION ADVERSE]
12	P_r/N_0 (DB-HZ) (10-11)	28.9	1.3	RSS TOLERANCES
<u>CARRIER TRACKING PERFORMANCE</u>				
13	CARRIER MODULATION LOSS (DB)	-6.1	1.7	1.05 ± 10% RAD
14	THRESHOLD LOOP BANDWIDTH (DB-HZ)	10.3	0.5	$2 B_{LO} = 10.8 ± 10% HZ$
15	LOOP SNR (DB) (12+13-14)	12.5	2.2	RSS TOLERANCES
16	REQUIRED LOOP SNR (DB)	10.0	0	RECOMMENDED 810-5
17	PERFORMANCE MARGIN (DB) (15-16)	2.5	2.2	RSS TOLERANCES
<u>DATA CHANNEL PERFORMANCE</u>				
18	DATA MODULATION LOSS (DB)	-1.2	0.6	1.05 ± 10% RAD
19	DATA BIT RATE (DB-BITS/S)	18.1	0	64 BITS/S
20	RECEIVER LOSS (DB)	-4.8	0.5	ESTIMATED FROM NASA/ARC DATA (10 DB LOOP SNR)
21	E_b/N_0 (DB) (12+18-19+20)	4.8	1.5	RSS TOLERANCES
22	REQUIRED E_b/N_0 (DB)	2.7	0	10^{-3} FRAME DELETION RATE
23	PERFORMANCE MARGIN (DB) (21-22)	2.1	1.5	RSS TOLERANCES

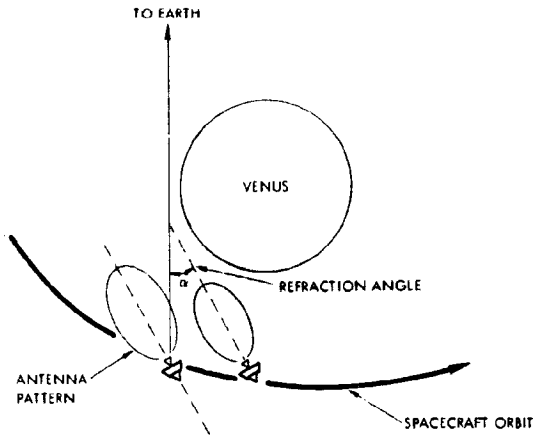


Figure 8.2-27. Spacecraft Occultation Positioning

Table 8.2-28. Uplink Command Design Control Table

NO.	PARAMETERS	NOMINAL	ADVERSE	NOTES
1	FREQUENCY (MHZ)	2115	-	
2	RANGE [GIGAMETERS (AU)]	254.32 (1.7)	-	
3	TRANSMITTER POWER (DBM)	73.0	0	20 KW
4	TRANSMITTER ANTENNA GAIN (DB)	51.8	0.9	26-METER DSS
5	SPACE LOSS	-267.1	-	
6	RECEIVER ANTENNA GAIN (DB)	27.5	0.3	1.52 METER (5-FOOT) DISH
7	POINTING LOSS (DB)	-2.3	0.2	CONSCAN (1 DB) + 0.017 RAD (1 DEG) POINTING ERROR
8	POLARIZATION LOSS (DB)	-3.2	0.1	
9	RECEIVER CIRCUIT LOSS (DB)	-1.9	0.2	
10	TOTAL RECEIVED POWER (DBM)(3+4+5+6+7+8+9)	119.2	1.0	
11	RECEIVER NOISE SPECTRAL DENSITY (DBM/HZ)	-169	1.0	$T_{SYS} = 910^{\circ}K$; $NF = 6$ DB
12	P_T/N_O (DB-HZ) (10-11)	49.8	1.4	
<u>CARRIER TRACKING PERFORMANCE</u>				
13	CARRIER MODULATION LOSS (DB)	-2.8	0.3	$\theta = 1.09$ RAD
14	THRESHOLD LOOP BANDWIDTH (DB-HZ)	13.0	1.0	$2 B_{LO} = 20$ HZ AT 6 DB SNR
15	LOOP SNR (DB) (12+13-14)	34.0	1.8	
16	REQUIRED LOOP SNR = LIMITER LOSS (DB)	6.3	-	LIMITER LOSS = 0.3 DB
17	PERFORMANCE MARGIN (DB) (15-16)	27.7	1.8	RSS TOLERANCES
<u>COMMAND CHANNEL PERFORMANCE</u>				
18	DATA MODULATION LOSS (DB)	-3.6	0.4	$\theta = 1.09$ RAD
19	DATA BIT RATE (DB-BITS/S)	0	-	1 BIT/S
20	RECEIVER LOSS (DB)	-1.1	-	RECEIVER, FILTER, AND LIMITER LOSS
21	E_b/N_O (DB) (12+18-19+20)	45.1	1.5	
22	REQUIRED E_b/N_O (DB)	17.3	1.0	10^{-5} BIT ERROR RATE
23	PERFORMANCE MARGIN	27.8	1.8	RSS TOLERANCES

Table

NO.	PARAMETER
1	FREQUENCY (MHZ)
2	RANGE [GIGAMETERS (AU)]
3	TRANSMITTER POWER (DBM)
4	TRANSMITTER CIRCUIT LOSS (DB)
5	TRANSMITTER ANTENNA GAIN (DB)
6	POINTING LOSS (DB)
7	POLARIZATION LOSS (DB)
8	SPACE LOSS (DB)
9	RECEIVER ANTENNA GAIN (DB)
10	TOTAL RECEIVED POWER (DBM)(3+4+5+6+7+8+9)
11	RECEIVER NOISE SPECTRAL DENSITY (DBM/HZ)
12	P_T/N_O (DB-HZ) (10-11)
<u>CARRIER TRACKING PERFORMANCE</u>	
13	CARRIER MODULATION LOSS (DB)
14	THRESHOLD LOOP BANDWIDTH (DB-HZ)
15	LOOP SNR (DB) (12+13-14)
16	REQUIRED LOOP SNR (DB)
17	PERFORMANCE MARGIN (DB) (15-16)
<u>DATA CHANNEL PERFORMANCE</u>	
18	DATA MODULATION LOSS (DB)
19	DATA BIT RATE (DB-BITS/S)
20	RECEIVER LOSS (DB)
21	E_b/N_O (DB) (12+18-19+20)
22	REQUIRED E_b/N_O (DB)
23	PERFORMANCE MARGIN (DB) (21-22)
<u>OFFLINE DIGITAL PROCESSING PERFORMANCE</u>	
24	CARRIER MODULATION LOSS (DB)
25	DIGITAL RECORDING LOSS (DB)
26	PROCESSING BANDWIDTH REQUIRED
27	REQUIRED SNR (DB) (IN 3 HZ)
28	PERFORMANCE MARGIN (DB)

NOTE: 4.2 DB LESS MARGIN AT 35 DAYS [9]

FOOT FRAME

Table 8.2-29. S-Band Occultation

PARAMETER	NOMINAL	ADVERSE	NOTES
	2300	-	
RANGE (AU)	59.84 (0.4)	-	ORBIT INSERTION
TRANSMITTER POWER (DBM)	37.8	0.4	6 WATTS NOMINAL
TRANSMITTER CIRCUIT LOSS (DB)	-1.2	0.1	
TRANSMITTER ANTENNA GAIN (DB)	15.5	0.5	AFT HORN
POINTING LOSS (DB)	-5	0.1	0.35 RAD (20 DEG) POINTING ERROR
POLARIZATION LOSS (DB)	-0.1	0.1	
SPACE LOSS (DB)	-255.2	0	59.84 GIGAMETERS (0.4 AU)
RECEIVER ANTENNA GAIN (DB)	61.6	0.4	64-METER [0.1 DB LOSS AT 0.35 RAD (20 DEG) ELEVATION]
TOTAL RECEIVED POWER (DBM) (3+4+5+6+7_8+9)	-146.6	0.8	RSS TOLERANCES
RECEIVER NOISE SPECTRAL DENSITY (DBM/HZ)	-184.0	0.6	29°K AT 0.35 RAD (20 DEG) ELEVATION [0.26 RAD (15 DEG) ELEVATION ADVERSE]
PERFORMANCE MARGIN (DB)	37.4	1.0	RSS TOLERANCES
<u>CARRIER TRACKING PERFORMANCE (REAL TIME)</u>			
CARRIER MODULATION LOSS (DB)	-1.3	0.3	0.54 ± 10% RAD
THRESHOLD LOOP BANDWIDTH (DB-HZ)	10.0	0.4	2 B _{LO} = 10 HZ
LOOP SNR (DB) (13-14)	26.1	1.1	RSS TOLERANCES
REQUIRED LOOP SNR (DB)	10.0	0	RECOMMENDED 810-5
PERFORMANCE MARGIN (DB) (15-16)	16.1	1.1	RSS TOLERANCES
<u>CARRIER TRACKING PERFORMANCE (REAL TIME)</u>			
CARRIER MODULATION LOSS (DB)	-5.8	0.9	0.54 ± 10% RAD
THRESHOLD LOOP BANDWIDTH (DB-HZ)	21.1	0	128 BITS/S
LOOP SNR (DB) (17-18)	-3.2	0.5	ESTIMATED FROM NASA/ARC DATA (25 DB LOOP SNR)
REQUIRED LOOP SNR (DB) (19-20)	7.3	1.4	RSS TOLERANCES
PERFORMANCE MARGIN (DB) (21-22)	2.8	0	10 ⁻³ FRAME DELETION RATE
THRESHOLD LOOP BANDWIDTH (DB-HZ)	4.5	1.4	RSS TOLERANCES
<u>DIGITAL PROCESSING PERFORMANCE</u>			
CARRIER MODULATION LOSS (DB)	-1.3	0.3	0.54 RAD ± 10%
THRESHOLD LOOP BANDWIDTH (DB-HZ)	-0.5	0.5	ESTIMATED
LOOP SNR (DB) (23-24)	4.8	1.2	3 HZ, ESTIMATED
REQUIRED LOOP SNR (DB) (25-26)	0	1.0	ESTIMATED
PERFORMANCE MARGIN (DB) (27-28)	35.8	1.9	THIS MARGIN ASSUMES POINTING LOSS (ITEM 6) IS 0 DB (TOTAL RECEIVED POWER = -141.6 DBM)

AT 35 DAYS [97.24 GIGAMETERS (0.65 AU)]

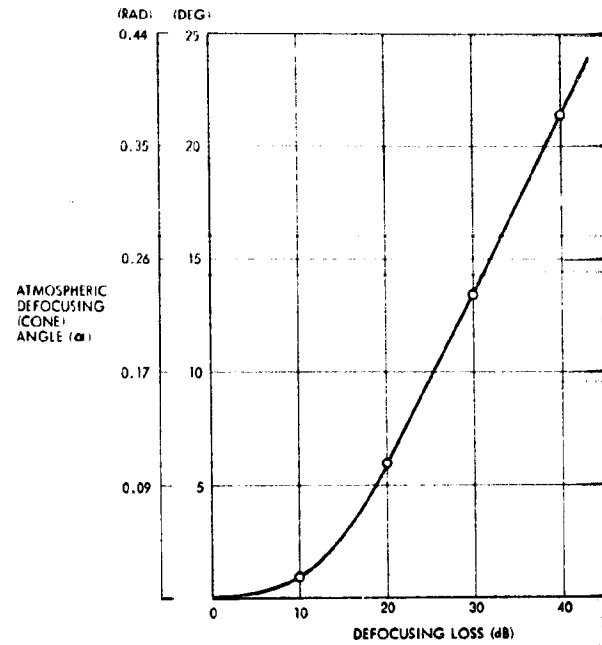


Table 8.2-30. X-Band

NO.	PARAMETER	NOMINAL	ADVERSE
1	FREQUENCY (MHZ)	8400	
2	RANGE [GIGAMETERS (AU)]	59.84 (0.4)	
3	TRANSMITTER POWER (DBM)	23.0	
4	TRANSMITTER CIRCUIT LOSS (DB)	-0.5	
5	TRANSMITTER ANTENNA GAIN (DB)	20.0	
6	POINTING LOSS (DB)	-0.1	
7	POLARIZATION LOSS (DP)	-0.1	
8	SPACE LOSS (DB)	-266.4	
9	ATMOSPHERIC LOSS (DB)	-0.2	
10	RECEIVER ANTENNA GAIN (DB)	71.6	
11	TOTAL RECEIVED POWER (DBM)	-152.7	
12	RECEIVER NOISE SPECTRAL DENSITY (DBM/HZ)	-182.7	
13	P _r /N ₀ (DB-HZ) (11-12)	30.0	
<u>CARRIER TRACKING PERFORMANCE (REAL TIME)</u>			
14	CARRIER MODULATION LOSS (DB)	0	
15	THRESHOLD LOOP BANDWIDTH (DB-HZ)	10	
16	LOOP SNR (DB) (13+14-15)	20.0	
17	REQUIRED LOOP SNR (DB)	10.0	
18	PERFORMANCE MARGIN (DB) (16-17)	10.0	
<u>OFFLINE DIGITAL PROCESSING PERFORMANCE</u>			
19	PROCESSING BANDWIDTH REQUIRED (DB-HZ)	4.8	
20	DIGITAL RECORDING LOSS (DB)	0.5	
21	REQUIRED SNR (DB)	0	
22	PERFORMANCE MARGIN (DB)	24.7	

NOTE: 4.2 DB LESS MARGIN AT 35 DAYS [97.24 GIGAMETERS (0.65 AU)]

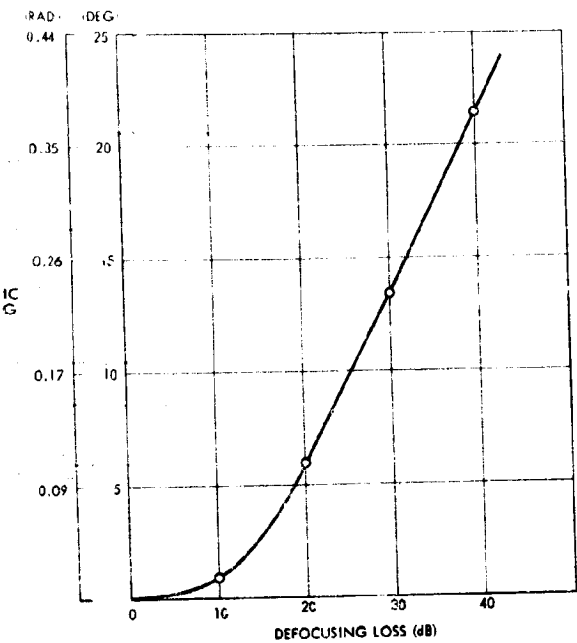


Figure 8.2-28. Occultation Defocusing Loss versus Defocusing Angle (S-band and X-band)

Table 8.2-30. X-Band Occultation

PARAMETER	NOMINAL	ADVERSE	NOTES
FREQUENCY (MHZ)	8400	-	
RANGE [GIGAMETERS (AU)]	59.84 (0.4)	-	ORBIT INSERTION
TRANSMITTER POWER (DBM)	23.0	1.0	200 MW
TRANSMITTER CIRCUIT LOSS (DB)	-0.5	0.2	
TRANSMITTER ANTENNA GAIN (DB)	20.0	0.3	BORESIGHT
POINTING LOSS (DB)	-0.1	-	0.017 RAD (1 DEG) ATTITUDE ERROR
POLARIZATION LOSS (DB)	-0.1	0.1	
SPACE LOSS (DB)	-266.4	-	
ATMOSPHERIC LOSS (DB)	-0.2	0.1	0.52 RAD (30 DEG) ELEVATION [0.17 RAD (10 DEG) ELEVATION ADVERSE]
RECEIVER ANTENNA GAIN (DB)	71.6	0.3	0.52 RAD (30 DEG) ELEVATION (30 MPH WIND) 64-METER
TOTAL RECEIVED POWER (DBM)	-152.7	1.2	RSS TOLERANCES
RECEIVER NOISE SPECTRAL DENSITY (DBM/HZ)	-182.7	2.3	39°K, 0.52 RAD (30 DEG) ELEVATION (66°K ADVERSE)
P_T/N_0 (DB-HZ) (11-12)	30.0	2.6	RSS TOLERANCES
CARRIER TRACKING PERFORMANCE (REAL TIME)			
CARRIER MODULATION LOSS (DB)	0	-	NO DATA OR RANGING
THRESHOLD LOOP BANDWIDTH (DB-HZ)	1	4	$2 B_{LO} = 10$ HZ
LOOP SNR (DB) (13+14-15)	20.0	2.6	RSS TOLERANCES
REQUIRED LOOP SNR (DB)	10.0	-	RECOMMENDED 810-5
PERFORMANCE MARGIN (DB) (16-17)	10.0	2.6	RSS TOLERANCES (MARGIN IS 4 DB WITH 0.21 RAD (1.2 DEG) OFFSET POINTING)
OFFLINE DIGITAL PROCESSING PERFORMANCE			
PROCESSING BANDWIDTH REQUIRED (DB-HZ)	4.8	1.2	3 HZ, ESTIMATED
DIGITAL RECORDING LOSS (DB)	0.5	0.5	ESTIMATED
REQUIRED SNR (DB)	0	1.0	ESTIMATED
PERFORMANCE MARGIN (DB)	24.7	3.1	RSS TOLERANCES

E: 4.2 DB LESS MARGIN AT 35 DAYS (97.24 GIGAMETERS (0.65 AU))

to John Love of TRW from Dr. Arrydas J. Kliore dated 2 April 1973. Tables 8.2-30 and 8.2-31 show that for received S- and X-band carrier levels of -142.9 and -152.7 dBm, respectively, defocusing losses of 35.8 and 24.7 dB can be tolerated. These numbers correspond to refraction angles of about 0.3 radian (18 degrees) for the S-band link and about 0.17 radian (10 degrees) for the X-band link. These calculations assume a required processing bandwidth of about 3 Hz and a required carrier-to-noise ratio in 3 Hz of 0 dB (a -178.7 dBm minimum S-band carrier level and a -177.4 dBm minimum X-band carrier level). Conversation with Dr. Fjeldbo has revealed that extraction of received signals with levels as low as -190 dBm or smaller is possible with increased processing integration time and a possible reduction of processing bandwidth. Also, under favorable conditions ground station noise levels may be lower than those used here, which were taken from JPL DSN Standard Practice, 810-5, Revision C. The increased integration times are possible under special situations where the received signal at the maximum defocusing angle may remain constant for several minutes, depending on the atmospheric and orbit geometry.

The occultation capability quoted in the previous paragraph [0.31 radian (18 degrees) at S-band, 0.17 radian (10 degrees) at X-band] assumed defocusing losses only. Atmospheric attenuation (absorption) also contributes to losses and may be several dB at S-band (up to 6 dB was experienced with Mariner 5 as shown in Figure 8.2-29) and possibly higher at X-band. These losses may somewhat reduce the proposed capability, but it can probably be regained with increased data processing. Atmospheric turbulence fading may also contribute to reduced received signal strength, but this effect is random and time varying and the average fading loss should be zero. This assumption is based on the conservation-of-energy approach to turbulence fading; for a more detailed discussion, see Appendix 7.6A, Probe Communications.

A question remains whether a one-way, two-way coherent, or two-way noncoherent mode of operation will be recommended for the S-band occultation experiment. Dr. Fjeldbo has indicated (in private communications) that because of atmospheric effects (defocusing, absorption,

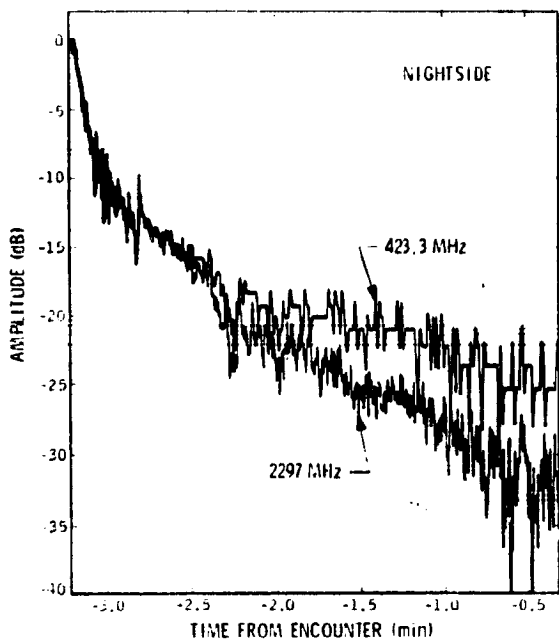


FIG. 8. Comparison of the amplitude variations produced by the atmosphere of Venus at 423.3 and 2297 MHz during immersion: No filtering was employed. The 423.3-MHz spacecraft receiver went out of lock 0.3 min before encounter.

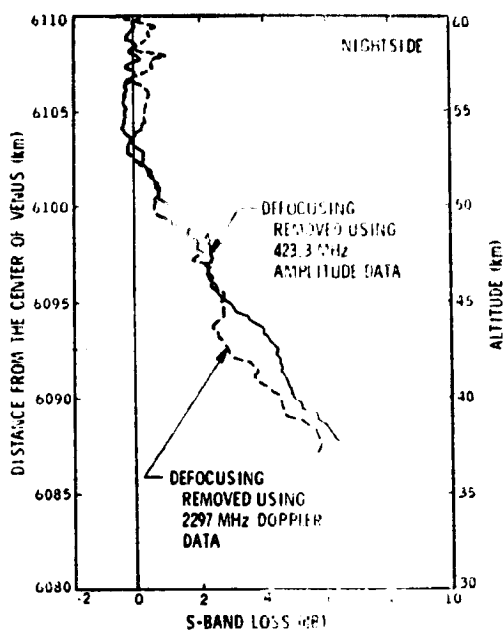


FIG. 9. Atmospheric propagation loss at S band versus the altitude of the lowest point on the radio ray: For the full-drawn curve, the defocusing was removed by using the 423.3-MHz amplitude data. For the stippled curve, the defocusing was computed from the Doppler data.

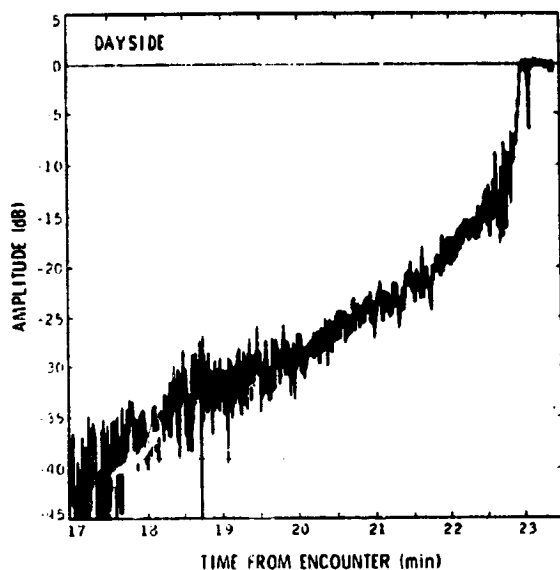


FIG. 13. Unfiltered amplitude perturbations produced by the atmosphere of Venus at 2297 MHz during emersion: Changes in the spacecraft antenna gain, caused by refraction, have been removed from the data.

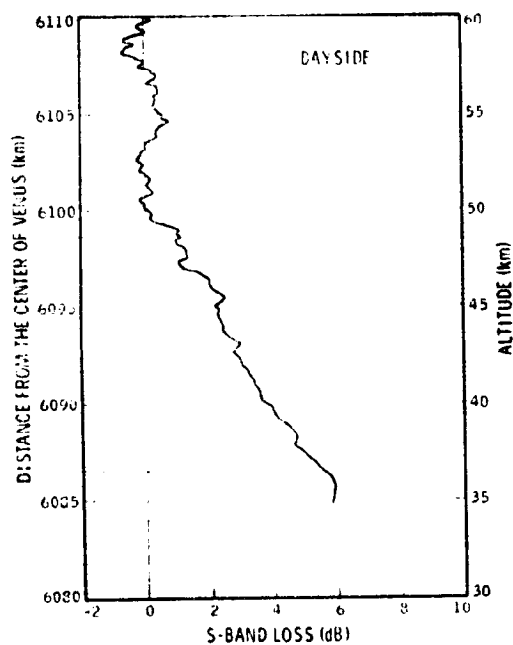


FIG. 18. Atmospheric propagation loss at S band versus the altitude of the lowest point on the radio ray.

Figure 8.2-29. Mariner V Occultation Data*

*Data from the Astronomical Journal, 76, No. 2, March 1971, No. 1387.

turbulence fading, etc.) a two-way coherent link may not be desirable; occasional loss-of-lock occurrences in the spacecraft receiver might possibly cause the spacecraft downlink to alternate between the coherent uplink and the auxiliary oscillator. If a two-way link is not recommended, a one-way link would want a stable oscillator; however, spacecraft ground operations may want a command uplink to the spacecraft during the occultation time period, hence the two-way noncoherent mode. But our recommended approach for occultation, repositioning the spacecraft prior to entry with no spacecraft precession or antenna gimbaling required, may reduce the desire for an uplink command capability at that time.

The choice of which mode of operation to implement may have a direct cost impact on the procurement of a spacecraft transponder. The only existing X-band transmitter has been an MVM 1973 unit built by Motorola to be compatible with the Motorola S-band receiver and transmitter driver. The X-band transmitter requires a 2F frequency drive signal (uplink is 221F), either in the coherent mode from the receiver or in the noncoherent mode from the S-band driver auxiliary oscillator. The preferred and possibly least expensive S-band transponder for the orbiter is the Viking Lander unit with an alternate being a TRW or Motorola design. Both the Viking unit and TRW development are presently noncompatible with the Motorola X-band transmitter, which represents a potential cost impact to accommodate X-band. For an approximate cost estimate, see Section 11.

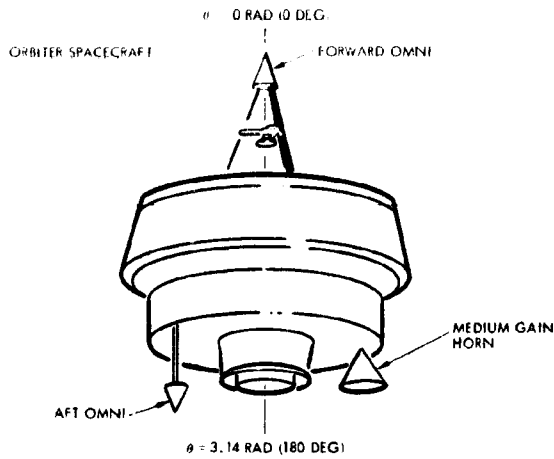
A question also exists on the desirability of turning off the data modulation for the occultation experiment, leaving all the transmitter power for the carrier. Our preferred orbiter configuration has a dual modulation index capability for data reasons. An extra advantage of this dual modulation index capability is that the low radian index can be used for occultation, leaving all but 1.3 dB of the total transmitted power in the carrier. This level is 4.8 dB higher than the carrier power in the normal communications mode, providing about 0.07 radian (4 degrees) more defocusing capability, and this mode is recommended for the occultation experiment.

The defocusing capabilities of the S- and X-band links are not the same and the respective horn beamwidths are not identical (based on low cost off-the-shelf antennas). Therefore, which angle to choose for prepositioning the spacecraft prior to occultation is not obvious. The optimum angle for X-band above would be 0.17 radian (10 degrees); at this angle the pointing loss due to the antenna pattern would be about 5 dB, but the EIRP would still be sufficient to maintain real time tracking prior to occultation. For S-band the optimum angle would be 0.31 radian (18 degrees), corresponding to about 5 dB pointing loss and real time tracking at 128 bits/s. A compromise offset angle recommended here for the chosen antennas is about 0.21 radian (12 degrees). At this offset angle, the X-band defocusing angle of 0.17 radian (10 degrees) is achieved within a few tenths of a dB of beam peak and the S-band 0.31-radian (18-degree) defocusing coverage is accomplished by "riding" up one side of the antenna beam 0.21 radian (12 degrees) to beam peak and 0.10 radian (6 degrees) over the other side, only 0.5 dB down. A slightly larger offset angle would be recommended if digital processing sensitivity were increased beyond the -178 dBm carrier level, as mentioned previously.

The recommended approach discussed here is to have occultation capability during entrance (immersion) only and none during exit (emersion) to minimize spacecraft operations. Also, no occultation capability is planned with the high gain dish, after the second flip maneuver, since the narrow beamwidth and the conscan mode would require spacecraft precession to follow the defocused ray.

Antennas. The preferred orbiter spacecraft antenna subsystem consists of four separate antennas which are used for conscan and TT&C during the transit, orbit insertion, and Venus orbit phases of the mission. As shown in Figure 8.2-30, the primary downlink antennas are the forward dish antenna and aft horn. An offset feed in the dish provides a 1 dB beam crossover reference for conscan, while an off axis aft omnidirectional antenna provides aft pattern coverage for launch and doppler attitude reference between 110 and 235 days of the mission. A forward omnidirectional antenna provides TT&C coverage during orbit insertion. Use of existing flight qualified designs was the major factor in the selection of

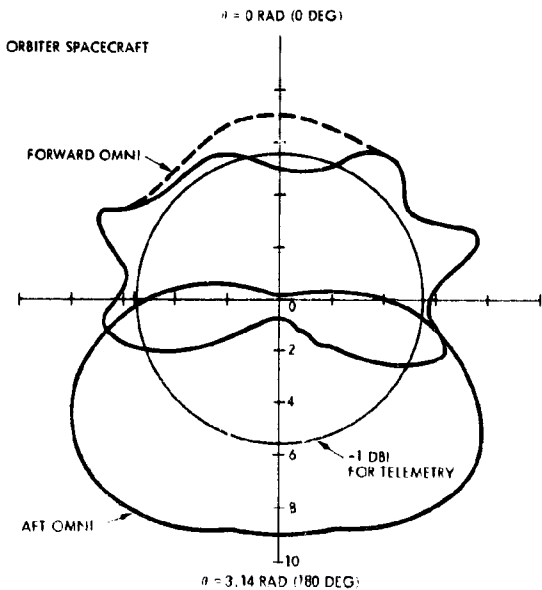
A ANTENNA LOCATIONS



C OMNI COVERAGE

NOTE:

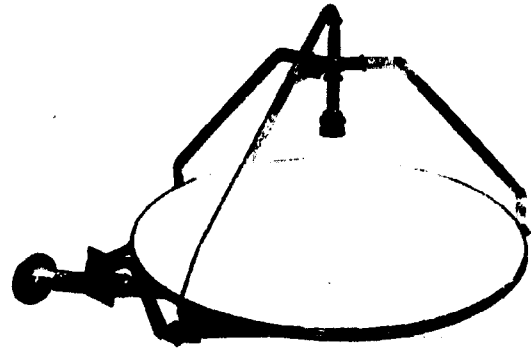
- SPHERICAL COVERAGE FOR TELEMETRY AND COMMAND IS PROVIDED
- THE SAME ANTENNAS ARE USED ON BOTH SPACECRAFT
- BOTH ANTENNAS HAVE BEEN FLOWN ON OTHER SPACECRAFT
- AFT COVERAGE OF THE ORBITER SPACECRAFT OMNI WILL BE SUPPLEMENTED BY THE MEDIUM GAIN HORN AND THE FORWARD COVERAGE BY THE HIGH GAIN ANTENNA
- PREVIOUS EXPERIENCE ON OTHER SIMILAR DESIGN SHOWS THAT SOME PATTERN ENHANCEMENT IS POSSIBLE ON THE ORBITER FORWARD OMNI AS SHOWN BY THE DOTTED LINE



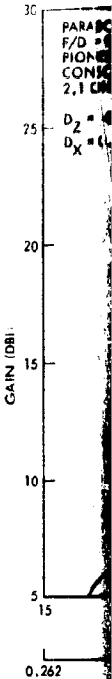
B ORBITER SPACECRAFT ANTENNAS

HIGH GAIN ANTENNA
(INCREASED DIAMETER DSCS DISH)

- FORWARD OMNI ANTENNA
(SAME AS THE PROBE BUS SPACECRAFT AFT OMNI ANTENNA)
- MEDIUM GAIN HORN
(SAME AS THE PROBE BUS SPACECRAFT MEDIUM GAIN HORN)
- AFT OMNI ANTENNA
(SAME AS THE PROBE BUS SPACECRAFT FORWARD OMNI ANTENNA)



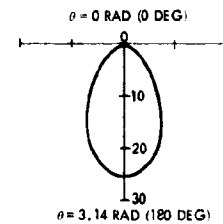
DSCS HIGH GAIN ANTENNA



MEDIUM GAIN HORN
(PIONEER 10 AND 11 MEDIUM GAIN HORN)



DB PATTERN (FREE SPACE)
f = 2.3 GHZ
POLARIZATION: RHCP
PLANE: theta = VAR., phi = 1.57 RAD (90 DEG)



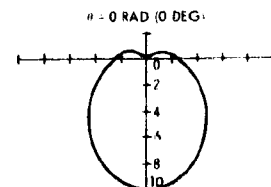
CHARACTERISTICS
FREQUENCY
POLARIZATION
PEAK GAIN
HALF POWER
VSWR
AXIAL RATIO
WEIGHT:

DESCRIPTION
• FLOWN
• CORNER
• CROSS

HIGH GAIN DISH FEED HORN
(PIONEER 10 AND 11 FEED HORN)

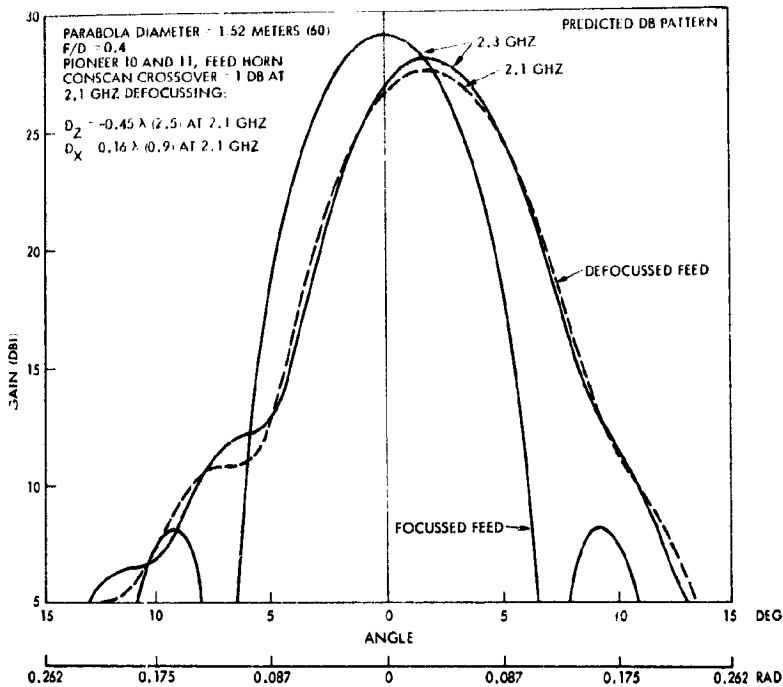


VOLTAGE PATTERN (FREE SPACE)
f = 2.3 GHZ
POLARIZATION: RHCP
PLANE: theta = VAR., phi = 1.57 RAD (90 DEG)



CHARACTERISTICS
FREQUENCY
POLARIZATION
PEAK GAIN
HALF POWER
VSWR
AXIAL RATIO
WEIGHT:

DESCRIPTION
• CONICAL
• CROSS



CHARACTERISTICS:

FREQUENCY:	2.1 GHZ	2.3 GHZ
POLARIZATION:	RHCP	RHCP
PEAK GAIN:	27.5 DBI	28.0 DBI
HALF POWER BW:	0.113 RAD (6.4 DEG)	0.105 RAD (5.8 DEG)
VSWR:	1.5:1	1.5:1
AXIAL RATIO (3°):	1.5 DB	1.5 DB
WEIGHT:	<6.0 KG	

DESCRIPTION:

- 1.52 M PARABOLIC HONEYCOMB SANDWICH DISH SIMILAR TO DSCS
- PIONEER 10 AND 11 HIGH GAIN FEED ON TRIPOD SUPPORT
- FEED DEFOCUSSED AND OFFSET Laterally for CONSCAN
- CONSCAN CROSS OVER AT 1 DB IS APPROXIMATELY 0.035 RAD (2.0 DEG)

CHARACTERISTICS:

FREQUENCY:	2.1 GHZ	2.3 GHZ
POLARIZATION:	RHCP	RHCP
PEAK GAIN:	>15.0 DBI	>15.5 DBI
HALF POWER BW:	>32 DEG	>28 DEG
VSWR:	<1.5:1	<1.5:1
AXIAL RATIO (±10°):	<1.5 DB	<4.5 DB
WEIGHT:	<1.5 DB	<1.7 KG

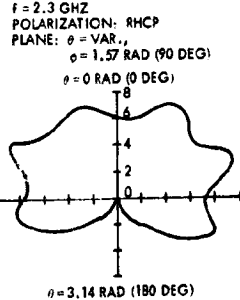
DESCRIPTION:

- FLOWN ON PIONEERS 10 AND 11
- CORRUGATED CONICAL HORN
- CROSS DIPOLE FEED

FORWARD-OMNI ANTENNA (PROJECT DSP CIRCUIT LOG SPIRAL)



VOLTAGE PATTERN (FREE SPACE)



CHARACTERISTICS:

FREQUENCY:	2.1 GHZ	2.3 GHZ
POLARIZATION:	RHCP	RHCP
PEAK GAIN:	>2 DBI	>2 DBI
VSWR:	<2:1	<2:1
AXIAL RATIO (±90°) (±1.57 RAD (90 DEG))	<4 DB	<4 DB
WEIGHT:	<0.41 KG	

DESCRIPTION:

- FLOWN ON DSP SPACECRAFT
- TWO ARM PRINTED CIRCUIT CONICAL LOG SPIRAL FEED WITH INFINITE BALLUN CABLE (2° = 0.26 RAD (15 DEG))
- EPOXY FIBERGLASS RADOME FOAM FILLED

CHARACTERISTICS:

FREQUENCY:	2.1 GHZ	2.3 GHZ
POLARIZATION:	RHCP	RHCP
PEAK GAIN:	7 DBI	7.5 DBI
HALF POWER BW:	1.397 RAD (79 DEG)	1.325 RAD (76 DEG)
VSWR:	<2.0:1	<1.5:1
AXIAL RATIO (±0.87 RAD (50 DEG))	<3.5 DB	<4 DB
WEIGHT:	0.5 KG	

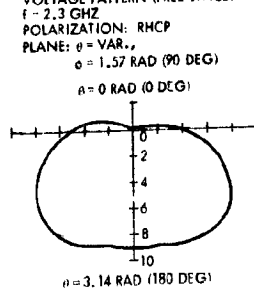
DESCRIPTION:

- CONICAL HORN EXCITED BY A CROSSED DIPOLE

AFT OMNI ANTENNA (PIONEER 10 AND 11 PROGRAM 169 CONICAL LOG SPIRAL)



VOLTAGE PATTERN (FREE SPACE)



CHARACTERISTICS:

FREQUENCY:	2.1 GHZ	2.3 GHZ
POLARIZATION:	RHCP	RHCP
PEAK GAIN:	>4 DBI	>4 DBI
VSWR:	<1.5:1	<1.5:1
AXIAL RATIO (±1.57 RAD (90 DEG))	<4.5 DB	<4.5 DB
WEIGHT:	<0.14 KG	

DESCRIPTION:

- FLOWN ON PIONEER 10 AND 11 AND PROJECT 169 SPACECRAFT
- TWO ARM PRINTED CIRCUIT CONICAL LOG SPIRAL FEED WITH ROBERT'S BALUN (2° = 0.35 RAD (20 DEG))
- EPOXY FIBERGLASS RADOME, FOAM FILLED

Figure 8.2-30. Baseline Orbiter Spacecraft Antennas

the baseline antenna subsystem configuration. All subsystem component designs have been flown on Pioneers 10 and 11, DSP, or DSCS spacecraft and represent lightweight, multiple use, lowest cost, and lowest design risk approaches compatible with the communications subsystem requirements. The high-gain dish feed, the aft omni antenna, the aft horn, the diplexers, and RF switches are all Pioneers 10 and 11 designs which are usable without modifications. The forward omni antenna is a DSP design which is usable without modifications and the dish is a larger diameter DSCS dish.

Transponder. As mentioned earlier, of the three companies developing lightweight S-band transponders, only Philco-Ford has units qualified for space use. Their Viking Lander unit is presently in the qualification cycle. Where weight is very important, such as with the Thor/Delta bus, probes, and orbiter described in following sections, the choice of a lightweight design is clear. For the Atlas/Centaur orbiter, where weight is not so critical, the choice is not so obvious, particularly since the Pioneers 10 and 11 has been selected for the probe bus. A lightweight transponder was selected because: 1) enough Pioneers 10 and 11 residuals are not available to supply both the bus and orbiter, and 2) the costs of new Pioneers 10 and 11 transponders are comparable to buying new lightweight designs.

A preliminary conclusion of the study is to use the Viking Lander transponder, based on its present development status. Since the contract awards for hardware development are at least a year away, this decision is subject to continuing review. To ensure the best available hardware, the procurement specifications have been written to allow units from any of the potential bidders. This preliminary specification was reviewed with both Motorola and Philco-Ford and it is TRW's understanding that both companies should be able to meet the requirements with existing or planned designs.

A summary of the requirements and characteristics of the lightweight transponders, i.e. receivers and transmitter driver, is given in the following sections.

1) Lightweight S-band Receiver. A short summary of the performance requirements for the orbiter receiver is given in Table 8.2-31. Designs from both Philco-Ford and TRW are covered in the next two sections.

Table 8.2-31. S-Band Receiver Performance Requirements

RECEIVING FREQUENCY RANGE (FACTORY PRESET):	2110-2120 MHZ
NOISE FIGURE (MAXIMUM):	6.5 DB
INPUT VSWR (MAXIMUM):	1.3:1
ACQUISITION THRESHOLD (LOOP SNR = 6.0 DB)	-148 DBM
LOOP NOISE BANDWIDTH AT THRESHOLD	20 HZ
LOOP NOISE BANDWIDTH - STRONG SIGNAL:	TBD
FREQUENCY OFFSET TRACKING CAPABILITY:	±126 KHZ
STATIC PHASE ERROR:	
±126 KHZ OFFSET AT -120 DBM	0.1 RAD
±63 KHZ OFFSET AT -148 DBM	0.2 RAD
DYNAMIC PHASE ERROR:	
±40 HZ/S OVER ±126 KHZ AT -120 DBM	0.7 RAD
±50 HZ/S OVER ±63 KHZ AT -148 DBM	0.7 RAD
±20 HZ/S OVER ±63 HZ AT -148 DBM	0.6 RAD
DYNAMIC RANGE:	100 DB
IMAGE REJECTION:	55 DB
VCO FREQUENCY STABILITY ALL CONDITIONS:	(± 5 PARTS/10 ⁶)/5 HR
PHASE STABILITY (COHERENT OUTPUT - S-BAND):	0.05 RAD (2.8 DEG RMS), 0.14 RAD (8.4 DEG) PEAK
COMMAND DEMODULATION:	"0" FOR 128 HZ, "1" FOR 204 HZ
COHERENT DRIVE TO TRANSMITTER:	REQUIRED
COHERENT MODE INHIBIT:	REQUIRED
DISABLE COHERENT DRIVE:	<-60 DBM
FSK SUBCARRIER OUTPUT:	10 ± 2 V PEAK TO PEAK
AGC CONSCAN OUTPUT:	
AC OUTPUT	100 MV ± 1 DB
S/N (-135 DBM 2 % AM)	-4 DB · HZ
SOURCE IMPEDANCE	10 KΩ
LOAD IMPEDANCE	165 KΩ
AUTOMATIC GAIN CONTROL CLOSED LOOP BANDWIDTH 3 DB	2 HZ ± 50%
TELEMETRY:	TBD
DESIGN AND CONSTRUCTION:	
SIZE	TBD
WEIGHT	1.6 KG (3.5 LB)
ENVIRONMENTAL:	
TEMPERATURE	5.6 TO 60°C
VIBRATION	TBD
SHOCK	TBD
INPUT VOLTAGE:	28 VDC ± 2%
INPUT POWER:	<3 WATTS

a) Philco-Ford Receivers. Philco-Ford has developed a product line of micro-miniature S-band hardware for both "near" and "deep" space applications. A deep space receiver being developed for the Viking Lander mission is presently being qualified. This unit appears to meet the Pioneer Venus mission requirements. The block diagram given in Figure 8.2-31 is similar to the Viking design.

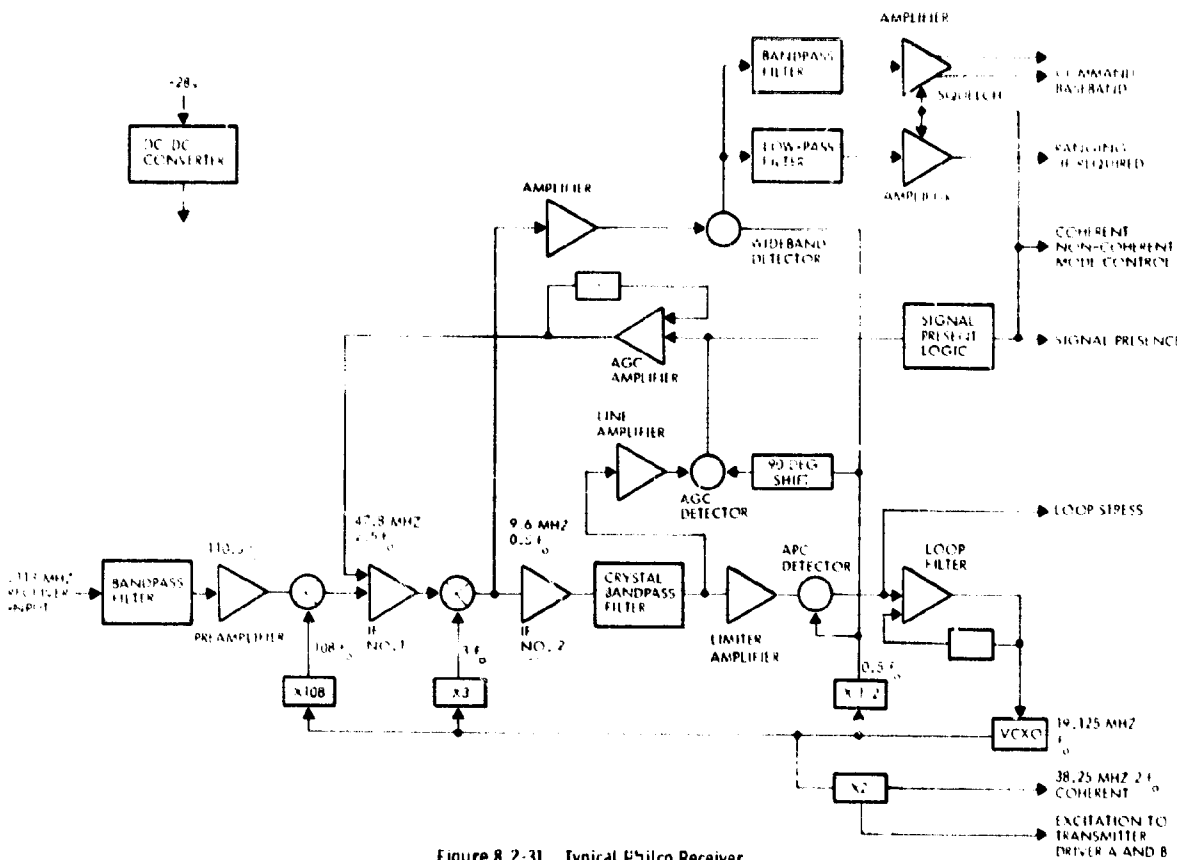


Figure 8.2-31. Typical Philco Receiver

The block diagram shows a double conversion, phase-locked loop design very similar to that originally developed for Defense Support Program (DSP) applications. It differs from the near space unified S-band system (USBS) designs in that a narrow 18 Hz loop noise bandwidth is utilized to reduce the acquisition threshold to about -150 dBm. To allow cross-strapping for redundancy, the receiver has two outputs to the command baseband circuitry and to the coherent transmitters. The present design is physically packaged with its companion transmitter and two

DC/DC converters. The receiver portion of the package (including converter) is made up of nine modules mounted on an interconnection chassis.

b) TRW Lightweight Receiver. In Figure 8.2-32, a block diagram is given for the DSN compatible receiver being developed at TRW. It is very similar in size, weight, and construction details to that being developed by Philco-Ford. Although this particular design is being developed during 1973, existing programs for similar type hardware have developed a solid technology and manufacturing base. The only noticeable difference in block diagrams given is that the TRW design utilizes an offset oscillator operating at f_r , the second IF frequency. This technique allows the second IF to be set at some frequency other than one subharmonically related to the first IF. This allows greater freedom in designing to reduce spurious responses and eliminates certain false lock problems. This design technique has been used on both DSP and USBS designs. TRW will compare its in-house design from both technical and cost standpoints to the Philco-Ford and the Motorola units.

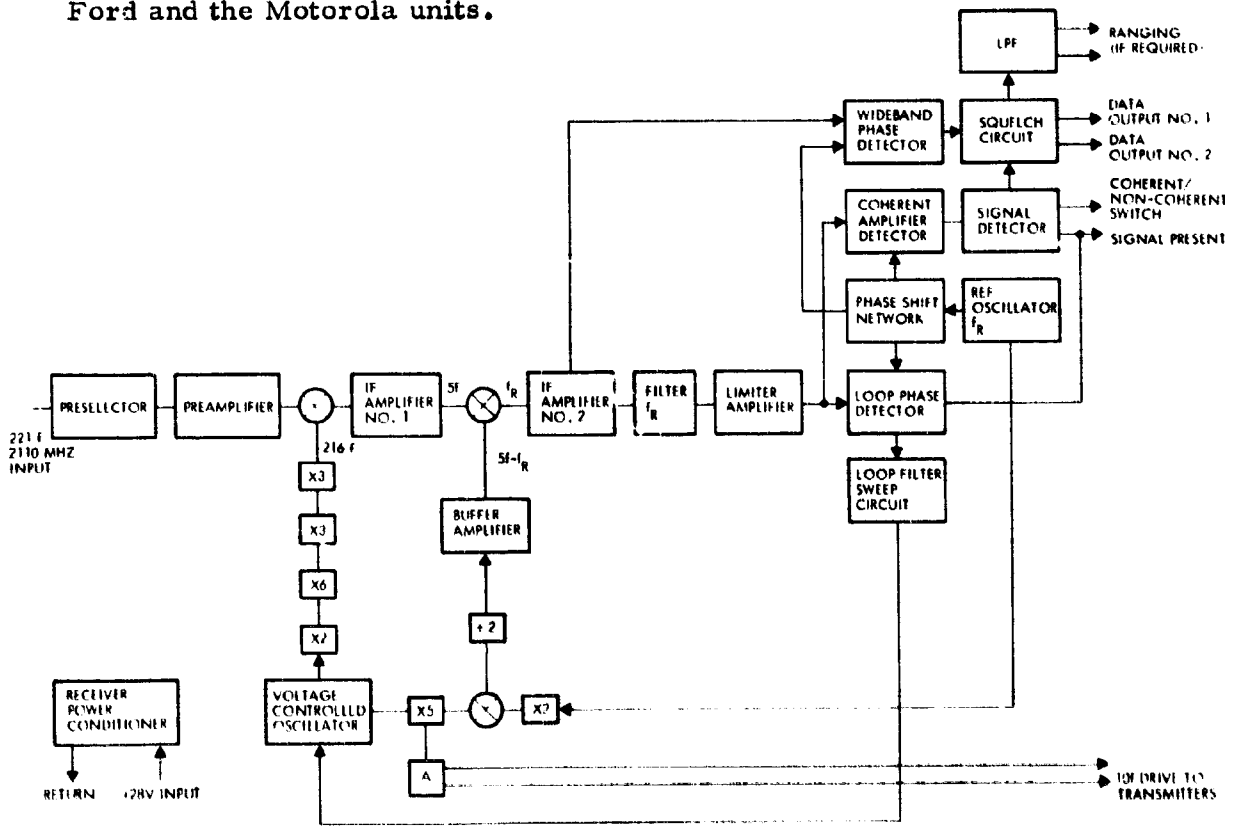


Figure 8.2-32. TRW Lightweight Receiver

2) Lightweight S-band Transmitter Drivers. The requirements for the transmitter driver and power amplifiers can be satisfied by modifications to existing designs from a number of companies. Any company with an SGLS design can easily modify the multiplication ratio to that required by the DSN. It has been TRW's experience, however, that the potential savings from separate bids on the receiver and transmitters is more than offset by contractual and interface problems. It is, therefore, TRW's intent to procure the transmitter driver from the same company that provides the transponder receiver. This limits the field, as previously discussed, to Philco-Ford, Motorola, and TRW. Block diagrams for a Philco-Ford and TRW lightweight transmitter driver are shown in Figure 8.2-33. Pertinent characteristics for each of these units are given in Table 8.2-32.

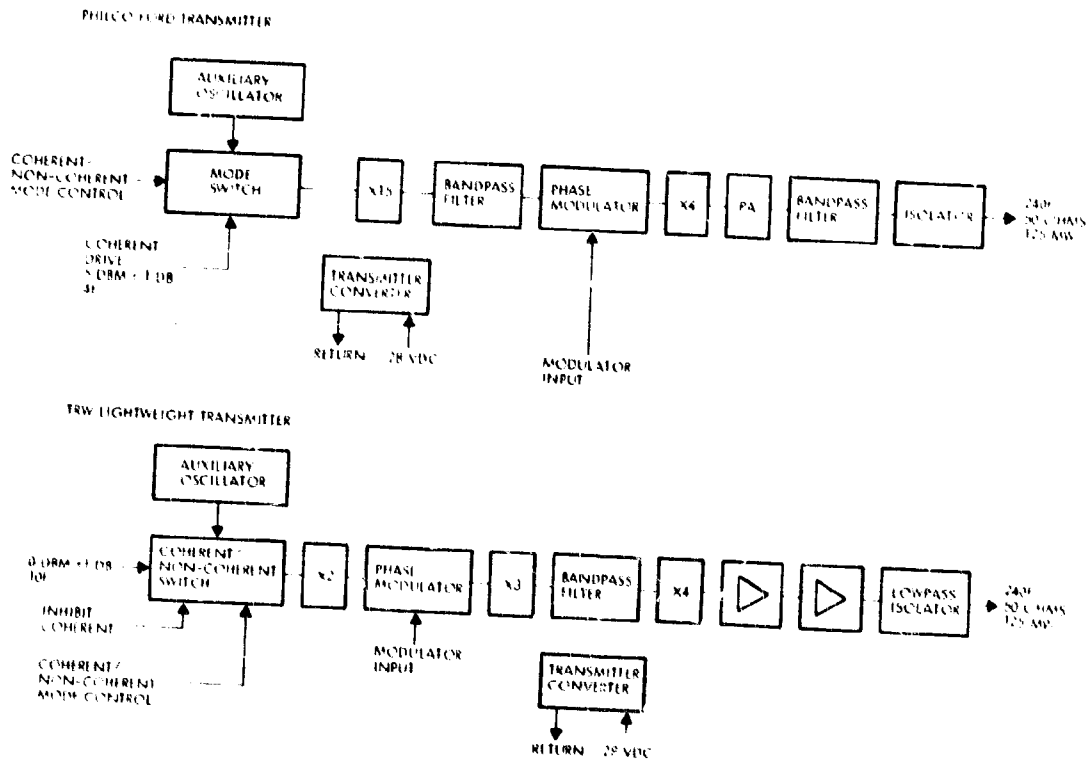


Figure 8.2-33. Transmitter Drivers

The baseline transmitter driver for the Atlas/Centaur orbiter is the Viking Lander. In its present state it is packaged together with the receiver in four modules (including a DC/DC converter) mounted on a

Table 8.2-32. Transmitter Driver Characteristics

	TRANSMITTER DRIVERS	
	VIKING LANDER	TRW LIGHTWEIGHT
FREQUENCY OF OPERATION		
INPUT	38.3 MHZ (4 f)	95.5 MHZ (10 f)
OUTPUT	2290 TO 2300 MHZ	2290 TO 2300 MHZ
DRIVE LEVEL REQUIRED	5 DBM ± 1 DB	0 DBM ± 1 DB
INPUT IMPEDANCE	50 Ω	50 Ω
INPUT VSWR	1.3:1	1.3:1
MODULATION		
TYPE	LINEAR PHASE	LINEAR PHASE
SENSITIVITY	±0.5 RAD/VOLT	±1.0 RAD/VOLT
STABILITY	±0.1 RAD	±0.1 RAD
OUTPUT POWER (MINIMUM)	125 MW	125 MW
SPURIOUS LEVELS	50 DB	40 DB
FREQUENCY STABILITY, AUXILIARY OSCILLATOR		
SHORT TERM (0.25 S)	3×10^{-10} (MUST MODIFY)	3×10^{-11}
LONG TERM	-	4×10^6 10 HR (-1 TO 32°C)
INPUT VOLTAGE	+28 VDC ± 25%	+28 VDC ± 15%
INPUT POWER	3 WATTS	3 WATTS
ENVIRONMENTAL		
TEMPERATURE	-11 TO 60°C	-9 TO 64°C
VIBRATION (SINE/RANDOM)	10/7.5	-/20
SHOCK	1200 G/3.2 KHZ	-

"mother" chassis common to the receiver. A review of the block diagram for a typical Philco transmitter shows it to be very similar to the TRW design. Both provide S-band power amplification to provide maximum efficiency. They differ primarily in the input frequency and the overall multiplication ratio. Both provide a receiver controlled noncoherent auxiliary oscillator.

3) Transponder Modifications, X-band Occultation Experiment. A requirement for an X-band occultation experiment has been reviewed during the study. The Version IV science payload includes a requirement for the X-band link using, for example, an existing (GFE) MVM 1973 X-band transmitter manufactured by Motorola. On reviewing the MVM 1973 design, it was established that the required coherent drive signal from the S-band receiver must be at 2/221 (2f) times the received S-band signal. This is compatible with the Mariner transponder, but not compatible with

the coherent drive available from the Viking Lander, TRW Lightweight, or Pioneers 10 and 11 transponders.

In each of these designs the basic VCXO frequency in the receiver is the required $2f$. It would appear that only a minor modification is required to the receivers to provide this $2f$ output through a buffer amplifier. These modifications would allow two-way coherent S- and X-band operation.

If it is required to provide one-way operation of S- and X-band (both coherent to the auxiliary oscillator in the S-band transponder), then modifications to the candidate transponder designs are more extensive. Only the Motorola designs will work with the MVM 1973 without any change.

The Viking Lander coherent drive and transmitter driver auxiliary oscillator work at $4f$, or twice that required by the MVM 1973 X-band transmitter. The TRW lightweight design coherent drive is at $10f$ and the Pioneers 10 and 11 design provides $12f$.

No proposals have been received for the transponders and no determination has yet been made of the cost that must be added to the S-band transponder to accommodate the X-band experiment.

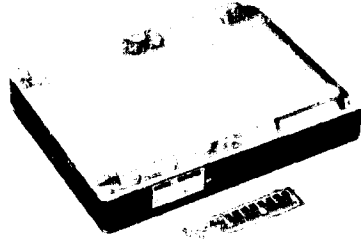
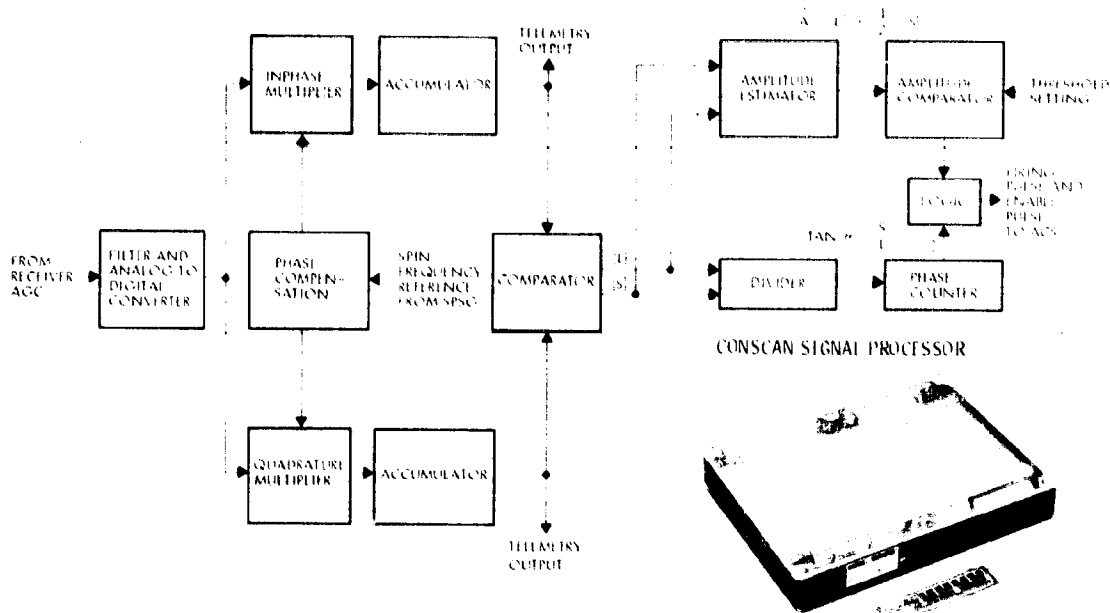
A preliminary estimate of at least \$25,000 to accommodate only the coherent two-way operation would appear reasonable. To provide both one-way and two-way X-band compatibility would probably cost at least \$50,000 additional. These costs should be recognized as costs to accommodate the science requirements; they are not a basic orbiter cost.

Power Amplifier

The power amplifier specified in the preferred Atlas/Centaur orbiter is identical to that described for the Atlas/Centaur bus, i.e., a 6-watt solid-state amplifier. A description of the unit was provided in the bus section.

Conscan Signal Processor

The selected digital conscan signal processor is the flight-proven unmodified Pioneers 10 and 11 unit (see Figure 8.2-34). It meets all Pioneer Venus functional requirements, is light [0.4 kilograms (0.8 pound)],



CONSCAN PROCESSOR CAPABILITY

CAPABILITY	CONSCAN PULSE FREQUENCY	THRESHOLD SETTING (DEAD ZONE)		PHASE COMPENSATION	
		MEDIUM-GAIN ANTENNA MODE	HIGH-GAIN ANTENNA MODE	MEDIUM-GAIN ANTENNA MODE	HIGH-GAIN ANTENNA MODE
	ONCE EVERY 3 REVOLUTIONS OR ONCE EVERY 2 REVOLUTIONS SELECTED BY JUMPER WIRE.	0 TO 90 MV, ADJUSTABLE IN 0.4 MV STEPS BY PROGRAMMABLE PLUG.		0.78 RAD - 45 DEG ADJUSTABLE IN 0.025 RAD - 1.4 DEG STEPS BY PROGRAMMABLE PLUG.	0.78 RAD - 45 DEG ADJUSTABLE IN 0.025 RAD - 1.4 DEG STEPS BY PROGRAMMABLE PLUG.
PIONEER VENUS REQUIREMENT	ONCE EVERY 2 REVOLUTIONS	28 MV	48 MV	LESS THAN 0.78 RAD - 45 DEG	LESS THAN 0.78 RAD - 45 DEG

Figure 8.2-34. Digital Conscan Signal Processor

low power (1.2 watts), and highly reliable. The processor estimates the phase and the amplitude of the 0.08 Hz (4.8 rpm) conscan signal embedded in noise and interference produced by wobble, antenna pattern distortion, and other sources. The conscan signal phase determines the precession thruster firing while the amplitude, which is proportional to earth aspect angle, terminates conscan when the selected threshold (deadzone) is reached. The digital implementation closely approximates an optimum maximum likelihood phase and amplitude estimator. The processor requires an accurate frequency (spin rate) reference which is supplied by the sun sensor. (See Section 8.5, Attitude Determination and Control, for the conscan functional description.)

Subsystem Weight and Power Summary

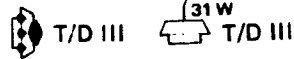
The preferred Atlas/Centaur orbiter communication subsystem weight and power is summarized in Table 8.2-33.

Table 8.2-33. Communications Subsystem Weight and Power Summary

ITEM	QUANTITY	WEIGHT KG (LB)	DC POWER (WATTS)
RECEIVER	2	1.4 (3.2)	7.0
CONSCAN PROCESSOR	1	0.4 (0.8)	1.2
TRANSMITTER DRIVER	2	1.1 (2.4)	3.5
POWER AMPLIFIER	2	0.2 (1.2)	22.0
HYBRID	1	0.05(0.1)	
DIPLEXERS	2	1.9 (4.3)	
SWITCHES	6	1.6 (3.6)	
AFT OMNI	1	0.1 (0.3)	
FORWARD OMNI	1	0.4 (0.9)	
ANTENNA (5-FOOT DISH)	1	3.3 (7.3)	
AFT HORN	1	1.5 (3.3)	
RF COAX AND CONNECTOR	A/R	1.4 (3.0)	
TOTAL		14.7 (32.4)	33.7

NOTE: THESE WEIGHTS WERE CHANGED SLIGHTLY SUBSEQUENT TO PREPARATION OF MASS PROPERTIES TABLES IN SECTION 6 OF THIS REPORT.

8.2.5 Recommended Communications Subsystem



8.2.5.1 Probe Bus (1977 Probe Mission Launch)



The recommended probe bus configuration is earth pointing for both the Thor/Delta and Atlas/Centaur versions for the 1977 launch and Version III science payload. For most of the cruise period and during entry the aft end of the spacecraft is pointed at earth, i.e., the spacecraft spin axis is pointed towards earth within an angle constrained by the beamwidth of the aft-pointing directional antenna. For launch, midcourse maneuvers, and probe release sequences, communication coverage is provided by a pair of omnidirectional antennas, one forward and one aft. The antennas are interconnected through switches and diplexers to redundant receivers, transmitter drivers, and power amplifiers. The block diagram is shown in Figure 8.2-35 along with a weight and power summary.

The Thor/Delta payload weight limitation constraints the communication subsystem to a low weight design, a 1.8-kilogram (1-pound) Viking transponder and a 0.45 kilogram (1-pound) solid-state power amplifier. The power amplifier will have a dual output power level capability (3 and 6 watts) to reduce the solar array sizing requirement. The output level will be controlled by the DC supply voltage, 28 volts for 6 watts and

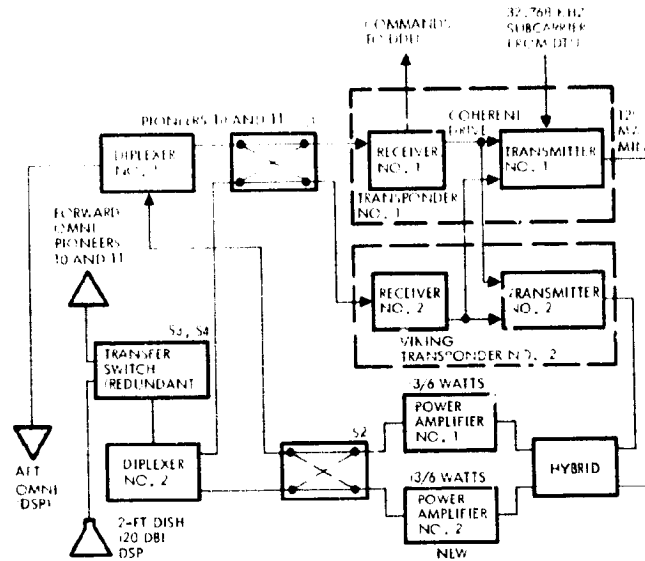


Figure 8.2-35. Thor Delta Communications Subsystem

21 volts for 3 watts. The Atlas/Centaur payload capability allows the use of residual Pioneers 10 and 11 transponders, 3.1-kilograms (6.8 pounds), and 8-watt TWTA's, 1.8-kilograms (4 pounds), without making any new units, resulting in considerable cost savings. The preferred directional antennas is a 0.35 meter (2-foot) diameter parabolic dish, flown on the Defense Support Program (DSP) with greater than 20 dBi gain and one sided half-power beamwidth of 0.113 radians (6.75 degrees). The 1977 launch allows bus entry with the ram and earth directions colinear and therefore permits use of such a narrowbeam antenna. The forward omni is a Pioneers 10 and 11 unit and the aft omni is a DSP unit. The diplexers and switches are also Pioneers 10 and 11 qualified units. The Viking Lander transponder is presently going through qualification but the solid-state power amplifiers, as required for this program, would have to be qualified for space use.

All three antennas are located off-axis because of the centered location of the large probe on the forward end and the launch vehicle adapter on the aft end. The off-axis antenna locations are advantageous for attitude control, however, as they provide spacecraft pointing information through doppler spin modulation.

During launch and through the first midcourse maneuver as a minimum, the two omni antennas will be separately connected to the two receivers and two transmitters through switches S1 and S2, respectively. The aft dish will be disconnected during this phase and will not be required until 55 days into the mission. By this time switches S3 or S4 will be activated to connect the dish to a receiver and transmitter as the forward omni is disconnected, nominally not to be required for the remainder of the mission. Switch S4 is included to prevent a single point bus-entry mission failure if switch S3 failed in the forward omni position.

The communications bit rate capability with the 26-meter network during cruise varies from 16 to 1024 bits/s as antennas, power levels, and range vary during the mission. Probe release and bus entry are handled by the 64-meter network at 16 and 1024 bits/s respectively.

DSN Configuration During Probe and Bus Entry

It is desirable, from the standpoint of the number of available receivers at the two 64-meter tracking stations at entry, to have the bus tracked in a two-way mode by the 26-meter stations. Two constraints prohibit the 26-meter stations from tracking the bus all the way through bus entry: two-way doppler rate and the entry high data rate requirement (512 bits/sec). The buildup of two-way doppler rate from 2 hours before bus entry (~ 0 Hz/s) to entry (~ 60 Hz/s) limits the Block III receiver tracking capability to about 1/2 to 1 hour before entry (10-25 Hz/s); see JPL Technical Report 32-1526, Vol. XIII, page 23 and also Vol. X, page 168. Also, the 26-meter station can support no more than 128 bits/s at bus entry for the preferred bus EIRP. For both these reasons the bus entry should be delayed from the last probe "touchdown" at the surface a minimum of 1/2 to 1 hour. This allows one receiver per probe per 64-meter station during simultaneous probe entry and two receivers per probe per station if a sequential probe entry sequence (two at a time) were used. Predetection recording would be accomplished at each 64-meter station with a fifth receiver operated in an open-loop mode. After the last probe impacts the surface, the 64-meter station with Block IV receivers would be available to track the last 1/2 to 1 hour bus entry with a programmable doppler rate capability and also to give a 1024 bits/s entry telemetry capability.

Performance Data

The mission data rate profile for the preferred Thor/Delta configuration is shown in Figure 8.2-36. Telemetry power budgets for probe release and bus entry are shown in Table 8.2-34, and an uplink power budget using a 26-meter station in a two-way tracking mode only is shown in Table 8.2-35. The uplink margin is greater than 30 dB, sufficient for a good two-way tracking data. The resulting receiver SNR of about 40 dB is sufficient for the bus to track uplink doppler rates up to 30 Hz/s with the receiver phase error remaining within ± 0.052 radian (± 3 degrees).

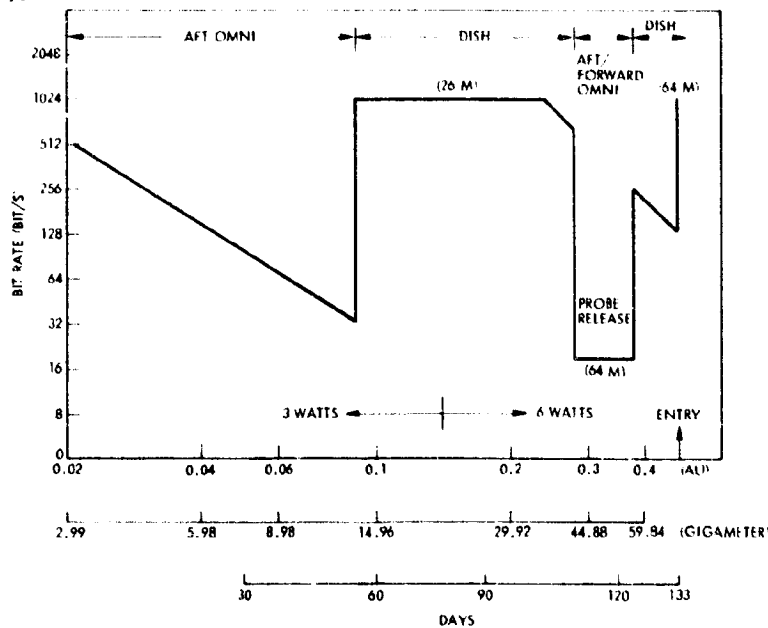


Figure 8.2-36. Bus Telemetry Rate History

The data rate profile shows two transmitter power output levels, 3 and 6 watts. The 6-watt power level is required for receiver carrier tracking with the 64-meter station during probe release while the bus is transmitting through an omni antenna of -2 dBi minimum gain. This mission design point also establishes the modulation index requirement at 0.66 radians. At probe release the link is sized at 16 bits/s, allowing for an 8 bits/s backup mode in case of any unforeseen performance degradations. The alternate 3-watt level is used to minimize the sizing of the solar array at 149.6-gigameters (1 AU) where the earth-spacecraft

Table 8.2-34. Bus Telemetry Design Control Tables

NUMBER	PARAMETER	PROBE RELEASE		ENTRY		NOTES	
		NOMINAL	ADVERSE	NOMINAL	ADVERSE	PROBE RELEASE	ENTRY
1	FREQUENCY (MHZ)	2300	0	2300	0		
2	RANGE GIGAWATT (AU)	10.38	0	10.40	0	6 WATTS NOMINAL	6 WATTS NOMINAL
3	TRANSMITTER POWER (DBM)	37.8	0.5	37.8	0.5		0.6 METER DISH
4	TRANSMITTER CIRCUIT LOSS (DB)	-1.3	0.1	-1.3	0.1	OMNI	0.03 RAD (2.1 DEG) POINTING ERROR
5	TRANSMITTER ANTENNA GAIN (DB)	-2.0	0	20.0	0.3		
6	POINTING LOSS (DB)	0	0	-0.3	0.2		
7	POLARIZATION LOSS (DB)	-0.2	0.1	-0.2	0.1		
8	SPACE LOSS	-254.8	0	-256.8	0		
9	RECEIVER ANTENNA GAIN (DB)	61.6	0.4	61.6	0.4	64 METER (0.1 DB LOSS AT 0.35 RAD (20 DEG) ELEVATION)	64 METER (0.1 DB LOSS AT 0.35 RAD (20 DEG) ELEVATION)
10	TOTAL RECEIVED POWER (DBM) (3-4-5-6-7-8-9)	-158.9	---	-159.2	---		
11	RECEIVER NOISE SPECTRAL DENSITY (HZ)	-184.0	1.0	-184.0	1.0	TSYS = 290°K, 0.35 RAD (20 DEG) ELEVATION, ADVERSE AT 0.26 RAD (15 DEG) ELEVATION.	TSYS = 290°K, 0.35 RAD (20 DEG) ELEVATION, ADVERSE AT 0.26 RAD (15 DEG) ELEVATION.
12	POINTING (DB-HZ) (10-11)	25.1	1.2	44.8	1.3	RSS	RSS
CARRIER TRACKING PERFORMANCE							
13	CARRIER MODULATION LOSS (DB)	-2.0	0.6	-2.0	0.6	J = 0.66 RAD = 10%	J = 0.66 RAD = 10%
14	THRESHOLD LOSS BANDWIDTH (DB-HZ)	10.0	0.4	10.0	0.4	2B _{LO} = 10 HZ = 10%	2B _{LO} = 10 HZ = 10%
15	LOOP SNR (DB) (12-13-14)	13.1	---	32.8	---		
16	REQUIRED LOOP SNR (DB)	10.0	0	10.0	0	RSS TOLERANCES	RSS TOLERANCES
17	PERFORMANCE MARGIN (DB) (15-16)	3.1	1.4	22.8	1.5		
DATA CHANNEL PERFORMANCE							
18	DATA MODULATION LOSS (DB)	-4.2	0.9	-4.2	0.4	J = 0.66 RAD = 10%	J = 0.66 RAD = 10%
19	DATA BIT RATE (DB-BITS-SEC)	12	0	30.1	0	16 BITS/S	1024 BITS/S
20	RECEIVER LOSS (DB)	-4.1	0.4	1.3	0.2	ESTIMATED	FROM NASA APC 17 DB SNR IN 2B _{LO}
21	DOPPLER LOSS (DB)	0	0	-0.1	0.1	---	MAXIMUM STATIC PHASE ERROR = 0.11 RAD (6 DEG) LOSS ESTIMATED.
22	E _s /N ₀ (DB) (12-18-19-20-21)	4.8	---	9.1	---		
23	REQUIRED E _b /N ₀ (DB)	2.4	0	3.6	0	10 ⁻³ DELETION RATE	10 ⁻³ DELETION RATE
24	PERFORMANCE MARGIN (DB) (22-23)	2.4	1.6	5.5	1.6	RSS TOLERANCES	RSS TOLERANCES

Table 8.2-35. Bus Entry Uplink Control Table

NUMBER	PARAMETER	NOMINAL	ADVERSE	NOTES
1	FREQUENCY (MHZ)	2115	0	
2	RANGE (GIGAMETER (AU))	(0.48)	0	
3	TRANSMITTER POWER (DBM)	73.0	0	20 W
4	TRANSMITTER ANTENNA GAIN (DB)	51.8	0.9	26 METER DSS
5	SPACE LOSS	-256.1	0	
6	RECEIVER ANTENNA GAIN (DB)	19.0	0.5	0.6 METER DISH
7	POINTING LOSS (DB)	-0.3	0.2	
8	POLARIZATION LOSS (DB)	-0.2	0.1	
9	RECEIVER CIRCUIT LOSS (DB)	-1.4	0.1	
10	TOTAL RECEIVED POWER (DBM) (3+4+5+6+7+8+9)	-114.2	---	
11	RECEIVER NOISE SPECTRAL DENSITY (DBM/ HZ)	-169	1.0	$T_{SYS} = 910^{\circ}K$, $NF = 6$ DB
12	$P_T N_O$ (DB-HZ) (10-11)	54.8	---	
<u>CARRIER TRACKING PERFORMANCE</u>				
13	CARRIER MODULATION LOSS (DB)	0	0	
14	THRESHOLD LOOP BANDWIDTH (DB-HZ)	13.0	1.0	$28_{LO} = 20$ HZ AT 6 DB SNR
15	LOOP SNR (DB) (12-13-14)	41.8	---	
16	REQUIRED LOOP SNR = LIMITER LOSS (DB)	6.3	0	LIMITER LOSS = 0.3 DB
17	PERFORMANCE MARGIN (DB) (15-16)	35.5	1.8	RSS TOLERANCES
<u>COMMAND CHANNEL PERFORMANCE</u>				
18	DATA MODULATION LOSS (DB)	---	---	} NO COMMAND MODULATION
19	DATA BIT RATE (DB-BITS/SEC)	---	---	
20	RECEIVER LOSS (DB)	---	---	
21	$E_B N_O$ (DB) (12+18+19+20)	---	---	
22	REQUIRED $E_B N_O$	---	---	
23	PERFORMANCE MARGIN	---	---	

communication range is small, requiring less EIRP. The 3-watt output of the solid-state power amplifier is implemented by switching a voltage-dropping power resistor into the 28 VDC supply line, thereby dropping the amplifier supply voltage to about 21 volts, resulting in a reduced RF output level of 3 watts.

During the first 55 days the aft omni is used to allow favorable sun aspect angles for probe thermal considerations. During this time normal tracking by the 26-meter network allows bit rates from 1024 to 32 bits/s.*

* For both the probe and orbiter missions the Pioneers 10 and 11 preferred DTU will be modified to generate bit rates from 8 to 1024 bits/s (instead of 16 to 2048 bits/s) since an 8 bits/s but not a 2048 bits/s requirement exists. For the modification see Section 8.3, Data Handling.

Except for the 2-week probe release sequence the remainder of the mission is accomplished using the aft 0.6-meter (2-foot) diameter dish. The power budget during entry with the 64-meter station shows sufficient margin (3.9 dB) above the RSS tolerances to allow the spacecraft to be pointed off the spacecraft-earth line up to the antenna half-power one sided beamwidth, about 0.122 radian (7 degrees), and still support a bit rate of 1024 bits/s. The entry EIRP at beam center is 56.0 dBm.

Antennas. The recommended Thor/Delta bus antennas are the same as the preferred Atlas/Centaur bus antennas described in Section 8.2.4.1 except for the medium-gain antenna. For the Thor/Delta bus, the medium-gain antenna is the 0.6-meter (2-foot) dish as shown in Figure 8.2-37. The dish was selected over the horn in this case primarily because of its higher gain since an offset entry angle was not required for the 1977 bus mission.

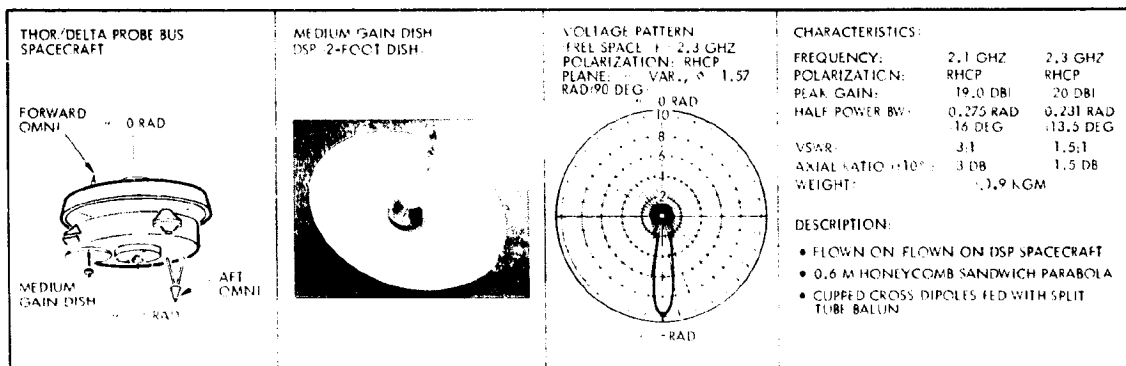


Figure 8.2-37. Thor/Delta Probe Spacecraft Medium-Gain Antenna

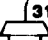
Transponder. The various transponders considered for Pioneer Venus have been described in previous sections. To minimize costs and to maximize commonality, it has been decided to baseline the Viking Lander transponder until cost and technical proposals are received from potential suppliers. As discussed earlier, both the S-band receiver and transmitter will be purchased from the same vendor to minimize interface problems.

Power Amplifier. The power amplifier specified for the bus is a 3/6-watt, dual mode, solid-state amplifier. It is identical to those described in Section 8.2.4.1.

T/D III Subsystem Weight and Power Summary. The recommended Thor/Delta probe bus communication subsystem weight and power is summarized in Table 8.2-36.

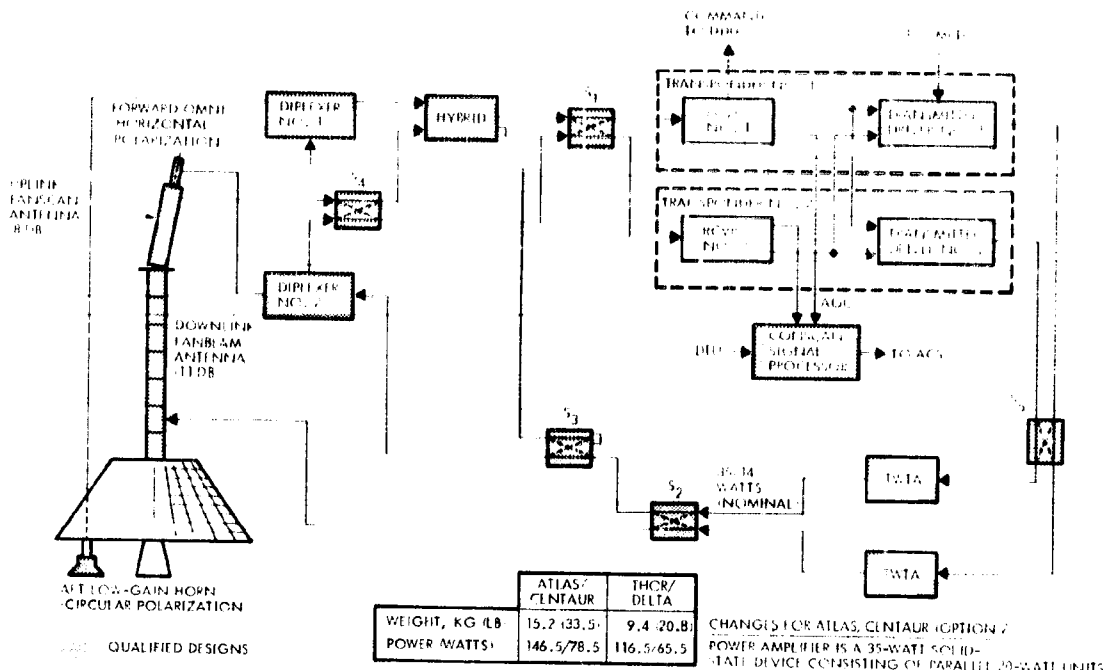
Table 8.2-36. Subsystem Weight and Power Summary

ITEM	QUANTITY	WEIGHT		DC POWER (WATTS)
		IF G	(LB)	
RECEIVER	2	2.4	(5.2)	7.0
TRANSMITTER DRIVER	2	1.1	(2.4)	3.5
POWER AMPLIFIER	2	0.6	(1.2)	22.0
HYBRID	1	0.05	(0.11)	
DIPLEXER	2	1.9	(4.3)	
SWITCHES	4	1.1	(2.4)	
FORWARD OMNI	1	0.1	(0.3)	
AFT OMNI	1	0.4	(0.9)	
MEDIUM GAIN				
ANTENNA (2-FT DISH)	1	0.9	(2.0)	
RF COAX AND CONNECTORS	A R	0.9	(2.0)	
TOTAL		9.4	(20.8)	32.5

8.2.5.2 Orbiter  T/D III

The recommended Thor/Delta orbiter spacecraft configuration has its spin axis perpendicular to the spacecraft-earth line, (the spin axis is also in a plane perpendicular to the Venus orbit plane). The primary downlink communications antenna is a 1.2-meter (4-foot) 11 dB Pioneers 6 through 9 Franklin array fanbeam antenna centered on the spacecraft spin axis. Together with a 35-watt TWTA (minimum 31 watts), the downlink supports 256 bits/s with the 64-meter network and 8 bits/s with the 26-meter network at 254.32 gigameter (1.7 AU). The primary spacecraft receive antenna is a 0.6 meter (2-foot) section of the same antenna, 8 dB gain, which is mounted on top of the downlink antenna. It is tilted 0.06 radian (3.5 degrees) off the spin axis to provide attitude control error signals to the conscan signal processor. This fanbeam antenna, which provides the beam scanning capability for attitude control, is referred to as the fanscan antenna. A block diagram of the subsystem, which includes these antennas, is shown in Figure 8.2-38.

A forward omni antenna is included; it is a Pioneers 6 through 9 unit with horizontal polarization and has a toroidal pattern which provides



Figur: 8.2-38. Orbiter Communication Subsystem Block Diagram

coverage at the 1.05 radian (60-degree) earth aspect angle during orbit insertion. The horizontal polarization provides some isolation from the vertical polarization of the fanbeam and fanscan antennas; it represents no ground station uplink/downlink operational problem, since both uplink and downlink will be handled by this antenna when in use. In the normal cruise attitude the uplink fanscan and downlink fanbeam antenna polarizations are essentially colinear [to within 0.06 radian (3.5 degrees)] and also provide compatibility with the simultaneous transmit (command) and receive (telemetry) colinear polarization limitation of the 26-meter stations. The forward omni, along with the aft low gain horn, provides near spherical coverage for launch and midcourse maneuvers. The only "hole" in the near-spherical omni coverage is a 0.35 radian (20-degree) half-angle cone (-5 dB point) along the forward axis where there is no mission requirement for communications. The aft low-gain horn is the feed from the Pioneers 10 and 11 high-gain dish and, together with the forward omni, provides -2 dBi near-spherical coverage except for a 0.58 radian (33-degree) half angle cone about the forward spin axis. The -2 dBi coverage includes a 3 dB circular/linear polarization loss and a 3 dB hybrid coupling loss for the low-gain horn.

The block diagram shows the coupling of the fanscan antenna and the aft low-gain horn in a 3 dB hybrid before the connection to Receiver 1, since the two patterns have essentially no overlap, any potential interferometer region is minimized. The forward omni is connected to Receiver 2, preventing any lock-out mode. After orbit insertion [at 59.84 gigameters (0.4 AU) communication range] and perpendicular spacecraft attitude is regained, switch S4 is activated to connect the fanscan antenna directly to one of the receivers, through switch S1, bypassing the coupler and gaining 3 dB more uplink sensitivity. The forward omni and low-gain horn will no longer be used except in some catastrophic attitude failure mode and then only an uplink capability would exist, since the omni downlink capability with the 64-meter station "runs out" shortly after orbit insertion. The fanbeam antenna is used for the downlink only to save diplexer and switch insertion losses. The insertion loss between the transmitter and antenna is then only 0.5 dB. A TWTA output bandpass filter would be required without the diplexer.

The preferred transponder is a Viking Lander unit and the power amplifier is a dual mode 35/14 watt TWTA unit made up of an MVM '73 tube and Helios power supply. Qualification would be required. When transmitting over the omni or low-gain horn the low-level output is used. This allows the use of existing Pioneers 10 and 11 switches and diplexers which are not rated for power levels up to 35 watts.

Performance Data

The bit rate capability of the orbit phase of the mission (see Figure 8.2-39) decreases from 1024 bits/s [59.84 to 1.27 gigameters (0.4 to 0.85 AU)] to 256 bits/s at 254.32 gigameters (1.7 AU) with the 64-meter stations. For the backup mode with the 26-meter network, the capability decreases from 256 bits/s at VOI to 8 bits/s at end-of-mission. A dual modulation index capability is implemented to provide the backup tracking mode by the 26-meter network. The index would be changed by command from 1.15 to 0.48 radians whenever this backup mode was required. During cruise the 26-meter stations are used with bit rate capability decreasing from 1024 bits/s near earth to 256 bits/s at VOI. The 1024 bit/s limitation is set by the implementation of the Pioneers 10 and 11 digital

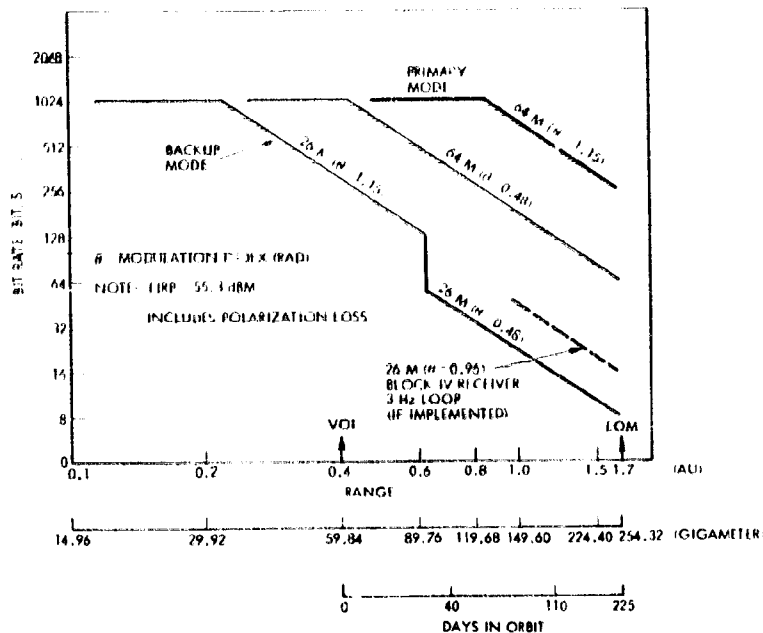


Figure 8.2-39. Orbiter Telemetry Rate History

telemetry unit which will be slightly modified to produce bit rates from 8 to 1024 bits/s. There does not appear to be a requirement for bit rates in excess of 1024 bits/s.

Tables 8.2-37 through 8.2-40 shows telemetry design control tables for the orbiter at the end-of-mission [254.32 gigameters (1.7 AU)] with an EIRP of 55.3 dBm. Table 8.2-37 assumes a slightly lower than nominal spacecraft transmitter power of 33 watts and a transmitting antenna gain of 11 db. Reception of the coded data with less than 10^{-3} frame deletion rate via the 26-meter stations of the DSN constrains the maximum bit rate to be 8 bits/s and the modulation index to be 0.48 (± 10 percent) radians.

Table 8.2-38 indicates that a data rate of 64 bits/s can be used with the 64-meter stations. Furthermore, the large carrier margin shown in Table 8.2-38 implies that an even larger data rate can be handled if the modulation index is increased.

Table 8.2-39 shows that the 64-meter stations can handle as high as 256 bits/s if the modulation index is switched to 1.15 radians.

Table 8.2-37. End-of-Mission Design Control Table
(26-Meter, 10.8 Hz Loop, $\theta = 0.48$ Rad)

NUMBER	PARAMETER	NOMINAL	ADVERSE	NOTES
1	FREQUENCY (MHZ)	2300		
2	RANGE (GIGAMETER (AU))	254.32 (1.7)	---	END-OF-MISSION (EOM)
3	TRANSMITTER POWER (DBM)	45.2	0.3	33-WATT NOMINAL (31-WATT ADVERSE)
4	TRANSMITTER CIRCUIT LOSS (DB)	-0.5	0.1	---
5	TRANSMITTER ANTENNA GAIN (DB)	11.0	0.3	FANBEAM (4 FT)
6	POINTING LOSS (DB)	-0.3	0.2	0.014 RAD (0.9 DEG) PITCH ERROR
7	POLARIZATION LOSS (DB)	-0.1	0.0	0.17 RAD (10 DEG) OFFSET LINEAR
8	SPACE LOSS (DB)	-267.8	---	---
9	RECEIVER ANTENNA GAIN (DB)	53.3	0.6	26 METER
10	TOTAL RECEIVED POWER (DBM) (3+4+5+6+7+8+9)	-159.2	---	---
11	RECEIVER NOISE SPECTRAL DENSITY (DBM/HZ)	-181.9	0.9	47°K, 0.26 RAD (15 DEG) ELEVATION 0.17 RAD (10 DEG) ELEVATION ADVERSE
12	$P_T N_O$ (DB-HZ) (10-11)	22.7	1.2	RSS TOLERANCES
<u>CARRIER TRACKING PERFORMANCE</u>				
13	CARRIER MODULATION LOSS (DB)	-1.0	0.3	0.48 ± 10% RAD
14	THRESHOLD LOOP BANDWIDTH (DB-HZ)	10.3	0.5	10.8 HZ LOOP
15	LOOP SNR (DB) (12+13-14)	11.4	---	---
16	REQUIRED LOOP SNR (DB)	10.0	0.0	---
17	PERFORMANCE MARGIN (DB) (15-16)	1.4	1.3	RSS TOLERANCES
<u>DATA CHANNEL PERFORMANCE</u>				
18	DATA MODULATION LOSS (DB)	-6.7	0.9	0.48 ± 10% RAD
19	DATA BIT RATE (DB-BITS SEC)	9.0	---	8 BITS SEC
20	RECEIVER LOSS (DB)	-3.2	0.5	ESTIMATED FROM PIONEER 9 DATA AND NEW SDA AND SSA
21	$E_B N_O$ (DB) (12+18-19+20)	3.8	---	---
22	REQUIRED $E_B N_O$ (DB)	2.2	---	10 ⁻³ DELETION RATE
23	PERFORMANCE MARGIN (DB) (21-22)	1.6	1.6	RSS TOLERANCE

Table 8

NUMBER	
1	FREQUENCY
2	RANGE (GIGAMETER (AU))
3	TRANSMITTER POWER (DBM)
4	TRANSMITTER CIRCUIT LOSS (DB)
5	TRANSMITTER ANTENNA GAIN (DB)
6	POINTING LOSS (DB)
7	POLARIZATION LOSS (DB)
8	SPACE LOSS (DB)
9	RECEIVER ANTENNA GAIN (DB)
10	TOTAL RECEIVED POWER (DBM)
11	RECEIVER NOISE SPECTRAL DENSITY (DBM/HZ)
12	$P_T N_O$ (DB-HZ)
<u>CARRIER TRACKING PERFORMANCE</u>	
13	CARRIER MODULATION LOSS (DB)
14	THRESHOLD LOOP BANDWIDTH (DB-HZ)
15	LOOP SNR (DB)
16	REQUIRED LOOP SNR (DB)
17	PERFORMANCE MARGIN (DB)
<u>DATA CHANNEL PERFORMANCE</u>	
18	DATA MODULATION LOSS (DB)
19	DATA BIT RATE (DB-BITS SEC)
20	RECEIVER LOSS (DB)
21	$E_B N_O$ (DB)
22	REQUIRED $E_B N_O$ (DB)
23	PERFORMANCE MARGIN (DB)

Table 8.2-38. End-of-Mission Design Control Table
(64-Meter, 10 Hz Loop, $\theta = 0.48$ Rad)

NUMBER	PARAMETER	NOMINAL	ADVERSE	NOTES
1	FREQUENCY (MHZ)	2300		
2	RANGE (GIGAMETER (AU))	254.32 (1.7)	0.3	
3	TRANSMITTER POWER (DBW)	45.2	0.3	38 WATTS NOMINAL (31 WATTS ADVERSE)
4	TRANSMITTER CIRCUIT LOSS (DB)	-0.5	0.1	
5	TRANSMITTER ANTENNA GAIN (DB)	11.0	0.3	FANBEAM
6	POINTING LOSS (DB)	-0.3	0.2	
7	POLARIZATION LOSS (DB)	-0.1	0.0	0.17 RAD (10 DEG) OFFSET LINEAR
8	SPACE LOSS (DB)	-267.8		
9	RECEIVER ANTENNA GAIN (DB)	61.6	0.4	64 METER (0.1 DB LOSS AT 0.35 RAD (20 DEG) ELEVATION)
10	TOTAL RECEIVED POWER (DBM) (3+4+5+6+7+8+9)	-150.9		
11	RECEIVER NOISE SPECTRAL DENSITY (DBM-HZ)	-184.0	0.6	29°K; 0.35 RAD (20 DEG) ELEVATION
12	$P_T N_O$ (DB-HZ) (10-11)	33.1	0.8	RSS
<u>CARRIER TRACKING PERFORMANCE</u>				
13	CARRIER MODULATION LOSS (DB)	-1.0	0.3	0.48 ± 10% RAD
14	THRESHOLD LOOP BANDWIDTH (DB-HZ)	10.0	0.4	10 HZ LOOP
15	LOOP SNR (DB) (12+13-14)	22.1		
16	REQUIRED LOOP SNR (DB)	10.0		
17	PERFORMANCE MARGIN (DB) (15-16)	12.1	1.0	RSS TOLERANCE
<u>DATA CHANNEL PERFORMANCE</u>				
18	DATA MODULATION LOSS (DB)	-6.7	0.9	0.48 ± 10% RAD
19	DATA BIT RATE (DB-BITS/SEC)	18.1		64 BITS/S
20	RECEIVER LOSS (DB)	-4.3	0.5	DUE TO 22.1 DB SNR IN $2\theta_{LO}$
21	$E_B N_O$ (DB) (12+18-19+20)	4.0		
22	REQUIRED $E_B N_O$	2.7		10^{-3} DELETION RATE
23	PERFORMANCE MARGIN (DB) (21-22)	1.3	1.3	RSS TOLERANCE

Table 8.2-

NUMBER	PARAMETER
1	FREQUENCY (MHZ)
2	RANGE (GIGAMETER (AU))
3	TRANSMITTER POWER (DBW)
4	TRANSMITTER CIRCUIT LOSS (DB)
5	TRANSMITTER ANTENNA GAIN (DB)
6	POINTING LOSS (DB)
7	POLARIZATION LOSS (DB)
8	SPACE LOSS (DB)
9	RECEIVER ANTENNA GAIN (DB)
10	TOTAL RECEIVED POWER (DBM)
11	RECEIVER NOISE SPECTRAL DENSITY (DBM-HZ)
12	$P_T N_O$ (DB-HZ) (10-11)
<u>CARRIER TRACKING PERFORMANCE</u>	
13	CARRIER MODULATION LOSS (DB)
14	THRESHOLD LOOP BANDWIDTH (DB-HZ)
15	LOOP SNR (DB) (12+13-14)
16	REQUIRED LOOP SNR (DB)
17	PERFORMANCE MARGIN (DB) (15-16)
<u>DATA CHANNEL PERFORMANCE</u>	
18	DATA MODULATION LOSS (DB)
19	DATA BIT RATE (DB-BITS/SEC)
20	RECEIVER LOSS (DB)
21	$E_B N_O$ (DB) (12+18-19+20)
22	REQUIRED $E_B N_O$ (DB)
23	PERFORMANCE MARGIN (DB) (21-22)

LDOUT FRAM

Table 8.2-39. End-of-Mission Design Control Table
(64-Meter, 10 Hz Loop, $\theta = 1.15$ Rad)

NUMBER	PARAMETER	NOMINAL	ADVERSE	NOTES
1	FREQUENCY (MHZ)	2300		
2	RANGE (GIGAMETER (AU))	254.32 (1.7)	0.3	
3	TRANSMITTER POWER (DBM)	45.2	0.3	33 WATTS NOMINAL (31 WATTS ADVERSE)
4	TRANSMITTER CIRCUIT LOSS (DB)	-0.5	0.1	
5	TRANSMITTER ANTENNA GAIN (DB)	11.0	0.3	FANBEAM
6	POINTING LOSS (DB)	-0.3	0.2	
7	POLARIZATION LOSS (DB)	-0.1	0.0	0.17 RAD (10 DEG) OFFSET LINEAR
8	SPACE LOSS (DB)	-267.8		
9	RECEIVER ANTENNA GAIN (DB)	61.6	0.4	64 METER [0.1 DB LOSS AT 0.35 RAD (20 DEG) ELEVATION]
10	TOTAL RECEIVED POWER (DBM) (3+4+5+6+7+8+9)	-150.9		
11	RECEIVER NOISE SPECTRAL DENSITY (DBM/HZ)	-184.0	0.6	29°K; 0.35 RAD (20 DEG) ELEVATION
12	P_r/N_0 (DB-HZ) (10-11)	33.1	0.8	RSS TOLERANCES
<u>CARRIER TRACKING PERFORMANCE</u>				
13	CARRIER MODULATION LOSS (DB)	7.8	2.8	1.15 ± 10% RAD
14	THRESHOLD LOOP BANDWIDTH (DB-HZ)	10.0	0.4	10 HZ LOOP
15	LOOP SNR (DB) (12+13-14)	15.3		
16	REQUIRED LOOP SNR (DB)	10.0		
17	PERFORMANCE MARGIN (DB) (15-16)	5.3	2.9	RSS TOLERANCE
<u>DATA CHANNEL PERFORMANCE</u>				
18	DATA MODULATION LOSS (DB)	-0.8	0.5	1.15 ± 10% RAD
19	DATA BIT RATE (DB-BITS/SEC)	24.1		256 BITS/S
20	RECEIVER LOSS (DB)	-2.7	0.5	
21	E_b/N_0 (DB) (12+18-19+20)	5.5		
22	REQUIRED E_b/N_0 (DB)	3.0		10^{-3} DELETION RATE
23	PERFORMANCE MARGIN (DB) (21-22)	2.5	1.1	RSS TOLERANCE

Table 8.2-40. End-of-Mission Design Control Table
(26-Meter, 3 Hz Loop, $\theta = 0.96$ Rad)

NUMBER	PARAMETER	NOMINAL	ADVERSE	NOTES
1	FREQUENCY (MHZ)	2360		
2	RANGE (GIGAMETER (AU))	254.32 (1.7)		
3	TRANSMITTER POWER (DBM)	45.2	0.3	33 WATTS (NOMINAL) (3) WATTS (ADVERSE)
4	TRANSMITTER CIRCUIT LOSS (DB)	-0.5	0.1	
5	TRANSMITTER ANTENNA GAIN (DB)	11.0	0.3	FANBEAM
6	POINTING LOSS (DB)	-0.3	0.2	
7	POLARIZATION LOSS (DB)	-0.0	0.0	0.17 RAD (10 DEG) OFFSET LINEAR
8	SPACE LOSS (DB)	-267.8		
9	RECEIVER ANTENNA GAIN (DB)	53.3	0.6	26 METER (BLOCK IV RECEIVER)
10	TOTAL RECEIVED POWER (DBM) (3+4+5+6+7+8+9)	-159.2		
11	RECEIVER NOISE SPECTRAL DENSITY (DBM/HZ)	-182.2	0.7	44°K; 0.35 RAD (20 DEG) ELEVATION (0.26 RAD (15 DEG) ADVERSE)
12	$P_T N_O$ (DB-HZ) (10-11)	23.0	1.0	RSS TOLERANCES
	<u>CARRIER TRACKING PERFORMANCE</u>			
13	CARRIER MODULATION LOSS (DB)	-4.8	1.4	0.96 ± 10% RAD
14	THRESHOLD LOOP BANDWIDTH (DB-HZ)	6.3	0.5	3 HZ LOOP WITH 1.5 DB DEG
15	LOOP SNR (DB) (12+13-14)	11.9		
16	REQUIRED LOOP SNR (DB)	10.0		
17	PERFORMANCE MARGIN (DB) (15-16)	1.9	1.8	RSS TOLERANCES
	<u>DATA CHANNEL PERFORMANCE</u>			
18	DATA MODULATION LOSS (DB)	-1.7	0.7	0.96 ± 10% RAD
19	DATA BIT RATE (DB-BITS/SEC)	12.0	---	16 BITS/S
20	RECEIVER LOSS (DB)	-5.6	0.5	
21	$E_B N_O$ (DB) (12+18-19+20)	5.7		
22	REQUIRED $E_B N_O$ (DB)	2.4		10^{-3} DELETION RATE
23	PERFORMANCE MARGIN (DB) (21-22)	3.3	1.3	RSS TOLERANCES

Table 8.2-

NUMBER	PARAMETER
1	FREQUENCY (MHZ)
2	RANGE (GIGAMETER (AU))
3	TRANSMITTER POWER (DBM)
4	TRANSMITTER CIRCUIT LOSS (DB)
5	TRANSMITTER ANTENNA GAIN (DB)
6	POINTING LOSS (DB)
7	POLARIZATION LOSS (DB)
8	SPACE LOSS (DB)
9	RECEIVER ANTENNA GAIN (DB)
10	TOTAL RECEIVED POWER (DBM)
11	RECEIVER NOISE SPECTRAL DENSITY (DBM/HZ)
12	$P_T N_O$ (DB-HZ) (10-11)
	<u>CARRIER TRACKING PERFORMANCE</u>
13	CARRIER MODULATION LOSS (DB)
14	THRESHOLD LOOP BANDWIDTH (DB-HZ)
15	LOOP SNR (DB) (12+13-14)
16	REQUIRED LOOP SNR (DB)
17	PERFORMANCE MARGIN (DB) (15-16)
	<u>DATA CHANNEL PERFORMANCE</u>
18	DATA MODULATION LOSS (DB)
19	DATA BIT RATE (DB-BITS/SEC)
20	RECEIVER LOSS (DB)
21	$E_B N_O$ (DB) (12+18-19+20)
22	REQUIRED $E_B N_O$ (DB)
23	PERFORMANCE MARGIN (DB) (21-22)

OUT FRAME

Table 8.2-41. Orbit Insertion Design Control Table

PARAMETER	NOMINAL	ADVERSE	NOTES
FREQUENCY (MHZ)	2300		
RANGE (GIGAMETER (AU))	59.84 (0.4)	---	
TRANSMITTER POWER (DBM)	41.5	0.2	14 WATTS NOMINAL
TRANSMITTER CIRCUIT LOSS (DB)	-1.1	0.1	---
TRANSMITTER ANTENNA GAIN (DB)	-0.5	0.0	FORWARD OMNI
POINTING LOSS (DB)	0.0	0.0	---
POLARIZATION LOSS (DB)	-0.1	0.0	---
SPACE LOSS (DB)	-255.2	---	(0.4 GIGAMETER AU)
RECEIVER ANTENNA GAIN (DB)	61.6	0.4	64 METER (0.1 DB LOSS AT 0.35 RAD (20 DEG) ELEVATION
TOTAL RECEIVED POWER (DBM) (3+4+5+6+7+8+9)	-153.8	---	---
RECEIVER NOISE SPECTRAL DENSITY (DBM/HZ)	-184.0	0.6	29°K, 0.35 RAD (20 DEG) ELEVATION
P_r/N_0 (DB-HZ) (10-11)	30.2	0.8	RSS TOLERANCE
<u>CARRIER TRACKING PERFORMANCE</u>			
CARRIER MODULATION LOSS (DB)	-1.0	0.3	0.48 = 10% RAD
THRESHOLD LOOP BANDWIDTH (DB-HZ)	10.0	0.4	10 HZ LOOP
LOOP SNR (DB) (12+13-14)	19.2	---	---
REQUIRED LOOP SNR (DB)	10.0	---	---
PERFORMANCE MARGIN (DB) (15-16)	9.2	1.0	RSS TOLERANCE
<u>DATA CHANNEL PERFORMANCE</u>			
DATA MODULATION LOSS (DB)	-6.7	0.9	0.48 = 10% RAD
DATA BIT RATE (DB-BITS/SEC)	15.1	---	32 BITS/S
RECEIVER LOSS (DB)	-4.1	0.5	ESTIMATED
E_b/N_0 (DB) (12+18-19+20)	4.3	---	---
REQUIRED E_b/N_0 (DB)	2.5	---	10^{-3} DELETION RATE
PERFORMANCE MARGIN (DB) (21-22)	1.8	1.3	RSS TOLERANCE

Table 8.2-42. Uplink

NUMBER	PARAMETER
1	FREQUENCY (MHZ)
2	RANGE (GIGAMETERS (AU))
3	TRANSMITTER POWER (DBM)
4	TRANSMITTER ANTENNA GAIN (DB)
5	SPACE LOSS (DB)
6	RECEIVER ANTENNA GAIN (DB)
7	POINTING LOSS (DB)
8	POLARIZATION LOSS (DB)
9	RECEIVER CIRCUIT LOSS (DB)
10	TOTAL RECEIVED POWER (DBM) (3+4+5+6+7+8+9)
11	RECEIVER NOISE SPECTRAL DENSITY (DBM/HZ)
12	P_r/N_0 (DB-HZ) (10-11)
<u>CARRIER TRACKING PERFORMANCE</u>	
13	CARRIER MODULATION LOSS (DB)
14	THRESHOLD LOOP BANDWIDTH (DB-HZ)
15	LOOP SNR (DB) (12+13-14)
16	REQUIRED LOOP SNR + LIMITER LOSS (DB)
17	PERFORMANCE MARGIN (DB) (15-16)
<u>COMMAND CHANNEL PERFORMANCE</u>	
18	DATA MODULATION LOSS (DB)
19	DATA BIT RATE (DB-BITS/SEC)
20	RECEIVER LOSS (DB)
21	E_b/N_0 (DB) (12+18-19+20)
22	REQUIRED E_b/N_0 (DB)
23	PERFORMANCE MARGIN (DB) (21-22)

OUTPUT FRAM

Table 8.2-42. Uplink at 254.32 Gigameters (1.7 AU)

NUMBER	PARAMETER	NOMINAL	ADVERSE	NOTES
1	FREQUENCY (MHZ)	2115		
2	RANGE [GIGAMETERS (AU)]	254.32 (1.7)		
3	TRANSMITTER POWER (DBM)	73.0	0.0	20 KW
4	TRANSMITTER ANTENNA GAIN (DB)	51.9	0.0	26 METERS
5	SPACE LOSS (DB)	-267.1	0.0	
6	RECEIVER ANTENNA GAIN (DB)	6.5	0.3	UPLINK FANSCAN
7	POINTING LOSS (DB)	-0.6	0.2	0.017 RAD (~1 DEG) POINTING ERROR
8	POLARIZATION LOSS (DB)	-0.1	0.1	0.17 RAD (10 DEG) OFFSET LINEAR
9	RECEIVER CIRCUIT LOSS (DB)	-1.3	0.2	
10	TOTAL RECEIVED POWER (DBM) (3+4+5+6+7+8+9)	-137.8		
11	RECEIVER NOISE SPECTRAL DENSITY (DBM/HZ)	-169.0	1.0	$T_{sys} = 910^{\circ}K$; NF = 6 DB
12	P_r/N_o (DB-HZ) (10-11)	31.2	1.4	RSS TOLERANCE
<u>CARRIER TRACKING PERFORMANCE</u>				
13	CARRIER MODULATION LOSS (DB)	-2.8	0.3	1.09 RAD
14	THRESHOLD LOOP BANDWIDTH (DB-HZ)	13.0	1.0	20 HZ LOOP AT 6 DB SNR
15	LOOP SNR (DB) (12+13-14)	15.4		
16	REQUIRED LOOP SNR + LIMITER LOSS (DB)	6.3		LIMITER LOSS = 0.3 DB
17	PERFORMANCE MARGIN (DB) (15-16)	9.1	1.7	RSS TOLERANCE
<u>COMMAND CHANNEL PERFORMANCE</u>				
18	DATA MODULATION LOSS (DB)	-3.6	0.4	1.09 RAD
19	DATA BIT RATE (DB-BITS/SEC)	0		1 BIT/S
20	RECEIVER LOSS (DB)	-1.1	0	RECEIVER, FILTER, AND LIMITER LOSS
21	$E_b N_o$ (DB) (12+18-19+20)	26.5		
22	REQUIRED $E_b N_o$ (DB)	17.3	1.0	10^{-5} BER
23	PERFORMANCE MARGIN (DB) (21-22)	9.2	1.7	RSS TOLERANCE

Table 8.2-40 indicates the performance that can be expected if Block IV receivers are used at the 26-meter stations (as proposed by the DSN). Assuming a 3-Hz ground receiver loop, a maximum data rate of 16 bits/s can be accommodated at an index of 0.96 radians.

Table 8.2-41 shows the telemetry budget for the orbiter at Venus orbit insertion with an earth aspect angle of 1.05 radian (60 degrees). For this case the spacecraft transmitter is operating at 14 watts nominal into the forward omni antenna with -0.5 db gain. For this configuration the 64-meter station can support 32 bits/s.

Table 8.2-42 shows the uplink performance at the end of the orbiter mission. Reliable reception of PCM/FSK/PM commands via the fanscan antenna is accomplished at 1 bit/s and a modulation index of 1.09 radians with greater than 7 db margin above the adverse tolerances.

Antennas. The recommended Thor/Delta orbiter antenna subsystem consists of four separate antennas which are used for TT&C and fanscan during transit, orbit insertion, and Venus orbit phases of the mission. The spacecraft configuration is the reduced EIRP option with the spin axis normal to the earth line. As shown in Figure 8.2-40, a fanbeam antenna is used as the primary downlink antenna, a tilted fanbeam antenna is used as the uplink and fanscan antenna, a forward omnidirectional antenna provides TT&C coverage during orbit insertion, and an aft horn provides TT&C coverage during launch. Use of existing flight-qualified designs and commonality of equipment with the probe bus spacecraft represented the lowest cost, lowest risk approach, and was therefore the major factor in establishing the antenna subsystem configuration.

The high-gain downlink antenna is the qualified Pioneers 6 through 9 Franklin array antenna, while the fanscan uplink antenna is a shortened Pioneers 6 through 9 antenna. The fanscan antenna will be tilted 0.06 radian (3.6 degrees) relative to the spin axis for a 1 dB fanscan cross-over reference. Each antenna in the stack will be separately fed by miniature coaxial cables to simplify the design relative to the existing Pioneers 6 through 9 design. Because of length, weight, and magnetic cleanliness constraints with the requirement for two omni antennas, the

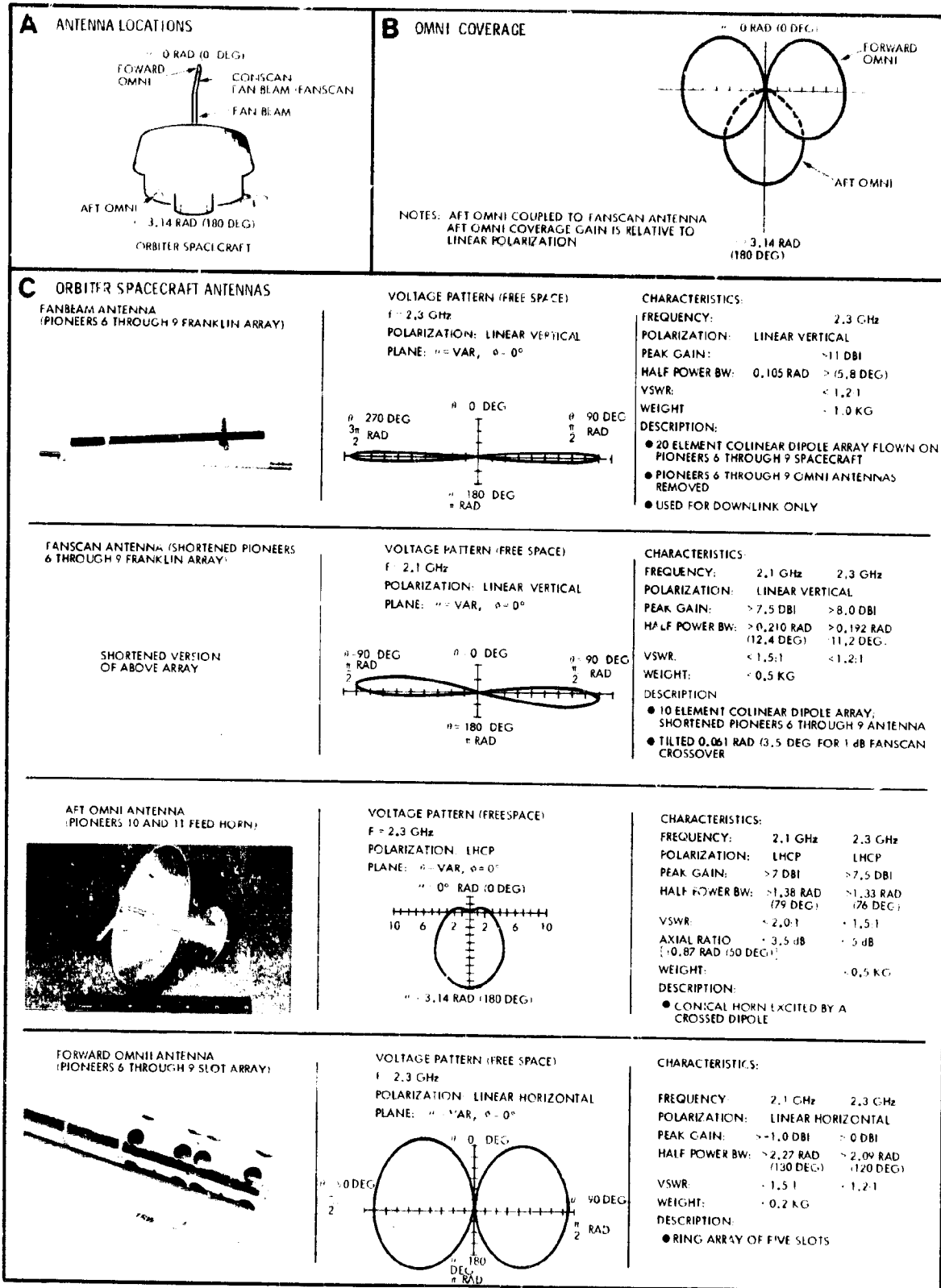


Figure 8.2-40. Recommended Thor/Delta Orbiter Spacecraft Antennas

existing Pioneers 6 through 9 antenna was a complex design. The design constraints led to a thin wall (0.13 mm) construction, an electrically short array (0.446 wavelength element spacing at 2.3 GHz), and a complex coaxial feed system to feed two omni antennas. The basic 20-element Pioneers 6 through 9 array design is simple, since all array elements are mechanically the same. Because of this feature, increasing or decreasing the array length is not a major modification. Operation at just the downlink or uplink frequency and incorporation of an independent feed system represents a significant design simplification which should result in lowering the assembly time and costs of the antenna.

The Pioneers 6 through 9 slot array omnidirectional antenna was selected as the forward omni antenna because its polarization is orthogonal to that of the fanbeam antennas. Maximum isolation between the forward omni antenna and the fanbeam antennas is achieved with non-aligned polarizations. The separate receive and transmit systems provide isolation between fanbeams, but RF chokes may be required to increase the isolation. The circularly polarized aft horn is used to fill in the radiation pattern coverage about the aft end of the spacecraft for the launch phase of the mission. Circular polarization provides constant gain relative to a linearly polarized ground station antenna as the spacecraft spins. With the switching and diplexing scheme employed, pattern interference between all antennas is minimized.

High RF power levels will not be applied to the diplexer nor will switching be formed in high RF power modes through critical altitudes; therefore, existing Pioneers 10 and 11 Type II diplexers and RF switches described in Section 8.2.4.1 can be used. All antennas are capable of handling RF power levels greater than 80 watts since minimum conductor spacing in any of the antenna designs is on the order of 0.2 cm.

Transponder. The transponder used on the orbiter will be identical to that specified for the probe bus. The present baseline is the Viking Lander unit, as described in Section 8.2.4.1.

Fanscan Signal Processor. The fanscan signal processor baselined for the Thor/Delta orbiter is identical to the unit flown on Pioneers 10 and 11. A description of the unit and a table of characteristics are given in Section 8.2.4.1.

Power Amplifier. The low gain of the fanbeam antenna used in the preferred orbiter configuration for the Thor/Delta requires that the power amplifier provide a nominal output of 36 watts (31 watts minimum). It has been shown that a solid state approach is more cost-effective and much lighter in weight than a TWTA. However, due to the lower efficiency of the solid state approach (parallel 20-watt units), the Thor/Delta launch will utilize the 36-watt TWTA from MVM '73 (modified). This reduces the power amplifier power input (compared to the solid state unit) by about 30 watts. Both the solid state and TWTA can be reduced in output power during the early part of the mission as required to accommodate the available dc power. The TWTA utilizes a dual mode tube to allow the reduction of output power to 16 watts.

Tradeoffs and characteristics for both the solid state and the TWTA power amplifier are given in Section 8.2.3.4.

Subsystem Weight and Power Summary. The recommended Thor/Delta orbiter communications subsystem weight and power is summarized in Table 8.2-43.

Table 8.2-43.
Communications Subsystem
Weight and Power Summary

ITEM	QUANTITY	WEIGHT (KG (LB))	DC POWER (WATTS)
RECEIVER	2	2.4 (5.2)	7.0
CONSCAN PROCESSOR	1	0.4 (0.8)	1.5
TRANSMITTER DRIVER	2	1.1 (2.4)	3.5
TWTA	2	5.4 (12.0)	106.0
DIPLEXERS	2	1.9 (4.3)	
HYBRIDS	2	0.1 (0.2)	
SWITCHES	4	1.1 (2.4)	
AFT OMNI	1	0.2 (0.5)	
FORWARD OMNI	1	0.1 (0.3)	
FANSCAN ANTENNA	1	0.5 (1.0)	
FANBEAM ANTENNA	1	1.1 (2.5)	
RF COAX AND CONNECTORS	A, R	1.1 (2.5)	
TOTAL		15.4 (34.1)	116.0
NOTE: THESE WEIGHTS WERE CHANGED SLIGHTLY SUBSEQUENT TO PREPARATION OF MASS PROPERTIES TABLES IN SECTION 6 OF THIS REPORT.			

During the course of the study three orbiter options were considered in fair detail and are summarized here for completeness. These options were based on the understanding of the science data requirements that existed prior to the Version IV update of the orbiter science definition (Version IV increased the amount of data to be taken per orbit and made X-band a primary science experiment). The understanding of these requirements with respect to desired real-time data rates varied enough to lead to the various options presented here. All three options have their spin axis perpendicular to the earth line and vary from a minimum 128 bits/s downlink despun reflector configuration using a 12-watt power amplifier (Atlas/Centaur and Thor/Delta Orbiter, Version III science payload) to a 35-watt, 11 dB fanbeam design with 8 bits/s minimum capability (Atlas/Centaur Orbiter, Version III science payload) to a 12-watt, 11 dB fanbeam alternate (Thor/Delta and Atlas/Centaur Orbiter, Version III science payload) that required the 64-meter network to achieve 64 bits/s minimum. Each configuration has a fanscan antenna that provides an attitude control function similar to Pioneers 10 and 11 by providing amplitude modulation on an uplink carrier which is extracted by the fanscan (conscan) signal processor. Also, each option is applicable to either the Atlas/Centaur or Thor/Delta launch vehicles.

8.2.6.1 Despun Reflector

A/C III



T/D III

The despun reflector option is essentially that which was presented at the Pioneer Venus Midterm Briefing on 2 March 1973. Only an uplink fanscan antenna and conscan signal processor were added to improve attitude control capability. Figure 8.2-41 is the subsystem block diagram. The aft horn and fanscan antenna are coupled together through a hybrid and together with the forward omni give the antenna coverage as shown in Figure 8.2-42. This is the same coverage as the recommended Thor/Delta orbiter version discussed in Section 8.2.4.2. A despun reflector similar to Helios is used to provide a real-time data rate at end-of-mission of 128 bits/s. At the time of the midterm, 128 bits/s was thought to be the real-time data requirement. This interpretation has since changed and is reflected in the lower FIRP options. The 12-watt power amplifier consists of two 6-watt units phase combined in a

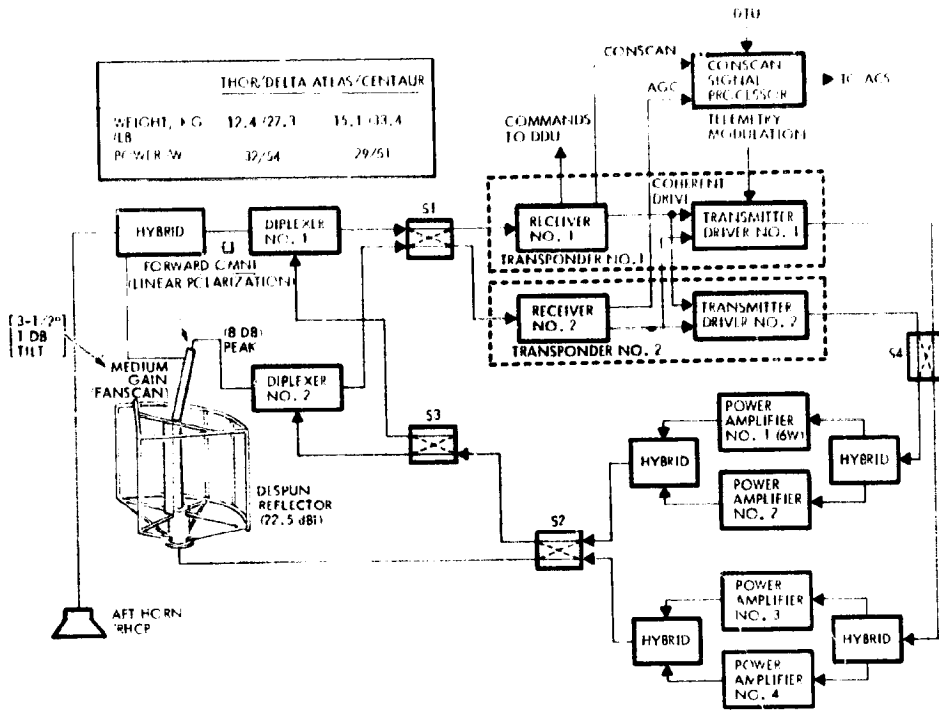


Figure 8.2-41. Communications Subsystem Block Diagram

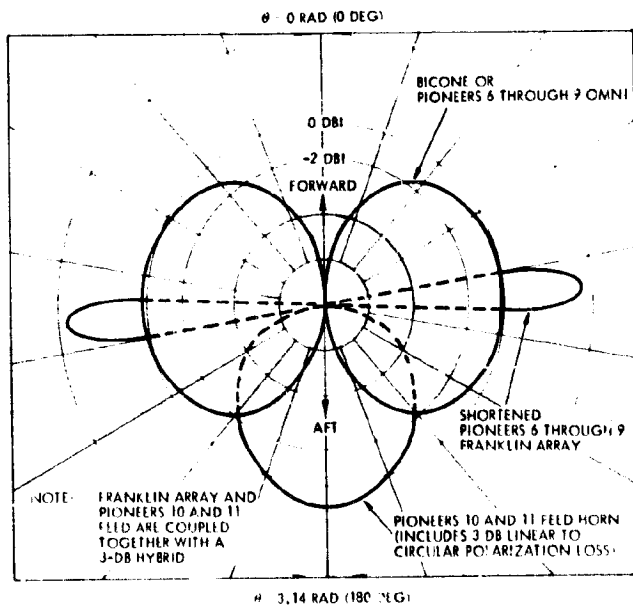




Figure 8.2-42. Linear Polarization Low-Gain (Omni) Coverage with Conscan



A/C III hybrid. The resulting EIRP of this configuration is 62 dBm. See Appendix 8.2C for a power amplifier/antenna sizing tradeoff that was performed for this option. During most of the cruise portion of the mission only one 6-watt module is activated to reduce the sizing of the solar array when the spacecraft is furthest from the sun (and closest to earth). Later on, just prior to orbit insertion, the other amplifier is activated. When only one amplifier is on, the resulting power out of the hybrid is a nominal 2.7 watts. A direct connection between the transmitter output and high gain antenna is made to maximize EIRP and reduce weight, i. e., eliminate a diplexer in that path. However, sufficient bandpass filtering must be included in the power amplifier to prevent it from overloading the receiver through antenna coupling. This feature is inherent in all the options presented here. Table 8.2-44 shows design control tables for orbit insertion with the omni (64-meter station) and end-of-mission with the high gain reflector (26-meter station) at 128 bits/s.

8.2.6.2 35-Watt/Fanbeam Fanscan Option  ^(31 W) A/C III  ^(31 W) T/D III

This Atlas/Centaur option is identical to the preferred Thor/Delta orbiter version presented in Section 8.2.4.2, except that the 35-watt TWTA is replaced by a less efficient (but less costly) 35-watt (31 watt minimum) solid-state power amplifier. The 35-watt amplifier would consist of two 20-watt units in parallel, as in the large probe, for commonality and lower cost. The reason the solid-state unit could not be used on the Thor/Delta configuration is that the extra solar array required to handle the increased DC power could not easily be accommodated on the small Thor/Delta conical solar array. Therefore, the Thor/Delta subsystem presented a higher cost than the corresponding Atlas/Centaur version.

The block diagram (except for the TWTA), the mission telemetry rate profile, and the design control tables for this option are the same as those presented in Section 8.2.4.2. The main reason a high transmitter power was used in both Atlas/Centaur and Thor/Delta versions of this option is that a letter from NASA/ARC (from John J. Hurt of Ames to W. H. Simmons of TRW, May 9, 1973, ASD:244-9/32-130) requested that the orbiter spacecraft be capable of performing the mission

Table 8. 2-44. Telemetry Design Control Table

PARAMETER	ORBIT INSERTION			END OF MISSION			NDC/E
	NOMINAL	ADVERSE	NOMINAL	ADVERSE	NOMINAL	ADVERSE	
1. FREQUENCY (MHZ)	2300	0	2300	0	2300	0	
2. RANGE (KILOMETERS /A.U.)	59.84 (0.4)	0	254.32 (1.7)	0			
3. TRANSMITTER POWER (DBM)	40.4	0.5	40.4	0.5	11 WATTS		11 WATTS
4. TRANSMITTER CIRCUIT LOSS (DB)	-1.1	0.1	-0.5	0.1			
5. TRANSMITTER ANTENNA GAIN (DB)	2.0	6	22.5	0.5	0 (MIN)		HIGH GAIN REFLECTOR
6. POINTING LOSS (DB)	0	0	-0.3	0.2			
7. POLARIZATION LOSS (DB)	-0.2	0.1	0	0			
8. SPACE LOSS	-255.2	0	-267.8	0			
9. RECEIVER ANTENNA GAIN (DB)	41.7	0.4	53.3	0.6	64 METERS DES		66 METERS DES
10. TOTAL RECEIVED POWER (DBM) (0-4-5-6-7-8-9)	-152.4	---	-152.4	---			
11. RF DRIVE NOISE SPECTRAL DENSITY (DBM/Hz)	-184.8	2.11	-183.0	1.5	TSYS = 24K, 0.75 RAD 149 DEG ELEVATION		TSYS = 24K, 0.75 RAD 149 DEG ELEVATION
12. P_{T/N_0} (DB-Hz) (0-11)	32.4	---	30.6	---			
<u>CARRIER TRACKING PERFORMANCE</u>							
13. CARRIER MODULATION LOSS (DB)	-7.2	2.3	-7.2	2.3	$\theta = 1.12$ RAD		$\theta = 1.12$ RAD
14. THREE HOLD LOOP BANDWIDTH (DB-Hz)	10.0	0.4	10.3	0.5	$2B_{LO} = 10$ HZ		$2B_{LO} = 10.3$ HZ
15. LOOP ST. LOSS (DB) (12-13-14)	15.2	---	13.1	---			
16. REQUIRED L. OP SNR (DB)	10.0	0	10.0	0			
17. PERFORMANCE MARGIN (DB) (15-16)	5.2	3.2	3.1	2.9	RSS TOLERANCE		RSS TOLERANCE
<u>DATA CHANNEL PERFORMANCE</u>							
18. DATA MODULATION LOSS (DB)	-0.9	0.5	-0.9	0.5	$\theta = 1.12$ RAD		$\theta = 1.12$ RAD
19. DATA RATE (DB-BITS/SEC)	21.1	0	21.1	0	128 BITS/S		128 BITS/S
20. RECEIVER LOSS (DB)	-3.7	1.0	-3.7	1.0			
21. DOPPLER LOSS (DB)	5	0	0	0	INSERTION BEHIND PLANET		
22. E_b/N_0 (DB) (18-19-20-21)	6.3	---	4.5	---			
23. REQUIRED E_b/N_0 (DB)	2.8	0	2.8	0	10^3 REJECTION RATE		10^3 REJECTION RATE
24. PERFORMANCE MARGIN (DB) (22-23)	3.9	2.5	2.1	2.1	RSS TOLERANCES		RSS TOLERANCES

^(31 W)
 A/C III with the 26-meter network, at least as a backup for daily operations. A
^(31 W)
 T/D III 35-watt output is required to do this with the existing Pioneers 6 through 9
 11 dB fanbeam antenna at 8 bits/s. The following option shows the lowest
 cost version of all three options presented here if the above request were
 waived, i. e., if use of the 64-meter network only were possible.

8.2.6.3 12-Watt Fanbeam/Fanscan Option ^(12 W)
 T/D III

This option represents the simplest spacecraft and lowest cost of
 all configurations that have their spin axis perpendicular to the earth-
 line. It is based on communication while in orbit with the 64-meter DSN
 only and will not work with the 26-meter DSN except for the cruise portion
 of the mission up to orbit insertion. From then on one 64-meter station
 is required each day for a few hours to read out an orbit of stored data.

The block diagram is the same as the preferred Thor/Delta orbiter
 shown in Section 8.2.4.2, except the 35-watt TWTA is replaced by a 12-
 watt solid-state power amplifier. The telemetry data rate profile is
 shown in Figure 8.2-43, 64 bits/s being the minimum capability. The
 downlink with the 26-meter network (10.8 loop bandwidth) expires shortly
 after orbit insertion, about [82.28 gigameters (0.55 AU)] (VOI + 22 days).
 From then on the 64-meter network is required. Resign control tables
 for the 26- and 64-meter downlinks are shown in Tables 8.2-45 and 8.2-46.

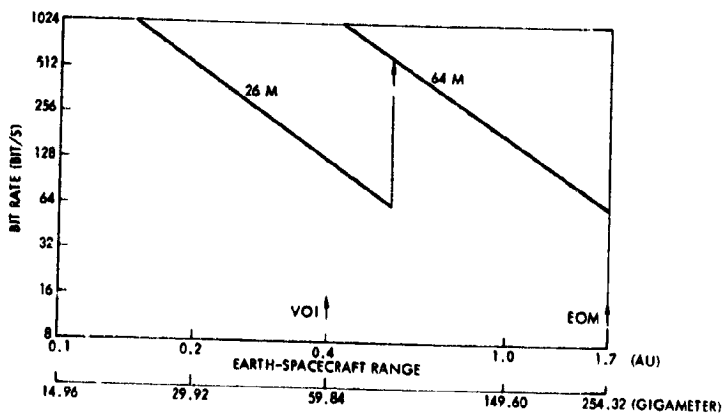


Figure 8.2-43. Orbiter Telemetry Rate Profile

Table 8.2-45. Early Orbit (26-Meter) Telemetry Design Control Table

NUMBER	PARAMETER	NOMINAL	ADVERSE	NOTES
1	FREQUENCY (MHZ)	2300		
2	RANGE [GIGAMETERS (AU)]	59.84 (0.4)		
3	TRANSMITTER POWER (DBM)	40.8	0.4	12 WATTS NOMINAL
4	TRANSMITTER CIRCUIT LOSS (DB)	-0.5	0.1	
5	TRANSMITTER ANTENNA GAIN (DB)	11.0	0.3	FANBEAM
6	POINTING LOSS (DB)	-0.3	0.2	
7	POLARIZATION LOSS (DB)	-0.1	0.0	0.17 RAD (10 DEG) OFFSET LINEAR
8	SPACE LOSS (DB)	-255.2	---	
9	RECEIVER ANTENNA GAIN (DB)	53.3	0.6	26 METERS
10	TOTAL RECEIVED POWER (DBM) (3+4+5+6+7+8+9)	-151.0	---	
11	RECEIVER NOISE SPECTRAL DENSITY (DBM, HZ)	-182.2	0.7	44°K; 0.35 RAD (20 DEG) ELEVATION [0.26 RAD (15 DEG) ADVERSE]
12	P_T/N_O (DB-HZ) (10-11)	31.2	1.0	RSS TOLERANCE
	<u>CARRIER TRACKING PERFORMANCE</u>			
13	CARRIER MODULATION LOSS (DB)	-5.9	1.7	1.04 ± 10% RAD
14	THRESHOLD LOOP BANDWIDTH (DB-HZ)	10.3	0.5	10.8 HZ LOOP
15	LOOP SNR (DB) (12+13-14)	15.0	---	
16	REQUIRED LOOP SNR (DB)	10.0	---	
17	PERFORMANCE MARGIN (DB) (15-16)	5.0	2.0	RSS TOLERANCE
	<u>DATA CHANNEL PERFORMANCE</u>			
18	DATA MODULATION LOSS (DB)	-1.3	0.5	1.0 ± 10% RAD
19	DATA BIT RATE (DB-BITS/SEC)	21.1	---	128 BITS/S
20	RECEIVER LOSS (DB)	-4.6	0.5	FROM NASA/ARC
21	E_B/N_O (DB) (12+18-19+20)	4.2	---	---
22	REQUIRED E_B/N_O (DB)	2.8	---	10^{-3} DELETION RATE
23	PERFORMANCE MARGIN (DB) (21-22)	1.4	1.2	RSS TOLERANCE

Table 8.2-46. End-of-Mission (64-Meter) Telemetry Design Control Table

NUMBER	PARAMETER	NOMINAL	ADVERSE	NOTES
1	FREQUENCY (MHZ)	2300		
2	RANGE (GIGAMETERS (AU))	254.32 (1.7)		
3	TRANSMITTER POWER (DBM)	40.8	0.1	12 WATTS NOMINAL
4	TRANSMITTER CIRCUIT LOSS (DB)	-0.5	0.1	
5	TRANSMITTER ANTENNA GAIN (DB)	11.0	0.3	FANBEAM
6	POINTING LOSS (DB)	-0.3	0.2	
7	POLARIZATION LOSS (DB)	-0.1	0.0	0.17 RAD (10 DEG) OFFSET LINEAR
8	SPACE LOSS (DB)	-267.8		
9	RECEIVER ANTENNA GAIN (DB)	61.6	0.4	64 METERS (0.1 DB LOSS AT 0.35 RAD (20 DEG) ELEVATION
10	TOTAL RECEIVED POWER (DBM) (3+4+5+6+7+8+9)	-155.3		
11	RECEIVER NOISE SPECTRAL DENSITY (DBM/HZ)	-184.0	0.6	29°N; 0.35 RAD (20 DEG) ELEVATION
12	$P_T N_O$ (DB-HZ) (10-11)	28.7	0.8	RSS TOLERANCE
<u>CARRIER TRACKING PERFORMANCE</u>				
13	CARRIER MODULATION LOSS (DB)	-5.9	1.7	1.04 x 10 ⁻⁶ RAD
14	THRESHOLD LOOP BANDWIDTH (DB-HZ)	10.0	0.4	10 HZ LOOP
15	LOOP SNR (DB) (12+13-14)	12.8		
16	REQUIRED LOOP SNR (DB)	10.0		
17	PERFORMANCE MARGIN (DB) (15-16)	2.8	1.9	RSS TOLERANCE
<u>DATA CHANNEL PERFORMANCE</u>				
18	DATA MODULATION LOSS (DB)	-1.3	0.5	1.04 x 10 ⁻⁶ RAD
19	DATA BIT RATE (DB-BITS/SEC)	18.1		64 BITS/S
20	RECEIVER LOSS (DB)	-5.3	0.5	FROM NASA ARC
21	$E_b N_O$ (DB) (12+18-19+20)	4.0		
22	REQUIRED $E_b N_O$ (DB)	2.7		
23	PERFORMANCE MARGIN (DB) (21-22)	1.3	1.1	RSS TOLERANCE

8.3 DATA HANDLING SUBSYSTEM

8.3.1 Introduction and Summary

During the study, data handling subsystem designs that would meet the constraints of the Thor/Delta launch vehicle were continually reviewed to see how they might be changed to take advantage of the additional capabilities allowed by the Atlas/Centaur. Each time, however, the requirements, interfaces and hardware were found to be essentially identical for both configurations; only the method of packaging the data storage unit changed. For this reason, reference to the launch vehicle is generally omitted from this section even though the effect of both vehicles on the subsystem were carefully considered.

The remainder of this introductory section summarizes the key feature of the preferred data handling subsystem (i. e., the one we have designed to meet the needs of the Version IV science payload). Section 8.3.2 summarizes the requirements analyses that were made for the probe bus designed for the Version III science payload, and the deltas required for Version IV. This is followed by summarized requirements for the orbiters designed for Version III and deltas for Version IV.

Section 8.3.3 covers our work on the pros and cons of using existing telemetry equipment as opposed to more advanced designs. This section also considers the use of centralized as opposed to conventional processing and compares various types of memories. It ends with a consideration of various ways of handling the interfaces between the science and this subsystem. These tradeoffs were aimed not so much at achieving high performance as at achieving low cost and (particularly when the Thor/Delta was under consideration) low weight.

Section 8.3.4 presents details on the bus and orbiter data handling systems designed for the Version III payload, while Section 8.3.5 presents the details on the subsystem designed for Version IV. A summary version of this last section is presented in Figure 8.3-1 and includes the following:

- The digital telemetry unit (DTU) fulfills all data handling functions except data storage. This DTU is the same unit used on Pioneers 10 and 11, with changes to only three of the nine circuit boards. The DTU is identical for both probe bus and orbiter,

and five of the nine subassemblies serve as the nucleus of the data subsystem for the probes as well.

- The data storage unit (DSU) is a new design based on current C-MOS technology that enhances the performance of several of the science instruments by providing multiple and simultaneous asynchronous buffering for high data rate measurements.
- Probe data storage uses the same components developed for the spacecraft DSU.
- Spacecraft/probe DTU commonality permits important savings in integration and operational software and training costs, particularly since the software requirements will be very similar to those developed for the Pioneers 10 and 11 program.

8.3.2 Requirements Analyses

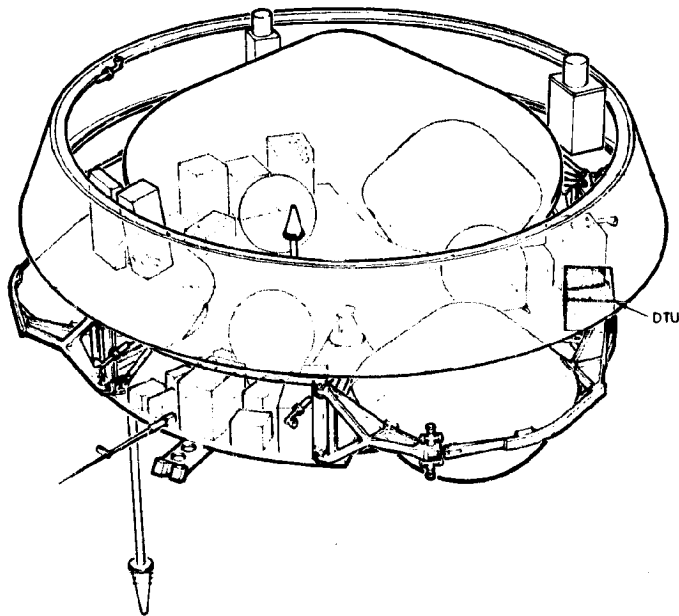
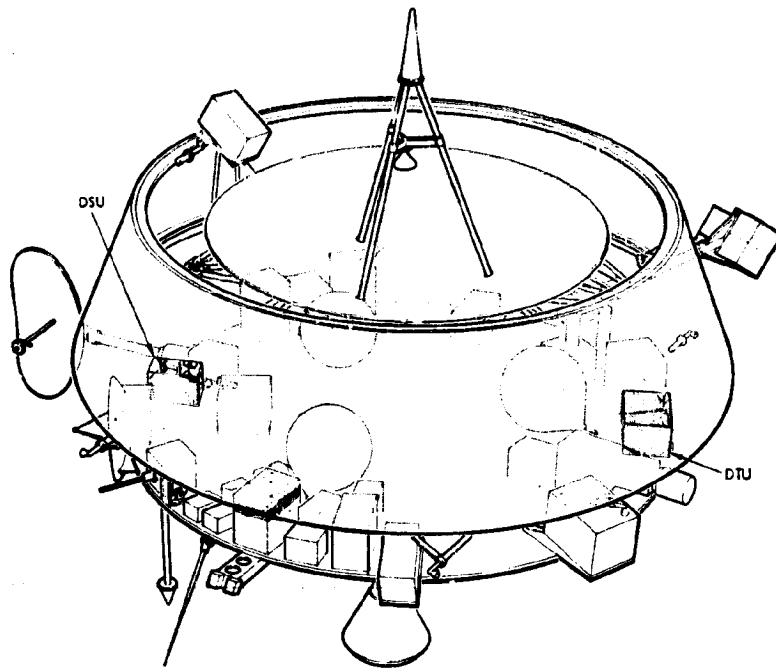
The analyses summarized in this section are presented first on the basis of the work done in response to the Version III science payload for each mission, and then on the basis of the work that was done in response to the Version IV payload.

The early work was based on bus and orbiter designs with quite low data rates because Version III did not impose high data rate requirements. In fact, the early versions of the payload were necessarily somewhat lacking in specific requirements so the study team made what it considered to be reasonable assumptions. For such considerations as timing and spin-sector determination, for example, or for downlink coding and formatting for DSN compatibility, requirements were actually "backfitted" from the hardware, so to speak, on the basis that use of Pioneers 10 and 11 hardware would keep costs to an absolute minimum.

With the advent of the Version IV payload's more specific and (in terms of data rate) more demanding science requirements, the team changed its approach accordingly.

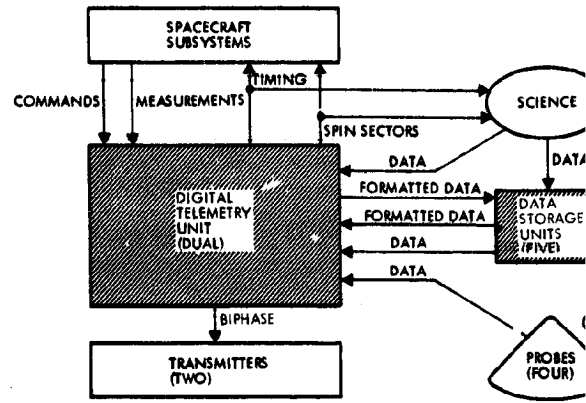
8.3.2.1 Probe Bus Requirements Analysis (Version III Science Payload 1977 Launch Opportunity)

The data handling subsystem acquires engineering data for subsequent telemetry transmission. The analog measurements should be quantized to at least 64 levels (6 bits) to obtain adequate information for spacecraft and instrument monitoring. A telemetry list is given in Appendix 8.3A. Table 8.3-1 summarizes this list.



FOLDOUT FRAME

A BLOCK DIAGRAM OF DATA HANDLING SUBSYSTEM



(1) ORBITER MISSION ONLY
(2) PROBE MISSION ONLY

DATA HANDLING FUNCTIONS:

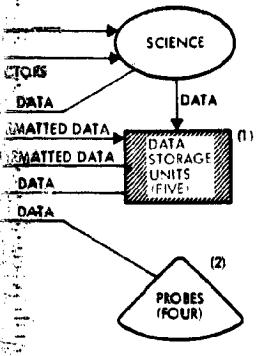
- GENERATE TIMING AND SPIN SECTOR DATA
- ACQUIRE SCIENCE AND ENGINEERING DATA
- QUANTIZE AND CONVERT DATA AS REQUIRED
- ENCODE AND PROCESS DATA INTO FORM SUITABLE FOR DOWNLINK MODULATION
- STORE DATA DURING OCCULTATION AND DATA PEAKS (ORBITER ONLY)

D DIGITAL TELEMETRY UNIT (DTU)



FLIGHT PROVEN PIONEER 10 AND 11
DIGITAL TELEMETRY UNIT (DTU)

SYSTEM



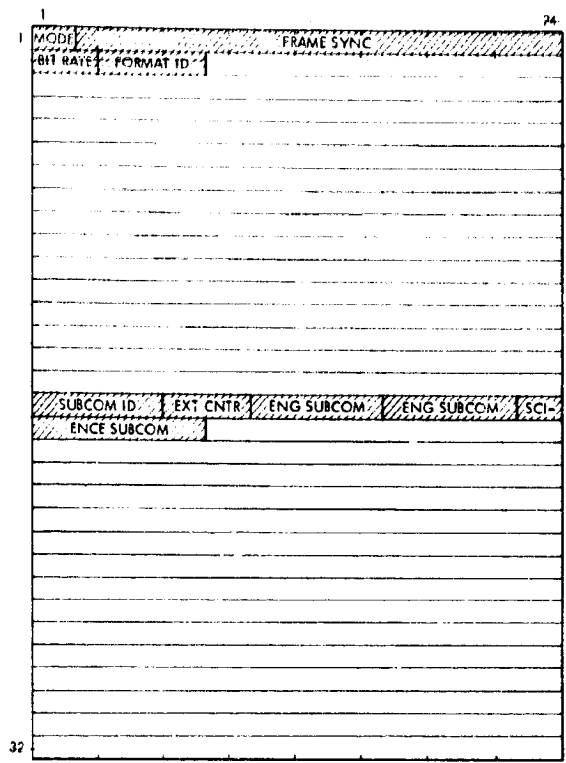
TIME AND PROCESS DATA INTO SUITABLE FOR DOWNLINK TRANSMISSION
 DATA DURING OCCUPATIONS
 DATA PEAKS - ORBITER ONLY*

B DATA HANDLING SUBSYSTEM PERFORMANCE SUMMARY

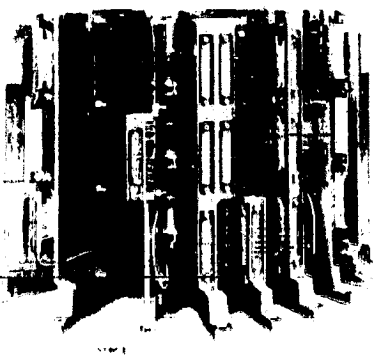
INPUTS	114 ANALOG (SCIENCE AND ENGINEERING) 102 DIGITAL (ENGINEERING) 86 DIGITAL (SCIENCE AND ENGINEERING)
ANALOG CONVERSION	SCIENCE AND INSTRUMENT HOUSEKEEPING: 10-BIT RESOLUTION, 0.5% ACCURACY ENGINEERING: 6-BIT RESOLUTION, 2% ACCURACY
OUTPUT	BIPHASE MODULATED THREE COMMANDABLE OUTPUT VOLTAGES (SELECTABLE MODULATION) INDEXES
CONVOLUTIONAL CODING	K = 32, 1/2 CODING CAN BE BYPASSED
DATA RATES	8, 16, 32, 64, 128, 256, 512, AND 1024 BITS/S (16 TO 2048 CODED SYMBOLS)
FORMATS	FOUR PRINCIPAL SCIENCE FORMATS SEVEN SPECIAL INTERLEAVED FORMATS TWO ENGINEERING SUBCOMS WHICH CAN ACCELERATE TO FIVE FORMATS ONE SCIENCE SUBCOM
CENTRAL TIMING	ACCURACY: ±0.02% 32.768 KHZ 2.048 KHZ BIT RATE (8 TO 1024 HZ) FRAME RATE (0.0104 TO 1.333 HZ)
SPIN PERIOD SECTORS	SUNPULSE REFERENCE ONE PULSE EACH REVOLUTION ONE PULSE 1/8TH, 1/64TH, AND 1/512TH REVOLUTION
STORAGE	1, 220, 800 BITS RECONFIGURABLE IN 245,760 BIT INCREMENTS UP TO 10 SIMULTANEOUS INPUTS UP TO 10 KBITS/S ON EACH INPUT
SUBSYSTEM WEIGHT	PROBE BUS 3.1 KG, (6.8 LB) ORBITER 12.6 KG, (27.8 LB)*
SUBSYSTEM REGULATED POWER	PROBE BUS 4.7 WATTS ORBITER 10.7 WATTS, PERIAPSIS: 6.8 WATTS, OTHER

*INCLUDES 9.5 KG (21 LB) FOR THE FIVE DSU'S. THIS IS A LAST MINUTE ADJUSTMENT AND IS NOT CONSISTENT WITH THE WEIGHT STUDIES ELSEWHERE IN THIS REPORT

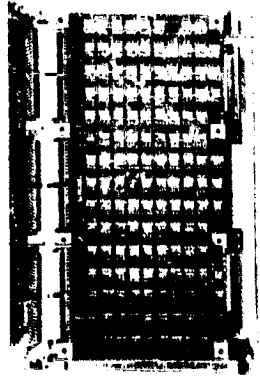
C BASIC FORMAT



COMMON DTU FORMAT PROPOSED FOR ORBITER, PROBE BUS AND PROBES

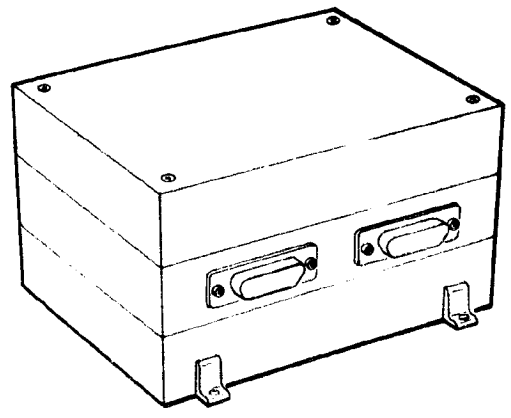


PIONEER DTU INTERNAL CONSTRUCTION



PC CARD AND CARD INTERCONNECTIONS AS USED IN PIONEER DTU

E DATA STORAGE UNIT (DSU)



ARTISTS CONCEPT OF 245,760-BIT SOLID STATE DATA STORAGE UNIT (DSU)

Figure 8.3-1. Preferred Data Handling Subsystem

Table 8.3-1. Engineering Measurements Summary

SUBSYSTEM	ANALOG	BILEVEL	DIGITAL
ELECTRICAL DISTRIBUTION	2	22	0
ELECTRICAL POWER	10	10	-
DATA HANDLING	3	7	10
COMMUNICATIONS	4	14	-
ATTITUDE CONTROL	10	8	4
THERMAL	5	1	-
SCIENCE	<u>1</u>	<u>16</u>	<u>6</u>
TOTAL REQUIRED	37	78	20

The data handling subsystem provides the spacecraft timing source. The timing requirement is set by the telemetry subcarrier frequency and stability requirements. In addition, data symbol transitions should be coherent with the subcarrier at all bit rates. The requirements for the Pioneer 10 and 11 subsystem were

used as a basis for the Pioneer Venus requirements; they meet or exceed the Pioneer Venus needs. They are:

Frequency	32.768 kHz \pm 0.02 percent
Jitter	<0.5 percent between any two cycles
Stability	200 ppm long-term
Asymmetry	<2.0 percent between adjacent half cycles.

A spin sector generator is required to provide angular resolution in the plane normal to the spin axis. This resolution should be better than 0.2 radian (± 0.5 degree) to provide the programming increments needed for spacecraft attitude control and for instrument sampling determination/control. The spin sector generator error contribution should not exceed 10 percent of the sun sensor error, minimize the effect on the overall roll attitude determination. That is, error between the sun pulse and a generated sector pulse should be less than 0.0002 radian (0.01 degree). Two spin sector operating modes are needed; an averaging mode to remove sun pulse jitter during normal flight, and a mode for times of spacecraft maneuvering where the sun pulse must be tracked regardless of jitter contributions.

Error correction coding of the telemetry downlink is strongly recommended to maximize the transmission bit rate at a given RF power within a maximum allowable error rate. The selected coding/decoding scheme must be compatible with the existing DSN capabilities. Rate one-half convolutional encoding with sequential decoding, as implemented on Pioneers

A/C III 10 and 11, offers an attractive low-cost approach because of the existing hardware and software.

T/D III

While the original study guidelines did not actually require that the probe bus be capable of relaying probe data in transit for the purpose of pre-separation checkout, it seemed likely to become a requirement. Consequently, the study team took it as a self-imposed requirement and designed the probes with an umbilical to the probe bus as well as designing the data format accordingly to accommodate probe data.

Critical probe bus data handling circuits should, of course, be redundant to maximize reliability.

For the Version III science payload it is assumed that the scientific data are digital for the neutral and ion mass spectrometers and the ultraviolet (UV) fluorescence experiment, and either analog or digital for the magnetometer and electron temperature probe. If analog is accepted, it should be quantized to 256 or more levels (8 bits), the Version III understanding of the instrument requirements. Except for the magnetometer, which operates throughout the mission, all data is acquired during the probe bus entry phase (approximately 10 minutes) as shown in Table 8.3-2.

Table 8.3-2. Probe Bus Instrument Data Rates (Version III Science Payload)

EXPERIMENT	BITS PER SAMPLE	SAMPLES PER MINUTE	BITS PER MINUTE	BITS PER SECOND
MAGNETOMETER	32	20	640	10.7
ELECTRON TEMPERATURE	30	60	1 800	30.0
NEUTRAL MASS SPECTROMETER	2500	2	5 000	83.3
ION MASS SPECTROMETER	2000	2	4 000	66.7
ULTRAVIOLET FLUORESCENCE	72	20	1 440	24.0
TOTAL			12 880	214.7

The added data handling requirements for the "other candidate" instruments are minimal. Several engineering measurements would be required plus the scientific data in Table 8.3-3.

A/C IV 8.3.2.2 Probe Bus Requirements Analyses (Version IV Science Payload)

The principal impact on the subsystem requirements is the increased data rate approaching Venus and during entry. The Version IV science

Table 8.3-3. Probe Bus Data Rates for "Other Candidate" Instruments (Version III Science Payload)

A/C III
T/D III

EXPERIMENT	BITS PER SAMPLE	SAMPLES PER MINUTE	BITS PER MINUTE	BITS PER SECOND
DAYGLOW PHOTOMETER	60	20	1200	20.0
SOLAR WIND PROB*	32	5	160	2.7
TOTAL			1360	22.7

* DURING CRUISE ALSO.

Table 8.3-4. Probe Bus Instrument Data Rates (Version IV Science Payload)

A/C IV

EXPERIMENT	BITS PER SAMPLE	BITS PER SECOND FROM ENTRY-4 DAYS	BITS PER SECOND FROM ENTRY-1 HOUR
NEUTRAL MASS SPECTROMETER	520	-	195
ION MASS SPECTROMETER	210	-	236.3
ELECTRON TEMPERATURE PROBE	90	-	33.8
RETARDING POTENTIAL ANALYZER	125	-	140.6
ULTRAVIOLET SPECTROMETER	7200 720	12 -	- 270
TOTAL		12	875.7

* DATA RATES ARE BASED ON THE PREFERRED DESCENT TRAJECTORY

requirements (see Table 8.3-4) increase the data rate from 214.7 to 875.7 bits/s at entry, a factor of four higher. Data acquisition and transmission are not required during cruise.

In addition to the science requirements given in Table 8.3-4, new instrument housekeeping requirements have been imposed. Significantly analog-to-digital conversion (to 10-bit resolution) is specified for the ion mass spectrometer. Table 8.3-5 gives the data requirements for the other candidate instruments.

All other probe bus data handling requirements remain as described in Section 8.3.2.1.

8.3.2.3 Orbiter Requirements Analysis (Version III Science Payload)

The orbiter engineering telemetry measurements list is given in Appendix 8.3A, and a summary is presented in Table 8.3-6.

ALL VERSION III
SCIENCE PAYLOAD

Table 8.3-5. Probe Bus Data Rates for "Other Candidate" Instruments (Version IV Science Payload)

A/C IV

EXPERIMENT	BITS PER SAMPLE	BITS PER SECOND DURING CRUISE	BITS PER SECOND FROM ENTRY-1 HOUR
SOLAR WIND ANALYZER	2500	57	57
MAGNETOMETER	30	15	30
TOTAL		72	87

Table 8.3-6. Engineering Measurements Summary

ALL ORBITER CONFIGURATIONS

SUBSYSTEM	ANALOG	BILEVEL	DIGITAL
ELECTRICAL DISTRIBUTION	2	18	3
ELECTRICAL POWER	11	6	-
DATA HANDLING	3	7	6
COMMUNICATIONS	6	18	-
ATTITUDE CONTROL	18	6	4
THERMAL	5	1	-
SCIENCE	1	21	6
TOTAL REQUIRED	46	77	19

ALL VERSION III SCIENCE PAYLOAD

The timing, data coding, DSN compatibility, and redundancy requirements are similar to those of the probe bus. The spin sector generation requirements are also similar except that a pseudo-sun pulse is necessary for science programming during periods of solar eclipse. The sector generator must "remember" the spin rate and continue to generate spin sector data in the absence of sun pulses for periods up to 85 minutes. This will occur during orbit day 170. The longest sun eclipse near periapsis is 28 minutes and occurs at day 41. Figure 8.3-2 depicts the sun occultation profile for the recommended orbit.

Other orbit characteristics such as time near periapsis and time in earth occultation which impact the orbiter data handling subsystem, are also shown in Figure 8.3-2. The earth occultation periods near periapsis during the first 71 days in orbit, are important since the majority of scientific information is acquired at low altitudes.

ALL ORBITER CONFIGURATIONS

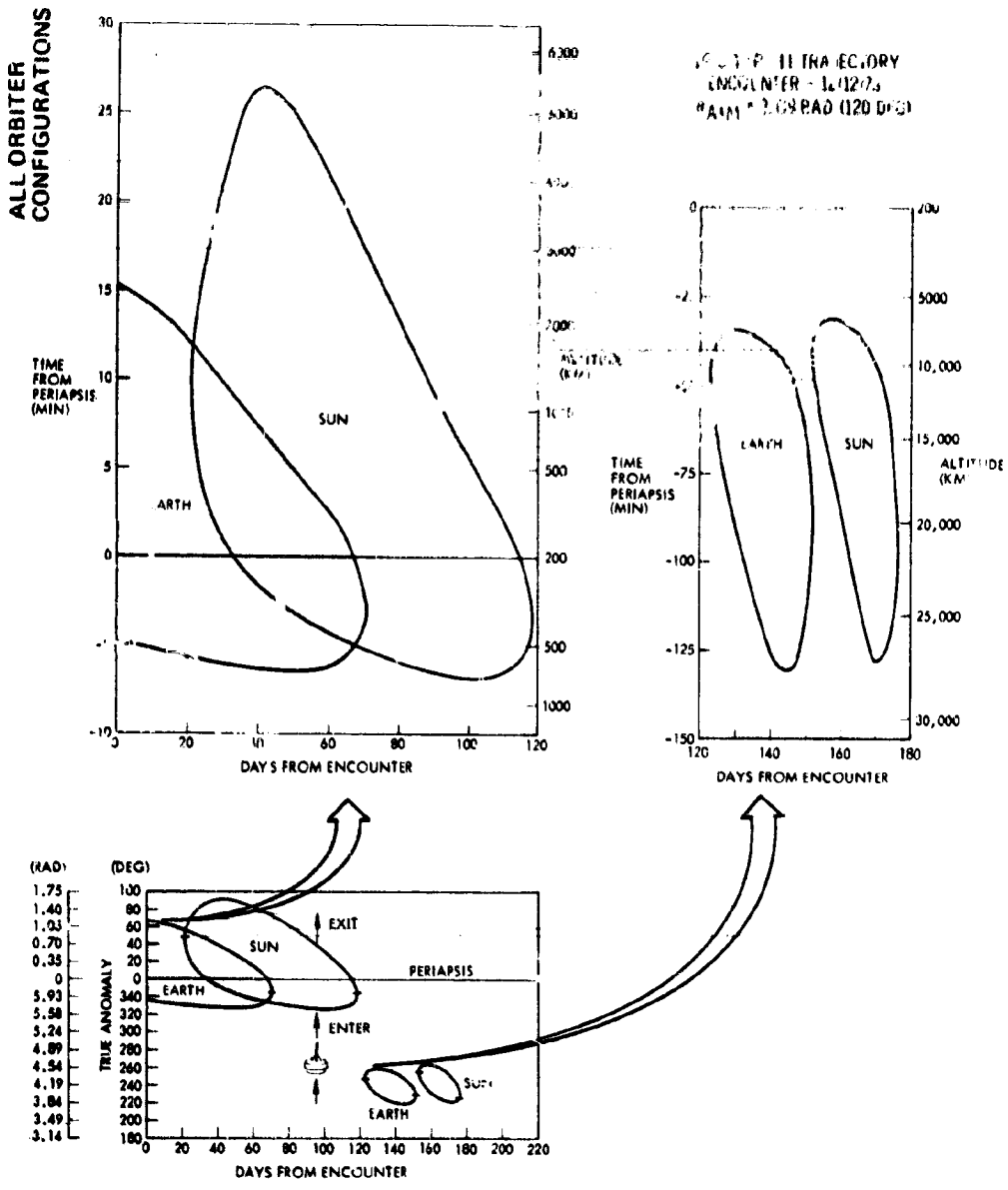


Figure 8.3-2. Orbiter Sun and Earth Occultation Profiles

ALL VERSION III SCIENCE PAYLOAD

Figure 8.3-3 illustrates the data acquisition profile by instrument. The magnetometer samples continuously during cruise and orbit. The electron temperature probe, neutral mass spectrometer, and ion mass spectrometer operate at altitudes where there is perceptible atmosphere. The radar altimeter can map below 1000 kilometers and may operate in a nonaveraging, high bit rate mode below 300 kilometers, where the received signal-to-noise ratio will be favorable. The infrared (IR) radiometer will sample when viewing the planet, probably the dark side only

ALL VERSION III ORBITERS

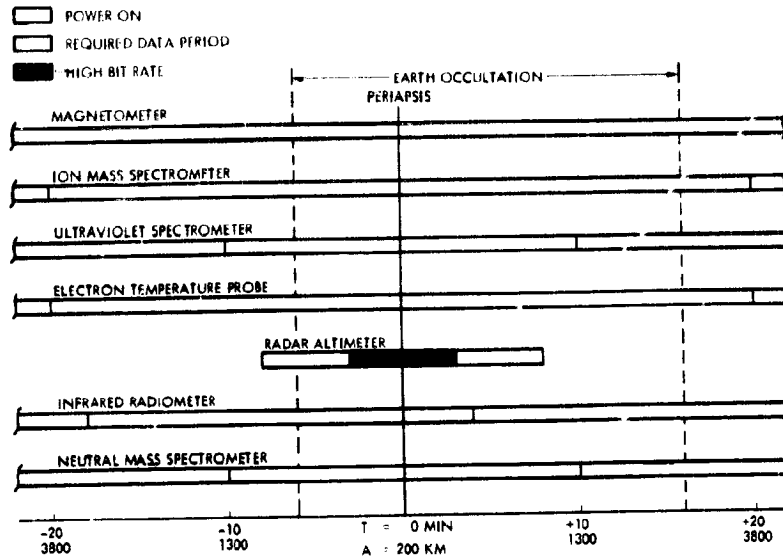


Figure 8.3-3. Orbiter Version III Science Payload Instrument Data Acquisition Profiles

and close to periapsis. The requirements for the ultraviolet (UV) spectrometer may vary depending on the selected instrument. The instrument will probably sample when viewing the nadir and zenith; possible sample periods are thus limited to two for a fixed mounted instrument but are essentially unlimited for a gimballed instrument. A reasonable requirement, adopted for our analysis, is to acquire UV spectrometer data when below 1500 kilometers, and to provide limited means of high altitude sampling.

From these considerations, representative data rate requirements, Table 8.3-7, were established which provide good science accommodation tempered by overall cost and risk considerations.

Table 8.3-7. Orbiter Instrument Data Rates (Version III Science Payload)

EXPERIMENT	BITS PER SAMPLE	SAMPLES PER MINUTE	BITS PER MINUTE	BITS PER SECOND
MAGNETOMETER	24	5	120	2
ELECTRON TEMPERATURE	30	60	1800	30
NEUTRAL MASS SPECTROMETER	5000	0.2	1000	16.7
ION MASS SPECTROMETER	2000	0.4	800	13.3
ULTRAVIOLET SPECTROMETER	400	2	800	13.3
INFRARED RADIOMETER	40	10	400	6.7
RADAR ALTIMETER	280	5	1400	23.7
TOTAL			6320	105.7

Requirements for special high bit rate modes are also included since such modes improve the scientific data return for the UV spectrometer and IR radiometer, with minimal impact on the data handling subsystem. In these modes, high bit rate data is stored and transmitted later at the prevailing telemetry link bit rate, as provided for the imaging photo polarimeter experiment on Pioneers 10 and 11. The special mode for the radar altimeter will be provided during all periapsis passes. The special modes for the UV and IR will be provided, by command, only when storage is available. Table 8.3-8 gives the special mode requirements. Memory is also needed to store normal formatted data during earth occultation periods which occur during the first 71 days in orbit. Finally, storage is necessary for the magnetometer data to preclude the need for continuous DSN coverage. Table 8.3-8 also gives the storage requirements. The total storage necessary is not the sum, since the special modes can time-share memory. However, since the DTU data is in line the first 71 days in orbit and the radar altimeter high bit rate mode is in line throughout the mission, redundancy is suggested for these functions.

Table 8.3-8. Orbiter Data Storage and Special Mode Requirements (Version III Science Payload)

USAGE	REQUIREMENTS (BITS)	COMMENTS
DIGITAL TELEMETRY UNIT (DTU)	168 960	22 MINUTES DURING OCCULTATION AT 128 BITS/S OF FORMATTED DATA
RADAR ALTIMETER	105 000	3500 BITS/S OF 1 SECOND EACH; 12 SECONDS FOR 6 MINUTES
ULTRAVIOLET SPECTROMETER	80 000	1600 BITS/S FOR 50 SECONDS
INFRARED RADIOMETER	40 960	2300 BITS/S FOR 18 SECONDS
MAGNETOMETER	-	2 BITS/S FOR UP TO 24 HOURS DEPENDING ON DSN AVAILABILITY AND MAGNETOMETER COVERAGE DESIRED

Additional requirements imposed by the other candidate instruments are summarized in Table 8.3-9.

8.3.2.4 Orbiter Requirements Analysis (Version IV Science Payload)

The orbiter subsystem requirements were impacted by Version IV science payload changes in data throughput rate and the amount and usage of storage. Table 8.3-10 summarizes the Version IV science data rate

Table 8.3-9. Orbiter Data Rates for "Other Candidate" Instruments (Version III Science Payload)

EXPERIMENT	BITS PER SAMPLE	SAMPLES PER MINUTE	BITS PER MINUTE	BITS PER SECOND
SOLAR WIND PROBE	32	5	160	2.7
THERMAL SUPERHERMAL PARTICLE DETECTOR	40	10	400	6.7
ELECTRIC FIELD DETECTOR	32	5	160	2.7
SOLAR ELECTRON DETECTOR	40	10	400	6.7
MICROWAVE RADIOMETER	600	2	1200	20
TOTAL			2320	38.8

Table 8.3-10. Orbiter Instrument Data Rates (Version IV Science Payload)

EXPERIMENT	BITS PER SAMPLE	BITS PER SECOND (CRUISE)	BITS PER SECOND (HIGH ALTITUDE)	BITS PER SECOND (PERIAPSIS)
MAGNETOMETER	32	3	3	32
SOLAR WIND ANALYZER	32	3	3	-
ELECTRON TEMPERATURE PROBE	24	-	-	24
NEUTRAL MASS SPECTROMETER	*	-	-	100
ION MASS SPECTROMETER	*	-	-	100
ULTRAVIOLET SPECTROMETER	*	-	1.7	34
INFRARED RADIOMETER	*	-	-	100
RADAR ALTIMETER	*	-	-	50
TOTAL		6	7.7	440

NOT AVAILABLE IN VERSION IV SCIENCE REQUIREMENTS

requirements during cruise, high altitude orbit, and at periapsis. Figure 8.3-4 presents a more detailed orbital data rate profile.

The data rate at periapsis has increased from 105.7 to 440 bits/s, a factor of four higher.

These higher data rates also increase the amount of storage required. Table 8.3-11 gives the minimum data storage necessary to buffer the unformatted data during occultation.

However, a cost-effective communications link requires a reduced telemetry data rate, which could be accomplished by storing low altitude data for later transmission at a lower data rate. The storage necessary for this is given in Table 8.3-12.

ALL VERSION IV SCIENCE PAYLOAD

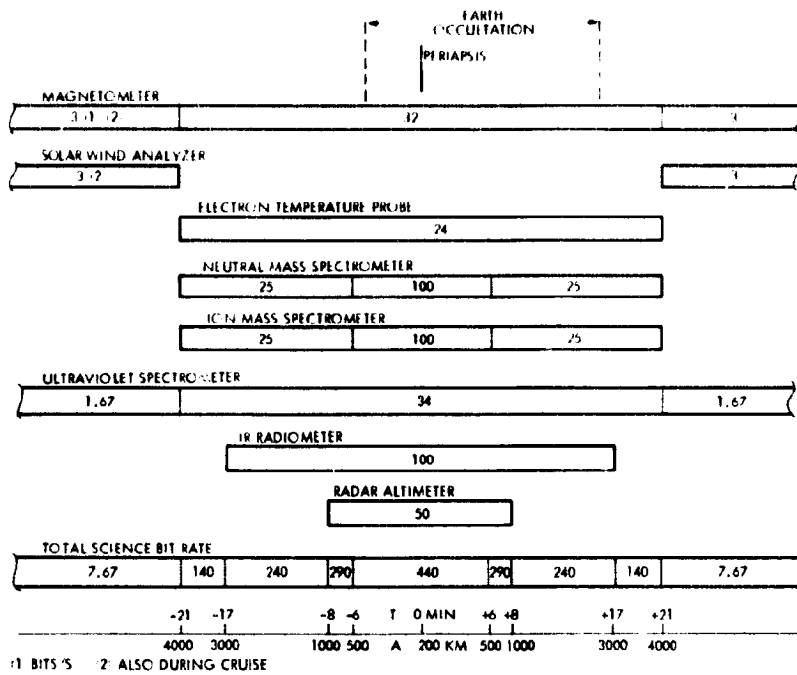


Figure 8.3-4. Orbiter Version IV Science Payload Data Rate Profile

Table 8.3-11. Minimal Orbiter Data Storage Requirements (Version III Science Payload)

USAGE	REQUIREMENTS (BITS)	COMMENTS
DIGITAL TELEMETRY UNIT (DTU)	7 600	HOUSEKEEPING DATA AT 5.8 BITS/S DURING 22 MINUTES OF OCCULTATION
MAGNETOMETER	42 240	32 BITS/S FOR 22 MINUTES
ELECTRON TEMPERATURE PROBE	31 680	24 BITS/S FOR 22 MINUTES
NEUTRAL MASS SPECTROMETER	82 500	100 BITS/S FOR 11 MINUTES AND 25 BITS/S FOR 11 MINUTES
ION MASS SPECTROMETER	82 500	100 BITS/S FOR 11 MINUTES AND 25 BITS/S FOR 11 MINUTES
ULTRAVIOLET SPECTROMETER	44 880	34 BITS/S FOR 22 MINUTES
INFRARED RADIOMETER	132 000	100 BITS/S FOR 22 MINUTES
RADAR ALTIMETER	39 000	50 BITS/S FOR 13 MINUTES
TOTAL	462 400	

The known data parameters of the other candidate instruments are given in Table 8.3-13.

The other orbiter data handling requirements are essentially unchanged from those defined for the Version III science payload in Section 8.3.2.3.

Table 8. 3-12. Cost-Effective (Delayed Transmission) Data Storage Requirements (Version IV Science Payload)

A/C IV

USAGE	REQUIREMENTS (BITS)	COMMENTS
DIGITAL TELEMETRY UNIT (DTU)	322 560	128 BITS/S FOR THE 42-MINUTE LOW-ALTITUDE PERIOD; INCLUDES FORMATTED MAGNETOMETER, ELECTRON TEMPERATURE, ULTRAVIOLET SPECTROMETER, AND HOUSEKEEPING DATA
NEUTRAL MASS SPECTROMETER	117 000	25 BITS/S FOR 30 MINUTES AND 100 BITS/S FOR 12 MINUTES
ION MASS SPECTROMETER	117,000	25 BITS/S FOR 30 MINUTES AND 100 BITS/S FOR 12 MINUTES
INFRARED RADIOMETER	204 000	100 BITS/S FOR 34 MINUTES
RADAR ALTIMETER	48 000	50 BITS/S FOR 16 MINUTES
TOTAL	808 560	

Table 8. 3-13. Orbiter Data Rates for "Other Candidate" Instruments (Version IV Science Payload)

ALL VERSION IV
SCIENCE PAYLOAD

EXPERIMENT	DATA ACQUISITION RANGE IN ORBIT (KM)	BITS PER ORBIT	BITS PER SAMPLE	BITS PER SECOND
AC ELECTRIC FIELD DETECTOR	>4000*	195 000	24	2.3
	<4000	5 600	24	2.3
MICROWAVE RADIOMETER	<2000	250 000	**	**
SPIN SCAN PHOTOMETER	>4000	3 600 000	**	**
	<4000	378 000	**	**

* ALSO DURING CRUISE

** NOT AVAILABLE IN VERSION IV SCIENCE REQUIREMENTS.

8.3.3 Tradeoff Studies

The tradeoff studies covered the following subjects:

- Off-the-shelf telemetry equipment
- Low weight, advanced technology alternate
- Centralized processing
- Memory alternatives
- Science interfaces.

All of the tradeoffs were conducted prior to the receipt of the Version IV science requirements. The results of the off-the-shelf telemetry equipment tradeoffs, and the science interface tradeoffs remain pertinent, however. The other three tradeoffs are less critical for the selected Atlas/Centaur launch vehicle, because of its large weight margin.

8.3.3.1 Off-the-Shelf Telemetry Equipment

ALL CONFIGURATIONS

A comprehensive survey of off-the-shelf telemetry equipment other than that derived from the Pioneers 10 and 11 program, was conducted. Although several provided good performance features and low basic costs, certain functions were lacking such as the convolutional coder and the spin sector generator. In addition, the interfaces with other subsystems were generally not compatible. It was concluded that the cost and risk advantages of using developed hardware could only be realized for this type of equipment if the entire equipment complement from the same program were used.

Since the Pioneers 10 and 11 DTU is flight-proven, meets the Pioneer Venus data handling requirements (with minor modifications) is compatible with the DSN and other spacecraft subsystems, and is well known to both NASA/ARC and TRW, it was selected as the preferred telemetry data processing unit. Table 8.3-14 summarizes the results of this equipment survey.

8.3.3.2 Low Weight, Advanced Technology Alternate

 T/D III  T/D III

It became obvious during the overall system studies that the weight margin for a Thor/Delta system was minimal, especially for the probe mission. An advanced data acquisition and command subsystem (DACS) was explored as a low-weight alternate. Figure 8.3-5 is a block diagram of a candidate DACS.

The DACS uses "P" channel MOS LSI and TTL MSI technology to achieve a flexible, low-weight, low-power subsystem. Key components have been developed and breadboarded at TRW. The subsystem uses the Pioneers 10 and 11 DDU to demodulate and authenticate commands and a central control unit (CCU) to distribute commands and collect and format telemetry data from remote terminal units (RTU). The RTU distributes commands received from the CCU and collects and performs analog-to-digital (A/D) conversion of telemetry data requested by the CCU in accordance with a program stored in the CCU read-only memory (ROM). When the probes are released, the telemetry format is determined by a program stored within a ROM in each probe RTU. Since the DACS processes commands, the Pioneers 10 and 11 CDU is simplified to provide only special

Table 8. 3-14. Telemetry Equipment Tradeoffs

TELEMETRY SYSTEM	MANUFACTURER	DEVELOPMENT STATUS	WEIGHT (KG (LB))	POWER (W (Amps))	ANALOG INPUTS	BILEVEL INPUTS	DIGITAL INPUTS	BIT RATES (BITS/S)	FORMATS	COMMENTS
<u>PIONEERS 10 AND 11</u>	TRW	FLOWN	3.40 (7.5)	4.5	111	102	86	(EIGHT), 16-2048	7 PRINCIPAL 28 TOTAL	USE AS IS. INTERNALLY REDUNDANT, I.E., 1.76 KG (3.75 LB) PER SIDE
<u>DSP</u>	DYNATRONICS	FLOWN	4.08 (9)	5.75	489	240	21	1K, 128K	1 FIXED	NO SPOKE-HEEL GENERATOR, NO CONVOLUTIONAL CODING, NO TIMING SIGNALS FOR SCIENCE, NO DSU INTERFACE
<u>PROGRAM 777</u>	DYNATRONICS	FLOWN	2.61 (5.75)	2.5	68	88	13	250	1 FIXED	NO SPOKE-HEEL GENERATOR, NO CONVOLUTIONAL CODING, NO TIMING SIGNALS FOR SCIENCE, NO DSU INTERFACE
<u>REMOTE MULTIPLEXER</u>	DYNATRONICS	FLOWN	2.47 (5.5)	2.5	79	88	6	SLAVED TO ENCODER	SLAVED TO ENCODER	
<u>HEAD</u>	TRW	IN DEVELOPMENT	0.45 (1)	0.5 TO 2	PROGRAMMABLE UP TO 128 FOR ANALOG/BILEVEL MIX AND 64 DIGITAL (EACH DIGITAL = 2) - UP TO 10 MULTIPLEXERS PER REDUNDANT STRING			SLAVED TO CPU	SLAVED TO CPU	NO SPOKE-HEEL GENERATOR, NO CONVOLUTIONAL CODING, NO TIMING SIGNALS FOR SCIENCE, NO DSU INTERFACE, RATE TOO HIGH, VERY FLEXIBLE
<u>CONTROL PROCESSOR</u>	TRW	IN DEVELOPMENT	1.13 (2.2)	3	-	-	-	25.6K	PROGRAMMABLE IN ROM'S	
<u>CENTRAL CLOCK</u>	TRW	IN DEVELOPMENT	0.91 (2)	5	-	-	-	1.024 MHZ	-	
<u>VIKING LANDER</u>	MMC	ADVANCED DEVELOPMENT	7.57 (16.7)	9	183	48	15	8-1/3, 33-1/3	MANY	NO SPOKE-HEEL GENERATOR, NO CONVOLUTIONAL CODING, NO TIMING SIGNALS FOR SCIENCE, NO DSU INTERFACE, INTERNALLY REDUNDANT
<u>OSO</u>	HAC	ADVANCED DEVELOPMENT	0.23 (0.5)	1.5	UP TO 32 TOTAL			SLAVED TO PCM	SLAVED TO PCM	NO SPOKE-HEEL GENERATOR, NO CONVOLUTIONAL CODING, NO DSU INTERFACE, VERY FLEXIBLE, CLOCK STABLE TO 1 PART IN 1 x 10 ⁹ , MORE COMPLICATED THAN NEEDED
<u>DUAL REMOTE MULTIPLEXER (4 TYPES)</u>	HAC	ADVANCED DEVELOPMENT	1.54 (3.4)	2.5	-	-	-	32K	MANY	
<u>PCM ENCODER</u>	HAC	ADVANCED DEVELOPMENT	1.32 (2.9)	-	-	-	-	-	MANY	
<u>FORMAT GENERATOR</u>	HAC	ADVANCED DEVELOPMENT	-	-	-	-	-	-	MANY	
<u>SPACECRAFT CLOCK</u>	HAC	ADVANCED DEVELOPMENT	3.40 (7.5)	-	-	-	-	-	-	

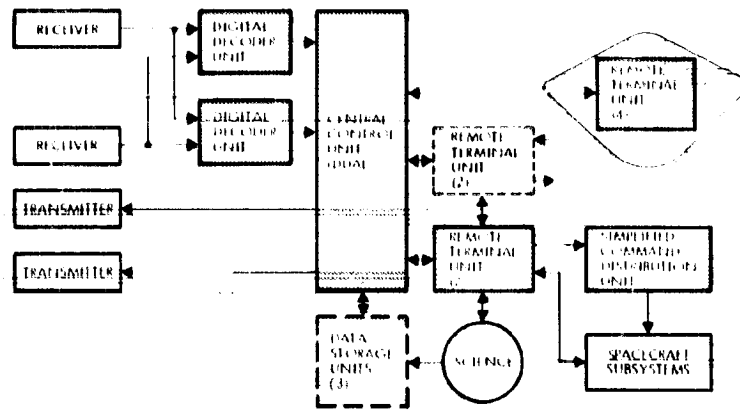


Figure 8.3.5 Alternate Data and Command Subsystem

functions, such as ordnance firing, high-level commands, and signal conditioning. Other CDU functions such as thruster firing, pulse counting, command storage, and sequencing and other DTU functions such as spin sector determination and convolutional coding are performed by the CCU. The key features of the DACS are:

- Low weight
- Low power consumption
- System flexibility (modular design, ROM programmable formats).

Table 8.3-15 compares the preferred command and data subsystem (derived from Pioneers 10 and 11) to the alternate DACS. Because of the increased use of microminiaturization (P-MOS LSI and bipolar MSI), the weight and power of the DACS are substantially reduced. However, the DACS requires further development with the attendant costs; the manufacturing costs are similar for the two approaches. The cost delta includes total program costs, including nonrecurring and recurring costs for the probe bus, the probes, and the orbiter. The \$730K difference assumes the availability of the prototype, qualification, and flight spare Pioneers 10 and 11 DTU's; only refurbishment and retest costs are included. The delta is reduced to \$430K if three new DTU's must be fabricated for the baseline.

Because of the lower costs and minimal risks associated with the developed approach, the Pioneers 10 and 11 subsystem is selected. However, the DACS remains a viable alternative for weight constrained Thor/Delta configurations.



Table 8.3-15. Baseline versus DACS Cost Tradeoffs

PARAMETER	BASELINE		DACS		DELTA FROM BASELINE	
	BUS PROBES	ORBITER	BUS PROBES	ORBITER	BUS PROBES	ORBITER
FLEXIBILITY	GOOD		VERY GOOD		-	-
STATUS	MINIMAL DEVELOPMENT REQUIRED		MODERATE DEVELOPMENT REQUIRED		-	-
WEIGHT (KG (LB))	12.1 (26.7)	9.5 (21.0)	7.3 (16.1)	7.7 (17.0)	-4.8 (-10.6)	-1.8 (-4.0)
POWER (WATTS)	16.2	11.7	11.2	11.5	-5.0	-0.2
RELIABILITY	-	0.998	-	0.985	-	-0.003
COST	-	-	-	-	-\$430K OR \$730K*	

* ASSUMES PIONEERS 10 AND 11 RESIDUAL UNITS AVAILABLE

A comprehensive analysis of the DACS is given in Appendix 8.3B.

8.3.3.3 Centralized Processing

Central processing was examined as an alternate to the conventional approach where each subsystem performs its own data processing. The concept is to execute in a single processor those functions presently performed in distributed hardware so that the overall spacecraft weight and cost will be minimized. Centralized functions would include:

- Telemetry formatting
- Convolutional encoding
- Spin sector generation
- Command storage
- Thruster pulse counting
- Programming for ΔV maneuvers
- Programming for precessions
- Programming for science instrument sampling
- Science gimbal controlling.

The subsystem model assumed the use of the DACS (described in Section 8.3.3.2) with the CCU replaced by a faster, general-purpose processor. In addition to hardware economies achieved with the DACS, the programming portions of the CEA and programming portions of the affected scientific instruments would be deleted.

T/D III

T/D III

Table 8.3-16 summarizes the comparative weight and power parameters. The weight saving is offset by the higher nonrecurring costs. Such a radical departure from proven approaches involves a development risk, however. In general, this risk derives from multiplexing many diverse functions by means of software within a single processor. The conventional subsystems lose their identity to the extent that classical management techniques are no longer applicable.

Table 8.3-16. Centralized versus Distributed Processing

	PROBE BUS			ORBITER		
	DISTRIBUTED	CENTRALIZED	DELTA	DISTRIBUTED	CENTRALIZED	DELTA
WEIGHT (KG (LB))	14.1 (31.0)	8.9 (19.7)	5.2 (11.3)	16.0 (35.3)	11.4 (25.2)	4.6 (10.1)
POWER (WATTS)	20.7	20.7	0	15.3	19.1	[3.8]

Appendix 8.3C documents additional details developed in this tradeoff study.

8.3.3.4 Memory Alternative

ALL ORBITER CONFIGURATIONS

The memories listed in Table 8.3-17 were investigated for use as the orbiter data storage unit. The Pioneers 10 and 11 DSU was rejected because of its unacceptably low capacity. There are other off-the-shelf core and plated wire memories with the capacity required for the orbiter but none can interface directly with the digital telemetry unit or the science. They are all heavier than the preferred C-MOS memory and, because of intricate fabrication techniques, cost more. Further, only one input or output is available while the selected approach is flexible and can be configured as a group of smaller memories, thus providing buffer storage for several science instruments simultaneously. Of course it is possible to use several core or wire memories to gain modularity, but the penalties are higher cost, weight, and power consumption. The P-MOS offers many of the same advantages as the static C-MOS but since it is dynamic timing problems limit the special buffer modes. Static P-MOS was not investigated because of the inherently high power consumption. The costs given in Table 8.3-17 include nonrecurring and recurring as well as the

ALL ORBITER CONFIGURATIONS

Table 8.3-17. Data Storage Tradeoffs

MEMORY TYPE	CAPACITY (BITS)	WEIGHT (KG (LB))	TOTAL COST (\$K)	POWER (WATTS)	REMARKS
CORE					
PIONEERS 10 AND 11	49 152	1.6 (3.5)	N/A	0.4 TO 1.2	OFF THE SHELF. HAS DTU INTERFACE. INSUFFICIENT CAPACITY. NEEDS THREE VOLTAGES.
EMI	1 100 000	6.4 (14.0)	630	2.0 TO 5.5	OFF THE SHELF. REQUIRES MAJOR MODIFICATION OR NEW INTERFACE UNIT. NEEDS THREE VOLTAGES.
HELIOS	524 288	4.7 (10.3)	?	3.0 TO 5.7	ADVANCED DEVELOPMENT. REQUIRES NEW INTERFACE UNIT. GERMAN MADE. NEEDS THREE VOLTAGES.
PLATED WIRE					
MINUTEMAN	580 000	7.4 (16.2)	644	1.5	OFF THE SHELF. REQUIRES NEW INTERFACE UNIT. NEEDS THREE VOLTAGES.
VIKING	500 000	4.3 (9.5)	655	1.5	ADVANCED DEVELOPMENT. REQUIRES NEW INTERFACE UNIT. NEEDS THREE VOLTAGES.
MOTOROLA	768 000	17.2 (38)	650	1.5 TO 2.5	REQUIRES NEW INTERFACE UNIT. NEEDS TWO VOLTAGES.
HONEYWELL	544 000	16.3 (36)	560	5	REQUIRES NEW INTERFACE UNIT. NEEDS POWER SWITCHING ADDED. NEEDS FOUR VOLTAGES.
SOLID STATE					
DYNAMIC P-MOS (MULTI-CHIP)	491 520	1.2 (2.7)	460	4.3	NEW DESIGN USING PROVEN TECHNOLOGY. BECAUSE OF TIMING PROBLEMS SPECIAL BUFFER MODES CANNOT BE SUPPLIED. NEEDS THREE VOLTAGES.
STATIC C-MOS (MULTI-CHIP)	491,520	1.2 (2.7)	415	0.4 TO 3.0	NEW DESIGN USING PROVEN TECHNOLOGY. GIVES SPECIAL MODES TO SCIENCE. NEEDS ONE VOLTAGE.
STATIC C-MOS (MULTI-CHIP)	737 280	1.8 (4.0)	465	0.6 TO 4.5	NEW DESIGN USING PROVEN TECHNOLOGY. GIVES SPECIAL MODES SIMULTANEOUSLY TO SCIENCE AND PROVIDES RECONFIGURABLE REDUNDANCY. OPERATIONALLY VERY FLEXIBLE. NEEDS ONE VOLTAGE.

*WEIGHT, COST, AND POWER COLUMNS INCLUDE DELTAS TO COVER INCREASED ELECTRONICS REQUIRED FOR ADDED INTERFACE MODULES. COSTS OF POWER REGULATION ALSO INCLUDED.

costs for required interface units, where applicable. The weight and power entries also include interface units, as required.

8.3.3.5 Science Interfaces ALL CONFIGURATIONS

The data handling subsystem can provide several interface services to the experiments. These include:

- Signal conditioning
- Asynchronous buffering
- Buffer storage
- Analog-to-digital conversion
- Analog multiplexing
- Programming.

ALL CONFIGURATIONS

Signal conditioning, asynchronous buffering, and programming are generally instrument-peculiar and, therefore, are usually performed by each instrument. This approach is recommended for Pioneer Venus in order to maintain standard interfaces with the resultant ease of interface specification and control.

Buffer storage is large and expensive, particularly when capacities approaching 100,000 bits are required. Time sharing of buffer storage yields obvious cost and weight advantages and is recommended and included in our preferred data handling subsystem approach.

Analog-to-digital conversion and analog multiplexing are functions which may be performed by either the individual instruments or centrally by the data handling subsystem since the tradeoffs are not sensitive in either direction. Modifications involving only a few boards will allow the Pioneers 10 and 11 DTU to provide 10-bit resolution analog-to-digital conversion for the instruments for both science and housekeeping data. Because other changes to the Pioneers 10 and 11 DTU are necessary, this is a cost-effective approach.

8.3.4 Data Handling Subsystem for Version III Science Payload

The subsystem designs discussed in this section were sized for use with the probe bus and two orbiter configurations: 1) a fanscan antenna with a 31-watt transmitter and, 2) a Franklin array with a despun reflector. Their sizing is also based on use of both 64- and 26-meter DSN subnets for time periods that vary according to what the team regarded as reasonable assumptions of availability.

These designs make use of the Pioneers 10 and 11 DTU and a new DSU. No distinction is made between Thor/Delta and Atlas/Centaur launch vehicles except in the area of DSU packaging.

ALL VERSION III
SCIENCE PAYLOAD

AC III 8.3.4.1 Probe Bus Data Handling Subsystem Description (Version III Science Payload)

T/D III

The probe bus data handling subsystem is comprised of a single internally redundant DTU. Figure 8.3-6 is a block diagram of the DTU.

The DTU can accept data as given in Table 8.3-18.

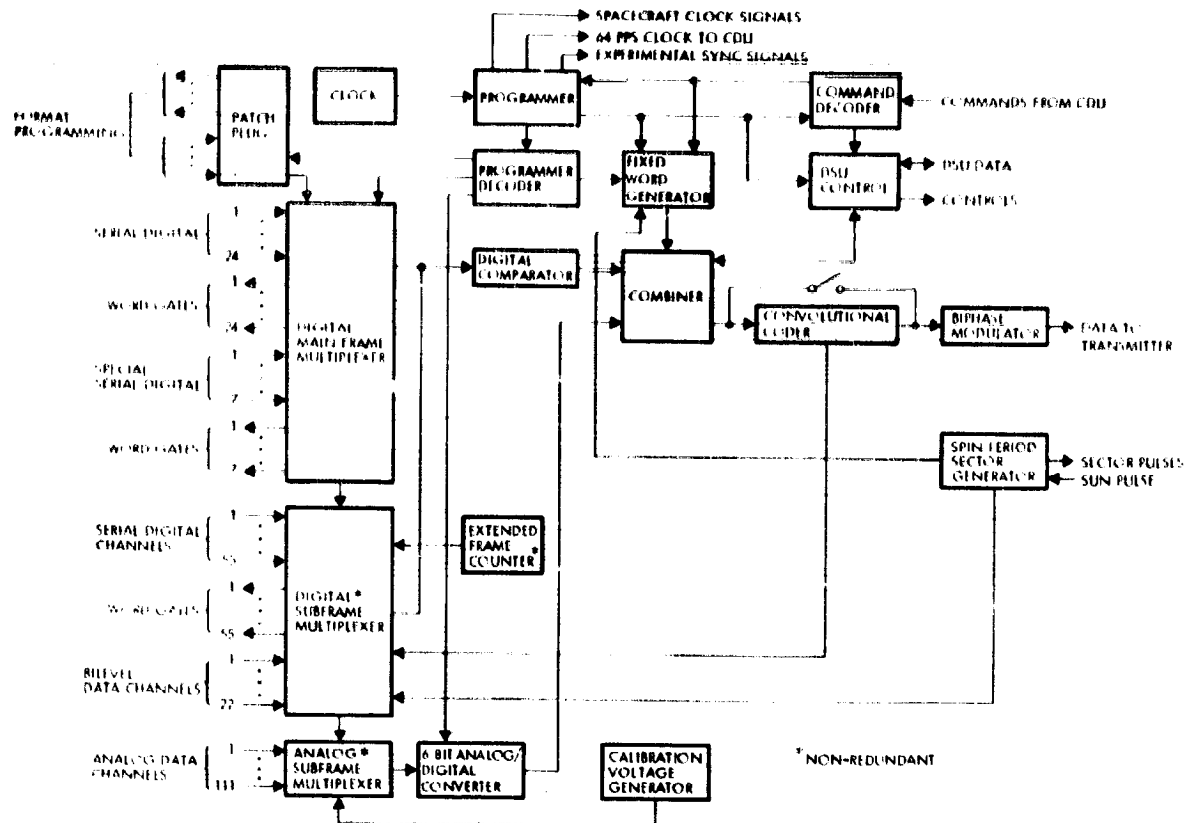


Figure 8.3-6. Digital Telemetry Unit (DTU)

Table 8.3-18. Version III DTU Inputs

TYPE OF CHANNEL	NUMBER OF CHANNELS
SERIAL DIGITAL INPUTS	
• SCIENCE FORMAT A	12
• SCIENCE FORMAT B	12
• SPECIAL D FORMATS	7
• ENGINEERING SUBCOM	35
• SCIENCE SUBCOM	20
	86
BILEVEL	
• ENGINEERING SUBCOM	78
• SCIENCE SUBCOM	24
	102
ANALOG	
• ENGINEERING SUBCOM	74
• SCIENCE SUBCOM	40
	114

The principal scientific data are required on 12 channels (Format A) in serial digital word lengths of 3 to 72 bits in 3-bit increments. A second set of 12 channels (Format B) is provided for use with an alternate selectable format. There are seven special serial inputs (Format D) which can be used to dump large buffers or other large data sources. The other inputs are for subcommutated housekeeping data. These data are acquired in 6-bit increments. Ten of the bilevel

channels are used internally in the DTU. Analog housekeeping data are accepted and digitized to 6 bits; three channels are used intentionally in the DTU. Word gates and shift clocks are supplied to synchronize serial data acquisition.

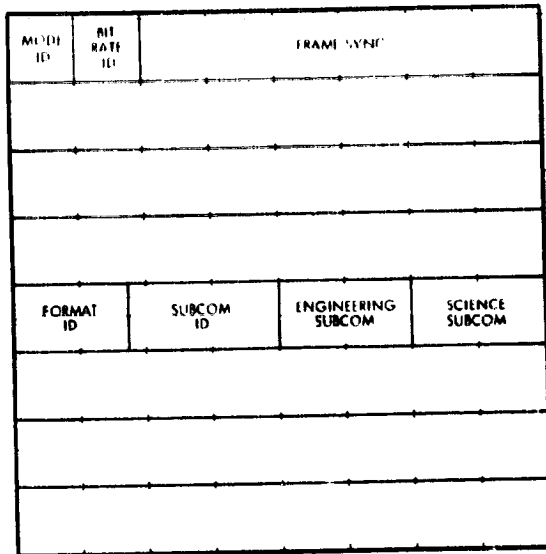


Figure 8.3-7. Basic Telemetry Format for Version 11 Science Payload

Data is arranged and formatted for telemetry in 192-bit mainframes. Figure 8.3-7 depicts this frame format comprised of eight 24-bit rows. One and a half rows are used for fixed words and a half is occupied by the subcommutated engineering and instrument housekeeping data. The remaining six rows are allocated to the science data. This allocation is controlled by external patching.

There are two principal science formats, designated as A and B. Each has its own patchable programming and each is selectable by ground command.

Special D formats are available where the A or B format is interleaved with an external source (such as checkout data from a probe). When in a D format, the external source is allocated every other 192-bit block. This external data is not formatted by the DTU, i.e., the fixed words and subcoms are not inserted.

The engineering subcom contains 128 words; each word is 6 bits. These words are in four groups designated C1 to C4. The C formats can be accelerated so as to replace the mainframe science data with engineering data. This allows a much faster engineering data rate for maneuvers or diagnostic purposes. Science housekeeping data is subcommutated with 64 words and 6-bit resolution and is designated E1 and E2.

The formatted data is convolutionally coded (rate 1/2, constraint length 32) and biphase modulated on a squarewave subcarrier for transmission. The encoder can be bypassed by ground command. The data is

transmitted at one of 8 bit rates from 8 to 1024 bits/s (16 to 2048 coded symbols per second). The subcarrier amplitude can be commanded to one of two accurately controlled voltage levels to achieve two modulation indices to optimize downlink telemetry acquisition and processing.

The DTU receives a sun pulse once per spacecraft revolution and generates spin sector pulses at four rates; one each revolution, one each 1/8 revolution, one each 1/64 revolution, and one each 1/512 revolution. An overflow flip-flop is added to the spin sector generator register to prohibit the use of the first sun pulse following an eclipse (while the flip-flop is only a requirement for the orbiter, its addition maintains maximum probe bus/orbiter DTU commonality). The DTU also acts as the central timing source and supplies several clock frequencies to other spacecraft subsystems and instruments.

The science data requirements occupy just over half the available frame at 512 bits/s; the remaining excess frame capacity, shown as spare, can accommodate growth of the science data rate requirements. Since the link can support 1024 bits/s during probe bus entry, a science data rate increase of approximately 300 percent is available.

Figure 8.3-8 shows the recommended format assignments for various phases of the probe mission and illustrates a possible word allocation for Format B.

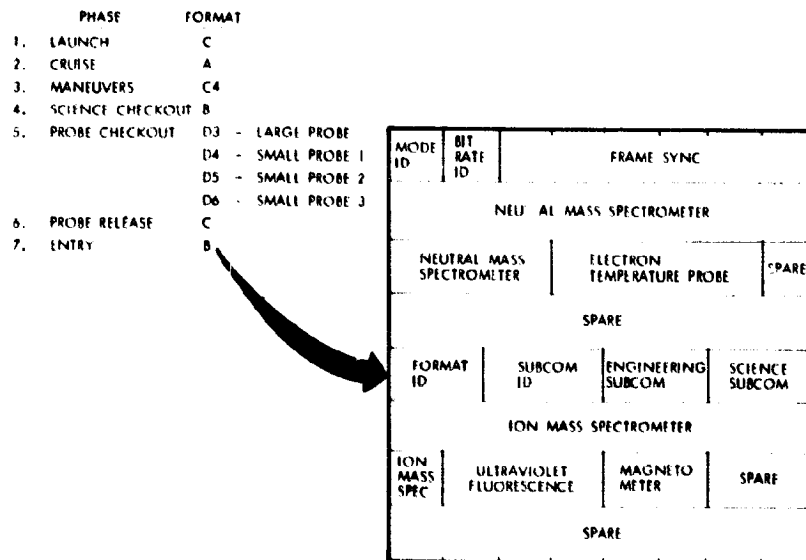


Figure 8.3-8. Telemetry formats for Probe Bus Version III Science Payload

A/C III

T/D III

The probe bus interfaces with the probes in order to provide commands and acquire telemetry data for sequencing, calibration and checkout. The DTU provides four separate serial input channels, one for each probe. There are three interface lines for each probe: an enable line to notify the probe that data is being transferred, a data line, and a chained clock line. The isolation shown in the DTU for the clock output will preclude propagation of line shorts that may be caused by the cable cutters at probe release. Figure 8.3-9 depicts this interface.

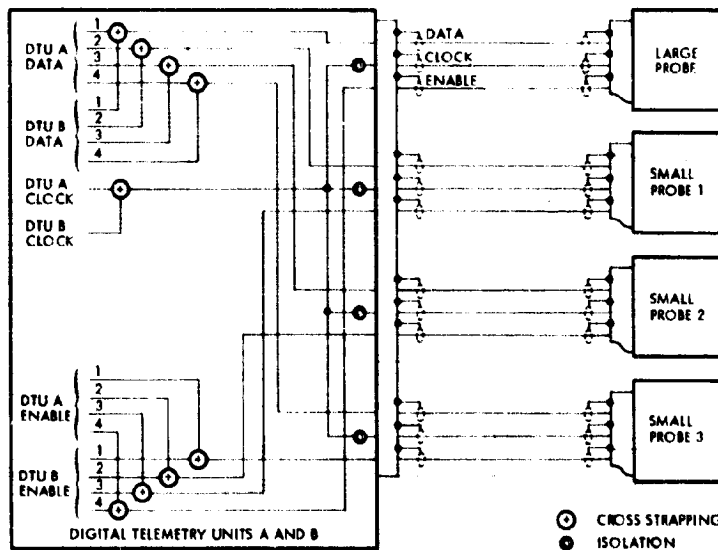


Figure 8.3-9. DTU/Probe Interface

A/C III 8.3.4.2 Orbiter Data Handling Subsystem Description (Version III Science Payload)

T/D III

The orbiter data handling subsystem is comprised of a single, inter-

^(31 W) A/C III nally redundant DTU and three DSU's. The DTU is described in Section

^(31 W) T/D III 8.3.4.1.

A recommended set of formats for the orbiter is given in Figure 8.3-10. For spacecraft option 1, the communications link can support 128 bits/s at end of mission. The principal orbiter format shown accommodates the Version III science low altitude data at this rate. The radar altimeter data is stored and read out after completion of the periapsis pass. The radar altimeter benefits from the use of a large buffer, particularly below 300 kilometers where a favorable signal-to-noise ratio

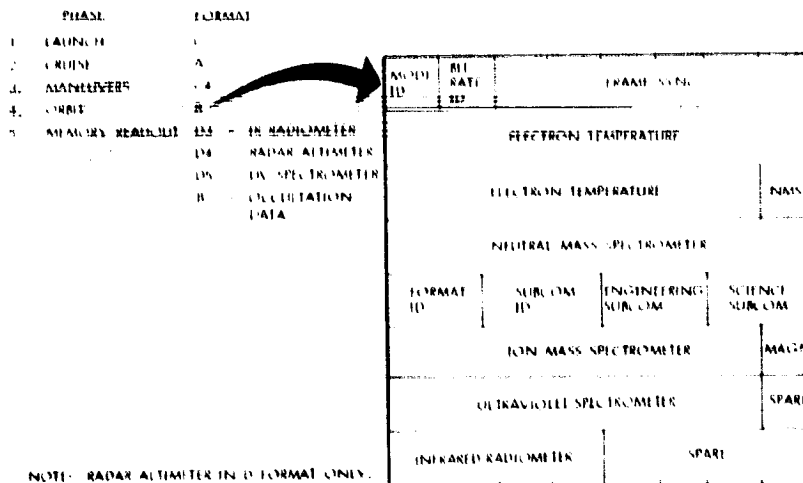


Figure 8.3-10 Orbiter Formats

allows high data sampling without data filtering. Greater data acquisition rates can be accommodated by storing at higher rates and telemetering in delayed time at 128 bits/s, or by using a 64-meter ground station. If storage is used for the high altitude data as well as for the radar altimeter, and all data during occultation, the duration of DSN station coverages is minimized. Figure 8.3-11 presents the time needed to transmit the data assuming the following data requirements:

- 491 520 (75 percent science, 25 percent housekeeping) near periapsis
- 245 760 (100 percent science) special modes, probably near periapsis
- 368 640 (75 percent science, 25 percent housekeeping) high altitude.

This profile could vary depending on the total science data taken each 24 hours. Additional station time is necessary for up to 2 hours from orbit days 1 to 71 and 125 to 144 for the RF occultation experiment. Several hours are needed on orbit days 30, 60, 150, and 185 for periapsis maintenance. Routine tracking is also required. The coverage needed during the orbiter cruise period could be minimized by storing the magnetometer data and transmitting for a short time once a day.

For the fanbeam orbiter spacecraft, the reduced telemetry rate capability necessitates greater DSN coverage. Figure 8.3-12 plots the time assuming the transmission of 1 105 920 stored bits cited above.

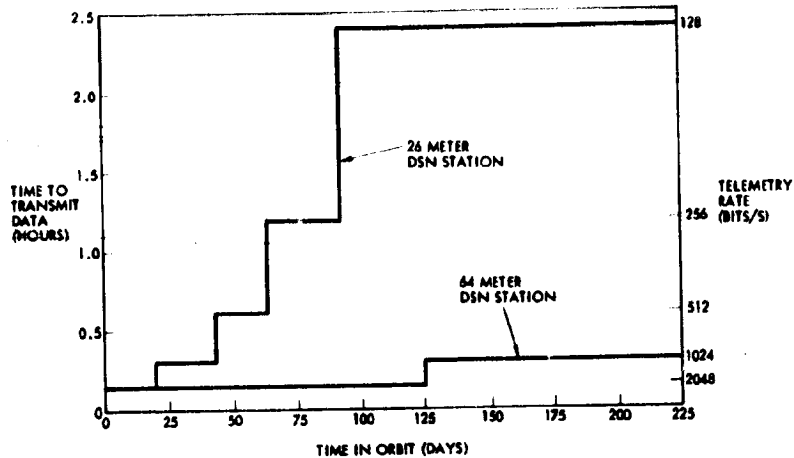
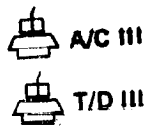


Figure 8.3-11. DSN Usage

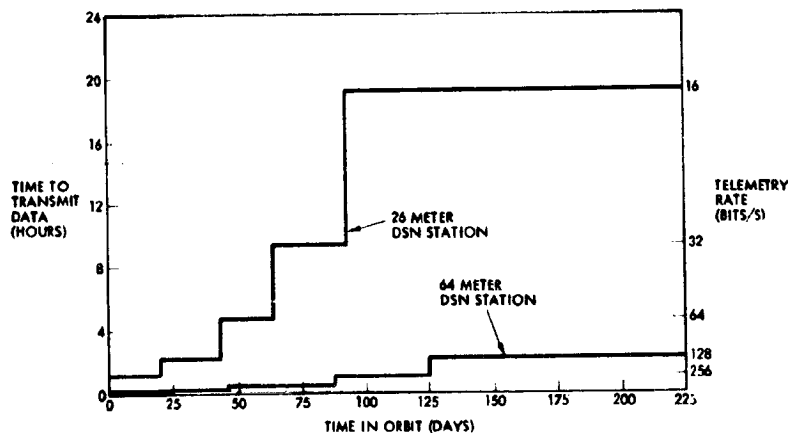
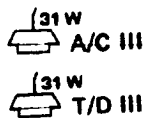


Figure 8.3-12. DSN Usage for Fanbeam Orbiter

The storage requirements are implemented by using three DSU's, each comprised of two 122 880 bit modules. These modules can be chained to form a single memory bank of 245 760 bits or they can be used independently. In this manner, the four data sources identified in Table 8.3-8 are accommodated simultaneously at low altitudes and the magnetometer (and perhaps the UV spectrometer) are assigned storage at high altitudes. Figure 8.3-13 shows the storage arrangement. In the event of a DSU failure, reconfiguration is accomplished by ground command. Any two of the three functions are chosen (the radar altimeter and IR radiometer are handled as a single function for reconfiguration since each requires half a DSU). Redundancy is provided for the formatted occultation period information and the nonformatted radar altimeter data (in line functions). The UV spectrometer and IR radiometer experiments are improved by the availability of the added storage.

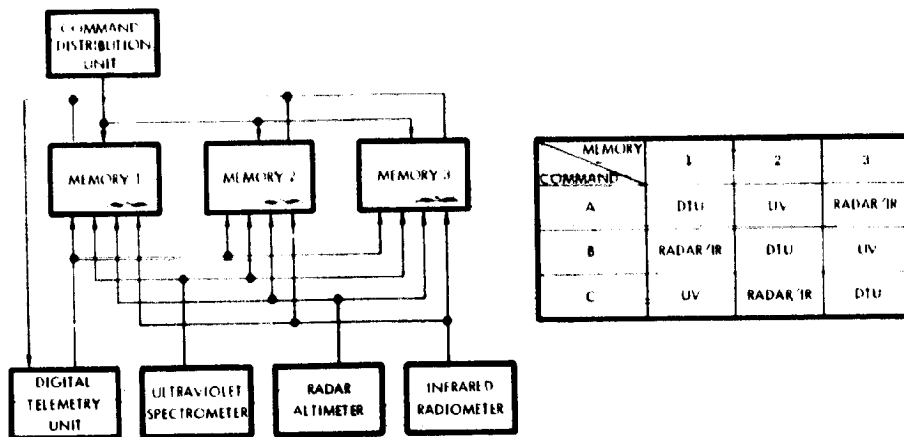


Figure 8.3-13. Data Storage Configuration

The proposed DSU is based on a 256-bit C-MOS random access memory chip. For the weight limited Thor/Delta orbiter, ten chips are placed in a single 24-lead flatpack. For the Atlas/Centaur configuration, conventional single chip 14-lead flatpacks are employed. Figure 8.3-14 is a block diagram of a memory module, two of which comprise a DSU. The memory is organized in a three-dimensional matrix, in the classical manner. There are forty 256-bit strings per plane and 12 planes. The memory module appears as 10 240 12-bit words. During memory load, data is shifted serially into the buffer shift register with the data source clock. On the twelfth clock, the contents of the buffer shift register are transferred in parallel to the addressed memory word. Since the address is selected by a counter, the module appears as a 122 880-bit serial memory to the "outside world."

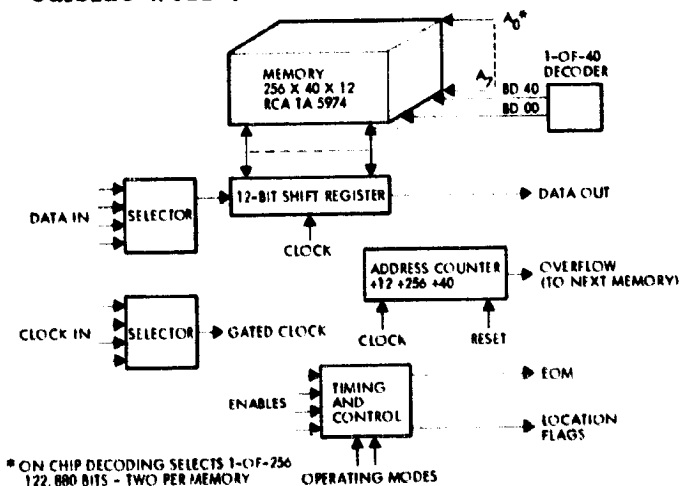




Figure 8.3-14. Memory Module Block Diagram

The selected DSU is the most cost-effective approach to satisfying both the orbiter mission requirements and the Pioneers 10 and 11 DTU interfaces. The new DSU design enhances the performance capability of several of the scientific instruments by providing multiple and simultaneous asynchronous buffering for high data rate measurements. This flexibility permits the use of a reasonably sized communications links and reduces ground operations time.

 A/C IV 8.3.5 Preferred Data Handling Subsystem for Atlas/Centaur Spacecraft (Version IV Science)

 A/C IV

The following data handling subsystems satisfy the Version IV science requirements and are sized for use with the preferred Atlas/Centaur earth-pointing configurations.

 A/C IV 8.3.5.1 Preferred Earth-Pointing Atlas/Centaur Version IV Science Probe Bus Data Handling Subsystem

The preferred probe bus data handling subsystem consists of a single, internally redundant, modified Pioneers 10 and 11 DTU. The following changes were made to the DTU described in paragraph 8.3.4.1.

Format

The Version IV science payload higher bit rate requirements necessitate a more efficient format than the Pioneers 10 and 11 DTU. The preferred, modified DTU uses 91 percent of its format for principal scientific data, versus 75 percent for the Pioneers 10 and 11 format. The basic format, Figure 8.1-C, is increased from 192 bits to 768 bits (from 8 to 32 rows of 24 bits each).

The new format is similar to the Pioneers 10 and 11 format, shown in Figure 8.3-8, facilitating the use of Pioneers 10 and 11 integration and operational software and eliminating considerable development costs.

Special Format

The special formats (D) are no longer interleaved with the A and B formats, as for Pioneers 10 and 11, but are placed into the main format. The principal format continues to be used, but 24 of the 32 rows are overlaid with D data (rows 5 to 16 and 21 to 32).

ALL VERSION IV SCIENCE PAYLOAD

Format Quantity

The number of principal science formats is increased from two (A and B) to eight. Four will be allocated to the probe bus and four to the orbiter. Therefore, one DTU spare is adequate for both the probe bus and the orbiter. These formats will be preloaded in read-only-memories (ROM's) providing programming versatility approaching patch connectors but with an increase in the number of formats.

Word Length

The preferred DTU program is not restricted by word length, increasing packing efficiency. The Pioneers 10 and 11 DTU had a 3-bit mainframe word length, which caused packing inefficiency for words whose length was not a multiple of three.

Analog-to-Digital (A/D)

The A/D conversion resolution is increased from 6 to 10 bits to accommodate the science requirements. Where less than 10 bits is necessary, as for the engineering subcommutators, the word length will be reduced. An integrated circuit, successive approximation A/D will replace the discrete component ramp converter now used.

Analog Main Frame

Routing of analog inputs to the main frame word slots allows accommodation of analog science. (This is not a requirement for the probe bus or orbiter but is necessary for the large and small probes. Commonality dictates its availability on the bus and orbiter for optional use.)

Science Subcommutator Word Length

The science subcommutator word length is increased from 6 to 10 bits to satisfy the ion mass spectrometer requirements.

Selectable Bit Rates

Eight commandable bit rates, from 8 to 1024 bits/s in binary increments, will be provided in lieu of the range from 16 to 2048 bits/s available on Pioneers 10 and 11. The 8 bits/s rate is required to support off earth-pointing maneuvers at extended ranges.

Multiple Level Biphase Outputs

Multiple modulation amplitudes are selectable by ground command to permit optimization of the downlink modulation index.

Spin Sector Generator Hold Mode

An overflow flip-flop prohibits pairing of the sun-pulses immediately before and after an eclipse. This allows smooth probe operation even with several hour sun eclipses.

The changes are principally confined to two board types, the programmer and the analog subcommutator. Only very minor modifications are necessary on other boards. These changes result in a cost-effective DTU that meets the Pioneer Venus requirements while retaining proven Pioneers 10 and 11 technology.

The format for the probe bus, Figure 8.3-15, shows an entry format sized for 1024 bits/s.

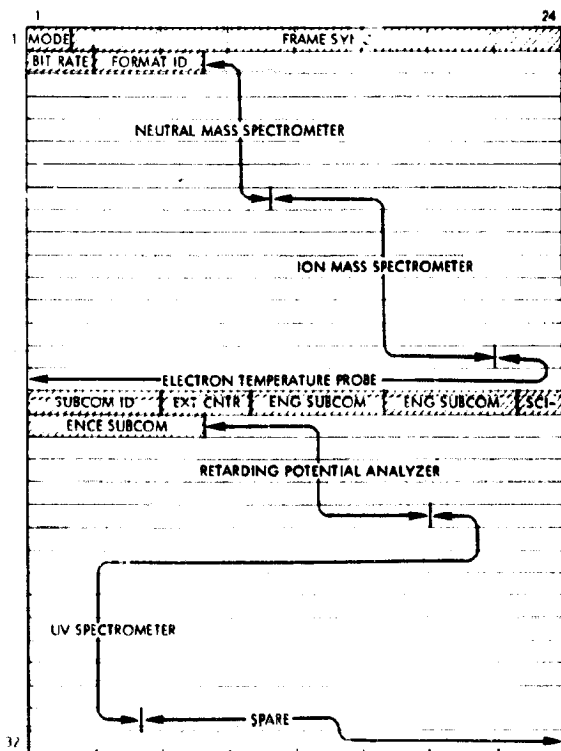
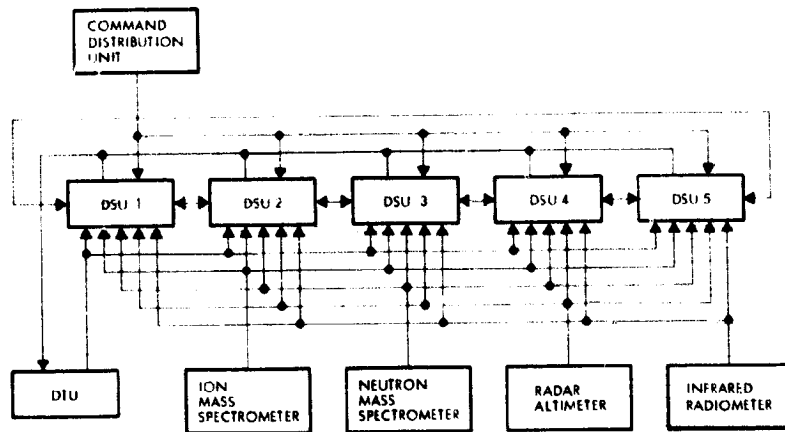


Figure 8.3-15. Probe Bus Entry Format (1024 bits/s)

If the "other candidate" instruments, Table 8.3-5, are both added, the science data rate will increase from 938.7 to 962.6 bits/s. The overall data rate could be increased the necessary 24 bits (but this would raise the rate just over the 1024 bits/s standard), or the DTU crystal frequency could be raised a few percent increasing the bit rates accordingly. Alternatively, the transmitter power may be increased to 12 watts; this would, however, impact other subsystems such as power and thermal. Either one of the two "other candidate" instruments could be added without impact to the probe bus data handling subsystem.

8.3.5.2 Preferred Atlas/Centaur Orbiter, Version IV Science, Data Handling Subsystem

The preferred orbiter data handling subsystem consists of a modified Pioneers 10 and 11 DTU (Section 8.3.5.1), and five DSU's (Section 8.3.4.2), two more than the Version III science subsystem. The DSU interconnections are shown in Figure 8.3-16. Data is stored at periapsis and transmitted later at slower rates, the most cost-effective method. The preferred DSU satisfies orbiter mission requirements, interfaces well with the preferred DTU, reduces ground operations time, and enhances the performance capability of several scientific instruments. Storage is available for use during the mission not just during occultation near periapsis.



MEMORY ORGANIZATION COMMAND MATRIX

MEMORY	1		2		3		4		5	
	1A	1B	2A	2B	3A	3B	4A	4B	5A	5B
LOW ALTITUDE										
A-1	DTU	DTU	DTU	IONS	NEUTRONS	RADAR	IR	IR	SPARE	
B-1		SPARE	DTU	DTU	DTU	IONS	NEUTRON	RADAR	IR	IR
C-1	IR	IR		SPARE	DTU	DTU	DTU	IONS	NEUTRONS	RADAR
D-1	NEUTRONS	RADAR	IR	IR		SPARE		DTU	DTU	DTU
E-1	DTU	IONS	NEUTRONS	RADAR	IR	IR		SPARE		DTU
HIGH ALTITUDE										
A-2	DTU	DTU	DTU	DTU	DTU	DTU	DTU	DTU	SPARE	
B-2		SPARE	DTU	DTU	DTU	DTU	DTU	DTU	DTU	DTU
C-2	DTU	DTU		SPARE	DTU	DTU	DTU	DTU	DTU	DTU
D-2	DTU	DTU	DTU	DTU		SPARE		DTU	DTU	DTU
E-2	DTU	DTU	DTU	DTU	DTU	DTU		SPARE		DTU

NOTE: COMMANDS A THROUGH E ROTATE DSU "POSITIONS"
COMMANDS 1 AND 2 SELECT ALTITUDE OPERATION

Figure 8.3-16. Storage Configuration

The available storage exceeds the requirements, as shown in Table 8.3-19. Figure 8.3-16 also shows the preferred storage configuration.

Table 8.3-19. Preferred Available Storage versus Requirements

USAGE	REQUIREMENTS (BITS)	IMPLEMENTATION (BITS)
DIGITAL TELEMETRY UNIT (DTU) (INCLUDES MAGNETOMETER, ELECTRON TEMPERATURE, AND ULTRAVIOLET DATA)	322 560	368 640
NEUTRAL MASS SPECTROMETER	117 000	122 880
ION MASS SPECTROMETER	117 000	122 880
INFRARED RADIOMETER	204 000	245 760
RADAR ALTIMETER	48 000	122 880
TOTAL	808 560	983 040

The total bits 983 040, are supplied by four DSU's, the fifth is a spare. Reconfiguration is accomplished by one of five ground commands which shift all five units to a new "position." This same command tells the DSU whether it is in a single module or chained modules mode. A sixth and seventh command place the DSU's in the high or low altitude configuration. The DSU's are in the read-in condition except when controlled for read-out by the DTU.

Figure 8.3-17 gives a periapsis pass in operational terms, illustrating the use of the DSU's.

The available telemetry link assumed is 64 bits/s. Data is stored for 42 minutes at low altitudes and telemetered later. Except during occultations, the magnetometer, electron temperature probe, UV spectrometer, and housekeeping data can be real time telemetered while the other periapsis storage take place. The 342 minutes shown to dump low altitude data, however, includes this formatted data. While the stored data is being read out to the ground, real time data is being interleaved so that no data is lost. The eight commands are stored, relieving the ground of much routine effort. Only the dump commands have to come from the ground. While these could be stored, the stored command programmer located in the CDU does not know when ground station availability exists. A more detailed discussion of the operational sequence is given in

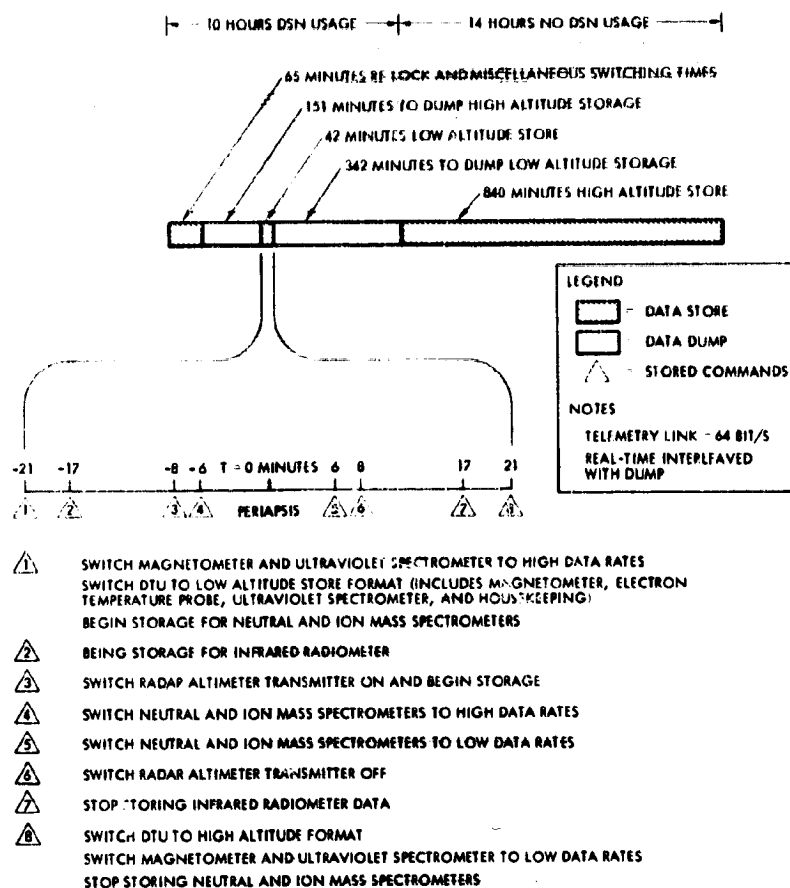
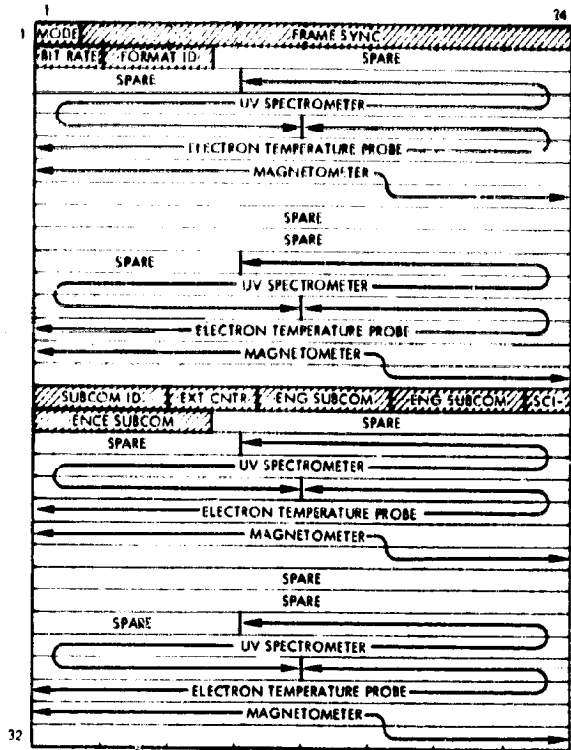


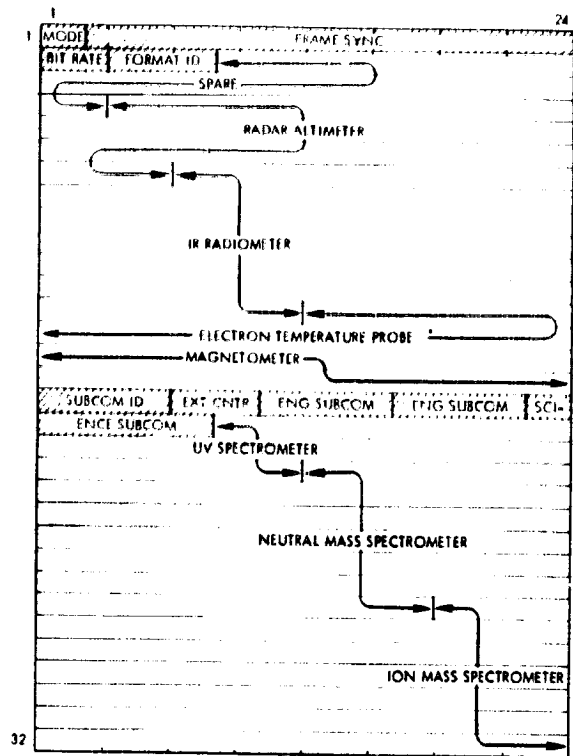
Figure 8.3-17. Orbiter Data Storage Timeline

section 10.5.7, and the command storage is described in Section 8.4. The formats derived for use with the subsystem hardware and operational procedures outlined are given in Figure 8.3-18.

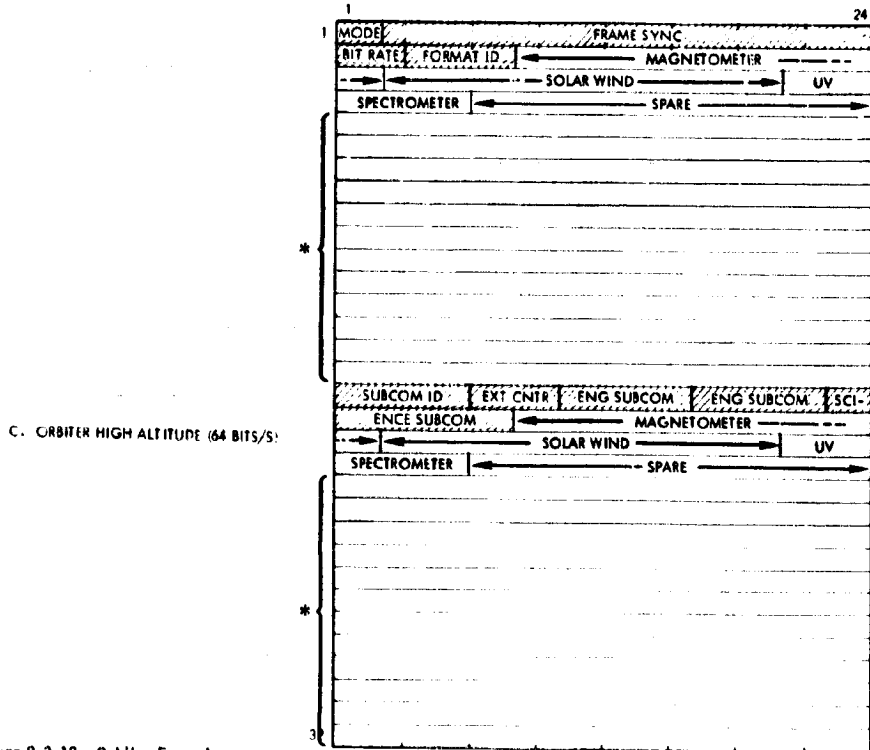
As shown in Table 8.3-13, the other candidate instruments are not well understood at this time. From a data handling viewpoint, the AC electric field detector could be added with no perceptible impact. The impact of the microwave radiometer also appears to be negligible. The spin scan photometer, however, will more than double the daily data. The effects of the added 3,978,000 bits will depend on the sample size, amount of storage in the instrument itself, and operational procedures. The photometer could be interleaved on every other orbit, for example, or one or two more DSU's could be added and continuous ground station coverage employed.



A. ORBITER LOW ALTITUDE - PARTIAL (128 BITS/S)



B. ORBITER LOW ALTITUDE - TOTAL (512 BITS/S)



C. ORBITER HIGH ALTITUDE (64 BITS/S)

* CAN BE USED FOR INTERLEAVING MEMORY DUMP VIA D FORMATS.

Figure 8.3-18. Orbiter Formats

8.4 COMMAND SUBSYSTEM

8.4.1 Introduction and Summary ALL CONFIGURATIONS

The preferred command subsystem design provides cost savings by using flight-proven Pioneers 10 and 11 hardware (either as-is or with minor modifications), which is highly reliable and flexible in its application. It consists of the digital decoder unit (DDU) and the command distribution unit (CDU), which process and distribute commands throughout the spacecraft and to the probes prior to their release.

The DDU and CDU consist of subassembly "slices" containing printed-circuit boards that facilitate modification of specific functions to meet new requirements or provision for growth. The key features of the proposed design, summarized in Figure 8.4-1, include:

- The DDU and CDU are redundant, the latter internally redundant in a single package.
- The DDU from Pioneers 10 and 11 can be used without change.
- The modifications required to the CDU involve the addition of one new slice, the redesign of an existing slice, and minor modifications to three other slices.
- The increased ordnance firing requirements of Pioneer Venus as compared to Pioneers 10 and 11 are accommodated by adding a slice containing the necessary firing circuitry. This is the most cost-effective approach to adding the required capability, and the small weight penalty is acceptable for the Atlas/Centaur mission. The majority of the additional ordnance firing requirements derive from the experiments and probe release operations.

The following sections derive the mission requirements imposed on the command subsystem, discuss the tradeoff analyses that were performed to select a cost-effective implementation, and describe the detailed preferred configuration recommended for the Pioneer Venus program.

8.4.2 Requirements Versus Capabilities

8.4.2.1 Commands A/C III A/C III

The function of the command processor in the Pioneers 10 and 11 CDU is to decode, process, and distribute real-time commands upon receiving digitally coded signals from the DDU. The three types of real-time commands are:

- Discrete pulse
- Discrete state
- Serial (routed to the DTU, ADCS, command memory, and to the probes)

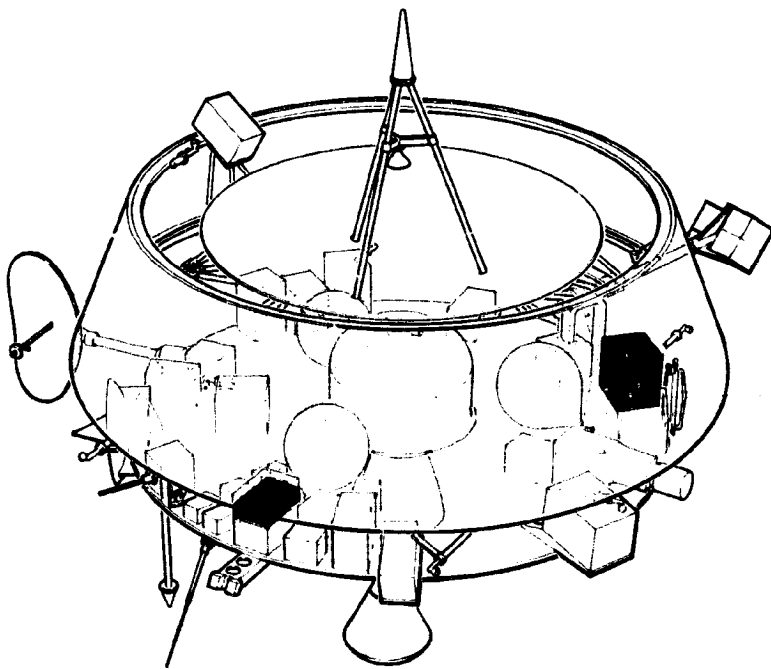
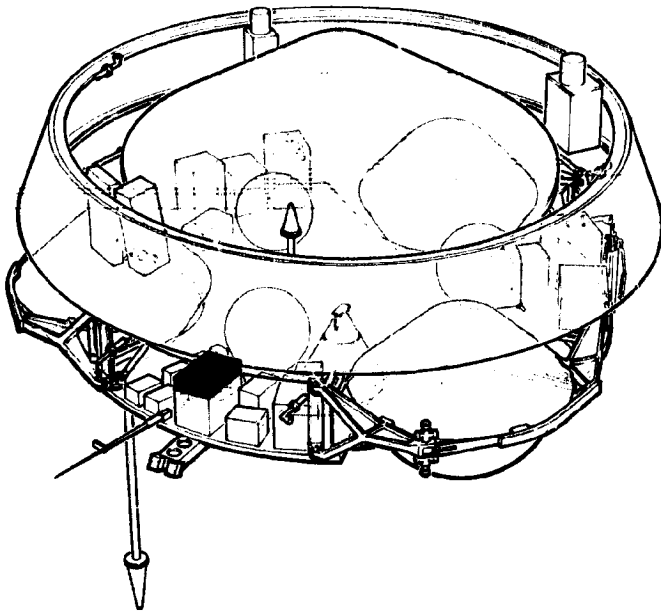
The existing real-time capability is adequate to meet all the Pioneer Venus requirements for the probe bus and orbiter missions without modification. Figure 8.4-1E summarizes the number of discrete commands required by each subsystem. Appendix 8-4A provides a detailed command list.

Provision must be made to command each of the four probes via a separate bus/probe interface connection (umbilical) during prelaunch testing and again during preseparation checkout. Approximately nine commands are required for each probe.

The serial command function of the CDU offers a convenient method of implementing these probe command requirements without impact to the existing design. Eight routing destinations are selectable with the 3-bit routing address in the command message. Spares are available, one of which may be assigned to the probes. By activating and commanding only one probe at a time, the single routing address serves all four probes.

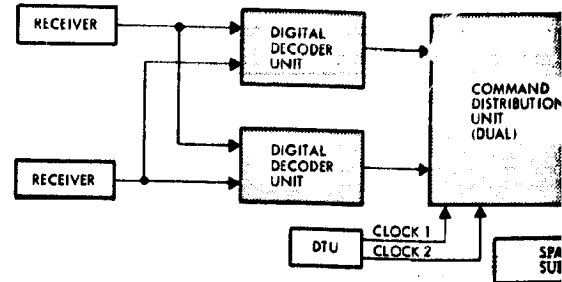
In addition to these real-time command requirements, the orbiter mission requires a command memory capability, permitting storage of commands for execution at a later time. Table 8.4-1 defines these requirements. Four commands are provided to arm and fire the solid rocket motor for Venus orbit insertion because the spacecraft is occulted by the planet during this critical operation. The timing error of the motor firing should not exceed approximately ± 60 seconds minimizing the perturbation to the desired orbit.

An additional requirement is to protect against premature, as well as late, motor firing that might preclude achieving a satisfactory orbit. Independent redundant time delay computation circuitry greatly enhances the reliability of this operation.

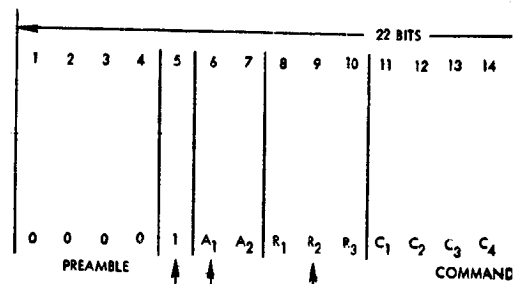


FOLDOUT FRAME

A COMMAND SUBSYSTEM COMPONENTS

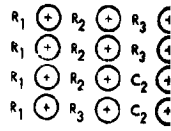


B COMMAND FORMAT

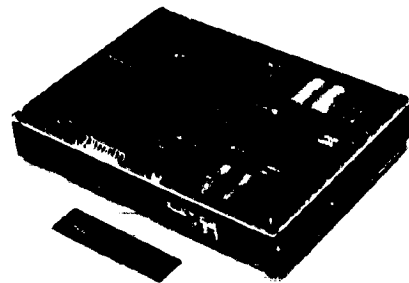


$R_1 R_2 R_3$

- 000 NOT USED
- 001 CDU REAL-TIME COMMANDS (DISCRETE COMMAND)
- 010 CDU COMMAND MEMORY, COMMAND
- 011 CDU COMMAND MEMORY, TIME
- 100 DTU SERIAL COMMAND DATA (8 BITS)
- 101 ACS SERIAL COMMAND
- 110 CDU COMMAND MEMORY, TIME
- 111 PROBE SERIAL COMMAND

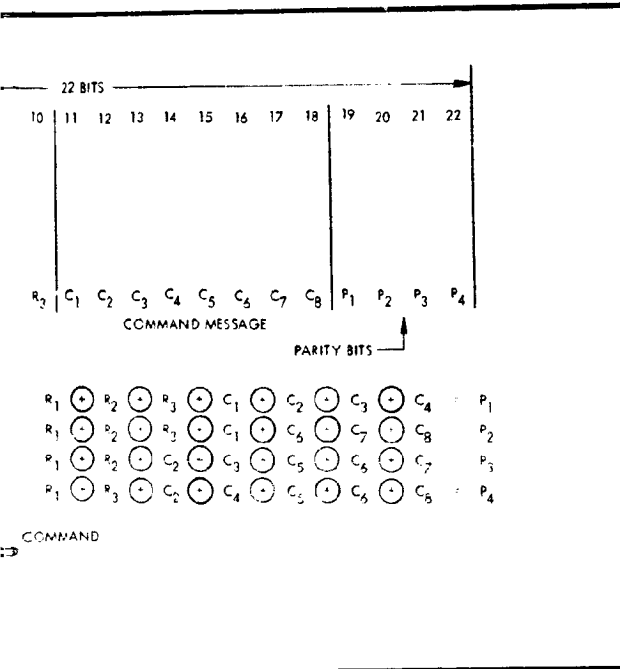
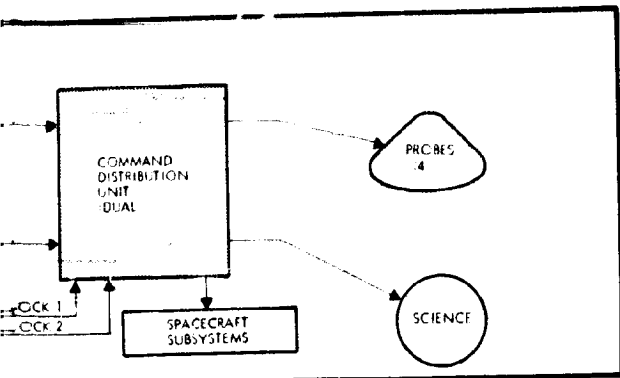


C PIONEERS 10 AND 11 DIGITAL DECODER UNIT



D SUBSYSTEM CHARACTERISTICS

SUMMARY DESCRIPTION
NUMBER USED
DIMENSIONS (CM)
WEIGHT (KG)
POWER (WATTS)
DERIVATION
REQUIRED MODIFICATIONS



D SUBSYSTEM CHARACTERISTICS SUMMARY

SUMMARY DESCRIPTION	DDU	CDU
NUMBER USED	2	1 (INTERNALLY REDUNDANT)
DIMENSIONS (CM)	20.4 x 15.2 x 2.5 (EACH)	20.4 x 17.8 x 25.4
WEIGHT (KG)	0.36 (EACH)	4.5
POWER (WATTS)	1.3	2.1
DERIVATION	PIONEERS 10 AND 11	PIONEERS 10 AND 11
REQUIRED MODIFICATIONS	NONE	<ol style="list-style-type: none"> 1. ADD EXTRA ORDNANCE FIRING SLICE 2. ADD STORED COMMAND SLICE 3. MINOR MODS TO FOUR EXISTING SLICES

E COMMAND REQUIREMENTS SUMMARY

SUBSYSTEM	ORBITER		BUS	
	STATE	PULSE	STATE	PULSE
ELECTRICAL DISTRIBUTION	2	21		24
ELECTRICAL POWER		12		20
DATA HANDLING		10		2
COMMUNICATIONS	6	24	4	12
ATTITUDE CONTROL		32		32
THERMAL		6		2
SCIENCE	16	29	10	6
TOTAL REQUIRED	24	134	14	98
CDU CAPABILITY	41	177	41	177
SPARES	17	43	27	79
PERCENT USED	58	76	34	55

F ORDNANCE FIRING CIRCUITS SUMMARY

SPACECRAFT	REQUIREMENTS	CAPABILITY	ADDITION
BUS	22	4	18
ORBITER	12	4	8

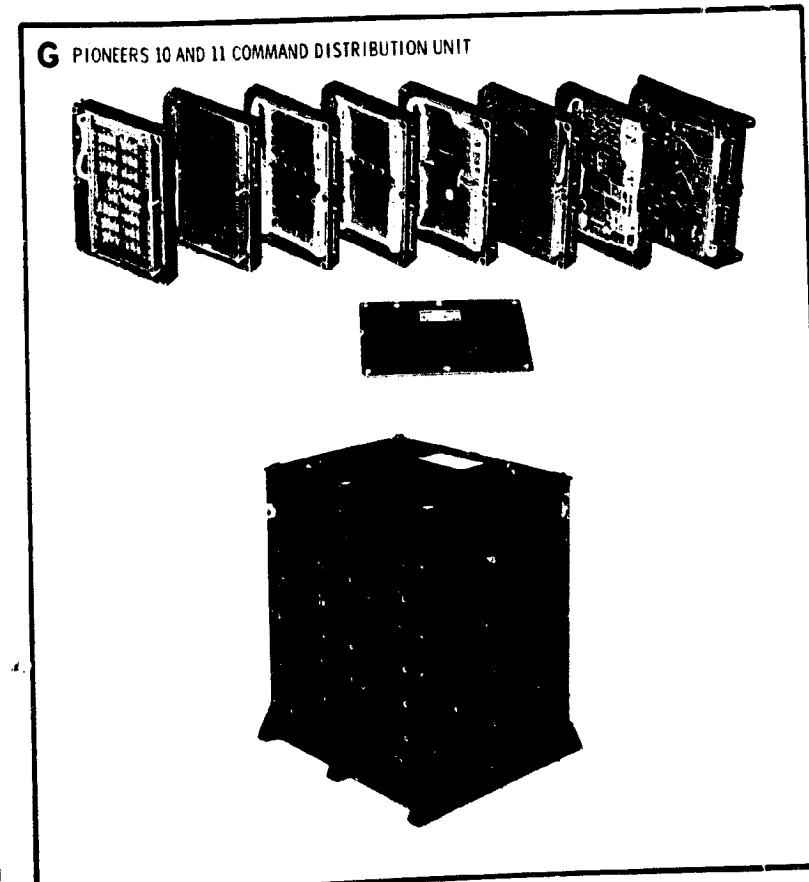


Figure 8.4-1. Command Subsystem

Table 8.4-1. Command Memory Requirements

COMMAND NAME	MISSION PH/SE	EXECUTE TIME (MIN)	TOTAL COMMANDS REQUIRED IN MEMORY	PROPOSED CAPACITY OF NEW MEMORY	SPARES
ARM ORBIT INSERTION MOTOR	ORBIT INSERTION ↓ ORBIT INSERTION	P-0.1	4	16	12
ARM ORBIT INSERTION MOTOR (REDUNDANT)		P-0.1			
FIRE ORBIT INSERTION MOTOR		P-0			
FIRE ORBIT INSERTION MOTOR (REDUNDANT)		P-0			
LOW ALTITUDE STORE FORMAT SELECT	EACH ORBIT ↓ EACH ORBIT	P-21	8	16	8
STORE INFRARED DATA		P-17			
RADAR ALTIMETER TRANSMITTER ENABLE AND STORE DATA		P-8			
NEUTRAL AND ION MASS SPECTROMETER TO HIGH BIT RATE		P-6			
NEUTRAL AND ION MASS SPECTROMETER TO HIGH BIT RATE		P+6			
RADAR ALTIMETER TRANSMITTER DISABLE		P+8			
HIGH ALTITUDE STORE FORMAT SELECT		P+21			
RESET STORED COMMAND COUNTER		P+25			

The spacecraft is occulted for periods up to 20 minutes during peri-apsis passage for the first 70 days in orbit. Stored commands reconfigure the instrument operating modes and the data storage formats during this period of high scientific interest when real-time commands cannot be transmitted. Approximately eight commands fulfill these functions. Timing execution of these events is less critical than the motor firing; an uncertainty of 2 minutes is acceptable.

The existing Pioneers 10 and 11 command memory in the CDU has the capability of storing up to five command messages and their associated time delays for later sequential execution. The maximum time delay capable of being stored in any given slot is 8320 seconds. Each command is executed sequentially after the associated time delay relative to the execution of the previous command in the stack. The resolution of each incremented time delay is 128 seconds for time delays between 384 and 8320 seconds. The existing memory is not redundant.

A tradeoff study, evaluating alternative approaches to meet the more stringent Pioneer Venus requirements, is discussed in Section 8.4.3.1.


8.4.2.2 Ordnance Firing Circuits  A/C III  A/C III

Table 8.4-2 identifies the ordnance firing function requirements applicable to the probe bus and orbiter spacecraft. Twenty-two firing circuits (including redundancy) initiate the scientific instrument and probe disconnect/release ordnance. The orbiter has 12 circuits to accommodate rocket motor ignition, ram platform release, and several experiment functions. Since the existing ordnance firing system has only four circuits, provision must be made to augment this capability to meet the new Pioneer Venus mission requirements. Several implementation approaches are evaluated in Section 8.4.3.2 and a preferred configuration is recommended.

Table 8.4-2. Ordnance Firing Requirements

	METHOD	ELECTRO-EXPLOSIVE DEVICE	FIRING CIRCUIT	ACTIVATION	
<u>ORBITER SPACECRAFT</u>					
	1 PIN PULLER	2	2	ORBIT	
	1 PIN PULLER	2	2	CRUISE	
	1 PIN PULLER	2	2	CRUISE	
	1 PIN PULLER	2	2	ORBIT	
	1 INITIATOR	2	2	VOI + 0	
	1 PIN PULLER	2	2	ORBIT	
	<u>FIRING CIRCUITS: 6 PRIMARY, 6 REDUNDANT, 12 TOTAL</u>				
	<u>PROBE BUS SPACECRAFT</u>				
	1 PIN PULLER	2	2	CRUISE	
	1 PIN PULLER	2	2	ORBIT	
	1 PIN PULLER	2	2	ORBIT	
	CABLE CUTTER	2	2	E - 25 DAY	
	3 BALL LOCKS	6	2	E - 25 DAY	
	1 PIN PULLER	2	2	E - 21 DAY	
	CABLE CUTTER	2	2	E - 21 DAY	
	1 PIN PULLER	2	2	E - 21 DAY	
	1 PIN PULLER	2	2	E - 19 DAY	
	CABLE CUTTER	2	2	E - 19 DAY	
	1 PIN PULLER	2	2	E - 19 DAY	
	1 PIN PULLER	2	2	F - 15 DAY	
	CABLE CUTTER	2	2	E - 15 DAY	
	1 PIN PULLER	2	2	E - 15 DAY	
	<u>FIRING CIRCUITS: 11 PRIMARY, 11 REDUNDANT, 22 TOTAL</u>				

ALL PROBE CONFIGURATIONS
ALL ORBITER CONFIGURATIONS

8.4.2.3 Thruster Firing Counters ALL CONFIGURATIONS

The preferred reaction control system for the probe bus and orbiter provides eight hydrazine thrusters: four axial thrusters for velocity and precession control and four transverse thrusters that may be used in a pulsed mode for lateral ΔV corrections (allowing the spacecraft to remain in an earth-pointing attitude) as well as for spin and despin control.

The CDU should be equipped with thruster firing counters to indicate the number of firings performed by each of the eight thrusters. In addition to the counting capability, real-time telemetry should indicate when the thrusters are firing.

The Pioneers 10 and 11 CDU includes counters for four axial thrusters, which count a maximum of 64 firings before recycling to zero. For the two spin control thrusters, however, the unambiguous counting capability is limited to two firings. The counting circuitry is activated when a pressure switch in the thruster propellant line is closed, indicating a firing condition. When the pressure switch again opens, the thruster counter increments by one.

The addition of four firing counters for the transverse thrusters (identical to the existing counters associated with the velocity/precession thrusters) is proposed to satisfy the new requirements.

8.4.3 Tradeoff Studies

8.4.3.1 Command Memory ALL ORBITER CONFIGURATIONS

The limitations of the Pioneers 10 and 11 command memory circuitry (five commands and associated time delays), timing resolution (128 seconds), and lack of redundancy led to the development of a new and more flexible design to meet Pioneer Venus mission requirements.

The new design of the stored command programmer:

- Allows for reasonable growth in command assignments.
- Simplifies and increases the flexibility of the ground operation procedures during the orbiter flip maneuvers and routine orbital operations, and if used on probe bus, during sequential probe release events.
- Minimizes the need for periodic mandatory real-time commands for each orbit cycle.


ALL ORBITER CONFIGURATIONS


- Is approximately equal to the cost of modifying the existing design.
- Provides redundancy with little increase in cost.

A detailed technical description of the preferred design for the command memory, incorporating the capabilities and features discussed above, is given in Appendix 8.4B. It is based on a random access C-MOS memory (256x2), which may be loaded in a random order with a maximum of 16 discrete commands and associated time codes. The time code provides a resolution of 2 seconds with a maximum delay of 36.4 hours.

The redundant 32-kHz clock signals from the DTU provide the independent timing sources for the master counter in each half of the stored command programmer. Thus, late execution of commands (or failure to execute) due to single-point failures in either circuit is precluded. A clock frequency detector circuit is incorporated to inhibit operation of the programmer if the clock has failed in a mode that would increase the frequency and cause a premature command execution.

A/C III 8.4.3.2 Ordnance Firing Circuit Augmentation

 T/D III Table 8.4-3 summarizes the key tradeoff considerations that were developed in evaluating four implementation concepts satisfying the increased requirements for ordnance firing circuits.

 A/C III




 T/D III

Table 8.4-3. Ordnance Firing Circuit Tradeoff Summary

OPTION	CONCEPT	CHARACTERISTICS	DELTA WEIGHT* (KG (LB))	DELTA COST (\$000)
1	USE EXISTING PIONEERS 10 AND 11 SLICE AND ADD A NEW SLICE	CAPACITOR DISCHARGE FIRING CIRCUITS; INDEPENDENT OF BATTERY	+0.45 (+0.98)	46
2	REDESIGN EXISTING PIONEERS 10 AND 11 SLICE TO USE THE 28-VDC BUS TO CHARGE CAPACITOR BANK	SAME AS OPTION 1	-0.47 (-1.03)	50
3	DEVELOP NEW SLICE DESIGN TO USE RELAYS THAT FIRE ORDNANCE DIRECTLY FROM 28-VDC BUS	REQUIRES A BATTERY TO HANDLE LARGE CURRENT PULSES	-0.42 (-0.93)	55
4	DEVELOP NEW SLICE DESIGN TO USE SCR'S THAT FIRE ORDNANCE DIRECTLY FROM 28-VDC BUS	SAME AS OPTION 3	-0.60 (-1.33)	52

* WEIGHT AND COST ENTRIES ARE RELATIVE TO THE UNMODIFIED EXISTING DESIGNS. COSTS ARE ESTIMATED TOTAL PROGRAM COST DELTAS (3 UNITS).

 A/C III Option 1 consists of retaining the existing ordnance slice and adding a new slice containing the additional firing circuits required. The weight and cost are increased slightly compared to the Pioneers 10 and 11 A/C III configuration.

 T/D III The second concept involves redesign of the existing ordnance slice to permit charging the capacitor bank directly from the 28-VDC bus. Elimination of the associated transformers and charging circuitry results in a small net weight reduction but at somewhat greater cost and design risk. This approach retains the capacitor discharge technique used successfully on Pioneers 10 and 11, with the important feature that operation is independent of battery degradation or failure. The new design allows for growth and includes provision for interface isolation circuits between the CDU and the probes.

Options 3 and 4 are designs based on relays or silicon-controlled rectifiers (SCR's) operating directly from the 28-VDC bus, omitting the capacitor bank for energy storage. This method places the battery in-line to support the transient load and increases the filtering requirements for units interconnected with the primary bus. Both options were rejected for this application because of the cost and risk associated with a new slice design and the potential impact on EMI filter modifications to existing units.

Option 1 is our preferred approach for the Atlas/Centaur configuration because of the low cost and risk, and an acceptably low weight penalty (0.45 kilogram).

Option 2 caters to the stringent weight constraints imposed by the Thor/Delta payload capability, while minimizing the redesign effort.

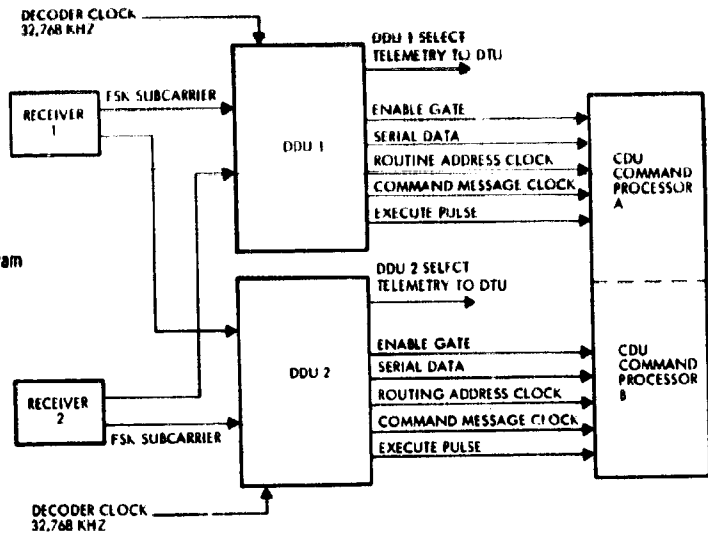
8.4.4 Preferred Subsystem Design A/C IV

The preferred command subsystem consists of the Pioneers 10 and 11 DDU and CDU interconnected as shown in Figure 8.4-2. A detailed description of the configuration is given in the following sections.

8.4.4.1 Digital Decoder Unit

Two redundant DDU's, identical to the Pioneers 10 and 11 units, fulfill the command demodulation requirements of both Pioneer Venus missions. The 8-bit command is authenticated by using a 4-bit parity

Figure 8.4-2. Command Subsystem Interface Diagram



Hamming code to provide a probability of executing a false command by less than 1.1×10^{-9} with a signal-to-noise ratio of 17.3 dB at the decoder input. The DDU provides a serial command output to the CDU, which includes 3 bits for routing serial commands to spacecraft and probe subsystems.

Figure 8.4-3 illustrates the basic DDU circuit functions, the fail-safe cross-strapped receiver inputs, and the CDU interface. Power gating is used in the digital section to conserve power when not processing a command. Power is applied to the analog portions of both redundant decoders at all times to prevent lockout modes.

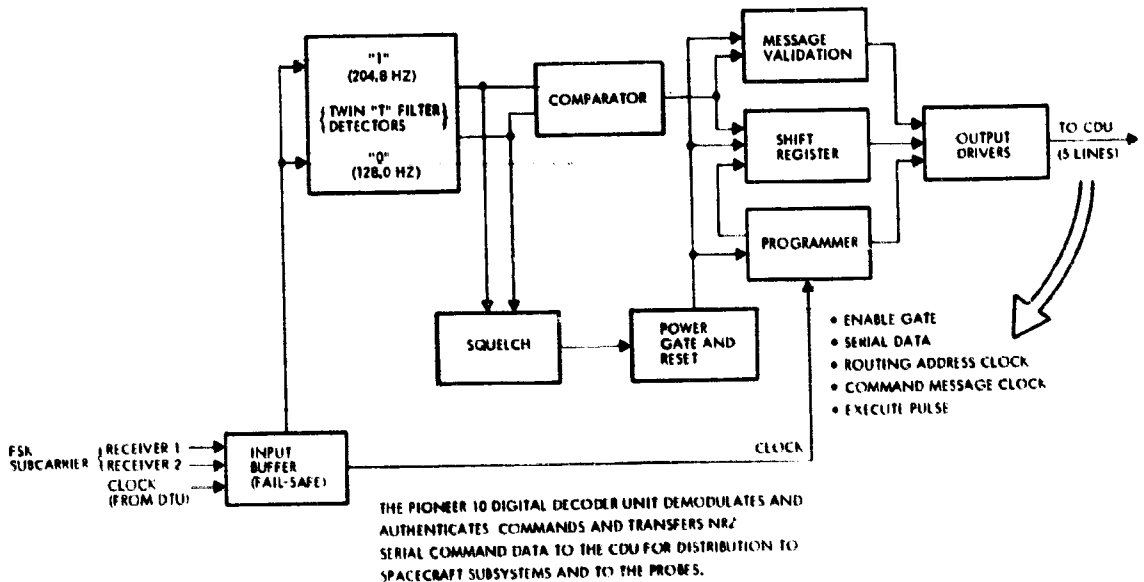


Figure 8.4-3. Pioneer Digital Decoder Unit

8.4.4.2 Command Distribution Unit

The key features of the CDU, consisting of subassembly slices containing printed-circuit boards, are summarized in Table 8.4-4 and described as follows.

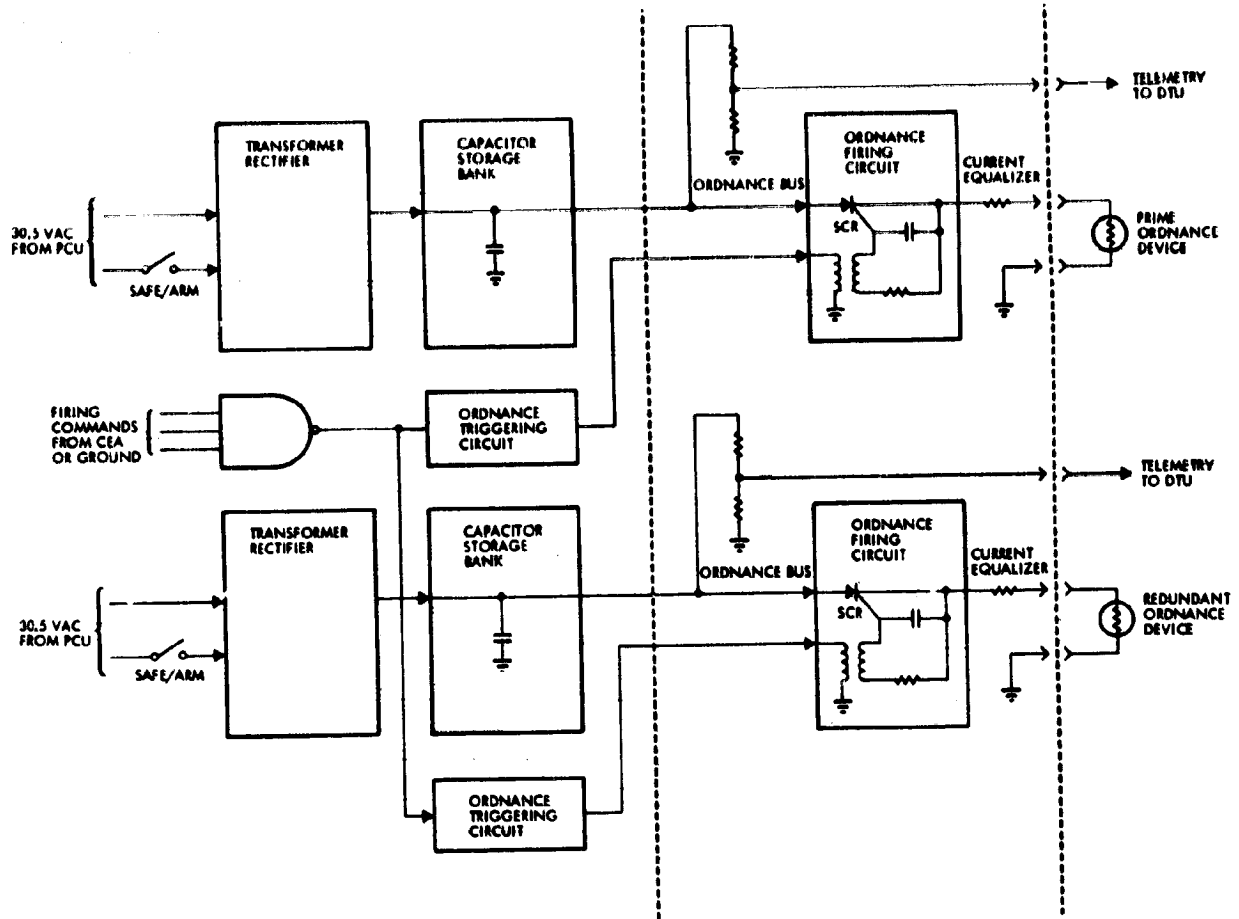
Ordnance Firing

The ordnance firing system (Figure 8.4-4) for rocket motor arming and ignition and various experiment and probe release functions is contained on two slices: one existing and one added to handle the increased requirements. This system includes redundant charging circuits and capacitor banks that provide power to fire ordnance devices, minimize battery requirements, and ensure probe separation in case of battery failure. Primary and backup ordnance must be ignited simultaneously for

Table 8.4-4. CDU Configuration

SPECIFICATION			
SIZE:			20.4 x 17.8 x 25.4 CM (8 x 7 x 10 IN.)
WEIGHT:			4.5 KG (9.8 LB)
POWER:			2.1 WATTS
PREVIOUS USE:			PIONEERS 10 AND 11
CIRCUIT TYPE:			LP-TTL MSI
REDUNDANCY:			INTERNAL
NO. OF SLICES:			9

MODIFICATION	SLICE NUMBER	WEIGHT KG (LB)	DESCRIPTION
MINOR	1	1.36 (3.0)	ORDNANCE - CAPACITOR DISCHARGE FUNCTION
MINOR	2	0.45 (0.99)	HIGH LEVEL OUTPUT CONTROL/SEQUENCER
MINOR	3	0.45 (0.98)	TELEMETRY CONDITIONING/UNDERVOLTAGE/ THRUSTER COUNTER
MINOR	4	0.35 (0.76)	SIGNAL PRESET CONTROL/TELEMETRY SIGNAL CONDITIONING
NONE	5	0.34 (0.74)	LOW LEVEL OUTPUT NO. 1
NONE	6	0.34 (0.74)	LOW LEVEL OUTPUT NO. 2
NONE	7	0.38 (0.84)	COMMAND PROCESSOR
NEW	8	0.34 (0.74)	COMMAND MEMORY PROGRAMMER (INCREASE CAPACITY)
NEW	9	0.45 (0.99)	ORDNANCE OF FIRING CIRCUITS, ISOLATORS, COUNTERS



FEATURES:

- THE ARM SIGNAL CONNECTS THE AC POWER SOURCE AND CHARGES CAPACITORS
- CAPACITORS FIRE THE ORDNANCE WHEN THE SCR SWITCHES ARE TRIGGERED
- RECHARGE OCCURS WITHIN 20 M/S
- EACH ORDNANCE CIRCUIT CAN FIRE UP TO SIX SQUIBS SIMULTANEOUSLY WITH ENERGY FROM ONE CAPACITOR BANK
- CAPACITOR CHARGE IS MONITORED BY TELEMETRY
- SAFE/ARM SWITCH STATUS ALSO MONITORED

Figure 8.4-4. Ordnance Firing System

release of the large probe from the six ball-lock retention mechanisms to avoid a tip-off condition. Delayed firing of redundant ordnance for the remaining functions is not required and may be bypassed.

The number of required firing circuits is minimized by parallel combining functions that occur simultaneously and do not interact. For example, the small probe thermal shield release and cable cutter actuation are initiated by the same trigger circuit. Sufficient space is available in this added slice to accommodate the increased quantity of thruster firing counters.

Output Control Logic

A third slice contains high-level output control logic to perform the commanded switching functions and a sequencer previously used to automatically initiate post launch functions prior to establishing the command link. The sequencer is not required for the Atlas/Centaur launched missions because the Centaur stage establishes the desired spacecraft spin rate and orientation. However, since the weight penalty is insignificant, it is recommended that the circuitry be retained to avoid the expense of its removal and to meet future requirements that may arise.

Signal Present Detection

A fourth slice contains signal-present detection circuitry to automatically switch antenna inputs to the appropriate spacecraft receiver (after a preset interval) to preclude a lock-out condition in case of receiver failure.

A limitation of the Pioneers 10 and 11 CDU design (which resulted in either a 36-hour or 72-hour period, depending on the previous position of the transfer switch) has been corrected. Replacement of the existing solid-state toggle function with a simple logic function that monitors the transfer switch position ensures that the preset delay remains invariant, regardless of the initial position of the switch.

The overvoltage sensing circuit monitors the 5.3-VDC power input voltage to each command processor. If the input voltage reaches +6.2 volts on the primary input voltage source, the sensing circuit automatically switches to the redundant input voltage source so that the command link will not be interrupted.

This slice also counts thruster firing pulses and delivers real time telemetry indication of when the thrusters are firing. There are 64 thruster firings counted before recycling the counter back to zero and starting over again. Provision is made to equip each of the eight thrusters with this capability.

Supplementary Functions

A fifth slice performs five more functions: signal conditioning, overload control, power reset, overvoltage sensing, and thruster pulse counting.

The signal conditioning circuits in the CDU provide signal compatibility with the digital telemetry unit (DTU) input characteristics. Each signal conditioning circuit consists of passive resistor circuits. Two types of signal conditioning are provided, thermistor conditioning using voltage divider resistors and switching event signals using current limiting resistors.

The overload control function turns off certain spacecraft loads in the event of an overload condition to the spacecraft main DC power bus. The loads turned off in sequence are science, data storage units (DSU), ACS to standby propellant heaters, and then the transmitter. The sensing of an overload condition is performed within the power control unit (PCU); an overload condition exists when the main DC power bus voltage falls to 26.5 ± 0.5 VDC for a time period of 200 ± 10 milliseconds. The above loads are turned off automatically by the CDU and remain off until restored by ground command.

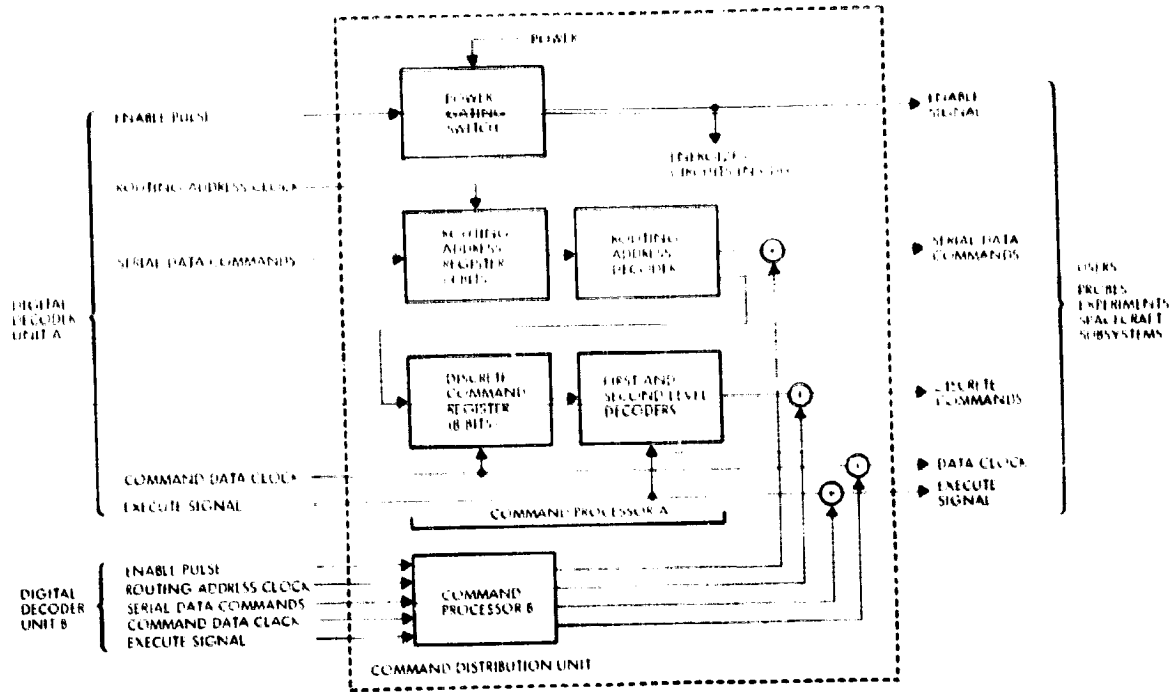
The power reset circuit is designed to reset all bistable functions in the CDU to a predetermined state. This function occurs during the initial application of power from the 5.3-VDC source. The power reset function can be simulated in flight by ground command.

Command Processing

The command distribution unit (CDU) command processor, Figure 8.4-5, decodes discrete commands from the associated DDU, processes them to produce user-compatible outputs, and then distributes the outputs. Both processors are contained in a single slice and the outputs are cross-strapped for added reliability. In the event of a failed command processor (A or B), the redundant processor must be addressed via the associated DDU to obtain a serial and/or discrete command output from the CDU.

A new slice contains the command memory, which stores up to 16 discrete commands and their associated time delays. In addition to the primary functions described in Section 8.4.3.1, it can also be used as a backup to stop maneuvers in the event of a malfunction.

Table 8.4-5 summarizes the CDU modes of operation. A functional block diagram of the CDU modified for the Pioneer Venus application is shown in Figure 8.4-6.



FEATURES:

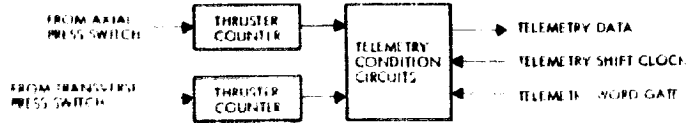
- DISCRETE COMMAND DECODING ACCOMPLISHED BY FIRST AND SECOND LEVEL DECODERS WHICH PRODUCE A TOTAL OF 256 OUTPUT STATES EASILY EXPANDABLE TO 512
- EXECUTE PULSE RECEIVED AFTER LAST DATA CLOCK PULSE INDICATING VERIFICATION OF GROUND COMMAND
- ACTIVATING ONE PROCESSOR AT A TIME CONSERVES POWER
- IN EVENT OF A FAILED PROCESSOR (A OR B), ALTERNATE PROCESSOR IS ADDRESSED BY ODU

Figure 8.4-5. Command Processor

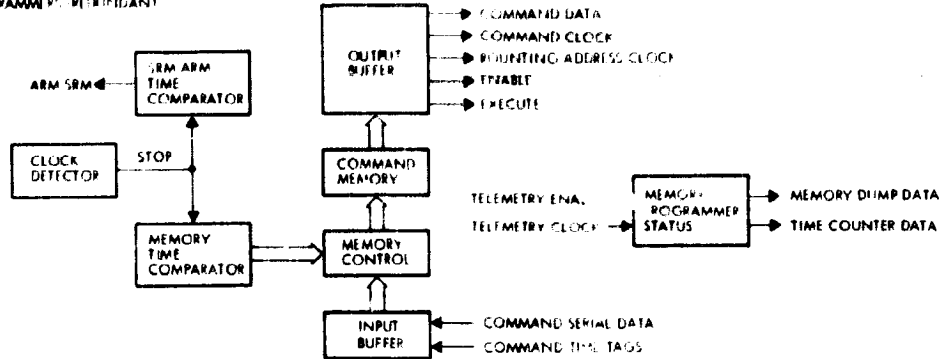
Table 8.4-5. CDU Modes of Operation

ITEM NO.	FUNCTION	INITIATION	OPERATING TIME	FUNCTION DESCRIPTION
1	COMMAND PROCESSING	UPON RECEIPT OF COMMAND SIGNAL FROM ODU VIA COMMAND LINK	22 SECONDS, MAXIMUM	ACCEPT, PROCESS, AND DISTRIBUTE REAL TIME COMMANDS
2	COMMAND MEMORY	GROUND COMMAND - "EXECUTE STORED SEQUENCE"	DEPENDENT TIME DELAYS STORED IN TIME REGISTERS	STORE 16 COMMANDS WHICH CAN BE INITIATED FOLLOWING STORED TIME DELAYS
3	ORDNANCE FIRING	GROUND COMMANDS	DURING ARMED PERIOD AND FIRING TIME	CONTROL ORDNANCE SAFE ARM AND FIRING FUNCTIONS
4	SIGNAL PRESENT DETECTION	ABSENCE OF SELECTOR INPUTS INDICATING LOSS OF LOCK	36-4 HOURS	SIGNAL PRESENT CONTACT FOR AUTOMATIC SWITCHING OF ANTENNAS
5	SIGNAL CONDITIONING	CONTINUOUS MONITORING	CONTINUOUS	SIGNAL CONDITIONING OF HIGH-LEVEL AND ANALOG TELEMETRY SIGNALS
6	OVERLOAD CONTROL	SIGNAL FROM PRIMARY PERSON IN PORT	300 MS, MAXIMUM	OVERLOAD CONTROL TO TURN OFF NONESSENTIAL POWER
7	45 VOLT SWITCHING AND OVERVOLTAGE SENSING	45 VOLT SWITCHING VIA GROUND COMMAND, OVERVOLTAGE SENSING IS AUTOMATIC	DISCRETE "OFF" SWITCHING TO 25 MS (MAX), OVERVOLTAGE SENSING CONTINUOUS	POWER RESET FUNCTION RELEASABLE CIRCUITS WHEN POWER IS RESTORED, OVERVOLTAGE SENSING FUNCTION
8	THRUSTER FIRING CONTROL	THRUSTER PRESSURE SWITCH CLOSED	THRUSTER THRUSTER FIRING PERIODS	DETECT AND STORE THRUSTER FIRING CONTROL

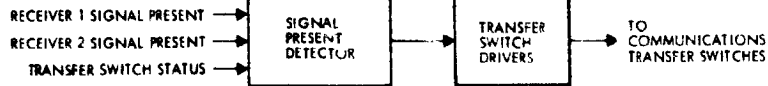
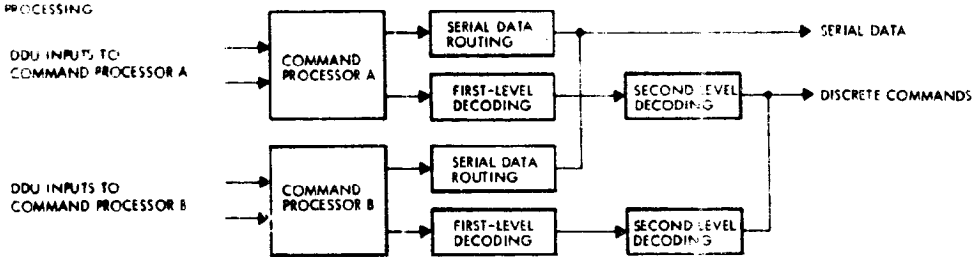
THRUSTER PRESS SWITCH



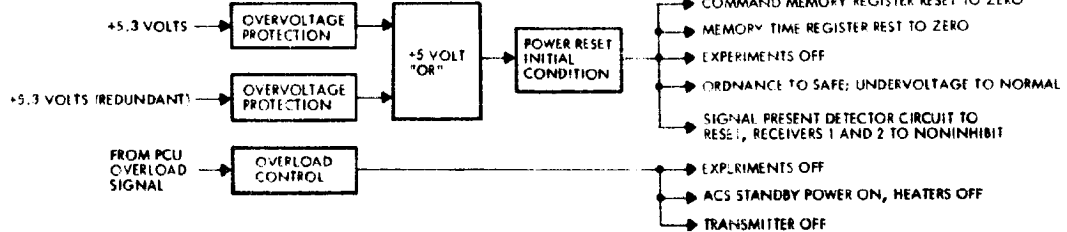
ARM AND MEMORY PROGRAMMER REDUNDANT



COMMAND PROCESSING



OVERLOAD CONTROL AND +5.3 VOLT "OR" SWITCHING



SIGNAL CONDITIONING



ORDNANCE FIRING

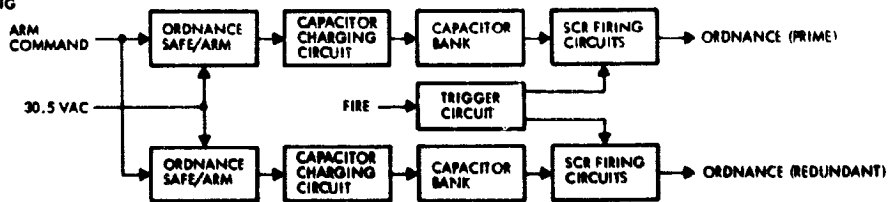


Figure 8.4-6. CDU Functional Block Diagram

Probe Interface

Each of the four probes operates under the control of the probe bus prior to separation for sequencing, calibration, and checkout. The command interface is comprised of three lines: command data, clock, and execute, as illustrated in Figure 8.4-7. Isolation is provided between the probes and the probe bus, as shown, to eliminate a possible electrical short condition from occurring when the umbilical to a probe is severed by the cable cutter prior to separation.

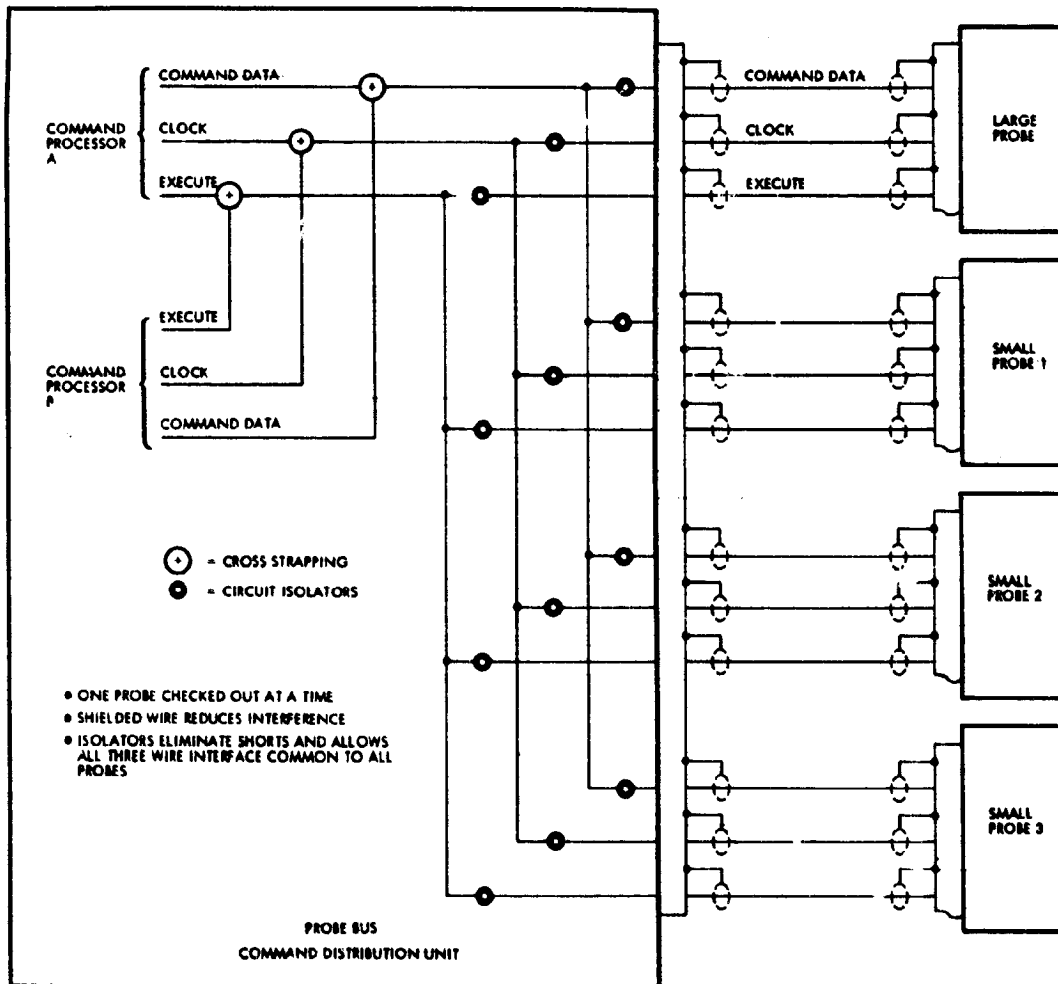


Figure 8.4-7. CDU/Probe Interface

8.5 Attitude Determination
and Control

8.5 ATTITUDE DETERMINATION AND CONTROL SUBSYSTEM (ADCS)

8.5.1 Introduction and Summary

Figure 8.5-1 summarizes the basic information on the ADCS that has been defined for the preferred Atlas/Centaur probe bus and orbiter carrying the Version IV science payload.

The most important characteristics of this ADCS from the cost point of view is that it is derived directly from the flight-proven Pioneers 10 and 11 and Intelsat III programs and uses a single subsystem design for both probe bus and orbiter. This commonality permits a further cost saving on spares since only one type of spare is needed for a given component. Preserving this commonality means that some functions are provided that are needed for only one mission and consequently are unused on the other; examples are the circuitry to generate small probe release signals, conscan logic, and ram platform motor control logic. The cost of these unused functions is minor compared to the savings effected by commonality of design.

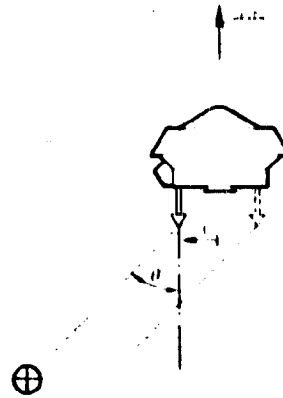
The requirements analysis indicates that attitude determination and control accuracies in the 0.017- to 0.035 radian (1- to 2-degree) range are adequate; this degree of accuracy is readily achieved without the use of sophisticated attitude references such as star mappers. The relatively low accuracy requirements stems in part from the use of sequential probe release, which has been adopted to permit entry of all probes with the desired zero angle of attack. From the attitude control point of view, sequential probe release is advantageous because high spin rates are not required, with their associated stringent requirements on release attitude.

Attitude determination is accomplished by a combination of sun sensor outputs (both sun aspect and roll reference) and one of three different RF sensing techniques (two of which impose virtually no weight or power requirements on the spacecraft); each is used under appropriate conditions, as outlined below:

A/C IV | -A/C IV

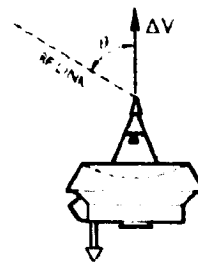
- Doppler Modulation

Rotation of the offset omni antenna about the spin axis produces a doppler modulation proportional to $r \sin \theta$ and allows the ground station to estimate θ with good accuracy for values of θ not in the vicinity of $\pi/2$ rad (90 deg). This technique is used on both probe bus and orbiter when the earth direction is not more than ~ 1 radian from the aft (negative) spin axis.



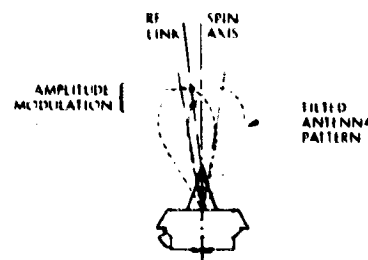
- Doppler Shift

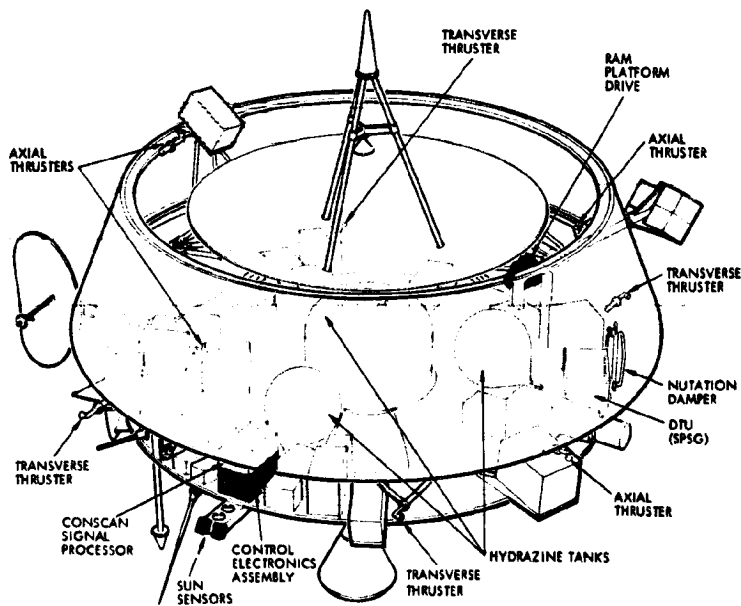
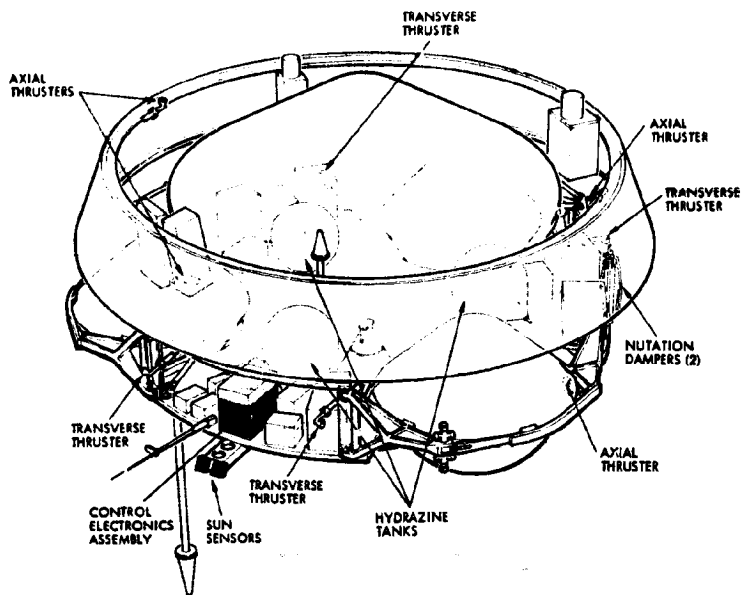
A deliberate axial ΔV maneuver (typically 1 meter/second) produces a doppler shift proportional to $\Delta V \cos \theta$, from which the ground station can estimate θ with good accuracy for values of θ in the vicinity of $\pi/2$ radians (90 degrees). This technique supplements the doppler modulation technique for cases where the earth direction is near $\pi/2$ radians, and also for determining the Venus orbit insertion attitude (at which time communication is through the on-axis forward omni antenna).



- Conical Scan (Conscan)

When the high-gain orbiter antenna is pointed at the earth, a measure of pointing error is determined onboard from the modulation of the uplink AGC voltage produced by rotation of the tilted antenna pattern about the spin axis. The onboard determination of two angles is based on this modulation combined with role reference pulses from the sun sensor; the two angles are telemetered to the ground, where pointing error is computed and appropriate commands transmitted to correct the error. An alternate mode of operation is provided, in which the attitude control pulses are computed onboard without ground intervention.





A KEY DESIGN FEATURES

ATTITUDE DETERMINATION AND CONTROL CONCEPTS HAVE BEEN SUCCESSFULLY PROVEN ON PIONEERS 10 AND 11 SPACECRAFT

ALL ADCS HARDWARE IS DERIVED FROM EXISTING, FLIGHT-PROVEN EQUIPMENT WITH MINOR MODIFICATIONS

ADCS DESIGNS FOR PROBE BUS AND ORBITER ARE COMPATIBLE WITH PIONEERS 10 AND 11 GROUND SOFTWARE AND MINIMIZE ADAPTION REQUIREMENTS

ONBOARD PROGRAMMING CAPABILITIES FOR AUTOMATIC EXECUTION OF MANEUVER SEQUENCES MINIMIZE DEPENDENCY ON REAL TIME CONTROL FOR CRITICAL EVENTS

SUN ASPECT SENSOR DATA PROVIDES CAPABILITY FOR IN-FLIGHT REACTION CONTROL SUBSYSTEM CALIBRATION

SIMPLE, RELIABLE, ATTITUDE DETERMINATION APPROACH, BASED ON SUN ASPECT SENSOR AND DOPPLER DATA, MEETS REQUIREMENTS OF ALL CRITICAL MANEUVERS AND EVENTS

CONSCAN SIMPLIFIES ATTITUDE DETERMINATION AND CONTROL IN ORBIT, THUS REDUCING TO A MINIMUM THE ENGINEERING SUPPORT REQUIRED FOR OPERATIONS

SUN SENSORS AND CRITICAL CEA CIRCUITS AND SUBASSEMBLIES ARE REDUNDANT FOR ENHANCED RELIABILITY

FAVORABLE SPACECRAFT MOMENT-OF-INERTIA RATIOS AND PASSIVE SPIN STABILIZATION APPROACH PRECLUDE INSTABILITY RISKS AND CROSS-COUPLED DYNAMIC PROBLEMS

NUTATION DAMPER FREQUENCY TUNING INSENSITIVE TO SPIN SPEED CHANGES WITHIN OPERATING RANGES

C REQUIREMENTS VERSUS CAPABILITIES

PROBE BUS ACCURACIES (3σ)		
	REQUIREMENT [RAD (DEG)]	CAPABILITY [RAD (DEG)]
SPIN SPEED CONTROL		
0.402 RAD/S (4.8 RPM) NOMINAL SPEED	1%	0.1 TO 0.5%
2.094 RAD/S (20 PRM) LARGE PROBE RELEASE	3%	0.5 TO 1.0%
1.047 RAD/S (10 RPM) SMALL PROBE RELEASE	3%	0.5 TO 1.0%
6.283 RAD/S (60 RPM) PROBE BUS ENTRY	3%	0.5 TO 1.0%
SPIN AXIS ALTITUDE DETERMINATION		
CRUISE-MIDCOURSE MANEUVERS	0.026 (1.5)	< 0.024 (1.4)
PROBE DEPLOYMENT RETARGETING	0.042 (2.5)	< 0.035 (2.1)
PROBE BUS ENTRY	0.009 (0.5)	0.003 TO (0.20 TO 0.32)
ANTENNA POINTING		
CRUISE	0.257 (15)	< 0.035 (2.1)
PROBE BUS ENTRY	0.017 (1)	< 0.14 (0.8)
VELOCITY INCREMENT DISPERSIONS		
MIDCOURSE MANEUVERS	0.005 (2)	< 0.026 (1.5)
RETARGETING MANEUVERS	0.052 (3)	< 0.018 (1.1)
EXPERIMENT POINTING		
CRUISE	0.052 (3)	< 0.028 (1.7)
PROBE BUS ENTRY	0.017 (1)	0.014 (0.8)
PROBE DEPLOYMENT ATTITUDE		
SPIN AXIS ORIENTATION	0.042 (2.5)	< 0.035 (2.1)
RELEASE SPIN ANGLE	0.009 (0.5)	0.007 (0.4)

FOLDOUT FRAME

...HAVE BEEN
...CRAFT
...PROVEN
...ADAPTION
...WITH
...CONTROL
...TIME CONTROL
...FLIGHT REACTION
...BASED ON SUN
...ALL CRITICAL
...CONTROL IN ORBIT,
...PORT REQUIRED FOR
...ASSEMBLY ARE
...PASSIVE SPIN
...AND CROSS-
...SPIN SPEED

B PRINCIPAL CHARACTERISTICS

FUNCTIONS:

- SUPPLY DATA FOR GROUND DETERMINATION OF SPIN AXIS ORIENTATION
- PROVIDE SPIN ANGLE ROLL REFERENCE TO SCIENCE AND ATTITUDE CONTROL LOGICS FOR TIMING THRUSTER OPERATION AND SMALL PROBE RELEASES
- PERFORM SPIN SPEED CONTROL BY GROUND COMMAND, EITHER PULSED OR CONTINUOUS FIRINGS CAN BE SELECTED
- CONTROL THRUSTERS FOR EXECUTING PRECESSION AND VELOCITY CORRECTION MANEUVERS; ALSO, COMBINED MANEUVER SEQUENCES CAN BE PROGRAMMED BY GROUND COMMAND
- CONTROL THRUSTERS FOR AUTOMATICALLY PRECESSING THE ORBITER TO EARTH-POINTING ORIENTATION
- PROVIDE TIMING SIGNALS FOR SMALL PROBE RELEASES, DELAYS FROM SUN SENSOR PULSES CAN BE SELECTED BY GROUND COMMAND

DESIGN DATA

	PROBE BUS	ORBITER
WEIGHT	2.7 KG (6 LB)	4.7 KG (10.3 LB)
POWER (AVERAGE) PEAK	2.1 WATT	2.1 WATT
RELIABILITY	0.99959 (115 DAYS)	0.99081 (425 DAYS)

INCREMENT (DEG)	CAPABILITY (RAD/DEG)
0.1	0.1 TO 0.5%
0.5	0.5 TO 1.0%
1.0	0.5 TO 1.0%
1.5	0.5 TO 1.0%
2.0	0.5 TO 1.0%
2.5	0.035 (2.1)
3.0	0.003 TO 0.20 TO 0.32
3.5	0.035 (2.1)
4.0	0.14 (0.8)
4.5	0.026 (1.5)
5.0	0.018 (1.1)
5.5	0.028 (1.7)
6.0	0.014 (0.8)
6.5	0.035 (2.1)
7.0	0.007 (0.4)

ORBITER ACCURACIES (3σ)

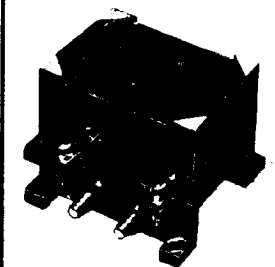
	REQUIREMENT (RAD/DEG)	CAPABILITY (RAD/DEG)
SPIN SPEED CONTROL		
0.402 RAD/S (4.8 RPM) NOMINAL SPEED	1%	0.1 TO 0.5%
6.283 RAD/S (60 RPM) ORBIT INSERTION	3%	0.5 TO 1.0%
SPIN AXIS ALTITUDE DETERMINATION		
CRUISE-MIDCOURSE MANEUVERS	0.026 (1.5)	< 0.024 (1.4)
ORBIT INSERTION MANEUVER IN ORBIT	0.042 (2.5) 0.017 (1.0)	< 0.041 (2.4) < 0.006 (0.36)
ANTENNA POINTING		
CRUISE (HIGH GAIN) (HORN)	0.070 (4.0)	0.004 (0.25)
IN ORBIT (HIGH GAIN) (HORN)	0.257 (15.0)	0.006 (0.35)
EARTH OCCULTATION	0.017 TO 0.070 (1 TO 4)	0.004 (0.25)
IN ORBIT (HORN)	0.257 (15)	0.006 (0.36)
VELOCITY INCREMENT DISPERSIONS		
MIDCOURSE MANEUVERS	0.035 (2)	< 0.026 (1.5)
ORBIT INSERTION	0.052 (3)	< 0.042 (2.5)
PERIAPSIS MAINTENANCE	0.052 (3)	< 0.04 (2.3)
EXPERIMENT POINTING		
CRUISE	0.052 (3)	0.004 TO 0.028 (0.25 TO 0.45)
IN ORBIT	0.035 (2)	0.004 TO 0.008 (0.25 TO 0.45)

D SUMMARY DESCRIPTION OF ATTITUDE DETERMINATION AND CONTROL SUBSYSTEM DESIGNS SELECTED FOR THE PREFERRED PROBE BUS AND ORBITER CONFIGURATIONS

SUN SENSOR ASSEMBLY

DESCRIPTION:
THE SSA CONSISTS OF A FUSED SILICA BLOCK WITH A PHOTO-VOLTAIC SILICON DETECTOR LOCATED ON THE BACK SURFACE, AND THE FRONT SURFACE HAVING PHOTOETCHED SLITS IN A VACUUM DEPOSITED NICKEL FILM.

ENV:
ROLL REFERENCE ASPECT 8 - 112 DEG
10 - 110 DEG



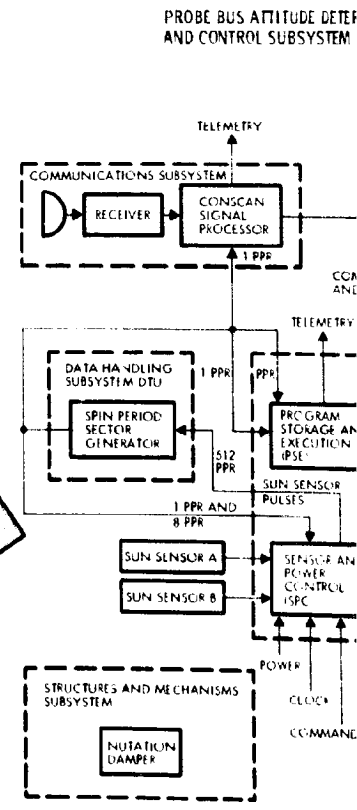
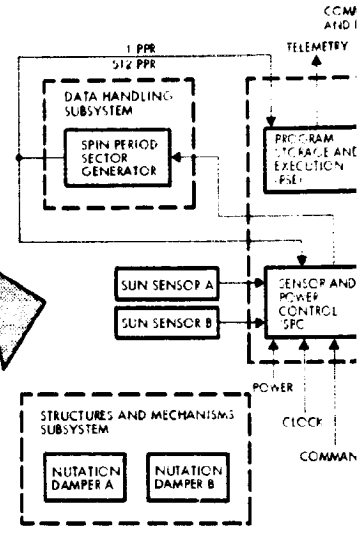
FUNCTION:
THE SSA PROVIDES ROLL INDEXING AND SUN ASPECT INFORMATION.

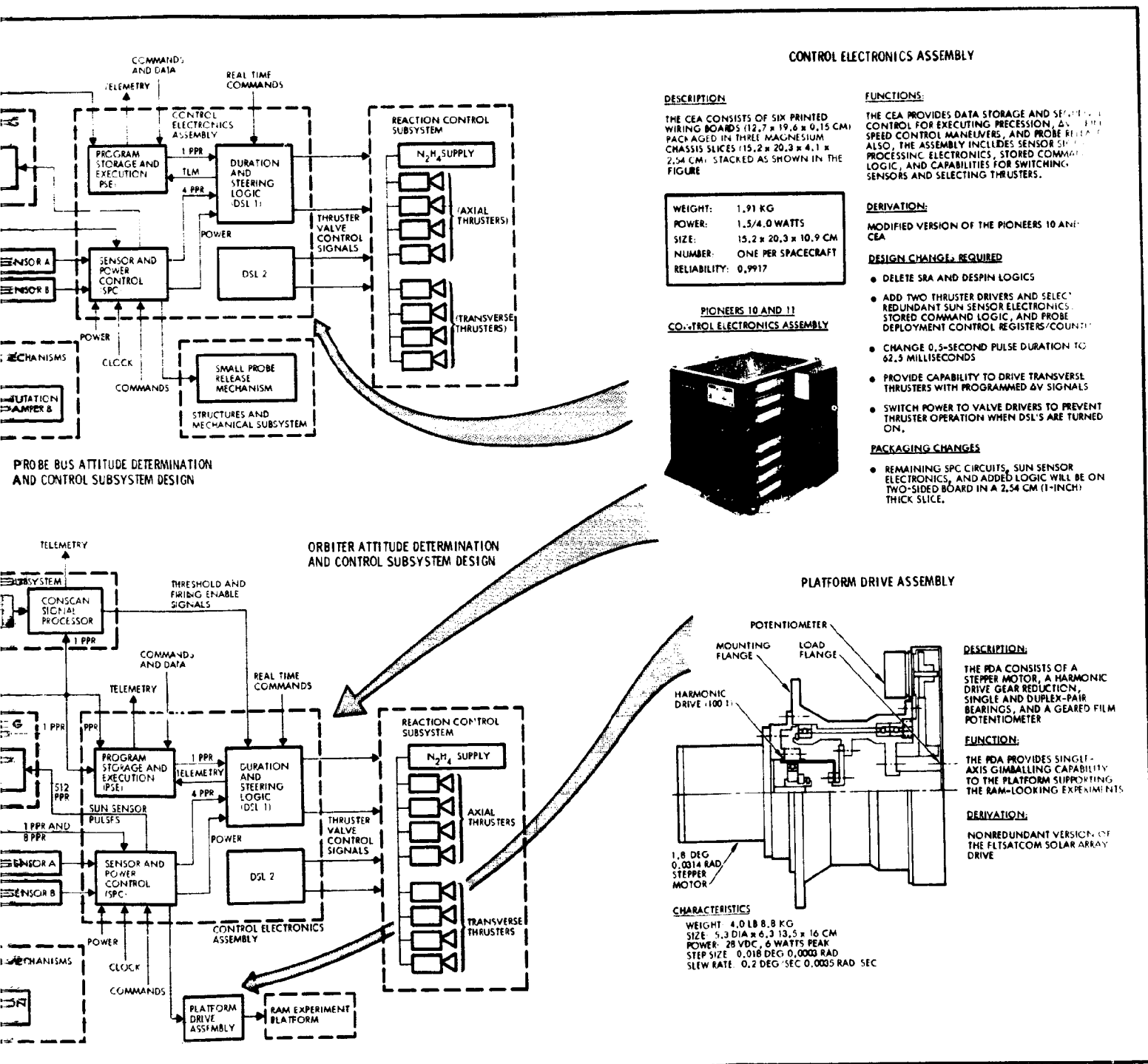
DERIVATION:
MODIFICATION OF INTELSAT III SSA BY CHANGING SLIT DESIGN.

ERROR ANALYSIS

SOURCE	ASPECT 1σ	ROLL 1σ
SENSOR TEST	0.044	0.034
RSS TOTAL 1σ	0.054	0.041

WEIGHT: 185 GRAMS
POWER: NONE
SIZE: 4.75 x 3.3 x 3 CM
NUMBER: TWO PER SPACECRAFT
RELIABILITY: 0.9993 (425 DAYS)





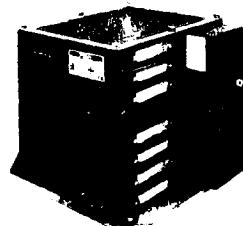
CONTROL ELECTRONICS ASSEMBLY

DESCRIPTION

THE CEA CONSISTS OF SIX PRINTED WIRING BOARDS (12.7 x 19.6 x 0.15 CM) PACKAGED IN THREE MAGNESIUM CHASSIS SLICES (15.2 x 20.3 x 4.1 x 2.54 CM) STACKED AS SHOWN IN THE FIGURE

WEIGHT:	1.91 KG
POWER:	1.5/4.0 WATTS
SIZE:	15.2 x 20.3 x 10.9 CM
NUMBER:	ONE PER SPACECRAFT
RELIABILITY:	0.9917

**PIONEERS 10 AND 11
CONTROL ELECTRONICS ASSEMBLY**



FUNCTIONS:

THE CEA PROVIDES DATA STORAGE AND SELECTION CONTROL FOR EXECUTING PRECESSION, AXIAL SPEED CONTROL MANEUVERS, AND PROBE RELEASE. ALSO, THE ASSEMBLY INCLUDES SENSOR SIGNAL PROCESSING ELECTRONICS, STORED COMMAND LOGIC, AND CAPABILITIES FOR SWITCHING SENSORS AND SELECTING THRUSTERS.

DERIVATION:

MODIFIED VERSION OF THE PIONEERS 10 AND 11 CEA

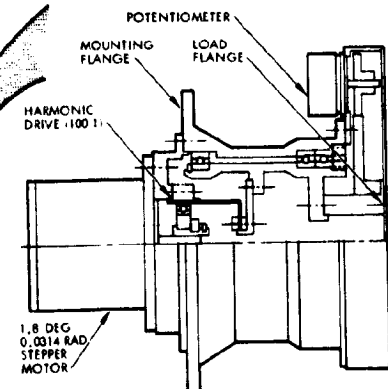
DESIGN CHANGES REQUIRED

- DELETE SRA AND DESPIN LOGICS
- ADD TWO THRUSTER DRIVERS AND SELECT REDUNDANT SUN SENSOR ELECTRONICS, STORED COMMAND LOGIC, AND PROBE DEPLOYMENT CONTROL REGISTERS/COUNTERS
- CHANGE 0.5-SECOND PULSE DURATION TO 62.9 MILLISECONDS
- PROVIDE CAPABILITY TO DRIVE TRANSVERSE THRUSTERS WITH PROGRAMMED ΔV SIGNALS
- SWITCH POWER TO VALVE DRIVERS TO PREVENT THRUSTER OPERATION WHEN DSL'S ARE TURNED ON.

PACKAGING CHANGES

- REMAINING SPC CIRCUITS, SUN SENSOR ELECTRONICS, AND ADDED LOGIC WILL BE ON TWO-SIDED BOARD IN A 2.54 CM (1-INCH) THICK SLICE.

PLATFORM DRIVE ASSEMBLY



DESCRIPTION:

THE PDA CONSISTS OF A STEPPER MOTOR, A HARMONIC DRIVE GEAR REDUCTION, SINGLE AND DUPLEX-PAIR BEARINGS, AND A GEARED FILM POTENTIOMETER

FUNCTION:

THE PDA PROVIDES SINGLE-AXIS GIMBALLING CAPABILITY TO THE PLATFORM SUPPORTING THE RAM-LOOKING EXPERIMENTS

DERIVATION:

NONREDUNDANT VERSION OF THE FLTSATCOM SOLAR ARRAY DRIVE

CHARACTERISTICS

WEIGHT:	4.0 LB 8.8 KG
SIZE:	5.3 DIA x 6.3 13.5 x 16 CM
POWER:	28 VDC, 6 WATTS PEAK
STEP SIZE:	0.018 DEG 0.0003 RAD
SLEW RATE:	0.2 DEG/SEC 0.0005 RAD/SEC

Figure 8.5-1. Attitude Determination and Control

A/C IV
A/C IV

The data rate requirements of the Version IV science payload for the orbiter led to the need for a high-gain antenna. It would have been possible to provide the required gain with a despun reflector antenna, but an earth-pointing spacecraft with fixed antenna was chosen because of the considerable cost saving (over \$1 million). This saving takes into account the gimbal mounting of the ram instruments required with the earth-pointing configuration. In addition to the cost saving, there is a lower risk factor, because there are no potential bearing problems or instabilities due to cross-coupling, with the fixed-antenna, earth-pointing configuration. The science aspects of the earth-pointing configuration were covered in Section 3.

Another point worthy of special mention is the sun sensor selected for the ADCS; this is an off-the-shelf design previously used successfully on Intelsat III. It has the advantage of providing both sun crossing pulses (as a roll reference) and sun aspect angle (for attitude determination) from a single instrument of simple design. It is planned to take advantage of sun sensor data to perform in-flight calibration of the reaction control system, thus effecting a considerable saving in ground testing costs. The calibration can be carried out at the time of the first midcourse correction and will reduce thruster impulse uncertainties to the 2 to 3 percent range. This is more than adequate for all pointing requirements, including the doppler shift attitude determination technique mentioned above.

The remaining sections, 8.5.2 through 8.5.6, cover respectively the requirements analyses, concept selection tradeoffs, the details of the preferred design summarized above, subsystem performance, and the science interface.

ALL VERSION III
SCIENCE PAYLOAD

8.5.2 Functions and Requirements, 1977 Probe Mission, Version III Science Payload and Both Thor/Delta and Atlas/Centaur Options

The attitude determination and control subsystem (ADCS) provides capabilities for performing the following functions:

- Attitude Determination. This function generates data from which the inertial orientation of the spin axis can be determined on the ground. Also, a spin angle (roll) reference is required onboard by the science experiments and for timing attitude control thrusting and small probe deployment.

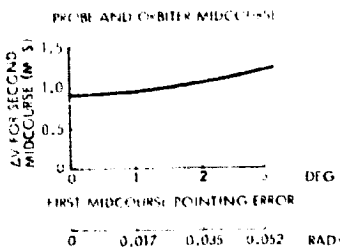
- **Spin Speed Control.** This function is required for initial despin (Thor/Delta configurations), nominal spin speed maintenance, spin-up/despin for orbiter deboost maneuver, and probe bus spin-up prior to entry. Additional spin-up/despin actions may be required during probe-bus retargeting maneuvers to reduce velocity dispersions caused by cm offsets. A set of redundant hydrazine thrusters (parts of the reaction control subsystem) provides control torque. The ADCS provides valve control signals, the duration and number of which are selectable by ground command.
- **Spacecraft Precession.** Spacecraft precessions are required for maintaining the desired cruise and orbiter attitudes and reorienting the vehicle for velocity corrections and probe deployment. The ADCS provides signals for thruster operation and includes a programmer to automatically execute an open-loop sequence of precession maneuvers for velocity corrections and probe deployment.
- **Velocity Control.** The ADCS provides signals to time the operation of the RCS thrusters to produce axial or transversal velocity corrections. Axial velocity corrections can be executed as part of an automatic sequence, including precession of the spacecraft to the desired orientation for firing and return to the initial position.
- **Small Probe Deployment Control.** Signals for initiating small probe deployment are provided to the separation mechanism. Delays relative to spin angle reference signals are adjustable by ground command.

Table 8.5-1 includes a more detailed list of functions and presents preliminary estimates of accuracy requirements.

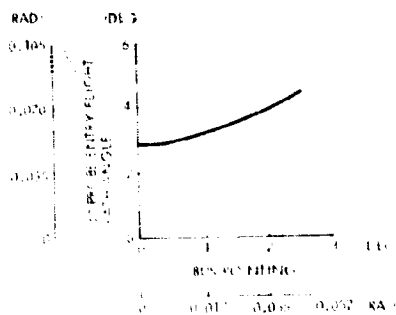
Table 8.5-1. Summary of Attitude Determination and Control Requirements

	PROBE BUS		ORBITER	
	ACCURACY (3σ)	REMARKS	ACCURACY (3σ)	REMARKS
SPIN SPEED CONTROL	1 PERCENT 3 PERCENT	0.50 RAD S (4.8 RPM) NOMINAL SPEED 6.28 RAD. S (60 RPM) PROBE BUS ENTRY	1 PERCENT 3 PERCENT	0.50 RAD S (4.8 RPM) NOMINAL SPEED 6.25 RAD. S (60 RPM) ORBIT INSERTION
SPIN AXIS ATTITUDE DETERMINATION	0.026 RAD (1.5 DEG) 0.017 RAD (1.0 DEG)	CRUISE-MIDCOURSE MANEUVERS PROBE DEPLOYMENT - RETARGETING	0.026 RAD (1.5 DEG) 0.035 RAD (2.0 DEG)	CRUISE-MIDCOURSE MANEUVERS ORBIT INSERTION
HIGH-GAIN ANTENNA POINTING (EARTH ASPECT COMPONENT)	0.009 RAD (0.5 DEG) 0.087 RAD (5.0 DEG) 0.017 RAD (1.0 DEG)	PROBE BUS ENTRY ATTITUDE CRUISE PROBE BUS ENTRY	0.017 RAD (1.0 DEG) 0.035 RAD (2.0 DEG) 0.016 TO 0.030 RAD (0.9 TO 1.7 DEG)	IN ORBIT CRUISE IN ORBIT
VELOCITY INCREMENT DISPERSIONS (OVERALL, INCLUDING DYNAMIC EFFECTS)	0.052 RAD (3.0 DEG) 0.035 RAD (2.0 DEG)	RETARGETING MANEUVERS MIDCOURSE MANEUVERS	0.052 RAD (3.0 DEG) 0.035 RAD (2.0 DEG)	ORBIT INSERTION MIDCOURSE-ORBIT TRIMS
EXPERIMENT POINTING	0.052 RAD (3.0 DEG) 0.009 RAD (0.5 DEG)	CRUISE PROBE BUS ENTRY	0.052 RAD (3.0 DEG) 0.035 RAD (2.0 DEG)	CRUISE IN ORBIT
PROBE DEPLOYMENT ATTITUDE	0.017 RAD (1.0 DEG) 0.009 RAD (0.5 DEG)	SPIN AXIS ORIENTATION SPIN ANGLE RELEASE	- -	- -
DESPIN REFLECTOR POINTING	-	-	0.013 RAD (0.75 DEG)	-

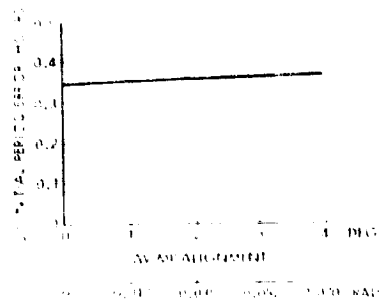
The functions that have greatest influence on ADCS requirements are 1) probe deployment and retargeting maneuvers and 2) orbiter antenna and science instrument pointing. A preliminary evaluation of sensitivities to attitude errors indicates that pointing accuracies on the order of 0.017 radian (1 degree) (3σ) would be adequate to perform all of the above mentioned functions. Less stringent requirements are anticipated for midcourse maneuvers, periapsis maintenance, and orbit insertion. Figure 8.5-2 shows that the effects of attitude errors on probe targeting accuracy, orbit parameters, and midcourse requirements are small compared to contributions from other sources.



A. EFFECTS OF POINTING ERRORS OF MIDCOURSE MANEUVERS
EFFECTS OF POINTING ERRORS DURING MIDCOURSE AV MANEUVERS ARE MORE SIGNIFICANT IF A LARGE FIRST MIDCOURSE MANEUVER IS REQUIRED. IN THAT CASE, POINTING AND OTHER EXECUTION ERRORS ADD TO THE TRACKING ERRORS IN DETERMINING THE RESULTANT SECOND MIDCOURSE REQUIREMENTS. AS A FIGURE OF MERIT, SECOND MIDCOURSE AV REQUIREMENTS ARE SHOWN AS A FUNCTION OF POINTING ERROR DURING FIRST MIDCOURSE. THE FIGURE SHOWS THAT SPACECRAFT POINTING ERRORS CONTRIBUTE ONLY SLIGHTLY TO OVERALL MIDCOURSE REQUIREMENTS. THIS PLOT IS FOR THOR DELTA. THE ATLAS CENTAUR IS LESS SENSITIVE.



B. EFFECTS OF POINTING ERRORS ON PROBE TARGETING
PROBE ENTRY ANGLES ARE CLOSELY RELATED TO FACTORS SUCH AS ACCELERATION, HEATING, ANGLE OF ATTACK, WHICH AFFECT PROBE PERFORMANCE AND ARE FUNCTIONS OF PROBE TARGETING. ENTRY ANGLE DISPERSIONS PROVIDE A FIGURE OF MERIT FOR THE DELIVERY SYSTEM. SEPARATION TIME ATTITUDE EFFECTS MUST BE SEPARATELY ASSESSED. AS SHOWN, BUT POINTING ERRORS DURING PROBE RETARGETING AND RELEASE MAKE A SMALL CONTRIBUTION TO OVERALL TARGETING ERRORS, WHICH ARE DOMINATED BY TRACKING UNCERTAINTIES.



C. EFFECTS OF POINTING ERRORS ON ORBIT PARAMETERS
INITIAL ORBIT PERIOD ERRORS ARE AFFECTED BY ARRIVAL VELOCITY, BY ARRIVAL VELOCITY AND POSITION ERRORS, AND BY EXECUTION ERRORS DURING THE ORBIT INSERTION MOTOR FIRING. THE FIGURE SHOWS THAT EXECUTION ERRORS HAVE AN ALMOST NEGLECTIBLE EFFECT COMPARED WITH ARRIVAL ERRORS.

THESE SENSITIVITIES ARE CALCULATED BY A MONTE CARLO TECHNIQUE WHICH INCLUDES ALL ERRORS AS STATISTICAL VARIABLES EXCEPT FOR THE ERROR UNDER CONSIDERATION (ABSCISSA). THIS TECHNIQUE IS NECESSARY BECAUSE SOME OF THE ERRORS ARE CORRELATED.

Figure 8.5-2. Maneuver Sensitivities to Spacecraft Attitude Errors

ALL FANBEAM, FANSCAN ORBITERS

Orbiter antenna-pointing requirements depend on communication distance, which determines the magnitude of the allowable attenuation. Assuming a 123-cm (48-inch) Franklin array (as in the recommended orbiter configurations for the Version III science payload) with a beamwidth of 0.101 radian (5.8 degrees) (between half-power points), the pointing errors corresponding to 0.3 and 1 dB attenuations are 0.016 and 0.030 radians (0.9 and 1.7 degrees), respectively. However, the allowable spin axis pointing errors may be larger (see Figure 8.5-3A) because component rotations about the spacecraft-earth line have no effect on antenna gain.

ALL ORBITERS EXCEPT EARTH-POINTING CONFIGURATIONS

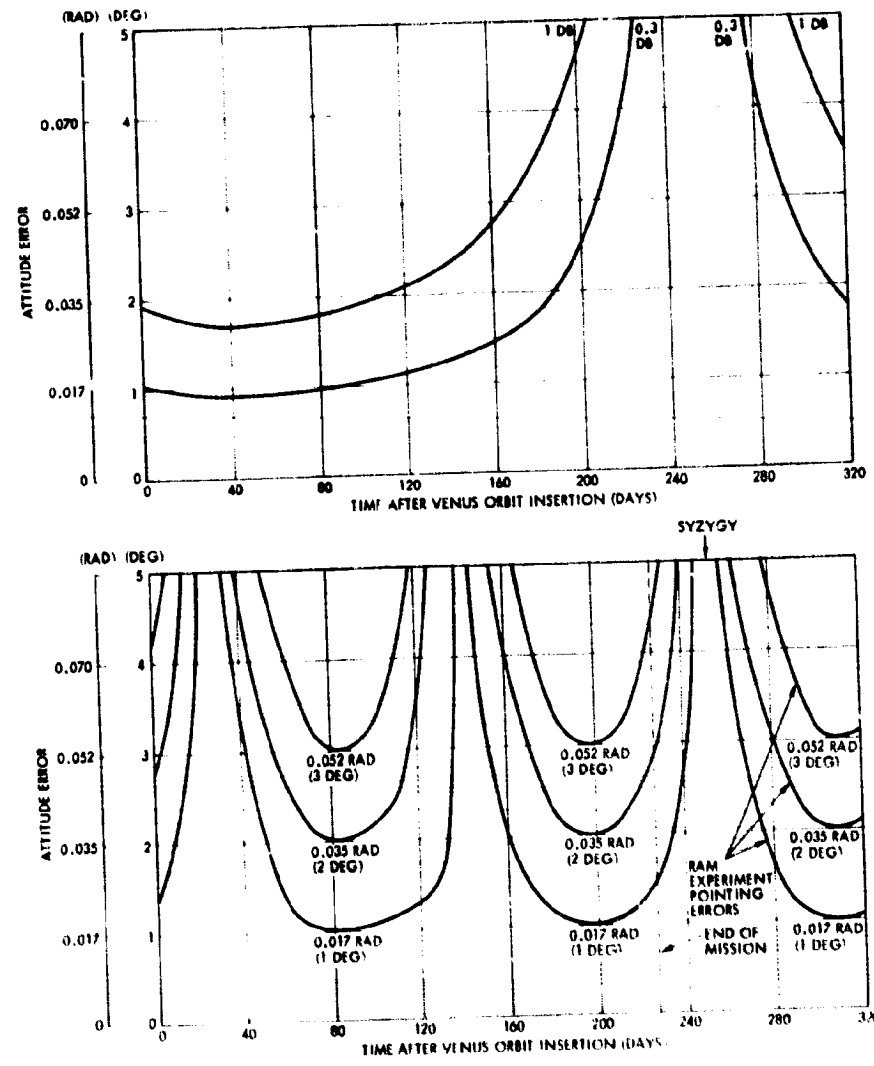


Figure 8.5-3. Maximum Allowable Attitude Errors

ALL ORBITERS EXCEPT
EARTH-POINTING
CONFIGURATIONS

A similar situation occurs with most experiments. As an example, Figure 8.5-3B shows the maximum allowable attitude errors for a given ram experiment pointing error. Here, as well as in Figure 8.5-3A, attitude deviations are assumed about the sun line, which is the direction of rotation typically associated with drifts induced by unbalanced solar pressure.

8.5.3 Functions and Requirements

Since Version IV science payload configurations are based on Atlas/Centaur launch vehicle systems, no initial despinn maneuvers are required. Prior to launch, each Centaur guidance and control system will be programmed to provide the required vehicle attitude and spin rate (after engine cutoff) so that, after separation (and magnetometer deployment, in the orbiter cases), the nominal cruise spin rate is attained.

Table 8.5-2 is an updated version of Table 8.5-1 listing requirements for attitude determination and control for the preferred configurations.

Table 8.5-2. Attitude Determination and Control Requirements

	PROBE BUS		ORBITER	
	ACCURACY (3 σ)	REMARKS	ACCURACY (3 σ)	REMARKS
SPIN SPEED CONTROL	1 PERCENT	0.50 RAD S (4.8 RPM) NOMINAL SPEED	1 PERCENT	0.50 RAD S (4.8 RPM) NOMINAL SPEED
	3 PERCENT	2.09 AND 1.05 RAD S (20 AND 10 RPM) PROBE RELEASES		
	3 PERCENT	6.28 RAD S (60 RPM) PROBE BUS ENTRY	3 PERCENT	6.28 RAD S (60 RPM) ORBIT INSERTION
SPIN AXIS ATTITUDE DETERMINATION	0.026 RAD (1.5 DEG)	CRUISE-MIDCOURSE MANEUVERS	0.026 RAD (1.5 DEG)	CRUISE-MIDCOURSE MANEUVERS
	0.044 RAD (2.5 DEG)	PROBE DEPLOYMENT - RETARGETING	0.044 RAD (2.5 DEG)	ORBIT INSERTION
	0.009 RAD (0.5 DEG)	PROBE BUS ENTRY ATTITUDE	0.017 RAD (1.0 DEG)	IN ORBIT
HIGH-GAIN ANTENNA POINTING	0.262 RAD (15 DEG)	CRUISE	0.070 RAD (4.0 DEG)	CRUISE
	0.009 RAD (0.5 DEG)	PROBE BUS ENTRY	0.017 RAD (1.0 DEG)	IN ORBIT
VELOCITY INCREMENT DISPERSIONS (OVERALL, INCLUDING DYNAMIC EFFECTS)	0.052 RAD (3.0 DEG)	RETARGETING MANEUVERS	0.052 RAD (3.0 DEG)	ONBIT INSERTION
	0.035 RAD (2.0 DEG)	MIDCOURSE MANEUVERS	0.035 RAD (2.0 DEG)	MIDCOURSE-ORBIT TRIMS
EXPERIMENT POINTING	0.052 RAD (3.0 DEG)	CRUISE	0.052 RAD (3.0 DEG)	CRUISE
	0.017 RAD (1.0 DEG)	PROBE BUS ENTRY	0.035 RAD (2.0 DEG)	IN ORBIT
PROBE DEPLOYMENT ATTITUDE	0.044 RAD (2.5 DEG)	SPIN AXIS ORIENTATION	-	-
	0.009 RAD (0.5 DEG)	SPIN ANGLE RELEASE	-	-
DESPUN REFLECTOR POINTING	-	-	+0.013 RAD (+0.75 DEG)	-

The probe bus spin speed has been raised to 2.09 rad/s (20 rpm) for large probe release and 1.05 rad/s (10 rpm) for small probe release to reduce subsequent probe precessions caused by solar light pressure. Entry spin speed is specified at 6.28 rad/s (60 rpm).

In the preferred earth-pointing orbiter configuration, the maximum allowable spin axis pointing errors for meeting communications requirements do not depend on celestial geometry, as in the case with fanbeam antennas.

Attitude error limits established by radially pointing science experiments are functions of earth position and, consequently, of time, as shown in Figure 8.5-4 for the ram experiments.

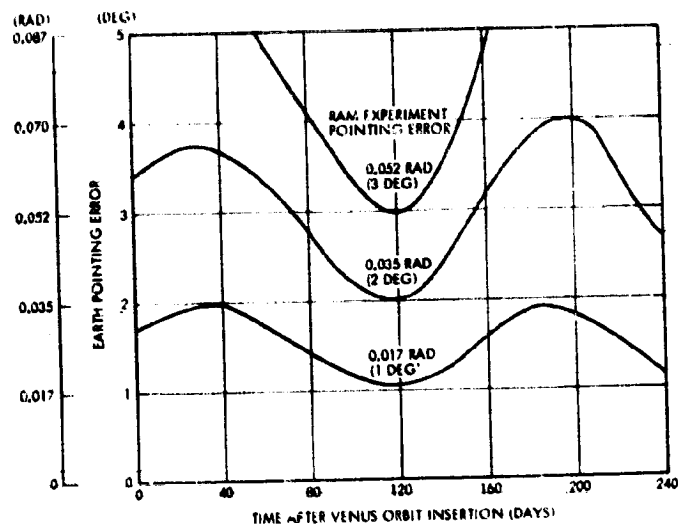


Figure 8.5-4. Maximum Attitude Errors Allowed by Ram Experiments

ALL VERSION IV SCIENCE PAYLOAD

Guiding criteria adopted for the ADCS design selection are to use existing flight-qualified hardware wherever possible and to provide:

- Electrical interface accommodation
- Growth potential
- Commonality of probe bus and orbiter vehicles
- Flight operations flexibility.

Commonality with Pioneers 10 and 11 hardware also implies commonality with Pioneers 10 and 11 software, which is an additional feature providing potential cost savings.

8.5.4 ADCS Concept Selection Tradeoffs ALL CONFIGURATIONS

Tradeoff studies were performed to select optimum attitude determination and control subsystem designs for the recommended and optional

configurations. These studies included:

- Selection of attitude control concept, and thruster control approach and hardware
- Selection of attitude determination approach and equipment
- Selection of antenna despin control concept and hardware
- Definition of maneuvering strategies for probe deployment and retargeting, and periapsis maintenance.

8.5.4.1 Thruster Control Tradeoffs (All Configurations)

The reaction control subsystem (RCS) selected for Pioneer Venus is identical to the Pioneers 10 and 11 RCS except for the following:

- The Pioneers 10 and 11 thrusters will be declustered to avoid plume impingement problems, and radioisotope elements will be replaced by resistive heaters. This change is being made for FLTSATCOM and will be available for Pioneer Venus.
- Two additional thrusters will provide a fully redundant spin/despin capability. Redundancy is also needed because the spin/despin thrusters will control velocity.

Various approaches for providing thruster control were surveyed, including those used in DSCS-II, Intelsat III, Pioneers A through E, and Pioneers 10 and 11. The Pioneers 10 and 11 control electronics assembly (CEA), with minor modifications and additions, was preferred because of:

- Similarity of design requirements
- Better performance and cost effectiveness
- Compatibility with power, data handling, and command and telemetry subsystem
- Minimum design changes.

The CEA is described in detail in Section 8.5.6 and attitude control performance data are given in Section 8.5.8.

8.5.4.2 Attitude Determination Tradeoffs (All Configurations)

At least two celestial references are needed to determine the inertial attitude of a spacecraft. For Pioneer Venus, it is necessary to define the spin axis orientation and to provide a spin angle (or roll) reference. Table 8.5-3 summarizes the reference alternatives.

Table 8.5-3. Attitude Determination References and Sensing Approaches
(The arrows indicate approaches preferred for Pioneer Venus)

REFERENCE	SENSING APPROACH	PROGRAM	PARAMETERS MEASURED/DEFINED	REMARKS
SUN	SUN PIPPER	PIONEERS 10 AND 11	ROLL REFERENCE PLANE	NO ASPECT MEASUREMENT CAPABILITY
	SUN ASPECT SENSOR	INTELSAT III	SUN ASPECT ROLL REFERENCE	
EARTH	RF PATTERN SEARCHING	PIONEERS 6 THROUGH 9	EARTH ASPECT	REQUIRES SPACECRAFT PRESSIONING
	RF POLARIZATION MEASUREMENT		POSITION ABOUT EARTH LINE	REQUIRES CORRECTION FOR FORWARD VELOCITY
	UPLINK CONSCAN FANSCAN	PIONEERS 10 AND 11	EARTH ASPECT AND PHASE	REQUIRES GROUND EQUIPMENT
	DOWNLINK CONSCAN FANSCAN		EARTH ASPECT AND PHASE	REQUIRES GROUND SUPPORT
	DOPPLER MODULATION	PIONEER 10	EARTH ASPECT AND PHASE	REQUIRES ANTENNA OFFSET FROM SPIN AXIS
	DOPPLER SHIFT		EARTH ASPECT	REQUIRES ΔV FIRING
STARS	STAR MAPPER	SAS-A, OSO	STAR AZIMUTH AND ELEVATION	REQUIRES DATA PROCESSING
	STAR TRACKER	MARINER, OAO	STAR GIMBAL ANGLES	REQUIRES ELECTRICAL MECHANICAL GIMBALLING

Sun Sensors

Since sun sensors provide by far the most reliable and inexpensive attitude reference, they have been selected as primary sources of attitude data on all Pioneer Venus configurations. We made a detailed survey of available sun sensors, including more than 12 units, and rejected those with extremely limited fields of view (FOV), or those applicable only to three-axis-stabilized spacecraft. Of the three potential candidates that remained, the DSP sun sensor was eliminated because, due to its small linear aspect range, it could not be adapted to Pioneer Venus without extensive modifications. The Pioneers 10 and 11 sensor was rejected because it has no aspect measurement capability at all. The Intelsat III sensor was preferred because it yields both roll and aspect information over its entire FOV, and adaptation to Pioneer Venus requires only minor changes. By a simple change of slit configuration, the FOV can be easily moved from the 0.45 to 2.70 radians (25 to 155 degrees) to the 0.17 to 1.92 radians (10 to 110 degrees) aspect range required by Pioneer Venus. Although the Intelsat III sensor is nonredundant, two units weigh and cost less than a single sensor from Pioneers 10 and 11. Table 8.5-4 summarizes the salient design characteristics of the candidate sun sensors mentioned above.

Table 8.5-4. Design Characteristics of Sun Sensor Alternatives

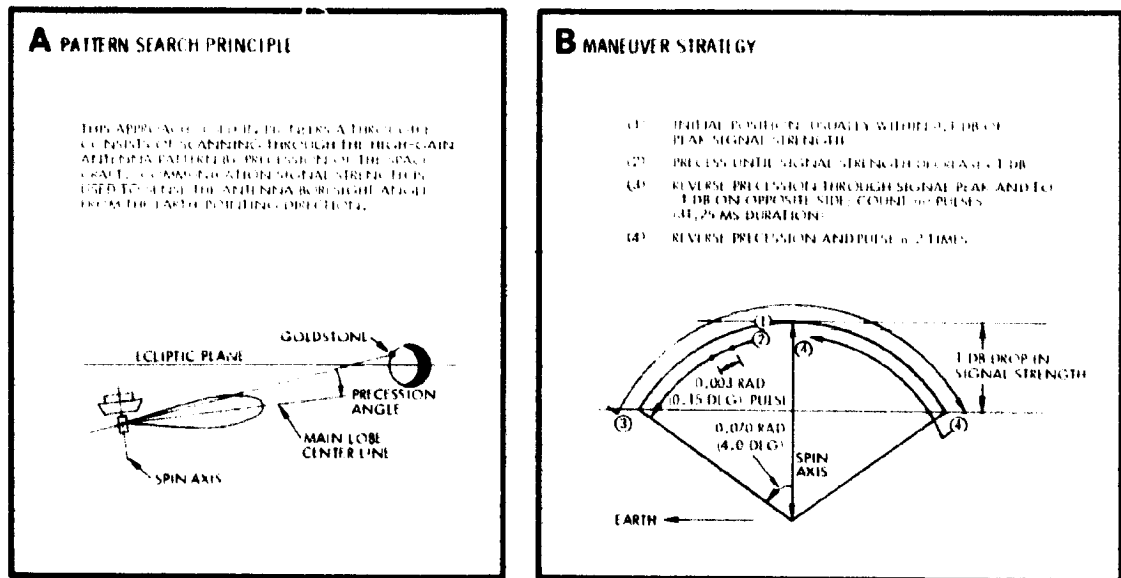
PARAMETER	UNITS	PIONEERS 10 AND 11	DSP	INTELSAT III	MODIFIED INTELSAT III
DEVELOPMENT STATUS	-	FLYING	FLYING	FLYING	MINOR MODIFICATIONS
WEIGHT	GRAMS	453.6	907.2	199.6	199.6
POWER	WATTS	0.3	0	0	0
REDUNDANCY	-	CHANNELS 2 AND 3 ONLY	NO	NO	NO
ROLL REFERENCE FOV	KAD (DEG)	0.017 TO 2.879 (1 TO 165)	0.331 TO 2.809 (19 TO 161)	0.436 TO 2.705 (25 TO 155)	0.175 TO 1.920 (10 TO 110)
ROLL REFERENCE ACCURACY	KAD (DEG)	≤ 0.017 (FOR VIEW ANGLE ≤ 0.034 RAD)	± 0.007 (± 0.4)	± 0.007 (± 0.4)	± 0.003 (± 0.2)
ASPECT FOV	KAD (DEG)	-	1.483 TO 1.658 (85 TO 95)	0.436 TO 2.705 (25 TO 155)	0.175 TO 1.920 (10 TO 110)
ASPECT ACCURACY	KAD (DEG)	-	± 0.012 (± 0.66) (AT NULL)	± 0.004 (± 0.25)	± 0.005 (± 0.3)
REMARKS		NO ASPECT MEASUREMENT CAPABILITY INCLUDES ELECTRONICS	NO ELECTRONICS	NO ELECTRONICS	NO ELECTRONICS V-TYPE SLIT

Earth Aspect Measurement Alternatives

The earth was selected as the second celestial reference. Earth aspect angle measurements, when used in conjunction with data provided by the selected sun sensor, are sufficient to provide complete attitude determination except in those instances where the earth and sun lines are nearly parallel.

Figure 8.5-5 illustrates the principle on which the antenna pattern searching approach is based and shows a typical maneuver sequence for repositioning the spin axis perpendicular to the earth line. This method is applicable to the orbiter configurations flying perpendicular to the Venus orbit plane. Its main advantage is that it does not require any onboard equipment, but it has the disadvantage of requiring a significant amount of ground support, particularly when solar pressure effects require frequent attitude corrections. It is considered a backup to fanscan or conscan techniques.

The orientation of the spacecraft about the earth line can be estimated on the basis of measurements of downlink signal polarization.



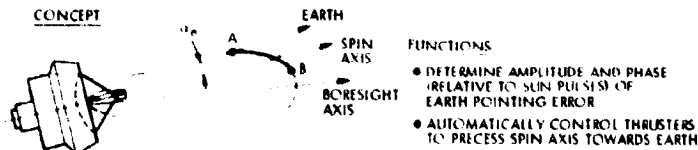
EARTH ASPECT ANGLE CAN TYPICALLY BE DETERMINED FROM THE HIGH-GAIN ANTENNA PATTERN WITHIN ONE-TENTH OF THE HALF-POWER BEAMWIDTH. THE SPIN-AXIS ORIENTATION IS FIRST CORRECTED IN SUN ASPECT TO ATTAIN THE DESIRED ATTITUDE NORMAL TO THE SPACECRAFT-SUN LINE. IN CONFIGURATIONS WITH DESPIN REFLECTOR, THE ROLL-TO-W POINTING IS NEXT CORRECTED TO MAXIMIZE SIGNAL STRENGTH. FINALLY, A SEQUENCE OF PRESSIONS AS IN B ABOVE IS EXECUTED TO ERASE THE SPIN AXIS INCORPORAL TO THE EARTH LINE. THESE PRESSIONS ARE TYPICALLY ABOUT THE SUN LINE, WHICH IS THE DIRECTION OF DRIFT PRODUCED BY UNBALANCED SOLAR PRESSURE TORQUES. OVERCOMPENSATION MAY BE DESIRABLE TO MINIMIZE THE FREQUENCY OF CORRECTIONS REQUIRED BY DRIFT. THE PROPELLANT CONSUMPTION PER MANEUVER SEQUENCE AS IN B IS ON THE ORDER OF 0.01 KG FOR THE THOR DELTA ORBITERS AND 0.04 KG FOR THE ATLAS CENTAUR CONFIGURATIONS. THE TECHNIQUE IS CONSIDERED TO BE A BACKUP TO FANSCAN OR CONSCAN.

Figure 8.5-5. Attitude Determination and Control By Antenna Pattern Searching

Corrections for Faraday rotation are necessary because deviations for S-band signals can be as high as 0.175 radian (10 degrees). These corrections involve measurements of free electron density along the communication path, which are not feasible at all times because calibration sources are not available (i.e., spacecraft with known attitudes at the right locations) or because solar activity is unusual. Under favorable ionospheric conditions, accuracies on the order of 0.017 to 0.026 radians (1 to 1.5 degrees) (3σ) may be attainable with calibration. Because of its disadvantages, it is not considered further.

Uplink conscan (used on Pioneers 10 and 11) is directly applicable to the probe bus spacecraft and the earth-pointing orbiter option. The principle of operation and functions performed by conscan are discussed briefly in Figure 8.5-6A. Uplink conscan requires an offset antenna (implying about 1 dB of signal loss) and signal processing onboard (conscan processors are off-the-shelf items weighing about 0.5 kg and requiring about 1.2 watts). Two advantages are that it 1) requires minimal ground software development and 2) greatly simplifies attitude determination and control operations. Downlink conscan also requires an offset antenna on the spacecraft, but attitude errors are computed on the

A CONSCAN ATTITUDE DETERMINATION AND CONTROL The CONSCAN concept has been successfully used on Pioneer 10 and 11. This approach is based on a pencil beam antenna intentionally offset from the spacecraft spin axis. If the Earth is on the spin axis, then the received signal will have a constant strength. If the Earth is offset from the spin axis, then the spacecraft spin will cause the gains to vary as the antenna pattern rotates about the spin axis. This causes the received signal to be amplitude modulated at the spin frequency. The amplitude of this modulation is a function of the angular distance of the Earth from the spin axis. The positive zero crossings of the modulation is detected and located relative to local reference, such as the sun reference. This defines the phase of spin angle relative to Earth and the angle is derived. The spacecraft can then be precessed by the spin axis control system to align the antenna with the spin axis. An amount of amplitude and phase will be derived for attitude determination on the ground. This technique is considered prime for the Atlas Centaur, Mars and Venus payload vehicles and for the high gain antenna.



B FANSCAN ATTITUDE DETERMINATION AND CONTROL FANSCAN is based on uplink reception with a fanbeam antenna offset in angle from the spin axis. This offset produces a signal loss of about 1 dB (typically). The figure shows a typical orbiter configuration including two antennas, an on-axis fanbeam for downlink communications, and an offset fanbeam for uplink communications and FANSCAN. If the spin axis is perpendicular to the Earth line, the received signal will exhibit an amplitude modulation, at twice the spin frequency, whose index is proportional to the offset angle. The CONSCAN processor design can be used for FANSCAN because it rejects even harmonics of the spin frequency. If the spin axis is offset from the plane normal to the Earth line, the AGC signal from the receiver will contain a component at the spin frequency whose amplitude will be a function of the pointing error. The technique has been considered prime for all configurations flying perpendicular to Earth and Sun lines.

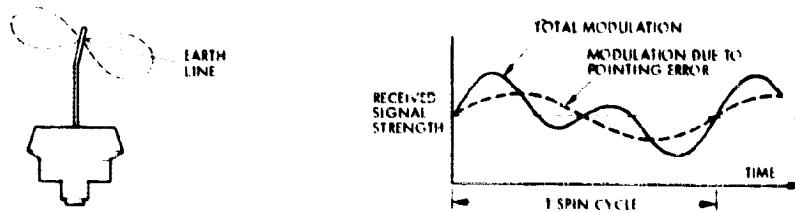
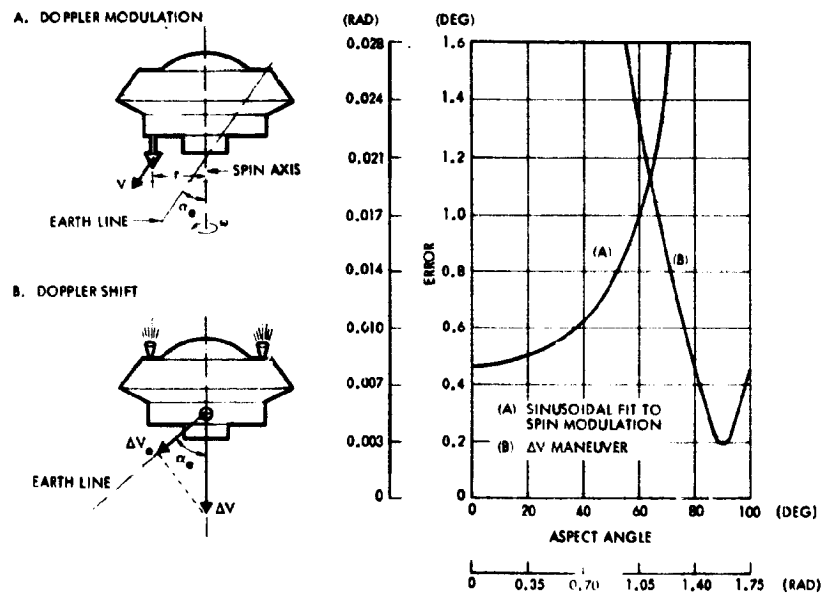


Figure 8.5-6. Conscan/Fanscan Attitude Determination and Control

ground. This method has not been used previously and requires new ground equipment or more ground software, but may be attractive as a potential backup to uplink conscan.

Uplink fanscan is identical in principle to conscan, except that it is implemented with an offset fanbeam antenna. This approach is applicable to the orbiter configurations with the spin axis perpendicular to the earth line. A brief description of the principle is given in Figure 8.5-6B and more details on design characteristics and performance can be found in Section 8.5.8 and in Appendix 8.5A. Downlink fanscan is also a viable alternative that may be attractive for backup purposes.

The first use of doppler effects for attitude determination is believed to be on Pioneers 10 and 11. Figure 8.5-7 discusses principles of operation and shows ranges of accuracy attainable with each approach. More



THE EARTH ASPECT ANGLE CAN BE DETERMINED FROM CHANGES PRODUCED BY THE SPIN ON THE FREQUENCY OF RF SIGNALS FROM AN OFFSET ANTENNA. IF THE SPIN AXIS IS MISALIGNED FROM THE EARTH LINE (BY ANGLE α_s), THE DOWNLINK SIGNAL IS FREQUENCY-MODULATED AT THE SPIN FREQUENCY, WITH THE MODULATION AMPLITUDE A FUNCTION OF α_s . WITH THE SPIN AXIS NEAR THE EARTHLINE, DOPPLER MODULATION CAN PROVIDE ATTITUDE INFORMATION WITHIN 0.009 RAD (0.5 DEG), BUT ACCURACY DEGRADES RAPIDLY FOR ANGLES GREATER THAN 1.05 RAD (60 DEG) AS SHOWN.

DOPPLER SHIFTS CAN ALSO BE USED FOR ATTITUDE DETERMINATION WITH ANGLES NEAR 1.57 RAD (90 DEG), BUT A Δv MANEUVER IS REQUIRED. THE COMPONENT OF VELOCITY CHANGE ALONG THE EARTHLINE IS OBTAINED BY DOPPLER MEASUREMENT, AND THE RATIO OF THIS COMPONENT TO THE PREDICTED VALUE OF THE MANEUVER EXECUTED GIVES THE COSINE OF THE ANGLE BETWEEN THE SPIN AXIS AND THE SPACECRAFT-EARTH LINE. THIS ATTITUDE DETERMINATION TECHNIQUE IS MOST SENSITIVE AT SPIN ANGLES NORMAL TO THE EARTHLINE, AS SHOWN. IT IS PREFERABLE TO USE DOPPLER SHIFT ONLY IN THOSE INSTANCES WHERE A Δv IS TO BE EXECUTED (MIDCOURSE, PERIAPSE MAINTENANCE, OR PROBE RETARGET MANEUVERS) TO MINIMIZE OPERATIONAL COMPLEXITY.

Figure 8.5-7. Doppler Measurement of Earth Aspect Angle

ALL CONFIGURATIONS detailed error analyses are presented in Appendix 8.5B. One of the main advantages of attitude determination by doppler measurements is that no onboard equipment is required. The DSN ground stations are needed for doppler signal analysis, but results are quickly obtainable with only simple processing of data. Doppler techniques are applicable to all Pioneer Venus configurations, particularly during probe deployment and velocity correction maneuvers, where omni antennas are used.

Star Mappers

ALL ORBITERS PERPENDICULAR TO THE EARTH LINE

Star mappers were considered for obtaining higher attitude determination accuracies if needed because of new requirements or changes in design ground rules. Star mapper operation is based on star aspect determinations by measurements of the transit times of stars across two slits. Some of the key factors considered in their design are star availability, spin rate range, sun/planet interference, and shade size and weight constraints.

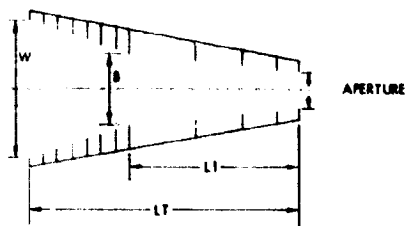
A survey of existing and proposed designs revealed no instrument directly applicable to the Pioneer Venus missions. On the assumption that developing a light, simple new design might be more cost effective than modifying an existing one, various configurations were examined to assess the impact of FOV and detector changes on shade size and weight, star availability, and sensor performance. The following preliminary requirements were established:

- Accuracy in the 0.009 to 0.017 radian (0.5 to 1.0 degree) range (without processing). Reducing accuracy requirements to this range minimizes aperture, shade size, and star availability, and software requirements.
- Use of sun aspect data for attitude determination. Only one star is required in FOV
- Northern hemisphere view in Venus orbit. This view minimizes planet interference and shade requirements.
- Nominal mapper operation restricted to orbit phase. This restriction simplifies the star availability problem and allows operation with at least one star of visual magnitude better than +1.0 at all times. Some degradation of performance in other orientations is assumed acceptable.

Figure 8.5-8 shows design data corresponding to four design examples based on the assumptions listed above. Inspection of the data

ALL ORBITERS PERPENDICULAR TO THE EARTH LINE

A SUN SHADE CONFIGURATION



B SUN SHADE DATA

DETECTOR	FIELD OF VIEW (RAD/DEG)	DIMMEST STAR (VISUAL MAGNITUDE)	APERTURE DIAMETER (CM)	W (CM)	LT (CM)	L1 (CM)	B (CM)	SUN ANGLE (RAD/DEG)	WEIGHT (G)
SILICON	0.33 (18)	ALTAIR +.77	4.26	22.96	21.56	17.89	9.93	0.79 (45)	830
	0.20 (11.3)	DUBHE +1.79	5.99	22.17	45.11	28.15	11.56	0.79 (45)	1630
S-20	0.33 (18)	ALTAIR +.77	1.86	10.01	14.97	7.80	4.33	0.79 (45)	160
	0.20 (11.3)	ALCAID +1.96	2.40	8.88	18.07	11.28	4.63	0.79 (45)	265

C SUMMARY OF DESIGN CHARACTERISTICS

	SILICON		S-20 (PMT)	
	0.33 (18)	0.20 (11.3)	0.33 (18)	0.20 (11.3)
FIELD OF VIEW (RAD (DEG))	0.33 (18)	0.20 (11.3)	0.33 (18)	0.20 (11.3)
SENSITIVITY	+0.77	+1.79	+0.77	+1.96
APERTURE (CM)	4.26	7.98	1.86	3.98
SPIN RATE (RAD/S (RPM))	0.50 (4.8)	0.50 (4.8)	0.50 (4.8)	0.50 (4.8)
BANDWIDTH (HZ)	30	30	30	30
ASPECT ANGLE (RAD (DEG))	0.60 (34.3)	0.66 (37.65)	0.60 (34.3)	0.66 (37.65)
MINIMUM SUN ANGLE (RAD (DEG))	0.79 (45.0)	0.79 (45.0)	0.79 (45.0)	0.79 (45.0)
SIZE * (CM)	8 x 8 x 16	10 x 10 x 20	6 x 6 x 16	8 x 8 x 20
WEIGHT (GRAMS) (SHADE INCLUDED)	2430	4030	1360	2265
POWER (WATTS)	0.9	0.9	1.5	1.5
ACCURACY (RAD (DEG))	0.01 TO 0.02	0.01 TO 0.02	0.01 TO 0.02	0.01 TO 0.02
(NO PROCESSING ASSUMED)	(0.6 TO 1) (30)	(0.6 TO 1) (30)	(0.6 TO 1) (30)	(0.6 TO 1) (30)

* DOES NOT INCLUDE SUN SHADE (SEE B)

FOUR PRELIMINARY STAR MAPPER DESIGNS HAVE BEEN PREPARED ON THE BASIS OF A MINIMUM SET OF REQUIREMENTS. TWO SENSOR CONFIGURATIONS USE SILICON DETECTORS AND THE OTHER TWO ARE BASED ON S-20 PHOTOMULTIPLIER TUBES. THE TABLES SHOW SHADE SIZES AND PRELIMINARY DESIGN CHARACTERISTICS AS FUNCTIONS OF DETECTOR TYPE AND FIELD-OF-VIEW WIDTH.

Figure 8.5-8. Star Mapper Design Requirements

in the tables shows aperture/shade size requirements can be significantly reduced by using photomultiplier tubes (PMT's). Silicon detectors are attractive because of their higher reliability, but there is not as much flight experience as with PMT's.

In general, star mappers are expensive (i.e., a star mapper development program for Pioneer Venus would cost at least \$350,000) and, in addition, they require elaborate (and costly) ground software.

More details on star mapper tradeoffs, surveys, and performance characteristics are given in Appendix 8.5C.

Selected Attitude Determination Approach ALL CONFIGURATIONS

The attitude determination approach selected for all Pioneer Venus configurations is based on sun and earth aspect measurements. The sun sensor selected for all configurations is the Intelsat III unit with a different slit configuration. This sensor provides both roll reference and aspect angle measurements. The selected earth aspect measurement approaches are:

- Doppler modulation and shift. These techniques will be used in all phases of the probe missions and during all phases of the orbiter mission except when using fanscan or conscan.
- Uplink fanscan. Fanscan will be used in all orbiter configurations flying perpendicular to the earth line during the cruise and orbit phases.
- Uplink conscan. This method will be used in the earth-pointing orbiter configuration when on the high-gain antenna.

Reasons for discarding star mappers and selecting these approaches are:

- Pioneer Venus attitude determination requirements [in 0.017 to 0.020 radian (1 to 1.5 degrees) range] can be met with simple, inexpensive, proven techniques based on sun and earth references.
- Star mapper hardware and software would require development costs. No existing, qualified, sensors are directly applicable.
- No onboard equipment is needed for using doppler methods. Simple, "eyeball"-type data processing can be used on the ground for quick action.
- Either fanscan or conscan can be implemented with the same processor, which is a flight-qualified off-the-shelf unit.

Performance data corresponding to all orientations for cruise, ΔV maneuvers, probe deployment, and orbital operations are given in Section 8.5.8.

Effect of Sun-Spacecraft-Earth Geometry on Attitude Determination Accuracy

One of the problems associated with sun and earth references for attitude determination is the degradation of accuracy occurring at times of syzygy or when the spin axis is near the plane determined by the sun, the earth, and the spacecraft. Figure 8.5-9A shows regions of attitude uncertainty (in stereographic projection) for the most favorable case [1.57 radian (90-degree) sun-spacecraft-earth angle] and for two conditions where losses of accuracy are caused by unfavorable geometry. Figure 8.5-9B relates attitude determination uncertainties to measurement errors, and Figure 8.5-9C is a typical time history of attitude determination accuracy for the orbiters, showing the improvements attainable during syzygy conditions by estimation of the drift rates produced by solar pressure. Even without corrections for drift, the accuracies attainable near the end of the mission meet the requirements of Section 8.5.2. In addition, all critical functions can be performed at times when attitude information quality is such that no degradation of mission objectives will occur. A star mapper is a viable alternative for providing additional attitude references during syzygy conditions, but it has not been included in the recommended baseline designs because of its relatively high cost and weight penalties compared to the mission benefits accrued on the basis of the science pointing requirements.

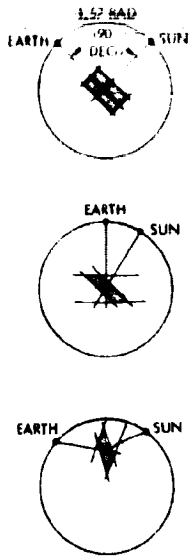
8.5.4.3 Antenna Despin Control Tradeoffs A/C III A/C IV T/D III

In the orbiter options with despun reflector antennas, a parabolic cylinder reflector is pointed at the earth by a closed-loop servo system operating with a sampled roll reference provided by the sun sensor.

The rotary interface between spacecraft and reflector is provided by a despin drive assembly including a brushless DC motor (with resolver commutation) and position and rate pickoffs. Four drive mechanizations were considered and the Helios assembly was selected because it meets requirements with minimum cost and weight. The selected drive is a

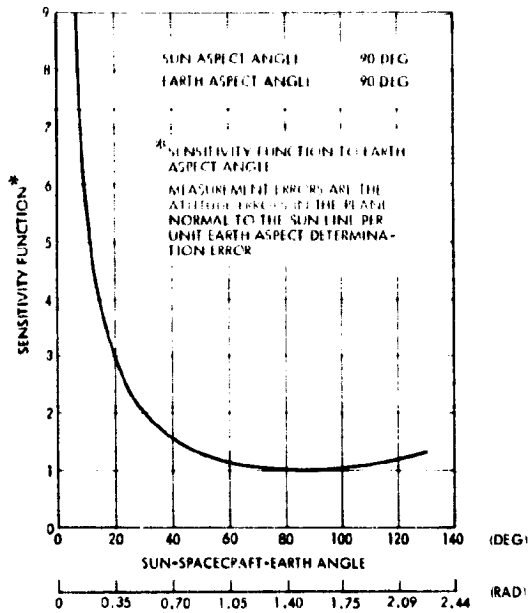
A ATTITUDE UNCERTAINTY REGIONS

MAXIMUM ACCURACY IS OBTAINED WITH 1.57 RAD (90 DEG) ANGLE BETWEEN SUN AND EARTH. DEGRADATION OCCURS WHEN THIS ANGLE APPROACHES 0 OR 1.74 RAD (0 OR 180 DEG) AND WHEN THE SPIN AXIS IS NEAR THE SUN-SPACECRAFT-EARTH PLANE.



B EFFECT OF SUN SPACECRAFT EARTH ANGLE ON ATTITUDE DETERMINATION ACCURACY

THE CURVE SHOWS THE EFFECT OF EARTH ASPECT ANGLE ON THE SENSITIVITY FUNCTION TO EARTH ASPECT MEASUREMENT ERROR AS A FUNCTION OF SUN-SPACECRAFT-EARTH ANGLE.



C TYPICAL TIME HISTORY OF ATTITUDE DETERMINATION ACCURACIES FOR ORBITERS

THE CURVE SHOWS ORBITER ATTITUDE DETERMINATION ACCURACY AS A FUNCTION OF TIME ON THE ASSUMPTION OF SUN ASPECT AND FANSCAN MEASUREMENTS. SOME DEGRADATION OCCURS NEAR SYZYG Y TIMES, BUT THERE ARE INSTANCES IN WHICH LARGER ATTITUDE ERRORS MAY BE TOLERABLE AS SHOWN IN SECTION 8.52. IMPROVEMENTS CAN BE OBTAINED BY ESTIMATION OF THE DRIFT RATES PRODUCED BY SOLAR PRESSURE.

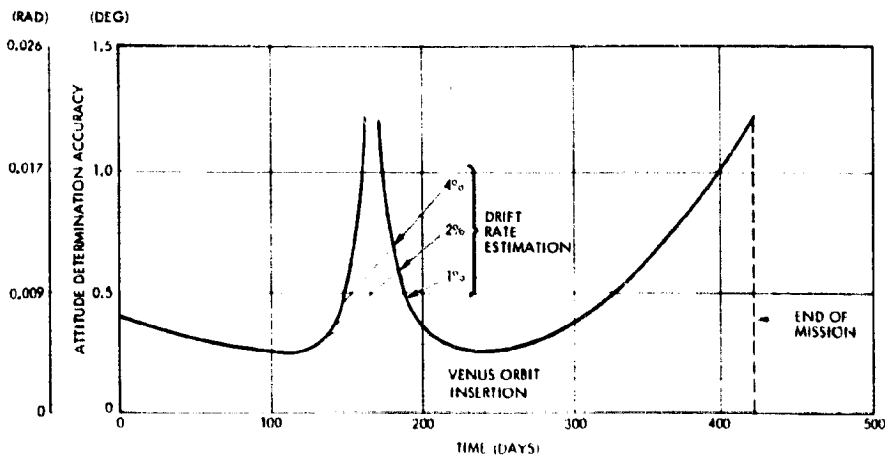


Figure 8.5-9. Effect of Sun-Spacecraft-Earth Geometry on Attitude Determination Accuracy

fully space-qualified unit that also includes the electronics for driving the motor and shaping the position reference and rate pulses. The only modification required for adapting this unit to the Pioneer Venus requirements (0.52 rad/s (5 rpm) instead of 6.28 rad/s (60 rpm)) is to increase the number of rate pulses from 5.09 to 81.5 per radian (32 to 512 per revolution). This modification will necessitate a change from the magnetic pickup now employed to a system consisting of light-emitting diodes, a mask, and detectors.

Despin electronics implementations for the Pioneer Venus antenna despin control system could be made with equipment developed for the Helios or the DSCS-II programs, or a combination of both.

The Helios system consists of two main assemblies:

- The despin drive assembly (DDA) includes electromechanical components and a nonredundant electronics package, the despin drive electronics (DDE). The DDE consists of motor power control amplifiers, resolver excitation and signal demodulation circuits, pulsewidth modulators for motor signal control, rate and pulse conditioning logic, and motor current telemetry interface circuit.
- The despin control electronics (DCE) is a nonredundant unit including digital position and rate error detectors, error signal holding registers, D/A converters, a proportional-plus-integral compensation amplifier, and a position reference function generator providing commandable piece-wise-linear approximations to the required offsets from the sun reference.

The DSCS-II despin electronics assembly is a nonredundant unit performing functions equivalent to the Helios DDE and DCE except that it has neither a rate loop nor a position reference function generator.

The despin electronics approach selected for Pioneer Venus consists of two Helios DCE assemblies (standby redundant) operating with the non-redundant DDE included in the despin drive assembly. This partially redundant scheme is preferred because:

- Total despin system reliability is increased from 0.928 (for a nonredundant system) to 0.981 at a cost of only \$50 000 and 1.8 kg.
- Going to fully redundant electronics would increase reliability by only 1 percent (relative to the selected approach) with a cost penalty greater than \$300 000.

A/C III
A/C IV
T/D III

The only internal modifications required to adapt the Helios DCE to the Pioneer Venus requirements are minor changes in loop gains and time constants. Clock frequencies, externally supplied to the DCE, will have to be changed for compatibility with the lower spin rate.

8.5.4.4 Probe Deployment and Retargeting Maneuver Tradeoffs (1977 Probe Missions, Atlas/Centaur and Thor/Delta)

As shown in Figure 8.5-10, the probe deployment sequence begins 25 days before encounter with the release of the large probe. The figure shows probe bus maneuvering requirements, alternatives for performing retargeting maneuvers, and the selected operations approach. The first retargeting is done by transverse thrusting because of propellant consumption considerations. If axial thrusting were used, the third retargeting orientation would be unfavorable for attitude determination purposes.

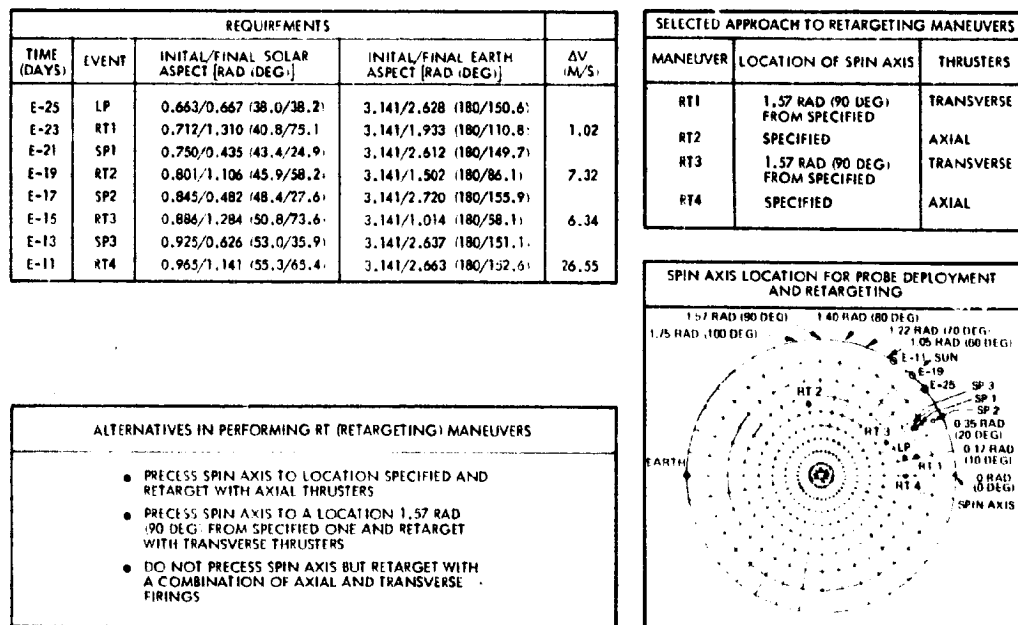


Figure 8.5-10. Probe Deployment and Retargeting Maneuver Tradeoffs

Spin axis orientations for the selected maneuvering approach are shown in the stereographic map on the lower right-hand side.

In addition to these alternatives, two choices of normal cruise orientations are:

- Earth pointing (tail of spacecraft pointed at earth)
- Perpendicular to the earth line and at maximum inclination relative to the Venus orbit plane.

A/C III The entire deployment sequence can be executed in any one of the following ways:
T/D III

- Return to cruise orientation after each maneuver
- Go from one required orientation to the next without returning to cruise attitude.

The preferred approach is to return to the cruise orientation after each maneuver for optimizing communications and improving initial attitude determination accuracy prior to each open-loop maneuver. The cruise orientation preferred is earth pointing because of the following reasons:

- Large probe thermal control during the first part of the cruise phase is facilitated.
- Attitude determination is considerably simplified. Doppler modulation provides sufficient accuracy and no additional onboard equipment is required.
- The total amount of precession required for probe deployment and retargeting is minimized.
- An additional fanbeam antenna is avoided since the medium-gain aft-looking antenna needed for probe bus entry can also serve for cruise communications.

Retargeting maneuvers will be performed as shown in the summary table included in Figure 8.5-10. The first retargeting is by transverse thrusting because it requires less propellant than an axial maneuver (I_{sp} loss is less than the impulse required for additional precession). Transverse thrusting is used for the third retargeting maneuver because the orientation required is more favorable for attitude determination by doppler modulation.

The stereographic map in Figure 8.5-10 shows spin axis locations for probe deployment and retargeting maneuvers relative to a coordinate system (centered on the spacecraft) where one axis points at the earth; the second axis is normal to the plane determined by the earth, the spacecraft, and the sun; and the third axis completes a right-handed set.

8.5.4.5 Orbiter Maneuver Tradeoffs (All Configurations, Version III Science Payload)

Velocity control maneuvers are required in orbit to maintain the altitude of periapsis within the 200 to 400 km range. These maneuvers

ALL VERSION III
ORBITERS

are most efficient when performed at apoapsis in a direction opposite to the velocity vector. Several ways of performing the maneuvers are:

- a) Precess the spacecraft to the desired orientation and fire the axial thrusters. The main disadvantage of this approach is due to the precession angles required [about 1.05 radians (60 degrees) from normal attitude], which cause loss of communications when the distance to earth exceeds the maximum range of the omni antenna.
- b) Precess the spacecraft to an orientation normal to the velocity direction at apoapsis and fire the transverse thrusters. This approach has the advantage that the precession can be made around the earth line, thus maintaining communications during the maneuver. One disadvantage is the large precession angles required [greater than 1.57 radians (90 degrees)] to avoid operation with sun aspect angles greater than 1.57 radians (90 degrees) during the first part of the orbit phase. This option is not available to earth-pointing spacecraft.
- c) Use a combination of axial and transverse thruster firing without precessing the spacecraft. The velocity change requirements increase by about 40 percent when this approach is followed.
- d) Fire axial thrusters only, with spacecraft in cruise attitude. Firings should be made at true anomalies of about 3.32 radians (190 degrees). Disadvantages of this method are the increased propellant requirements and the resulting changes in orbit parameters.

A comparison of the last three alternatives (acceptable from the communications standpoint) is made in Figure 8.5-11 in terms of propellant requirements. Alternative b) has been selected because of its lower propellant requirements.

8.5.5 ADCS Concept Selection Tradeoffs A/C IV A/C IV

Additional tradeoffs for selecting preferred attitude determination and control designs for the Atlas/Centaur, 1978 probe bus and orbiter, Version IV science payload configurations were performed in the following areas:

- Probe deployment and retargeting maneuver strategy
- Periapsis maintenance maneuver strategy
- Ram experiment platform drive
- Occultation experiment strategy.

ALL ORBITERS PERPENDICULAR TO THE EARTH LINE

DAYS FROM VOI	SELECTED APPROACH				ALTERNATE APPROACH			
	PRECSSION ± TO ⊙ TRANSVERSE FIRINGS				AXIAL + TRANSVERSE FIRINGS CRUISE ATTITUDE		AXIAL FIRING CRUISE ATTITUDE	
	ONE-WAY PRECSSION [RAD (DEG)]	ΔV [M/S]	SUN ASPECT [RAD (DEG)]	EARTH ASPECT [RAD (DEG)]	AXIAL ΔV [M/S]	TRANS- VERSE ΔV [M/S]	TRUE ANOMALY	ΔV [M/S]
30	2.60 (149)	12.3	1.01 (58)	1.57 (90)	6.31	10.6	190	20.0
60	2.57 (147)	10.2	1.01 (58)	1.57 (90)	5.25	8.8	190	16.6
150	0.77 (44)	12.3	1.10 (63)	1.57 (90)	6.31	10.6	190	20.0
180	0.56 (32)	8.7	1.31 (75)	1.57 (90)	4.47	7.5	190	14.1
TOTALS	12.78 (744)	43.5			22.34	37.5		70.7
N ₂ H ₄ MASS (KG)	0.45	1.30			2.03	3.71		7.00
TOTAL MASS (KG)		4.75				5.74		7.00

VENUS ORBIT INSERTION MANEUVER		
ΔV [M/S]	SUN ASPECT [RAD (DEG)]	EARTH ASPECT [RAD (DEG)]
954	1.17 (67)	1.06 (61)

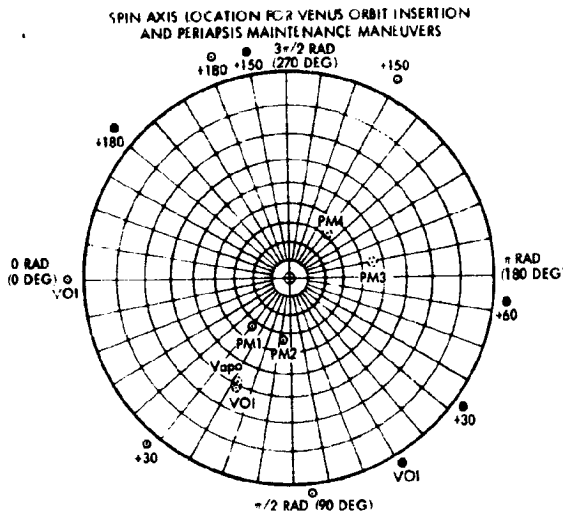


Figure 8.5-11. Probe Deployment and Retargeting Maneuver Tradeoffs



The attitude control requirements of these configurations are similar to those of the earlier spacecraft and, therefore, the same approach has been selected.

Attitude determination requirements are also similar, except for the sun sensor FOV. The first small probe release has to be made in an orientation where the sun aspect angle will be 1.90 radians (10.9 degrees). Therefore, to provide some margin during the precession maneuver to reach this attitude, the roll indexing FOV will be extended at least 0.03 radian (2 degrees) (on each side) beyond the 0.17 to 1.92 radian (10 to 110 degree) solar aspect measurement range previously selected. The advantage of operation with two different ranges for aspect measurement and roll indexing is that the logic for precession control can be designed for automatically stopping maneuvers when either of the ends of the sun aspect measurement range is reached.

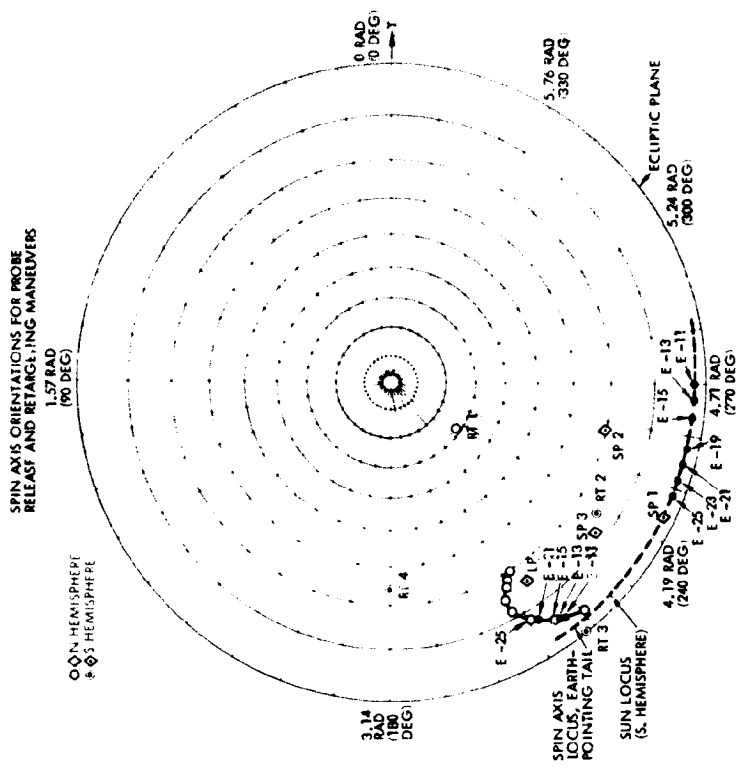
Probe deployment and retargeting maneuvers will be made with the earth in the rear hemisphere starting from, and returning to, the earth-pointing orientation for optimum communications. Doppler and sun aspect measurements will provide attitude information after each precession maneuver.

To reduce probe precession due to solar pressure after release to acceptable limits, it has been calculated that 2.09 and 1.045 rad/s (20 and 10 rpm) are appropriate for large and small probe release, respectively.

Requirements and details about the probe deployment and bus targeting sequence are given in Figure 8.5-12.

Earth-pointing configurations utilizing conscan for attitude determination provide consistently good spin axis attitude determination accuracies even at syzygy times. This is not the case with fanscan because this approach does not provide information for rotations about the earth line. The only problem with conscan is the angle limitation due to antenna gain and beamwidth constraints. As shown in Figure 8.5-13, periapsis maintenance maneuvers can be executed by precessing the spacecraft to orientations where transverse thruster firings can provide the required increments along the velocity vector direction at periapsis. The preferred approach, eliminating the need for spacecraft precessions, consists in firing axial and transverse components while in the earth-pointing attitude. The main advantage of this approach is that communications are not interrupted at any time during the orbit phase of the mission.

Existing gimbal actuators were surveyed to select a unit to drive the platform for the ram-looking experiments. Among the units considered, the most attractive candidates were the DSCS-II antenna drive assembly (a single axis module only), the OGO solar array drive, and the solar array drive being developed for FLTSATCOM (a single, nonredundant version only). The FLTSATCOM solar array drive was selected because it is less complex and its lower cost and weight. The DSCS-II drive is over-designed for this application, and its resolver position indicator requires complex electronics (the accuracy provided by this resolver is not needed). The OGO solar array drive is expensive, requires complex electronics (because a closed servo loop is required to control it), and operates continuously to hold the desired orientation.



TIME DAYS	EVENT	REQUIREMENTS			SPIN SPEED (RAD S)
		INITIAL SCALAR ASPECT	FINAL EARTH ASPECT	ΔV (M S)	
E-25	LP	0.644/0.635 37.0/36.4	3.14/2.706 180.0/155.1	-	2.1
E-23	RT 1	0.75/1.13 40.0/65.0	3.14/2.16 180.0/140.0	1.21	1.05
E-21	SP 1	0.733/0.016 42.0/10.9	3.14/2.534 180.0/143.5	-	1.05
E-19	RT 2	0.73/0.40 43.0/23.3	3.14/2.56 180.0/148.0	16.07	1.05
E-17	SP 2	0.930/0.000 47.0/22.9	3.14/1.382 180.0/136.5	-	1.05
E-15	RT 3	0.892/0.802 45.0/46.1	3.14/1.110 180.0/116.0	6.12	1.05
E-13	SP 3	0.907/0.080 52.0/34.6	3.14/2.678 180.0/154.0	-	1.05
E-11	RT 4	0.94/1.22 54.0/37.0	3.14/2.34 180.0/134.0	25.72	1.05

SELECTED APPROACH TO RETARGETING MANEUVERS	
MANEUVER	THRUSTERS
RT 1	AXIAL
RT 2	AXIAL
RT 3	TRANSVERSE
RT 4	AXIAL

Figure 8.5-12. Probe Deployment and Retargeting Maneuver Tracks

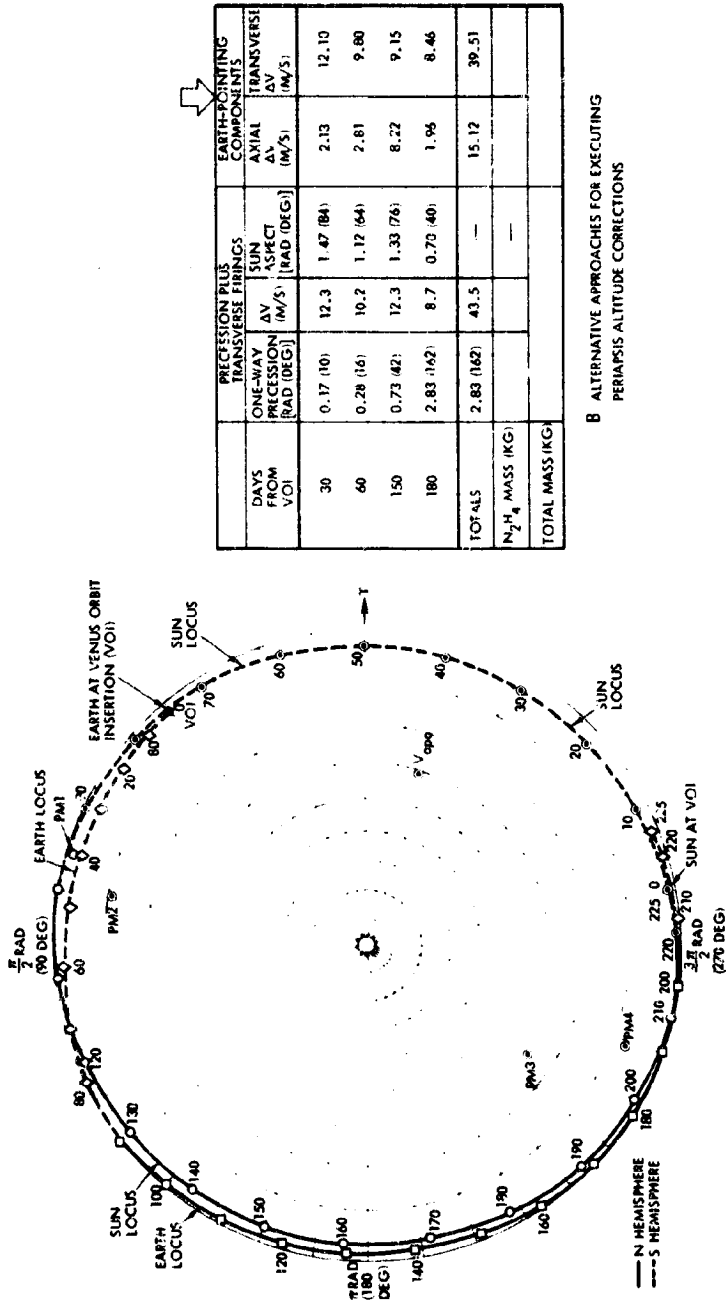


Figure 8.5-13. Periapsis Maintenance Maneuver Tradeoffs

Figure 8.5-14 shows the selected platform drive assembly, which includes a stepper motor, a harmonic-drive gear reduction, single and duplex-pair bearings, and an unlimited rotation film potentiometer for shaft position indication. The curve included in the figure shows the ideal drive offset angles (from the forward spin axis direction) required to point the platform-mounted experiments in the ram direction at periapsis (once per revolution). The actual gimballed angle function will not be continuous because adjustments will be made only about once per week. The maximum rate of gimballed angle change will be about 0.03 radian (1.75 degrees)/day during the first 10 days in orbit. Afterwards, it will not exceed 0.017 radian (1 degree)/day.

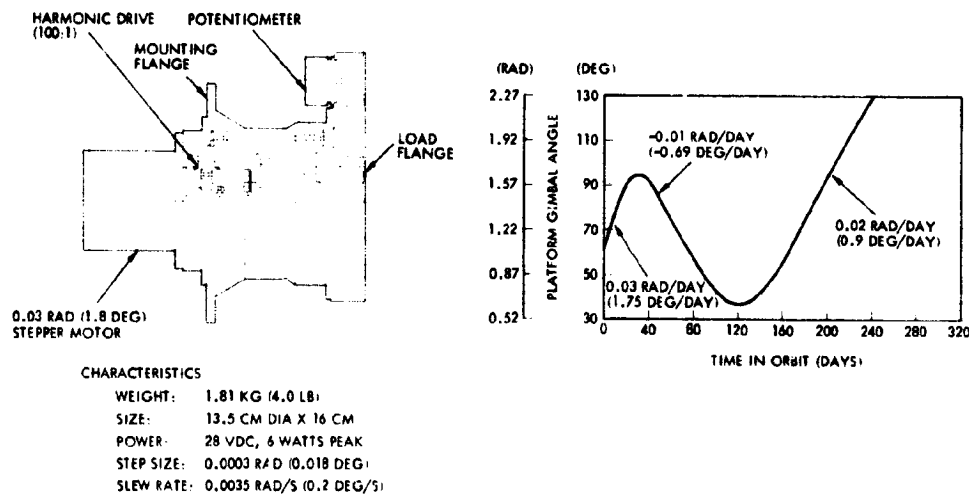


Figure 8.5-14. Selected Platform Drive Assembly Design

Various strategies will perform earth occultation experiments. The simplest one consists in offsetting the spacecraft in advance so that, near the end of the occultation, the antennas are pointing in the direction of the refracted rays. The most complex approach consists of programming the precessions of the spacecraft for continuously tracking the refracted rays during both entry to and exit from occultation.

The selected approach is based on a fixed offset of about 0.21 radian (12 degrees), which is a compromise between the capabilities of the X- and S-band antennas. This method was preferred because it meets occultation experiment requirements with minimum cost and complexity, while still providing good performance (out to 0.31 radian (18 degrees) refraction

ACIV angle for S-band and 0.26 radian (15 degrees) for X-band). Section 8.5.10.3 discusses requirements and design implications of tracking the refracted rays which could provide somewhat better performance if high-gain antennas are used.

Limitation of X-band occultation experiments to the first 37 days in orbit has the advantage of requiring only one additional (X-band) antenna (on the aft end of the spacecraft). Attitude determination in the offset pointing orientation can be made on the basis of sun sensor and doppler modulation data.

Occultation experiments performed after 37 days, the time at which the spacecrafts flips to present its high-gain antenna to earth, are more difficult because of the increasing range and because of the narrowness of the high-gain antenna pattern. A further high-gain X-band antenna and programmed ray tracking would be appropriate.

8.5.6 Preferred ADCS Design Description ALL VERSION III SCIENCE PAYLOAD

The ADCS designs selected for the preferred and optional Pioneer Venus spacecraft configurations are based on equipment developed for the Pioneers 10 and 11, Intelsat III, and Helios programs, with minor modifications.

Table 8.5-5 summarizes the attitude determination approaches selected for each spacecraft configuration and the component assemblies used in each ADCS design. Also, the table shows which equipment from other subsystems is used for attitude determination and control functions in each case.

Conceptually, there is no difference between designs for Atlas/Centaur and Thor/Delta configurations of the same type. The only difference would be in the CEA's because the Thor/Delta version would be repackaged to save weight.

The earth-pointing orbiter configurations have a single-axis gimbaled platform where ram-viewing experiments will be located. Actuation power and shaft position indication are provided by a platform drive assembly (PDA). Power control and signal processing for the PDA will be made by additional circuits in the CEA.

Table 8.5-5. ACDS Equipment and Approaches for Pioneer Venus

ALL VERSION III SCIENCE PAYLOAD

	ATLAS/CENTAUR AND THOR/DELTA PROBE BUSES	ATLAS, CENTAUR AND THOR/DELTA ORBITERS			
		PREFERRED	OPTION 1	OPTION 2	OPTION 3
ATTITUDE DETERMINATION APPROACH					
FANSCAN	NO	YES	YES	NO	YES
CONSCAN	NO	NO	NO	YES	NO
DOPPLER (CRUISE)	YES	NO	NO	YES	NO
DOPPLER (MANEUVERS)	YES	YES	YES	YES	YES
ADCS EQUIPMENT					
PIONEERS 10 AND 11 CONTROL ELECTRONICS ASSEMBLY	YES	YES	YES	YES*	YES
INTELSAT III SUN SENSOR ASSEMBLY	YES	YES	YES	YES	YES
PLATFORM DRIVE ASSEMBLY	NO	NO	NO	YES	NO
HELIOS ANTENNA DESPIN CONTROL EQUIPMENT	NO	NO	NO	NO	YES
EQUIPMENT FROM OTHER SUBSYSTEMS					
PIONEERS 10 AND 11 CONTROL ELECTRONICS ASSEMBLY	YES	YES	YES	YES	YES
CONSCAN, FANSCAN PROCESSOR	NO	YES	YES	YES	YES
SPIN PERIOD SECTOR GENERATOR	YES	YES	YES	YES	YES
NUTATION DAMPER QUANTITIES (PER SPACECRAFT)	2	1	1	1	1

*THIS UNIT INCLUDES ELECTRONICS FOR RAM PLATFORM DRIVE ASSEMBLY

The Pioneer 10 and 11 CEA (common to all designs) centralizes all subsystem interfaces, thus providing better commonality with other subsystems, also based on Pioneer designs. Modifications required include deletions of star sensor and despin logics and additions of sun sensor electronics, DEA switching logic (Option 3 only), probe deployment control capabilities, drivers for additional spin/despin thrusters, and drivers for platform drive assembly (Option 2 only).

The selection of the Intelsat III sun sensor is a significant cost saving (on the order of \$200 K to \$300 K) because it allows inflight calibration of the reaction control subsystem, thereby reducing ground testing requirements. The only modification to this unit presently considered is a change in the slit geometry.

Adaptation of the Helios antenna despin equipment to the Pioneer Venus requirements involves minor modifications, such as changing clock frequencies, loop gains, and the number of rate pulses per spin revolution.

A/C III 8. 5. 6. 1 ADCS Design for the Preferred Probe Bus Configurations

A/C IV Figure 8. 5-15 shows the ADCS configuration recommended for the probe bus spacecraft. The CEA is the primary control system for both the orbiter and the probe missions. It is composed of three subassemblies:

- Program storage and execution (PSE)

- Duration and steering logic (DSL)
- Sensor and power control (SPC).

The PSE subassembly permits an entire maneuver sequence to be performed without ground commands. A maneuver sequence normally consists of an open-loop precession to a new attitude, execution of a ΔV , and an open-loop precession back to the original attitude. Maneuver accuracy is obtained by controlling execution error sources and by in-flight calibration of thruster performance. This operation sequence has been successfully used on Pioneers 10 and 11. The PSE will be used on Pioneer Venus with no modification.

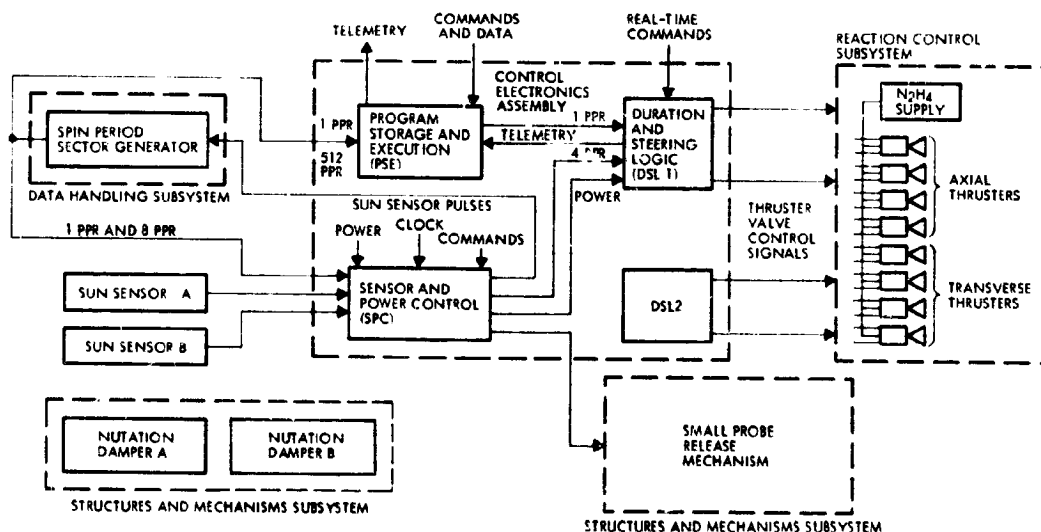


Figure 8.5-15. Attitude Determination and Control Subsystem for the Preferred Probe Bus Configurations

The DSL subassembly is redundant and contains logic for selecting thruster combinations and pulsewidths to be used. The DSL can be used without the PSE for real time, or quadrature-pulse firing (precession pulses at 0, 1.57, 3.14 or 4.71 radians (0, 90, 180 or 270 degrees) in roll relative to the sun). Modifications include additional logic for two more thrusters, deletion of the despun logic, and a change in pulsewidth selection.

The SPC subassembly is that of Pioneers 10 and 11 except that all star logic circuits will be deleted. Electronics for the redundant sun sensors will be added along with logic to control the small probe release

mechanism. This logic provides capability to trigger the probe release at preselected (by ground command) angles from the roll reference defined by the sun sensor.

The spin period sector generator (a part of the data handling subsystem described in Section 8.2) measures the spin period and generates pulse trains consisting of 1, 8, 64 and 512 pulses per 6.28 radians (spin revolution). The spin period sector generator is updated every revolution in a mode called the ACS mode in Pioneer's 10 and 11. This mode is used during precession maneuvers and small probe deployment because the one pulse per revolution signal is synchronous with the sun sensor pulses and therefore gives an accurate base from which to control the release time. The hold mode is entered by stored command prior to sun occultation in the orbiter. In this mode, the spin period is determined onboard on the basis of averaging measurements during 402.05 radians (64 spin revolutions). The period obtained by this averaging process is used to generate a roll reference during such occultation. No updating of the period measurement takes place until exit from the hold mode is ordered by another stored command.

The reaction control subsystem (see Section 8.6.2) includes eight hydrazine thrusters and the corresponding valves, supply, and instrumentation. Precession maneuvers and velocity corrections are performed by means of a set of four axial thrusters located in the same plane with the spin axis. During precessions, thrusters are fired impulsively to produce couples (thus minimizing velocity changes). Velocity corrections are made by continuous firing of two thrusters to minimize disturbance torques. Spin speed control and impulsive velocity corrections (normal to the spin axis) are executed by means of a set of four transverse thrusters located on a plane perpendicular to the spin axis at the location of the center of mass after large probe deployment.

The nutation dampers proposed for the proposed bus configurations consist of mercury-filled U-tubes with expanded end chambers to enable their natural frequencies to be tuned to the required spacecraft nutation frequencies. Two devices are used on each spacecraft to minimize the degradation of performance caused by inertia ratio changes during probe deployment.

8. 5. 6. 2 ADCS Design for the Fanbeam, Fanscan Orbiter Configurations

(31W) A/C III (31W) T/D III

The ADCS design recommended for the preferred orbiter configurations is shown schematically in Figure 8. 5-16.

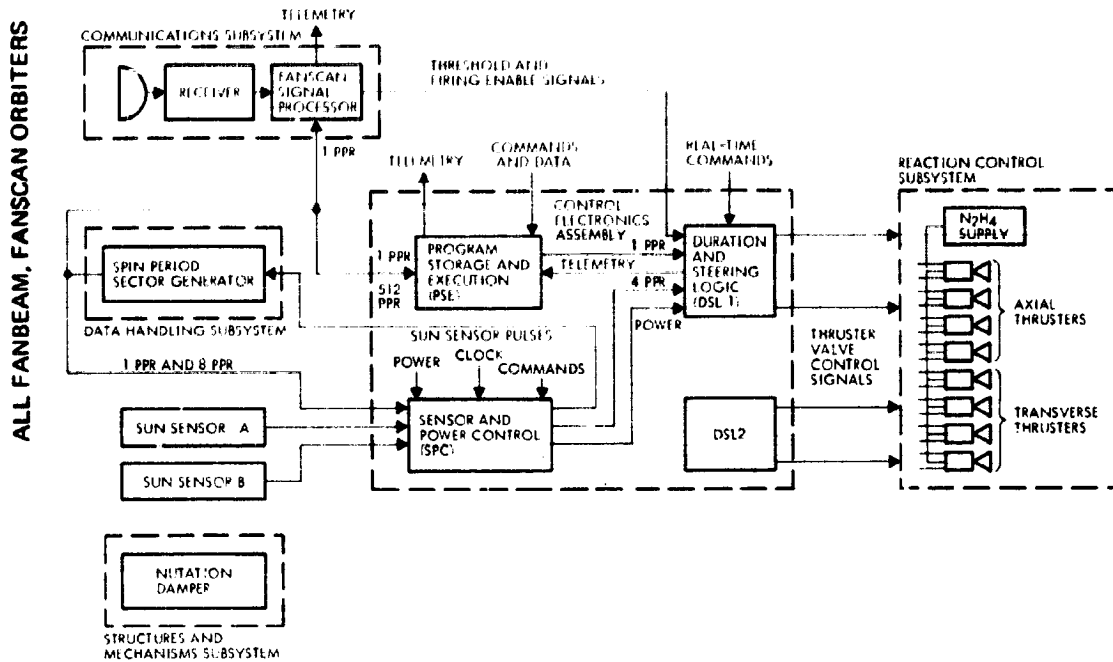


Figure 8.5-16. Attitude Determination and Control Subsystem Configuration for the Fanbeam, Fanscan Orbiters

The CEA is the same unit proposed for the probe bus configurations except that the logic for probe release, included in the sensor and power control subassembly, will not be used.

Attitude determination data from the fanscan signal processor is provided directly to telemetry. Threshold and firing enable signals are input to the duration and steering logic subassemblies to provide automatic precession control capability. The direction of precession (to be selected a priori by command) is determined by the fixed-angle precession logic included in the DSL's.




A single nutation damper is used because the ranges of inertia ratios in the orbiters are not so wide as in the probe bus configurations.

8. 5. 6. 3 ADCS Designs for the Optional Orbiter Configurations

(12W) A/C III

(12W) T/D III

As shown in Table 8. 5-5, the Option 1 design is identical to the configuration proposed for the preferred orbiters except in the transmitter power.

-  - A/C III
-  - A/C IV
-  - T/D III

The subsystem design recommended for the earth-pointing orbiters is shown in Figure 8.5-17. Essentially, it is the same design proposed for the fanbeam, fanscan orbiters except for the additions of a ram platform drive assembly and the associated control electronics.

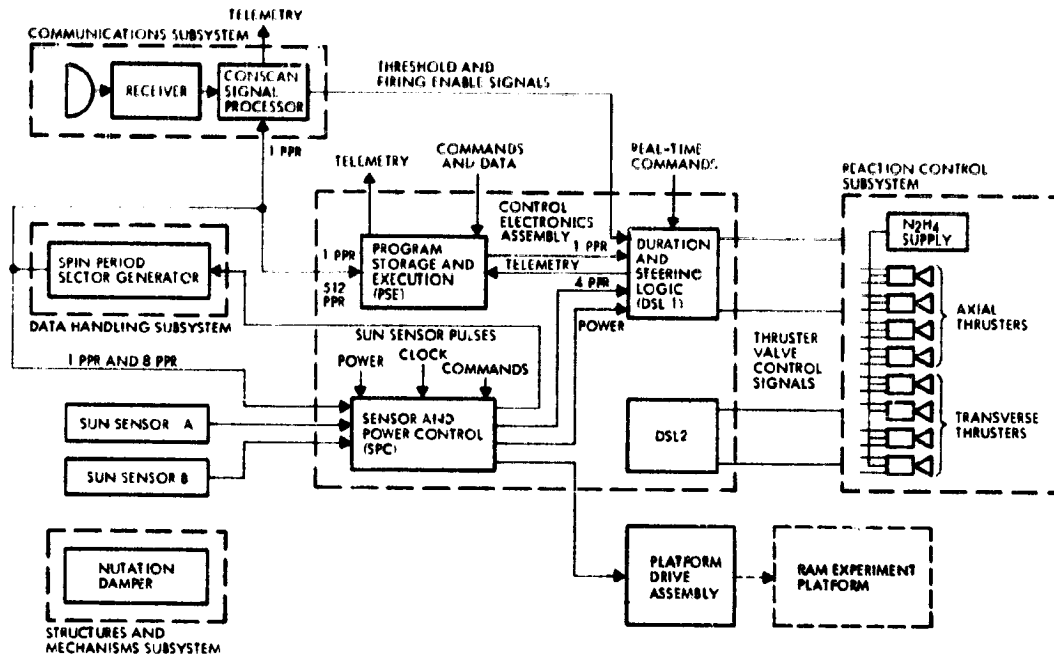





Figure 8.5-17. Attitude Determination and Control Subsystem Configuration for the Earth-Pointing Orbiters

-  A/C III
-  A/C IV
-  T/D III

As shown in Figure 8.5-18, the ADCS design recommended for the orbiter options with despun antenna reflector includes the Helios despun drive assembly and two Helios despun electronics assemblies. Additional logic is required in the CEA to provide DEA power control and redundancy switching. The DDA includes electromechanical components and a non-redundant electronics package consisting of motor driver circuits and pippier pulse conditioning logics. Each DEA comprises electronic circuits for implementing both rate and position control loops, and a position function generator providing commandable piece-wise-linear approximations to the required offsets from the sun reference.

8.5.6.4 Functional Block Diagram

ALL VERSION III SCIENCE PAYLOAD

Figure 8.5-19 is an all-inclusive functional block diagram which applies to a specific configuration if the corresponding block deletions are made. This diagram is intended to show signal flow, the operations

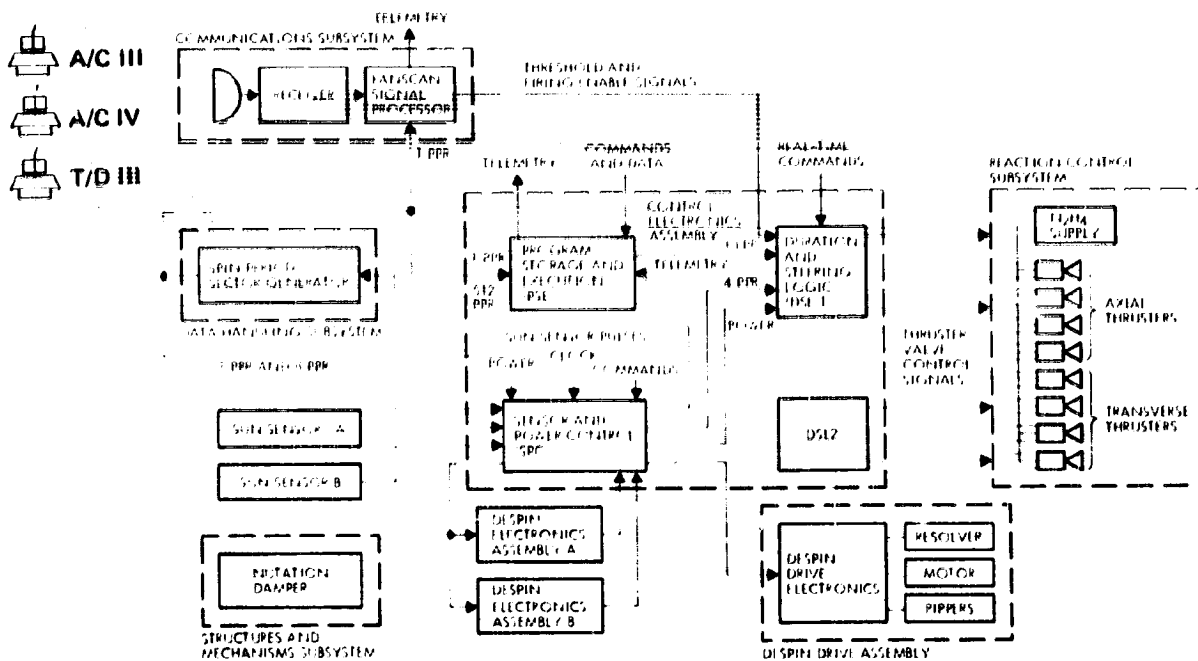


Figure 8.5-18. Altitude Determination and Control Subsystem Configuration for the Orbiters with Despin Antenna Reflector

performed in each control mode, and the interfaces of the CEA with the spin period sector generator, the conscan/fanscan processor, the despin control equipment, and the platform drive assembly.

Redundant sun sensors provide 1) roll reference pulses to the spin period sector generator and 2) sun aspect information to telemetry. The spin period sector generator (part of the data handling subsystem) generates sequences of 1, 8, and 512 pulses per spin cycle and operates in the four modes listed. The programmer includes data storage registers and counters for executing maneuver sequences. The fixed-angle precession logic defines four orthogonal precession directions selectable by ground command. The pulse generator has logic for selecting pulse durations and preventing thruster firing due to single failures. The valve select logic includes command storage latches and decoder gates for selecting thrusters. The valve drivers are series redundant, power on and operation of two drivers are required for firing. Probe deployment is controlled by delay logic, adjustable by command.

ALL VERSION III SCIENCE PAYLOAD

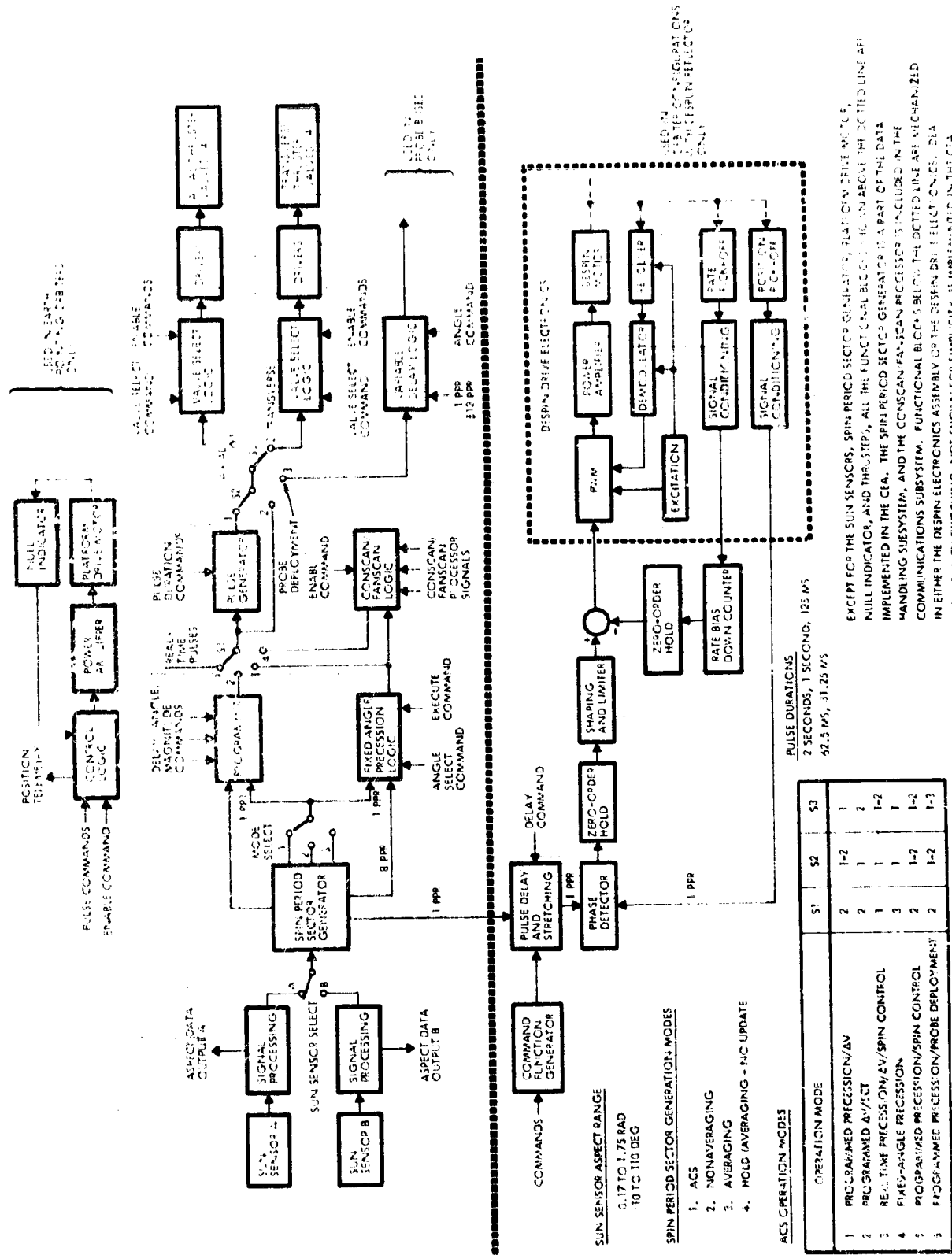


Figure 8.5-19. ADCS Functional Block Diagram

The conscan processor generates firing pulses and, in addition, provides a threshold signal to the conscan logic for stopping precession when the pointing error is less than the deadzone value. In the fanscan case, timing pulses for thruster firing are generated by the fixed-angle precession logic. The fanscan logic outputs a firing pulse when it gets a permissive level from the fanscan processor (once every two revolutions) and an enable command from the ground.

The despin control system maintains the high-gain antenna reflector in an earth-pointing orientation. The required antenna angle from the sun is provided either by command or by an onboard function generator. In either case, the commanded angle is computed with respect to the sun sensor phase reference. Using a piece-wise-linear approximation to the changing sun-spacecraft-earth angle, the function generator automatically updates the control loop position command to keep the antenna reflector pointing at the earth.

The antenna control loop receives a pointing command once per spacecraft revolution. The antenna position error is computed digitally, then converted to an analog signal. The total control error, which drives the despin motor, includes an antenna rate feedback signal. Antenna rate is measured by a digital tachometer operating with pulses generated by photoelectric rate pickup devices. The main functions of the rate loop are to improve system stability and to reduce antenna pointing errors caused by periodic torque fluctuations.

During acquisition, the antenna position error is limited to 0.39 radian (22.5 degrees) and maximum motor torque is applied to despin the antenna. When the control errors are small, the antenna position loop employs proportional-plus-integral control. Integral control is necessary to minimize errors caused by constant torque operation, such as bearing friction.

8.5.6.5 Sun Sensor Assembly

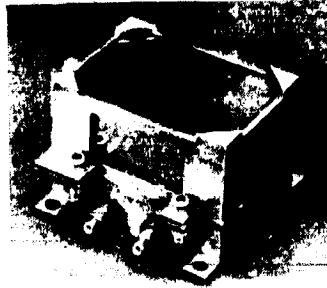
ALL CONFIGURATIONS

The sun sensor assembly (Figure 8.5-20) selected for all ADCS designs is essentially the Intelsat III unit with a different slit geometry. A V-type slit configuration has been preferred to the Intelsat III arrangement to 1) improve accuracy over the entire aspect angle range of the sensor, 2) simplify the signal processing logic, and 3) eliminate polarity

DESCRIPTION

THE SSA CONSISTS OF A FUSED SILICA BLOCK WITH A PHOTO-VOLTAIC SILICON DETECTOR LOCATED ON THE BACK SURFACE. THE FRONT SURFACE HAS PHOTOETCHED SLITS IN A VACUUM-DEPOSITED NICKEL FILM.

INTELSAT III SUN SENSOR



FUNCTION

THE SSA PROVIDES ROLL INDEXING AND SUN ASPECT INFORMATION.

DERIVATION

MODIFICATION OF INTELSAT III SSA BY CHANGING SLIT DESIGN.

ERROR ANALYSIS

SOURCE	ASPECT (1 σ)	ROLL (1 σ)
SENSOR	0.044	0.034
TEST	0.031	0.022
RSS TOTAL (1 σ)	0.054	0.041

WEIGHT:	185 G
POWER:	NO/4E
SIZE:	4.75 x 3.3 x 3 CM
NUMBER:	2 PER SPACECRAFT
RELIABILITY:	0.9993 (425 DAYS)

Figure 8.5-20. Sun Sensor Assembly Summary Description

ambiguities. An important feature of the proposed design is the resulting scale factor linearity that minimizes ground software requirements.

When the sun is in the FOV of the sensor, the output consists of two pulses per spin revolution (reference and timing pulses). Sun aspect angle is measured by the time separation between the thresholded trailing edges of the reference and timing pulses, and roll indexing is provided by the thresholded reference pulses only.

The sun sensor signal processing electronics (to be incorporated into the CEA) are described in Figure 8.5-21.

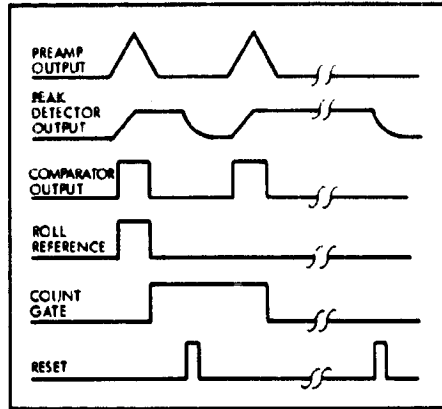
8.5.6.6 Control Electronics Assembly (CEA)

The Pioneer 10 and 11 CEA (Figure 8.5-22) is directly applicable to all mission functions required for Pioneer Venus. It contains three functional subassemblies: program storage and execution (PSE), duration and steering logic (DSL), and sensor and power control (SPC).

The sun sensor signal processing electronics amplifies the sun pulses, detects the amplitude of the peak signal, and sets a threshold in the comparator so that the trailing edge of the sun pulse is always sensed at the same percentage of peak. The two sun pulses are separated in the logic circuitry and gate a clock frequency into a 15-bit binary counter for aspect information. The roll timing reference is a single pulse out of the logic circuitry.

ALL CONFIGURATIONS

WAVEFORMS



CHARACTERISTICS

POWER	0.5 W
SIZE (PRINTED CIRCUIT BOARD)	100 cm ²
RELIABILITY	0.9889 (425 DAYS)

BLOCK DIAGRAM

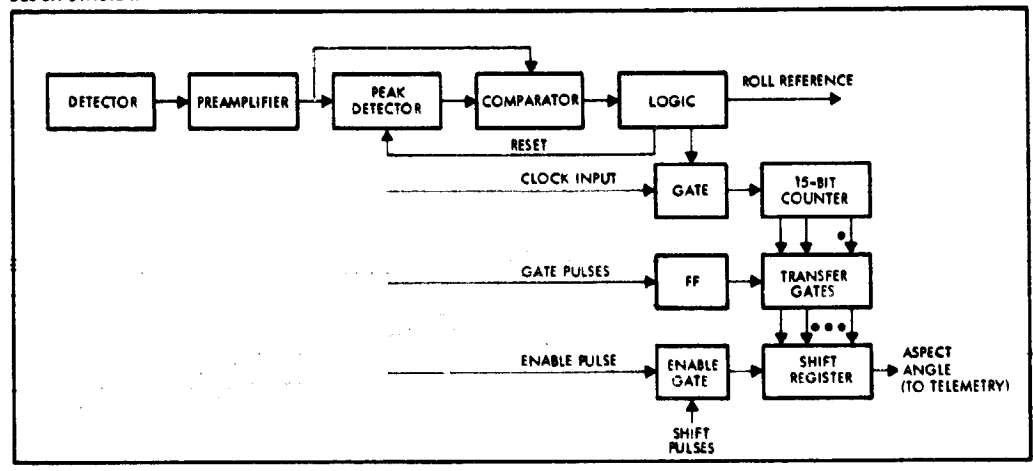


Figure 8.5-21. Sun Sensor Signal Processing Electronics (CEA)

DESCRIPTION

THE CEA CONSISTS OF SIX PRINTED WIRING BOARDS (12.7 x 19.6 x 0.15 CM) PACKAGED IN THREE MAGNESIUM CHASSIS SLICES (15.2 x 20.3 x 4.1 OR 2.54 CM) STACKED AS SHOWN BELOW.

WEIGHT:	1.91 KG
POWER:	1.5/4.0 W
SIZE:	15.2 x 20.3 x 10.9 CM
NUMBER:	1 PER SPACECRAFT
RELIABILITY:	0.9917

PIONEER F AND G CONTROL ELECTRONICS ASSEMBLY



FUNCTIONS

THE CEA PROVIDES DATA STORAGE AND SEQUENCE CONTROL FOR EXECUTING PRECESSION, ΔV, SPIN SPEED CONTROL MANEUVERS, AND PROBE RELEASE. ALSO, THE ASSEMBLY INCLUDES SENSOR SIGNAL PROCESSING ELECTRONICS, STORED COMMAND LOGIC, AND CAPABILITIES FOR SWITCHING SENSORS AND SELECTING THRUSTERS.

DERIVATION

MODIFIED VERSION OF THE PIONEER F AND G CEA.

DESIGN CHANGES REQUIRED

- DELETE SRA AND DESPIN LOGICS
- ADD TWO SGT DRIVERS AND SELECT LOGIC, REDUNDANT SUN SENSOR ELECTRONICS, STORED COMMAND LOGIC, AND PROBE DEPLOYMENT CONTROL REGISTERS COUNTER
- CHANGE 0.5-SECOND PULSE DURATION TO 62.5 MS
- PROVIDE CAPABILITY TO DRIVE TRANSVERSE THRUSTERS WITH PROGRAMMED ΔV SIGNALS
- SWITCH POWER TO VALVE DRIVERS TO PREVENT THRUSTER OPERATION WHEN DN'S ARE TURNED ON.

PACKAGING CHANGES

- REMAINING SPC CIRCUITS, SUN SENSOR ELECTRONICS, AND ADDED LOGIC WILL BE ON TWO-SIDED BOARD IN A 2.54 CM (1 IN.) THICK SLICE

Figure 8.5-22. Control Electronics Assembly Summary Description

ALL VERSION III SCIENCE PAYLOAD

The PSE contains data storage registers and state logic that controls the stored program to execute a maneuver. The seven "states" are normally executed in order:

- 1) Delay
- 2) First precession
- 3) Delay
- 4) ΔV execution
- 5) Delay
- 6) Return precession
- 7) Program complete.

The delay states allow ground intervention, attitude determination, and wobble decay. The program can be interrupted, stepped to the next state, or reset on command. Precession magnitude is controlled via calibrated thrusters pulsing once per revolution for a programmed period of time. Pulse counting is unsatisfactory because of spin coupling effects. Pulses occur at a fixed roll angle such that the spin axis describes a rhumb line during reorientation.

Since the PSE is internally redundant, no single failure can result in improper ΔV or precession execution. No modification of the PSE is required for Pioneer Venus.

The DSL contains pulsewidth and thruster selection logic plus an independent capability for thruster firing, either in real time or a roll angle of 0, 1.37, 3.14, or 4.71 radians (0, 90, 180, or 270 degrees) relative to the sun pulse. This enables all mission functions (precession, ΔV , and spin control) to be completely executable without the PSE using only ground commands. The minor improvements in the DSL assemblies are 1) expansion of valve drivers and selection logic for two additional thrusters and 2) separate power switching for the valve drivers to prevent inadvertent pulse firings during power switching.

The SPC contains power switching logic for the other assemblies plus star sensor logic that will be deleted in all Pioneer Venus designs. Circuits for small probe release control will be added. Sun sensor electronics added to the SPC will provide roll reference pulses for the spin

period sector generator, which in turn provides the reference signals for experiments and attitude control. Aspect information from the sun sensor electronics is telemetered.

Most CEA changes are made in the SPC, with minimal changes for the DSL's. The PSE, which is by far the most complex electronic design, will be unmodified.

8. 5. 6. 7 Despin Drive Assembly A/C III A/C IV T/D III

The despin drive (Figure 8. 5-23) consists of an inside-out, resolver-commutated, 16-pole brushless DC motor; position and rate pickup; and integral motor drive electronics. VacKote dry-film bearing lubrication allows operation from -50 to 75°C (-58 to 167°F). The drive is derived from the Helios solar probe satellite and will be modified to provide 512 rate pulses per 6.28 radians (per revolution). A 4.32 cm (1.7 in.) hole through the drive allows passage of wave guide, structure, and cabling.

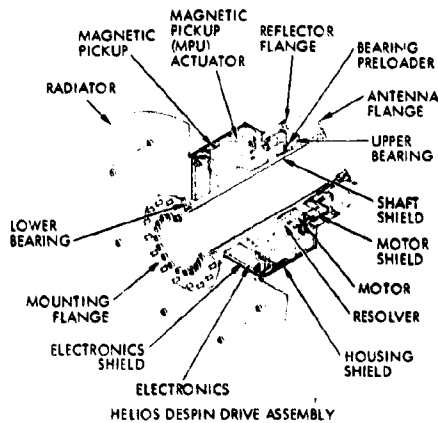


DESPIN DRIVE ASSEMBLY

PICKUPS

POSITION PICKUP: REDUNDANT, ONCE PER REVOLUTION PULSES GENERATED BY MAGNETIC PICKUPS, PEAK VOLTAGE IS 180 MV AND SLOPE IS 1.6 MV/ARC MINUTE OF SHAFT ROTATION AT 0.52 RAD/S (5 RPM).

RATE PICKUP: LIGHT-EMITTING DIODES WILL BE USED IN CONJUNCTION WITH A MASK AND OPTICAL PICKUP TO YIELD 512 PULSES PER 2 RADIANS (512 PULSES PER REVOLUTION). THE CHARACTERISTICS OF THESE PULSES ARE CURRENTLY UNDEFINED.



HELIOS DESPIN DRIVE ASSEMBLY

MOTOR CHARACTERISTICS

STALL TORQUE:	4680.52 G-CM (65 IN.-OZ) AT 28 VOLTS
BACK EMF CONSTANT:	1.13 V-RAD/S
TORQUE CONSTANT:	11521.29 G-CM (160 IN.-OZ) /AMP
RESISTANCE:	68 OHMS PHASE
INDUCTANCE:	100 MILLIHENRIES /PHASE

Figure 8. 5-23. Despin Drive Assembly Summary Description

The design uses a single-piece titanium shaft that attaches to the reflector. The shaft also connects to the despun section through a set of preloaded angular contact bearings, and a three-piece housing of aluminum and titanium.

The bearing spacing has been maximized, within the constraints of the envelope, to minimize any angular offset between the reflector and spacecraft. The bearing pair have outward-directed thrust capacity which, coupled with the spacing, maximizes the bearing rotational spring rate.

Both bearings have light interference fits in their outer race mount. The upper bearing has a slip fit inner race mount, while the lower bearing has a slight interference fit inner race. A small unbalance radial load may be produced by the motor magnet ring, which makes press fits on the bearings outer races desirable to prevent creep and possible fretting. The upper bearing inner race is a sliding fit to simplify assembly and disassembly, to provide the bearing system constant preload loop, and to allow for differential axial expansions.

Bearing preload is achieved with eight helical compression springs applying 22.24 to 44.48 newtons (5 to 10 pounds) of force on the upper bearing inner race through the preload ring.

The bearings and the slip fit bearing and shaft interface will be lubricated with the BBRC dry VacKote process. Dry VacKote, which is used on the Helios drive, produces lower and more constant bearing drag torques than does the wet VacKote process.

The motor and resolver stators are attached to the same housing section. Arc-shaped slotted holes are provided at the resolver and housing interface to provide precise external angular alignment of the motor and resolver electrical zero. The resolver is attached to the shaft and housing with machine screws. The motor rotor is similarly attached to the shaft but is keyed to the housing and clamped in place when the upper and middle housing sections are joined.

To generate the required number of 512 pulses per 6.28 radians (revolution), the magnetic pickups are replaced by light-emitting diodes, a mask, and a solid-state photoelectric detector. The mask (located between light source and detector) intermittently interrupts the light beam, thus producing a pulse train with very short rise and decay times.

All electrical leads exit the DMA from the upper housing section. This design simplifies the structural assembly and disassembly by minimizing the risk of lead damage.



Angular contact ball bearings (AFBMA Class ABEC 7) used in the despin drive are manufactured by Fafnir. The slim-line type of bearing is used because of its low weight. Both races and balls are made from 400C stainless steel, hardened to a minimum of Rockwell C58. Raceway surface finish is obtained by honing (polishing is not permitted). The ball separators are made from Ruion A material containing 5-percent molybdenum disulfide. This separator is a sacrificial type in that it replenishes any lubrication removed from contacting metal surfaces.

BBRC uses dry VacKote lubrication on all bearings and sliding surfaces. VacKote is the generic name for several proprietary lubricant formulations and application processes developed by BBRC for use in hard vacuum. VacKote development was begun in 1959 when the first OSO was being designed. At that time, it was discovered that the available lubricants for vacuum service were not effective at the hard vacuum levels of orbiting satellites. Two basic systems resulted from this early work, one based on a fluid and one based on a dry lubricant.

After an investigation of fluid, semifluid, and dry lubrication systems, dry VacKote lubrication was selected for the DDA. Dry VacKote has an extremely low evaporation rate. Hard vacuum poses no danger of material loss. Potential contamination outside the DDA is minimized. Labyrinths and other flow restrictions are not necessary, thus simplifying the mechanical design. Common components requiring wet lubrication (brushes and slip rings) are not present. And, finally, but most significantly, the dry VacKote system is characterized by extremely low torque and is insensitive to torque variation with temperature.

The dry VacKote process desposits an unbonded but adherent coating of MoS_2 about 0.001 cm (10 microinches) thick. It is unbonded in the sense that no resins or adhesives are employed. This dry coating will be applied to the balls, race surfaces, retainers, and the slip fit bearing interface. Dry VacKote prevents metallic contact and fretting, thus preventing cold welding and the generation of metallic debris. It tends to relieve surface concentration factors, which reduces the chance of spalling. It further has the tendency to improve the surface finish of the treated parts by reducing the surface roughness.

A block diagram of the electronics included in the despinner drive assembly is shown in Figure 8.5-24. The rate and position pulse conditioning logics include priority circuits such that pulses from only one of each pickoff pair are delivered to the DEA. Pulses from the redundant pickups will be automatically delivered if any one of the priority units fails. The sine and cosine motor driving signals are obtained by pulsewidth modulation of the DC supply voltage. Driving signals are derived by demodulation of the sine and cosine output signals from a resolver mounted on the same shaft as the motor. The amplitude of the resolver excitation signal is controlled by the drive signal input from the DEA. Motor current is measured by sensing logic included in the power output stages. The resulting analog signal is conditioned for direct output to telemetry.

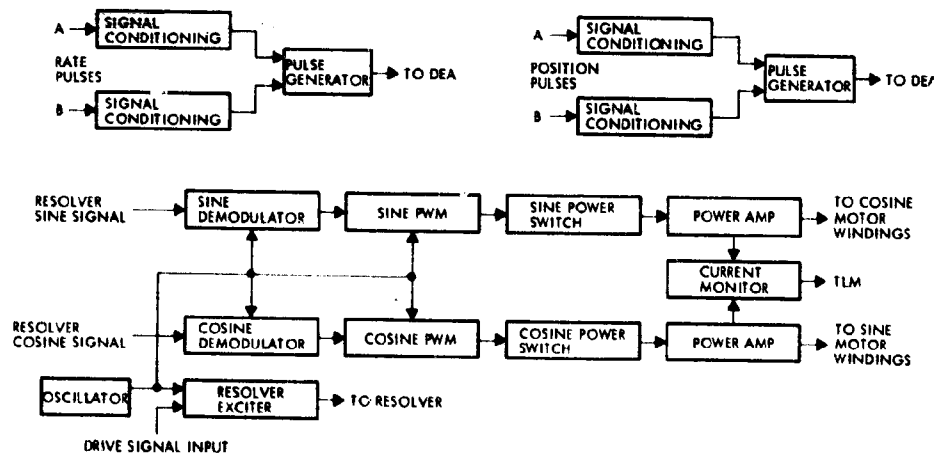


Figure 8.5-24. Despin Drive Electronics Block Diagram

The only modifications to the despinner drive electronics required for adaptation to Pioneer Venus are minor changes in the pulse conditioning circuits. The position pulse channel requires adjustments to the signal levels for 0.52 rad/s (5 rpm) operation. The rate pulse channel will be modified to provide excitations to the pickoff light sources and to operate with the new photoelectric sensors.

8.5.6.8 Despin Electronics Assembly

A block diagram of the DEA is shown in Figure 8.5-25. The angle command generator provides adjustable linear functions of time (in digital form) to approximate the required offset angles from the sun for maintaining the antenna reflector pointed at the earth. Initial angles within the

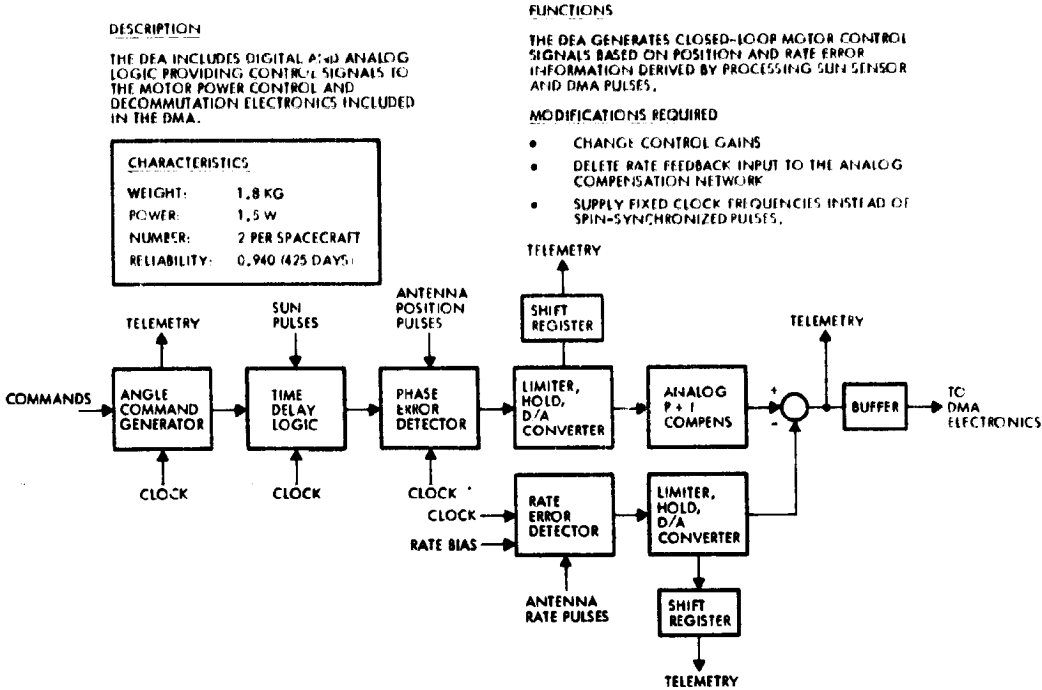


Figure 8.5-25. Despin Electronics Assembly Summary Description

0 to 6.23 radian (0 to 360 degree) range can be established by command with a quantization of 0.003 radian (0.175 degree). Positive or negative increment rates can be selected by command within the following ranges:

X1: 0.004 to 0.127 radian (0.24 to 7.25 degree)/day


X2: 0.007 to 0.253 radian (0.48 to 14.5 degree), day


Each range consists of 32 levels.

The time delay logic delays each sun sensor pulse by an interval proportional to the output from the angle command generator.

The phase error detector is an 11-bit downcounter providing a sampled measure of the antenna pointing error by measurement of the phase shift between the delayed sun sensor pulses and the position pulses from the DDA.

An 8-bit sample-and-hold register provides limiting to ± 0.39 radian (± 22.5 degrees). Sample-and-hold updating is synchronized to the antenna position pulses. Thus, the D/A converter output between consecutive antenna position pulses is constant.

 A/C III

 A/C IV

 T/D III

Position loop stabilization and steady-state error minimization are provided by an analog amplifier, which introduces proportional-plus-integral compensation.

The rate error detector is an 11-bit upcounter that provides a sampled measure of antenna inertial rate on the basis of a commanded rate bias and clock pulse counts between consecutive rate pulses.

Limiting to 8 bits is provided by a sample-and-hold register, to which digital data transfer is made after each antenna rate pulse.

Adaptation of the Helios assembly to Pioneer Venus requires only minor modifications (see Figure 8.5.25). Redundancy switching will be performed in the CEA, which also handles the command and telemetry interfaces.

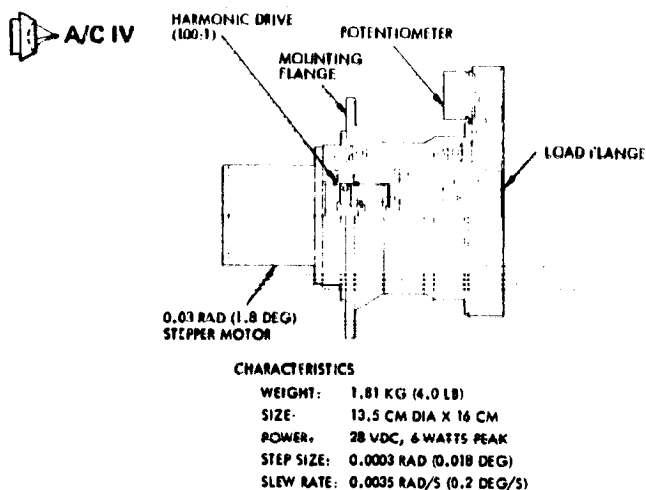
8.5.7 Descriptions of ADCS Designs for the Preferred Atlas/Centaur Configurations for the Version IV Science Payload

 A/C IV

 A/C IV

The ADCS design selected for the preferred probe bus configuration is as described in Section 8.5.6.1. The design selected for the preferred orbiter configuration is as described in Section 8.5.6.3 for the earth-pointing orbiters.

A summary description of the selected platform drive assembly is given in Figure 8.5-26. The layout design of the platform drive assembly (PDA) is based upon a solar array drive currently being developed for FLTSATCOM. The drive unit consists of a 0.03 radian (1.8 degree)-per-step stepper motor, which is coupled to the input of a harmonic drive reducer. The harmonic drive ratio is 100:1, which results in an output step size of 0.0003 radian (0.018 degree) per step. The output shaft is supported in the housing by a duplex pair of angular contact bearings fixed at one end. The other end of the shaft is supported by a single-row deep-groove bearing, which floats axially in the housing to accommodate axial thermal expansion. This bearing arrangement has been selected to positively control the shaft location under load, specifically under vibration during launch. The bearings are of 440C stainless steel with phenolic retainers, impregnated with NPT-4 oil. Other bearings for the harmonic drive and motor are similarly impregnated with NPT-4 oil. Nylasint



DESCRIPTION

THE PDA CONSISTS OF A STEPPER MOTOR, A HARMONIC DRIVE GEAR REDUCTION, SINGLE AND DUPLEX-PAIR BEARINGS, AND A GEARED FILM POT.

FUNCTION

THE PDA PROVIDES SINGLE-AXIS GIMBALLING CAPABILITY TO THE PLATFORM SUPPORTING THE RAM-LOOKING EXPERIMENTS.

DERIVATION

NONREDUNDANT SINGLE-AXIS VERSION OF THE ELTSATCOM SOLAR ARRAY DRIVE.

Figure 8.5-26. Platform Drive Assembly Summary Description

reservoirs, impregnated with NPT-4 oil, are mounted in several locations throughout the assembly. The shaft and housing and other structural parts are made from 2024 aluminum alloy.

For position indication, one single-turn potentiometer is mounted to the housing. Input rotation of the potentiometer is taken from the output shaft with a set of antibacklash gears. The potentiometer will contain a conductive plastic or film-type resistive element, which needs no additional lubrication. Bartemp bearings will be used so that lubricant reservoirs need not be built into the potentiometer.

8.5.8 Attitude Determination and Control Performance, Version III Science Payload

8.5.8.1 Probe Mission (1977 Launch) A/C III T/D III

Detailed analyses were performed to derive quantitative assessments of the performance attainable with the recommended ADCS design in all critical phases of the probe mission. Particular attention was given to the determination of drift rates caused by solar pressure; the calculation of attitude errors and dynamic perturbations originated by separation (from booster), midcourse, probe release, and retargeting maneuvers; the analysis of reaction control subsystem performance; the computation of attitude determination accuracies during cruise and probe release and retargeting maneuvers; and the computation of velocity errors during retargeting maneuvers.

A/C III

T/D III

This section summarizes the results of the above mentioned analyses. Wherever possible, the material is organized chronologically. Data are given separately for the Thor/Delta and the Atlas/Centaur preferred configurations appropriate to the Version III science payload and the 1977 probe mission launch.

Separation from Booster T/D III

The Thor/Delta-launched spacecraft will be spinning at $9.42^{+2.83}_{-1.47}$ rad/s (90^{+27}_{-14} rpm) at third-stage burnout. Spacecraft nutation will have induced by the third-stage motor thrust vector misalignments and by center-of-mass offsets of the combined third stage and spacecraft. Assuming a third-stage motor thrust of 7.1×10^4 newtons (16 000 pounds), a thrust vector to center-of-mass offset of 1.83 mm (0.006 foot), a spin axis moment of inertia (for third-stage and spacecraft combination) of $155 \text{ kg} \cdot \text{m}^2$ (114 slug-ft^2), an inertia parameter $\lambda = 0.4$, and a spin rate of 8 rad/s (76.4 rpm), the peak nutation angle at burnout is approximately 0.07 radian (4 degrees).

The nutation angle following separation from the third stage is a function of spin rate, nutation angle before separation, mass properties, axial and lateral spring force differentials, moment arms, and separation time. A nutation angle of 0.0314 radian (1.8 degrees) is predicted after separation on the basis of the following assumptions:

- Nutation angle before separation = 0.07 radian (4 degrees)
- Average transverse MOI after separation = $122 \text{ kg} \cdot \text{m}^2$ (90 slug-ft^2)
- Average transverse MOI before separation = $258 \text{ kg} \cdot \text{m}^2$ (190 slug-ft^2)
- Spin MOI of spacecraft after separation = $145.5 \text{ kg} \cdot \text{m}^2$ (107 slug-ft^2)
- Spin MOI before separation = $155 \text{ kg} \cdot \text{m}^2$ (114 slug-ft^2)
- Separation time $\cong 0.1$ second
- Axial force differential per pair of springs = 17.8 newtons (4 pounds)
- Lateral force differential per pair = 8.9 newtons (2 pounds)

A/C III

- Radial distance from centerline to separation springs = 0.305 meter (1 foot)

T/D III

- Axial distance from spacecraft center of mass to separation springs = 0.244 meter (0.8 foot).

A pictorial representation of the spin axis attitude error during separation is shown in Figure 8.5-27. For the Thor/Delta, the momentum shift will be approximately 0.0374 radian (2.2 degrees), and the nutation damper time constant after separation will be on the order of 15 minutes.

T/D III

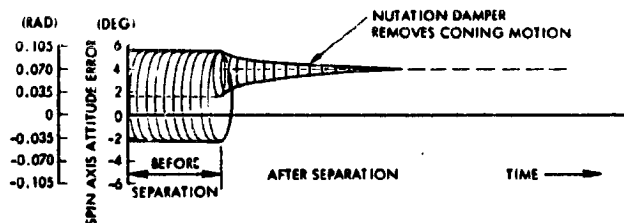


Figure 8.5-27. Pictorial Representation of Spin Axis Attitude Errors During Separation from Third Stage

The Atlas/Centaur-launched spacecraft will be spun up to 5 rpm by the Centaur prior to separation. An analysis of the separation dynamics is not included at the present time because the pertinent Centaur data are not available.

Despin Maneuver T/D III

The Thor/Delta configuration initially spins at $9.42 \begin{matrix} +2.83 \\ -1.47 \end{matrix}$ rad/s ($90 \begin{matrix} +27 \\ -14 \end{matrix}$ rpm). Assuming a nominal cruise spin speed of about 0.5 rad/s (4.8 rpm), the spacecraft will be initially despun down to a rate of approximately 0.55 rad/s (5.25 rpm) by the transverse thrusters (so that the desired rate is attained after magnetometer boom deployment).

Assuming a constant deceleration of 0.0565 rad/s^2 (0.54 rpm) for stead-firing conditions, the thrusting time required for the initial despin maneuver is in the range from 132 to 208 seconds.

During deployment, the magnetometer boom will be subject to lateral loading due to nutation and Coriolis acceleration. Assuming a boom length of 3.5 meters (136 inch), an inertia parameter $\lambda = 0.2$, a spin speed of 0.5 rad/s (5 rpm) and a nutation angle of 0.07 radian (4 degrees), the resulting acceleration is on the order of 0.006 g. With a

T/D III deployment rate of 1 meter/s, the Coriolis acceleration is 0.0017 g. At the nominal spin rate of 0.5 rad/s (5 rpm), the axial load due to centrifugal force is about 0.09 g.

Cruise Phase Attitude Determination and Control ALL CONFIGURATIONS

Three-dimensional angular geometry will be described in terms of stereographic projections. The spacecraft is assumed positioned at the center of a sphere with its equator parallel to the ecliptic plane. The spin axis and the spacecraft-sun and spacecraft-earth lines are next projected onto the sphere. The sphere is divided in 0.17 rad (10 deg) increments both in longitude (meridians) and latitude (parallels) to indicate angular measure. Figure 8.5-28 shows how the stereographic projection of this imaginary sphere surrounding the spacecraft is obtained. An important property of this projection is that it is conformal (angles measured on the projection are equal to the corresponding angles on the sphere).

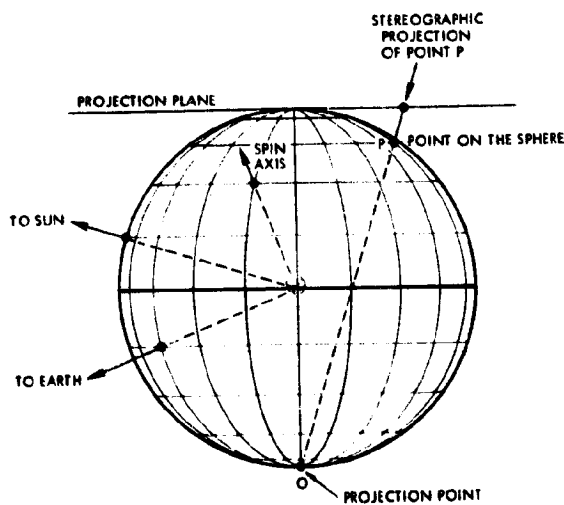


Figure 8.5-28. Stereographic Projection Method for Plane Representation of Three-Dimensional Angular Geometry

A/C III T/D III Figure 8.5-29 is a stereographic projection showing locations of the sun and earth as functions of time and the spin axis orientation profile during the probe bus cruise phase. After launch and trans-Venus injection, the spin axis (point A) is about 0.49 rad (28 deg) from the sun. From the thermal, power, and communications view, this attitude is desirable; no initial orientation is needed. The spacecraft therefore could remain in this position until day 5, when the first midcourse maneuver is planned.

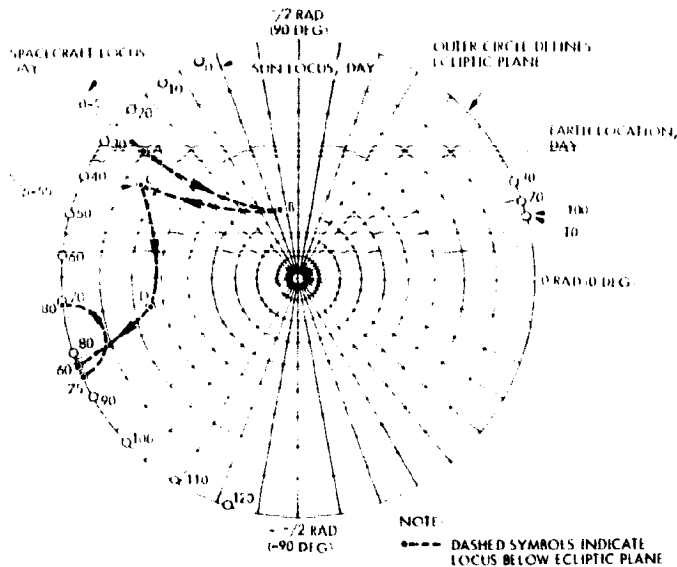


Figure 8.5-29. Stereographic Projection Showing Sun-Earth-Spacecraft Geometry During Probe Bus Cruise

At this time the vehicle is precessed to the required attitude (i. e., point B) and the ΔV is executed. Instead of returning to the initial position, the vehicle is precessed to a new location (point C), where it can remain from day 5 until time for the second midcourse on day 55. After the second midcourse (assumed at orientation D), the communications signal strength decreases until the medium-gain (0.6 meter) antenna is required. At this point, the spacecraft becomes an earth pointer and remains earth pointing until probe deployment.

On about day 75, syzygy begins (where the sun, earth, and spacecraft are most closely aligned). At this time, another option occurs: either the spacecraft can remain as it is such that the sun passes through the sun sensor deadzone, or the spacecraft can be precessed around the sun, always keeping the sun aspect angle greater than 0.17 radian (10 degrees) and the earth within the range of the 0.6-meter medium-gain antenna.

Disturbance torques produced by unbalanced solar pressure are the main cause of attitude drift during probe bus cruise. The curves presented in Figure 8.5-30 provide current estimates of attitude drift rate as functions of time for the Thor/Delta and Atlas/Centaur spacecraft configurations. Drift rates are generally low because thermal reasons require

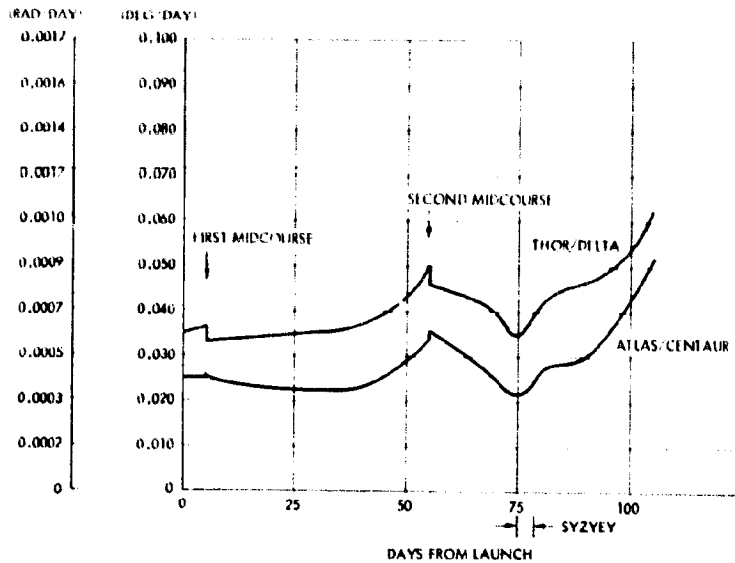


Figure 8.5-30. Solar Pressure Drift Rate Versus Time, Probe Bus Cruise Phase

orientations with sun aspect angles in the 0.26 to 0.61 radian (15 to 35 degree) range during cruise and the effective offset between centers of pressure and mass decreases with aspect angle. For instance, if the attitude of the spacecraft is not corrected during the 50-day period between first and second midcourse maneuvers, the total precession due to solar pressure would be less than 0.035 radian (2 degrees).

Attitude determination accuracy is a function of solar and earth aspect angles and the sun-vehicle-earth angle. The sun sensor provides sun aspect measurements with an accuracy given approximately by the following expression

$$\Delta\alpha(\text{rad}, 3\sigma) = 0.00349/\sin \alpha_s$$

where α_s is the sun aspect angle. Doppler modulation provides earth aspect angle information with accuracies as shown in Figure 8.5-7. Based on these assumptions and the geometry shown in Figure 8.5-29, attitude determination accuracies for the most significant cruise events are as follows:

Initial attitude after launch	± 0.014 rad (± 0.80 deg)
Initial attitude before maneuvers for first midcourse correction	± 0.014 rad (± 0.80 deg)

First midcourse attitude	± 0.008 to ± 0.021 rad (± 0.44 to ± 1.2 deg)
Cruise attitude (after first midcourse)	± 0.012 rad (± 0.67 deg)
Cruise attitude (35 days after launch)	± 0.017 rad (± 1.0 deg)
Cruise attitude before second midcourse)	± 0.024 rad (± 1.4 deg)
Second midcourse attitude	± 0.008 to 0.021 rad (± 0.44 to ± 1.2 deg)
Earth-pointing attitude	± 0.008 rad (± 0.44 deg)

Midcourse Maneuvers

The attitude errors, velocity dispersions, and spin rate variations that may occur during midcourse maneuvers are summarized in Tables 8.5-6 and 8.5-7 for the Thor/Delta and Atlas/Centaur probe bus configurations. Attitude determination errors are not included because the orientations required for these corrections are not known at the present time.

During midcourse correction ΔV maneuvers utilizing the axial thrusters, the most significant disturbance producing attitude errors is due to the difference in thrust level of the thrusters. A ± 4 percent thrust level uncertainty was assumed for this case. The alignment of the thrusters is the most significant cause of spin rate changes during these maneuvers. A thrust vector alignment accuracy of approximately 0.5 deg (~ 9 milliradian) was assumed for this analysis. Experience of Pioneer 10 has shown a much larger error, on the order of 1 degree (~ 17 milliradian) although flight data from Intelsat III has shown errors of less than 1/8 degree (~ 2 milliradian). For either case, the spin rate variations are sufficiently large during the large ΔV maneuvers that an in-orbit calibration should be performed prior to a ΔV maneuver, and the maneuver then be controlled in such a manner as to prevent unacceptable spin rate changes. For the probe mission, utilization of a pair of the spin thrusters for a ΔV maneuver is impractical before large probe release due to the large axial center of mass offset before large probe release. The summary table assumes that the spin thrusters lie nominally in the center of mass plane after large probe release.

Table 8.5-6. Thor/Delta Probe Mission Spacecraft Dynamic Disturbances

T/D III

EVENT	ΔV (M/S)	THRUST EACH THRUSTER (N (LB))	SPIN RATE CHANGE (RAD/S (RPM))	ANGLE OF ATTACK ERROR (RAD (DEG))	MOMENTUM VECTOR SHIFT (RAD (DEG))	VELOCITY DISPERSION ANGLE (RAD (DEG))	VELOCITY DEGRADATION (M/S)	NUTATION ANGLE (RAD (DEG))
SEPARATION FROM BOOSTER	0.2		0 (0)		0.038 (2.2)			0.031 (1.8)
FIRST MIDCOURSE ¹	73	5.2 (1.17)	± 1.05 (110)	0.077 (4.4)	0.014 (0.8)	0.070 (0.4)	0.1	0.065 (3.7)
SECOND MIDCOURSE ¹	7	3.1 (0.7)	± 0.01 (± 0.1)	0.045 (2.6)	0.009 (0.5)	0.004 (0.25)	0.004	0.038 (2.2)
THIRD MIDCOURSE ¹	2	3.1 (0.7)	± 0.03 (± 0.3)	0.045 (2.6)	0.009 (0.5)	0.004 (0.25)	0.001	0.038 (2.2)
THIRD MIDCOURSE ²	2	3.1 (0.7)	± 0.15 (± 1.4)	2.443 (140)	2.443 (± 40)	LARGE		0.003 (0.2)
FIRST RETARGETING ¹	1.02	3.1 (0.7)	± 0.01 (± 0.1)	0.023 (1.3)	0.010 (0.6)	0.005 (0.3)	---	0.012 (0.7)
FIRST RETARGETING ²	1.02	3.1 (0.7)	± 0.04 (± 0.4)	0.009 (0.5)	0.009 (0.5)	0.004 (0.25)		0.00007 (0.004)
SECOND RETARGETING ¹	7.32	3.1 (0.7)	± 0.07 (± 0.7)	0.209 (12)	0.070 (4)	0.035 (2)	0.041	0.140 (8)
THIRD RETARGETING ¹	6.34	3.1 (0.7)	± 0.06 (± 0.6)	0.140 (8)	0.067 (5)	0.041 (2.5)	0.066	0.070 (4)
THIRD RETARGETING ²	6.34	3.1 (0.7)	± 0.23 (± 2.3)	0.075 (4.3)	0.075 (4.3)	0.038 (2.2)	---	NEGLIGIBLE
FOURTH RETARGETING ¹	26.55	3.1 (0.7)	± 0.29 (± 2.8)	0.038 (2.2)	0.017 (1)	0.009 (0.5)	0.008	0.021 (1.2)

0.524 RAD/S (5 RPM) SPIN RATE ASSUMED FOR ALL CASES.

¹UTILIZING PAIR OF AXIAL THRUSTERS WITH 9 MILLIRADIAN MISALIGNMENT.

²UTILIZING PAIR OF SPIN THRUSTERS.

Table 8.5-7. Atlas/Centaur Probe Mission Spacecraft Dynamic Disturbances

A/C III

EVENT	ΔV (M/S)	THRUST EACH THRUSTER (N (LB))	SPIN RATE CHANGE (RAD/S (RPM))	ANGLE OF ATTACK ERROR (RAD (DEG))	MOMENTUM VECTOR SHIFT (RAD (DEG))	VELOCITY DISPERSION ANGLE (RAD (DEG))	VELOCITY DEGRADATION (M/S)	NUTATION ANGLE (RAD (DEG))
FIRST MIDCOURSE ¹	13	5.2 (1.17)	± 0.16 (15)	0.030 (1.7)	0.007 (0.4)	0.003 (0.2)	0.0026	0.024 (1.4)
SECOND MIDCOURSE ¹	7	5.2 (1.17)	± 0.08 (8)	0.030 (1.7)	0.007 (0.4)	0.003 (0.2)	0.0014	0.024 (1.4)
THIRD MIDCOURSE ¹	2	5.2 (1.17)	± 0.02 (2)	0.030 (1.7)	0.007 (0.4)	0.003 (0.2)	0.0004	0.24 (1.4)
THIRD MIDCOURSE ²	2	5.2 (1.17)	± 0.12 (11)	1.920 (110)	1.920 (± 10)	LARGE	LARGE	
FIRST RETARGETING ¹	1.02	5.2 (1.17)	± 0.01 (1)	0.017 (1)	0.007 (0.4)	0.003 (0.2)	NEGLIGIBLE	0.009 (0.5)
FIRST RETARGETING ²	1.02	5.2 (1.17)	± 0.04 (4)	± 0.014 (0.8)	0.014 (0.8)	NEGLIGIBLE	NEGLIGIBLE	0.003 (0.2)
SECOND RETARGETING ¹	7.32	5.2 (1.17)	± 0.06 (6)	0.157 (9)	0.052 (3)	0.026 (1.5)	0.04	0.105 (6)
THIRD RETARGETING ¹	6.34	5.2 (1.17)	± 0.06 (6)	0.171 (9.8)	0.062 (4.2)	0.042 (2.4)	0.04	0.106 (6.2)
THIRD RETARGETING ²	6.34	5.2 (1.17)	± 0.28 (2.7)	0.096 (5.6)	0.096 (5.6)	0.049 (2.8)	NEGLIGIBLE	0.002 (0.1)
FOURTH RETARGETING ¹	26.55	5.2 (1.17)	± 0.24 (2.3)	0.035 (2)	0.017 (1)	0.009 (0.5)	0.01	0.017 (1)

0.524 RAD/S (5 RPM) SPIN RATE ASSUMED FOR ALL CASES.

¹UTILIZING PAIR OF AXIAL THRUSTERS.

²UTILIZING PAIR OF SPIN THRUSTERS.

The following is a summary of parameter definitions and nomenclature used in Tables 8.5-6 and 8.5-7.

- Angle of attack (α_1)—the angle between the spin axis just prior to thruster firing and the spin axis during thruster firing
- Nutation angle (θ)—the angle between the spacecraft spin axis and the angular momentum vector
- Attitude angle (α)—the angle between the spin axis prior to thruster firing and the angular momentum vector
- Velocity degradation (ΔV_d)—the loss in magnitude of the velocity increment due to the coning motion of the spacecraft
- Velocity increment dispersion angle (α_V)—the angle between the intended direction of the velocity increment and the actual velocity increment.

Probe Deployment and Retargeting Maneuvers

Figure 8.5-31 includes results of an analysis of attitude determination accuracies obtainable during probe deployment and retargeting based on measurements of sun and earth aspect angles. Estimation accuracies are given in terms of error ellipse parameters defined in the figure. Earth aspect angle measurements are made by the doppler techniques described in a preceding section, where determination errors are given as functions of aspect angle. Solar aspect measurement errors are assumed given by an inverse sine function of aspect angle with a minimum value of 0.0035 radian (0.2 degree) (3σ) for orientations perpendicular to the spacecraft-sun line.

In all cases the peak errors are less than the assumed requirement of 0.017 radian (1 degree) (3σ).

Retargeting maneuver execution errors are given in Tables 8.5-6 and 8.5-7 for the Thor/Delta and Atlas/Centaur configurations. The first retargeting maneuver will be made by a pair of transverse thrusters. Relatively large attitude errors [(0.209 radian)(up to 12 degrees)] are induced during the second retargeting maneuver due to the radial center of mass offset occurring after release of the first small probe. These errors can be reduced by either increasing the spin rate or by operating with the transverse thrusters in the pulsed mode. The third retargeting maneuver is based on transverse thruster firings because the required attitude is more favorable for attitude determination. The fourth retargeting is made by the axial thrusters because of the large velocity change required.

Figure 8.5-32 shows the locations of the spin axis during the entire probe deployment and retarget sequence. Using the probe bus as an earth pointer during this period permits maximum communications utilization prior to maneuvers. It is an excellent starting point for maneuvers since the precession magnitudes required are reasonably small. Two options for mission operations are apparent: first, maneuvers can be minimized by orientation to a position (say the large probe release), executing, and staying there until the next maneuver two days later. The next maneuver is the first retarget, which is only an 0.14 radian (8 degree) precession. The spacecraft can now remain in this position until time to maneuver for the first small probe release, again a short maneuver. This process can be continued for the entire sequence since the baseline design permits the resultant sun angles for indefinite periods. Power and thermal designs are ideal for this process. However, if high-bit-rate communication using only the 26-meter DSN is desired, the second option can be used, that is, spacecraft can be precessed back to earth pointing at any time (aft of spacecraft to earth). With this modified earth-pointing approach, all probe release maneuvers are shortened considerably from the Venus orbit plane normal position.

Tables 8.5-8 and 8.5-9 show differences between the actual and desired velocity changes during ΔV maneuvers. Velocity errors associated with the probe retargeting (RT) maneuvers are resultants of axial and radial vector components.

Axial velocity errors are caused by uncertainties in the thruster impulse, which have been assessed as ranging from 3 to 6 percent of the desired level. Radial velocity errors result from a combination of attitude errors incurred prior to thrusting and velocity dispersions caused by effects of misalignments while thrusting. Attitude determination errors are caused by solar and earth aspect measurement errors and the associated geometry. Velocity dispersion errors were estimated assuming a 9-milliradian thrust vector misalignment for the probe bus configurations. Four percent thruster imbalance was assumed in both cases.

⊕ A/C III

⊕ T/D III

Presented in Tables 8.5-10 and 8.5-11 are current estimates of performance characteristics of the reaction control system (RCS). These include the abilities to precess the spin axis, spin-up and spin-down, and change the spacecraft velocity vector. Precessions and axial velocity changes are performed by a set of four thrusters located at the top and bottom of the spacecraft. Spin control and radial velocity changes are made by a set of four thrusters located on a plane perpendicular to the spin axis and located near the spacecraft's center of mass. RCS performance varies as a function of propellant remaining (blowdown effects) and mass properties. Calculations are shown for the spinning, precessing, and velocity trimming of the Thor/Delta and Atlas/Centaur probe and orbiter missions. The peak nutation factor is a function of mass properties and thruster firing policy. This factor determines the maximum nutation amplitude based on the precession step size.

Pulse sizes available to the RCS are of 2.0; 1.0; 0.125; 0.0625- and 0.03125-second duration. The 125 millisecond pulse duration is used as a general reference in the table and other values are included where appropriate due to preferred mode of operation.

Small Probe Release Dynamics ⊕ T/D III

The trajectories of the small probes relative to the bus are described by the equations for an involute, i. e. ,

$$\Delta R = R_o (\cos \phi + \phi \sin \phi)$$

$$\Delta T = -R_o (\sin \phi - \phi \cos \phi)$$

where

ΔR = radial displacement between probe and bus

ΔT = tangential displacement between probe and bus

R_o = distance between probe center of mass and bus-plus-remaining-probe center of mass at time of separation

ϕ = angle of rotation after time of separation.

A/C III
T/D III

EVENT	SYMBOL	LP	RT1	SP1	RT2	SP2	RT3	SP3	
DAYS BEFORE ENCOUNTER		25	23	21	19	17	15	13	
-SPACECRAFT- ANGLE IN VOP RAD (DEG)	α	2.478 (142.0)	2.429 (139.2)	2.384 (136.6)	2.340 (134.1)	2.296 (131.6)	2.255 (129.2)	2.216 (127.0)	2.177
SPIN AXIS ANGLE CELESTIAL SPHERE RAD (DEG)	β	1.918 (109.9)	1.740 (99.7)	1.302 (74.4)	2.612 (149.7)	0.686 (39.9)	1.735 (99.4)	1.191 (67.7)	2.000
-ASPECT RAD (DEG)	A	0.667 (38.2)	0.698 (40.0)	0.435 (24.9)	1.016 (58.2)	0.462 (27.6)	0.750 (43.0)	0.626 (35.9)	1.140
ERROR RAD (DEG) "E"	E	0.006 (0.32)	0.005 (0.31)	0.008 (0.48)	0.004 (0.24)	0.0075 (0.43)	0.0051 (0.29)	0.006 (0.34)	0.000
DETERMINATION MODE*		A	A	A	B	A	A	A	
PROBABILITY ELLIPSE ON CELESTIAL SPHERE RAD (DEG)									
SEMI-MAJOR AXIS	a	0.0105 (0.60)	0.0091 (0.52)	0.0108 (0.62)	0.0112 (0.64)	0.0173 (0.99)	0.0136 (0.78)	0.0120 (0.69)	0.010
SEMI-MINOR AXIS	b	0.0054 (0.31)	0.0037 (0.21)	0.0079 (0.45)	0.0030 (0.17)	0.0061 (0.35)	0.0051 (0.29)	0.0058 (0.33)	0.000
ANGLE BETWEEN "E" AND "a"	c	0.1413 (28.1)	0.2618 (15.0)	0.6666 (38.2)	1.3192 (75.6)	1.1447 (65.6)	0.1902 (10.9)	0.5200 (29.8)	0.570

* A - DOPPLER MODULATION
B - DOPPLER SHIFT

Figure 8.5-31. Probe Deployment and Retargeting Attitude Determination Accuracies

T/D III ^(31 W) T/D III Table 8.5-10. Re Th

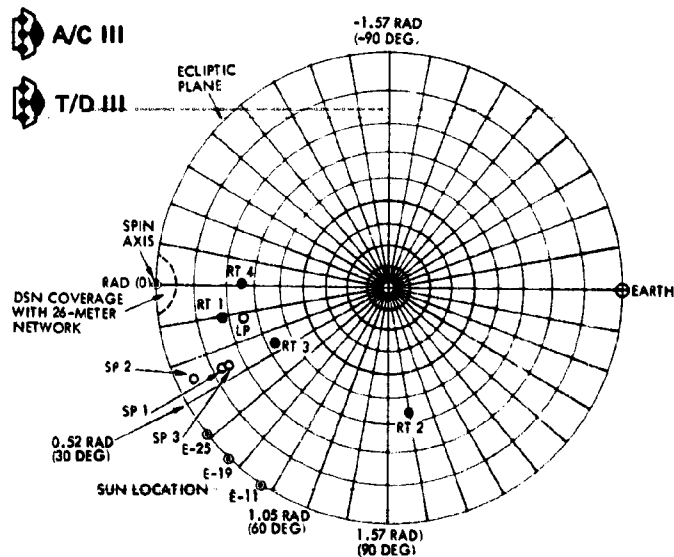
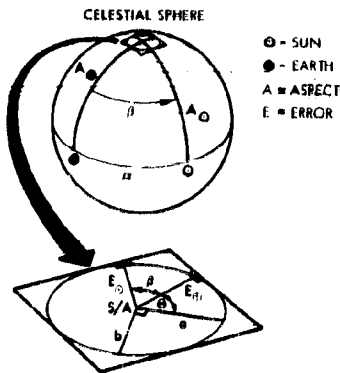


Figure 8.5-32. Stereographic Projection Showing Locations of the Spin Axis, Sun, and Earth During Probe Release and Probe Bus Retargeting Maneuvers

CONDITION	SPIN SPEED CHANGE	
	125 MS (RAD/S)/PULSE (RPM/PULSE)	CONTINUOUS (RAD/S ²)/RPM/S
PROBE		
CRUISE:		
100 PERCENT N ₂ H ₄	0.0071 (0.068)	0.056 [*] (0.54)
50 PERCENT	0.0040 (0.038)	0.0314 (0.030)
20 PERCENT	0.0032 (0.031)	0.0262 (0.25)
AFTER:		
LP	0.0037 TO 0.0073 (0.035 TO 0.070)	0.0293 TO 0.0586 (0.28 TO 0.56)
SP1	0.0043 TO 0.0086 (0.041 TO 0.082)	0.0346 TO 0.0691 (0.33 TO 0.66)
SP2	0.0057 TO 0.0113 (0.054 TO 0.108)	0.0450 TO 0.0901 (0.43 TO 0.86)
SP3	0.0069 TO 0.0138 (0.066 TO 0.132)	0.0555 TO 0.0111 (0.53 TO 1.06)
END OF MISSION	0.0062 TO 0.0124 (0.059 TO 0.118)	0.0492 TO 0.0984 (0.47 TO 0.94)
ORBITER		
CRUISE:		
100 PERCENT N ₂ H ₄	0.1131 (0.108)	0.0901 (0.86)
50 PERCENT	0.0063 (0.060)	0.0503 (0.48)
20 PERCENT	0.0052 (0.050)	0.0419 (0.40)
ENCOUNTER*	0.0052 TO 0.0104 (0.050 TO 0.100)	0.0419 TO 0.0838 (0.40 TO 0.80)
IN ORBIT*	0.0052 TO 0.0104 (0.050 TO 0.100)	0.0429 TO 0.0858 (0.41 TO 0.82)
IN ORBIT**	0.0053 TO 0.0105 (0.051 TO 0.102)	0.0387 TO 0.0775 (0.37 TO 0.74)
END OF MISSION	0.0048 TO 0.0105 (0.046 TO 0.092)	0.0398 TO 0.0796 (0.38 TO 0.76)

* MAGNETOMETER RETRACTED.
** MAGNETOMETER DEPLOYED.

	RT3	SP3	RT4
	15	13	11
	2.255 (129.2)	2.216 (127.0)	2.176 (124.7)
	1.735 (99.4)	1.191 (67.7)	2.068 (118.5)
	0.750 (43.0)	0.626 (35.9)	1.141 (65.4)
	0.0051 (0.29)	0.006 (0.34)	0.0038 (0.22)
	A	A	A
	0.0136 (0.78)	0.0120 (0.69)	0.0110 (0.63)
	0.0051 (0.29)	0.0058 (0.33)	0.0038 (0.22)
	0.1902 (10.9)	0.5200 (29.8)	0.5741 (32.9)



FOR $\alpha > 1.57$ RADIANS (90 DEGREES),
"a" LIES BETWEEN
 E_C AND E_{θ}

Table 8.5-8. Velocity Errors During Thor Probe Maneuvers

	PROBE EVENT			
	RT1	RT2	RT3	RT4
ΔV (M/S)	1.02	7.32	6.34	26.55
ATTITUDE DETERMINATION ERROR [RAD (DEG)]	0.0091 (0.52)	0.0112 (0.64)	0.0136 (0.78)	0.0109 (0.62)
VELOCITY DISPERSION ANGLE [RAD (DEG)]	0.0044 (0.25)	0.0369 (2.0)	0.0436 (2.5)	0.0087 (0.50)
COMBINED VELOCITY ERROR ANGLE [RAD (DEG)]	0.0101 (0.58)	0.0366 (2.10)	0.0455 (2.61)	0.0140 (0.80)
RADIAL VELOCITY ERROR (M/S)	0.01	0.27	0.29	0.37
AXIAL VELOCITY ERROR (M/S)	0.03 TO 0.06	0.22 TO 0.44	0.19 TO 0.38	0.77 TO 1.00
TOTAL VELOCITY ERROR (M/S)	0.032 TO 0.061	0.35 TO 0.52	0.35 TO 0.48	0.86 TO 1.00

Table Determination Accuracies

Table 8.5-10. Reaction Control System Performance of Thor/Delta Configurations



Table 8.5-1

SPIN SPEED CHANGE		PRECESSION [RAD (DEG)]		PEAK NUTATION FACTOR	ΔV (M/S)		TRANSVERSE THRUSTER ΔV (M/S) REV 2-SECOND PULSES TWO FIRINGS/REV
125 MS (RAD/S) PULSE (RPM, PULSE)	CONTINUOUS (RAD/S) (RPM, S)	125 MS PULSE	31.25 MS PULSE		125 MS PULSE	CONTINUOUS (PER SECOND)	
0.0071 (0.068)	0.0565 (0.54)	0.0138 (0.79)	0.0035 (0.20)	1.46	0.0054	0.026	0.104
0.0040 (0.038)	0.0314 (0.030)	0.0077 (0.44)	0.0019 (0.11)	1.46	0.0018	0.014	0.056
0.0032 (0.031)	0.0262 (0.25)	0.0065 (0.37)	0.0016 (0.09)	1.46	0.0015	0.012	0.048
0.0037 TO 0.0073 (0.035 TO 0.070)	0.0293 TO 0.0586 (0.28 TO 0.56)	0.0070 TO 0.0140 (0.40 TO 0.80)	0.0017 TO 0.0035 (0.10 TO 0.20)	1.88	0.0023 TO 0.0046	0.018 TO 0.036	0.072 TO 0.144
0.0043 TO 0.0086 (0.041 TO 0.082)	0.0346 TO 0.0691 (0.33 TO 0.66)	0.0086 TO 0.0171 (0.49 TO 0.98)	0.0021 TO 0.0042 (0.12 TO 0.24)	1.55	0.0026 TO 0.0052	0.021 TO 0.042	0.084 TO 0.168
0.0057 TO 0.0113 (0.054 TO 0.108)	0.0450 TO 0.0901 (0.43 TO 0.86)	0.0108 TO 0.0216 (0.62 TO 1.24)	0.0026 TO 0.0052 (0.15 TO 0.30)	1.35	0.0031 TO 0.0062	0.025 TO 0.050	0.100 TO 0.200
0.0069 TO 0.0138 (0.066 TO 0.132)	0.0555 TO 0.0111 (0.53 TO 0.106)	0.0136 TO 0.0272 (0.78 TO 1.56)	0.0033 TO 0.0066 (0.19 TO 0.38)	1.27	0.0039 TO 0.0078	0.031 TO 0.062	0.124 TO 0.248
0.0062 TO 0.0124 (0.059 TO 0.118)	0.0492 TO 0.0984 (0.47 TO 0.94)	0.0120 TO 0.0241 (0.69 TO 1.38)	0.0030 TO 0.0059 (0.17 TO 0.34)	1.31	0.0035 TO 0.0070	0.028 TO 0.056	0.112 TO 0.224
0.1131 (0.108)	0.0901 (0.86)	0.0222 (1.27)	0.0058 (0.33)	1.04	0.0043	0.034	0.136
0.0063 (0.060)	0.0503 (0.48)	0.0124 (0.71)	0.0031 (0.18)	1.05	0.0024	0.019	0.076
0.0052 (0.050)	0.0419 (0.40)	0.0105 (0.60)	0.0026 (0.15)	1.05	0.0020	0.016	0.064
0.0052 TO 0.0104 (0.050 TO 0.100)	0.0419 TO 0.0838 (0.40 TO 0.80)	0.0105 TO 0.0209 (0.60 TO 1.20)	0.0026 TO 0.0052 (0.15 TO 0.30)	1.10	0.0018 TO 0.0036	0.014 TO 0.028	0.056 TO 0.112
0.0052 TO 0.0104 (0.050 TO 0.100)	0.0424 TO 0.0858 (0.41 TO 0.82)	0.0106 TO 0.0213 (0.61 TO 1.22)	0.0026 TO 0.0052 (0.15 TO 0.30)	1.08	0.0025 TO 0.0050	0.020 TO 0.040	0.80 TO 1.60
0.0053 TO 0.0105 (0.051 TO 0.102)	0.0387 TO 0.0775 (0.37 TO 0.74)	0.0096 TO 0.0192 (0.55 TO 1.10)	0.0024 TO 0.0049 (0.14 TO 0.28)	1.04	0.0025 TO 0.0050	0.020 TO 0.040	0.80 TO 1.60
0.0048 TO 0.0105 (0.046 TO 0.092)	0.0398 TO 0.0796 (0.38 TO 0.76)	0.0098 TO 0.0195 (0.56 TO 1.12)	0.0024 TO 0.0049 (0.14 TO 0.28)	1.05	0.0024 TO 0.0048	0.019 TO 0.038	0.072 TO 0.144

CONDITION	SPIN SPEED CHANGE	
	125 MS [RAD/S]/PULSE (RPM/PULSE)	CONTINUOUS [RAD/S]
PROBE		
CRUISE:		
100 PERCENT N_2H_4	0.0031 (0.030)	0.0251
50 PERCENT	0.0018 (0.017)	0.0147
20 PERCENT	0.0016 (0.015)	0.0126
AFTER:		
LP	0.0018 TO 0.0034 (0.017 TO 0.032)	0.0147 TO 0.0294 (0.14 TO 0.28)
SP1	0.0020 TO 0.0040 (0.019 TO 0.038)	0.0157 TO 0.0314 (0.15 TO 0.30)
SP2	0.0027 TO 0.0054 (0.026 TO 0.052)	0.0208 TO 0.0416 (0.20 TO 0.40)
SP3	0.0036 TO 0.0071 (0.034 TO 0.068)	0.0283 TO 0.0566 (0.27 TO 0.54)
END OF MISSION	0.0025 TO 0.0050 (0.024 TO 0.048)	0.0199 TO 0.0398 (0.19 TO 0.38)
ORBITER		
CRUISE:		
100 PERCENT N_2H_4	0.0057 (0.054)	0.0450
50 PERCENT	0.0031 (0.030)	0.0251
20 PERCENT	0.0026 (0.025)	0.0209
ENCOUNTER*	0.0029 TO 0.0059 (0.028 TO 0.056)	0.0230 TO 0.0460 (0.22 TO 0.44)
IN ORBIT*	0.0029 TO 0.0059 (0.028 TO 0.056)	0.0230 TO 0.0460 (0.22 TO 0.44)
IN ORBIT**	0.0024 TO 0.048 (0.023 TO 0.046)	0.0188 TO 0.0376 (0.18 TO 0.36)
END OF MISSION	0.0022 TO 0.0044 (0.021 TO 0.042)	0.0170 TO 0.0340 (0.17 TO 0.34)

* MAGNETOMETER RETRACTED.
** MAGNETOMETER DEPLOYED.

5-8. Velocity Errors During Thor/Delta Probe Maneuvers

Table 8.5-9. Velocity Errors During Atlas/Centaur Probe Bus Maneuvers

	PROBE EVENT			
	RT1	RT2	RT3	RT4
	1.02	7.32	6.34	26.55
TERMINATION (DEG)	0.0091 (0.52)	0.0112 (0.64)	0.0136 (0.78)	0.0109 (0.63)
DISPERSION (DEG)	0.0044 (0.25)	0.0349 (2.0)	0.0436 (2.5)	0.0087 (0.50)
VELOCITY ERROR (RAD (DEG))	0.0101 (0.58)	0.0756 (2.10)	0.0455 (2.61)	0.0140 (0.80)
VELOCITY ERROR	0.01	0.27	0.29	0.37
VELOCITY ERROR	0.03 TO 0.06	0.22 TO 0.44	0.19 TO 0.38	0.77 TO 1.54
VELOCITY ERROR	0.032 TO 0.061	0.35 TO 0.52	0.35 TO 0.48	0.86 TO 1.58



	PROBE EVENT			
	RT1	RT2	RT3	RT4
ΔV (M/S)	1.02	7.32	6.34	26.55
ATTITUDE DETERMINATION ERROR (RAD (DEG))	0.0091 (0.52)	0.0112 (0.64)	0.0136 (0.78)	0.0109 (0.63)
VELOCITY DISPERSION ANGLE (RAD (DEG))	0.000 (0.00)	0.0762 (1.50)	0.0489 (2.80)	0.0087 (0.50)
COMBINED VELOCITY ERROR ANGLE (RAD (DEG))	0.0091 (0.52)	0.0284 (1.63)	0.0508 (2.91)	0.0140 (0.80)
RADIAL VELOCITY ERROR (M/S)	0.01	0.21	0.32	0.37
AXIAL VELOCITY ERROR (M/S)	0.03 TO 0.06	0.22 TO 0.44	0.19 TO 0.38	0.77 TO 1.54
TOTAL VELOCITY ERROR (M/S)	0.32 TO 0.061	0.32 TO 0.51	0.37 TO 0.50	0.85 TO 1.58



Table 8.5-11. Reaction Control System Performance of Atlas/Centaur Configuration

CONDITION	SPIN SPEED CHANGE		PRECESSION (RAD (DEG))		PEAK MUTATION FACTOR	ΔV (M/S)		TRANSVERSE THRUSTER ΔV (M/S)/REV 2-SECOND PULSES TWO FIRINGS/REV
	125 MS (RAD/S)/PULSE (RPM/PULSE)	CONTINUOUS (RAD/S ² (RPM/S ²))	125 MS PULSE	31.25 MS PULSE		125 MS PULSE	CONTINUOUS (PER SECOND)	
PROBE								
CRUISE:								
100 PERCENT N_{2H_4}	0.0031 (0.030)	0.0251 (0.24)	0.0063 (0.36)	0.0016 (0.090)	1.48	0.0016	0.014	0.056
50 PERCENT	0.0018 (0.017)	0.0147 (0.14)	0.0035 (0.20)	0.0009 (0.050)	1.48	0.0009	0.007	0.028
20 PERCENT	0.0016 (0.015)	0.0126 (0.12)	0.0031 (0.18)	0.0008 (0.045)	1.48	0.008	0.006	0.024
AFTER:								
LP	0.0018 TO 0.0034 (0.017 TO 0.032)	0.0147 TO 0.0293 (0.14 TO 0.28)	0.0033 TO 0.0066 (0.19 TO 0.38)	0.008 TO 0.0017 (0.048 TO 0.096)	1.79	0.0011 TO 0.0022	0.009 TO 0.018	0.036 TO 0.072
SP1	0.0020 TO 0.0040 (0.019 TO 0.038)	0.0157 TO 0.0314 (0.15 TO 0.30)	0.0040 TO 0.0080 (0.23 TO 0.46)	0.0010 TO 0.0020 (0.058 TO 0.116)	1.56	0.0014 TO 0.0028	0.012 TO 0.024	0.048 TO 0.096
SP2	0.0027 TO 0.0054 (0.026 TO 0.052)	0.0209 TO 0.0419 (0.20 TO 0.40)	0.0054 TO 0.0108 (0.31 TO 0.62)	0.0014 TO 0.0027 (0.078 TO 0.156)	1.38	0.0019 TO 0.0038	0.014 TO 0.028	0.56 TO 0.112
SP3	0.0036 TO 0.0071 (0.034 TO 0.068)	0.0283 TO 0.0565 (0.27 TO 0.54)	0.0072 TO 0.0143 (0.41 TO 0.82)	0.0018 TO 0.0036 (0.102 TO 0.204)	1.34	0.0024 TO 0.0048	0.019 TO 0.038	0.076 TO 0.152
END OF MISSION	0.0025 TO 0.0050 (0.024 TO 0.048)	0.0199 TO 0.0398 (0.19 TO 0.38)	0.0051 TO 0.0101 (0.29 TO 0.58)	0.0013 TO 0.0025 (0.072 TO 0.144)	1.51	0.0022 TO 0.0044	0.018 TO 0.036	0.072 TO 0.144
ORBITER								
CRUISE:								
100 PERCENT N_{2H_4}	0.0057 (0.034)	0.0450 (0.43)	0.0113 (0.65)	0.0028 (0.162)	1.06	0.0029	0.024	0.096
50 PERCENT	0.0031 (0.030)	0.0251 (0.24)	0.0063 (0.36)	0.0016 (0.090)	1.06	0.0016	0.014	0.056
20 PERCENT	0.0026 (0.025)	0.0209 (0.20)	0.0052 (0.30)	0.0013 (0.075)	1.06	0.0014	0.011	0.044
ENCOUNTER*	0.0029 TO 0.0059 (0.028 TO 0.056)	0.0230 TO 0.0461 (0.22 TO 0.44)	0.0059 TO 0.0119 (0.34 TO 0.68)	0.0015 TO 0.0030 (0.085 TO 0.170)	1.01	0.0013 TO 0.0026	0.010 TO 0.020	0.040 TO 0.080
IN ORBIT*	0.0029 TO 0.0059 (0.028 TO 0.056)	0.0230 TO 0.0461 (0.22 TO 0.44)	0.0059 TO 0.0119 (0.34 TO 0.68)	0.0015 TO 0.0030 (0.085 TO 0.170)	1.03	0.0018 TO 0.0036	0.014 TO 0.028	0.056 TO 0.112
IN ORBIT**	0.0024 TO 0.048 (0.023 TO 0.046)	0.0188 TO 0.0377 (0.18 TO 0.36)	0.0049 TO 0.0098 (0.28 TO 0.56)	0.0012 TO 0.0024 (0.070 TO 0.140)	1.09	0.0018 TO 0.0036	0.014 TO 0.028	0.056 TO 0.112
END OF MISSION	0.0022 TO 0.0044 (0.021 TO 0.042)	0.0178 TO 0.0356 (0.17 TO 0.34)	0.0044 TO 0.0087 (0.25 TO 0.50)	0.0011 TO 0.0022 (0.062 TO 0.124)	1.07	0.0015 TO 0.0030	0.012 TO 0.024	0.048 TO 0.096

* MAGNETOMETER RETRACTED.
** MAGNETOMETER DEPLOYED.

HOLDOUT PRA

The relative trajectories shown in Figure 8.5-33 show only one probe interferes with the deployed magnetometer boom, thereby requiring retraction of the boom for release of this probe. The relative trajectories of the first and third probes released begin in a direction along a radial line passing through the spacecraft centerline; however, the relative trajectory of the second probe released begins in a direction approximately 0.157 rad (9 deg) off a radial line due to the center-of-mass offset of the bus and last remaining probe at that time.

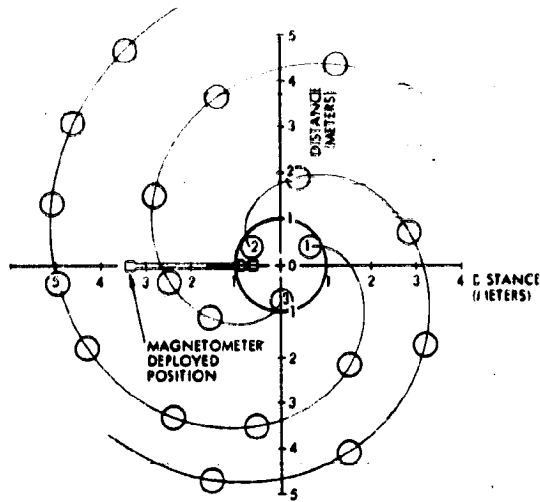


Figure 8.5-33. Small Probe Trajectories Relative to Probe Bus Coordinate System

The small probes are released sequentially from the bus with no impulse imparted to the probe by the release mechanism. As a result,

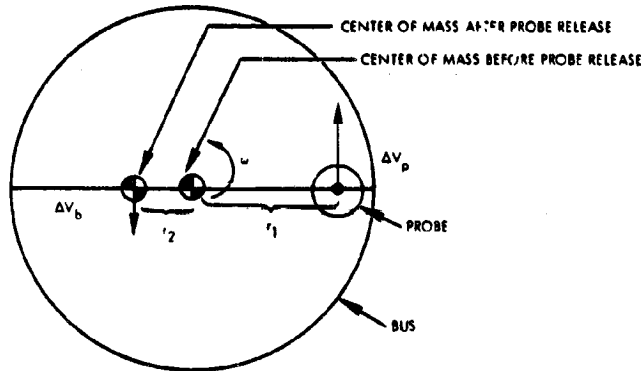


Figure 8.5-34. Small Probe Release Geometry

Table 8.5-12. Velocity Increments Produced by Small Probe Releases

EVENT	R ₁ (M)	R ₂ (M)	ΔV _{PROBE} (M/S)	ΔV _{BUS} (M/S)
FIRST SMALL PROBE RELEASE	0.83	0.13	0.43	-0.069
SECOND SMALL PROBE RELEASE	0.77	0.145	0.40	-0.076
THIRD SMALL PROBE RELEASE	0.68	0.15	0.35	-0.078

*THE ΔV'S IMPARTED DURING THE SECOND PROBE RELEASE WILL BE IN A DIRECTION APPROXIMATELY 0.157 RADIAN (9 DEGREES) OFF PERPENDICULAR TO THE RADIAL LINE CONNECTED TO THE CENTER OF THE PROBE AND THE CENTER OF THE SPACECRAFT DUE TO THE CENTER OF MASS LOCATION PRIOR TO SECOND PROBE RELEASE.

each probe travels in an inertial direction perpendicular to a radial line connecting the spacecraft and the probe centers of mass at the instant of release as shown in Figure 8.5-34. No change of either probe or bus spin rate occurs as a result of probe release. The velocity changes imparted to the probe and bus are $\Delta V_p = \omega r_1$; $\Delta V_b = \omega r_2$; where ω is the spin rate. Nominal values for the velocity increments expected in the Thor/Delta configuration are given in Table 8.5-12.

During small probe release, disturbances can induce transverse rates that will cause precession of the momentum vector and nutation of the spin axis. One source of disturbance torques is the preload energy in the release mechanism. This energy can produce a force misaligned with the probe center of mass as shown in Figure 8.5-35.

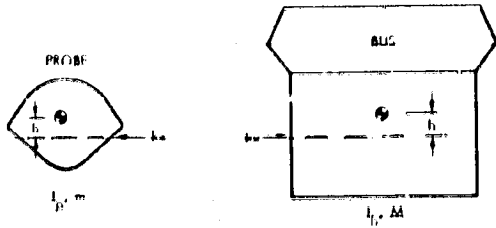


Figure 8.5-35. Forces Inducing Traverse Rates During Small Probe Release

The curves in Figure 8.5-36 indicate the magnitude of the errors as a function of the various parameters. Since the center of mass of the small probe lies approximately 2 centimeters above the plane of the release

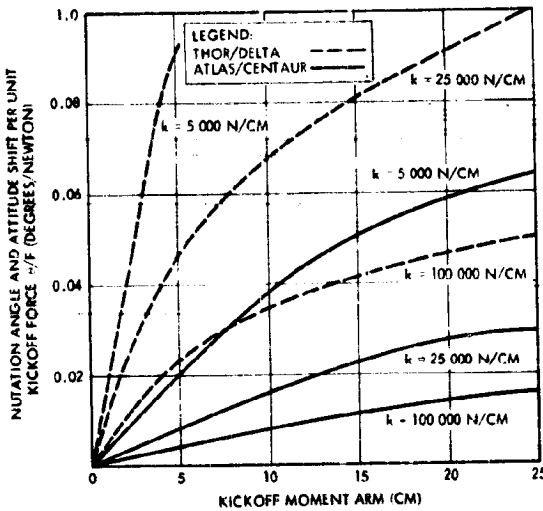



Figure 8.5-36. Small Probe Tipoff Errors for a Preloaded Release System

mechanism, it can be determined from the curves that only small preload forces can be allowed. For example, using a relatively stiff release mechanism structure, i.e., $k = 1.05 \times 10^7$ N/m, a preload force of approximately 50 newtons (11 pounds) will induce 0.017 rad (1 deg) of attitude shift and nutation. Softer structures will induce higher errors for the same preload. Therefore, a design was conceived to release the probe in two stages. The first stage releases the preload, which is necessary to hold the probe firmly during boost. After this preload is released, the probe is restrained in the release mechanism, with only loads due to centrifugal force acting on the structure. This load is approximately 6.5 N (1.5 lb). Therefore, the probe and release mechanism structure is required to produce a stiffness of only 440 N/cm (250 lb/in.) to limit the attitude shift and nutation to less than 0.017 rad (1 deg). This can be achieved easily.


Another source of attitude disturbance is the shift of the spacecraft principal axis after each probe is released, due to the errors in aligning

the probe center of mass and the spacecraft center of mass in the same plane perpendicular to the spin axis. The small probe attitude shift and nutation will be equal to the spacecraft principal axis tilt due to this effect.

 T/D III The large probe is separated from the bus by unlocking three ball-lock bolts, thereby allowing the three separation springs to impart an axial relative velocity of about 0.3 m/s (1 ft/s) to both probe and bus. The resulting inertial velocity changes are 0.196 m/s (0.65 ft/s) for the probe and -0.124 m/s (0.41 ft/s) for the bus. Uncertainties in these values can be limited to less than ± 5 percent by calibrating the separation springs.

The separation event will also produce disturbances that will precess the probe momentum vector and induce nutation. A summary of the error analysis including contributions from various sources is given in Table 8.5-13.

Table 8.5-13. Large Probe Separation Tipoff Errors

 T/D III

DISTURBANCE	TRANSVERSE ANGULAR RATE (RAD/S)	MOMENTUM VECTOR SHIFT AND NUTATION ANGLE (RAD/DEG)
NET LATERAL SPRING FORCE (1 NEWTON (0.22 POUND))	0.005	0.009 (0.5)
ANGULAR SPRING RATE DIFFERENTIAL (.2 PERCENT)	0.006	0.010 (0.6)
COMPRESSED HEIGHT OF EACH SPRING (0.25 CENTIMETER (0.02 INCH))	0.005	0.009 (0.5)
SPRING RADIAL LOCATION (0.15 CENTIMETER (0.06 INCH))	0.001	0.002 (0.1)
BALL-LOCK RELEASE DIFFERENTIAL (5 MILLISECONDS)	0.003	0.005 (0.3)
RSS TOTAL	0.01	0.017 (1.0)

8.5.8.2 Orbiter Mission A/C III T/D III

Detailed attitude determination and control performance analyses have been done for both the Thor/Delta and Atlas/Centaur configurations. The subjects considered include disturbance torque analyses during cruise and orbit, dynamic analyses of all maneuvers, reaction control subsystem performance evaluation, attitude determination accuracy analyses, and an analysis of the communications antenna and science instrument pointing requirements.

Following the approach used in the preceding section, results are presented in chronological order. Where applicable, data for the Thor/Delta and the Atlas/Centaur configurations are given separately.

Separation from Booster $\begin{matrix} \leftarrow (31W) \\ \rightarrow \end{matrix}$ A/C III $\begin{matrix} \leftarrow (31W) \\ \rightarrow \end{matrix}$ T/D III

A third stage burnout, the Thor/Delta-launched orbiter spacecraft will be spinning at $9.42 \begin{matrix} +2.83 \\ -1.47 \end{matrix}$ rad/s ($90 \begin{matrix} +27 \\ -14 \end{matrix}$ rpm). Assuming a combined spin moment of inertia of $96.5 \text{ kg}\cdot\text{m}^2$ ($71 \text{ slug}\cdot\text{ft}^2$), an inertia parameter $\lambda = 0.45$, and other parameters as in the probe bus case, the peak nutation angle will be on the order of 0.087 radian (5 degrees) at the maximum spin speed of 7.95 rad/s (76 rpm).

After separation, a nutation angle of 0.035 radian (2 degrees) is predicted when the following assumptions are made:

- Nutation angle before separation = 0.087 radian (5 degrees)
- Average transverse MOI after separation = $65.5 \text{ kg}\cdot\text{m}^2$ ($46 \text{ slug}\cdot\text{ft}^2$)
- Average transverse MOI before separation = $177 \text{ kg}\cdot\text{m}^2$ ($130 \text{ slug}\cdot\text{ft}^2$)
- Spin MOI after spacecraft separation = $91.1 \text{ kg}\cdot\text{m}^2$ ($64 \text{ slug}\cdot\text{ft}^2$)
- Spin MOI before separation = $101.1 \text{ kg}\cdot\text{m}^2$ ($71 \text{ slug}\cdot\text{ft}^2$)
- Other parameters same as for probe bus.

The momentum shift will be approximately 0.087 radian (5 degrees) and the nutation damper time constant for the Thor/Delta orbiter after separation is on the order of 15 minutes at 0.52 rad/s (5 rpm).

The Atlas/Centaur-launched spacecraft will be initially oriented and spun up to 0.52 rad/s (5 rpm) by the Centaur. Since no data on Centaur operation at 0.52 rad/s (5 rpm) are available at the present time, the corresponding analysis of separation dynamics could not be completed.

Despin Maneuver $\begin{matrix} \leftarrow (31W) \\ \rightarrow \end{matrix}$ T/D III

The initial spin rate of the Thor/Delta spacecraft after separation is $9.42 \begin{matrix} +2.83 \\ -1.47 \end{matrix}$ rad/s ($90 \begin{matrix} +27 \\ -14 \end{matrix}$ rpm). By command, the control system will be operated to reduce the spin speed down to 0.61 rad/s (5.8 rpm). The nominal rate of 0.5 rad/s (4.8 rpm) will be attained after the magnetometer boom is deployed (Version III science payload).

Assuming an average deceleration rate of 0.09 rad/s^2 (0.86 rpm/s), the required firing time will be in the range from 82 to 129 seconds.

Based on calculations made for the probe bus, it follows that magnetometer boom deployment loads due to nutation and Coriolis effects will be small for the orbiter also.

Cruise Phase Attitude Determination and Control $\leftarrow \begin{matrix} 31 W \\ \text{A/C III} \end{matrix} \leftarrow \begin{matrix} 31 W \\ \text{T/D III} \end{matrix}$

Figure 8.5-37 is a stereographic projection showing locations of the sun and earth and spin axis orientations during orbiter cruise. Initially, the spacecraft will point south in the orientation designated A in the figure. During the first 5 days, this attitude will allow communications with the omni and the high-gain antennas. After the first midcourse correction, planned on day 5, the spacecraft will be precessed to the B orientation, near which it will remain for the next 50 days until the second midcourse correction is executed. After the second midcourse maneuver, the cruise attitude will be C. After 200 days, the cruise orientation will be D. From there, the vehicle will be precessed to point E for Venus orbit insertion. A syzygy condition occurs on day 168, when the sun, the earth, and the spacecraft are almost aligned.

ALL FANBEAM, FANSCAN ORBITERS

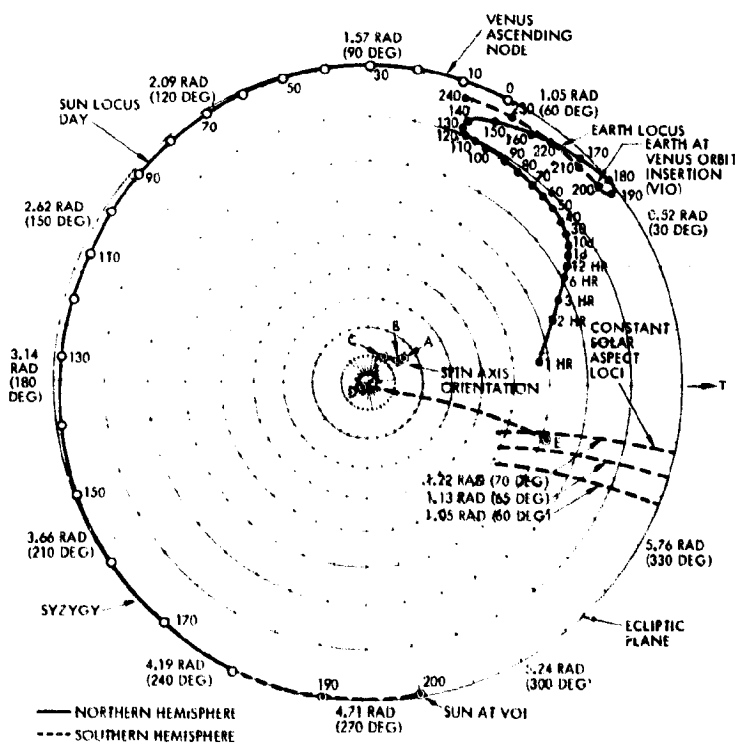


Figure 8.5-37. Stereographic Projection Showing Sun-Earth-Spacecraft Geometry During Orbiter Cruise

Attitude drift during cruise is produced by solar pressure torques. Disturbance torque analysis results for the Thor/Delta and Atlas/Centaur configurations are given in Figure 8.5-38. Drift rates are larger in the Thor/Delta configuration because the solar array height and, consequently, the offset between centers of pressure and mass are greater than in the Atlas/Centaur configurations. Precession caused by solar pressure is always about the line joining the spacecraft and the sun. Consequently, at any given point in time, the solar pressure drift will change the earth aspect angle at a rate dependent on the earth-vehicle-sun angle. As the inertial location of the sun (in a vehicle-centered coordinate system) changes with time, any accumulated precession due to solar pressure will also include a small component, which will appear as a sun aspect drift.

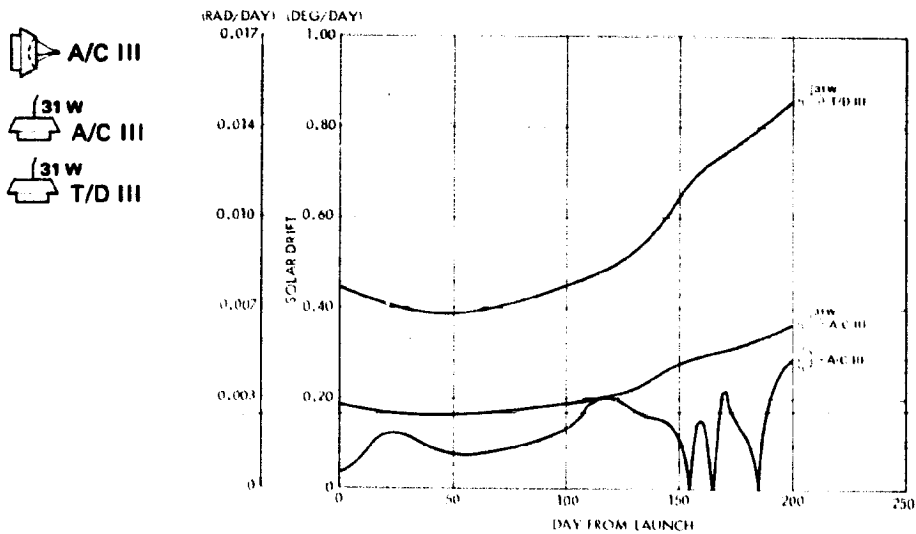


Figure 8.5-38. Solar Pressure Drift Rate Versus Time Orbiter Cruise Phase

Figure 8.5-37 shows that precession caused by the solar pressure during the 50-day period following the first midcourse correction will be almost along the desired locus from B to C. During this period, the Thor/Delta configuration would precess about 0.35 radian (20 degrees), while the Atlas/Centaur spacecraft would drift only 0.15 radian (8.5 degrees).

The frequency with which attitude corrections have to be made depends on the pointing error allowance during cruise. Assuming a maximum pointing error of 0.0524 radian (3 degrees) and corrections to bias

31 W
 A/C III solar pressure effects, intervals between maneuvers for the Thor/Delta
 31 W
 T/D III orbiter would vary from 7 to 15 days. For the Atlas/Centaur configura-
 tion, the corresponding intervals would be in the range from 17 to 35 days.
 Consequently, for the Atlas/Centaur configuration, only one attitude
 correction may be necessary during the interval between first and second
 midcourse corrections.

The sun aspect sensor and the fanscan system provide attitude
 determination information. Sun aspect measurements are made with
 accuracies estimated by the same model assumed for the probe bus space-
 craft. During cruise, fanscan will provide data from which earth aspect
 angle can be determined with an accuracy better than 0.0044 radian
 (0.25 degree), 3σ . The overall attitude determination accuracy is also a
 function of the sun-vehicle-earth angle. Figure 8.5-39 is a plot of attitude
 determination accuracy during orbiter cruise. Except during syzygy con-
 ditions, attitude determination errors will be well below the 0.0175-radian
 (1-degree) limit. All critical functions can be performed at times when
 attitude information quality is such that no degradation of mission objec-
 tives will occur.

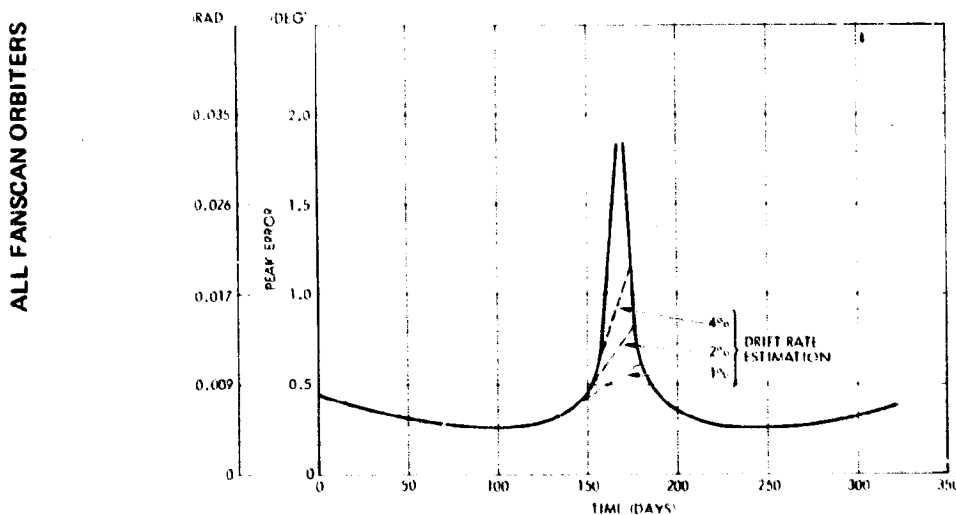


Figure 8.5-39. Attitude Determination Accuracy During Orbiter Cruise

The attitude determination accuracy during syzygy can be improved
 by prediction of the drift due to solar pressure effects as shown in Fig-
 ure 8.5-39, where a 2-percent estimation accuracy (easily attainable
 after 150 days of tracking) is shown bounding the error to less than the
 required 0.0175 radian (1 degree) limit.

Earth aspect angle information during midcourse maneuvers is obtained by doppler measurements. Consequently, the corresponding attitude determination accuracies will be in the ± 0.0077 to ± 0.0209 radian (± 0.44 to ± 1.2 degree) as in the probe bus configurations.

Midcourse Maneuvers

Tables 8.5-14 and 8.5-15 contain summaries of attitude errors, velocity dispersions, and spin rate variations that may occur during midcourse maneuvers with the Thor/Delta and the Atlas/Centaur orbiter configurations. Attitude determination errors are not included because the orientations at which these maneuvers should be executed are not defined at present. Assumptions made in the error analyses are shown

Table 8.5-14. Thor/Delta Orbiter Dynamic Disturbances

(31 W) T/D III

EVENT	ΔV (M/S)	THRUST EACH THRUSTER (N (LB))	SPIN RATE CHANGE (RAD/S (RPM))	ANGLE OF ATTACK ERROR (RAD (DEG))	MOMENTUM VECTOR SHIFT (RAD (DEG))	VELOCITY DISPERSION ANGLE (RAD (DEG))	VELOCITY DEGRADATION (M/S)	NUTATION ANGLE (RAD (DEG))
SEPARATION FROM BOOSTER	0.25*		0 (0)		0.087 (5)			0.035 (2)
FIRST MIDCOURSE	7	5.2 (1.17)	± 0.31 (± 12.5)	0.084 (4.8)	0.023 (1.3)	0.012 (0.7)	0.11	0.061 (3.5)
SECOND MIDCOURSE	7	3.1 (0.7)	± 0.13 (± 1.2)	0.051 (2.9)	0.014 (0.8)	0.007 (0.4)	0.004	0.037 (2.1)
THIRD MIDCOURSE	2	3.1 (0.7)	± 0.03 (± 0.35)	0.051 (2.9)	0.014 (0.8)	0.007 (0.4)	0.001	0.037 (2.1)
DEBOOST		28 500 (6400)	0 (0)	0.154 (8.8)	0.042 (2.4)	0.021 (1.2)	(0.5%)	0.112 (6.4)
PERIAPSIS TRIM ΔV (TOTAL)	43.5	3.1 (0.7)	± 0.52 (± 5)	0.037 (2.1)	0.010 (0.6)	0.005 (0.3)	0.013	0.026 (1.5)

* ASSUMES 1 M/S RELATIVE VELOCITY AT SEPARATION.

OTHER ASSUMPTIONS: 9-MILLIRADIAN THRUSTER MISALIGNMENT
 +4 PERCENT THRUST LEVEL UNCERTAINTY FOR EACH THRUSTER
 0.32 RAD/S (5 RPM) SPIN RATE DURING MIDCOURSE AND PERIAPSIS TRIM MANEUVERS
 6.28 RAD/S (60 RPM) SPIN RATE DURING DEBOOST (VENUS ORBIT INSERTION).

Table 8.5-15. Atlas/Centaur Orbiter Dynamic Disturbances

(31 W) A/C III

EVENT	ΔV (M/S)	THRUST EACH THRUSTER (N (LB))	SPIN RATE CHANGE (RAD/S (RPM))	ANGLE OF ATTACK ERROR (RAD (DEG))	MOMENTUM VECTOR SHIFT (RAD (DEG))	VELOCITY DISPERSION ANGLE (RAD (DEG))	VELOCITY DEGRADATION (M/S)	NUTATION ANGLE (RAD (DEG))
FIRST MIDCOURSE	14.5	5.2 (1.17)	± 0.293 (± 2.8)	0.072 (4.1)	0.024 (1.4)	0.012 (0.7)	0.015	0.047 (2.7)
SECOND MIDCOURSE	7	5.2 (1.17)	± 0.147 (± 1.4)	0.072 (4.1)	0.024 (1.4)	0.012 (0.7)	0.007	0.047 (2.7)
THIRD MIDCOURSE	2	5.2 (1.17)	± 0.042 (± 0.4)	0.072 (4.1)	0.024 (1.4)	0.012 (0.7)	0.002	0.047 (2.7)
DEBOOST		21 300 (4800) MAXIMUM	0 (0)	0.065 (3.7)	0.021 (1.2)	0.010 (0.6)	(0.1%)	0.045 (2.5)
PERIAPSIS TRIM ΔV (TOTAL)	43.5	5.2 (1.17)	± 0.785 (± 7.5)	0.072 (4.1)	0.024 (1.4)	0.012 (0.7)	0.04	0.047 (2.7)

ASSUMPTIONS: 9-MILLIRADIAN THRUSTER MISALIGNMENT
 +4 PERCENT THRUST LEVEL UNCERTAINTY FOR EACH THRUSTER
 0.32 RAD/S (5 RPM) SPIN RATE FOR MIDCOURSE AND PERIAPSIS TRIM MANEUVERS
 6.28 RAD/S (60 RPM) SPIN RATE FOR DEBOOST MANEUVER (VENUS ORBIT INSERTION).

with the tables, and considerations of the magnitude of the various error sources and definitions of parameters are similar to those for the probe bus spacecraft.

Venus Orbit Insertion Maneuver

The Venus orbit insertion maneuver will be executed on day 200. The orientation required for this maneuver is shown as point E in Figure 8.5-37, where the sun aspect angle will be about 1.19 radian (68 degrees) and the earth aspect angle will be 1.045 radian (60 degrees), approximately. The spacecraft precession required (from D to E) is on the order of 1.08 radians (62 degrees).

Since the earth will be on the forward side of the spacecraft, where the omni antenna is on center, no doppler information will be available for attitude determination unless a small ΔV maneuver is executed. The approach proposed consists in executing an open-loop precession maneuver from D to E. Assuming an impulse bit predictability error of 3 percent, the execution error along the constant rhumb path would be about 0.03 radian (1.9 degrees). However, the accuracy of execution can be improved significantly by information provided by the sun aspect sensor. For instance, the sun aspect angle at the end of the constant-rhumb maneuver is known, and the angles between the precession path and the constant solar aspect loci are predictable. For the assumed geometry, the sun sensor error is about 0.0038 radian (0.22 degree) and the angle between the rhumb line and the constant sun aspect locus at E is on the order of 0.47 radian (27 degrees). Consequently, the uncertainty along the rhumb line could be theoretically reduced to about 0.0085 radian (0.49 degree). If other effects such as dispersion across the rhumb line direction and trim maneuver errors are included, the overall error will be in the 0.01 to 0.012 radian (0.6 to 0.7 degree) range.

Attitude Determination and Control in Orbit

Figure 8.5-40 shows sun and earth locations (in ecliptic coordinates) during the orbit phase. Point E represents the spin axis orientation after the deboost maneuver. Point F corresponds to the attitude that would optimize communications, while point G is the preferred orientation for science instrument pointing (perpendicular to the Venus orbit plane).

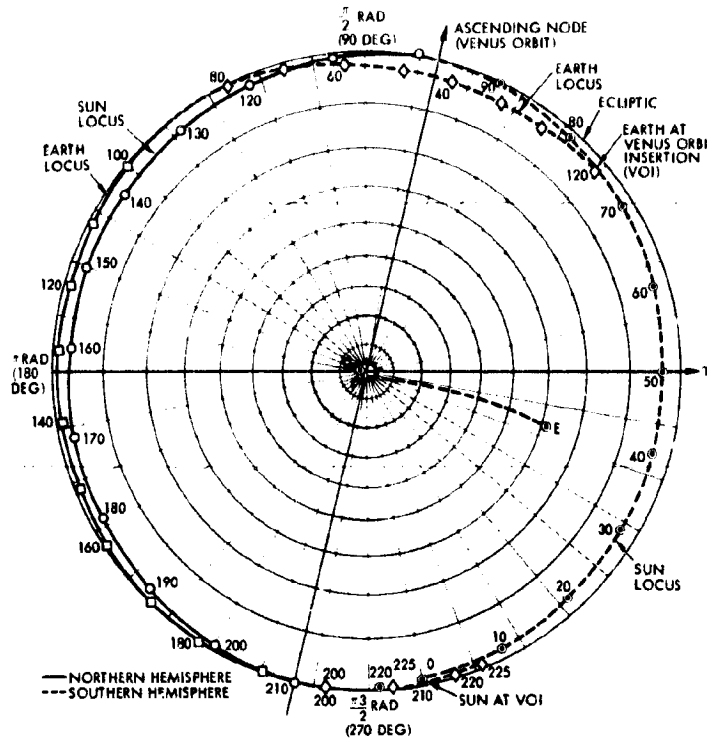


Figure 8.5-40. Sterographic Projection Showing Sun-Earth-Spacecraft Geometry in Orbit

Inspection of the graph shows that there are periods during which the spacecraft can be normal to the Venus orbit plane without affecting communications (i. e., 140 days after VOI). Therefore, the selected orientation policy consists of pointing as close to G as allowed by communication constraints.

(31 W)
T/D III

Disturbance torques in Venus orbit are mainly due to solar pressure [0.014 radian (0.80 deg)/day drift rate for the Thor/Delta orbiter]. Drift rates caused by gravity gradient and aerodynamic torques are at least one order of magnitude lower than the effects of solar pressure [i. e., the drift rate induced by gravity gradient is of the order of 0.0008 radian (0.045 deg)/day and aerodynamic torques cause precessions of the order of 0.0002 radian (0.011 deg)/day at 200 km periapsis altitudes]. Attitude drifts produced by environmental disturbance torques are shown in Figure 8.5-41.

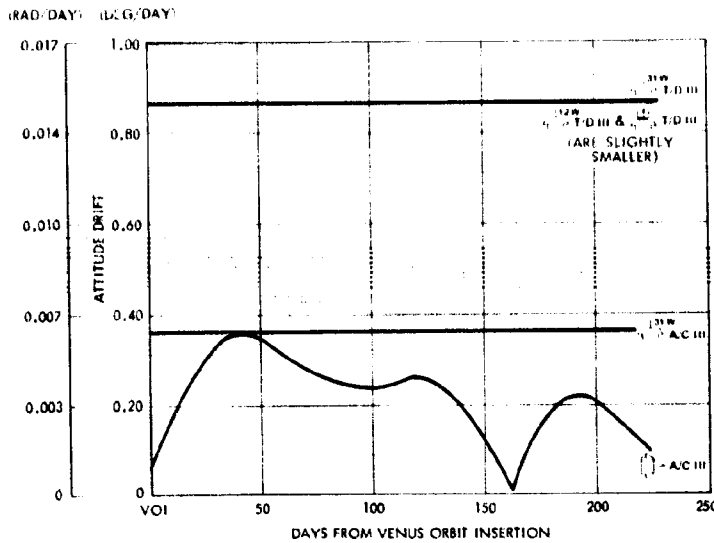


Figure 8.5-41. Attitude Drift Produced by Environmental Disturbance Torques in Orbit

Drift rates caused by solar pressure can be reduced (in the Thor/Delta orbiter case) by either raising the center of mass (requires redistributing equipment) or lowering the center of pressure (by attaching a solar sail or fin to the lower part of the spacecraft).

Antenna-pointing requirements depend on the communication link budget allocations for effects of pointing errors that, in general, are a function of range. Assuming a 1-dB tolerance during the early part of the orbit phase and a maximum loss of 0.3 dB at end of mission, the corresponding earth aspect angle components of the pointing error are 0.029 radian (1.67 degrees) and 0.016 radian (0.9 degree). These maximum allowable errors are based on the assumption of a 1.22-meter (48-inch) Franklin array with a half-power beamwidth of about 0.1 radian (5.8 degrees).

If only communications requirements are considered, the allowable spin-axis-pointing errors may be larger than the above limits because component rotations about the spacecraft-earth line have no effect on antenna gain. Figure 8.5-3A shows, as functions of time, the maximum rotations about the sun line that can be tolerated without exceeding the 1 dB and 0.3 dB attention limits assumed. For the Thor/Delta configuration, the minimum interval between attitude corrections will be 4 days

(31 W) A/C III if precessions are made to bias the pointing in a direction opposite to the expected drift. The Atlas/Centaur configuration will not require attitude corrections more often than once every 9 or 10 days, assuming the same control policy.

(31 W) T/D III

Figure 8.5-3B shows how much the spacecraft may be allowed to precess due to solar pressure effects while still maintaining the ram experiments within specified pointing error limits at periapsis. One interesting conclusion derived from comparing Figures 8.5-3A and 8.5-3B is that, during the first half of the orbit phase, the communications and ram experiment pointing requirements are compatible. After 185 days in orbit, both requirements could be made compatible if the ram experiment pointing error tolerance is increased from 0.35 radian (2 degrees) to 0.525 radian (3 degrees).

Attitude determination accuracies attainable in orbit on the basis of telemetered sun aspect and fanscan information are shown in Figure 8.5-42. The maximum limit of 0.0175 radian (1 degree) is exceeded only during the last 6 days of the mission, when the pointing error can be allowed to be as high as 0.049 radian (2.8 degrees) without violating the assumed ram experiment and communications pointing constraints.

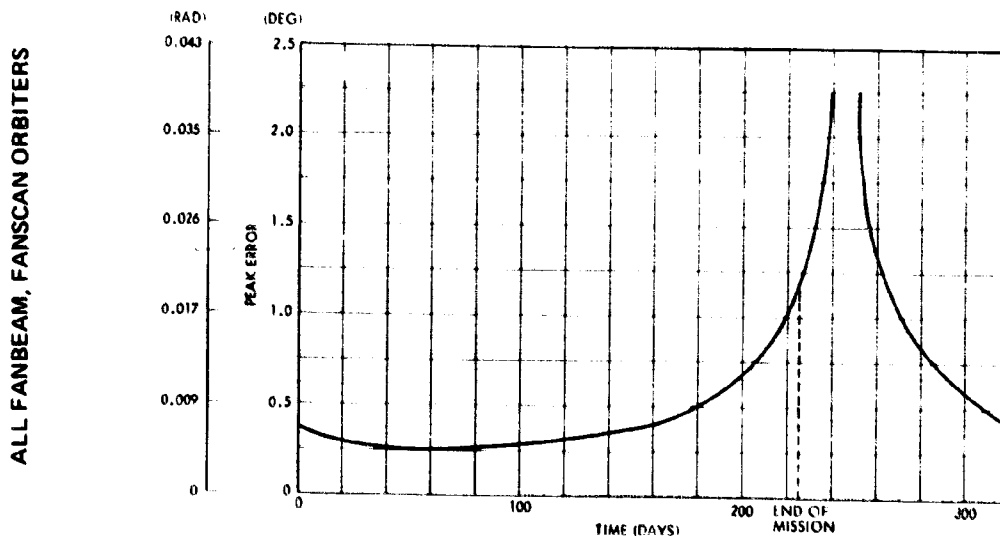


Figure 8.5-42. Attitude Determination Accuracy in Orbit

RCS performance data for the orbiter configurations are given in Tables 8.5-10 and 8.5-11, which include the abilities to precess the spin axis, spin-up and spin-down, and change the spacecraft velocity vector. Precessions and axial velocity changes are performed by a set of four thrusters located at the top and bottom of the spacecraft. Spin control and radial velocity changes are made by a set of four thrusters located on a plane perpendicular to the spin axis and located near the spacecraft's center of mass. RCS performance varies as a function of propellant remaining (blowdown effects) and mass properties. The peak nutation factor is a function of mass properties and thruster firing policy. This factor determines the maximum nutation amplitude based on the precession step size.

Periapsis Maintenance Maneuvers

Orientations for periapsis maintenance maneuvers are shown in Figure 8.5-13. Spin axis attitude determination accuracy calculations for periapsis maintenance are based on the same assumptions and procedures used for the probe mission. Results are included in Table 8.5-16 in terms of total attitude determination errors, which corresponds to the semi-major axes of the associated error ellipses. Peak attitude errors range from 0.007 radian (0.04 degree) to 0.0175 radian (1 degree).

Table 8.5-16. Velocity Errors During Thor/Delta and Atlas/Centaur Orbiter Maneuvers

	THOR DELTA ORBITER EVENT				ATLAS CENTAUR ORBITER EVENT			
	PM1	PM2	PM3	PM4	PM1	PM2	PM3	PM4
ΔV (M/S)	12.3	10.2	12.3	8.7	12.3	10.2	12.3	8.7
ATTITUDE DETERMINATION ERROR RAD (DEG)	0.0070 (0.40)	0.0073 (0.42)	0.0150 (0.86)	0.0171 (0.98)	0.0070 (0.40)	0.0073 (0.42)	0.0150 (0.86)	0.0171 (0.98)
VELOCITY DISPERSION ANGLE RAD (DEG)	0.0052 (0.30)	0.0052 (0.30)	0.0052 (0.30)	0.0052 (0.30)	0.0122 (0.70)	0.0122 (0.70)	0.0122 (0.70)	0.0122 (0.70)
COMBINED VELOCITY ERROR ANGLE RAD (DEG)	0.0087 (0.50)	0.0092 (0.53)	0.0159 (0.91)	0.0178 (1.02)	0.0141 (0.81)	0.0143 (0.82)	0.0192 (1.11)	0.0209 (1.20)
RADIAL VELOCITY ERROR (M/S)	0.11	0.10	0.20	0.16	0.17	0.15	0.24	0.18
AXIAL VELOCITY ERROR (M/S)	0.37 TO 0.74	0.31 TO 0.61	0.37 TO 0.74	0.26 TO 0.52	0.37 TO 0.74	0.31 TO 0.61	0.37 TO 0.74	0.26 TO 0.52
TOTAL VELOCITY ERROR (M/S)	0.39 TO 0.75	0.32 TO 0.62	0.42 TO 0.77	0.31 TO 0.54	0.41 TO 0.76	0.35 TO 0.63	0.44 TO 1.20	0.32 TO 0.55

Periapsis maintenance maneuver execution errors are given in Table 8.5-16 for the Thor/Delta and Atlas/Centaur configurations. Axial velocity errors are caused by uncertainties in the thruster

(31 W)

→ A/C III

(31 W)

→ T/D III

impulse, which have been assessed as ranging from 3 to 6 percent of the desired level. Radial velocity errors result from a combination of attitude errors incurred prior to thrusting and velocity dispersions caused by effects of misalignments while thrusting. Attitude determination errors are due to solar and earth aspect measurement errors and the associated geometry. Velocity dispersion errors were estimated assuming a 9-milliradian thrust vector misalignment for the orbiter configurations, and four percent thruster imbalance was assumed in both cases.

8.5.9 Attitude Determination and Control Performance, Version IV Science Payload, 1978 Probe Mission Launch

8.5.9.1 1978 Probe Mission A/C IV

This section contains ADCS performance data corresponding to the 1978 probe mission. The Version IV science payload preferred spacecraft configuration is assumed here.

Separation From Booster

The spacecraft will be initially oriented and then spun up to 0.5 rad/s (4.8 rpm) by the Centaur control system prior to separation. An analysis of the separation dynamics is not included at present because the pertinent Centaur data are not available.

Cruise Phase Attitude Determination and Control

The geometry during probe bus cruise is shown in Figure 8.5-43. During the first 5 days, the spacecraft will be pointing in the direction designated as A. After the first midcourse maneuver, the spacecraft will be precessed to position B, where it will remain during the following 45 days. These orientations have been selected for facilitating thermal control of the large probe during cruise. After the second midcourse maneuver the spacecraft will be precessed to point C, at which the earth pointing phase begins (aft end points at earth).

Syzygy occurs at about 60 days from launch, but it is not a problem any more because the sun aspect angle (while earth pointing) will be about 0.35 radian (20 degrees), and doppler modulation of the offset omni antenna provides attitude information with accuracy independent from the earth-spacecraft-sun angle.

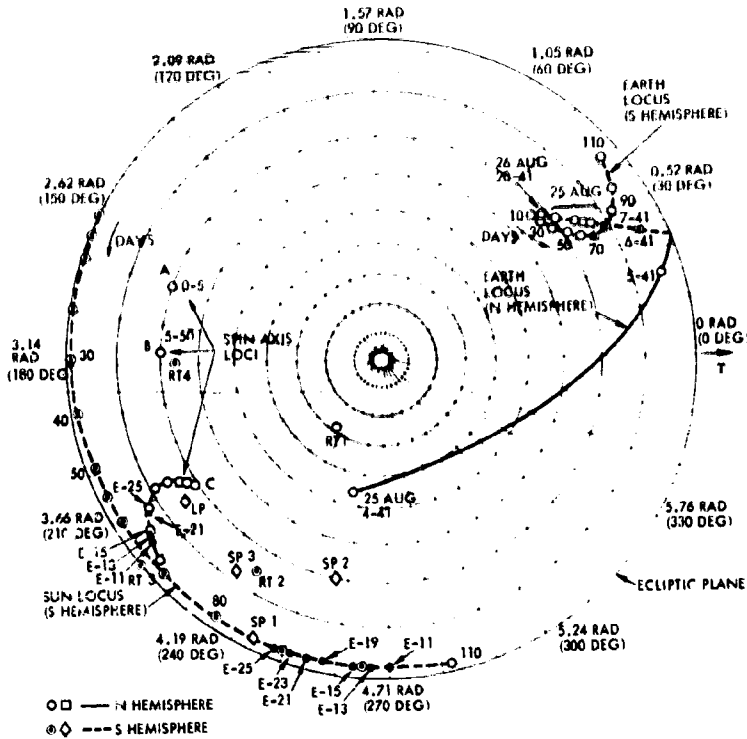


Figure 8.5-43. Stereographic Projection Showing Angular Geometry During Probe Bus Cruise and Probe Deployment and Retargeting Maneuvers

Precession rates caused by solar pressure and required for earth tracking are shown in Figure 8.5-44 as functions of time. The solar pressure drifts are significantly lower than earlier configurations due to a lowering and size reduction of the solar array.

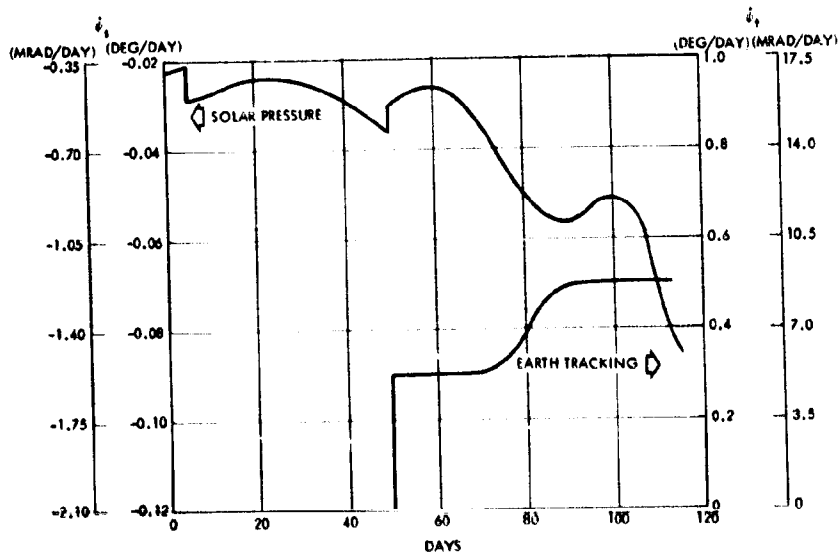


Figure 8.5-44. Precession Rates During 1978 Probe Bus Cruise

Attitude determination accuracies for the most significant cruise events are as follows:

Initial attitude after launch	± 0.0115 radian (± 0.66 degree)
Initial attitude before first midcourse	± 0.0117 radian (± 0.67 degree)
First midcourse	± 0.004 radian to 0.021 radian (± 0.25 to ± 1.2 degree)
Cruise (after first midcourse)	± 0.011 radian (± 0.62 degree)
Second midcourse	± 0.004 radian to ± 0.021 radian (± 0.25 to ± 1.2 degrees)
Cruise (after second midcourse)	± 0.004 radian (± 0.25 degree)

Midcourse Maneuvers

Table 8.5-17 contains a summary of attitude errors, velocity dispersions, and spin rate variations that may occur during midcourse corrections. Parameter definitions and assumptions made are as described for Tables 8.5-6 and 8.5-7.

Table 8.5-17. Atlas/Centaur Probe Bus Dynamic Disturbances Due to Thruster Firings

EVENT	ΔV [M/S (FT/SEC)]	NOMINAL SPIN RATE [RAD/S (RPM)]	CHANGE IN SPIN RATE [RAD/S (RPM)]	ANGLE OF ATTACK [RAD (DEG)]	MOMENTUM VECTOR SHIFT [RAD (DEG)]	VELOCITY DISPERSION [RAD (DEG)]	VELOCITY DEGRADATION [M/S]	NUTATION ANGLE [RAD (DEG)]
FIRST MIDCOURSE (1)	7 (23)	0.52 (5)	+0.073 (+0.7)	0.016 (0.9)	0.005 (0.3)	0.0026 (0.15)	NEGLECTIBLE	0.0010 (0.6)
SECOND MIDCOURSE (1)	1 (3.28)	0.52 (5)	-0.0105 (+0.1)	0.016 (0.9)	0.005 (0.3)	0.0026 (0.15)	NEGLECTIBLE	0.0010 (0.6)
(2)	1 (3.28)	0.52 (5)	+0.052 (+0.5)	0.698 (40)	0.698 (40)	0.35 (20)		
THIRD MIDCOURSE (1)	2 (6.56)	0.52 (5)	+0.021 (+0.2)	0.016 (0.9)	0.005 (0.3)	0.0026 (0.15)	NEGLECTIBLE	0.0010 (0.6)
(2)	2 (6.56)	0.52 (5)	+0.105 (+1.0)	1.394 (80)	1.394 (80)	0.698 (40)		
SPIN-UP	+0.005 (+0.017)	0.52 - 2.09 (5 - 20)	+1.57 (+15)	0.0019 (0.11)	0.0010 (0.06)	N/A	N/A	0.0010 (0.06)
DESPIN	-0.005 (-0.017)	2.09 - 1.05 (20 - 10)	-1.05 (-10)	0.0005 (0.03)	0.00017 (0.01)	N/A	N/A	0.00035 (0.02)
FIRST RETARGETING (1)	1.21 (4)	1.05 (10)	-0.0105 (+0.1)	0.0033 (0.19)	0.0014 (0.08)	0.0007 (0.04)	NEGLECTIBLE	0.0019 (0.11)
(2)	1.21 (4)	1.05 (10)	-0.042 (+0.4)	0.0087 (0.5)	0.0087 (0.5)	0.0044 (0.25)	NEGLECTIBLE	
SECOND RETARGETING (1)	16.07 (53)	1.02 (10)	+0.126 (+1.2)	0.033 (1.9)	0.0012 (1.9)	0.0012 (0.7)	NEGLECTIBLE	0.023 (1.3)
THIRD RETARGETING (1)	6.12 (19.7)	1.05 (10)	+0.048 (+0.45)	0.031 (1.8)	0.017 (1.8)	0.0087 (0.5)	NEGLECTIBLE	0.016 (0.9)
(2)	6.12 (19.7)	1.05 (10)	+0.230 (+2.2)	0.05 (3)	0.05 (3)	0.026 (1.5)	0.001	
FOURTH RETARGETING (1)	25.72 (84.5)	1.05 (10)	+0.188 (1.8)	0.0087 (0.5)	0.0028 (0.16)	0.0014 (0.08)	N/A	0.00017 (0.01)
SPIN-UP	+0.025 (+0.081)	1.05 - 6.29 (10 - 60)	+5.2 (+50)	0.0005 (0.03)	0.00035 (0.02)	N/A	N/A	

NOTE: THRUST LEVEL = 5.2 NEWTONS (1.17 LB) PER THRUSTER
 (1) UTILIZING PAIR OF AXIAL THRUSTERS
 (2) UTILIZING PAIR OF SPIN CONTROL THRUSTERS

Probe Deployment and Retargeting Maneuvers

The geometry during probe deployment and retargeting maneuvers is shown in Figure 8.5-43. All maneuvers will start from and return to the earth-pointing attitude.

Attitude determination during this sequence of maneuvers is based on sun sensor aspect data and doppler modulation measurements. A summary of attitude determination accuracies at the probe release and retargeting orientations is presented in Table 8.5-18.

Table 8.5-18. Probe Deployment and Retargeting Attitude Determination Accuracies

EVENT	SYMBOLS**	LP	RT1	SP1	RT2	SP2	RT3	SP3	RT4
DAYS BEFORE ENCOUNTER		25	23	21	19	17	15	13	11
SUN-SPACECRAFT-EARTH ANGLE [RAD (DEG)]	α	2.495 (143)	2.443 (140)	2.408 (138)	2.355 (135)	2.321 (133)	2.286 (131)	2.234 (128)	2.198 (126)
SUN-SPIN AXIS-EARTH ANGLE CELESTIAL SPHERE [RAD (DEG)]	β	1.735 (99.4)	2.352 (134.8)	0.567 (32.5)	1.143 (65.5)	1.621 (92.9)	2.951 (169.1)	2.021 (115.8)	2.445 (140.1)
SUN-ASPECT [RAD (DEG)]	A_s	0.635 (36.4)	1.134 (65)	0.190 (10.9)	0.401 (23)	0.310 (22.9)	0.803 (46)	0.604 (34.6)	1.518 (87)
ERROR [RAD (DEG)]	E_s	0.0080 (0.46)	0.0038 (0.22)	0.0183 (1.05)	0.0089 (0.51)	0.0089 (0.51)	0.0049 (0.28)	0.0065 (0.37)	0.0035 (0.20)
EARTH-ASPECT [RAD (DEG)]	A_e	2.713 (155.5)	2.164 (124)	2.539 (145.5)	2.583 (148)	2.382 (136.5)	1.501 (86)	2.688 (154)	2.339 (134)
ERROR [RAD (DEG)]	E_e	0.0066 (0.38)	0.0199 (1.14)	0.0092 (0.53)	0.0092 (0.53)	0.0127 (0.73)	0.0040 (0.23)	0.0077 (0.44)	0.0136 (0.78)
DETERMINATION MODE*		A	A	A	A	A	B	A	A
PROBABILITY ELLIPSE ON CELESTIAL SPHERE [RAD (DEG)]									
SEMI-MAJOR AXIS	a	0.0070 (0.40)	0.0288 (1.62)	0.0272 (1.53)	0.0119 (0.68)	0.9127 (51.7)	0.0333 (1.91)	0.0096 (0.55)	0.0216 (1.24)
SEMI-MINOR AXIS	b	0.0056 (0.33)	0.0038 (0.22)	0.0086 (0.49)	0.0077 (0.44)	0.0089 (0.51)	0.0031 (0.18)	0.0058 (0.33)	0.0035 (0.20)
ANGLE BETWEEN E_s AND α	θ	0.5724 (32.8)	0.8010 (45.9)	1.4675 (84.1)	0.9562 (54.8)	0.0995 (5.7)	1.4937 (85.6)	0.8393 (48.1)	0.9057 (51.9)

* A - DOPPLER MODULATION

B - DOPPLER SHIFT

** MAGNITUDES ARE DEFINED IN FIGURE 8.5-31.

Retargeting maneuver execution errors are given in Table 8.5-17, and velocity errors due to combined effects of attitude determination and execution errors are shown in Table 8.5-19.

Reaction control subsystem performance will be approximately as given in Table 8.5-11 since changes in mass properties are small.

Probe Release Dynamics

Table 8.5-20 is an updated version of Table 8.5-12 giving velocity increments produced by small probe releases.

Large probe tipoff errors produced during separation are given in Table 8.5-21.

Table 8.5-19. Velocity Errors During Probe and Orbiter Maneuvers

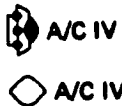


	PROBE EVENT				ORBITER EVENT			
	RT1	RT2	RT3	RT4	PM1	PM2	PM3	PM4
ΔV (M/S)								
AXIAL	1.21	16.07	0	25.72	2.13	2.81	8.22	1.96
RADIAL	0	0	6.12	0	12.10	9.80	9.15	8.46
TOTAL	1.21	16.07	6.12	25.72	12.3	10.2	12.3	8.7
ATTITUDE DETERMINATION ERROR [RAD (DEG)]	0.0283 (1.62)	0.0119 (0.68)	0.0333 (1.90)	0.0216 (1.24)	0.0063 (0.36)	0.0063 (0.36)	0.0063 (0.36)	0.0063 (0.36)
VELOCITY DISPERSION ANGLE [RAD (DEG)]	0.0007 (0.04)	0.0061 (0.35)	0.026 (1.5)	0.0014 (0.08)	0.0079 (0.45)	0.0079 (0.45)	0.0079 (0.45)	0.0079 (0.45)
COMBINED VELOCITY ERROR ANGLE [RAD (DEG)]	0.0283 (1.62)	0.0132 (0.76)	0.424 (2.43)	0.0216 (1.24)	0.0101 (0.58)	0.0101 (0.58)	0.0101 (0.58)	0.0101 (0.58)
VELOCITY ERROR (M/S)								
RADIAL**	0.03	0.21	0.26	0.56	0.36	0.29	0.28	0.25
AXIAL*	0.04 0.07	0.48 0.96	0.18 0.37	0.77 1.54	0.14 0.18	0.13 0.20	0.28 0.50	0.10 0.15
TOTAL	0.05 0.08	0.52 0.98	0.32 0.45	0.95 1.64	0.39 0.75	0.32 0.62	0.40 0.75	0.27 0.33

* INCLUDES THRUST UNCERTAINTY OF AXIAL THRUSTING AND VELOCITY ERROR ANGLE EFFECTS OF RADIAL THRUSTING

** INCLUDES THRUST UNCERTAINTY OF RADIAL THRUSTING AND VELOCITY ERROR ANGLE EFFECTS OF AXIAL THRUSTING

Table 8.5-20. Small Probe Separation Velocities,
= 1.048 rad/s (10 rpm)*



EVENT	r ₁ (M)	r ₂ (M)	V _p (M/S)	V _b (M/S)
FIRST SMALL PROBE RELEASE	0.87	0.18	0.91	-0.19
SECOND SMALL PROBE RELEASE	0.81	0.22	0.85	-0.23
THIRD SMALL PROBE RELEASE	0.67	0.25	0.7	-0.26

* THESE ΔV 'S ARE IN A DIRECTION PERPENDICULAR TO A RADIAL LINE FROM THE SPACECRAFT CENTERLINE TO THE SEPARATING PROBE CENTER OF MASS EXCEPT FOR THE SECOND PROBE RELEASE, WHICH IS APPROXIMATELY 0.17 RADIAN (10 DEGREES) OFF THIS LINE DUE TO THE SPACECRAFT CENTER-OF-MASS LOCATION AT THAT TIME.

8.5.9.2 Orbiter Mission

Separation From Booster

The spacecraft will be initially oriented and then spun up to 0.5 rad/s (4.8 rpm) by the Centaur control system prior to separation. An analysis of the separation dynamics is not included at present because the pertinent data are not available.

Table 8.5-21. Large Probe Separation Tipoff Errors

A/C IV

PERTURBANCE	INVERSE ANGULAR RATE (RAD/SEC)	MOMENTUM FOR FLUTTER FLUTTER ANGLE (DEGREES)	
		10 RPM	30 RPM
NET LATERAL SPRING FORCE (2.74 IN/IN) (0.44)	0.004	0.2	0.1
AXIAL SPRING RATE DIFFERENTIAL (2 PERCENT)	0.005	0.25	0.125
COMPRESS HEIGHT OF EACH SPRING (0.05 CM) (0.02 IN.)	0.003	0.15	0.08
SPRING RADIAL LOCATION (0.15 CM) (0.06 IN.)	0.001	0.05	0.025
BALL LOCK RELEASE DIFFERENTIAL (5 MILLISECOND)	0.003	0.15	0.08
855 TOTAL	0.008	0.4	0.2

Cruise Phase Attitude Determination and Control A/C IV

The cruise phase geometry is as shown in Figure 8.5-37 except that the spacecraft will be initially placed in the earth-pointing orientation corresponding to the fifth day. After the first midcourse maneuver the spacecraft will be returned to the earth pointing orientation.

During the first 110 days, the forward end of the spacecraft will be pointed at earth, except for the second midcourse maneuver (planned on day 55). Attitude determination during this phase will be provided by the conscan system. During maneuvers, attitude determination will be on the basis of sun aspect sensor and doppler modulation data.

After 110 days, a spacecraft flip maneuver is required to point the aft end at earth, which is necessary to maintain the solar aspect angle less than 1.57 radians (90 degrees).

There are several options regarding the flip maneuver. The approach favored at present consists in programming a 1.57-radian (90-degree) open loop maneuver, at the end of which antennas will be switched and, if required, a small ΔV firing will be made for doppler attitude determination. A second 1.57-radian (90-degree) maneuver will be programmed afterwards for attaining the desired earth-pointing attitude. The open-loop maneuvers can be executed with accuracies in the 0.047- to 0.063-radian (2.7- to 3.6-degree) range, on the basis of in-flight reaction control subsystem calibration data.

Attitude determination during the remainder of the cruise phase will be on the basis of sun sensor and doppler modulation data.

Figure 8.5-45 shows precession rates due to solar pressure effects and earth tracking. Figure 8.5-46 shows attitude determination accuracies attainable by doppler measurements. The curves designated A correspond to spin modulation effects, while the curves labeled B are based on a 1 m/s velocity maneuver. Curves designated A were obtained by assuming an antenna phase center uncertainty of 17.7 mm (0.5 inch) on a plane normal to the spin axis.

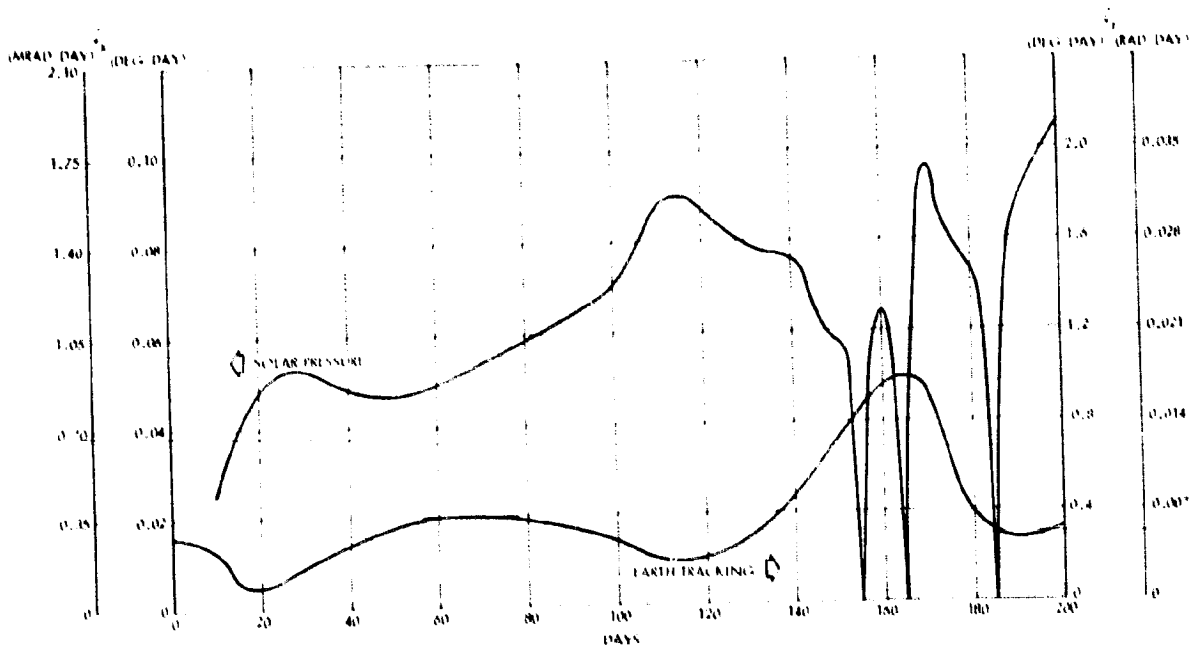


Figure 8.5-45. Precession Rates Due to Solar Pressure and Earth Tracking

Midcourse Maneuvers

Table 8.5-22 contains summaries of attitude errors, velocity dispersions, and spin rate variations that may occur during midcourse maneuvers. The assumptions made are as described for Tables 8.5-14 and 8.5-15.

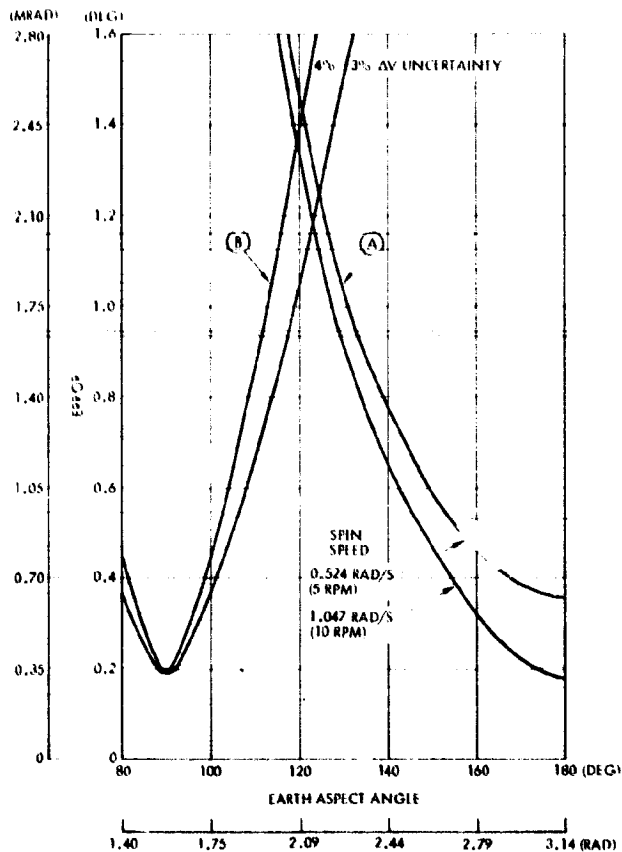


Figure 8.5-46. Doppler Attitude Determination Accuracies

Table 8.5-22. Atlas/Centaur Orbiter Dynamic Disturbances Due to Thruster Firings

EVENT	ΔV [M/S (FT/SEC)]	NOMINAL SPIN RATE [RAD/S (RPM)]	CHANGE IN SPIN RATE [RAD/S (RPM)]	ANGLE OF ATTACK [RAD (DEG)]	MOMENTUM VECTOR SHEP [RAD (DEG)]	VELOCITY DISPERSION [RAD (DEG)]	VELOCITY DEGRADATION [RAD (DEG)]	NUTATION ANGLE [RAD (DEG)]
FIRST MID-COURSE	(1) 7 (23)	0.52(5)	-0.126 (-1.21)	0.024 (1.4)	0.0087 (0.5)	0.0046 (0.25)	0.0006	0.016 (0.9)
	(2) 7 (23)	0.52(5)	-0.461 (-4.41)	0.16 (91)	0.16 (91)			0.0017 (0.11)
SECOND MID-COURSE	(1) 1 (3.28)	0.52(5)	-0.0189 (-0.17)	0.024 (1.4)	0.0087 (0.5)	0.0046 (0.25)	0.0001	0.016 (0.9)
	(2) 1 (3.28)	0.52(5)	-0.063 (-0.6)	0.023 (1.3)	0.0222 (1.3)			0.0017 (0.11)
THIRD MID-COURSE	(1) 2 (6.56)	0.52(5)	-0.056 (-0.54)	0.024 (1.4)	0.0087 (0.5)	0.0046 (0.25)	0.0002	0.016 (0.9)
	(2) 2 (6.56)	0.52(5)	-0.126 (-1.21)	0.045 (2.6)	0.045 (2.6)			0.0017 (0.11)
VELOCITY ORBIT INSERTION		6.29(60)		0.017 (1)	0.007 (0.4)	0.0035 (0.2)	NEGLECTIBLE	0.0122 (0.7)
PERIAPSIS MAINTENANCE								
	ΔV NO. 1							
ΔV NO. 1	(1) 12.3(40.4)	0.52(5)	-0.084 (-0.8)	0.042 (2.4)	0.016 (0.9)	0.0078 (0.45)	0.005	0.026 (1.5)
	(2) 12.3(40.4)	0.52(5)	-0.344 (-3.2)	0.21 (12)	0.21 (12)			0.0017 (0.11)
ΔV NO. 2	(1) 10.2(33.5)	0.52(5)	-0.073 (-0.7)	0.042 (2.4)	0.016 (0.9)	0.0078 (0.45)	0.004	0.026 (1.5)
	(2) 10.2(33.5)	0.52(5)	-0.450 (-4.3)	0.12 (10)	0.017 (10)			0.0017 (0.11)
ΔV NO. 3	(1) 12.3(40.4)	0.52(5)	-0.084 (-0.8)	0.042 (2.4)	0.016 (0.9)	0.0078 (0.45)	0.005	0.026 (1.5)
	(2) 12.3(40.4)	0.52(5)	-0.344 (-3.2)	0.21 (12)	0.21 (12)			0.0017 (0.11)
ΔV NO. 4	(1) 8.7(28.5)	0.52(5)	-0.083 (-0.8)	0.042 (2.4)	0.016 (0.9)	0.0078 (0.45)	0.004	0.026 (1.5)
	(2) 8.7(28.5)	0.52(5)	-0.387 (-3.7)	0.14 (8)	0.14 (8)			0.0017 (0.11)

NOTES: (1) UTILIZING AXIAL THRUSTERS.
(2) UTILIZING PAIR OF SPIN CONTROL THRUSTERS.

Venus Orbit Insertion Maneuver

The orientation required for this maneuver is shown in Figure 8.5-47. At this attitude, the sun aspect angle is 1.172 radians (67 degrees) and the earth is on the forward end of the spacecraft at an angle of about 1.047 radians (60 degrees). The spacecraft precession required is on the order of 2.37 radians (136 degrees).

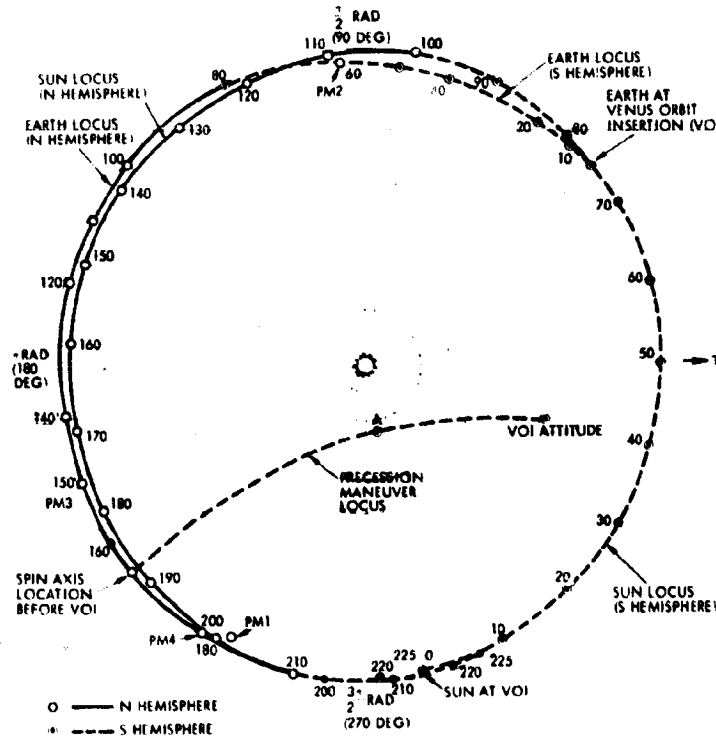


Figure 8.5-47. Venus Orbit Insertion and Orbit Phase Geometry

Because the earth is on the side of the spacecraft where the omni antenna is on center, no doppler information will be available for attitude determination unless a small velocity maneuver is executed. Sun sensor data cannot be used to improve the open-loop maneuver accuracy as in the fanbeam fanscan configurations because, near the end, the sun aspect is almost constant. The approach proposed consists in first precessing to a point such as A (in Figure 8.5-47) where the earth aspect angle [about 1.4 radians (80 degrees)] is favorable for doppler attitude determination by means of a small ΔV maneuver. The orientation at A can be estimated with an accuracy on the order of 0.013 radian (0.74 degree).

From this point, a precession maneuver of about 0.995 radian (57 degrees) is executed to reach the VOI attitude. Assuming an execution uncertainty of ± 0.030 radian (± 1.7 degree), the total error will be approximately 0.016 radian (1.9 degrees).

Attitude Determination and Control in Orbit

The angular geometry during the orbit phase is shown in Figure 8.5-47. During the first 37 days in orbit the aft end of the spacecraft will be pointed at earth. After a flip maneuver, the forward end of the spacecraft will be maintained earth pointing through the rest of the mission.

As shown in Figure 8.5-48, the main source of attitude drift in orbit is earth motion. Solar pressure effects produce precession rates which are approximately one order of magnitude lower.

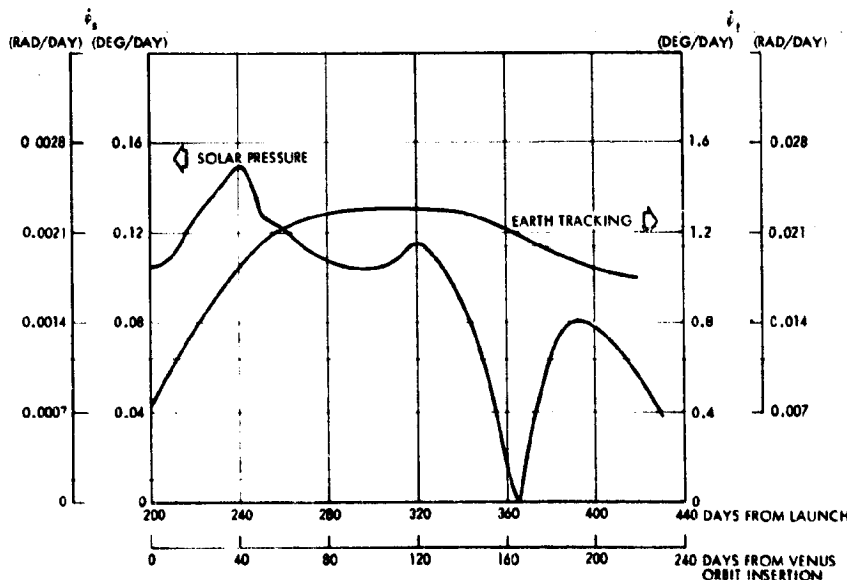


Figure 8.5-48. Attitude Drift Rates in Orbit Due to Solar Pressure and Earth Motion

During the first 37 days in orbit, antenna-pointing errors up to 0.205 radian (12 degrees) can be allowed except during occultation experiments. Therefore, the frequency of attitude corrections during this period will depend on the occultation experiment schedule.

The communications link budget allows a maximum pointing error of 0.017 radian (1 degree) during earth occultation experiments. This



A/C IV requirement can easily be met since the attitude determination accuracies attainable with sun sensor and doppler data will range from 0.0066 to 0.0070 radian (0.44 to 0.46 degree).

After the flip maneuver, antenna-pointing requirements will vary from ± 0.070 to ± 0.017 radian (± 4 to ± 1 degrees), depending on communications range. Consequently, intervals between attitude corrections will be in the range from 8 down to 1.7 days.

Reaction control subsystem performance in the preferred Atlas/Centaur, Version IV, science payload orbiter configuration will be approximately as given in Table 8.5-11.

Periapsis Maintenance Maneuvers

Periapsis maintenance maneuvers will be made in the earth pointing orientations shown in Figure 8.5-47. Combinations of axial and radial firings will produce the required velocity increments as described in Figure 8.5-13.

Execution errors are mostly due to dynamic effects and uncertainties in the orientation and magnitude of the transverse thrust pulses. Table 8.5-22 presents a summary of attitude errors, velocity dispersions, and spin rate variations that may occur during periapsis maintenance maneuvers.

8.5.10 ADCS/Science Interface

8.5.10.1 Radar Altimeter and Ram Experiment Gimballing Requirements

ALL ORBITERS EXCEPT EARTH-POINTING CONFIGURATIONS

In the spacecraft configurations with the spin axis oriented approximately normal to the Venus orbit plane, the science instrument pointing geometry at periapsis is fixed as long as orbit parameters are maintained close to the nominal design values. Therefore, if measurements are made at periapsis only, the corresponding instruments can be mounted directly on the spacecraft at the required angles from the spin axis.

If tracking capability and/or insensitivity to orbit parameter changes are required, then the affected instruments may have to be gimbaled for changing the angles between their lines of sight and the spin axis.

ALL ORBITERS EXCEPT
EARTH-POINTING CONFIGURATIONS

Figure 8.5-49 shows the gimballed angles required to point the radar altimeter antenna and the ram-viewing experiments during the time period within 8 minutes from periapsis crossing. This period corresponds to the orbit sector where the spacecraft altitudes are lower than 1000 km. The spacecraft spin axis is assumed perpendicular to the Venus orbit plane. The radar altimeter antenna is assumed gimballed about an axis perpendicular to the spin axis and the gimballed angles are chosen so that the boresight axis points at nadir once per revolution. The ram-viewing experiments are also assumed gimballed about an axis perpendicular to the spin axis. Gimballed angles are chosen so that the lines of sight point in the direction of the spacecraft velocity vector once per 2π radians (once per revolution).

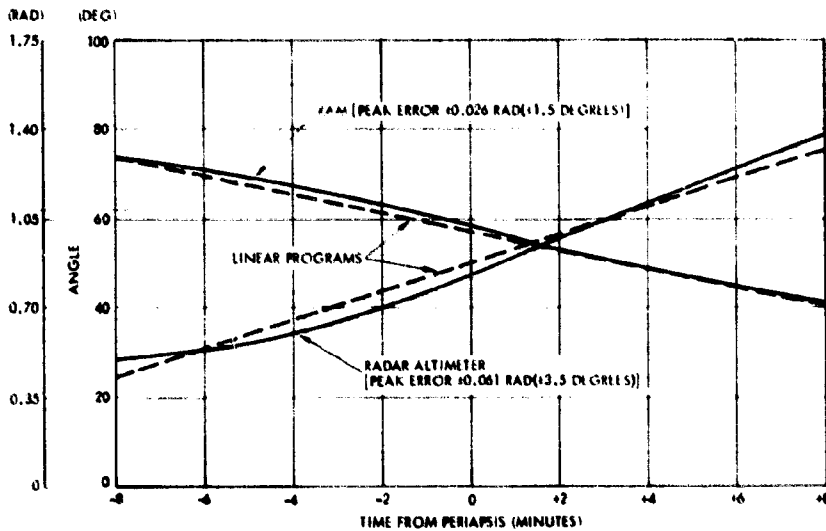


Figure 8.5-49. Radar Altimeter and Ram Experiment Gimballed Angles for Tracking, Spin Axis Normal To Venus Orbit Plane (Solid Lines Represent Requirements)

Use of a single gimballed drive for both the radar altimeter and the ram experiment package is not feasible because, while the nadir pointing vector scans ± 0.7 radian (± 40 degrees) over the 16-minute period, the ram vector sweeps through an angle of ± 0.384 radian (± 22 degrees) only.

If linear approximations to the required gimballed angle functions are used, the peak-pointing errors incurred (without including spacecraft attitude errors) will be of the order of 0.006 radian (± 3.5 degrees) for the radar altimeter and 0.0026 radian (1.5 degrees) for the ram experiment package.

An interesting conclusion that may be derived from Figure 8.5-49 is that a single programmer (or drive control logic) can be used for gimbaling both experiments simultaneously.

The earth-pointing configurations require gimbaling of both the radar altimeter and the ram-looking experiments, irrespective of tracking requirements, because the pointing geometry varies with time in orbit.

Figure 8.5-50 shows the radar altimeter gimbal angle profiles required for nadir tracking with earth-pointing spacecraft configurations. Parameters shown on the graph are times in days from Venus orbit insertion. The required pointing functions can be approximately by linear programs with errors within the 0.053-radian (3-degree) to 0.175-radian (10 degree) range (neglecting spin-axis-pointing errors). The programming logic required should have the capability to select initial values and slopes by ground command.

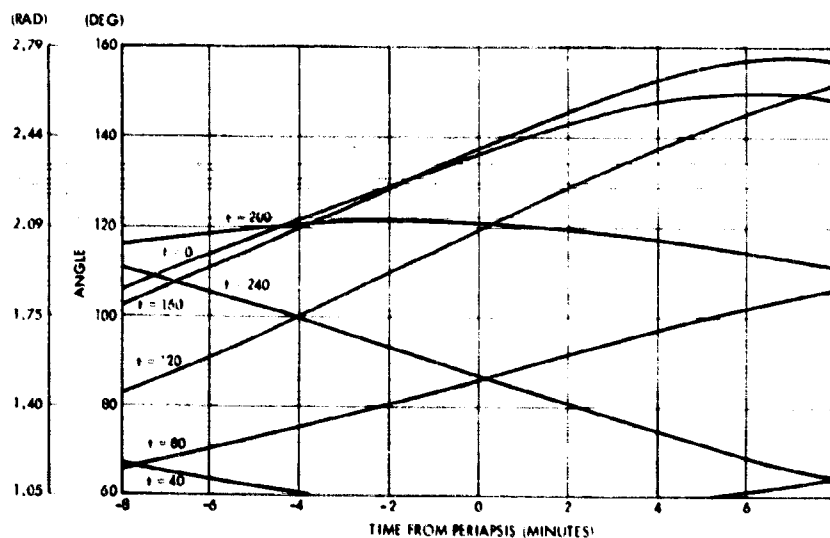


Figure 8.5-50. Radar Altimeter Gimbal Angles for Tracking, Earth-Pointing Configurations

Gimbal angles required to point the ram-viewing experiments (between 1000-km points) with the earth-pointing spacecraft are shown in Figure 8.5-51. These functions can also be approximated by linear programs, and the resulting errors (neglecting spacecraft altitude errors) would be in the range from 0.0175 radian (1 degree) to 0.087 radian (5 degrees).

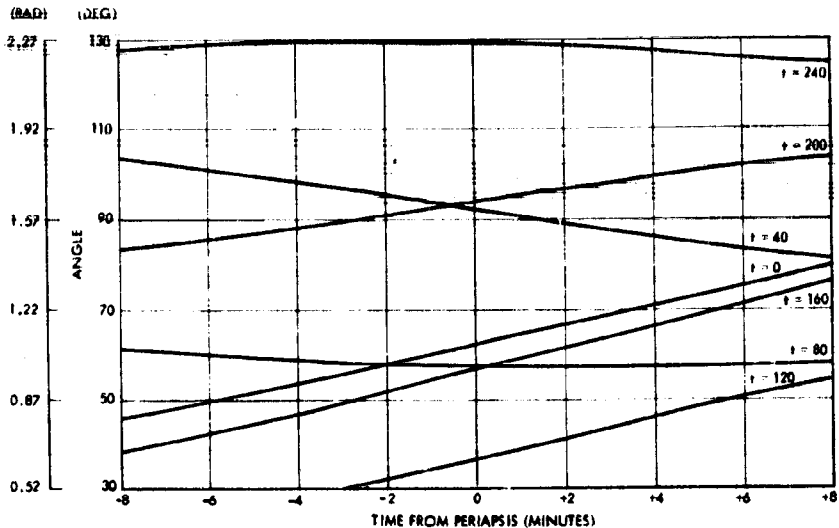


Figure 8.5-51. Ram Experiment Gimbal Angles for Tracking, Earth-Pointing Configurations

8.5.10.2 Gimbal Actuator Design Example

Figure 8.5-52 shows a simple mechanization suggested for gimbaling the radar altimeter that employs a size 8 stepper motor, a spur gearhead, and a harmonic drive final reduction. The motor basic step angle is 1.57 radians (90 degrees), which is reduced by 15:1 in the gearhead and an additional 120:1 through the harmonic drive. Thus, the output motion per input pulse is 0.0009 radian (0.05 degree).

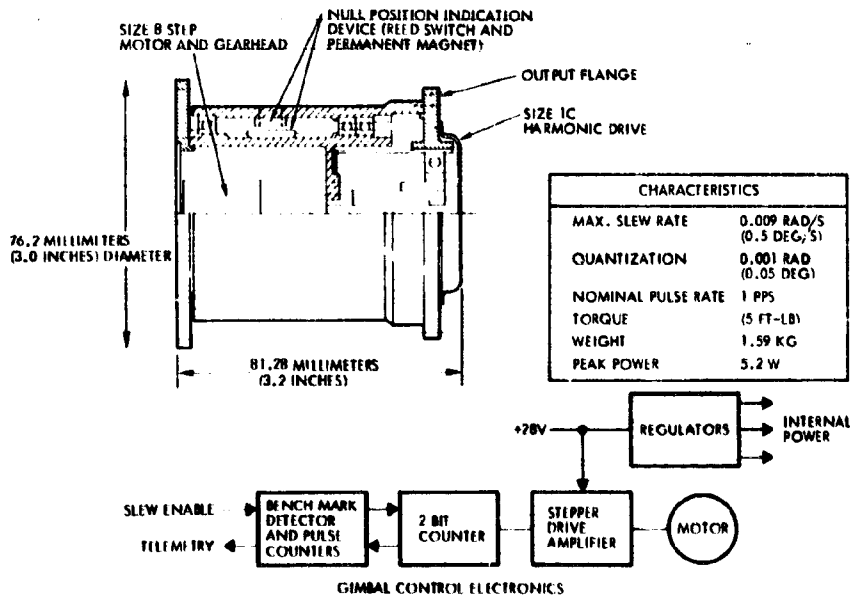


Figure 8.5-52. Gimbal Actuator Design Example for Altimeter and Ram Platform

To determine output shaft position, a permanent-magnet-operated reed switch is used for the null position indication, and pulses to the motor are counted and stored in a register. At switch closure, the register is set to zero and the count in the register at any given time is proportional to the drive output travel. This type of position indication has advantages over other types, such as resolvers or potentiometers, because no complex electronics are required or wear elements are involved.

The drive would employ lubrication techniques that were successfully flown by TRW on the DSCS-II antenna drives of a similar design. NPT-4 oil would be used on all wear surfaces and oil/vacuum impregnated nylasint reservoirs would be strategically placed to assure replenishment of the oil lost by evaporation or creep. The pinions would be 440C stainless steel with porous phenolic ball separators.

8.5.10.3 Refracted Ray Tracking During Occultation Experiments ALL ORBITERS

As the Pioneer Venus spacecraft becomes occulted from the earth, RF signals will be refracted by the Venus atmosphere. High-gain antenna orientations required to track the refracted signals are plotted in Figure 8.5-53, which is a stereographic polar diagram with time from VOI as a parameter. Inspection of the graph shows that various spin axis precession maneuvers are required, in most cases, if both entry and exit occultations are to be tracked.

One possible maneuvering approach is shown in the graph and consists of precessing only in the plane of the earth and the initial spin axis orientation. The required precession rates, of the order of 0.0017 rad/s (0.1 deg/s), can be attained by either using pulse durations greater than 125 milliseconds or by operating with multiple firings per spin revolution. Other strategies eliminating the need for spacecraft precessions during tracking have been considered and discarded because of the large precession amplitudes and rates required for repositioning after completing occultation entry.

The graph presented on the right-hand side of the chart shows the spacecraft precessions required 30 days after VOI. Superimposed on the graph are examples of precession command profiles providing piecewise-linear approximations to the required time functions.

ALL ORBITERS

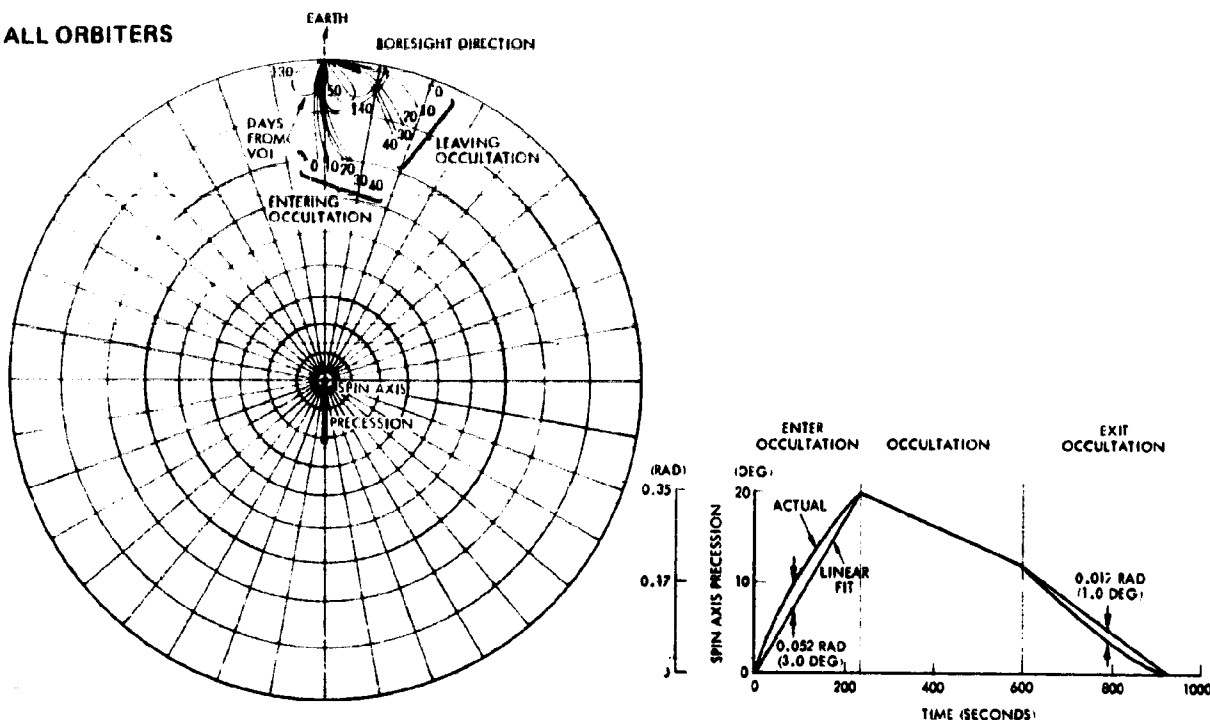


Figure 8.5-53. Earth Occultation Experiment Tracking Requirements

8.5.10.4 Dual Frequency Occultation ADCS Interface A/C IV

The preferred way of accommodating this Version IV science payload experiment is to limit the experiment to the first 37 days in orbit, when the tail of the spacecraft is earth pointing. The same medium-gain (Pioneers 10 and 11 derived) horn that is used on the probe bus provides S-band communications, and a slightly narrower pattern X-band horn is added (derived from DSCS-II).

Prior to occultation, the spacecraft is repositioned away from earth to the communication angle limit [about 0.205 radian (12 degrees)]. As the rays refract during occultation, they ride up the pattern. Actually, the occultation experiment can continue (with postfacto data processing) beyond the point of downlink loss and it is expected that S-band to 0.31 radian (18 degrees) and X-band to 0.205 radian (12 degrees) can be achieved.

This implementation limits the experiment to the entering (or exiting, but not both) occultations, but requires no maneuvers commanded in real time. It impacts the ADCS system only in an operational sense.

8.6 PROPULSION

The propulsion subsystem consists of a common design, monopropellant hydrazine reaction control system (RCS) for both the probe bus and orbiter, and a solid fuel orbit insertion motor (OIM) for the orbiter. Figure 8.6-1 summarizes the propulsion subsystem for the preferred Atlas/Centaur Version IV science payload.

The preferred subsystems minimize development risk and cost and offer high reliability. The RCS consists of flight-proved components, principally from Pioneers 10 and 11. Blowdown pressurization and centrifugal forces resulting from spacecraft spin provide positive propellant expulsion with simple, inexpensive tanks. Eight Pioneer-type catalytic thrusters provide redundancy for all spacecraft RCS maneuvers. The flight-proven Aerojet SVM-2 solid rocket motor, selected for the orbiter, provides the required propellant load capability.

Requirements, tradeoff studies, and preferred subsystem descriptions for the Atlas/Centaur and Thor/Delta are discussed below. Additional details of the OIM are presented in Appendices 8.6A, 8.6B, and 8.6C.

8.6.1 Reaction Control System

The preferred blowdown pressurization monopropellant hydrazine RCS provides the thrust required by the attitude control subsystem to adjust spacecraft spin rate, precess the spin axis to control spacecraft attitude, and perform ΔV maneuvers. Because the RCS consists mainly of flight-proven hardware from Pioneers 10 and 11, it provides minimum cost, minimum development risk, and high reliability.

8.6.1.1 RCS Requirements

The RCS requires 1) energy to change spacecraft spin speed, attitude, and velocity; 2) use of existing hardware to achieve a cost-effective system; and 3) a system design that interfaces with the attitude control subsystem.

The energy requirements for the probe and orbiter missions are of approximately the same magnitude. However, the energy requirements for the Atlas/Centaur probe and orbiter missions are somewhat lower

than those of the similar Thor/Delta missions. This results from the high degree of injection accuracy afforded by the Atlas/Centaur which is reflected in reduced miscourse ΔV and spin control requirements as shown in Table 8.6-1. Because Atlas/Centaur weights are considerably higher than those for the Thor/Delta mission, there is not a wide difference in RCS propellant needs.

Maximum use of existing (off-the-shelf) hardware achieves a cost-effective subsystem that meets the spacecraft and trajectory energy requirements. The major development and test costs and risks associated with a new RCS are eliminated, minimizing hardware design costs.

Because of the weights involved, selection of effective off-the-shelf hardware for Thor/Delta is more difficult than for the less weight-constrained Atlas/Centaur.

The RCS system design requirements reflect the interface with the attitude control system, predicted on mission requirements involving velocity changes, precession maneuvers, and spin-rate changes.

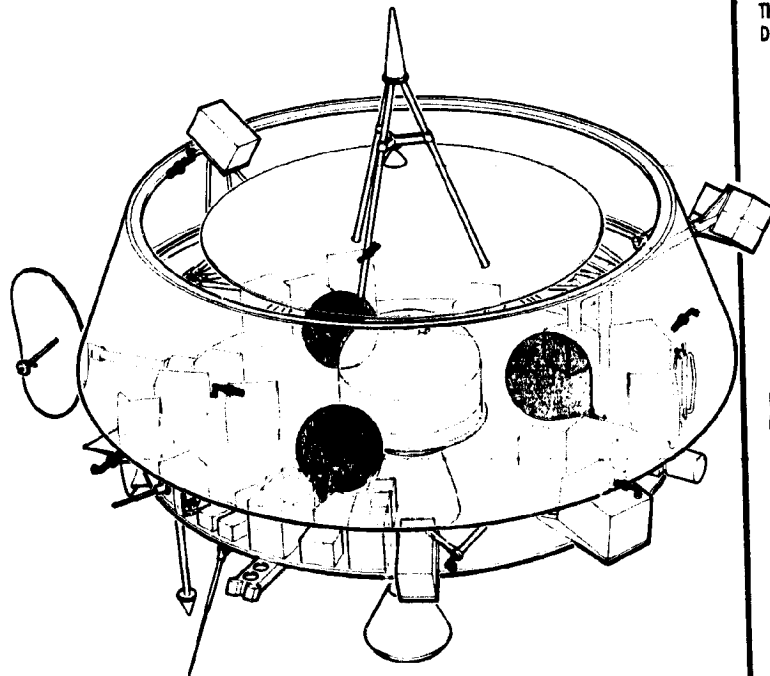
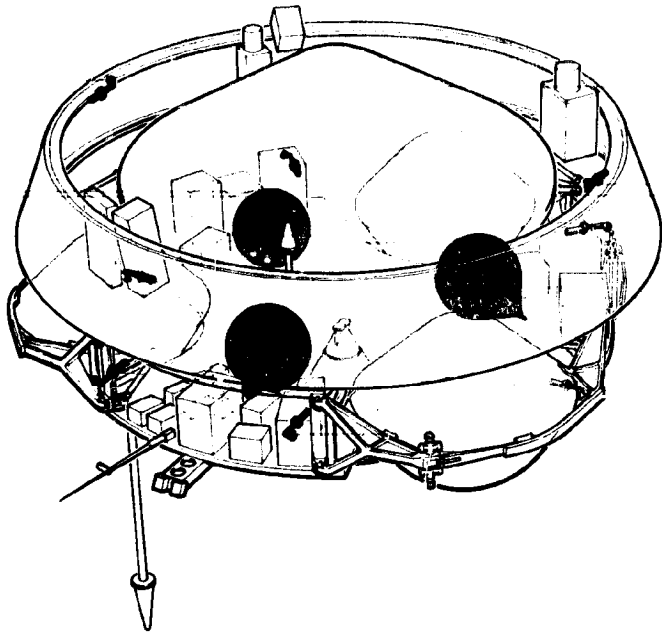
The velocity increment changes are best achieved by axial thrusters, which can be fired continuously, and are not subjected to the specific impulse degradation associated with pulsed radial or transverse thrusters.

To minimize unbalanced torques during thruster operations, the axial thrusters must be parallel to the spacecraft spin axis. Thrust level and thruster location are defined by the goal that the spacecraft precession should not exceed approximately 0.017 radian (1 degree) during a 125-millisecond pulse.

Both the transverse (spin) thrusters and the propellant tanks centers of mass are located in the plane of the spacecraft center of gravity to minimize precession in the pulsed lateral translation mode.

Three propellant tanks are required to improve spacecraft stability and to accommodate the basic structural layout.

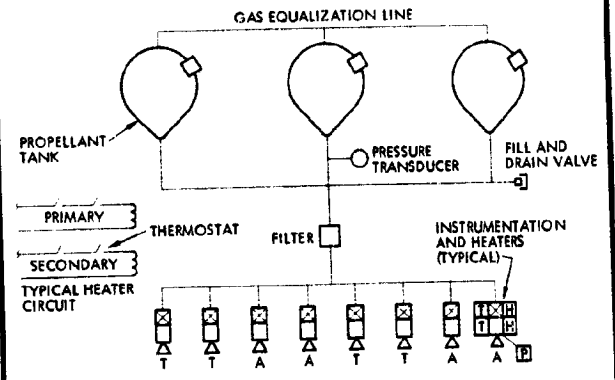
A further system requirement is that no probable single-point malfunction will cause loss of the mission.



FOLDOUT FRAME

THE PREFERRED BLOWDOWN PRESSURIZATION MONOPROPELLANT HYDRAZINE RCS PROVIDES THE THRUST FOR:

- MIDCOURSE AND CRUISE VELOCITY CONTROL
- ATTITUDE CONTROL
- SPIN/DESPIN CONTROL
- PRESSION = 0.017 RAD (1 DEG) FOR 0.125 SECC ND PULSE



- T TRANSVERSE THRUSTER FOR SPIN AND LATERAL ΔV
- A AXIAL THRUSTER FOR PRESSION AND AXIAL ΔV
- H HEATER THERMOSTAT
- TS TEMPERATURE SENSOR
- PS PULSE COUNTER PRESSURE SWITCH

THE PREFERRED DESIGN ASSURES MINIMUM COST, MINIMUM DEVELOPMENT RISK, AND HIGH RELIABILITY

RCS COMMON TO PROBE BUS AND ORBITER DRAWINGS EXIST	MINIMUM COST
PROVEN COMPONENTS	MINIMUM DESIGN EFFORT
RELAXED REQUIREMENTS	NO DEVELOPMENT
EXTENSIVE EXPERIENCE AT TRY	NO QUALIFICATION
TOOLING AND TEST EQUIPMENT AVAILABLE	MINIMUM COST AND RISK
DOCUMENTATION AVAILABLE	MINIMUM COST
COMPATIBLE WITH PROPELLANT LOADING CART USED FOR PIONEERS 10 AND 11	MINIMUM COST AND RISK
	MINIMUM COST

FLIGHT-PROVEN HARDWARE GIVES HIGH RELIABILITY AND MAXIMUM SIMPLICITY, AND ELIMINATES TEST COSTS

REDUNDANT THRUSTERS (8)	FLTSATCOM TYPE BASED ON PIONEERS 10 AND 11
TEARDROP SHAPE TANKS (3)	TEARDROP SHAPE SIMPLIFIES PIPING AND PROVIDES AMPLE PROPELLANT GROWTH
PRESSURE TRANSDUCER (1)	PIONEERS 10 AND 11
FILL AND DRAIN VALVE (1)	PIONEERS 10 AND 11
PROPELLANT FILTER (1)	PIONEERS 10 AND 11

BLOWDOWN LOW-COST

THE PREFERRED EXCELLENCE

66
1-
16
OR
18
12
6 E

THE PREFERRED USING

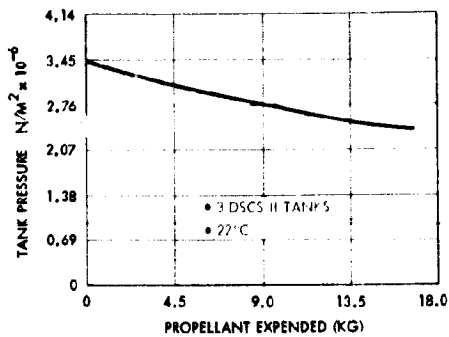
PROPELLANT THROUGH FILTER PRESSURE FILL LINE TO PROPELLANT TANK

CENTRAL

PROPELLANT

ALL CONFIGURATIONS

BLOWDOWN PRESSURIZATION IS LIGHT, RELIABLE, AND LOW-COST



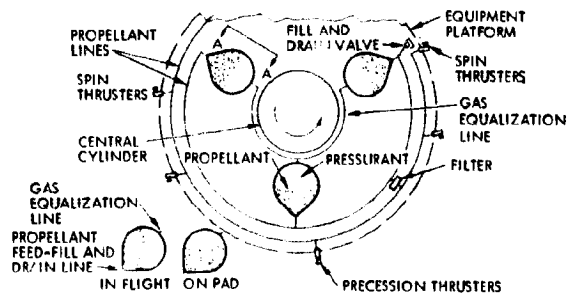
THE PREFERRED RCS IS DESIGNED SO THAT ITS CAPABILITIES EXCEED MISSION REQUIREMENTS

CAPABILITY	REQUIREMENTS
60,700 N (5,415,000 LB) S-I IMPULSE	31,300 N (5,47,026 LB) S-I IMPULSE
1.4:1 BLOWDOWN RATIO	2.4:1 BLOWDOWN RATIO, MAX
15.3 KG (36 LB) N ₂ H ₄ THROUGH ONE THRUSTER	9 KG (20 LB) THROUGH ONE THRUSTER
18,500 PULSES	6,000 PULSES
120 LC-TEMPERATURE STARTS	114 LC-TEMPERATURE STARTS
6,500 SECOND STEADY-STATE BURN	3,000 SECOND STEADY-STATE BURN

THE RCS WEIGHT BREAKDOWN REFLECTS THE ACCURACY OF USING FLIGHT-TESTED COMPONENTS WITH KNOWN WEIGHTS

ITEM	NUMBER REQUIRED	PER COMPONENT (KG / LB)	TOTAL (KG / LB)	
			ORBITER	PROBE
PROPELLANT TANK	3	1.54 (3.4)	4.62 (10.2)	4.62 (10.2)
THRUSTER	8	0.27 (0.6)	2.17 (4.8)	2.17 (4.8)
FILTER	1	0.18 (0.4)	0.18 (0.4)	0.18 (0.4)
PRESSURE TRANSDUCER	1	0.17 (0.4)	0.18 (0.4)	0.18 (0.4)
FILL AND DRAIN VALVE	1	0.1 (0.2)	0.09 (0.2)	0.09 (0.2)
PIPES AND FITTINGS	-	-	0.77 (1.7)	0.77 (1.7)
TOTAL HARDWARE	-	-	8.03 (17.7)	8.03 (17.7)
PRESSURANT	-	-	0.41 (0.9)	0.41 (0.9)
PROPELLANT	-	-	15.06 (33.2)	16.60 (36.6)
TOTAL LOADED	-	-	23.49 (51.8)	25.04 (55.2)

CENTRIFUGAL EXPULSION ELIMINATES THE NEED FOR A BLADDER



THE PREFERRED AEROJET SVM-2 IS A LOW-COST, FLIGHT-PROVEN, HIGHLY RELIABLE ENGINE

FULLY QUALIFIED WITH SAFE AND ARM DEVICE FLOWN ON MINUTEMAN USES MINUTEMAN PROPELLANT, FLOWN SUCCESSFULLY AFTER 8 YEARS STORAGE HAS LOWEST PROGRAM COST OF QUALIFIED ENGINES

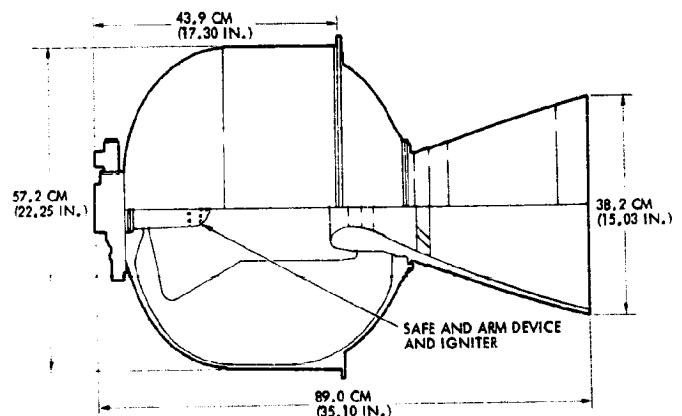
FEATURES

- RELIABLE FOR 8000 SAFE AND ARM DEVICE REPLENISHMENT (4.4 ARMS)
- MINUTEMAN PROPELLANT (5% ALUMINUM)
- GLASS, TITANIUM AND CASE
- BURST OPERATING PRESSURE RATIO OF 1.4
- GUN-GARD V-45 INSULATION
- PARTIALLY SUBMERGED, 28:1 EXPANSION RATIO NOZZLE
- THRUST PARALLELISM, MAX $\pm 0.0064 \text{ CM (} \pm 0.0025 \text{ IN.)}$
- THRUST OFFSET $\pm 0.05 \text{ CM (} \pm 0.020 \text{ IN.)}$
- STORAGE LIFE 3 YEARS
- RELIABILITY > 0.98

WEIGHT FOR VERSION IV SCIENCE MISSION

LOADED WEIGHT (WITH SAFE AND ARM)	162.2 KG (361.1 LB)
PROPELLANT WEIGHT	145.9 KG (321.4 LB)

AEROJET SVM-2 ORBIT INSERTION MOTOR PROVIDES ORBITER VELOCITY CHANGE



PERFORMANCE CHARACTERISTICS

TOTAL IMPULSE, NOMINAL (IN-S)	405,560 (91,137 LB-S)
TOTAL IMPULSE REPRODUCIBILITY, 3 σ	$\pm 1\%$
TOTAL DURATION (SECONDS)	23
THRUST LEVEL	
NOMINAL	15,000 N (3,370 LBF)
MAXIMUM	21,500 N (4,840 LBF)
MAXIMUM EFFECTIVE OPERATING PRESSURE	3.51×10^6 (514 PSIA)
SPECIFIC DELAY TIME (SECONDS)	283.6
IGNITION DELAY TIME (SECONDS)	± 0.100

SERVICE LIMITS

OPERATING TEMPERATURE	-7 TO +43°C (+20 TO +110°F)
STORAGE TEMPERATURE	-12 TO +43°C (+20 TO +110°F)
IMPOSED AXIAL ACCELERATION (G)	14
IMPOSED LATERAL ACCELERATION (G)	2
HUMIDITY	98% AT +49°C (+120°F) FOR 120 HR
TEMPERATURE CYCLING LIMITS	+7 TO +43°C (+20 TO +110°F)
SPIN RATE	0 TO 11.5 RAD/S (0 TO 111 RPM)

Figure 8.6-1. Preferred Atlas/Centaur Reaction Control Subsystem and Orbit Insertion Motor

Table 8.6-1. Energy Requirements for the Probe and Orbiter Missions

	THOR/DELTA		ATLAS/CENTAUR		VERSION IV ATLAS/CENTAUR	
	PROBE	ORBITER	PROBE	ORBITER	PROBE	ORBITER
MIDCOURSE ΔV (M/S)	82	82	10	23.5	10	10
PROBE DEPLOYMENT ΔV (M/S)	41.23	0	49.12	0	49.12	0
PERIAPSIS ΔV (M/S)	0	43.5	0	43.5	0	43.5
ATTITUDE CONTROL PRECESSION (RAD (DEG))	21.485 (1231)	21.031 (1205)	25.865 (1482)	21.031 (1205)	25.865 (1482)	25.446 (1458)
SPIN CONTROL CHANGE IN SPIN RATE (RAD/S (RPM))	16.860 (161)	23.143 (221)	6.912 (66)	12.881 (123)	6.912 (66)	12.881 (123)
TOTAL PROPELLANT REQUIRED (KG)	18.2	16.3	16.7	13.0	17.1	14.7

ALL CONFIGURATIONS

8.6.1.2 RCS Tradeoff Studies

ALL CONFIGURATIONS

Tradeoff studies were performed to determine the best approach to use in configuring the RCS. These studies determined:

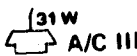
- The required number and locations of the thrusters
- Thruster position outboard from the spacecraft spin axis
- The most desirable propellant
- Whether blowdown or regulated pressurization was optimum
- Whether a bladder was needed to maintain propellant position or whether spacecraft spin forces would be sufficient to ensure continuous propellant feed for the thrusters
- The most applicable propellant tank.

Determination of Thruster Required Number and Location

Figure 8.6-2 shows thruster locations for three to eight thrusters and indicates that more than five are required to ensure mission success with the failure of a single thruster. If amplification of the coning angle is important, then eight thrusters are required; if not, six could be used.

Thruster Position Outboard from the Spacecraft Spin Axis

The most desirable position for RCS thruster mounting is at the outboard edge of the spacecraft platform. This position minimizes exhaust gas impingement on the spacecraft. However, the requirement that the



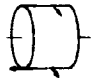


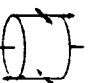
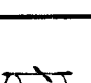
THRUST ARRANGEMENT					
NUMBER OF THRUSTERS	3	4	5	6	8
MISSION CONSTRAINTS	MUST PRECESS SPACECRAFT LARGE ANGLE TO PERFORM ΔV MANEUVERS (=3.142 RAD (=180 DEG))	MUST PRECESS SPACECRAFT MEDIUM ANGLE TO PERFORM ΔV MANEUVERS (=1.571 RAD (=90 DEG))	MUST PRECESS SPACECRAFT SMALL ANGLE TO PERFORM ΔV MANEUVERS (=0.785 RAD (=45 DEG))		
RELIABILITY	ONE FAILURE LOSES MISSION	ONE ROLL THRUSTER FAILURE LOSES MISSION		MISSION SUCCESS WITH ONE FAILURE	MISSION SUCCESS WITH TWO FAILURES
OPERATIONAL EFFECTS	AMPLIFIES CONING ANGLE DURING ΔV				NO AMPLIFICATION OF CONING ANGLE DURING ΔV
	ΔV RESULTING DURING SPIN AND PRECESSION				MINIMUM ΔV DURING SPIN AND PRECESSION

Figure 8.6-2. Required Number and Location of Thrusters Tradeoff

A/C III spacecraft precess 0.017 radian (1 degree) or less with each precession pulse firing must also be considered. At a nominal moment of inertia of $176 \text{ kg} \cdot \text{m}^2$ ($130 \text{ slug} \cdot \text{ft}^2$), during all portions of the mission, the Atlas/Centaur thrusters could be positioned at the spacecraft's outboard edge and operated at 125-millisecond pulses without exceeding this requirement (Figure 8.6-3).

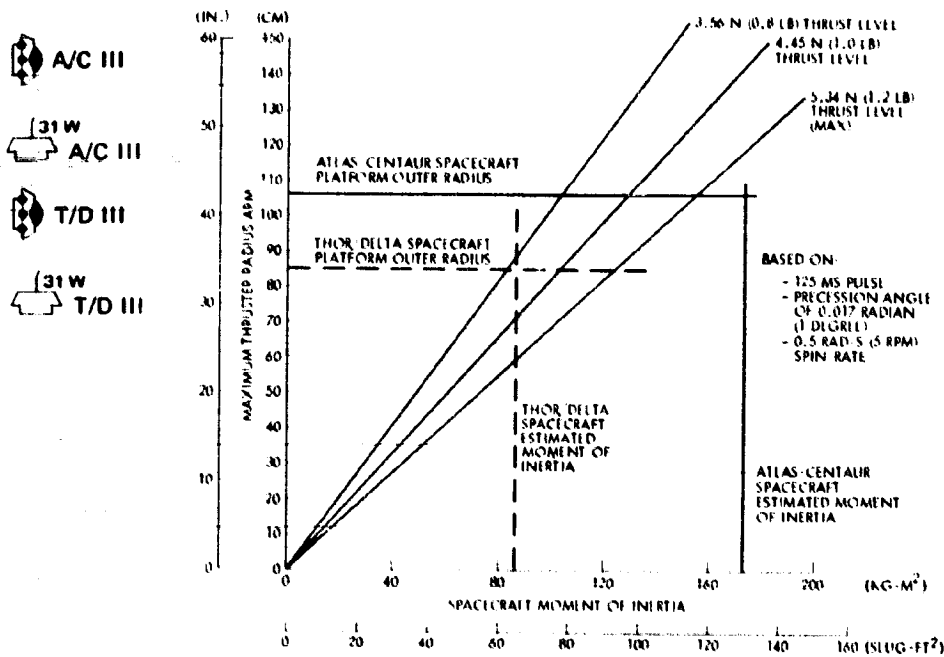


Figure 8.6-3. Maximum Allowable Precession Thruster Radius Arm to Meet 0.017 Radian (1 Degree) Precession Limit at 0.125 Second Pulsewidth as a Function of Thrust Level and Spacecraft Moment of Inertia

T/D III
(31 W) T/D III

For the Thor/Delta, at a nominal moment of inertia of $88 \text{ kg} \cdot \text{m}^2$ ($65 \text{ slug} \cdot \text{ft}^2$), when the thrust level is 5.34 N, the precession requirement of 0.017 radian (<1 degree) or less could be met by using a shorter pulsewidth (64 ms @ 2.2 N). Only after the system supply pressure drops to approximately 300 psia could the desired 0.125-millisecond pulsewidth be used.

Other items influencing thruster location are structural, thermal, and impingement considerations. Structural aspects are not critical because the thruster weights and thrust levels are relatively low and do not present design problems.

The thermal considerations are somewhat more important. While it would be desirable to locate all thrusters so that solar and/or spacecraft conductive heating could be used, this is not practical with either spacecraft configuration. Therefore, some of the thrusters will be shaded and will require heaters. Wherever possible, the thrusters are thermally coupled to the warmer spacecraft structure, and all thrusters are insulated to minimize radiative heat losses and heater power requirements.

Plume impingement was a key consideration in thruster location. The outboard locations selected tend to minimize plume impingement on critical surfaces.

Propellant Selection

The propellant tradeoff was made early in the study, but since the propellant weights involved span the final selected weights, the results are still valid.

Figure 8.6-4 shows that, regardless of launch vehicle or mission, the use of monopropellant hydrazine results in the lightest systems. The other systems show less direct cost, but the ammonia systems exceed the spacecraft power capability and the nitrogen systems are far too heavy. Monopropellant hydrazine is the best choice.

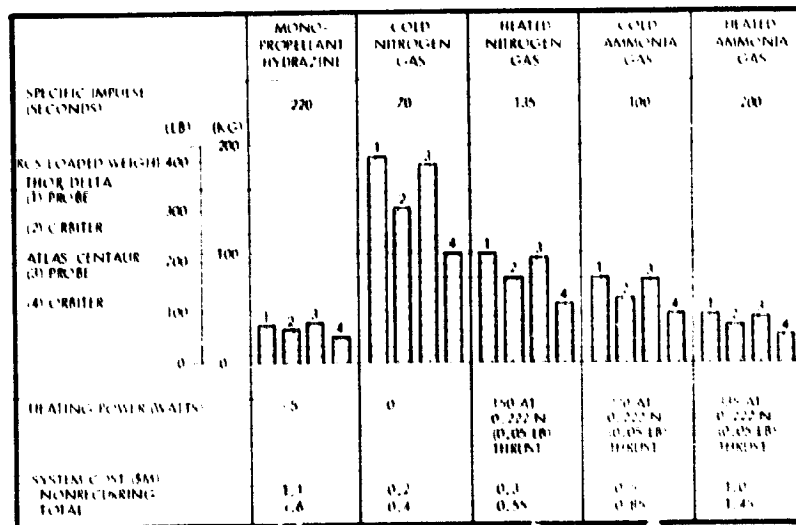


Figure 8.6-4. RCS Propellant Tradeoffs

Blowdown Versus Regulated Pressurization ALL CONFIGURATIONS

As was the case for propellant selection, the blowdown versus regulated pressurization tradeoff study was done early. However, since the weight of propellants studied encompassed the selected final propellant loading, the results remain valid.

The weights are based on use of the 27.9 cm (11 inch) diameter Mariner '69 tank and Pioneers 10 and 11 type FLTSATCOM thrusters. As shown in Figure 8.6-5, the selected blowdown system is lighter. It is also more reliable and less costly.

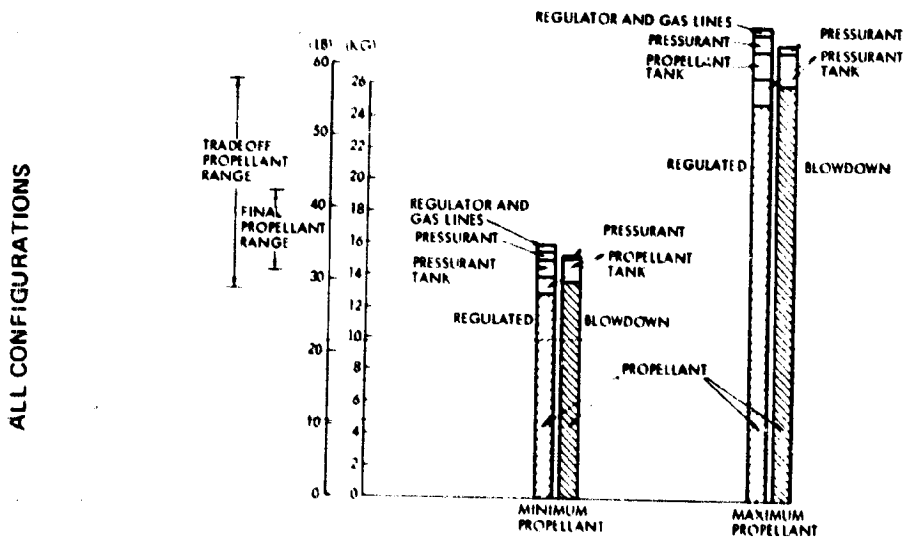
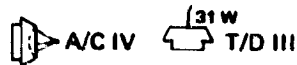


Figure 8.6-5. Blowdown Versus Regulated Pressurization Tradeoff

Bladder Versus Centrifugal Forces for Continuous Propellant Feed



The use of centrifugal force for propellant feed eliminates the need for a bladder and its associated components. Bladders are not required when there is a bond number greater than 10 (when centrifugal forces dominate over surface tension). The bond number is defined as:

$$B_o = \frac{\text{body force}}{\text{surface tension force}} = \frac{R^3 g}{\sigma / \rho}$$

where

- ρ = liquid density
- σ = surface tension
- g = acceleration due to spin
- R = tank radius

The properties of hydrazine over the spacecraft temperature ranges are:

$$\rho = 1.009 \text{ g/cm}^3$$

$$\sigma = 74.76 \text{ dyne/cm}$$

With tank diameters of 27.9 cm (11 in.), therefore, the bond number for the Thor/Delta vehicle (with its 0.5 rad/s spin rate) is:

$$B_o = \frac{(13.9 \text{ cm})^2 \cdot 12.9 \text{ cm/s}^2}{74.1 \text{ cm}^3/\text{s}^2} = 34$$

The Atlas/Centaur has an even greater margin because of its larger diameter Defense System Communications Satellite (DSCS) II tanks. Figure 8.6-6 shows how the bond number varies with spin rate for the Atlas/Centaur and Thor/Delta configurations.

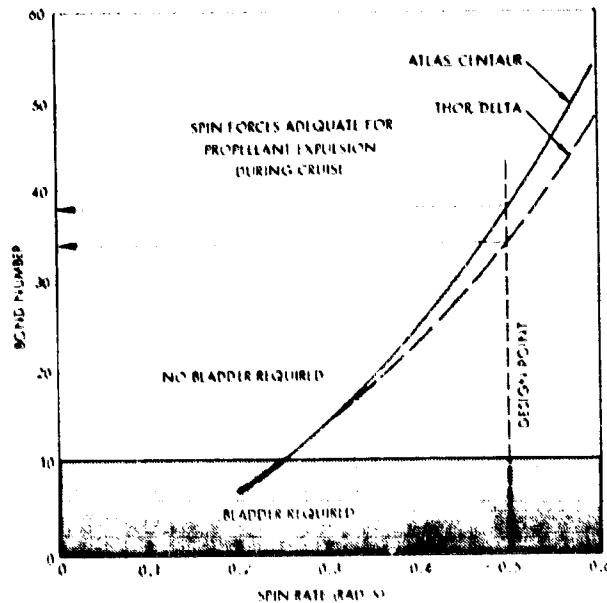


Figure 8.6-6. Bladder Versus Spin Forces

Propellant Tank Selection  A/C IV  T/D III  - A/C IV  T/D III ^(31W)



The hydrazine quantities to be stored for the various missions and spacecraft are shown in Table 8.6-2.

Table 8.6-2 Propellant Requirements

LAUNCH VEHICLE	MISSION	USABLE PROPELLANT KG (LB)	RESIDUAL KG (LB)	TOTAL KG (LB)	PRESSURANT KG (LB)
THOR DELTA	PROBE ORBITER	17.9 (39.3)	0.4 (0.8)	18.3 (40.1)	0.3 (0.6)
		15.9 (35.0)	0.4 (0.8)	16.3 (35.8)	0.3 (0.6)
ATLAS CENTAUR	PROBE ORBITER	15.6 (34.4)	1.5 (3.2)	17.1 (37.6)	1.5 (3.4)
		12.6 (27.8)	1.5 (3.2)	14.1 (31.0)	1.7 (3.8)
VERSION IV ATLAS CENTAUR	ORBITER	13.2 (29.3)	1.5 (3.2)	14.7 (32.5)	1.6 (3.7)





Three candidate tanks were considered. These were the Mariner '69 tank ($1.14 \times 10^4 \text{ cm}^3$, 697 in.³), the Skynet tank ($8.14 \times 10^3 \text{ cm}^3$, 497 in.³), and the DSCS II tank ($1.89 \times 10^4 \text{ cm}^3$, 1100 in.³). Each candidate tank has been qualified and flown on hydrazine subsystems. The DSCS II tanks are the most attractive for the Atlas/Centaur spacecraft, while the Mariner '69 tank is best for the Thor/Delta.

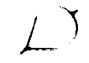


Table 8.6-3 shows a comparison of the candidate tanks. The key considerations in selecting the DSCS II tanks for the Atlas/Centaur spacecraft were the adequacy of the existing design (600 psia operating pressure), the piping system simplicity and high reliability, and minimum platform outboard area committed to the RCS piping. The Mariner '69 tank was selected for the Thor/Delta spacecraft because the Skynet tanks provided insufficient volume to meet the desired 3.4:1 blowdown pressure ratio and the DSCS II tanks present packaging problems because of the large tank envelope.

Maintenance of Positive Propellant Head During the Mission  A/C IV  - A/C IV



The 0.5 rad/s (5 rpm) spacecraft spin rate produces centrifugal forces adequate to maintain a positive propellant head at the tank outlet ports with 0.42 kg (0.92 lb) residual hydrazine per tank. The most critical period of the mission relative to propellant unporting (exposure of the

Table 8.6-3. RCS Tank Tradeoffs

-  A/C IV
-  T/D III
-  A/C IV
-  (31 W) T/D III

TANK	MATERIAL	VOLUME (m^3 (IN. ³))	ATLAS CENTAUR BLOWDOWN RATIO	THOR DELTA BLOWDOWN RATIO	WEIGHT (KG (LB))	OPERATING BOOST PRESSURE ($N/m^2 \times 10^6$ (PSIA))	REMARKS
 DYNA II 33 x 40 x 6 CM (13 x 16 IN.)	Ti	16 027 (976)	1.4:1	1.3:1	1.5 (3.4)	4.14 8.20 (600 1200)	PROS: SATISFACTORY PRESSURE CAPABILITY AMPLE PROPELLANT GROWTH MARGIN (-100%) SIMPLE PIPING, ONE OUTBOARD LIQUID FEED TUBE AND ONE INBOARD GAS TUBE EASIEST TO MOUNT (POLAR MOUNTS) CONS: DIFFICULT TO PACKAGE ON THOR DELTA SPACECRAFT GREATEST WEIGHT AND ENVELOPE
 MARINER '69 27.9 CM (11 IN.) DIAMETER	Ti	11 420 (697)	1.9:1	2.1:1	1.0 (2.3)	2.76 5.52 (400 800)	PROS: AMPLE PROPELLANT GROWTH (-20%) NOMINAL WEIGHT AND ENVELOPE CONS: REQUIRES REDESIGN TO • ELIMINATE BLADDER • ADD DIP TUBES • INCREASE PRESSURE CAPABILITY EXTRA TUBING NEEDED FOR ON PAD DRAIN DIFFICULT TO MOUNT
 SKYNET 23.4 CM (10 IN.) DIAMETER	T	8 140 (497)	3.0:1	3.8:1	0.7 (1.5)	3.10 6.20 (450 900)	PROS: LEAST WEIGHT AND ENVELOPE CONS: REQUIRES REDESIGN TO INCREASE PRESSURE CAPABILITY MARGINAL GROWTH CAPABILITY (-10%)

*GREATER THAN DESIRED 3.4:1 BLOWDOWN RATIO.

-  A/C IV liquid outlet port to gas during RCS operation) occurs at end-of-life. At this time the spacecraft is at its lowest weight and axial thruster firings
-  A/C IV have the greatest effect on the in-tank propellant position.

Propellant position in the preferred Atlas/Centaur tanks at end-of-life, i.e., with the +X axis thrusters firing is shown in Figure 8.6-7. The propellant position is approximately 0.19 radian (11 degrees) from the vertical at 0.5 rad/s, and represents an unavailable volume of 415 cm³, or 0.42 kg of hydrazine per tank. Firing the +X axis thrusters is worst-case, as acceleration from the -X axis thrusters would orient the propellant toward the liquid outlet port in a conospheroid tank.

The sensitivity of the residual propellant to spacecraft spin rate in a conospheroid tank is shown in Figure 8.6-8. Unporting can be prevented by on-loading the proper amount of propellant. With a 0.5 rad/s spin rate, 0.42 kg of residual propellant, an acceptable quantity, is sufficient. At spin rates below the 0.4 rad/s range, the necessary residual quantities become excessive. Spin rates above 0.5 rad/s would reduce the hydrazine required.

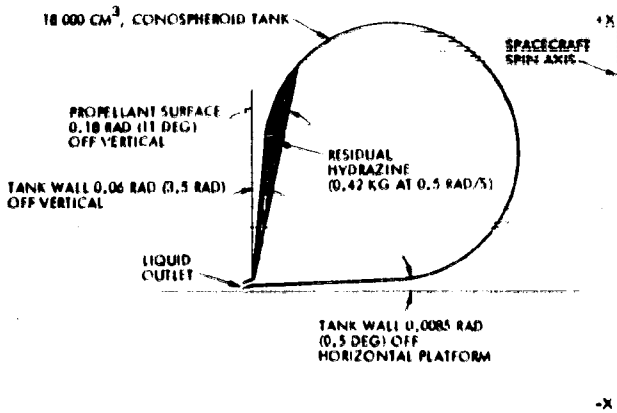


Figure 8.6-7. Atlas/Centaur Propellant Position at End of Life With +X Axis Thrusters Firing

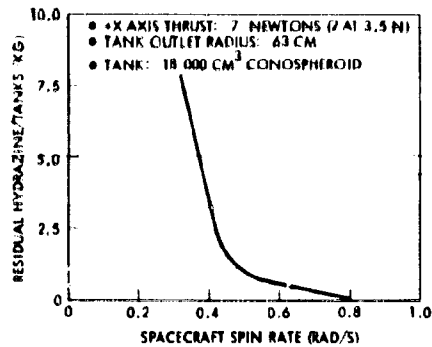


Figure 8.6-8. Residual Propellant Necessary to Prevent Propellant Unporting in Atlas/Centaur Conospheroid Tanks

8.6.1.3 Preferred Atlas/Centaur RCS Description

The selected RCS, Figure 8.6-9, is common to the probe bus and orbiter. Eight thrusters are used to provide redundancy and to prevent coning angle amplification; the transverse thrusters also simplify ground station operation by retaining spin-axis orientation during lateral maneuvers.

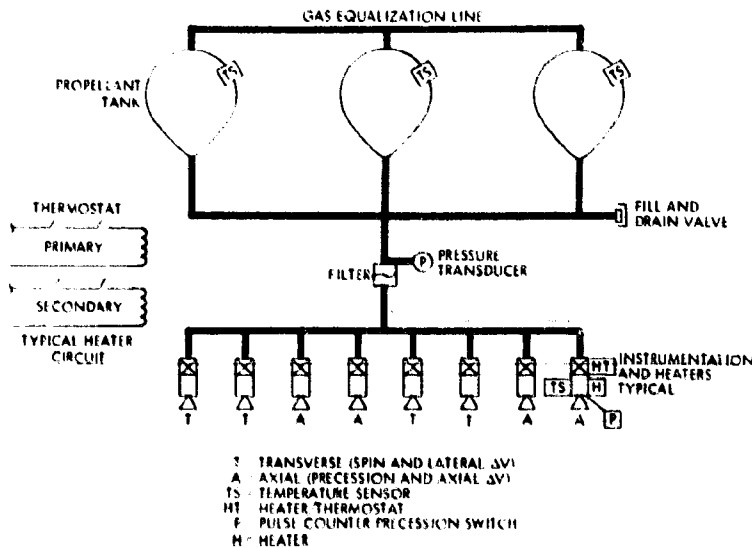


Figure 8.6-9. Preferred Atlas/Centaur RCS

Pioneer 10 and 11 flight-qualified components are used throughout the subsystem to eliminate development risk and to minimize cost. Minor design changes, incorporated for FLTSATCOM, adapt the Pioneer 10 and 11 hardware to this specific, unclustered engine application.

The propellant and pressurant lines and fittings are welded or brazed (between the thrusters and tanks) to ensure leak-free assemblies. Blow-down pressurization and centrifugal force for propellant positioning and expulsion eliminates the need for a bladder and the associated regulators and pressurization components. This simplified RCS minimizes cost and provides high reliability.

General Arrangement

The RCS is composed of three propellant tanks with temperature sensors, and eight thrusters (four axial thrusters for large ΔV maneuvers and precessions, and four transverse thrusters for spin control and small lateral ΔV maneuvers) as shown in Figure 8.6-9. Each thruster has a propellant valve heater, thermostat, and temperature sensor. The catalyst bed and a pressure-switch pulse counter have heaters and temperature sensors.

There are primary and secondary thermostat circuits for all heating elements, providing series-parallel redundancy. While conservative temperature-control limits on all heaters increase the needed power, they assure a positive deadband between the primary and secondary heaters so that both circuits do not come on simultaneously, causing excessive power drain. Integration and test costs are minimal. The use of tighter control limits, with secondary heater power turn-on close to the hydrazine freezing point, would require additional verification testing to assure that parts of the system away from the thermostat do not actually freeze.

The tanks and thrusters are connected by plumbing without heaters, but containing temperature sensors. They are within the thermally controlled equipment compartment. A filter is located upstream of the thrusters. A fill and drain valve provides for loading and draining the propellant. Common gas and propellant lines maintain equal quantities of propellant in the three tanks for spacecraft balance.

Piping

Proper line sizing and routing are essential to maintain equal propellant loads among tanks and, therefore, spacecraft balance. For the preferred RCS piping, Figure 8.6-10, as for all TRW spin-stabilized hydrazine systems, the tanks are interconnected with flight-proven 0.95 cm (0.375 inch) diameter piping. The plumbing is routed to maintain equal levels (loads) in the three tanks during static and dynamic conditions. Gas bubbles in the liquid lines will migrate into the tanks, as will liquid in the gas lines.

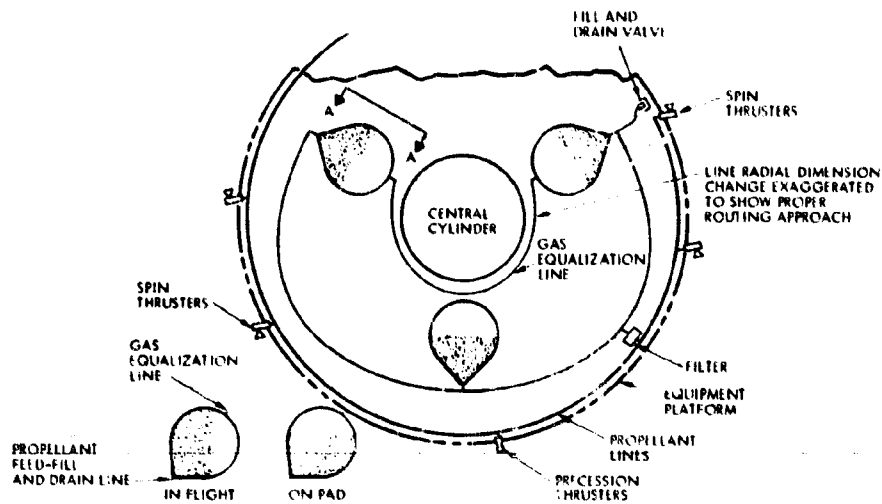


Figure 8.6-10. Atlas/Centaur RCS Piping Diagram

To prevent bubble traps, the liquid supply piping on the probe bus is routed over the small probes. Inboard routing is not recommended because bubbles could be trapped in these inboard piping segments, preventing liquid-to-liquid communication between tanks. This could result in unequal tank loading. The lines are also oriented to maximize the amount of propellant that can be drained from the tanks while the spacecraft is on-pad.

The orbiter liquid piping would be routed in the same manner. However, it is possible to route the orbiter piping along the platform.

The DSCS II tank does not require dip tubes for propellant draining or ullage interconnect because the tank outlet is down and outboard and the gas port is up and inboard. The liquid port is covered by liquid and the gas port is uncovered in both spin and static environments.

RCS Performance

The following three tables (Tables 8.6-4, 8.6-5, and 8.6-6) illustrate the RCS performance for the Atlas/Centaur spacecraft. They show the propellant required, thruster operations, and tank pressures for each mission mode. Table 8.6-4 presents the RCS performance for the 508 kg (1120 lb) orbiter payload and Table 8.6-5, the 434 kg (955 lb) orbiter. The probe data presented in Table 8.6-6 is representative (within one percent) of either the 1977 launched probe at 773 kg (1703 lb) or the 1978 launch Version IV science payload probe at 783 kg (1724 lb).

Table 8.6-4. Science Version IV Atlas/Centaur Configuration — RCS Performance, Orbiter Mission, 508 kg (1120 pounds)

MISSION MODE	THRUSTER DUTY CYCLE ON/OFF TIME (SECONDS)	NUMBER OF PULSES PER TWO THRUSTERS	TOTAL IMPULSES N·S (LB·S)	AVERAGE SPECIFIC IMPULSE (SECONDS)	PROPELLANT CONSUMED [KG (LB)]	TANK PRESSURE (N/M ² × 10 ⁻⁶)
FIRST MIDCOURSE						
PRECESS 1.70 RAD (100 DEG)	0.125-12.5	240	378 (62.5)	180	0.16 (0.35)	3.10
SW 7 M/S	CONTINUOUS	770 SECONDS	2 556 (800)	227	1.60 (3.52)	
PRECESS 1.70 RAD (100 DEG)	0.125-12.5	240	278 (62.5)	180	0.16 (0.35)	
CRUISE						
[SOLAR TORQUE 0.20 RAD (12 DEG) EARTH TRACK 1.63 RAD (80 DEG)]	0.125-12.5	240	272 (61)	180	0.15 (0.34)	
SECOND MIDCOURSE						
PRECESS 1.70 RAD (100 DEG)	0.125-12.5	240	278 (62.5)	180	0.16 (0.35)	2.99
SW 1 M/S	CONTINUOUS	110 SECONDS	508 (114)	227	0.23 (0.50)	
PRECESS 1.70 RAD (100 DEG)	0.125-12.5	240	278 (62.5)	180	0.16 (0.35)	
FLIP 3.06 RAD (180 DEG)	0.125-12.5	430	500 (113)	180	0.29 (0.63)	
THIRD MIDCOURSE						
PRECESS 0.77 RAD (45 DEG)	0.125-12.5	110	124 (28)	180	0.07 (0.16)	2.83
SW 2 M/S	CONTINUOUS	220 SECONDS	1 016 (228)	227	0.46 (1.00)	
PRECESS 0.77 RAD (45 DEG)	0.125-12.5	110	124 (28)	180	0.07 (0.16)	
INSERTION						
PRECESS 2.07 RAD (122 DEG)	0.125-12.5	300	339 (76.3)	180	0.20 (0.43)	2.76
SPIN TO 6.3 RAD/S	CONTINUOUS	395 SECONDS	1 756 (395)	225	0.80 (1.76)	
SPIN TO 0.5 RAD/S	CONTINUOUS	345 SECONDS	1 529 (344)	223	0.70 (1.54)	
PRECESS 2.07 RAD (122 DEG)	0.125-12.5	278	296 (66.7)	177	0.17 (0.38)	
FLIP 3.06 RAD (180 DEG)	0.125-12.5	410	437 (98.4)	177	0.25 (0.56)	2.69
ON-ORBIT						
[EARTH TRACK 4.25 RAD (250 DEG) SOLAR TORQUE 0.37 RAD (22 DEG)]	0.125-12.5	620	660 (149)	177	0.39 (0.85)	2.26
PERIAPSIS MAINTENANCE 12.3 M/S	CONTINUOUS	1100 SECONDS	4 472 (1006)	222	2.05 (4.52)	
70.2 M/S	CONTINUOUS	960 SECONDS	4 009 (902)	222	1.70 (3.75)	
12.3 M/S	CONTINUOUS	1100 SECONDS	4 472 (1006)	222	2.05 (4.52)	
8.7 M/S	CONTINUOUS	760 SECONDS	3 160 (711)	222	1.45 (3.20)	
TOTALS		3498 PULSES 5300 SECONDS	28 343 (6300.4)		13.3 (29.22)	

Table 8.6-5. Atlas/Centaur Configuration RCS Performance, Orbiter Mission

MISSION MODE	THRUSTER DUTY CYCLE ON/OFF TIME (SECONDS)	NUMBER OF PULSES PER TWO THRUSTERS	TOTAL IMPULSES (N · S (LB · S))	AVERAGE SPECIFIC IMPULSE (SECONDS)	PROPELLANT CONSUMED (KG (LB))
INITIAL ATTITUDE					
DESPIN	CONTINUOUS		60 (11.5)	225	0.03 (0.06)
PRECES	0.125/12.5	151	174 (39)	175	0.10 (0.22)
TRIM SPIN	0.125/12.5		NEGATIVE		
MIDCOURSE 14.5 M/S, 7 M/S, 2 M/S					
PRECES	0.125/12.5	840	939 (211)	173	0.55 (1.22)
ΔV	CONTINUOUS		9 496 (2134)	222	4.37 (9.62)
TRIM SPIN	VARIES		165 (37)	170	0.10 (0.22)
CRUISE	0.125/12.5	105	58 (13)	170	0.04 (0.08)
ORBIT INSERTION					
PRECES	0.125/12.5	131	76 (17)	170	0.04 (0.10)
SPIN UP	CONTINUOUS		1 157 (260)	220	0.54 (1.19)
DESPIN	CONTINUOUS		1 157 (260)	220	0.54 (1.19)
PRECES	0.125/12.5	135	76 (17)	170	0.04 (0.10)
PERIAPSIS MANEUVERS AND ATTITUDE MAINTENANCE					
PRECES	0.125/12.5	583	654 (147)	160	0.42 (0.92)
ΔV	CONTINUOUS		11 935 (2683)	218	5.58 (12.30)
TRIM SPIN	VARIES		209 (47)	160	0.14 (0.30)
CRUISE	0.125/12.5	270	182 (41)	160	0.12 (0.26)
TOTAL			26 342 (5919.5)		12.6 (27.78)

Table 8.6-6. Science Version III and IV Atlas/Centaur Configuration RCS Performance, Probe Mission

MISSION MODE	THRUSTER DUTY CYCLE ON/OFF TIME (SECONDS)	NUMBER OF PULSES PER TWO THRUSTERS	TOTAL IMPULSES (N · S (LB · S))	AVERAGE SPECIFIC IMPULSE (SECONDS)	PROPELLANT CONSUMED [KG (LB)]	TANK PRESSURE (IN 10^{-6})
FIRST MIDCOURSE						
PRECES 1.70 RAD (1.70 DEG) (100 DEG) 100 DEG	0.125/12.5	640	738 (166)	180	0.42 (0.92)	3.10
ΔV 7 M/S	CONTINUOUS	575 SECONDS	5 498 (1237)	227	2.47 (5.45)	2.86
SOLAR TORQUE AND EARTH TRACK 10.65 RAD (38 DEG)	0.125/12.5	120	140 (31.4)	180	0.08 (0.17)	
SECOND MIDCOURSE						
PRECES 1.70 RAD (1.70 DEG) (100 DEG) 100 DEG	0.125/12.5	640	738 (166)	180	0.42 (0.92)	
ΔV 1 M/S	CONTINUOUS	85 SECONDS	795 (177)	227	0.35 (0.78)	2.81
THIRD MIDCOURSE						
PRECES 0.77 RAD (0.77 DEG) (45 DEG) 45 DEG	0.125/12.5	288	388 (75)	180	0.19 (0.42)	
ΔV 2 M/S	CONTINUOUS	165 SECONDS	1 370 (354)	227	0.71 (1.56)	2.75
LARGE PROBE RELEASE						
SPIN TO 2.1 RAD/S	CONTINUOUS	290 SECONDS	662 (149)	180	0.30 (0.66)	
PRECES 0.43 RAD (0.43 DEG) (25 DEG) 25 DEG	0.125/12.5	660	702 (158)	178	0.40 (0.88)	
DESPIN TO 1 RAD/S	CONTINUOUS	45 SECONDS	384 (86.5)	225	0.17 (0.38)	
RETARGET RELEASE SMALL PROBE NO. 1						
PRECES - Δ 3.60 RAD (212 DEG)	0.125/12.5	1390	1 467 (330)	177	0.80 (1.76)	2.70
ΔV 1.21 M/S	CONTINUOUS	65 SECONDS	373 (129)	224	0.27 (0.58)	
RETARGET RELEASE SMALL PROBE NO. 2						
PRECES - Δ 3.68 RAD (216.2 DEG)	0.125/12.5	1070	1 125 (253)	177	0.64 (1.41)	
ΔV 16.07 M/S	CONTINUOUS	790 SECONDS	6 294 (1416)	223	2.89 (6.36)	2.43
RETARGET RELEASE SMALL PROBE NO. 3						
PRECES - Δ 5.85 RAD (344 DEG)	0.125/12.5	1325	1 391 (313)	177	0.80 (1.72)	
ΔV 6.12 M/S	CONTINUOUS	260 SECONDS	1 942 (437)	222	0.89 (1.97)	2.33
RETARGET BUS						
PRECES 0.44 RAD (0.44 DEG) (25.8 DEG) 25.8 DEG	0.125/12.5	155	163 (36.6)	177	0.10 (0.22)	
ΔV 25.72 M/S	CONTINUOUS	1000 SECONDS	7 263 (1634)	221	2.80 (6.17)	2.19
SPIN TO 63 RAD/S	CONTINUOUS	120 SECONDS	902 (203)	221	0.43 (0.91)	
UV EXPERIMENT - 1.36 RAD (80 DEG)	0.125/12.5	245	258 (58)	176	0.15 (0.33)	
SPIN CONTROL	CONTINUOUS (0.03 RAD/S M/S)	100 SECONDS	738 (166)	221	0.34 (0.75)	2.10
TOTALS		6533 PULSES 3495 SECONDS	33 673 (7575.5)		15.6 (34.3)	

Other RCS Features  A/C IV  A/C IV

Figure 8.6-11 summarizes other features of the preferred Atlas/Centaur RCS.

8.6.1.4 Preferred Thor/Delta RCS Description  T/D III  T/D III

The selected RCS is common to both the probe bus and the orbiter. The design is similar to the Atlas/Centaur RCS described in Section 8.6.1.3. Flight-qualified hardware is used throughout; eight thrusters are used to provide redundancy and to prevent coning angle amplification; and blowdown pressurization/centrifugal expulsion are used. The preferred Thor/Delta power and telemetry requirements and design are identical to the preferred Atlas/Centaur, Figure 8.6-11. Figure 8.6-12 summarizes other features of the preferred Thor/Delta RCS subsystem.

8.6.2 Orbit Insertion Motor  A/C IV  T/D III

A solid rocket was selected for both the Atlas/Centaur and the Thor/Delta orbiter missions. The Aerojet SVM-2 is optimum for both the earlier and Version IV science Atlas/Centaur orbiters. The existing, qualified motor design has the necessary propellant load capability. The Hercules BE-3-A motor, selected for the Thor/Delta orbiter, is also qualified, and the existing design is totally adequate with the addition of a safe and arm device.

Bipropellant rockets were evaluated and found to present higher risk and cost than solid rockets, although the bipropellant showed a small performance advantage.


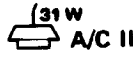
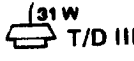
Appendices 8.6A and 8.6B discuss the details of the selected Atlas/Centaur and Thor/Delta solid motors. Appendix 8.6C discusses the contamination aspects of solid motors in general.

8.6.2.1 Requirements  A/C IV  T/D III

The mission requirements shown in Table 8.6-7 are payload weight and velocity change, the key performance requirements. Because each candidate motor was compatible with the applicable spacecraft design, additional performance requirements (envelope, weight, etc.) were not considered critical.

Table 8.6-7. Mission Requirements

A/C IV (31 W) T/D III	LAUNCH VEHICLE	VELOCITY CHANGE				PAYLOAD WEIGHT			
		MIDCOURSE		ORBIT INJECTION		SEPARATION		INJECTION IGNITION	
		(M/S)	(FT/S)	(M/S)	(FT/S)	(KG)	(LB)	(KG)	(LB)
	THOR/DELTA	82	(269)	954	(3130)	292.6	(645)	280.3	(618)
	ATLAS/CENTAUR	23.5	(77)	854	(3130)	463	(960)	429.3	(946.5)
	ATLAS/CENTAUR VERSION IV SCIENCE PAYLOAD	23.5	(77)	854	(3130)	509	(1120)	505	(1115)

8.6.2.2 Tradeoffs   

Tradeoff studies were made to determine whether existing rocket motor systems could meet the Pioneer Venus Type II trajectory for both the Atlas/Centaur and the Thor/Delta launch vehicles. Only motors that had been successfully flown in space were considered. Primary criteria for selection were:

- Magnitude of changes to meet Pioneer Venus requirements
- Demonstrated reliability in flight
- Overall cost of procurement
- Design limitations

Atlas/Centaur  

Solid Rocket Motor for Use with Hydrazine System. Tables 8.6-8 and 8.6-9 show the key features of the candidate motors for the initial Atlas/Centaur orbiter and the Atlas/Centaur Version IV science payload orbiter.

The Hercules BE-3-B motor required such a large addition to the cylindrical portion of the chamber that it was dropped from contention early because requalification would be necessary. The increased cost and risk are not warranted.

The Thiokol TE-M-521 motor is acceptable for the initial Atlas/Centaur, but requires 4.22 cm additional length in the cylindrical portion of the motor case plus an increase in throat area to accommodate the increased propellant weight and burning surface area. The TE-M-521 would have to be lengthened 12.5 cm for the Version IV science payload,

A THE PREFERRED RCS USES FLIGHT-QUALIFIED THRUSTER HARDWARE

ITEM	USE AS IS	MODIFIED	REMARKS
PROPELLANT TANK	X		DCSC II
THRUSTER	X		FLTSATCOM
THRUSTER VALVE	X		FLTSATCOM
FILTE?	X		PIONEERS 10 AND 11
PRESSURE TRANSDUCER	X		PIONEERS 10 AND 11
FILL AND DRAIN VALVE	X		PIONEERS 10 AND 11
LINE AND FITTINGS		X	PIONEERS 10 AND 11 WITH MODIFIED LINE RUNS/SIZE

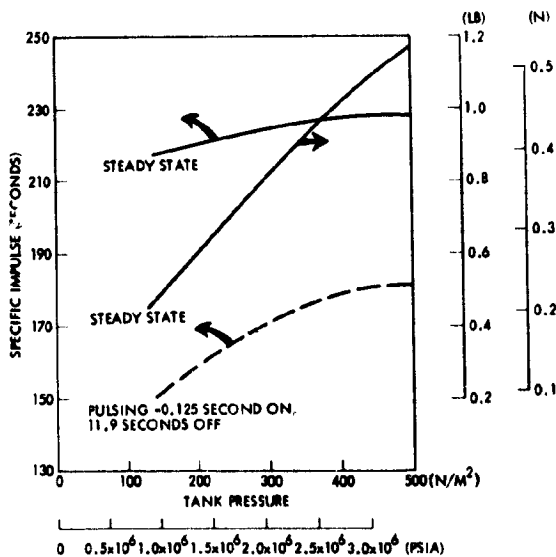
* DERIVED FROM PIONEER 10 AND 11 ISOTOPE-HEATED, DUAL THRUSTER UNIT. REMOVED FROM EXPENSIVE, COMPLEX CLUSTER UNIT, MOUNTED SEPARATELY; VALVE AND DECOMPOSITION CHAMBER MECHANICALLY ATTACHED WITH PERFORATED METAL THERMAL STANDOFF; ISOTOPE HEATING ELEMENT DELETED. THRUSTER VALVE SEAL MATERIAL IMPROVED, ELIMINATING DRY SEAL LEAKAGE EXPERIENCED DURING PIONEER 10 AND 11 SUBSYSTEM TESTING. REDUCED UNIT COMPLEXITY LOWERS COSTS AND INCREASES RELIABILITY.

B THE RCS WEIGHT BREAKDOWN REFLECTS THE ACCURACY OF USING FLIGHT KNOWN WEIGHTS *

ITEM	NUMBER REQUIRED	WEIGHT	
		PER COMPONENT (KG-LB.)	TOTAL ORBITER
PROPELLANT TANK	3	1.54 (3.4)	4.62 (10.2)
THRUSTER	8	0.27 (0.6)	2.17 (4.8)
FILTER	1	0.18 (0.4)	0.18 (0.4)
PRESSURE TRANSDUCER	1	0.18 (0.4)	0.18 (0.4)
FILL AND DRAIN VALVE	1	0.09 (0.2)	0.09 (0.2)
LINE AND FITTINGS	-		0.77 (1.7)
TOTAL HARDWARE			8.03 (17.7)
PRESSURANT			0.41 (0.9)
PROPELLANT			15.06 (33.3)
TOTAL LOADED WEIGHT			23.49 (51.7)

* WEIGHTS OF THE HARDWARE FOR MOUNTING THE TANKS, THRUSTERS, VALVES ARE NOT SHOWN HERE; THEY ARE PARTS OF OTHER SUBSYSTEMS.

D THE SELECTED TRW MRE-1 THRUSTER GIVES EXCELLENT PERFORMANCE OVER A WIDE BLOWDOWN RANGE, AS VERIFIED BY ACTUAL TEST DATA FROM PIONEERS 10 AND 11 *



* THRUSTER PERFORMANCE DATA, IN CONJUNCTION WITH PROPELLANT TANK BLOWDOWN, VERIFIED INITIAL PROPELLANT ESTIMATES TO WITHIN ONE PERCENT.

E RCS POWER

ITEM	MAXIMUM POWER (WATTS)		
	PER UNIT	SYSTEM AVERAGE	
THRUSTER VALVE ACTUATION POWER	5	10	BASED ON DURING MAXIMUM SECOND FIRING
PRESSURE TRANSDUCER	0.3	0.3	CONTIN
THRUSTER VALVE HEATERS			CONTIN
SPIN	0.3	1.2	ON USE
ΔV UPPER	0.6	1.2	AND TH
ΔV LOWER	0.2	0.4	PRIMARY
THRUSTER CATALYST BED			12.78°C
SPIN	0.3	1.2	SECOND
ΔV UPPER	0.4	0.8	(45°F)
ΔV LOWER	0.2	0.4	
TOTAL CONTINUOUS POWER		5.5	

NO HEATERS ARE NEEDED FOR PROPELLANT TANK AND LINES WHICH ARE LOCATED IN THE (+44°C/+40°F+) EQUIPMENT COMPARTMENT. PROTRUDING PORTS ARE INSULATED.

NOTE: HYDRAZINE FREEZES AT -1.67°C (-35°F).

ACCURACY OF USING FLIGHT-TESTED COMPONENTS WITH

PER COMPONENT (KG-LB)	WEIGHT	
	TOTAL (KG-LB)	
	CRIBTER	PROBE
1.54 (3.4)	4.62 (10.2)	4.62 (10.2)
0.27 (0.6)	2.17 (4.8)	2.17 (4.8)
0.18 (0.4)	0.18 (0.4)	0.18 (0.4)
0.18 (0.4)	0.18 (0.4)	0.18 (0.4)
0.09 (0.2)	0.09 (0.2)	0.09 (0.2)
	0.77 (1.7)	0.77 (1.7)
	8.03 (17.7)	8.03 (17.7)
	0.41 (0.9)	0.41 (0.9)
	15.06 (33.2)	16.6 (36.6)
	23.49 (51.8)	25.04 (55.2)

TANKS, THRUSTERS, VALVES, ETC., AND WIRING
SUBSYSTEMS.

C THE PIONEER VENUS THRUSTER REQUIREMENTS ARE LESS SEVERE THAN PIONEERS 10 AND 11 OR FLTSATCOM, GIVING A HIGH LEVEL OF CONFIDENCE IN THE SELECTED THRUSTER

ITEM	MISSION REQUIREMENTS					
	PIONEERS 10 AND 11		FLTSATCOM		PIONEER VENUS	
	(LB)	(KG)	(LB)	(KG)	(LB)	(KG)
MAXIMUM PROPELLANT THROUGHPUT						
SINGLE THRUSTER	12.25	(27)	16.33	(36)	9.07	(20)
TOTAL ALL THRUSTERS	26.76	(59)	63.50	(140)	15.9	(35)
NUMBER OF THRUSTERS PER SPACECRAFT	6		16		8	
MAXIMUM HOT PULSES, SINGLE THRUSTER	18 500		21 133		6 600	
MINIMUM TEMPERATURE STARTS, SINGLE THRUSTER	120		1 104		114	
MAXIMUM CONTINUOUS FIRING, SINGLE THRUSTER (SECONDS)	6 500		220		3 000	

* NOT REALLY A COLD START BECAUSE HEATERS LIMIT MINIMUM TEMPERATURE TO 121°C (250°F). REQUIRES ONE WATT HEATER POWER PER THRUSTER WITH 4.4°C (40°F) PROPELLANT.

WATTS	REMARKS
10	BASED ON FIRING TWO THRUSTERS DURING OPERATION. POWER ONLY DURING FIRING. 3300 SECONDS MAXIMUM STEADY STATE; TWO SECONDS MAXIMUM PULSING PER FIRING
0.3	CONTINUOUS
1.2	CONTINUOUS POWER VALUES BASED ON USE OF THERMAL STANDOFFS AND THERMOSTATIC CONTROL.
0.4	PRIMARY HEATER POWER ON AT 12.78°C (55°F), OFF AT 13.34°C (65°F).
0.2	SECONDARY HEATER ON AT 7.22°C (45°F), OFF AT 12.78°C (55°F).
0.8	
0.4	
0.5	

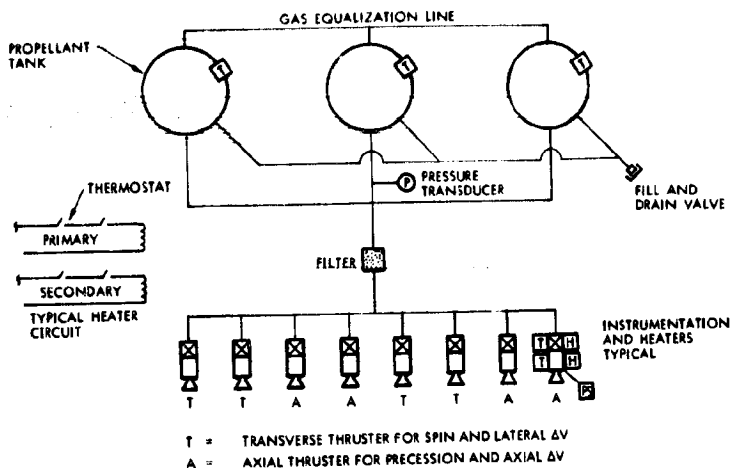
AND LINES WHICH ARE KEPT IN THE HEATED PROTRUDING PORTIONS ARE COPPER-COATED

F THE RCS TELEMETRY PROVIDES INSTRUMENTATION NEEDED FOR PERFORMANCE PREDICTIONS (BURN TIMES/PULSES), DIAGNOSTIC PURPOSES, AND MONITORING NORMAL RCS OPERATION

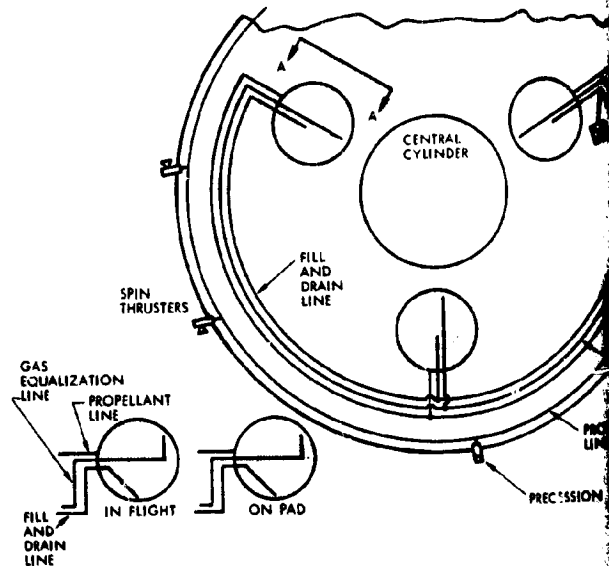
ITEM	ALLOWABLE RANGE	CONTROL SETTING	REMARKS
TEMPERATURE	[°C (°F)]	[°C (°F)]	
PROPELLANT TANK	10 TO 49 (40 TO 120)	12.8 TO 18.2 (55 TO 65)	TEMPERATURES ARE TAKEN AT LOCATIONS WHERE FREEZING OF HYDRAZINE COULD OCCUR. TEMPERATURE INDICATES THRUSTER OPERATION.
PROPELLANT LINE	10 TO 49 (40 TO 120)	12.8 TO 18.2 (55 TO 65)	
PROPELLANT VALVE CATALYST BED	10 TO 109 (40 TO 230)	12.8 TO 18.2 (55 TO 65)	
	10 TO 980 (40 TO 1800)	NONE	
PRESSURE	[N/M ² (PSIA)]		
PROPELLANT TANK	10 x 10 ⁶ TO 3.45 x 10 ⁶ (145 TO 500)	NONE	INDICATES THRUSTER BURN TIME. INDICATES PULSES NECESSARY TO DELIVER REQUIRED IMPULSE. PRESSURE SWITCH DELIVERS A PULSE FOR EACH THRUSTER FIRING.
THRUST CHAMBER		NONE	

Figure 8.6-11. Other Features of the Preferred Atlas/Centaur RCS

A THE PREFERRED THOR/DELTA RCS, WITH THE EXCEPTION OF THE SPHERICAL TANK, USES THE SAME HARDWARE AS THE PREFERRED ATLAS/CENTAUR, AND THE SAME THERMAL CONTROL APPROACH.



C THE PREFERRED RCS PIPING ARRANGEMENT ACCOMMODATES THE SELECTED PROPPELLANT TANK, WHICH HAS BEEN MODIFIED TO ELIMINATE THE BLADDER AND INSTEAD USES THREE TUBES AT THE TANK'S OUTBOARD END: (1) FOR THRUSTER PROPPELLANT SUPPLY, (2) FOR ON-PAD PROPPELLANT DRAINING, AND (3) FOR ULLAGE INTERCONNECT IN STATIONARY CONDITIONS. PIPING IS 0.95 CM (0.375 IN.) IN DIAMETER, AND ROUTED TO PREVENT VIBRATION AND TO MAINTAIN EQUAL PROPPELLANT HEADS IN THE TANKS.*



* PROPER LINE SIZING/ROUTING IS ESSENTIAL IN MAINTAINING SPACECRAFT BALANCE.

B THE RCS WEIGHT BREAKDOWN REFLECTS THE ACCURACY OF USING FLIGHT-TESTED COMPONENTS WITH KNOWN WEIGHTS. * THE PROBE AND ORBITER HARDWARE WEIGHTS ARE IDENTICAL; HOWEVER, THE ORBITER PROPPELLANT TANKS ARE LOADED TO ONLY 16.24 KG (35.8 LB).

ITEM	NUMBER REQUIRED	WEIGHT [KG (LB)]	
		PER COMPONENT	TOTAL
PROPPELLANT TANK	3	1.04 (2.3)	3.12 (6.9)
THRUSTER	8	0.27 (0.6)	2.17 (4.8)
FILTER	1	0.18 (0.4)	0.18 (0.4)
PRESSURE TRANS	1	0.18 (0.4)	0.18 (0.4)
FILL AND DRAIN VALVE	1	0.09 (0.2)	0.09 (0.2)
LINES AND FITTINGS	-	-	0.90 (2.0)
TOTAL HARDWARE			6.67 (14.7)
PRESSURANT			0.27 (0.6)
PROPPELLANT			18.19 (40.1)
TOTAL LOADED			25.13 (55.4)

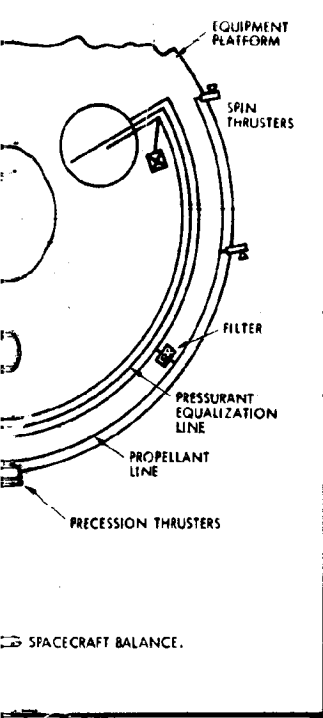
* WEIGHTS OF THE HARDWARE FOR MOUNTING THE TANKS, THRUSTERS, VALVES, ETC. AND WIRING ARE NOT SHOWN HERE; THEY ARE PARTS OF OTHER SUBSYSTEMS.

D THE PREFERRED RCS USES FLIGHT-QUALIFIED THRUSTER HARDWARE.

ITEM	USE AS IS	CHANGED	REMARKS
PROPPELLANT TANK		X	MARINER '69 WITHOUT A BLADDER AND WITH MODIFICATION TO TANK MOUNTING
THRUSTER	X		FLTSATCOM*
THRUSTER VALVE	X		FLTSATCOM*
FILTER	X		PIONEERS 10 AND 11
PRESSURE TRANSDUCER	X		PIONEERS 10 AND 11
FILL AND DRAIN VALVE	X		PIONEERS 10 AND 11
LINES AND FITTINGS		X	PIONEERS 10 AND 11 WITH LINE RUNS/SIZE

* DIVIDED FROM PIONEERS 10 AND 11; MODIFIED THE SAME AS ATLAS/CENTAUR TO REDUCE UNIT COMPLEXITY, HIGHER RELIABILITY, AND LOWER COSTS.

LOCATES THE SELECTED MARINER '69
 THE BLADDER AND INCORPORATE
 PROPELLANT SUPPLY, 12: AS A DIP TUBE
 INTERCONNECT IN STATIC AND DYNAMIC
 AND ROUTED TO PREVENT BUBBLE TRAPS



SPACECRAFT BALANCE.

REMARKS

'69 WITHOUT A BLADDER
 MODIFICATION IN
 COUNTING
 13M*
 13M*
 10 AND 11
 10 AND 11
 10 AND 11
 10 AND 11 WITH MODIFIED
 SIZE

CENTAUR THRUSTER VALVE;
 COSTS.

E RCS PERFORMANCE

PREFERRED ORBITER MISSION RCS PERFORMANCE

MISSION MODE	TIME SPENT IN MODE (SECONDS)	AVERAGE THRUSTER DUTY CYCLE PER PULSE TIME (SECONDS)		NUMBER OF PULSES	TOTAL IMPULSE [N * S (LB-S)]	AVERAGE SPECIFIC IMPULSE (SECONDS)	PROPELLANT CONSUMED [KG (LB)]	
		ON	OFF					
INITIAL ATTITUDE	DESPIN	96		CONTINUOUS	850 (191)	225	0.39 (0.85)	
	PRECESS	946	0.125	12.5	76	85 (19)	0.05 (0.11)	
	TRIM SPIN					NEG		
MIDCOURSE 73 M/S 7 M/S 2 M/S	PRECESS	5 150	0.125	12.5	448	516 (116)	173	0.30 (0.67)
	ΔV	~2 500		CONTINUOUS		22 237 (4 999)	222	10.20 (22.50)
	TRIM SPIN	REAL-TIME PULSES	0.032 TO 0.125	SEVERAL RESOLUTIONS		391 (88)	170	0.24 (0.52)
	CRUISE		0.125	12.5		58 (13)	170	0.04 (0.08)
ORBIT INSERTION	PRECESS	736	0.125	12.5	61	36 (8)	170	0.02 (0.05)
	SPIN UP	60		CONTINUOUS		534 (120)	220	0.25 (0.55)
	DESPIN	60		CONTINUOUS		525 (118)	220	0.24 (0.54)
	PRECESS		0.125	12.5		36 (8)	170	0.02 (0.05)
PERIAPSIS MANEUVERS AND ATTITUDE MAINTENANCE	PRECESS	3 594	0.125	12.5	288	320 (72)	160	0.20 (0.45)
	ΔV	900		CONTINUOUS		8 016 (1 802)	218	3.75 (8.27)
	TRIM SPIN	REAL-TIME	0.032 TO 0.125	VARIES		142 (32)	160	0.09 (0.20)
	CRUISE	REAL-TIME	0.125	12.5		89 (20)	160	0.06 (0.13)
TOTAL					33 835 (7 606)		15.85 (34.97)	

PREFERRED PROBE MISSION RCS PERFORMANCE

MISSION MODE	TIME SPENT IN MODE (SECONDS)	AVERAGE THRUSTER DUTY CYCLE PER PULSE TIME (SECONDS)		NUMBER OF PULSES	TOTAL IMPULSE [N * S (LB-S)]	AVERAGE SPECIFIC IMPULSE (SECONDS)	PROPELLANT CONSUMED [KG (LB)]	
		ON	OFF					
INITIAL ATTITUDE	DESPIN	160		CONTINUOUS	1 415 (318)	225	0.64 (1.42)	
	PRECESS	1 050	0.125	12.5	84	93 (21)	0.05 (0.12)	
	TRIM SPIN					NEG		
MIDCOURSE 73 M/S 7 M/S 2 M/S	PRECESS	7 988	0.125	12.5	640	716 (161)	173	0.42 (0.93)
	ΔV	~3 200		CONTINUOUS		28 335 (6 370)	222	13.01 (28.70)
	TRIM SPIN	REAL-TIME		VARIES		444 (100)	170	0.27 (0.59)
	CRUISE	REAL-TIME	0.125	12.5		133 (30)	170	0.08 (0.18)
PROBE DEPLOYMENT	PRECESS	9 161	0.125	12.5	733	841 (189)	160	0.53 (1.18)
	ΔV	~640		CONTINUOUS		5 680 (1 277)	220	2.63 (5.80)
	SPIN TRIM		0.032 TO 0.125	12.5		89 (20)	160	0.06 (0.13)
ATTITUDE MAINTENANCE *	PRECESS		0.125	12.5		169 (38)	170	0.10 (0.23)
TOTAL					37 915 (8 524)		17.79 (39.28)	

* EARTH TRACK AND ATTITUDE DRIFT

Figure 8.6-12. Preferred Thor/Delta RCS

Table 8.6-8. Orbit Injection Rocket Details for Initial Atlas/Centaur Configuration

CANDIDATE ORBIT INJECTION ROCKET	SPACECRAFT WEIGHT AT IGNITION (NOT INCLUDING ORBIT INSERTION ROCKET) (KG) (LB)	DELIVERED IMPULSE (N·S) (LBF·S)	PROPELLANT WEIGHT (KG) (LB)		MOTOR WEIGHT (KG) (LB)		PROPELLANT WEIGHT CHANGE (KG) (LB)		THRUST		DESIGN CHANGES	CRITICAL DESIGN LIMITATIONS (WITHIN PIONEER VENUS DESIGN REQUIREMENTS)
							MAXIMUM (N) (LBF)	AVERAGE (N) (LBF)				
HERCULES BE-3-B												
PIONEER VENUS REQUIREMENT	286.9 (632.7)	343 577 (77 243)	126.96 (279.9)	142.34 (313.8)	-27.62 (-60.9)	40 704 (10 500)	42 902 (9870)	ADD 12.70 CM (5.0 IN.) TO CASE, INCREASE THROAT AREA	MINIMUM FIRING TEMPERATURE			
EXISTING ROCKET CAPABILITIES	N/A (N/A)	269 549 (60 600)	99.34 (219.0)	112.31 (247.6)	0 (0)	36 474 (8 200)	34 250 (7700)	NONE	MINIMUM FIRING TEMPERATURE (°C (-32°F))			
THIOLKOL TE-M-521												
PIONEER VENUS REQUIREMENT	291.43 (642.5)	346 752 (77 957)	122.61 (270.3)	137.89 (304.0)	+10.57 (+23.3)	18 815 (4 230)	17 570 (3950)	ADD 4.22 CM (1.66 IN.) TO CASE	NONE			
EXISTING ROCKET CAPABILITIES	N/A (N/A)	318 477 (71 600)	112.04 (247.1)	125.74 (277.2)	0 (0)	17 125 (3 850)	16 013 (3600)	NONE	NONE			
AEROJET SVM-2												
PIONEER VENUS REQUIREMENT	284.58 (267.4)	346 201 (44 833)	124.51 (274.5)	144.74 (319.0)	14.11 (-31.1)	21 528 (4 840)	14 990 (3370)	NONE	NONE			
EXISTING ROCKET CAPABILITIES	N/A (N/A)	386 531 (86 900)	138.62 (305.6)	158.85 (350.2)	0 (0)	21 484 (4 830)	13 967 (3140)	NONE	NONE			

HERCULES BE-3-B
 STATUS: PRODUCTION
 FLIGHT HISTORY: 9 FLIGHTS
 STRYPE (AEC)
 ADVANCED VELA
 PROGRAM COST (EST): \$215K
 DELIVERY: 10 MONTHS ARO

THIOLKOL TE-M-521
 STATUS: PRODUCTION
 FLIGHT HISTORY: 7 FLIGHTS
 SKYNET I
 NATO I
 IMP H
 PROGRAM COST (EST): \$328K
 DELIVERY: 17 MONTHS ARO

AEROJET SVM-2
 STATUS: PRODUCTION
 FLIGHT HISTORY: 5 FLIGHTS
 INTELSAT III
 PROGRAM COST (EST): \$307K
 DELIVERY: 10 MONTHS ARO

Table 8.6-9. Orbit Injection Rocket Details for the Atlas/Centaur Version IV Science Payload Configuration

CANDIDATE ORBIT INJECTION ROCKET	SPACECRAFT WEIGHT AT IGNITION (NOT INCLUDING ORBIT INSERTION ROCKET) (KG) (LB)	DELIVERED IMPULSE (N·S) (LBF·S)	PROPELLANT WEIGHT (KG) (LB)		MOTOR WEIGHT (KG) (LB)		PROPELLANT WEIGHT CHANGE (KG) (LB)		THRUST		DESIGN CHANGES	CRITICAL DESIGN LIMITATIONS (WITHIN PIONEER VENUS DESIGN REQUIREMENTS)
							MAXIMUM (N) (LBF)	AVERAGE (N) (LBF)				
THIOLKOL TE-M-521												
PIONEER VENUS REQUIREMENT	346.72 (762.8)	405 729 (91 218)	143.77 (316.3)	160.09 (352.2)	+31.50 (+69.3)	18 815 (4230)	17 570 (3950)	ADD 12.5 CM (4.9 IN.) TO CASE	NONE			
EXISTING ROCKET CAPABILITIES	N/A (N/A)	318 477 (71 600)	112.04 (247.0)	125.74 (277.2)	0 (0)	17 125 (3850)	16 013 (3600)	NONE	NONE			
AEROJET SVM-2												
PIONEER VENUS REQUIREMENT	340.41 (748.9)	405 368 (91 137)	146.09 (321.4)	166.41 (366.1)	+7.18 (+15.8)	21 528 (4840)	14 990 (3370)	NONE	NONE			
EXISTING ROCKET CAPABILITIES	N/A (N/A)	386 531 (86 900)	138.62 (305.6)	158.85 (350.2)	0 (0)	21 484 (4830)	13 967 (3140)	NONE	NONE			

THIOLKOL TE-M-521
 STATUS: PRODUCTION
 FLIGHT HISTORY: 7 FLIGHTS
 SKYNET I
 NATO I
 IMP H
 PROGRAM COST (EST): \$328K
 DELIVERY: 17 MONTHS ARO

AEROJET SVM-2
 STATUS: PRODUCTION
 FLIGHT HISTORY: 5 FLIGHTS
 INTELSAT III
 PROGRAM COST (EST): \$307K
 DELIVERY: 10 MONTHS ARO

requiring requalification testing and unnecessary costs. The weight in orbit is about 6.80 kg (15 lb) greater for the TE-M-521 than for the selected motor, but in a non-weight-limited system this is not a significant parameter.

The selected Aerojet SVM-2 offers:

- No anticipated changes to any hardware
- Ability to accommodate a ± 10 percent propellant load variation. Requirements to the earlier Atlas/Centaur are a -14.1 kg (-31.1 lb) or 10.2 percent propellant off-loaded. For the Version IV science payload, the requirements are a +7.18 kg (+15.8 lb) or 4.6 percent propellant on-load.
- Successful flight history
- Program costs and risks lower than the TE-M-521 (10 percent lower cost).

Bipropellant Versus Solid/Hydrazine RCS Systems Tradeoff, Atlas/Centaur Orbiter. In Table 8.6-10, three liquid bipropellant systems are compared, and the best bipropellant system is compared to the mono-propellant/solid rocket system.

Table 8.6-10. Comparison of Bipropellant Versus Solid Hydrazine RCS Systems for Atlas/Centaur

SYSTEM	USABLE PIONEER VENUS SPACECRAFT WEIGHT IN ORBIT*		RCS SYSTEM BURNOUT WEIGHT		PROPELLANT WEIGHT REQUIRED		PROPELLANT SPECIFIC IMPULSE		IMPULSE DELIVERED		
	(KG)	(LB)	(KG)	(LB)	(KG)	(LB)	(N · S/KG)	(LBF · S/LBM)	(N · S)	(LBF · S)	
MARINER '71 (N ₂ O ₄ /MMH)	156.2	(344.0)	150.0	(331.0)	129.4	(285.0)	2775.7	(283.0)	358 749	(80 654)	
MMBPS (N ₂ O ₄ /MMH)	216.9	(477.7)	91.0	(207.0)	125.0	(275.3)	2893.4	(295.0)	361 178	(81 200)	
SYMPHONIE (N ₂ O ₄ /A-50)	294.0	(647.5)	20.4	(44.9)	121.5	(267.6)	2991.5	(305.0)	363 072	(81 626)	
SELECTED {	TRW (N ₂ H ₄)	288.2	(634.8)			4.5	(9.9)	2157.8	(220.0)	21 362	(2 178)
	SVM-2 (SOLID)	288.2	(634.8)			124.5	(274.5)	2781.6	(283.6)	346 201	(77 833)
ERSC {	SYMPHONIE (N ₂ O ₄ /A-50)	294.0	(647.5)			121.5	(267.6)	2991.5	(305.0)	363 072	(81 626)

* REQUIRED PIONEER VENUS SPACECRAFT WEIGHT IN ORBIT IS 285 KG (628 LB).

(31 W)
A/C III

The ESRO Symphonie, the MMBPS (multi-mission spacecraft), and the U.S. Mariner '71 bipropellant systems were compared to determine which would best supply enough impulse to perform both midcourse and orbit injection maneuvers. All three supplied enough impulse. The MMBPS and Mariner, however, are too large and must be grossly off-loaded. Neither allows adequate usable spacecraft weights in orbit. The Symphonie is favored by a good margin.

Other liquid bipropellant systems could be assembled from existing qualified components such as the Marquardt R4D Apollo thrusters of the Rocketdyne or Bell tankage. In the interest of minimizing costs, this study considered only complete systems that could be used in their existing qualified configurations.


The selected liquid bipropellant system was then compared to the hydrazine/solid rocket system in terms of relative complexity (reliability), cost, and flight experience. In all three areas, the hydrazine/solid system is favored. Because bipropellant systems are more complex than hydrazine/solid systems, they are less reliable. Bipropellant systems historically cost two to three times as much as equivalent monopropellant systems. Finally, the flight history of satellite propulsion systems is overwhelmingly in favor of hydrazine/solid systems.

The study results indicate that the ESRO Symphonie has a small weight advantage (6 kg lighter) over the solid system, but for a non-weight-limited system, this is not a significant parameter. The bipropellant system may have some advantage in terms of its relatively long burn time which would produce lower gravity forces and might, therefore, permit lighter deployable structural elements. In terms of all the criteria, however, simplicity, and historical performance record of the hydrazine/solid rocket system makes it the preferred choice.

Thor/Delta (31 W)
T/D III

Solid Rocket Motor for Use With Hydrazine System. Table 8.6-11 shows the key features of the candidate motors for the Thor/Delta orbiter.

Only two known existing rocket motors meet the mission requirements without gross changes in design, requiring requalification of the

 (31 W) T/D III motor. The first, the Aerojet SVM-1, meets the mission requirements with the following changes to the existing design:

- The addition of 2.54 cm (1 in.) to the cylindrical section of the motor case
- A slight increase in the throat area to accommodate the increase in propellant burning area and weight.

These changes are considered minor and would not require motor requalification.

The anticipated \$250K program cost of the Aerojet SVM-1 is nearly twice as high as that for the Hercules BE-3-A, the second and preferred motor, which offers:

- No changes to the existing hardware design other than the addition of a safe and arm device
- Off-loading of 3.58 kg (7.0 lb), which represents only a 4.1 percent change to the propellant load and no changes to the motor. The off-loading can be accomplished by machining the internal surfaces of the propellant grain with existing tooling after it has been cast.
- A larger number of successful flights (161 as opposed to three for the SVM-1)
- Program costs of only \$135K.

Bipropellant Versus Solid/Hydrazine RCS System Tradeoff, Thor/Delta Orbiter. In Table 8.2-12, three liquid bipropellant systems are compared, and the best bipropellant system is compared to the monopropellant hydrazine system. As for the Atlas/Centaur orbiters, the ESRO Symphonie is favored.

When the Symphonie system is compared to a hydrazine/solid propellant system, neither exhibits clear-cut performance advantages. However, as for the Atlas/Centaur orbiters, the hydrazine/monopropellant system is simpler, more reliable, less costly, and has superior flight experience to the bipropellant system.

8.6.2.3 Preferred Atlas/Centaur Subsystem A/C IV (31 W) A/C III

The Aerojet SVM-2 solid rocket was selected for either the earlier or Atlas/Centaur Version IV science payload orbiter. The existing motor

Table 8.6-11. Orbit Insertion Rocket Details for Thor/Delta Configuration, Orbiter Mission

CANDIDATE ORBIT ROCKET	SPACECRAFT WEIGHT AT LAUNCH (NOT INCLUDING ORBIT INSERTION WEIGHT)		DELIVERED IMPULSE		PROPELLANT WEIGHT		MOTOR WEIGHT		PROPELLANT WEIGHT CHARGE		THRUST		DESIGN CHANGES	CRITICAL DESIGN LIMITATIONS (WITHIN PIONEER VENUS DESIGN REQUIREMENTS)		
	(KG)	(LB)	(KG)	(LBF)	(KG)	(LB)	(KG)	(LB)	(KG)	(LB)	MAXIMUM (KG)	AVERAGE (LBF)				
AEROJET SVM-1																
PIONEER VENUS REQUIREMENT	184.52	(406.8)	225 905	(50 788)	79.92	(176.2)	95.80	(211.2)	+5.99	(+13.2)	15 568	(3500)	13 957	(3140)	ADD 2.54 CM (1.0 IN.) TO CASE, INCREASE THROAT AREA	NONE
EXISTING ROCKET CAPABILITIES	N/A	(N/A)	209 425	(47 083)	73.94	(163.0)	89.58	(197.5)	0	(0)	14 412	(3240)	12 925	(2900)	NONE	NONE
HERCULES BE-3-A																
PIONEER VENUS REQUIREMENT	186.83	(411.9)	224 838	(50 548)	83.05	(183.1)	93.48	(206.1)	-3.58	(-7.9)	28 467	(6400)	26 243	(5900)	NONE	MINIMUM FIRING TEMPERATURE 0°C (+32°F)
EXISTING ROCKET CAPABILITIES	N/A	(N/A)	234 854	(52 800)	86.64	(191.0)	97.07	(214.0)	0	(0)	28 467	(6400)	26 243	(5900)	NONE	MINIMUM FIRING TEMPERATURE 0°C (+32°F)

AEROJET SVM-1
STATUS: PRODUCTION
FLIGHT HISTORY: 3 FLIGHTS
COMSAT
PROGRAM COST (EST): \$250K
DELIVERY: 10 MONTHS ARO

HERCULES BE-3-A
STATUS: PRODUCTION
FLIGHT HISTORY: 161 FLIGHTS
VELA (USAF), RANGER (NASA),
ATHENA (AFBSD), AMRAD (ARMY),
SPARTA (ARMY)
PROGRAM COST (EST): \$135K
DELIVERY: 10 MONTHS ARO

Table 8.6-12. Comparison of Bipropellant Versus Solid/Hydrazine RCS Systems for Thor/Delta


SYSTEM	USABLE PIONEER VENUS SPACECRAFT WEIGHT IN ORBIT*		RCS SYSTEM BURNOUT WEIGHT		PROPELLANT WEIGHT REQUIRED		PROPELLANT SPECIFIC IMPULSE		IMPULSE DELIVERED		
	(KG)	(LB)	(KG)	(LB)	(KG)	(LB)	(N·S/KG)	(LBF·S/LBM)	(N·S)	(LBF·S)	
MARINER 71 (N ₂ O ₄ /MMH)	51.3	(113.1)	150.3	(331.0)	91.2	(200.9)	2775.7	(283.0)	252 944	(56 867)	
MMBPS (N ₂ O ₄ /MMH)	53.6	(118.8)	110.7	(243.0)	88.2	(194.2)	2893.4	(295.0)	254 755	(57 274)	
SYMPHONIE (N ₂ O ₄ /A-50)	186.7	(411.3)	20.4	(44.9)	85.7	(188.8)	2991.5	(305.0)	256 169	(57 592)	
SELECTED	TRW (N ₂ H ₄)	187.8	(413.7)			10.67	(23.5)	2157.8	(220.0)	22 996	(5 170)
	BE-3-A (SOLID)	187.8	(413.7)			83.05	(183.1)	2707.0	(276.0)	224 838	(50 548)
ESRO	SYMPHONIE (N ₂ O ₄ /A-50)	186.7	(411.3)			85.7	(188.8)	2991.5	(305.0)	256 169	(57 592)

*REQUIRED PIONEER VENUS SPACECRAFT WEIGHT IN ORBIT IS 187 KG (413 POUNDS) FOR SOLID AND 186 KG (411 POUNDS) FOR BI-PROPELLANT.

design is unique in that the ± 10 percent propellant load variation capability encompasses the requirements of both of these spacecraft. The preferred motor does not require requalification and is lower in cost than the Thiokol TE-M-521 candidate.

Atlas/Centaur Orbit Insertion Rocket Description  A/C IV  ^(31 W) A/C III

A detailed description of the selected Aerojet SVM-2 motor is contained in Appendix 8.6A.

8.6.2.4 Preferred Thor/Delta Subsystem  ^(31 W) T/D III

The Hercules BE-3-A motor was selected for the Thor/Delta orbiter. The existing motor design meets the orbiter requirements with only minor changes to incorporate a safe and arm device and to reduce the propellant load by 7.9 kg. These changes are straightforward and requalification is not necessary. The Hercules motor also has an impressive history of flight service and is low in cost.

Thor/Delta Orbit Insertion Rocket Description  ^(31 W) T/D III

A detailed description of the Hercules BE-3-A motor and the recommended safe and arm device are covered in Appendix 8.6B.

8.7 Thermal Control

8.7 THERMAL CONTROL.

8.7.1 Introduction

The thermal control system design for the preferred Atlas/Centaur configuration, as well as all optional configurations, consists of bimetallic-actuated louver assemblies, multilayer insulation blankets, electrical heaters, and selected surface coatings. Thermal system hardware and coatings will in most instances be common to both the probe bus and orbiter spacecraft when each is launched by the same type of booster. Hardware commonality is stressed in the system selection to reduce over-all fabrication, integration, and test costs. Certain individual insulation blankets, such as those which enclose the orbit insertion motor, and the number of required louver assemblies will vary between the probe bus and orbiter designs. The alternate modified DSCS-II configuration thermal system design utilized electric heaters to maintain a constant power level in the equipment mounting area, and does not require louvers. All other features of the preferred design are retained for the alternate configuration.

Temperature control of the large and small probes prior to separation can be accomplished by controlling the transit solar aspect angle, providing probe internal heaters, insulating the probes during transit, or combining two or three of these systems. To minimize the electrical power requirements for the mission, it is recommended that the small probes be insulated from the external environment and radiatively coupled to the equipment compartment. Furthermore, heaters can be eliminated in the large probe by controlling the solar aspect angle throughout the mission. This technique eliminates heater circuits with 1) their associated wiring and electrical connections between the probe and spacecraft, 2) their ground command switching hardware, and 3) avoids an increase in solar array size.

The 6-watt S-band transmitter selected for the preferred Atlas/Centaur design requires no special thermal provisions. However, the 31-watt transmitter used in one optional design requires a thermal fin insert in the platform under the transmitter assemblies to conduct heat away from the concentrated energy source and radiate excess heat to space through the louver assemblies. The thermal fin insert can be eliminated in the Thor/Delta 12-watt transmitter configuration by locally thickening the mounting platform face sheets.

8.7.2 Preferred Atlas/Centaur Configurations A/C IV -A/C IV

The preferred Atlas/Centaur probe bus and orbiter thermal control systems utilize common hardware and surface coatings wherever possible. The thermal system and its inherent performance are described below for both missions. The related thermal environment and analysis techniques used to determine system performance are also provided.

8.7.2.1 Probe Bus Spacecraft A/C IV

System Description

The preferred Atlas/Centaur probe bus spacecraft thermal control system description and pertinent operational features are presented in Figure 8.7-1. Specific hardware and thermal provisions are identified and the purpose of each item defined. Hardware is designed to be common with both mission configurations wherever possible. One exception to this goal is the outer conical section of the forward thermal shield which is fabricated of 24 aluminized kapton layers instead of the mylar/teflon film used for the other thermal shields. The aluminized side faces outward because the forward facing experiments need a metallic potential reference plane on the forward end of the spacecraft. This orientation produces high surface temperatures on the outer insulation layers which protect the solar array.

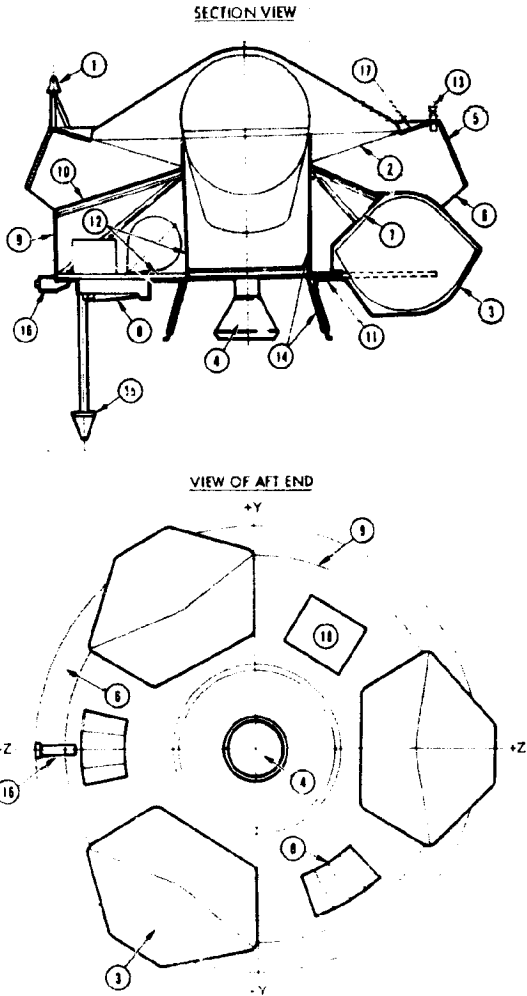
Thermal Control System Performance

Figure 8.7-2 lists the maximum predicted temperature variation of each component during the entire mission. All components, including the scientific experiments, meet the specified acceptance temperature limits. The figure also describes the earth-to-Venus transit temperatures for the solar array, large probe, battery, and potential reference plane.

All thruster valves and catalyst beds have to be heated when not being fired to prevent the temperature of the hydrazine from falling below 4°C (40°F). Figure 8.7-2C lists valve and catalyst bed temperatures for various heater power combinations for the three thruster types. The selected heater power levels and temperatures are indicated on the unshaded lines. A total power requirement of 5.2 watts is needed to keep the four transverse, two aft ΔV , and two forward ΔV thrusters warm. The powers are quite low because the thruster surface exposed to the

A THERMAL CONTROL SYSTEM HARDWARE DESCRIPTION

THE PROBE BUS USES RELIABLE AND FLIGHT-PROVEN THERMAL CONTROL HARDWARE. LOCATIONS OF HARDWARE ARE KEYED TO THE ADJACENT TABLE FOR DETAILED DESCRIPTIONS



B THERMAL CONTROL SYSTEM FEATURES

- INSULATED EQUIPMENT COMPARTMENT WITH LOUVERS TO MINIMIZE SOLAR INTENSITY VARIATION DURING TRANSIT TO VENUS
- REAR SURFACE OF SOLAR ARRAY THERMALLY COUPLED INDIRECTLY TO SPACE TO REDUCE ARRAY TEMPERATURE
- LOW ABSORBANCE/HIGH EMITTANCE SHIELDS TO PREVENT SOLAR IRRADIATION ON ARRAY REAR SURFACE
- HEATED THRUSTERS WITH COPPER-PLATED LINES TO PREVENT HYDRAZINE FROM FREEZING
- WHITE PAINTED SURFACES TO LOWER OPERATING TEMPERATURE LEVELS
- SOLAR ASPECT ANGLE CONTROLLED TO MAINTAIN ACCEPTABLE LARGE PROBE TEMPERATURE
- LARGE PROBES COUPLED RADIATIVELY TO SOLAR ARRAY
- SMALL PROBES COUPLED RADIATIVELY TO EQUIPMENT COMPARTMENT
- HEATED, JETTISONABLE PANELS AROUND SMALL PROBES TO MAINTAIN ACCEPTABLE PROBE TEMPERATURES DURING TRANSIT

ID NO.	NAME OF ITEM	DESCRIPTION OF HARDWARE
1	FORWARD OMNI ANTENNA THERMAL COATING	3-MIL COAT OF 5-13G WHITE PAINT ON EXTERNAL SURFACES OF OMNI ANTENNA
2	LARGE PROBE CLOSEOUT	ONE OUTER LAYER OF 2-MIL SILVER TEFLON (SILVER SIDE FACING INWARD) LAMINATED TO 2-MIL INNER LAYER OF CLEAR MYLAR
3	SMALL PROBE INSULATION COVER	ONE 10-MIL FIBERGLASS JETTISONABLE COVER FOR EACH PROBE. EXTERNAL SURFACE INSULATED WITH 22 LAYERS OF ALUMINIZED MYLAR SANDWICHED BETWEEN ONE OUTER 2-MIL ALUMINIZED KAPTON AND ONE INNER 2-MIL ALUMINIZED MYLAR COVER SHEET (ALUMINIZED SURFACES INWARD). SIMILAR INSULATION BLANKET WITH 7-MIL MYLAR FACE SHEETS INSULATES EACH PROBE FROM THE SPACECRAFT INTERIOR EXCEPT AT THERMAL WINDOW PENETRATION. ITEM K/X, SEE FIGURE B.7-4
4	MEDIUM-GAIN ANTENNA COATING	3-MIL COAT OF 5-13G WHITE PAINT ON EXTERNAL SURFACE
5	SOLAR ARRAY SUBSTRATE THERMAL COATING	3-MIL COAT OF JM BLACK VELVET PAINT ON BACK SURFACE OF SUBSTRATE
6	MIDSIELD	ONE OUTER LAYER OF 2-MIL SILVER TEFLON (SILVER SIDE FACING INWARD) LAMINATED TO 2-MIL INNER LAYER OF CLEAR MYLAR
7	SMALL PROBE THERMAL WINDOW	ONE 2-MIL, 0.047 M ² (0.5 FT ²) SHEET OF BLACKENED KAPTON BETWEEN EACH SMALL PROBE AND THE EQUIPMENT COMPARTMENT
8	BIMETAL ACTUATED LOUVERS	TOTAL BLADE AREA 0.145 M ² (1.56 FT ²) CLOSED EFFECTIVE EMITTANCE 0.20 FULL CLOSED AT 4°C (40°F) OPEN EFFECTIVE EMITTANCE 0.74 FULL OPEN AT 29°C (85°F) 3-MIL COATS OF Z-93 WHITE PAINT ON PLATFORM UNDER LOUVERS
9	EQUIPMENT COMPARTMENT SIDE INSULATION	22 LAYERS OF 1/4-MIL ALUMINIZED MYLAR SANDWICHED BETWEEN ONE OUTER 2-MIL ALUMINIZED MYLAR COVER SHEET (ALL ALUMINIZED SURFACES EXCEPT INSIDE COVER SHEET INWARD) K/X, SEE FIGURE B.7-4
10	EQUIPMENT COMPARTMENT TOP INSULATION	22 LAYERS OF 1/4-MIL ALUMINIZED MYLAR SANDWICHED BETWEEN TWO 2-MIL ALUMINIZED MYLAR COVER SHEETS (ALL ALUMINIZED SURFACES EXCEPT AFT COVER SHEET FACE INWARD) K/X, SEE FIGURE B.7-4
11	EQUIPMENT COMPARTMENT AFT INSULATION	22 LAYERS OF 1/4-MIL ALUMINIZED MYLAR SANDWICHED BETWEEN ONE OUTER 2-MIL ALUMINIZED KAPTON AND ONE INNER 2-MIL ALUMINIZED MYLAR COVER SHEETS (ALUMINIZED SURFACE FACE FORWARD) K/X, SEE FIGURE B.7-4
12	EQUIPMENT COMPARTMENT RADIATIVE AND CONDUCTIVE THERMAL COUPLING REQUIREMENTS	3-MIL COATING OF 3M BLACK VELVET PAINT ON EQUIPMENT PLATFORM AND HEAT DISSIPATING EQUIPMENT BARE METAL SURFACE ON CENTRAL COLUMN AND HYDRAZINE TANKS. TANKS CONDUCTIVELY COUPLED TO MOUNTING PLATFORM AND ISOLATED FROM COLUMN PROVIDE GOOD CONDUCTIVE THERMAL COUPLING BETWEEN HIGH HEAT DENSITY COMPONENTS (I.E., TRANSMITTER) AND PLATFORM WITH RTV INTERFACE FILLER MATERIAL. H = 142 W/M ² (25 BTU/HR-FT ² -°F)
13	RCS THRUSTER VALVE BODY AND SUPPLY LINE INSULATION, VALVE AND CATALYST BED HEATERS, AND THRUSTER ISOLATION REQUIREMENTS	LOWER ΔV THRUSTER INSULATED COMPLETELY WITH HIGH TEMPERATURE MOLYBDENUM FOAM ALL FUEL LINES ARE COPPER PLATED, LINES EXTERNAL TO THE EQUIPMENT COMPARTMENT INSULATED WITH 10 LAYERS OF NRCL INSULATION K/X, 0.056 W/M ² -°C (0.01 BTU/HR-FT ² -°F) DUAL RANGE THERMOSTATICALLY CONTROLLED HEATERS ON VALVE AND CATALYST BED WITH GROUND CONTROL BACKUP. PRIMARY HEATER CONTROL RANGE 13°C (55°F) TO 18°C (65°F) RANGE 7°C (45°F) TO 13°C (55°F). HEATER POWER REQUIREMENT 3.2 WATTS. THRUSTERS ISOLATED FROM STRUCTURES WITH TITANIUM STANDOFFS
14	CENTRAL COLUMN INSULATION	22 LAYERS OF 1/4-MIL ALUMINIZED MYLAR SANDWICHED BETWEEN TWO 2-MIL ALUMINIZED MYLAR COVER SHEETS (MYLAR SURFACES FACE OUTWARD) K/X, SEE FIGURE B.7-4
15	AFT OMNI ANTENNA THERMAL COATING	3-MIL COAT OF 5-13G WHITE PAINT ON EXTERNAL SURFACES OF OMNI ANTENNA
16	SMALL PROBE INSULATION	22 LAYERS OF 1/4-MIL ALUMINIZED MYLAR SANDWICHED BETWEEN ONE OUTER 2-MIL ALUMINIZED KAPTON AND ONE INNER 2-MIL ALUMINIZED MYLAR COVER SHEETS (ALUMINIZED SURFACES INWARD) K/X, SEE FIGURE B.7-4
17	PLATFORM THERMAL REFLECTIVE COATING	22 LAYERS OF 1/4-MIL ALUMINIZED MYLAR SANDWICHED BETWEEN ONE OUTER 2-MIL ALUMINIZED KAPTON AND ONE INNER 2-MIL ALUMINIZED MYLAR COVER SHEETS (ALUMINIZED SURFACES INWARD) K/X, SEE FIGURE B.7-4
18	THRUSTER VALVE	3-MIL COAT OF 5-13G WHITE PAINT ON EXTERNAL SURFACES OF THRUSTER VALVE

HARDWARE	PURPOSE	SURFACE THERMAL PROPERTIES					
		INSIDE			OUTSIDE		
		α_{NEW}	α_{DEG}	ϵ	α_{NEW}	α_{DEG}	ϵ
FRONT SURFACES OF OMNI ANTENNA	MINIMIZE ABSORBED SOLAR HEAT INPUT TO REDUCE VARIATION IN TEMPERATURE DURING MISSION. LOCATION ENSURES SOLAR HEATING TO LIMIT MINIMUM TEMPERATURES FOR ALL SOLAR ASPECT ANGLES ENCOUNTERED	--	--	--	0.24	0.31	0.88
FRONT SURFACES FACING INWARD LAMINATED TO ONE	SHIELD BACK SIDE OF SOLAR ARRAY FROM DIRECT SOLAR IMPINGEMENT AFTER LARGE PROBE RELEASE	--	--	0.66	0.08	0.12	0.66
SMALL PROBE, EXTERNAL SURFACE INSULATED BETWEEN ONE OUTER 2-MIL ALUMINIZED COVER SHEET (ALUMINIZED SURFACES FACE) AND MYLAR FACE SHEETS INSULATES EACH SMALL WINDOW PENETRATION, ITEM 7	MINIMIZE SMALL PROBE HEAT LEAKS DURING CRUISE TO MAINTAIN PROBE TEMPERATURES ABOVE MINIMUM LIMITS	--	--	0.90	0.45	0.48	0.69
FRONT SURFACE	MAXIMIZE RADIATION COUPLING FROM ANTENNA TO INSULATION	--	--	--	0.24	0.31	0.88
FRONT SURFACE OF SUBSTRATE	MAXIMIZE RADIANT HEAT TRANSFER FROM BACK SURFACE OF SOLAR ARRAY	--	--	0.90	0.80	0.80	0.80 AT ZERO ARRAY OUTPUT
FRONT SURFACES FACING INWARD LAMINATED TO ONE	SHIELD BACK SIDE OF SOLAR ARRAY FROM DIRECT SOLAR IMPINGEMENT. PROVIDE LOW TEMPERATURE BOUNDARY (LOW ϵ) TO MAXIMIZE HEAT TRANSFER FROM BACK SURFACE OF SOLAR ARRAY	--	--	0.66	0.08	0.12	0.66
KAPTON BETWEEN EACH SMALL PROBE AND	COUPLES SMALL PROBES TO EQUIPMENT COMPARTMENT TO CONTROL PROBE TEMPERATURE VARIATION DURING TRANSIT. LOCATION OF WINDOWS PREVENT DIRECT SOLAR IMPINGEMENT	--	--	0.90	--	--	0.90
TEMPERATURE RANGE: 4°C (40°F) TO 18°C (65°F) WITH SHUTTER COVERS	CONTROL EQUIPMENT COMPARTMENT HEAT LEAKS TO OFFSET THE VARIATION IN EQUIPMENT AND ENVIRONMENTAL HEAT INPUT EXPERIENCED DURING THE MISSION TO MAINTAIN COMPONENT TEMPERATURES WITHIN ACCEPTABLE LIMITS	--	--	--	0.50	0.50	0.20 CLOSED 0.74 OPEN
KAPTON BETWEEN ONE OUTER 2-MIL SURFACES EXCEPT INSIDE COVER SHEET FACE	MINIMIZE SOLAR HEAT LEAK INTO AND UNCONTROLLED HEAT LEAKS OUT OF THE EQUIPMENT COMPARTMENT. STABLE ALUMINIZED KAPTON MINIMIZES EXTERNAL SURFACE PROPERTY DEGRADATION	--	--	0.69	0.45	0.48	0.69
KAPTON BETWEEN TWO 2-MIL ALUMINIZED PARTIAL COVER SHEET FACE INWARD	MINIMIZE UNCONTROLLED HEAT LEAKS INTO AND OUT OF THE EQUIPMENT COMPARTMENT AND THERMALLY DECOUPLE COMPARTMENT FROM SOLAR ARRAY	--	--	0.69	--	--	0.69
KAPTON BETWEEN ONE OUTER 2-MIL ALUMINIZED COVER SHEETS (ALUMINIZED)	MINIMIZE UNCONTROLLED HEAT LEAKS OUT OF THE EQUIPMENT COMPARTMENT. STABLE ALUMINIZED KAPTON MINIMIZES EXTERNAL SURFACE PROPERTY DEGRADATION	--	--	--	0.45	0.48	0.69
EQUIPMENT PLATFORM AND HEAT DISSIPATING COMPONENTS	EQUALIZE TEMPERATURE GRADIENTS WITHIN EQUIPMENT COMPARTMENT BY MAXIMIZING RADIATIVE THERMAL COUPLING BETWEEN STRUCTURE AND HEAT DISSIPATING COMPONENTS	--	--	--	--	--	0.90
THRUSTER TANKS, TANKS CONDUCTIVELY COUPLED TO COLUMN	THERMALLY DECOUPLE ZERO HEAT DISSIPATING COMPONENT FROM SURROUNDING TO MINIMIZE TEMPERATURE VARIATIONS DURING TRANSIT ENVIRONMENTAL CONDITIONS	--	--	--	--	--	0.10
THRUSTERS WITH HIGH HEAT DENSITY COMPONENTS AND FILLER MATERIAL, $H = 142 \text{ W/M}^2\text{-}^\circ\text{C}$	MINIMIZE COMPONENT TO EQUIPMENT PLATFORM TEMPERATURE GRADIENTS TO MINIMIZE MAXIMUM COMPONENT TEMPERATURE LEVEL ABOVE SURROUNDINGS	--	--	--	--	--	--
THRUSTERS WITH TEMPERATURE MCLYBDENUM FOIL	MINIMIZE UNCONTROLLED THRUSTER HEAT LEAK TO SPACE	--	--	--	0.12	0.12	0.05
THRUSTERS WITH THE EQUIPMENT COMPARTMENT	MINIMIZE TEMPERATURE GRADIENT IN SUPPLY LINES AND HEAT LEAKS INTO OR OUT OF THRUSTER AND LINES	--	--	--	--	--	0.05
THRUSTERS WITH IGNITION VALVE AND CATALYST BED WITH TEMPERATURE RANGE 13°C (55°F) TO 18°C (65°F), BACKUP THRUSTERS AT 1.2 WATTS, THRUSTERS MOUNTED	MAINTAIN THRUSTER AND SUPPLY LINE TEMPERATURES ABOVE MINIMUM TEMPERATURE LIMITS ISOLATES THRUSTER FROM STRUCTURE TO MINIMIZE HEATER POWER REQUIREMENTS	--	--	--	--	--	--
KAPTON BETWEEN TWO 2-MIL ALUMINIZED	MINIMIZES UNCONTROLLED HEAT LEAKS INTO AND OUT OF THE EQUIPMENT COMPARTMENT	--	--	0.69	--	--	0.69
FRONT SURFACES OF OMNI ANTENNA	MINIMIZE ABSORBED HEAT INPUT TO REDUCE VARIATION IN TEMPERATURE DURING MISSION	--	--	--	0.24	0.31	0.88
KAPTON BETWEEN ONE OUTER 2-MIL ALUMINIZED COVER SHEETS (ALUMINIZED SURFACES FACE)	MINIMIZE SOLAR HEAT LEAK INTO AND UNCONTROLLED HEAT LEAKS OUT OF THE SENSOR ASSEMBLY. STABLE ALUMINIZED KAPTON MINIMIZES EXTERNAL SURFACE PROPERTY DEGRADATION	--	--	--	0.45	0.48	0.69
KAPTON BETWEEN ONE OUTER 2-MIL ALUMINIZED COVER SHEET (ALUMINIZED SURFACES FACE)	MINIMIZE HEATING OF SOLAR ARRAY BY BACK SURFACE	--	--	0.04	0.11	0.11	0.04
FRONT SURFACE OF SUBSTRATE	MAXIMIZE RADIANT HEAT TRANSFER AND MINIMIZE ABSORBED SOLAR INPUT	--	--	0.04	0.24	0.31	0.88

Figure 8.7-1. Preferred Atlas/Centaur Probe Bus Spacecraft Thermal Control System Description

MOLDOUT FRAME

A COMPONENT TEMPERATURE CONTROL CAPABILITY VERSUS TEMPERATURE REQUIREMENTS

ALL COMPONENTS ARE MAINTAINED WITHIN SPECIFIED TEMPERATURE LIMITS. FOR SOME OF THE EXPERIMENTS THE SPECIFIED LIMITS ARE TENTATIVE. THESE LIMITS MUST BECOME MORE CLEARLY DEFINED DURING THE HARDWARE PHASE.

SUBSYSTEM AND SCIENCE COMPONENTS	PREDICTED TEMPERATURES		ACCEPTANCE OPERATING TEMPERATURE LIMITS	
	MINIMUM	MAXIMUM	MINIMUM	MAXIMUM
	°C (°F)	°C (°F)	°C (°F)	°C (°F)
COMMUNICATIONS				
MEDIUM-GAIN ANTENNA	-129 (-200)	24 (75)	-157 (-250)	93 (200)
OMNI ANTENNA	-129 (-200)	24 (75)	-145 (-230)	93 (200)
S-BAND TRANSMITTERS	7 (45)	41 (105)	4 (40)	52 (125)
POWER AMPLIFIER	7 (45)	41 (105)	4 (40)	52 (125)
S-BAND RECEIVERS	7 (45)	36 (97)	-4 (25)	43 (110)
DATA HANDLING				
DTU	7 (45)	26 (78)	-7 (20)	41 (105)
DDU	7 (45)	16 (61)	-7 (20)	41 (105)
ELECTRICAL POWER				
BATTERY	7 (45)	22 (72)	-1 (30)	29 (85)
PCU	7 (45)	33 (92)	-20 (-4)	65 (149)
CTRF/INVERTER	7 (45)	21 (70)	-18 (0)	49 (120)
SHUNT RADIATOR	-94 (-137)	132 (270)	-157 (-250)	132 (270)
SOLAR ARRAY	-101 (-150)	63 (145)	-148 (-235)	107 (225)
CDU	7 (45)	28 (83)	-7 (20)	41 (105)
ACS/PROPULSION				
CEA	7 (45)	16 (61)	-7 (20)	41 (105)
SUN SENSOR	-7 (20)	52 (125)	-15 (5)	60 (140)
THRUSTER VALVE BODYS	13 (55)	82 (180)	13 (55)	93 (200)
HYDRAZINE LINES	4 (40)	82 (180)	4 (40)	82 (180)
HYDRAZINE TANKS	5 (43)	24 (75)	4 (40)	43 (110)
SCIENCE				
ION MASS SPECTROMETER	-18 (0)	52 (125)	-30 (-22)	60 (140)
UV SPECTROMETER	-18 (0)	52 (125)	-30 (-22)	60 (140)
ELECTRON TEMPERATURE PROBE ELECTRONICS	7 (45)	32 (89)	4 (40)	43 (110)
NEUTRAL MASS SPECTROMETER	-18 (0)	52 (125)	-30 (-22)	60 (140)
LARGE PROBE PAYLOAD	7 (45)	32 (89)	-18 (0)	35 (95)
SMALL PROBE PAYLOAD	-9 (15)	24 (76)	-18 (0)	35 (95)
RETARDING POTENTIAL ANALYZER	-18 (0)	52 (125)	-30 (-22)	60 (140)

C ATTITUDE CONTROL SYSTEM TEMPERATURES AND POWER REQUIREMENTS

A STUDY OF THRUSTER TEMPERATURE RESPONSE IN BOTH FIRING AND NONFIRING MODES WAS PERFORMED TO DETERMINE HEATER POWER REQUIREMENTS. HEATERS WILL BE THERMOSTATICALLY CONTROLLED.

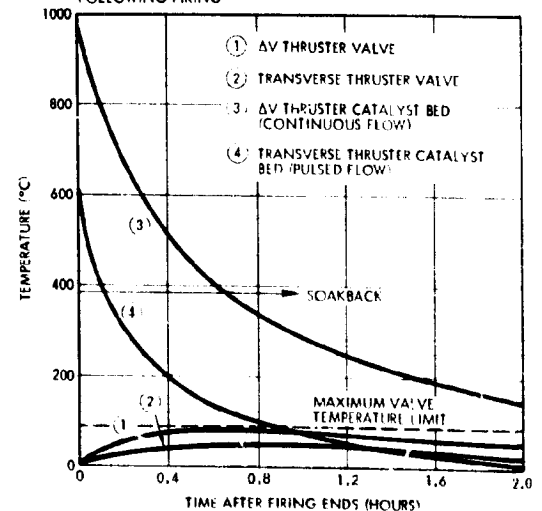
THRUSTER NONFIRING EQUILIBRIUM TEMPERATURE VERSUS HEATER POWER (MAXIMUM HEATER POWER REQUIREMENT DURING MISSION)

THRUSTER	VALVE HEATER POWER (WATTS)	VALVE TEMPERATURE *		CATALYST BED HEATER POWER (WATTS)	CATALYST BED TEMPERATURE **	
		°C	°F		°C	°F
TRANSVERSE	0.3	20	68	0.3	24	75
	0.4	24	78	0.3	26	79
	0.5	29	84	0.2	13	55
	0.5	31	88	0.3	29	83
AFT ΔV	0.2	21	70	0.2	45	113
	0.5	34	93	0	10	49
	0.5	46	115	0.2	63	145
FORWARD ΔV	0.6	18	65	0.4	36	97
	0.5	7	45	0.4	31	89
	0.5	2	35	0.2	-2	29
	0.5	4	39	0.3	16	60

* MINIMUM VALVE TEMPERATURE LIMIT 18°C (65°F) TO ACCOMMODATE DUAL THERMOSTAT CONTROL SYSTEM.

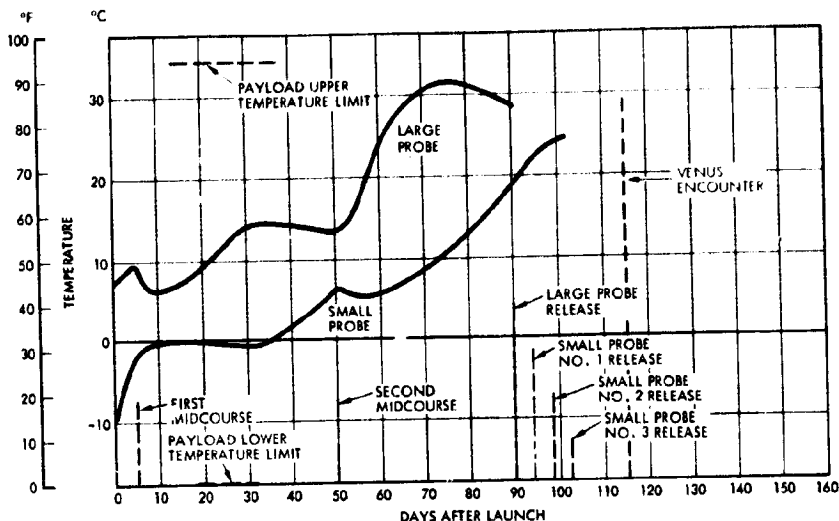
** MINIMUM BED TEMPERATURE LIMIT 24°C (75°F).

THRUSTER TEMPERATURE RESPONSE FOLLOWING FIRING



B PROBE PAYLOAD TEMPERATURES PRIOR TO RELEASE

LARGE PROBE PAYLOAD TEMPERATURE IS MAINTAINED WITHIN ACCEPTABLE LIMITS BY SOLAR ASPECT ANGLE CONTROL. SMALL PROBES ARE INSULATED FROM THE EXTERNAL ENVIRONMENT AND COUPLED TO THE LOUVER CONTROLLED EQUIPMENT COMPARTMENT BY THERMAL WINDOWS.



D TEMPERATURE HISTORY OF BUS COMPONENTS DURING EARTH/VENUS TRANSIT

BUS COMPARTMENT COMPONENTS ARE CONTROLLED BY LOUVERS AND INSULATION. THE PLASMA POTENTIAL REFERENCE SURFACE IS ALUMINIZED KAPTON AND REACHES A PEAK TEMPERATURE OF 230°C (446°F). ALL COMPARTMENT LOCATED COMPONENTS ARE MAINTAINED BETWEEN 4 AND 40°C (40 TO 104°F).

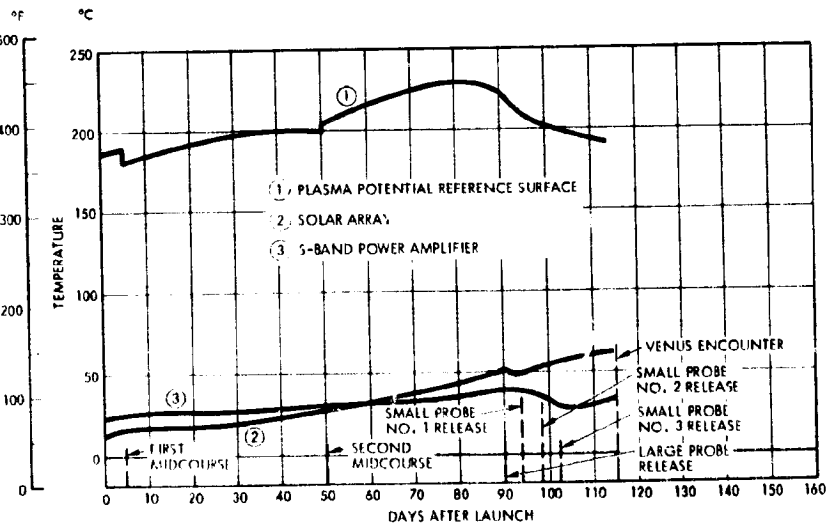


Figure 8.7-2. Preferred Atlas/Centaur Probe Bus Spacecraft Thermal Performance

ambient environment is kept small and three 0.03-meter (1-inch) long titanium standoffs are used to attach the thruster valve to the structure. Additional heater power is not required for the lines and fuel tanks since the equipment compartment level is maintained above 4°C (40°F) and fuel lines external to the compartment are wrapped with multilayer insulation. Copper plated (10 mil) lines are used to enhance thermal conduction and prevent local cold spots from occurring. Figure 8.7-2C also indicates that the valves will not overheat after firing has been completed.

Thermal Environment

The design thermal environment for the entire probe bus spacecraft mission is shown in Figure 8.7-3. Adequate on-stand spacecraft temperature control is provided by supplying 45 kg/min (100 lb/min) of conditioned air into the fairing. The air supply is controlled between 16°C (60°F) and 38°C (100°F) with a relative humidity less than 50 percent (Figure 8.7-3A).

Figure 8.7-3B also specifies typical ascent temperature histories for the inner and outer surfaces of the Atlas/Centaur fairing. Since the shroud is constructed with a 0.04 meter (1.75-inch) thick phenolic honeycomb wall, the interior surface temperature is unaffected by external aerodynamic heating during ascent. Therefore extra thermal protection is not required for ascent temperature control. Low heat capacitance spacecraft surfaces such as solar cells, silver teflon thermal shields, and aluminized insulation blankets are prevented from exceeding their respective maximum temperature limits after shroud separation by jettisoning the fairing 275 seconds after liftoff when the free-molecular heating is below 342 watts/meter² (0.03 BTU/ft²-sec).

The transit thermal environment from booster separation to Venus encounter considers that the spacecraft orientation is inertially fixed, with the exception of solar pressure perturbations, between the first and second midcourse maneuvers, and then remains earth pointing until encounter. The resultant orientation provides sun aspect angles that will maintain acceptable temperatures of the large probe without the use of electric heaters (Figure 8.7-3C).

Probe bus heat dissipations for all components are tabulated in Figure 8.7-3E. A representative mission power profile is also included to indicate the overall variation in spacecraft heat dissipation, Figure 8.7-3D.

Thermal Analysis Techniques A/C IV

Figure 8.7-4 presents the probe bus spacecraft and typical thruster analytical computer models used in the study. Component temperatures for various operating conditions were calculated with these models, using the TRW thermal analyzer computer program. Critical "configuration factors" input into these programs were determined by the TRW "VIEWFAC" program, which generates a hemispherical view from one surface to all adjacent surfaces. A typical computer generated picture is shown in Figure 8.7-4B.

8.7.2.2 Orbiter Spacecraft A/C IV

System Description

A description of the preferred Atlas/Centaur orbiter thermal control system design is shown in Figure 8.7-5. The specific hardware and thermal provisions are identified along with the purpose of each item.

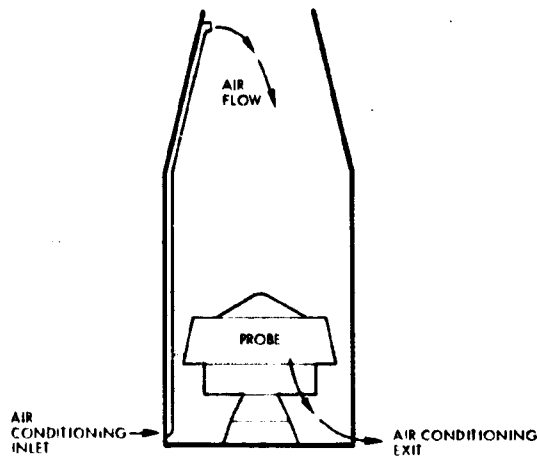
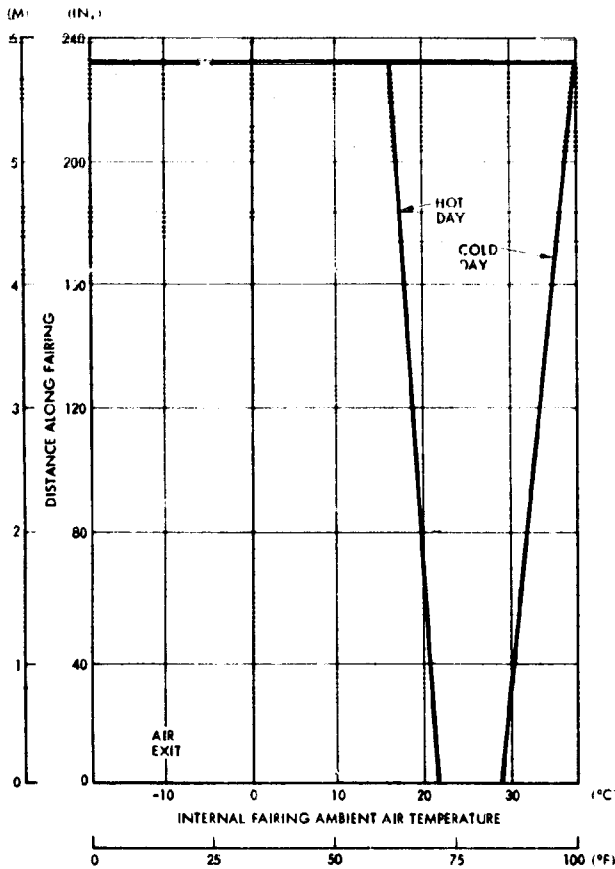
Thermal Control System Performance

Prelaunch orbiter spacecraft temperatures are identical to probe bus spacecraft temperature for that period. The hydrazine system power requirements and temperature levels are also identical to the probe bus system throughout the mission. Other orbiter spacecraft component temperatures will vary between the levels listed in Figure 8.7-6A. Earth/Venus transit and Venus orbit temperature histories of selected components are presented in Figure 8.7-6B.

All component temperatures, including all scientific experiments located within the equipment compartment, except the infrared radiometer, remain within their respective acceptance temperature range. The infrared radiometer temperature will exceed its upper acceptance limit, which is much lower than other experiment temperature limits, during the mission. If the upper temperature limit can be raised without degrading the instrument performance, platform mounting will be acceptable. Otherwise, the instrument will have to be isolated from the equipment compartment and provided with its own thermal control system. A multi-layer insulation and electric heater system combined with a dedicated radiator panel is best for this arrangement.

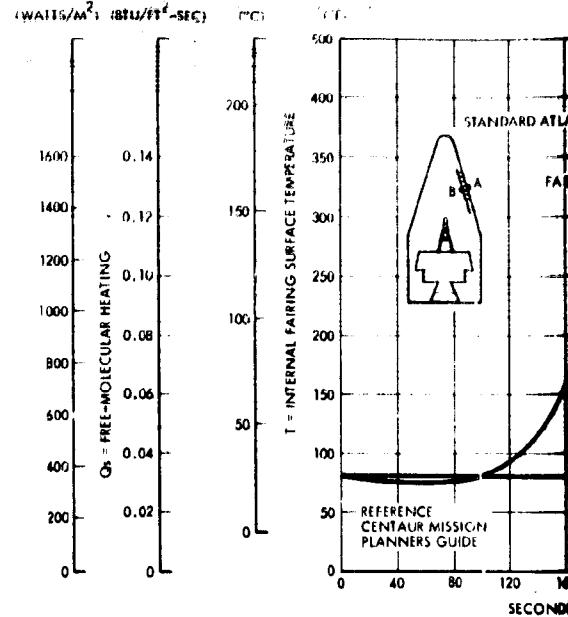
A TYPICAL FAIRING INTERNAL AMBIENT AIR TEMPERATURE PROFILE PRIOR TO LAUNCH

APPROXIMATELY 68 KG/MIN (150 LB/MIN.) OF TEMPERATURE AND HUMIDITY CONTROLLED AIR IS REQUIRED TO MAINTAIN SPACECRAFT COMPONENTS WITHIN ACCEPTANCE LIMITS PRIOR TO LAUNCH. THE AIR SUPPLY TEMPERATURE CONTROL RANGE IS 16 TO 18°C (60 TO 100°F) WITH A RELATIVE HUMIDITY BELOW 50 PERCENT.



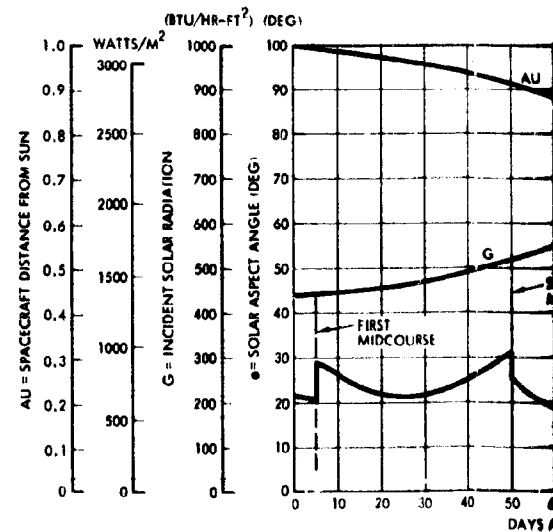
B TYPICAL UNINSULATED FAIRING TEMPERATURES AND STAGNATION FREE-MOLECULAR HEATING DURING ASCENT

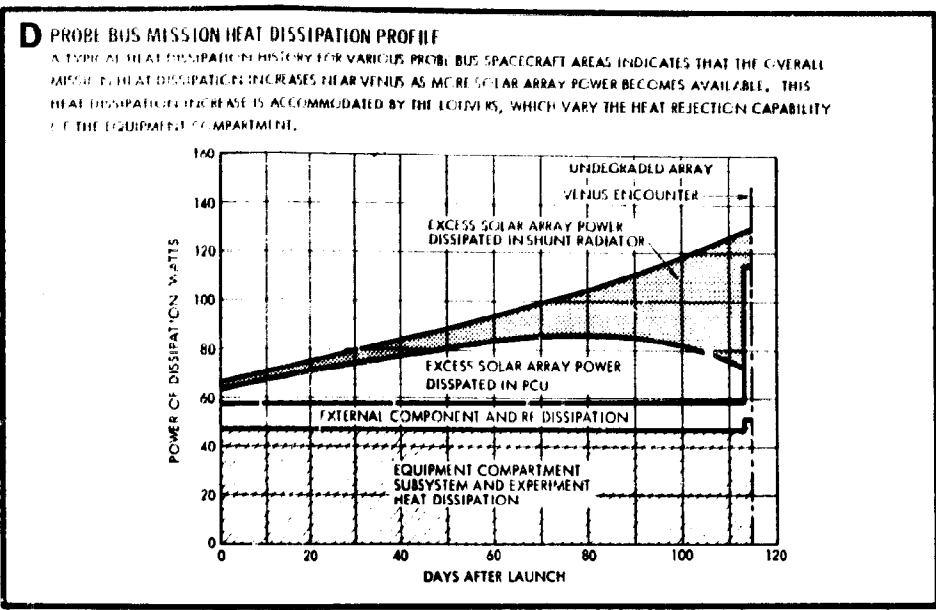
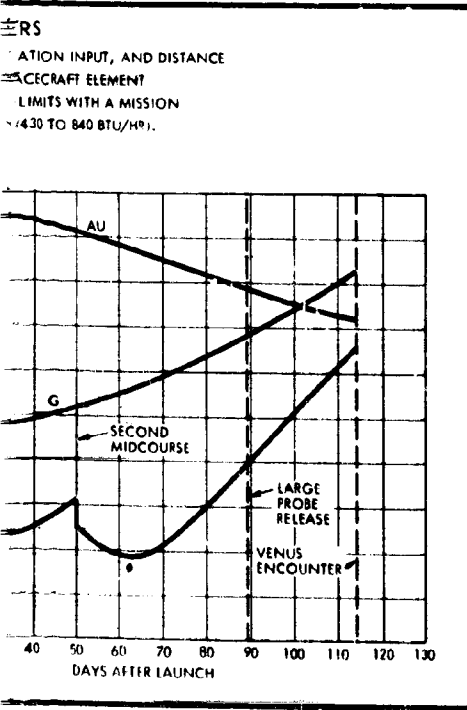
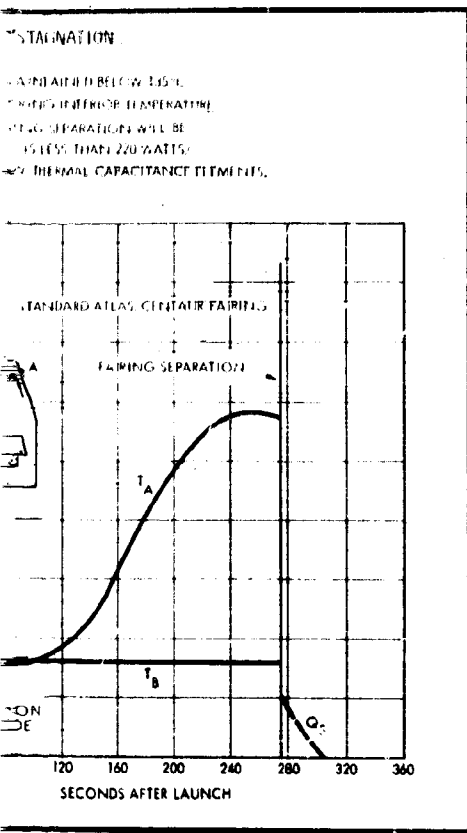
SPACECRAFT TEMPERATURE SENSITIVE ELEMENTS HAVE TO BE MAINTAINED BELOW 100°C DURING ASCENT. THE STANDARD ATLAS/CENTAUR FAIRING INTERIOR HAS A NEGLECTIBLE TEMPERATURE RISE DURING LAUNCH. FAIRING SEPARATION IS DELAYED UNTIL THE STAGNATION FREE-MOLECULAR HEATING IS LESS THAN 20 WATTS/METER² (0.02 BTU/FT²-SEC) TO PREVENT OVERHEATING OF LOW THERMAL CAPACITY ELEMENTS.



C PROBE BUS SPACECRAFT TRANSIT THERMAL PARAMETERS

THE SPACECRAFT SOLAR ASPECT ANGLE, INCIDENT SOLAR RADIATION INPUT, FROM THE SUN IMPACT THE THERMAL SYSTEM DESIGN. THE SPACECRAFT ELEMENT TEMPERATURES HAVE TO BE MAINTAINED WITHIN ACCEPTANCE LIMITS WITH A MAXIMUM SOLAR HEAT FLUX VARIATION OF 1370 TO 2660 WATTS/METER² (430 TO 840 BTU/HR-FT²) DURING TRANSIT.





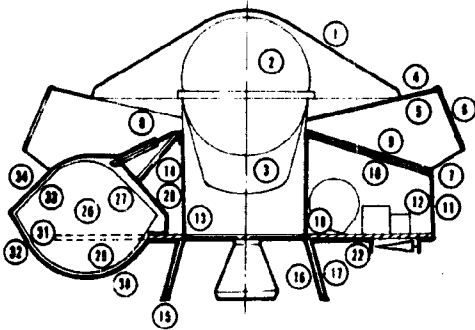
E COMPONENT HEAT DISSIPATIONS

SUBSYSTEM AND EXPERIMENT COMPONENTS ARE LOCATED SUCH THAT HEAT DISSIPATION IS DISTRIBUTED THROUGHOUT THE PLATFORM AREA. LOUVERS ACCOMMODATE VARIATIONS IN HEAT DISSIPATION AND ARE LOCATED TO FURTHER EQUALIZE PLATFORM TEMPERATURES.

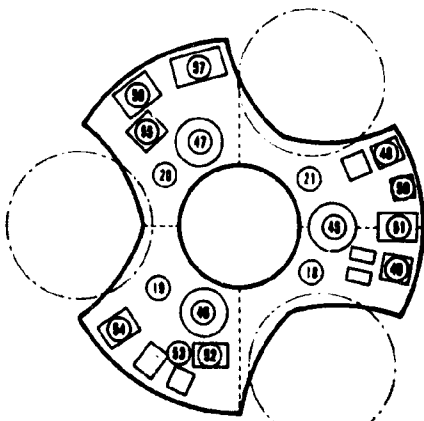
COMPONENT	HEAT DISSIPATION (WATTS)		
	LAUNCH	TRANSIT	ENCOUNTER
SCIENCE			
NEUTRAL MASS SPECTROMETER	0.0	0.0	14.4
ION MASS SPECTROMETER	0.0	0.0	3.0
ELECTRON TEMPERATURE PROBE	0.0	0.0	3.6
UV SPECTROMETER	0.0	0.0	1.8
RECORDING POTENTIAL ANALYZER	0.0	0.0	3.0
DATA HANDLING			
DIGITAL TELEMETRY UNIT	3.6	3.6	3.6
DIGITAL DECODER UNIT	0.3	0.3	0.3
COMMUNICATIONS			
S-BAND RECEIVERS	3.4	3.4	3.4
S-BAND TRANSMITTER DRIVER	1.3	1.3	1.3
S-BAND POWER AMPLIFIER	16.5	16.5	16.5
ACS/PROPULSION			
CONTROL ELECTRONIC ASSEMBLY	1.7	1.7	1.7
PRESSURE TRANSDUCER	0.4	0.4	0.4
ELECTRICAL POWER CONTROL			
PCU ELECTRONICS	4.0	4.0	4.0
COMMAND DISTRIBUTION UNIT	2.1	2.1	2.1
CONVERTER	8.1	8.1	8.1

Figure 8.7.3. Preferred Atlas/Centaur Probe Bus Spacecraft Thermal Environment

A PROBE BUS SPACECRAFT ANALYTICAL THERMAL MODEL
 AN ANALYTICAL THERMAL MODEL WAS CONSTRUCTED TO CONFIRM THE ADEQUACY OF THE SELECTED PROBE BUS THERMAL CONTROL DESIGN



SECTION VIEW



VIEW OF PLATFORM

NODE NUMBER	DESCRIPTION
1	EXPOSED BEARING SURFACE
2	LARGE PROBE PAYLOAD, SEE SECTION 7.4 FOR COMPLETE NCDALIZATION
3	LARGE PROBE PAYLOAD
4	PLASMA BOUNDARY REFERENCE SURFACE - EXTERNAL
5	PLASMA BOUNDARY REFERENCE SURFACE - INTERNAL
6	SEPARATION
7	INTERNAL SURFACE
8	LARGE PROBE PAYLOAD
9	EQUIPMENT COMPARTMENT TOP INSULATION - EXTERNAL
10	EQUIPMENT COMPARTMENT TOP INSULATION - INTERNAL
11	EQUIPMENT COMPARTMENT SIDE INSULATION - EXTERNAL
12	EQUIPMENT COMPARTMENT SIDE INSULATION - INTERNAL
13	CENTRAL CORE INSULATION - EXTERNAL
14	CENTRAL CORE INSULATION
15	CENTRAL CORE SURFACE
16	CENTRAL CORE INSULATION - AFT - EXTERNAL
17	CENTRAL CORE INSULATION - AFT - INTERNAL
18	PLATFORM SEGMENT -Z, -Y
19	PLATFORM SEGMENT -Z, -Z
20	PLATFORM SEGMENT -Z, -Y
21	PLATFORM SEGMENT -Y, -Z
22	EQUIPMENT COMPARTMENT AFT INSULATION, PLAT NODE 18 - EXTERNAL
23	EQUIPMENT COMPARTMENT AFT INSULATION, PLAT NODE 19 - EXTERNAL
24	EQUIPMENT COMPARTMENT AFT INSULATION, PLAT NODE 20 - EXTERNAL
25	EQUIPMENT COMPARTMENT AFT INSULATION, PLAT NODE 21 - EXTERNAL
26	SMALL PROBE PAYLOAD -Z, SEE SECTION 7.4 FOR COMPLETE NCDALIZATION
27	SMALL PROBE TOP INSULATION - INTERNAL
28	SMALL PROBE TOP INSULATION - EXTERNAL
29	SMALL PROBE BOTTOM INSULATION - INTERNAL
30	SMALL PROBE BOTTOM INSULATION - EXTERNAL
31	SMALL PROBE BOTTOM INSULATION - INTERNAL
32	SMALL PROBE BOTTOM INSULATION - EXTERNAL
33	SMALL PROBE TOP INSULATION - INTERNAL
34	SMALL PROBE TOP INSULATION - EXTERNAL
35	SMALL PROBE PAYLOAD -Y, -Z, SEE SECTION 7.4 FOR COMPLETE NCDALIZATION
36	SMALL PROBE TOP INSULATION - INTERNAL
37	SMALL PROBE TOP INSULATION - EXTERNAL
38	SMALL PROBE BOTTOM INSULATION - INTERNAL
39	SMALL PROBE BOTTOM INSULATION - EXTERNAL
40	SMALL PROBE BOTTOM INSULATION - INTERNAL
41	SMALL PROBE BOTTOM INSULATION - EXTERNAL
42	SMALL PROBE TOP INSULATION - INTERNAL
43	SMALL PROBE TOP INSULATION - EXTERNAL
44	SMALL PROBE PAYLOAD -Z, -Y, SEE SECTION 7.4 FOR COMPLETE NCDALIZATION
45	SMALL PROBE TOP INSULATION - INTERNAL
46	SMALL PROBE TOP INSULATION - EXTERNAL
47	SMALL PROBE BOTTOM INSULATION - INTERNAL
48	SMALL PROBE BOTTOM INSULATION - EXTERNAL
49	SMALL PROBE TOP INSULATION - INTERNAL
50	SMALL PROBE TOP INSULATION - EXTERNAL
51	HYDRAZINE TANK (-Z)
52	HYDRAZINE TANK (-Y)
53	HYDRAZINE TANK (-Z, -Y)
54	S-BAND RECEIVERS
55	S-BAND TRANSMITTERS AND POWER AMPLIFIERS
56	ELECTRON TEMPERATURE PROBE ELECTRONICS
57	CLA AND DDU
100	BATTERY
	CTR AND INVERTER
	PCU
	MAGNETOMETER ELECTRONICS
	CDU
	DTU
	SPACE

B CONFIGURATION
 CONFIGURATION PROJECTIONS BY COMPUTER FACTOR MAP

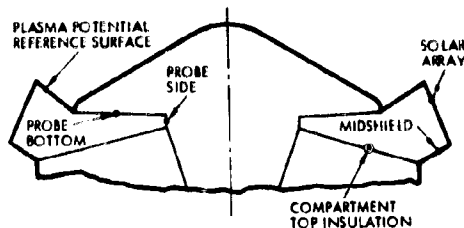
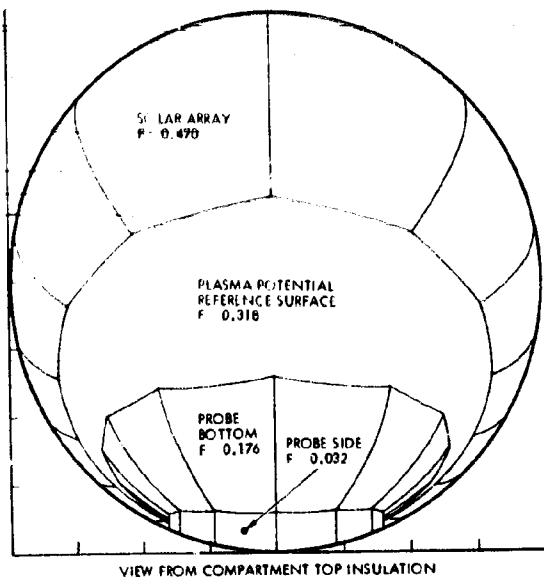
C THRUSTER
 A DETAILED REQUIREMENT ADEQUACY ANALYTICAL



FOLDOUT FRAME

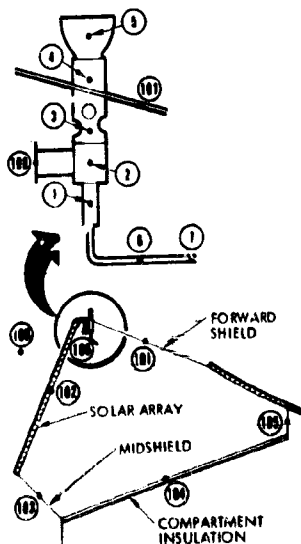
B CONFIGURATION FACTOR DETERMINATION

CONFIGURATION FACTORS WERE DETERMINED BY A GRAPHICS COMPUTER PROGRAM, WHICH PRODUCES A VIEW FACTOR PROJECTION DRAWING SHOWING ALL SURFACES AS SEEN FROM A GIVEN LOCATION. VIEW FACTORS ARE DETERMINED BY COMPUTING THE AREAS VISIBLE IN THE DRAWING. ENOUGH VIEWS WERE TAKEN TO DETERMINE A COMPLETE VIEW FACTOR MATRIX FOR THE VEHICLE. A TYPICAL VIEW IS SHOWN BELOW.



C THRUSTER THERMAL MODEL

A DETAILED THRUSTER ANALYSIS MODEL WAS CONSTRUCTED TO DETERMINE HEATER REQUIREMENTS AND CONFIRM THE OVERALL THRUSTER THERMAL CONTROL DESIGN ADEQUACY. BOUNDARY TEMPERATURES WERE CALCULATED WITH THE BUS SPACECRAFT ANALYTICAL THERMAL MODEL.



NODE NUMBER	DESCRIPTION
1	INLET VALVE FITTING
2	VALVE
3	THERMAL BARRIER
4	CATALYST BED
5	NOZZLE
6	FUEL LINE
7	FUEL LINE (BOUNDARY NODE)
100	SPACE
101	FORWARD THERMAL SHIELD (BOUNDARY NODE)
102	SOLAR ARRAY (BOUNDARY NODE)
103	MIDTHERMAL SHIELD (BOUNDARY NODE)
104	COMPARTMENT INSULATION (BOUNDARY NODE)
105	BRACKETS (BOUNDARY NODE)
106	ATTACH BRACKET BOUNDARY NODE

D INSULATION CONDUCTANCE

INSULATION CONDUCTANCE VALUES USED IN THE ANALYTICAL MODEL WERE OBTAINED FROM PIONEERS 10 AND 11 SPACECRAFT TESTS. DATA (SHOWN BELOW) WAS CORRELATED AS A FUNCTION OF INSULATION OUTER SURFACE TEMPERATURE

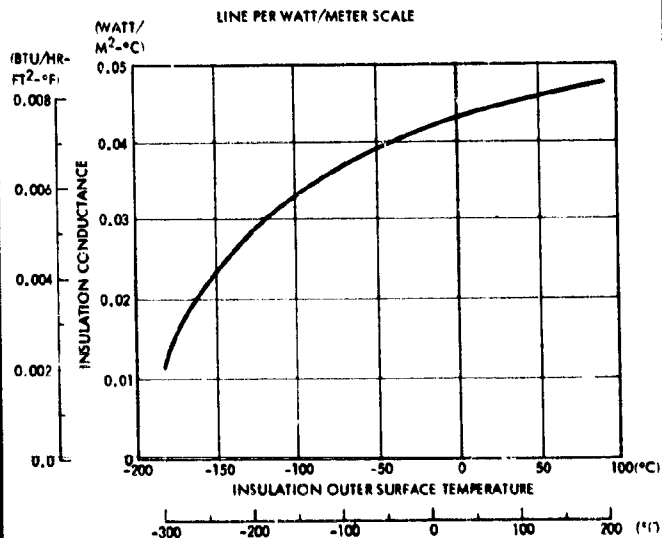
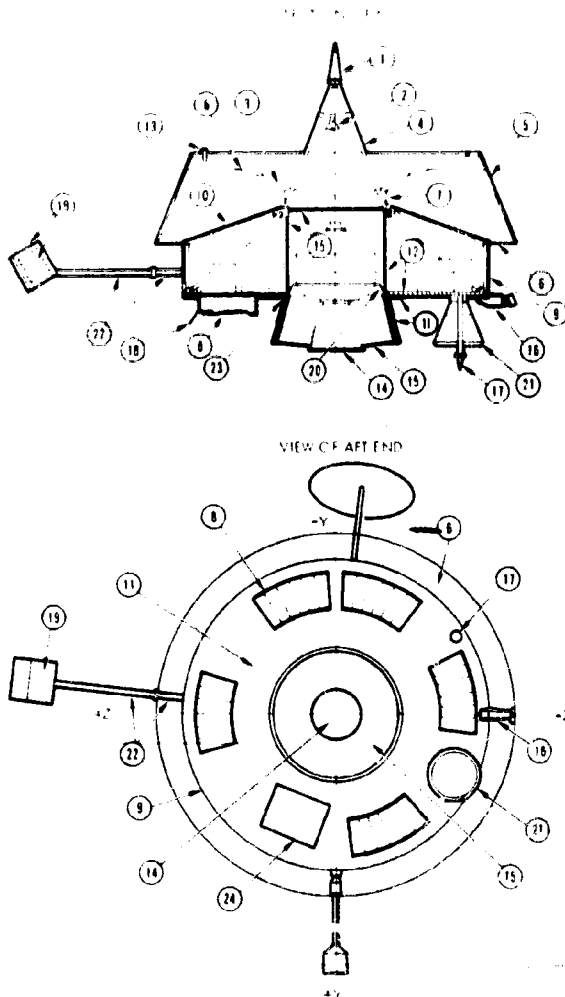


Figure 8.7-4. Pioneer Atlas/Centaur Probe Bus Spacecraft Thermal Analysis

A THERMAL CONTROL SYSTEM HARDWARE DESCRIPTION

THE WRITER USES THERMAL CONTROL HARDWARE COMMON TO THE DEEP SPACE PROGRAM. PARTICULAR HARDWARE ARE REFERRED TO IN THE ADJUNCT TABLES ATTACHED TO THIS REPORT.



B THERMAL CONTROL SYSTEM FEATURES

- INSULATED EQUIPMENT COMPARTMENT WITH LOUVERS TO MINIMIZE SOLAR INTENSITY VARIATION DURING TRANSIT TO VENUS
- REAR OF SOLAR ARRAY THE "MIL" COUPLED INDIRECTLY TO SPACE TO REDUCE ARRAY TEMPERATURE
- LOW ABSORBANCE HIGH EMITTANCE SHIELDS TO PREVENT SOLAR IRRADIATION ON ARRAY REAR SURFACE
- HEATED THRUSTERS WITH COPPER-PLATED LINES TO PREVENT HYDRATION FROM FREEZING
- WHITE PAINTED SURFACES TO LOWER OPERATING TEMPERATURE LEVELS
- SUN SHIELDS TO PREVENT SUN IRRADIATION ON AFT-MOUNTED LOUVER ASSEMBLIES
- INSULATED HEATED SOLE MOTOR COMPARTMENT TO MAINTAIN ACCEPTABLE MOTOR TEMPERATURE DURING TRANSIT. A JETTISONABLE INSULATED CAP IS PROVIDED OVER THE NOZZLE OPENING
- INSULATED RASA PLATFORM COMPARTMENT WITH INTEGRAL SECOND SURFACE RADIATION PANELS. ELECTRIC HEATERS PROVIDED TO MAINTAIN ACCEPTABLE TEMPERATURES WHEN EXPERIMENTS ARE NOT OPERATING

ID. NO.	NAME OF ITEM	DESCRIPTION OF HARDWARE	FUNCTION
1	FORWARD CONICAL ANTENNA THERMAL COATING	1-MIL COAT OF 5-1130 WHITE PAINT ON EXTERNAL SURFACE OF CONICAL ANTENNA	MINIMIZE TO REDUCE LOCATION TEMPERATURE
2	HIGH-GAIN ANTENNA FEED THERMAL COATING	1-MIL COAT OF 5-1130 WHITE PAINT ON EXTERNAL SURFACE OF FEED	MINIMIZE TO REDUCE LOCATION TEMPERATURE
3	HIGH-GAIN ANTENNA REFLECTOR THERMAL COATING	1-MIL COAT OF 5-1130 WHITE PAINT ON EXTERNAL SURFACE OF ANTENNA	MINIMIZE TO REDUCE LOCATION TEMPERATURE
4	FEED SUPPORT THERMAL COATING	1-MIL COAT OF 5-1130 WHITE OF SUPPORT EXTERNAL SURFACE	MINIMIZE HEAT INPUT
5	SOLAR ARRAY SUBSTRATE THERMAL COATING	1-MIL COAT OF 3M BLACK VELVET PAINT ON BACK SURFACE OF SUBSTRATE	MAXIMIZE OF SOLAR
6	FORWARD AND MIDSIELD	ONE OUTER LAYER OF 2-MIL ALUMINIZED REFLECTOR (ALUMINIZED SIDE FACING INWARD). LAMINATED TO ONE 2-MIL INNER LAYER OF CLEAR MYLAR	SHIELD AND REFLECTED LOW TEMP HEAT TRAP
7	CENTRAL CYLINDER THERMAL COATING	COLORLESS CHEM FILM SURFACE	RADIATIVE AND FORM
8	BIMETAL ACTUATED LOUVERS	0.50 M ² (5.4 FT ²) TOTAL BLADE AREA CLOSED EFFECTIVE EMITTANCE 0.20 FULL CLOSED AT 4°C (40°F) OPEN EFFECTIVE EMITTANCE 0.74 FULL OPEN AT 29°C (85°F) 3-MIL COAT OF Z-93 WHITE PAINT ON PLATFORM UNDER LOUVERS	CONTROL OF SET POINT. ACCEPTABLE MAINTAINANCE ACCEPTABLE
9	EQUIPMENT COMPARTMENT SIDE INSULATION	22 LAYERS OF 1.4-MIL ALUMINIZED MYLAR SANDWICHED BETWEEN ONE OUTER 2-MIL ALUMINIZED KAPTON AND ONE INNER 2-MIL ALUMINIZED MYLAR COVER SHEET. ALL ALUMINIZED SURFACES EXCEPT INSIDE COVER SHEET FACE INWARD. K/X, SEE FIGURE 8.7-4	MINIMIZE UNDESIRABLE COMPARTMENT EXTERNAL
10	EQUIPMENT COMPARTMENT TOP INSULATION	22 LAYERS OF 1.4-MIL ALUMINIZED MYLAR SANDWICHED BETWEEN TWO 2-MIL ALUMINIZED MYLAR COVER SHEETS. ALL ALUMINIZED SURFACES EXCEPT AFT COVER SHEET FACE INWARD. K/X, SEE FIGURE 8.7-4	MINIMIZE OF THE EQUIPMENT COUPLE
11	EQUIPMENT COMPARTMENT AFT INSULATION	22 LAYERS OF 1.4-MIL ALUMINIZED KAPTON SANDWICHED BETWEEN ONE OUTER 2-MIL ALUMINIZED KAPTON AND ONE INNER 2-MIL ALUMINIZED MYLAR COVER SHEET. ALL ALUMINIZED SURFACES FACE FORWARD. K/X, SEE FIGURE 8.7-4	MINIMIZE EQUIPMENT PERFORMANCE MAINTAINANCE EXTERNAL
12	EQUIPMENT COMPARTMENT RADIATIVE AND CONDUCTIVE THERMAL COUPLING REQUIREMENTS	3-MIL COATING OF 3M BLACK VELVET PAINT ON EQUIPMENT PLATFORM AND HEAT DISSIPATING EQUIPMENT BAR METAL SURFACE ON CENTRAL COLUMN AND HYDRAZINE TANKS. TANKS CONDUCTIVELY COUPLED TO MOUNTING PLATFORM AND ISOLATED FROM COLUMN. PROVIDE GOOD CONDUCTION THERMAL COUPLING BETWEEN HIGH HEAT DENSITY COMPONENTS. TRANSMITTER AND PLATFORM WITH RTV INTERFACE FILLER MATERIAL. H-142 WATTS M ² -C (22 BTU HR-FT ² -°F)	EQUALIZE COMPARTMENT COUPLING REQUIREMENTS THERMALLY MINIMIZE PERIODIC CONDITION
13	RCS THRUSTER VALVE BODY AND SUPPLY LINE INSULATION. VALVE HEATERS, AND THRUSTER ISOLATION PROVISIONS	LOWER ΔV THRUSTER INSULATED COMPLETELY WITH HIGH TEMPERATURE ACRYLONITRILE FOIL. ALL FUEL LINES ARE COPPER PLATED. LINES EXTERNAL TO THE EQUIPMENT COMPARTMENT INSULATED WITH 10 LAYERS OF MRL-1 INSULATION. K/X 0.056 WATTS M ² -C (0.01 BTU HR-FT ² -°F) DUAL-RANGE THERMOSTATICALLY CONTROLLED HEATERS ON VALVE AND CATALYST BED WITH GROUND CONTROL BACKUP. PRIMARY HEATER CONTROL RANGE 13°C (55°F) TO 18°C (65°F). BACKUP RANGE 7°C (45°F) TO 13°C (55°F). HEATER POWER REQUIREMENT 5.2 WATTS THRUSTERS MOUNTED TO STRUCTURE WITH TITANIUM STANDOFFS	MINIMIZE SPACE MINIMIZE AND HEAT MAINTAIN ABOVE MINIMUM HEATER POWER

7010047 PRAISE

PURPOSE	SURFACE THERMAL PROPERTIES						
	INSIDE			OUTSIDE			
	"NEW	"DEG	"	"NEW	"DEG	"	
EXTERNAL	MINIMIZE ABSORBED SOLAR AND ALBEDO HEAT INPUT TO REDUCE VARIATION IN TEMPERATURE DURING MISSION. IC CATHODE ENSURES SOLAR HEATING TO LIMIT MINIMUM TEMPERATURES FOR ALL SOLAR ASPECT ANGLES ENCOUNTERED.	--	--	--	0.24	0.39	0.88
EXTERNAL	MINIMIZE ABSORBED SOLAR AND ALBEDO HEAT INPUT TO REDUCE VARIATION IN TEMPERATURE DURING MISSION. IC CATHODE ENSURES SOLAR HEATING TO LIMIT MINIMUM TEMPERATURES FOR ALL SOLAR ASPECT ANGLES ENCOUNTERED.	--	--	--	0.24	0.39	0.88
EXTERNAL	MINIMIZE ABSORBED SOLAR AND ALBEDO HEAT INPUT TO REDUCE VARIATION IN TEMPERATURE AND REFLECTOR DISTORTION DURING MISSION.	--	--	--	0.24	0.39	0.88
EXTERNAL	MINIMIZE DIRECT AND REFLECTED SOLAR AND ALBEDO HEAT INPUT TO LIMIT MAXIMUM SUPPORT TEMPERATURES	--	--	--	0.24	0.39	0.88
ON BACK	MAXIMIZE RADIANT HEAT TRANSFER FROM BACK SURFACE OF SOLAR ARRAY	--	--	0.90	0.80	0.80	0.80
TEFLON LAMINATED TO SOLAR	SHIELD BACKSIDE OF SOLAR ARRAY FROM DIRECT OR REFLECTED SOLAR AND ALBEDO IMPINGEMENT. PROVIDE LOW TEMPERATURE BOUNDARY (LOW ϵ) TO MAXIMIZE HEAT TRANSFER FROM BACK SURFACE OF SOLAR ARRAY	--	--	0.66	0.08	0.18	0.66
	RADIATIVELY DECOUPLE CYLINDER FROM SOLAR ARRAY AND FORWARD SHIELD	--	--	0.05	--	--	0.05
FULL CLOSED	CONTROL EQUIPMENT COMPARTMENT HEAT LEAK TO OFFSET THE VARIATION IN EQUIPMENT AND ENVIRONMENTAL HEAT INPUT EXPERIENCED DURING THE MISSION TO MAINTAIN COMPONENT TEMPERATURES WITHIN ACCEPTABLE LIMITS	--	--	--	0.50	0.50	0.20
FULL OPEN AT PLATFORM							CLOSED 0.74 OPEN
SOLAR SANDWICHED MYLAR LAYERS EXCEPT	MINIMIZE SOLAR AND ALBEDO HEAT LEAK INTO AND UNCONTROLLED HEAT LEAKS OUT OF THE EQUIPMENT COMPARTMENT. STABLE ALUMINIZED KAPTON MINIMIZES EXTERNAL SURFACE PROPERTY DEGRADATION.	--	--	0.69	0.45	0.50	0.69
SOLAR SANDWICHED MYLAR LAYERS EXCEPT	MINIMIZES UNCONTROLLED HEAT LEAKS INTO AND OUT OF THE EQUIPMENT COMPARTMENT AND THERMALLY DECOUPLES COMPARTMENT FROM SOLAR ARRAY	--	--	0.69	--	--	0.69
KAPTON SANDWICHED KAPTON FACE FORWARD	MINIMIZE UNCONTROLLED HEAT LEAKS OUT OF THE EQUIPMENT COMPARTMENT. MINIMIZE SOLID MOTOR PLUME RADIANT HEAT INPUT TO EQUIPMENT COMPARTMENT. STABLE ALUMINIZED KAPTON MINIMIZE EXTERNAL SURFACE PROPERTY DEGRADATION.	--	--	--	0.45	0.50	0.69
PAINT ON	EQUALIZE TEMPERATURE GRADIENTS WITHIN EQUIPMENT COMPARTMENT BY MAXIMIZING RADIATIVE THERMAL COUPLING BETWEEN STRUCTURE AND HEAT DISSIPATING COMPONENTS	--	--	--	--	--	0.90
EQUIPMENT ISOLATED	THERMALLY DECOUPLE ZERO HEAT DISSIPATING COMPONENTS FROM SURROUNDING TO MINIMIZE TEMPERATURE VARIATIONS DURING TRANSIENT ENVIRONMENTAL CONDITIONS	--	--	--	--	--	0.10
HEAT COUPLING COMPONENTS AT INTERFACE	MINIMIZE COMPONENT TO EQUIPMENT PLATFORM TEMPERATURE GRADIENTS TO MINIMIZE MAXIMUM COMPONENT TEMPERATURE ABOVE SURROUNDINGS	--	--	--	--	--	--
ISOLATED WITH	MINIMIZE UNCONTROLLED THRUSTER HEAT LEAK TO SPACE	--	--	--	0.12	0.12	0.05
ISOLATED WITH	MINIMIZE TEMPERATURE GRADIENTS IN SUPPLY LINES AND HEAT LEAKS INTO OR OUT OF THRUSTER AND LINES	--	--	--	--	--	0.05
ISOLATED WITH	MAINTAINS THRUSTER AND SUPPLY LINE TEMPERATURES ABOVE MINIMUM TEMPERATURE LIMITS	--	--	--	--	--	--
ISOLATED WITH	ISOLATES THRUSTER FROM STRUCTURE TO MINIMIZE HEATER POWER REQUIREMENT	--	--	--	--	--	--
TITANIUM							

ID NO.	NAME OF ITEM	DESCRIPTION OF MATERIAL
14	MOTOR NOZZLE CAP INSULATION	22 LAYERS OF 1/4-MIL ALUMINIZED KAPTON SANDWICHED BETWEEN TWO 2-MIL ALUMINIZED KAPTON COVER SHEETS (ALUMINIZED SURFACES FACE INWARD) K/X, SEE FIGURE 8.7-4
15	SOLID MOTOR INSULATION	22 LAYERS OF 1/4-MIL ALUMINIZED KAPTON SANDWICHED BETWEEN TWO 2-MIL ALUMINIZED KAPTON COVER SHEETS (ALUMINIZED SURFACES FACE INWARD) K/X, SEE FIGURE 8.7-4
16	SUN SENSOR INSULATION	22 LAYERS OF 1/4-MIL ALUMINIZED MYLAR SANDWICHED BETWEEN ONE OUTER 2-MIL ALUMINIZED KAPTON AND ONE INNER 2-MIL ALUMINIZED MYLAR COVER SHEETS (ALUMINIZED SURFACES FACE INWARD) K/X, SEE FIGURE 8.7-4
17	AFT OMNI ANTENNA THERMAL COATING	3-MIL COAT OF S-13G WHITE PAINT ON EXTERNAL SURFACES OF OMNI ANTENNA
18	AFT SUN SHIELD	ONE 5-MIL SHEET OF WHITE PAINTED KAPTON (PAINTED SIDE FACING INWARD)
19	RAM PLATFORM INSULATION/RADIATOR SURFACES	22 LAYERS OF 1/4-MIL ALUMINIZED MYLAR SANDWICHED BETWEEN ONE OUTER 2-MIL ALUMINIZED KAPTON AND ONE INNER 2-MIL ALUMINIZED MYLAR COVER SHEETS (ALUMINIZED SURFACES FACE INWARD) K/X = SEE FIGURE 8.7-4 TWO 0.037 M ² (0.4 FT ²) SECOND SURFACE MIRROR COVERED SURFACES ON EITHER END OF PLATFORM 8-WATT ELECTRIC HEATER
20	MOTOR HEATER	5-WATT ELECTRIC HEATER WITH THERMOSTATIC CONTROL
21	MEDIUM-GAIN ANTENNA COATING	3-MIL COAT OF S-13G WHITE PAINT ON EXTERNAL SURFACE
22	RAM BCOM INSULATION	22 LAYERS OF 1/4-MIL ALUMINIZED MYLAR SANDWICHED BETWEEN ONE OUTER 2-MIL ALUMINIZED KAPTON AND ONE INNER 2-MIL ALUMINIZED MYLAR COVER SHEETS. K X, SEE FIGURE 8.7.4.
23	MOTOR/PLATFORM ATTACHMENT RING	FIBERGLASS SUPPORT STRUCTURE
24	SHUNT RADIATOR	3 MIL COAT OF S 13G WHITE PAINT ON AFT SURFACE, FORWARD SURFACE UNCOATED

UNCLASSIFIED

NAME OF ITEM	DESCRIPTION OF HARDWARE	PURPOSE	SURFACE THERMAL PROPERTIES					
			INSIDE			OUTSIDE		
			NEW	DEG	'	NEW	DEG	'
NOZZLE INSULATION	22 LAYERS OF 1/4-MIL ALUMINIZED KAPTON SANDWICHED BETWEEN TWO 2-MIL ALUMINIZED KAPTON COVER SHEETS (ALUMINIZED SURFACES FACE INWARD) K X, SEE FIGURE 8.7-4	MINIMIZE UNCONTROLLED HEAT LEAK FROM SOLID MOTOR TO MAINTAIN MOTOR WITHIN ACCEPTABLE TEMPERATURE LIMITS PRIOR TO FIRING. NOZZLE CAP IS JETISONED WHEN MOTOR FIRES	--	--	0.05	0.45	0.50	0.69
MOTOR ISOLATION	22 LAYERS OF 1/4-MIL ALUMINIZED KAPTON SANDWICHED BETWEEN TWO 2-MIL ALUMINIZED KAPTON COVER SHEETS (ALUMINIZED SURFACES FACE INWARD) K X, SEE FIGURE 8.7-4	MINIMIZE UNCONTROLLED HEAT LEAK FROM SOLID MOTOR TO MAINTAIN MOTOR WITHIN ACCEPTABLE TEMPERATURE LIMITS PRIOR TO FIRING. MINIMIZE UNCONTROLLED HEAT LEAK FROM THE EQUIPMENT COMPARTMENT, MINIMIZE SOLID MOTOR RADIANT HEAT/ SCAK-BACK TO EQUIPMENT COMPARTMENT AFTER MOTOR FIRING, KAPTON REQUIRED TO PREVENT DEGRADATION OF INSULATION THERMAL PROPERTIES DUE TO HEAT/ SCAK-BACK FROM MOTOR CASE	--	--	0.69	--	--	0.05
SENSOR ISOLATION	22 LAYERS OF 1/4-MIL ALUMINIZED MYLAR SANDWICHED BETWEEN ONE OUTER 2-MIL ALUMINIZED KAPTON AND ONE INNER 2-MIL ALUMINIZED MYLAR COVER SHEETS (ALUMINIZED SURFACES FACE INWARD) K X, SEE FIGURE 8.7-4	MINIMIZE SOLAR AND ALBEDO HEAT LEAK INTO AND UNCONTROLLED HEAT LEAK OUT OF THE SENSOR ASSEMBLY. STABLE ALUMINIZED KAPTON MINIMIZES EXTERNAL SURFACE PROPERTY DEGRADATION	--	--	--	0.45	0.50	0.69
OMNI ANTENNA THERMAL COATING	3-MIL COAT OF S-13G WHITE PAINT ON EXTERNAL SURFACES OF OMNI ANTENNA	MINIMIZE ABSORBED SOLAR AND ALBEDO HEAT INPUT TO REDUCE VARIATION IN TEMPERATURE DURING MISSION. LOCATION ENSURES SOLAR HEATING THROUGH MOST OF MISSION TO LIMIT MINIMUM TEMPERATURE DURING NORMAL OPERATION	--	--	--	0.24	0.39	0.88
SUN SHIELD	ONE 5-MIL SHEET OF WHITE PAINTED KAPTON (PAINTED SIDE FACING INWARD)	SHIELD LOUVERS FROM DIRECT SOLAR HEAT INPUT FOR SOLAR ASPECT ANGLES AS LARGE AS 1.75 RADIAN (100 DEGREES)	0.20	0.35	0.68	0.45	0.50	0.69
PLATFORM ISOLATION/ RADIATOR SURFACES	22 LAYERS OF 1/4-MIL ALUMINIZED MYLAR SANDWICHED BETWEEN ONE OUTER 2-MIL ALUMINIZED KAPTON AND ONE INNER 2-MIL ALUMINIZED MYLAR COVER SHEETS (ALUMINIZED SURFACES FACE INWARD) K X, SEE FIGURE 8.7-4 TWO 0.037 M ² (0.4 FT ²) SECOND SURFACE MIRROR COVERED SURFACES ON EITHER END OF PLATFORM 8-WATT ELECTRIC HEATER	MINIMIZE SOLAR AND ALBEDO HEAT LEAK INTO AND UNCONTROLLED HEAT LEAK OUT OF RAM PLATFORM. STABLE ALUMINIZED KAPTON MINIMIZES EXTERNAL SURFACE PROPERTY DEGRADATION PROVIDES CONTROLLED HEAT LOSS TO SPACE MAINTAIN ACCEPTABLE TEMPERATURE LEVEL WHEN EXPERIMENTS NOT OPERATING	--	--	0.05	0.45	0.50	0.69
MOTOR HEATER	5-WATT ELECTRIC HEATER WITH THERMOSTATIC CONTROL	MAINTAIN ACCEPTABLE MOTOR TEMPERATURE LEVEL DURING TRANSIT PRIOR TO MOTOR FIRING	--	--	--	--	--	--
LOW-GAIN ANTENNA COATING	3-MIL COAT OF S-13G WHITE PAINT ON EXTERNAL SURFACE	MINIMIZE SOLAR AND ALBEDO HEAT INPUT TO REDUCE VARIATION IN TEMPERATURE DURING MISSION.	--	--	--	0.24	0.39	0.88
RAM ISOLATION	22 LAYERS OF 1/4-MIL ALUMINIZED MYLAR SANDWICHED BETWEEN ONE OUTER 2-MIL ALUMINIZED KAPTON AND ONE INNER 2-MIL ALUMINIZED MYLAR COVER SHEETS. K X, SEE FIGURE 8.7-4.	MINIMIZE SOLAR AND ALBEDO HEAT INPUT AND UNCONTROLLED HEAT LEAKS OUT OF RAM PLATFORM AND EQUIPMENT COMPARTMENT	--	--	--	0.45	0.50	0.69
MOTOR PLATFORM ATTACHMENT RING	FIBERGLASS SUPPORT STRUCTURE	MINIMIZE HEAT LOSS FROM SOLID ROCKET MOTOR OUT OF SUPPORT COLUMN	--	--	--	--	--	--
NOZZLE RADIATOR	1 MIL COAT OF S-13G WHITE PAINT ON AFT SURFACE, FORWARD SURFACE UNCOATED	MAXIMIZE RADIANT LOSS TO SPACE AND MINIMIZE ABSORBED SOLAR AND ALBEDO HEAT INPUTS	--	--	0.04	0.24	0.39	0.88

Figure 8.7-5. Preferred Atlas/Centaur Orbiter Spacecraft Thermal Control System Description

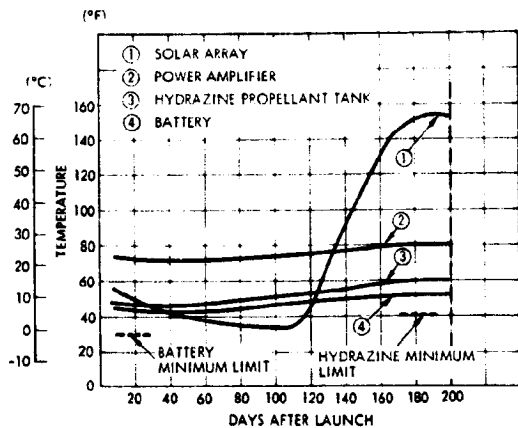
A COMPONENT TEMPERATURE CONTROL CAPABILITY VERSUS TEMPERATURE REQUIREMENTS

ALL EQUIPMENT TEMPERATURES EXCEPT THE IR RADIOMETER MEET THE SPECIFIED ACCEPTANCE TEMPERATURE LIMITS. THE IR RADIOMETER TEMPERATURE WILL REACH 28°C (82°F), 16°C (78°F) ABOVE THE 12°C (54°F) SPECIFICATION LIMIT. TO CONTROL TO THE ABOVE LIMIT WOULD REQUIRE THAT THE UNIT BE ISOLATED FROM THE SPACECRAFT AND PROVIDED WITH A HEATER. SINCE THIS IS A SIGNIFICANT CHANGE THE UPPER EXPERIMENT TEMPERATURE LIMIT SHOULD BE REVIEWED TO DETERMINE WHETHER IT CAN BE RAISED.

SUBSYSTEM AND SCIENCE COMPONENTS	PREDICTED TEMPERATURES		ACCEPTANCE OPERATING TEMPERATURE LIMITS	
	MINIMUM	MAXIMUM	MINIMUM	MAXIMUM
	°C F	°C F	°C F	°C F
COMMUNICATIONS				
OMNI ANTENNAS	-129 -200	24 75	-145 -230	93 200
HIGH-GAIN ANTENNA FEED	-131 -200	21 69	-206 -349	171 340
S-BAND TRANSMITTER	-115 -175	24 75	-185 -300	38 100
POWER AMPLIFIER	10 49	43 110	4 40	52 125
S-BAND RECEIVER	10 49	42 110	4 40	52 125
MEDIUM-GAIN ANTENNA	-129 -200	24 75	-185 -300	38 100
DATA HANDLING				
DTU	9 47	21 69	-7 20	41 105
DSU	6 43	19 67	-7 20	41 105
DDU	9 48	20 68	-7 20	41 105
ELECTRICAL POWER				
BATTERY	9 47	24 75	-1 30	29 85
PCU	10 49	38 100	-20 -4	55 149
CTRF/INVERTER	8 46	28 83	-18 0	49 120
SHUNT RADIATOR	-102 -153	132 270	-157 -250	132 270
SOLAR ARRAY	-148 -235	107 225	-148 -235	107 225
CDU	10 49	21 70	-7 20	41 105
ACS PROPULSION				
CEA	9 48	20 68	-7 20	41 105
SUN SENSOR	4 39	57 125	-15 5	60 140
THRUSTER VALVE BODIES	13 55	82 180	13 55	93 200
HYDRAZINE TANKS	7 44	21 70	4 40	43 110
HYDRAZINE LINES	4 40	82 180	4 40	82 180
SOLID ROCKET MOTOR	4 41	16 62	-7 20	38 100
SCIENCE				
MAGNETOMETER ELECTRONICS	7 45	21 69	0 32	60 140
RADAR ALTIMETER ELECTRONICS	5 42	24 75	-30 -22	60 140
ELECTRON TEMPERATURE PROBE ELECTRONICS	5 42	26 79	-4 40	43 110
UV SPECTROMETER	10 45	36 100	0 32	40 104
ION MASS SPECTROMETER	-25 -13	18 65	-30 -22	60 140
IR RADIOMETER	8 46	28 82	-22 -22	12 54
NEUTRAL MASS SPECTROMETER	-25 -13	19 67	-30 -22	60 140
X-BAND OCCULTATION ELECTRONICS	7 45	24 75	-30 -22	60 140

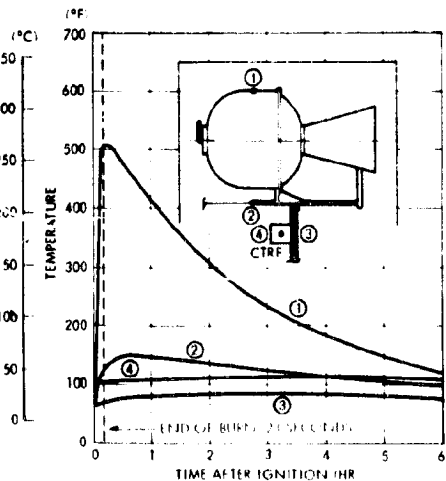
B TEMPERATURE HISTORY OF CRITICAL COMPONENTS DURING EARTH/VENUS TRANSIT

SPACECRAFT TEMPERATURES INITIALLY DECREASE WITH MISSION TIME AS THE SPACECRAFT GOES OUT TO 1.07 AU AND THEN INCREASE AS THE INCIDENT SOLAR HEATING MORE THAN DOUBLES FROM ITS MINIMUM VALUE. THIS EFFECT IS DRAMATICALLY SHOWN BY THE SOLAR ARRAY TEMPERATURE BELOW.



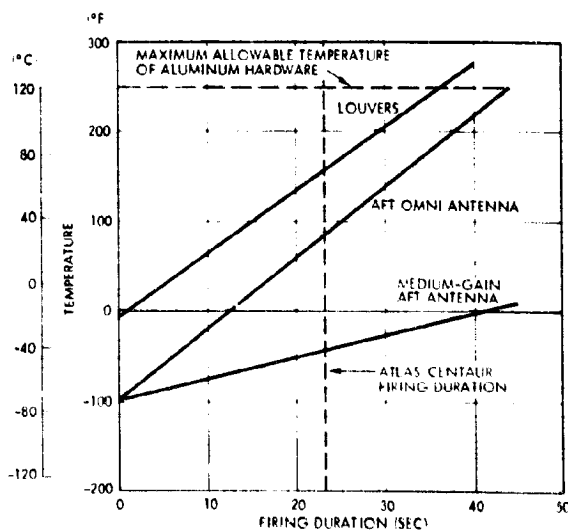
E VENUS ORBIT INSERTION SPACECRAFT TEMPERATURES FOLLOWING MOTOR IGNITION

COMPONENT AND STRUCTURE HEATING BY THE ENGINE WILL NOT BE EXCESSIVE DURING ORBIT INSERTION FIRING. PLATFORM MOUNTED ELECTRONIC COMPONENTS WILL EXHIBIT ONLY A SLIGHT TEMPERATURE RISE AND REMAIN WITHIN ACCEPTANCE LIMITS.



F TEMPERATURE RISE OF AFT-MOUNTED COMPONENTS DURING VENUS INSERTION MOTOR FIRING

AFT-LOCATED HARDWARE SUCH AS THE LOUVERS AND OMNI ANTENNA HEAT-UP DURING MOTOR FIRING. THE RATE OF TEMPERATURE RISE IS DEPENDENT UPON THE VIEW OF THE PLUME AND THE THERMAL CAPACITANCE OF THE EQUIPMENT. EXCESSIVE HEATING WILL NOT OCCUR DURING FIRING.



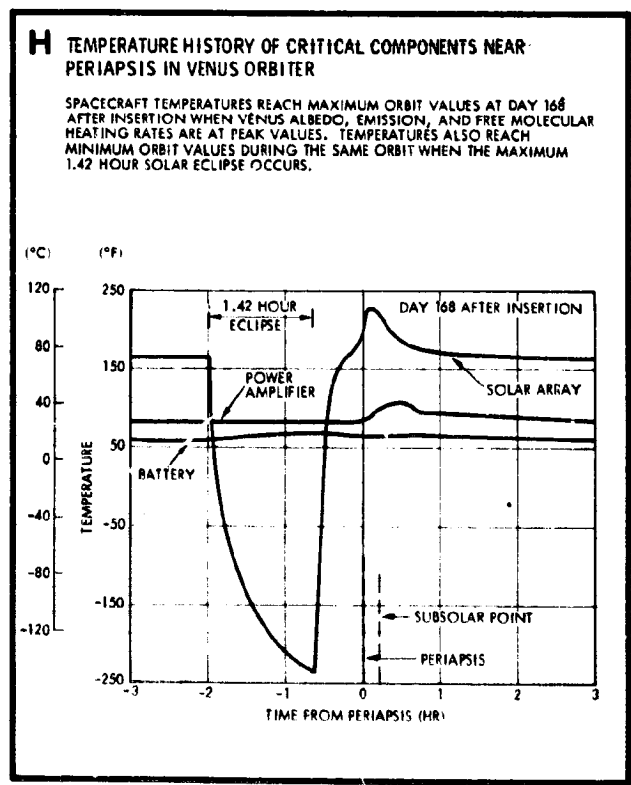
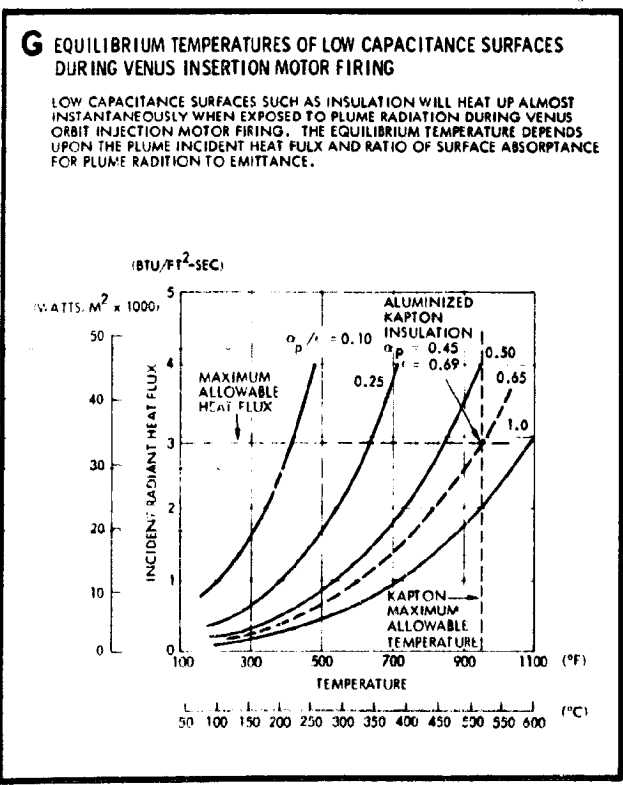
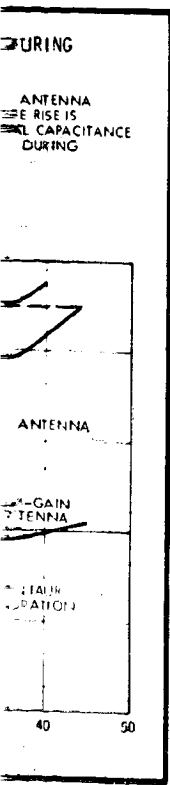
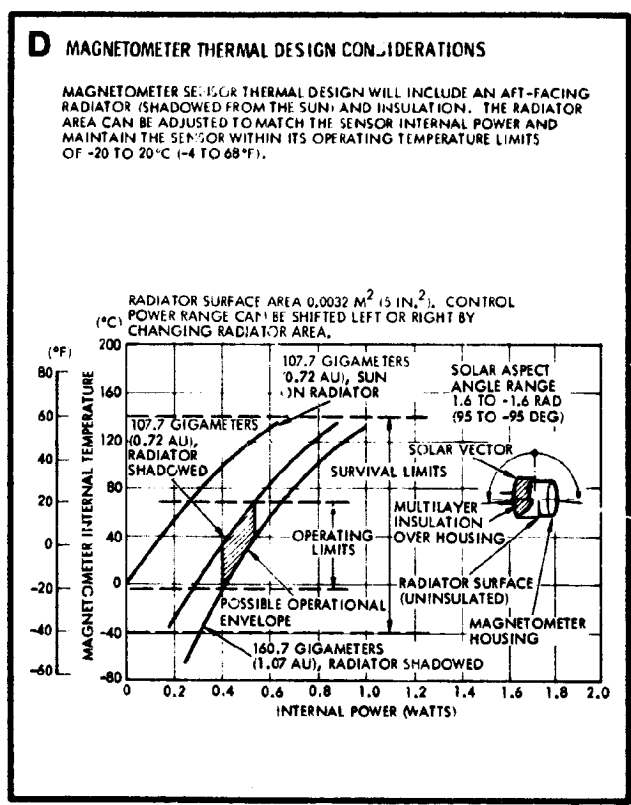
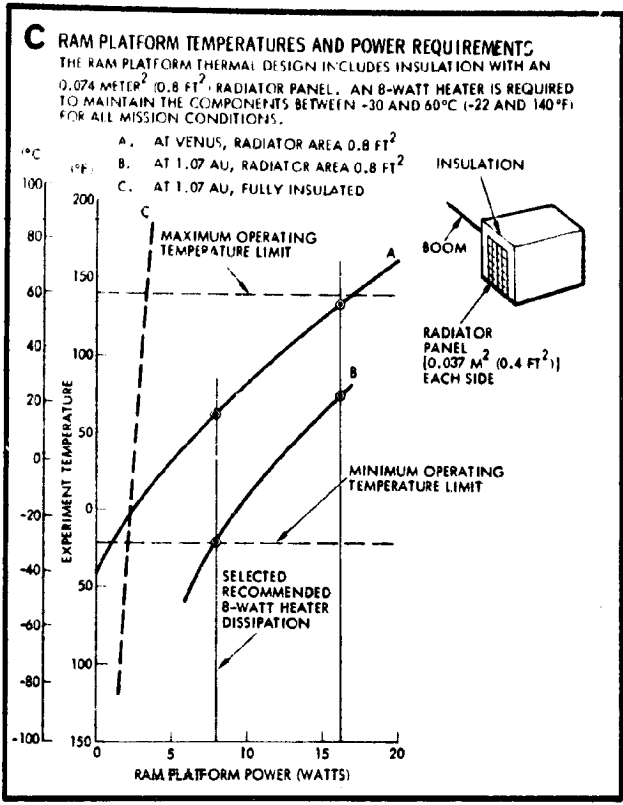
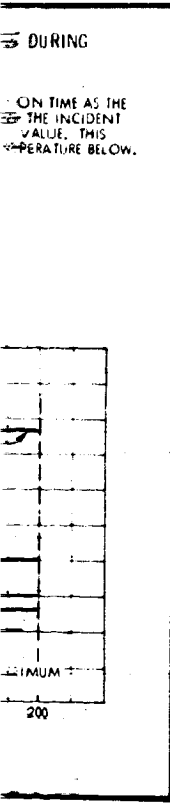


Figure 8.7-6. Preferred Atlas/Centaur Orbiter Spacecraft Thermal Performance

The magnetometer, IMU, and NMU are isolated experiments that require separate temperature control provisions. The IMU and NUM are located together on the ram platform and can be thermally controlled by providing an insulation enclosure around the experiments with 0.037 m^2 (0.4 ft^2) surface mirror radiator panels on either end. An 8-watt heater mounted on the ram platform is operated whenever the experiments are turned off. The operating temperature extremes are shown in Figure 8.7-6C. A fully insulated design (Curve C) would reduce the heater power requirement, but produce excessively high experiment temperature when the experiments are operated.

Typical magnetometer temperature levels that can be achieved in practice are presented in Figure 8.7-6D. These temperatures can be maintained within the magnetometer package by using a radiator surface in conjunction with unit internal power dissipation, possibly supplemented by an electric heater. The figure indicates that the experiments can, through proper design, such as locating radiator surfaces to limit sun exposure, provide acceptable magnetometer operating temperatures. However, the design will be sensitive to electrical lead losses, insulation shorting, and other physical considerations.

Positive temperature control of the Venus injection motor is achieved by mounting a 5-watt electric heater to the motor attachment flange. Excess solar array power is available prior to engine ignition and there is little impact in providing a heater. The heater is thermostatically controlled to compensate for the inherent inaccuracies in the ability to predict small heat losses out of the motor compartment.

Antenna distortion is not a severe constraint for this mission. However, it is desirable to reduce the overall antenna temperature variation so that dimensional change is not excessive. For a white antenna surface the temperature will be between -131°C (-204°F) and 71°C (160°F).

Firing of the solid rocket motor for Venus orbit insertion produces plume radiant heating of aft facing surfaces and internal heating by the nozzle and casing temperature increase. Figure 8.7-6G specifies the temperatures at which low capacitance surfaces, such as multilayer insulation sheets, will stabilize when heated by radiation from the aluminum particles in the motor plume. The figure indicates that, for the expected

heat flux value identified in Figure 8.7-6E, it will be necessary to use aluminized kapton material for the equipment platform aft-facing insulation assemblies. The rear surface of the cylinder closeout section which has a heat flux greater than the permissible $34\ 000\ \text{watts/m}^2$ ($3\ \text{BTU/ft}^2\text{-sec}$), will be constructed with the insulation attached to the inside of an aluminum collar. The aluminum collar will have sufficient thermal capacitance to limit the temperature rise in the area and protect the insulation from being damaged. Other aft facing aluminum surfaces, as shown in Figure 8.7-6F, will not be excessively heated by plume radiation. Heating within the spacecraft will also be maintained within acceptable levels by the central cylinder insulation. Figure 8.7-6E presents the soakback temperature response of the structure near the motor attachment and a typical electronic component mounted to the honeycomb platform. All temperatures are well within limits.

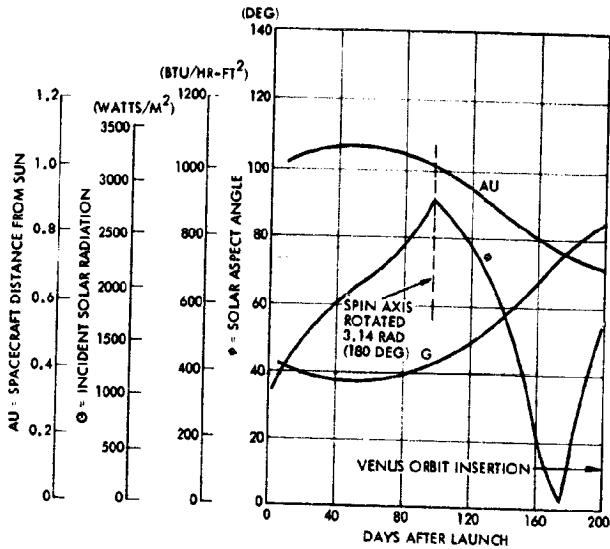
During the 24-hour Venus orbit the spacecraft can approach within 200 kilometers of the planet's surface. At these heights the spacecraft is exposed to planetary emission heating which, as shown in Figure 8.7-7G, is relatively small. After approximately 168 days in Venus orbit, the spacecraft is also subjected to reflected solar, or albedo heating. Figure 8.7-7G indicates that this heat is much greater than that produced by planetary emission. The effect of these combined Venus heat inputs on normal spacecraft operation at 106.96 gigameters (0.715 AU), as well as the maximum 1.4-hour eclipse that occurs at the same time, is shown in Figure 8.7-6H. It is in this period that the compartment interior reaches its peak temperature and the solar array is exposed to both its minimum and maximum mission temperatures.

Thermal Environment

Figure 8.7-7 presents the earth/Venus transit and Venus orbit thermal environment for the preferred Atlas/Centaur orbiter spacecraft. The on-stand and ascent environments are identical to those specified for the probe bus configuration in Figure 8.7-3. Figure 8.7-7A, H, B and C also identify the trajectory and solar aspect angle parameters for transit and Venus orbit operation of the earth-pointer spacecraft, as well as heat dissipations utilized in the design. It should be noted that the spacecraft will be flipped 3.14 radians (180 degrees) two times in the mission to maintain proper sun position for the solar array.

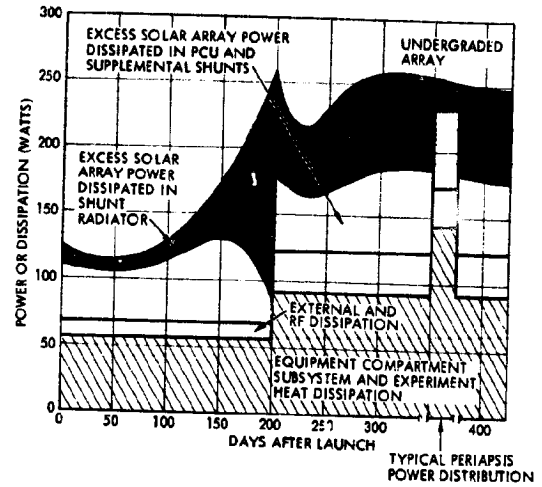
A ORBITER SPACECRAFT TRANSIT THERMAL PARAMETERS

THE SPACECRAFT SOLAR ASPECT ANGLE, INCIDENT SOLAR RADIATION INPUT, AND DISTANCE FROM THE SUN IMPACT THE THERMAL SYSTEM DESIGN. THE SPACECRAFT ELEMENT TEMPERATURES MUST BE MAINTAINED WITHIN ACCEPTANCE LIMITS WITH A SOLAR HEAT FLUX VARIATION OF 1160 TO 2260 WATTS/METER² (380 TO 840 BTU/HR-FT²)



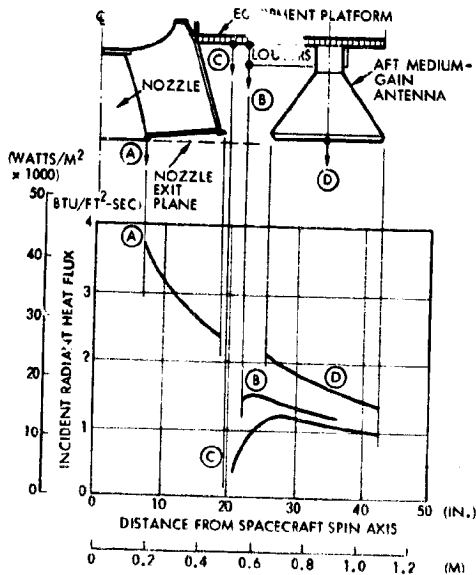
B ORBITER MISSION HEAT DISSIPATION PROFILE

A TYPICAL HEAT DISSIPATION HISTORY FOR VARIOUS ORBITER SPACECRAFT AREAS INDICATES THAT THE OVERALL MISSION HEAT DISSIPATION INCREASES NEAR VENUS AS MORE SOLAR ARRAY POWER BECOMES AVAILABLE. THIS HEAT DISSIPATION INCREASE IS ACCOMMODATED BY THE LOUVERS WHICH VARY THE HEAT REJECTION CAPABILITY OF THE EQUIPMENT COMPARTMENT



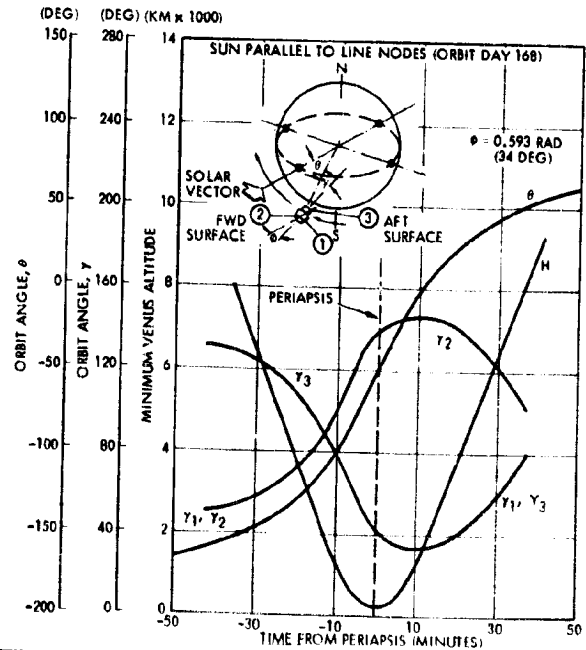
E INJECTION MOTOR PLUME INCIDENT RADIANT HEAT FLUX

THE AFT SURFACES OF THE ORBITER SPACECRAFT RECEIVE RADIANT HEATING FROM THE SOLID MOTOR PLUME FOR THE 23 SECONDS THAT THE ATLAS/CENTAUR MOTOR FIRES AT VENUS ORBIT INSERTION. CRITICAL SPACECRAFT SURFACES ARE POSITIONED TO REDUCE THE INCIDENT HEAT RATE TO ACCEPTABLE LEVELS CONSIDERING THE HEAT CAPACITY AND SURFACE ABSORPTANCE THE PLUME



F VENUS ORBIT ANGLE AND ALTITUDE PARAMETERS NEAR PERIAPSIS

WHEN THE SUN IS PARALLEL TO THE LINE OF NODES (ORBIT DAY 168), THE MOST SEVERE VENUS ALBEDO HEAT INPUT OCCURS. ORBIT ALTITUDE AND VEHICLE ORIENTATION ARE REQUIRED INPUTS TO HEAT INPUT CALCULATIONS



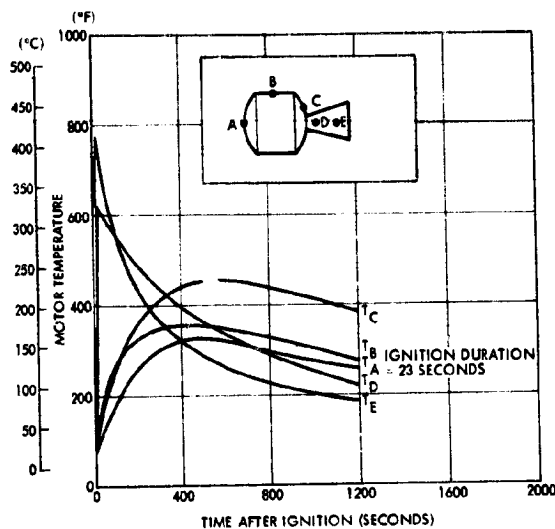
C COMPONENT HEAT DISSIPATIONS

SUBSYSTEM AND EXPERIMENT COMPONENTS ARE LOCATED SUCH THAT HEAT DISSIPATION IS DISTRIBUTED THROUGHOUT THE PLATFORM AREA. TOWERS ACCOMMODATE VARIATIONS IN DISSIPATION AND ARE LOCATED TO FURTHER EQUALIZE PLATFORM TEMPERATURES.

COMPONENT	HEAT DISSIPATION (WATTS)				
	LAUNCH	TRANSIT	ECLIPSE	PERIAPSIS	POST ECLIPSE
SCIENCE					
MAGNETOMETER	0.0	4.8	4.8	4.8	4.8
SOLAR WIND ANALYZER	0.0	0.0	6.0	6.0	6.0
ELECTRON TEMPERATURE PROBE	0.0	0.0	0.0	3.0	3.0
NEUTRAL MASS SPECTROMETER	0.0	0.0	14.4	14.4	14.4
ION MASS SPECTROMETER	0.0	0.0	2.4	2.4	2.4
UV SPECTROMETER	0.0	0.0	7.2	7.2	7.2
IR RADIOMETER	0.0	0.0	0	7.2	7.2
X-BAND OCCULTATION	0.0	0.0	14.4	14.4	14.4
RADAR ALTIMETER	0.0	0.0	0.0	43.2	0.0
DATA HANDLING					
DIGITAL TELEMETRY UNIT	3.9	3.9	3.9	3.9	3.9
DATA STORAGE UNIT	0.0	0.0	0.0	4.5	0.0
DIGITAL DECODER UNIT	0.3	0.3	0.3	0.3	0.3
COMMUNICATIONS					
S-BAND RECEIVERS	7.0	7.0	7.0	7.0	7.0
S-BAND TRANSMITTER DRIVER	3.5	3.5	3.5	3.5	3.5
S-BAND POWER AMPLIFIER	16.5	16.5	16.5	16.5	16.5
ACS PROPULSION					
CONTROL ELECTRONICS ASSEMBLY AND SUN SENSOR	1.7	1.7	1.7	1.7	1.7
PRESSURE TRANSDUCER	0.4	0.4	0.4	0.4	0.4
ELECTRICAL POWER AND CONTROL					
PCU ELECTRONICS	4.0	4.0	4.0	4.0	4.0
COMMAND DISTRIBUTION UNIT	2.1	2.1	2.1	2.1	2.1
CONVERTER	5.1	5.1	5.1	8.1	5.1
BATTERY	0.0	4.2	22.0	0.0	6.5

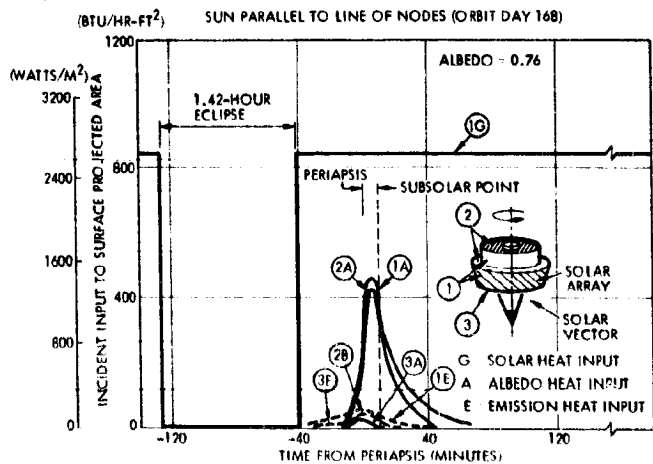
D INJECTION MOTOR CASE TEMPERATURE HISTORY AFTER IGNITION

MOTOR CASING TEMPERATURE RISE DURING VENUS ORBIT INSERTION CAN HEAT THE ADJACENT ORBITER STRUCTURE. MOTOR MOUNTING IS DESIGNED TO MINIMIZE THE EFFECTS OF MOTOR HEATING TO SENSITIVE SPACECRAFT ELEMENTS



G SOLAR AND VENUS HEAT INPUTS NEAR PERIAPSIS

MAXIMUM ORBITER SPACECRAFT TEMPERATURES OCCUR NEAR VENUS PERIAPSIS WHILE MINIMUM TEMPERATURES FOR OTHER SPACECRAFT ELEMENTS EXCEPT COMPONENTS IN THE EQUIPMENT COMPARTMENT OCCUR AT THE END OF THE 1.42-HOUR MAXIMUM ECLIPSE. SOLAR ASPECT ANGLE IS 0.59 RADIAN (34 DEGREES) AT THIS TIME IN THE MISSION



H VENUS ORBIT PERIAPSIS ALTITUDE, SOLAR ASPECT ANGLE, AND ECLIPSE DURATION

DAY 168 REPRESENTS THE MOST SEVERE THERMAL DESIGN CONDITION DURING VENUS ORBIT. ON THIS DAY, THE ORBITER SPACECRAFT IS EXPOSED TO THE MAXIMUM ECLIPSE (1.42 HOURS) AND THEN SUBJECTED WITHIN THE HOUR TO THE WORST ALBEDO HEATING CONDITION

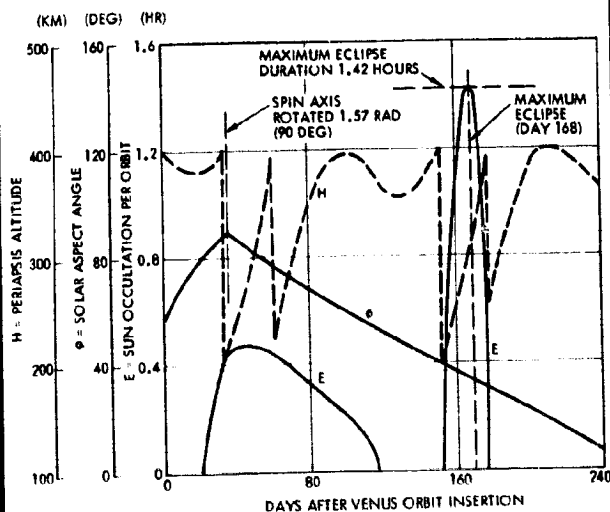


Figure 8.7-7. Preferred Atlas/Centaur Orbiter Thermal Environment

Solid particle plume radiant heat flux rates and solid motor case temperature histories for Venus orbit insertion motor firing are shown in Figure 8.7-7D and E. Maximum albedo and planetary emission heat rates that will be encountered in orbit for a Venus albedo of 0.76 are also defined in Figure 8.7-7F and G. The maximum heating rates occur for a few days approximately 168 days after orbit insertion. The occurrence period is shown, along with the design periapsis altitude variation, in Figure 8.7-7H.

Thermal Analysis Techniques

The preferred Atlas/Centaur analytical computer model is presented in Figure 8.7-8. Thruster heater requirements are identical with those determined for the probe bus spacecraft.

8.7.3 Thor/Delta Configurations

As with the Atlas/Centaur configurations common hardware/surface coatings are used wherever possible for the Thor/Delta probe bus and orbiter spacecraft designs. Descriptions of two Thor/Delta configurations appropriate to the Version III science payload are presented below. Similar Atlas/Centaur designs were also analyzed in detail to select the equivalent thermal hardware.

8.7.3.1 Probe Bus Spacecraft, 1977 Launch T/D III

System Description

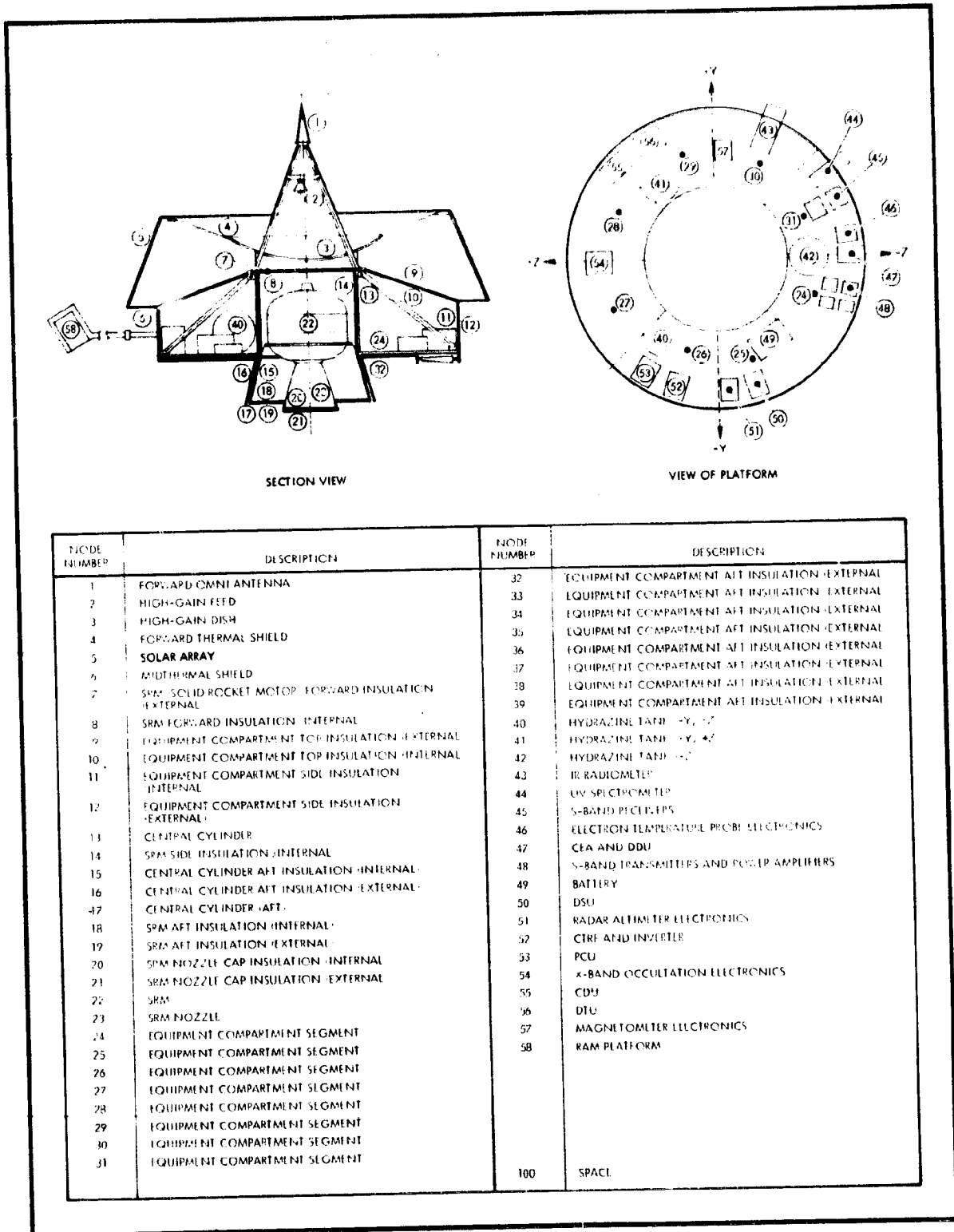
Figure 8.7-9 describes the design Thor/Delta probe bus thermal control system configuration. The description uses the previously presented Atlas/Centaur format, and presents both Thor/Delta and Atlas/Centaur Version III louver area requirements.

Thermal Control System Performance

Predicted mission operational temperatures are presented in Figure 8.7-10 for the Thor/Delta probe bus configuration. All spacecraft temperatures are maintained within acceptance limits by the reduced thermal control system design.

Thermal Environment

The Thor/Delta prelaunch and ascent environment is much different than that experienced on the Atlas/Centaur launch vehicle. Figure



AN ANALYTICAL THERMAL MODEL WAS CONSTRUCTED TO CONFIRM THE ADEQUACY OF THE SELECTED ORBITER THERMAL CONTROL DESIGN.

Figure 8.7-8 Preferred Atlas/Centaur Orbiter Spacecraft Thermal Model

8.7-11A defines the spacecraft prelaunch thermal environment for the Thor/Delta fairing. Adequate on-stand spacecraft temperature control is provided in the Thor/Delta design by supplying approximately 68 kg/min (150 lb/min) of conditioned air into the fairing. The air supply is controlled between 10°C (50°F) and 32°C (90°F) with a relative humidity less than 50 percent.

Figure 8.7-11B also specifies ascent temperature histories for three points on the standard Thor/Delta fairing. Since excessively high fairing temperatures exist adjacent to the spacecraft during ascent, insulation will be required on the inside surface of the fairing to prevent local shroud surfaces from exceeding 135°C (175°F). The free-molecular heating rate that occurs after fairing jettison is included in the figure. Fairing jettison is delayed until the free-molecular heating is below 1140 watts/meter² (0.1 BTU/ft²-s) to prevent low heat capacity spacecraft surfaces such as solar cells, silver teflon thermal shields, and aluminized insulation from exceeding maximum temperature limits.

For the Thor/Delta configuration, low heat capacitance surfaces that face aft can be heated by third-stage engine firing. Figure 8.7-11C describes the engine case temperature response for the 144-second period following ignition until the spacecraft separates from the boost vehicle. Temperature increases are small, however, because the engine is located a significant distance from the sensitive surfaces.

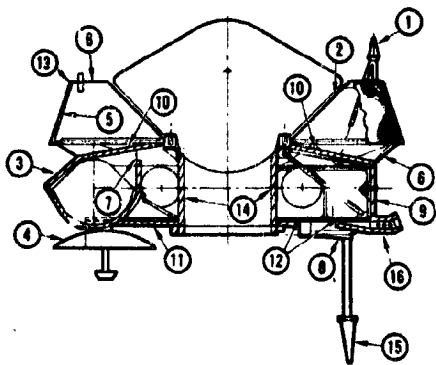
The probe bus thermal environment encountered during transit from earth to Venus is provided in Figure 8.7-11D. Representative component and system power dissipations are also presented in Figures 8.7-11E and F.

Thermal Analysis Techniques

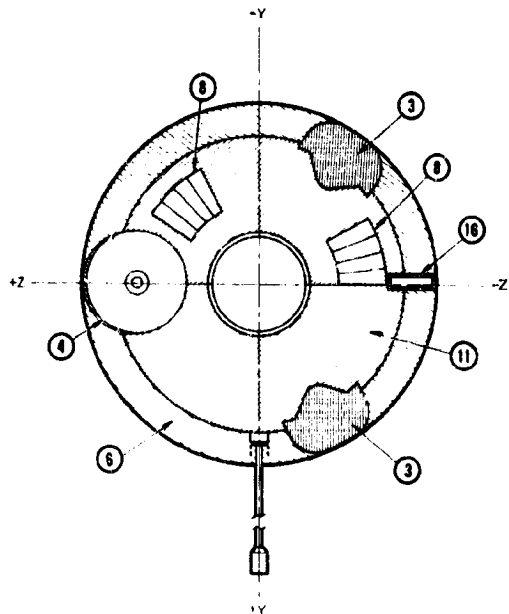
All Thor/Delta probe bus temperatures were calculated using a computer model similar to that used for the Atlas/Centaur configuration. Thermal environment, dimensional, and physical property differences were accounted for in the analysis. The thruster computer model was identical in both the Thor/delta and Atlas/Centaur configurations. An equivalent Atlas/Centaur Version III spacecraft was also studied.

THE PROBE BUS USES RELIABLE AND FLIGHT PROVEN HARDWARE. LOCATIONS OF THE HARDWARE ARE KEYED TO THE ADJACENT TABLE FOR DETAILED DESCRIPTION.

SECTION VIEW



VIEW OF AFT END



I.D. NO.	NAME OF ITEM	DESCRIPTION OF HARDWARE
1	FORWARD OMNI ANTENNA THERMAL COATING	3-MIL COAT OF S-13G WHITE PAINT ON EXTERNAL SURFACES
2	LARGE PROBE CLOSEOUT	ONE OUTER LAYER OF 2-MIL SILVER TEFLON (SILVER SIDE FACI TO ONE 2-MIL INNER LAYER OF CLEAR MYLAR
3	SMALL PROBE INSULATION COVER	ONE 10-MIL FIBERGLASS JETTISONABLE COVER FOR EACH PROBE INSULATED WITH 22 LAYERS OF ALUMINIZED MYLAR SANDWIC 2-MIL ALUMINIZED KAPTON AND ONE INNER 2-MIL ALUMINI (ALUMINIZED SURFACES FACE INWARD). SIMILAR INSULATION MYLAR FACE SHEETS INSULATES EACH PROBE FROM THE SPACEC AT THERMAL WINDOW PENETRATIONS, ITEM 7 K/X - SEE FIGURE 8.7-4
4	MEDIUM-GAIN ANTENNA COATING	BARE FIBERGLASS CONVEX SURFACE; BARE ALUMINUM CONCA
5	SOLAR ARRAY SUBSTRATE THERMAL COATING	3-MIL COAT OF 3M BLACK VELVET PAINT ON BACK SURFACE C
6	FORWARD AND MIDSHIELD	ONE OUTER LAYER OF 2-MIL SILVER TEFLON (SILVER SIDE FACI TO ONE 2-MIL INNER LAYER OF CLEAR MYLAR
7	SMALL PROBE THERMAL WINDOW	ONE 2-MIL, 0.0186M ² (0.2 FT ²) SHEET OF BLACKENED KAPTON PROBE AND THE EQUIPMENT COMPARTMENT
8	BIMETAL ACTUATED LOUVERS	TOTAL BLADE AREA = 0.22 M ² (2.34 FT ²); A/C, 0.15 M ² (1.56 FT ²) CLOSED EFFECTIVE EMITTANCE = 0.20 FULL CLOSED AT 4°C (40°F) OPEN EFFECTIVE EMITTANCE = 0.74 FULL OPEN AT 29°C (85°F) 3-MIL COATS OF Z-93 WHITE PAINT ON PLATFORM UNDER LOU
9	EQUIPMENT COMPARTMENT SIDE INSULATION	22 LAYERS OF 1/4-MIL ALUMINIZED MYLAR SANDWICHED BETW 2-MIL ALUMINIZED KAPTON AND ONE INNER 2-MIL ALUMINI SHEET (ALL ALUMINIZED SURFACES EXCEPT INSIDE COVER SHEE K/X, SEE FIGURE 8.7-4
10	EQUIPMENT COMPARTMENT TOP INSULATION	22 LAYERS OF 1/4-MIL ALUMINIZED MYLAR SANDWICHED BETW ALUMINIZED MYLAR COVER SHEETS (ALL ALUMINIZED SURFACE COVER SHEET FACE INWARD) K/X, SEE FIGURE 8.7-4
11	EQUIPMENT COMPARTMENT AFT INSULATION	22 LAYERS OF 1/4-MIL ALUMINIZED MYLAR SANDWICHED BETW 2-MIL ALUMINIZED KAPTON AND ONE INNER 2-MIL ALUMINI COVER SHEETS (ALUMINIZED SURFACE FACE FORWARD) K/X, SEE FIGURE 8.7-4
12	EQUIPMENT COMPARTMENT RADIATIVE AND CONDUCTIVE THERMAL COUPLING REQUIREMENTS	3-MIL COATING OF 3M BLACK VELVET PAINT ON EQUIPMENT DISSIPATING EQUIPMENT BARE METAL SURFACE ON CENTRAL COLUMN AND HYDRAZINE DUCTIVELY COUPLED TO MOUNTING PLATFORM AND ISOLATE PROVIDE GOOD CONDUCTIVE THERMAL COUPLING BETWEEN COMPONENTS (I.E., TRANSMITTER) AND PLATFORM WITH RTV MATERIAL. H > 142 W/M ² -°C (25 BTU/HR-FT ² -°F)
13	RCS THRUSTER VALVE BODY AND SUPPLY LINE INSULATION, VALVE AND CATALYST BED HEATERS, AND THRUSTER ISOLATION PROVISIONS	LOWER ΔV THRUSTER INSULATED COMPLETELY WITH HIGH TEMP FOIL ALL FUEL LINES ARE COPPER PLATED. LINES EXTERNAL TO THE MENT INSULATED WITH 10 LAYERS OF NRC-L INSULATION K/X = 0.056 W/M ² -°C (0.01 BTU/HR-FT ² -°F) DUAL RANGE THERMOSTATICALLY-CONTROLLED HEATERS ON WITH GROUND CONTROL BACKUP. PRIMARY HEATER CONTROL 18°C (65°F). BACKUP RANGE 7°C (45°F) TO 13°C (55°F). HEAT 5.2 WATTS THRUSTERS MOUNTED TO STRUCTURES WITH TITANIUM STANDC
14	CENTRAL CYLINDER INSULATION	22 LAYERS OF 1/4-MIL ALUMINIZED MYLAR SANDWICHED BETW ALUMINIZED MYLAR COVER SHEETS (MYLAR SURFACES FACE O K/X - SEE FIGURE 8.7-4
15	AFT OMNI ANTENNA THERMAL COATING	3-MIL COAT OF S-13G WHITE PAINT ON EXTERNAL SURFACES
16	SUN SENSOR INSULATION	22 LAYERS OF 1/4-MIL ALUMINIZED MYLAR SANDWICHED BETW ALUMINIZED KAPTON AND ONE INNER 2-MIL ALUMINIZED M (ALUMINIZED SURFACES FACE INWARD) K/X - SEE FIGURE 8.7-4

DESCRIPTION OF HARDWARE	PURPOSE	SURFACE THERMAL PROPERTIES					
		INSIDE			OUTSIDE		
		"NEW	"DEC	"	"NEW	"DEC	"
WHITE PAINT ON EXTERNAL SURFACES OF OMNI ANTENNA	MINIMIZE ABSORBED SOLAR HEAT INPUT TO REDUCE VARIATION IN TEMPERATURE DURING MISSION. LOCATION ENSURES SOLAR HEATING TO LIMIT MINIMUM TEMPERATURES FOR ALL SOLAR ASPECT ANGLES ENCOUNTERED	--	--	--	0.24	0.39	0.88
2-MIL SILVER TEFLON (SILVER SIDE FACING INWARD) LAMINATED COVER OF CLEAR MYLAR	SHIELD BACKSIDE OF SOLAR ARRAY FROM DIRECT SOLAR IMPINGEMENT AFTER LARGE PROBE RELEASE	--	--	0.66	0.08	0.12	0.90
JETTISONABLE COVER FOR EACH PROBE. EXTERNAL SURFACE CONSISTS OF ALUMINIZED MYLAR SANDWICHED BETWEEN ONE OUTER COVER SHEET AND ONE INNER 2-MIL ALUMINIZED MYLAR COVER SHEET (FACE INWARD). SIMILAR INSULATION BLANKET WITH 2-MIL ALUMINIZED MYLAR SANDWICHED BETWEEN TWO 2-MIL ALUMINIZED MYLAR COVER SHEETS (ALL ALUMINIZED SURFACES EXCEPT AIR EXPOSURE SURFACES, ITEM 7)	MINIMIZE SMALL PROBE HEAT LEAKS DURING CRUISE TO MAINTAIN PROBE TEMPERATURES ABOVE MINIMUM LIMITS	--	--	0.90	0.45	0.48	0.69
BLACK VELVET PAINT ON BACK SURFACE OF SUBSTRATE	MAXIMIZE RADIATION COUPLING FROM ANTENNA TO PLATFORM INSULATION. MINIMIZE HEAT LOSS TO SPACE FROM CONCAVE SURFACE	0.70	0.70	0.85	0.15	0.15	0.05
BLACK VELVET PAINT ON BACK SURFACE OF SUBSTRATE	MAXIMIZE RADIANT HEAT TRANSFER FROM BACK SURFACE OF SOLAR ARRAY	--	--	0.90	0.80	0.80	0.80
2-MIL SILVER TEFLON (SILVER SIDE FACING INWARD) LAMINATED COVER OF CLEAR MYLAR	SHIELD BACKSIDE OF SOLAR ARRAY FROM DIRECT SOLAR IMPINGEMENT. PROVIDE LOW TEMPERATURE BOUNDARY (LOW α/ϵ) TO MAXIMIZE HEAT TRANSFER FROM BACK SURFACE OF SOLAR ARRAY	--	--	0.66	0.08	0.12	0.66
2 FT ² SHEET OF BLACKENED KAPTON BETWEEN EACH SMALL EQUIPMENT COMPARTMENT	COUPLES SMALL PROBES TO EQUIPMENT COMPARTMENT TO CONTROL PROBE TEMPERATURE VARIATION DURING TRANSIT. LOCATION OF WINDOWS PREVENT DIRECT SOLAR IMPINGEMENT	--	--	0.90	--	--	0.90
2 M ² (2.34 FT ² A/C, 0.15 M ² (1.56 FT ²) T/D) WINDOW. COEFFICIENT OF TRANSMITTANCE = 0.20 FULL CLOSED AT 4°C (40°F). COEFFICIENT OF TRANSMITTANCE = 0.74 FULL OPEN AT 29°C (85°F)	CONTROL EQUIPMENT COMPARTMENT HEAT LEAKS TO OFFSET THE VARIATION IN EQUIPMENT AND ENVIRONMENTAL HEAT INPUT EXPERIENCED DURING THE MISSION TO MAINTAIN COMPONENT TEMPERATURES WITHIN ACCEPTABLE LIMITS	--	--	--	0.50	0.50	0.20
WHITE PAINT ON PLATFORM UNDER LOUVERS							0.74
ALUMINIZED MYLAR SANDWICHED BETWEEN ONE OUTER COVER SHEET AND ONE INNER 2-MIL ALUMINIZED MYLAR COVER SHEET (SURFACES EXCEPT INSIDE COVER SHEET FACE INWARD)	MINIMIZE SOLAR HEAT LEAK INTO AND UNCONTROLLED HEAT LEAK OUT OF THE EQUIPMENT COMPARTMENT. STABLE ALUMINIZED KAPTON MINIMIZES EXTERNAL SURFACE PROPERTY DEGRADATION	--	--	0.69	0.45	0.48	0.69
ALUMINIZED MYLAR SANDWICHED BETWEEN TWO 2-MIL ALUMINIZED MYLAR COVER SHEETS (ALL ALUMINIZED SURFACES EXCEPT AIR EXPOSURE SURFACES)	MINIMIZE UNCONTROLLED HEAT LEAKS INTO AND OUT OF THE EQUIPMENT COMPARTMENT AND THERMALLY DECOUPLE COMPARTMENT FROM SOLAR ARRAY	--	--	0.69	--	--	0.69
ALUMINIZED MYLAR SANDWICHED BETWEEN ONE OUTER COVER SHEET AND ONE INNER 2-MIL ALUMINIZED MYLAR COVER SHEET (EXPOSED SURFACE FACE FORWARD)	MINIMIZE UNCONTROLLED HEAT LEAKS OUT OF THE EQUIPMENT COMPARTMENT. STABLE ALUMINIZED KAPTON MINIMIZES EXTERNAL SURFACE PROPERTY DEGRADATION	--	--	--	0.45	0.48	0.69
BLACK VELVET PAINT ON EQUIPMENT PLATFORM AND HEAT DISSIPATING COMPONENTS	EQUALIZE TEMPERATURE GRADIENTS WITHIN EQUIPMENT COMPARTMENT BY MAXIMIZING RADIATIVE THERMAL COUPLING BETWEEN STRUCTURE AND HEAT DISSIPATING COMPONENTS	--	--	--	--	--	0.90
CENTRAL COLUMN AND HYDRAZINE TANKS. TANKS COUPLING TO PLATFORM AND ISOLATED FROM COLUMN	THERMALLY DECOUPLE ZERO HEAT DISSIPATING COMPONENT FROM SURROUNDING TO MINIMIZE TEMPERATURE VARIATIONS DURING TRANSIENT ENVIRONMENTAL CONDITIONS	--	--	--	--	--	<0.10
POSITIVE THERMAL COUPLING BETWEEN HIGH HEAT DENSITY COMPONENTS (SMITTER) AND PLATFORM WITH RTV INTERFACE FILLER (25 BTU/HR-FT ² -°F)	MINIMIZE COMPONENT TO EQUIPMENT PLATFORM TEMPERATURE GRADIENTS TO MINIMIZE MAXIMUM COMPONENT TEMPERATURE ABOVE SURROUNDINGS	--	--	--	--	--	--
PLATED COMPLETELY WITH HIGH TEMPERATURE MOLYBDENUM	MINIMIZE UNCONTROLLED THRUSTER HEAT LEAK TO SPACE	--	--	--	0.12	0.12	0.05
INSULATED LINES EXTERNAL TO THE EQUIPMENT COMPARTMENT WITH LAYERS OF NiC-L INSULATION (25 BTU/HR-FT ² -°F)	MINIMIZE TEMPERATURE GRADIENT IN SUPPLY LINES AND HEAT LEAKS INTO OR OUT OF THRUSTER AND LINES	--	--	--	--	--	0.05
HEATERS ON VALVE AND CATALYST BED BACKUP. PRIMARY HEATER CONTROL RANGE 13°C (55°F) TO 13°C (55°F). HEATER POWER REQUIREMENT	MAINTAINS THRUSTER AND SUPPLY LINE TEMPERATURES ABOVE MINIMUM TEMPERATURE LIMITS						
STRUCTURES WITH TITANIUM STANDOFFS	ISOLATES THRUSTER FROM STRUCTURE TO MINIMIZE HEATER POWER REQUIREMENT						
ALUMINIZED MYLAR SANDWICHED BETWEEN TWO 2-MIL ALUMINIZED MYLAR COVER SHEETS (MYLAR SURFACES FACE OUTWARD)	MINIMIZES UNCONTROLLED HEAT LEAKS INTO AND OUT OF THE EQUIPMENT COMPARTMENT	--	--	0.69	--	--	0.69
WHITE PAINT ON EXTERNAL SURFACES OF OMNI ANTENNA	MINIMIZE ABSORBED HEAT INPUT TO REDUCE VARIATION IN TEMPERATURE DURING MISSION	--	--	--	0.24	0.31	0.88
ALUMINIZED MYLAR SANDWICHED BETWEEN ONE OUTER 2-MIL ALUMINIZED MYLAR COVER SHEET AND ONE INNER 2-MIL ALUMINIZED MYLAR COVER SHEET (FACE INWARD)	MINIMIZE SOLAR HEAT LEAK INTO AND UNCONTROLLED HEAT LEAKS OUT OF THE SENSOR ASSEMBLY. STABLE ALUMINIZED KAPTON MINIMIZES EXTERNAL SURFACE PROPERTY DEGRADATION	--	--	--	0.45	0.48	0.69

Figure 8.7-9. Thor/Delta Bus Spacecraft Thermal Control System Description

A COMPONENT TEMPERATURE CONTROL CAPABILITY VERSUS TEMPERATURE REQUIREMENTS

PROBE SPACECRAFT TEMPERATURE PREDICTIONS INDICATE THAT THE SELECTED THERMAL CONTROL DESIGN CAN SATISFY ALL TEMPERATURE REQUIREMENTS WITH MARGIN.

SUB-SYSTEM AND SCIENCE COMPONENTS	PREDICTED TEMPERATURES		ACCEPTABLE OPERATING TEMPERATURE LIMITS	
	MINIMUM	MAXIMUM	MINIMUM	MAXIMUM
	(°C)	(°F)	(°C)	(°F)
COMMUNICATIONS				
MEDIUM-GAIN ANTENNA	-94 (-135)	32 (90)	-157 (-250)	93 (200)
CANDID ANTENNA	-64 (-120)	31 (75)	-145 (-230)	75 (200)
S-BAND TRANSMITTERS	7 (45)	41 (105)	4 (40)	52 (125)
POWER AMPLIFIER	7 (45)	41 (105)	4 (40)	52 (125)
S-BAND RECEIVERS	7 (45)	36 (97)	-4 (25)	43 (110)
DATA HANDLING				
DTU	7 (45)	26 (78)	-7 (20)	41 (105)
DDU	7 (45)	16 (61)	-7 (20)	41 (105)
ELECTRICAL POWER				
BATTERY	7 (45)	22 (72)	-1 (30)	29 (85)
PCU	7 (45)	33 (92)	20 (-4)	65 (149)
DC-DC CONVERTER	7 (45)	21 (70)	-18 (0)	49 (120)
SHUNT RADIATOR	-94 (-137)	132 (270)	-157 (-250)	132 (270)
SOLAR ARRAY	-101 (-150)	58 (137)	-143 (-225)	102 (215)
CDU	7 (45)	28 (83)	-7 (20)	41 (105)
ACS PROPULSION				
CEA	7 (45)	15 (61)	-7 (20)	41 (105)
SUN SENSOR	7 (20)	52 (125)	15 (5)	60 (140)
THRUSTER VALVE BODIES	13 (55)	82 (180)	13 (55)	93 (200)
HYDRAZINE LINES	4 (40)	82 (180)	4 (40)	82 (180)
HYDRAZINE TANKS	6 (43)	24 (75)	4 (40)	43 (110)
SCIENCE				
MAGNETOMETER ELECTRONICS	7 (45)	31 (88)	0 (32)	60 (140)
ION MASS SPECTROMETER	-12 (10)	49 (120)	-30 (-22)	60 (140)
UV FLUORESCENCE	7 (45)	24 (75)	-30 (-22)	40 (104)
ELECTRON TEMPERATURE PROBE ELECTRONICS	7 (45)	32 (89)	4 (40)	43 (110)
NEUTRAL MASS SPECTROMETER	-9 (15)	57 (135)	-30 (-22)	60 (140)
LARGE PROBE PAYLOAD	-7 (20)	28 (82)	-18 (0)	29 (85)
SMALL PROBE PAYLOAD	-15 (5)	27 (80)	-18 (0)	29 (85)

B PREDICTED TEMPERATURES DURING EARTH-VENUS TRANSIT

SPACECRAFT COMPONENT TEMPERATURES INCREASE WITH MISSION TIME AS INCIDENT SOLAR HEATING AND EQUIPMENT HEAT DISSIPATION NEARLY DOUBLE FROM NEAR-EARTH VALUES.

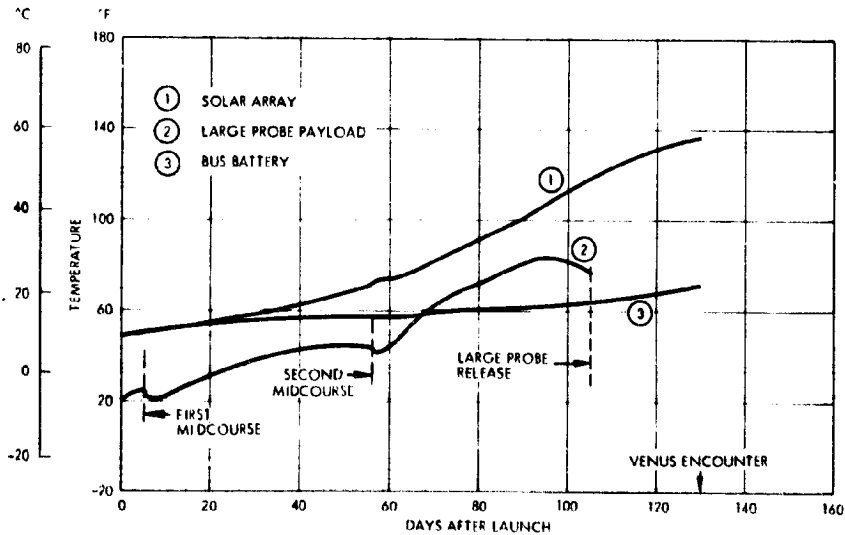
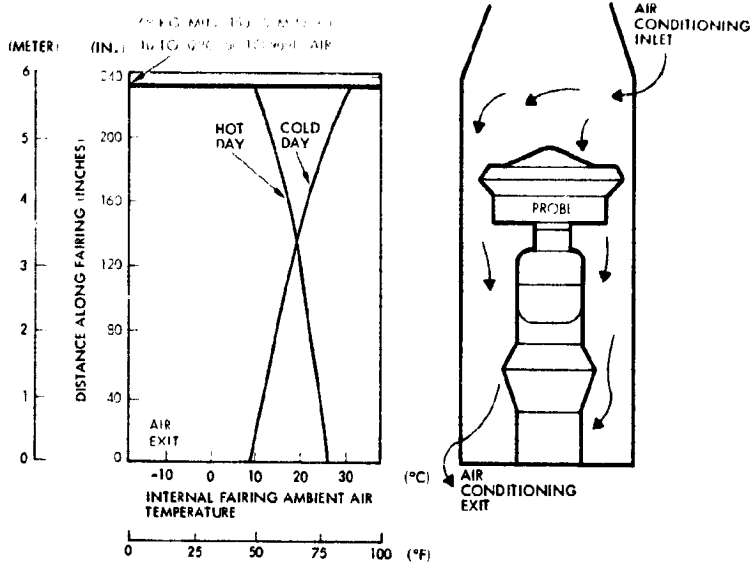


Figure 8.7-10. Thor/Delta Probe Bus Spacecraft Thermal Performance

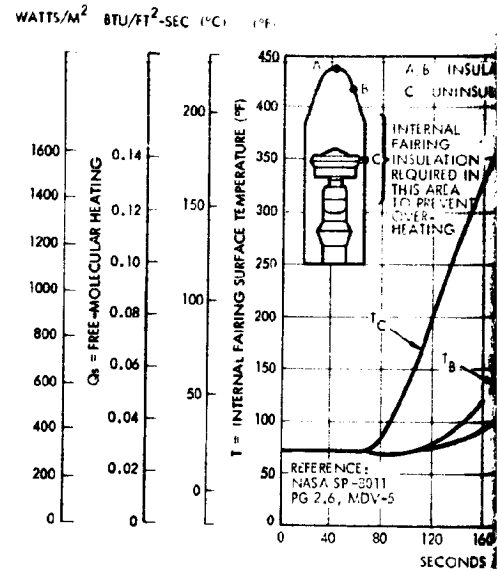
A TYPICAL FAIRING INTERNAL AMBIENT AIR TEMPERATURE PROFILE PRIOR TO LAUNCH

APPROXIMATELY 2000 LBS OF AIR IS SUPPLIED TO THE FAIRING AND REMOVED BY CONTROLLABLE AIR EXITS TO MAINTAIN SPACECRAFT TEMPERATURES WITHIN APPROXIMATELY 20°F TO 30°F. AIR SUPPLY TEMPERATURES RANGE FROM 10°C TO 20°C WITH AIR FLOW CONTROLLABILITY BEING 10 PERCENT.



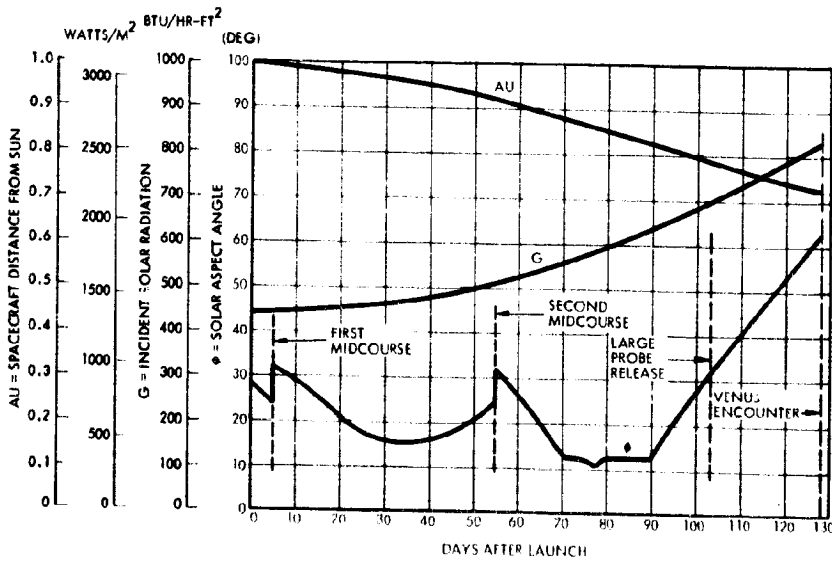
B TYPICAL UNINSULATED FAIRING TEMPERATURES AND STAGNATION MOLECULAR HEATING DURING ASCENT

SPACECRAFT TEMPERATURES DURING ASCENT ARE MAINTAINED TO 20°C TO 30°C BY CONTROLLABLE AIR EXITS TO MAINTAIN SPACECRAFT TEMPERATURES WITHIN APPROXIMATELY 20°F TO 30°F. AIR SUPPLY TEMPERATURES RANGE FROM 10°C TO 20°C WITH AIR FLOW CONTROLLABILITY BEING 10 PERCENT.



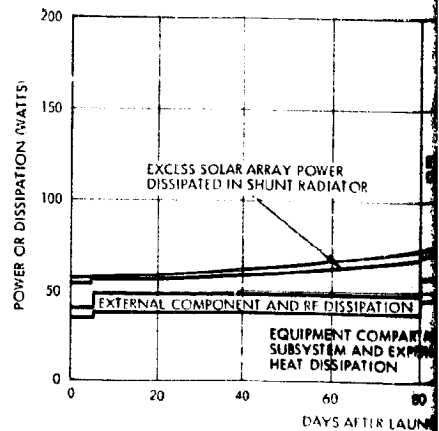
D PROBE SPACECRAFT TRANSIT THERMAL PARAMETERS

THE PROBE SPACECRAFT SOLAR ASPECT ANGLE IS SELECTED TO MAINTAIN THE SUN ON THE LARGE PROBE THROUGHOUT THE MISSION. A HEAT FLUX VARIATION OF 1330 TO 2660 WATTS/METER² (430 TO 840 BTU/HR-FT²) WILL OCCUR DURING TRANSIT.



E PROBE SPACECRAFT MISSION HEAT DISSIPATING PROFILE

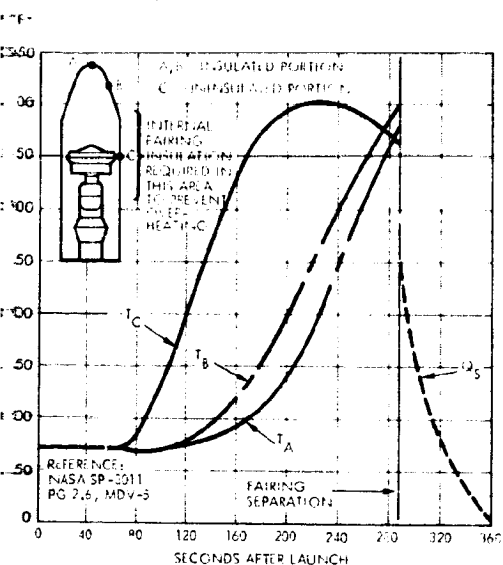
A TYPICAL HEAT DISSIPATION HISTORY FOR VARIOUS PROBE SPACESHUTTLES IS SHOWN. THAT THE OVERALL MISSION HEAT DISSIPATION INCREASES AS THE MISSION PROGRESSES. THE HEAT DISSIPATION IS CONTROLLED BY THE LOUVERS WHICH VARY THE HEAT REJECTION CAPABILITY OF THE COMPARTMENT.



FOLDOUT FRAME

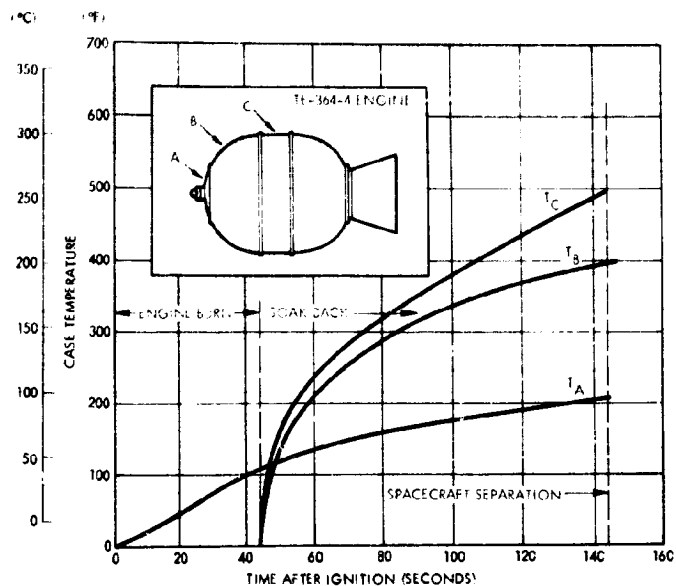
TEMPERATURES AND STAGNATION FREE-STREAM

TEMPERATURES AND STAGNATION FREE-STREAM VELOCITY FOR THE THIRD-STAGE ENGINE CASING FOR 145 SECONDS AFTER IGNITION, 100 SECONDS AFTER THIRD-STAGE SEPARATION. SPECIAL PROTECTIVE COATINGS ON THE ENGINE CASING SURFACE ARE NOT REQUIRED BECAUSE THE HEAT LOAD IS LOW.



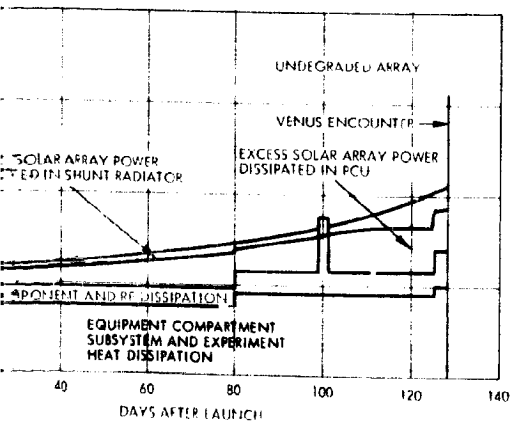
C TYPICAL THIRD-STAGE ENGINE TEMPERATURE HISTORY AFTER IGNITION

TEMPERATURE HISTORY FOR THE THIRD-STAGE ENGINE CASING FOR 145 SECONDS AFTER IGNITION, 100 SECONDS AFTER THIRD-STAGE SEPARATION. SPECIAL PROTECTIVE COATINGS ON THE ENGINE CASING SURFACE ARE NOT REQUIRED BECAUSE THE HEAT LOAD IS LOW.



ION HEAT DISSIPATING PROFILE

TEMPERATURE HISTORY FOR VARIOUS PROBE SPACECRAFT APAS INDICATES HEAT DISSIPATION INCREASES NEAR VENUS AS MORE SOLAR RADIATION IS RECEIVED. THIS HEAT DISSIPATION INCREASE IS ACCOMMODATED BY THE HEAT REJECTION CAPABILITY OF THE EQUIPMENT.



F COMPONENT HEAT DISSIPATIONS

SUBSYSTEM AND EXPERIMENT COMPONENTS ARE LOCATED SUCH THAT HEAT DISSIPATION IS DISTRIBUTED THROUGHOUT THE PLATFORM AREA. LOUVERS ACCOMMODATE VARIATIONS IN HEAT DISSIPATION AND ARE LOCATED TO FURTHER EQUALIZE PLATFORM TEMPERATURES.

COMPONENT	HEAT DISSIPATION (WATTS)		
	LAUNCH	TRANSIT	ENCOUNTER
SCIENCE			
MAGNETOMETER	0.0	3.5	3.5
NEUTRAL MASS SPECTROMETER	0.0	0.0	3.9
ION MASS SPECTROMETER	0.0	0.0	2.0
ELECTRON TEMPERATURE PROBE	0.0	0.0	2.0
UV FLUORESCENT	0.0	0.0	2.5
DATA HANDLING			
DIGITAL TELEMETRY UNIT	3.8	3.8	3.8
DIGITAL DECODER UNIT	0.3	0.3	0.3
COMMUNICATIONS			
S-BAND RECEIVERS	4.0	4.0	4.0
S-BAND TRANSMITTER DRIVER	1.3	1.3	1.3
S-BAND POWER AMPLIFIER	16.5	16.5	16.5
ACS, PROPULSION			
CONTROL ELECTRICAL ASSEMBLY	1.5	1.5	1.5
PRESSURE TRANSDUCER	0.4	0.4	0.4
ELECTRICAL POWER CONTROL			
PCU/ELECTRONICS	4.0	4.0	4.0
COMMAND DISTRIBUTION UNIT	2.5	2.5	2.5
CONVERTER	5.5	5.5	5.5

Figure 8.7-11. Thor/Delta Probe Bus Spacecraft Thermal Environment

8. 7. 3. 2 Orbiter Spacecraft

System Description

A detailed description of the Thor/Delta thermal control system design is presented in Figure 8. 7-12. This spacecraft had a boom-mounted magnetometer, but did not require an experiment ram platform.

Thermal Control System Performance

Figure 8. 7-13A lists the maximum predicted temperature variation of each component during the complete mission. The actual earth/Venus transit temperature fluctuations of the selected components are also shown in Figure 8. 7-13B. All components except the infrared radiometer will remain within acceptance limits, although the Venus orbit insertion motor will be below the required 4°C (40°F) minimum ignition temperature during the first 110 days of the mission. This is acceptable since the allowable motor cold soak temperature is -18°C (0°F).

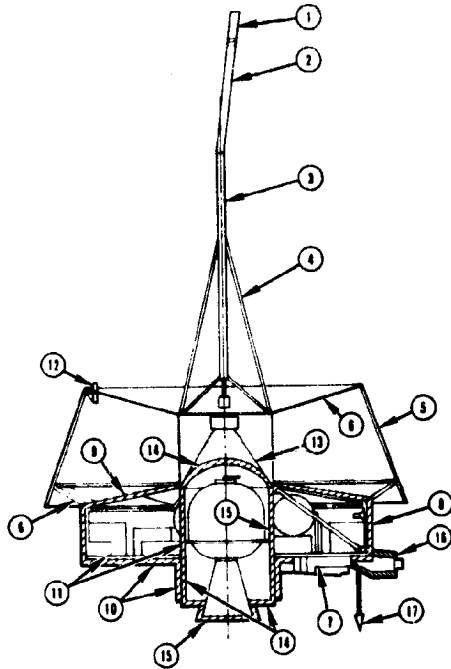
The infrared radiometer will, as in the Atlas/Centaur orbiter design, exceed its upper acceptance temperature limit during the mission. The conclusions and recommendations discussed in the preceding paragraph for the Atlas/Centaur design are also valid for this application.

Thermal Environment

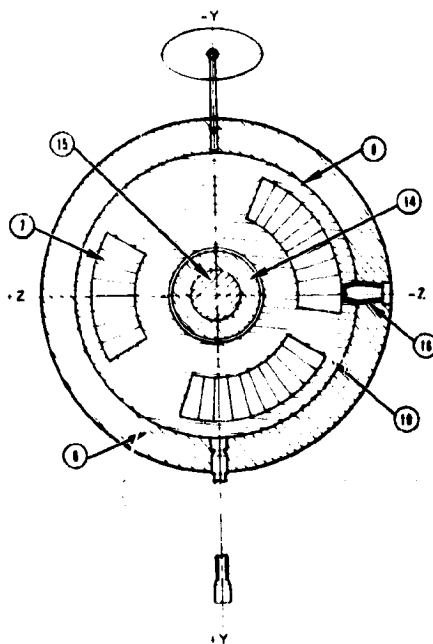
The Thor/Delta orbiter spacecraft prelaunch, ascent and third-stage engine firing thermal environments are identical to those described for the probe bus spacecraft in Figure 8. 7-11. The transit thermal environment from separation to Venus orbit insertion is given in Figure 8. 7-14A. The solar aspect angle is quite different than specified for the preferred Atlas/Centaur configuration because the recommended Thor/Delta orbiter has its spin axis always normal to the Venus orbit plane. This means that the sun is always at right angles to the spin axis instead of continuously varying like the earth-pointing Atlas/Centaur configuration.

Typical power dissipations, orbit parameters, and injection motor heating characteristics for the Thor/Delta orbiter spacecraft are also included in Figure 8. 7-14. The maximum Venus heat inputs occur 168 days after orbit insertion as discussed in Section 8. 7. 2. 2.

SECTION VIEW



VIEW OF AFT END



I.D. NO.	NAME OF ITEM	DESCRIPTION OF HARDWARE
1	FORWARD OMNI ANTENNA THERMAL COATING	3-MIL COAT 5-13G WHITE PAINT ON EXTERNAL SURFACES OF OMNI ANTENNA
2	FANBEAM ANTENNA THERMAL COATING	3-MIL COAT OF 5-13 G WHITE PAINT ON EXTERNAL SURFACE OF ANTENNA
3	HIGH-GAIN ANTENNA THERMAL COATING	3-MIL COAT OF 5-13G WHITE PAINT ON EXTERNAL SURFACE OF ANTENNA
4	ANTENNA SUPPORT THERMAL COATING	3-MIL COAT OF 5-13G WHITE PAINT ON EXTERNAL SURFACE OF SUPPORT
5	SOLAR ARRAY SUBSTRATE THERMAL COATING	3-MIL COAT OF 3M BLACK VELVET PAINT ON BACK SURFACE OF SUBSTRATE
6	FORWARD AND MIDSHIELD	ONE OUTER LAYER OF 2-MIL ALUMINIZED TEFLON (INWARD) LAMINATED TO ONE 2-MIL INNER LAYER OF ALUMINIZED MYLAR
7	BIMETAL ACTUATED LOUVERS	TOTAL BLADE AREA = 0.65 M ² (7.05 FT ²); A/C, 0.50 M ² CLOSED EFFECTIVE EMITTANCE = 0.20 FULL CLOSED OPEN EFFECTIVE EMITTANCE = 0.74 FULL OPEN AT 1000 K; 3-MIL COAT OF 2-93 WHITE PAINT ON PLATFORM UNDER SURFACE
8	EQUIPMENT COMPARTMENT SIDE INSULATION	22 LAYERS OF 1/4-MIL ALUMINIZED MYLAR SANDWICHED BETWEEN 2-MIL ALUMINIZED KAPTON AND ONE INNER 2-MIL ALUMINIZED MYLAR COVER SHEET (ALUMINIZED SURFACES EXCEPT INSIDE COVER SHEET FACE INWARD); K/X SEE FIGURE 8.7-4
9	EQUIPMENT COMPARTMENT TOP INSULATION	22 LAYERS OF 1/4-MIL ALUMINIZED MYLAR SANDWICHED BETWEEN 2-MIL ALUMINIZED KAPTON AND ONE INNER 2-MIL ALUMINIZED MYLAR COVER SHEET (ALUMINIZED SURFACES EXCEPT INSIDE COVER SHEET FACE INWARD); K/X SEE FIGURE 8.7-4
10	EQUIPMENT COMPARTMENT AFT INSULATION	22 LAYERS OF 1/4 MIL ALUMINIZED MYLAR SANDWICHED BETWEEN 2 MIL ALUMINIZED KAPTON AND ONE INNER 2-MIL ALUMINIZED MYLAR COVER SHEETS (ALUMINIZED SURFACES EXCEPT INSIDE COVER SHEET FACE INWARD); K/X SEE FIGURE 8.7-4
11	EQUIPMENT COMPARTMENT RADIATIVE AND CONDUCTIVE THERMAL COUPLING REQUIREMENTS	3-MIL COATING OF 3M BLACK VELVET PAINT ON EXTERNAL SURFACES OF HEAT DISSIPATING EQUIPMENT; BARE METAL SURFACE ON CENTRAL COLUMN AND THERMAL COUPLING PLATE; PROVIDE GOOD CONDUCTION THERMAL COUPLING BETWEEN COMPONENTS (I.E., TRANSMITTER) AND PLATFORM; MATERIAL: H = 142 WATTS/M ² -°C (25 BTU/HR -FT ² -°F)
12	RCS THRUSTER VALVE BODY AND SUPPLY LINE INSULATION, VALVE AND CATALYST BED HEATERS, AND THRUSTER ISOLATION PROVISIONS	LOWER DV THRUSTER INSULATED COMPLETELY WITH 10 LAYERS OF MOLYBDENUM FOIL; ALL FULL LINES ARE COPPER PLATED; LINES EXTERNAL TO EQUIPMENT COMPARTMENT INSULATED WITH 10 LAYERS OF MOLYBDENUM FOIL; K/X = 0.56 WATTS/M ² -°C (0.01 BTU/HR-FT ² -°F); DUAL-RANGE THERMOSTATICALLY CONTROLLED HEATERS WITH GROUND CONTROL BACKUP. PRIMARY RANGE 5 TO 18°C (45°F); BACKUP RANGE 7°C (45°F) TO 13°C (55°F); 5.0 WATTS THRUSTERS MOUNTED TO STRUCTURE WITH TITANIUM
13	SUPPORT CONE THERMAL COATING	COLORLESS CHEM FILM SURFACE
14	SOLID MOTOR INSULATION	22 LAYERS OF 1/4-MIL ALUMINIZED KAPTON SANDWICHED BETWEEN 2-MIL ALUMINIZED KAPTON COVER SHEETS (ALUMINIZED SURFACES EXCEPT INSIDE COVER SHEET FACE INWARD); K/X SEE FIGURE 8.7-4
15	MOTOR NOZZLE CAP INSULATION	22 LAYERS OF 1/4-MIL ALUMINIZED KAPTON SANDWICHED BETWEEN 2-MIL ALUMINIZED KAPTON COVER SHEETS (ALUMINIZED SURFACES EXCEPT INSIDE COVER SHEET FACE INWARD); K/X SEE FIGURE 8.7-4
16	SUN SENSOR INSULATION	22 LAYERS OF 1/4-MIL ALUMINIZED MYLAR SANDWICHED BETWEEN 2-MIL ALUMINIZED KAPTON AND ONE INNER 2-MIL ALUMINIZED MYLAR COVER SHEETS (ALUMINIZED SURFACES EXCEPT INSIDE COVER SHEET FACE INWARD); K/X SEE FIGURE 8.7-4
17	AFT OMNI ANTENNA THERMAL COATING	3-MIL COAT OF 5-13G WHITE PAINT ON EXTERNAL SURFACE OF ANTENNA

OUTLINE FRAME

DESCRIPTION OF HARDWARE	PURPOSE	SURFACE THERMAL PROPERTIES					
		INSIDE			OUTSIDE		
		NEW	DEG	'	NEW	DEG	'
13G WHITE PAINT ON SURFACE OF OMNI ANTENNA	MINIMIZE ABSORBED SOLAR AND ALBEDO HEAT INPUT TO REDUCE VARIATION IN TEMPERATURE DURING MISSION. LOCATION ENSURES SOLAR HEATING TO LIMIT MINIMUM TEMPERATURES FOR ALL SOLAR ASPECT ANGLES ENCOUNTERED.	-	-	-	0.24	0.39	0.88
13G WHITE PAINT ON SURFACE OF ANTENNA	MINIMIZE ABSORBED SOLAR AND ALBEDO HEAT INPUT TO REDUCE VARIATION IN TEMPERATURE DURING MISSION. LOCATION ENSURES SOLAR HEATING TO LIMIT MINIMUM TEMPERATURES FOR ALL SOLAR ASPECT ANGLES ENCOUNTERED.	-	-	-	0.24	0.39	0.88
13G WHITE PAINT ON SURFACE OF ANTENNA	MINIMIZE ABSORBED SOLAR AND ALBEDO HEAT INPUT TO REDUCE VARIATION IN TEMPERATURE DURING MISSION. LOCATION ENSURES SOLAR HEATING TO LIMIT MINIMUM TEMPERATURES FOR ALL SOLAR ASPECT ANGLES ENCOUNTERED.	-	-	-	0.24	0.39	0.88
13G WHITE PAINT ON SURFACE OF SUPPORT	MINIMIZE ABSORBED SOLAR AND ALBEDO HEAT INPUT TO LIMIT MAXIMUM SUPPORT TEMPERATURES	-	-	-	0.24	0.39	0.88
3M BLACK VELVET PAINT SURFACE OF SUBSTRATE	MAXIMIZE RADIANT HEAT TRANSFER FROM BACK SURFACE OF SOLAR ARRAY	-	-	0.90	0.80	0.80	0.80 AT ZFRC ARRAY OUTPUT
FRONT OF 2-MIL ALUMINIZED TEFLON (ALUMINIZED SIDE FACING) MOUNTED TO ONE 2-MIL INNER LAYER OF CLEAR MYLAR	SHIELD BACK SIDE OF SOLAR ARRAY FROM DIRECT SOLAR AND ALBEDO IMPINGEMENT. PROVIDE LOW TEMPERATURE BOUNDARY (LOW α/ϵ) TO MAXIMIZE HEAT TRANSFER FROM BACK SURFACE OF SOLAR ARRAY	-	-	0.66	0.08	0.18	0.66
AREA: 0.65 M ² (7.05 FT ²); A/C, 0.50 M ² (5.4 FT ²), T/D EMISSANCE = 0.20 FULL CLOSED AT 4°C (40°F), EMISSANCE = 0.74 FULL OPEN AT 29°C (85°F) 13G WHITE PAINT ON PLATFORM UNDER LOUVERS	CONTROL EQUIPMENT COMPARTMENT HEAT LEAKS TO OFFSET THE VARIATION IN EQUIPMENT AND ENVIRONMENTAL HEAT INPUT EXPERIENCED DURING THE MISSION TO MAINTAIN COMPONENT TEMPERATURES WITHIN ACCEPTABLE LIMITS	-	-	-	0.50	0.50	0.20 CLOSED 0.74 OPEN
2-MIL ALUMINIZED MYLAR SANDWICHED BETWEEN ONE OUTER 2-MIL KAPTON AND ONE INNER 2-MIL ALUMINIZED MYLAR COVER SHEET (ALL SURFACES EXCEPT INSIDE COVER SHEET FACE INWARD); 8.7-4	MINIMIZE SOLAR AND ALBEDO HEAT LEAK INTO AND UNCONTROLLED HEAT LEAKS OUT OF THE EQUIPMENT COMPARTMENT. STABLE ALUMINIZED KAPTON MINIMIZES EXTERNAL SURFACE PROPERTY DEGRADATION	-	-	0.69	0.45	0.50	0.69
4-MIL ALUMINIZED MYLAR SANDWICHED BETWEEN TWO 2-MIL KAPTON COVER SHEETS (ALL ALUMINIZED SURFACES EXCEPT INSIDE COVER SHEET FACE INWARD); 8.7-4	MINIMIZE UNCONTROLLED HEAT LEAKS INTO AND OUT OF THE EQUIPMENT COMPARTMENT AND THERMALLY DECOUPLE COMPARTMENT FROM SOLAR ARRAY	-	-	0.69	-	-	0.69
4-MIL ALUMINIZED MYLAR SANDWICHED BETWEEN ONE ALUMINIZED KAPTON AND ONE INNER 2-MIL ALUMINIZED MYLAR COVER SHEETS (ALUMINIZED SURFACES FACE FORWARD); 8.7-4	MINIMIZE UNCONTROLLED HEAT LEAKS OUT OF THE EQUIPMENT COMPARTMENT. MINIMIZE SOLID MOTOR PLUME RADIANT HEAT INPUT TO EQUIPMENT COMPARTMENT. STABLE ALUMINIZED KAPTON MINIMIZES EXTERNAL SURFACE PROPERTY DEGRADATION	-	-	-	0.45	0.50	0.69
3M BLACK VELVET PAINT ON EQUIPMENT PLATFORM AND SURFACE OF EQUIPMENT COUPLING TO CENTRAL COLUMN AND HYDRAZINE TANKS. TANKS COUPLING TO MOUNTING PLATFORM AND ISOLATED FROM COLUMN REDUCES THERMAL COUPLING BETWEEN HIGH HEAT DENSITY COMPONENTS (TRANSMITTER) AND PLATFORM WITH RTV INTERFACE FILLER 13G WHITE PAINT ON SURFACE OF THRUSTER THRUSTER INSULATED COMPLETELY WITH HIGH TEMPERATURE INSULATION THRUSTER LINES ARE COPPER PLATED. LINES EXTERNAL TO THE EQUIPMENT COMPARTMENT ARE INSULATED WITH 10 LAYERS OF NRC-L INSULATION HEATER POWER REQUIREMENT: 133 W (0.10 BTU/HR-FT ² -°F) HEATER CONTROL BACKUP. PRIMARY HEATER CONTROL RANGE 13°C (55°F) TO 17°C (63°F). BACKUP RANGE 7°C (45°F) TO 13°C (55°F). HEATER POWER REQUIREMENT: 133 W (0.10 BTU/HR-FT ² -°F) THRUSTER MOUNTED TO STRUCTURE WITH TITANIUM STANDOFFS	EQUALIZE TEMPERATURE GRADIENTS WITHIN EQUIPMENT COMPARTMENT BY MAXIMIZING RADIATIVE THERMAL COUPLING BETWEEN STRUCTURE AND HEAT DISSIPATING COMPONENTS THERMALLY DECOUPLE ZERO HEAT DISSIPATING COMPONENTS FROM SURROUNDING TO MINIMIZE TEMPERATURE VARIATIONS DURING TRANSIENT ENVIRONMENTAL CONDITIONS MINIMIZE COMPONENT TO EQUIPMENT PLATFORM TEMPERATURE GRADIENTS TO MINIMIZE MAXIMUM COMPONENT TEMPERATURE ABOVE SURROUNDINGS	-	-	-	-	-	0.90 0.10
THRUSTER INSULATED COMPLETELY WITH HIGH TEMPERATURE INSULATION THRUSTER LINES ARE COPPER PLATED. LINES EXTERNAL TO THE EQUIPMENT COMPARTMENT ARE INSULATED WITH 10 LAYERS OF NRC-L INSULATION HEATER POWER REQUIREMENT: 133 W (0.10 BTU/HR-FT ² -°F) HEATER CONTROL BACKUP. PRIMARY HEATER CONTROL RANGE 13°C (55°F) TO 17°C (63°F). BACKUP RANGE 7°C (45°F) TO 13°C (55°F). HEATER POWER REQUIREMENT: 133 W (0.10 BTU/HR-FT ² -°F) THRUSTER MOUNTED TO STRUCTURE WITH TITANIUM STANDOFFS	MINIMIZE UNCONTROLLED THRUSTER HEAT LEAK TO SPACE MINIMIZE TEMPERATURE GRADIENTS IN SUPPLY LINES AND HEAT LEAKS INTO OR OUT OF THRUSTER AND LINES MAINTAINS THRUSTER AND SUPPLY LINE TEMPERATURES ABOVE MINIMUM TEMPERATURE LIMITS ISOLATES THRUSTER FROM STRUCTURE TO MINIMIZE HEATER POWER REQUIREMENT	-	-	-	0.12	0.17	0.05 0.05
3M BLACK VELVET PAINT ON EQUIPMENT PLATFORM AND SURFACE OF EQUIPMENT COUPLING TO CENTRAL COLUMN AND HYDRAZINE TANKS. TANKS COUPLING TO MOUNTING PLATFORM AND ISOLATED FROM COLUMN REDUCES THERMAL COUPLING BETWEEN HIGH HEAT DENSITY COMPONENTS (TRANSMITTER) AND PLATFORM WITH RTV INTERFACE FILLER 13G WHITE PAINT ON SURFACE OF THRUSTER THRUSTER INSULATED COMPLETELY WITH HIGH TEMPERATURE INSULATION THRUSTER LINES ARE COPPER PLATED. LINES EXTERNAL TO THE EQUIPMENT COMPARTMENT ARE INSULATED WITH 10 LAYERS OF NRC-L INSULATION HEATER POWER REQUIREMENT: 133 W (0.10 BTU/HR-FT ² -°F) HEATER CONTROL BACKUP. PRIMARY HEATER CONTROL RANGE 13°C (55°F) TO 17°C (63°F). BACKUP RANGE 7°C (45°F) TO 13°C (55°F). HEATER POWER REQUIREMENT: 133 W (0.10 BTU/HR-FT ² -°F) THRUSTER MOUNTED TO STRUCTURE WITH TITANIUM STANDOFFS	RADIATIVELY DECOUPLE CONE FROM SOLAR ARRAY AND FORWARD SHIELD	-	-	0.05	-	-	0.05
4-MIL ALUMINIZED KAPTON SANDWICHED BETWEEN TWO 2-MIL KAPTON COVER SHEETS (ALUMINIZED SURFACES FACE INWARD); 8.7-4	MINIMIZE UNCONTROLLED HEAT LEAKS FROM SOLID MOTOR TO MAINTAIN MOTOR WITHIN ACCEPTABLE TEMPERATURE LIMITS PRIOR TO FIRING. MINIMIZE UNCONTROLLED HEAT LEAKS FROM THE EQUIPMENT COMPARTMENT. MINIMIZE SOLID MOTOR RADIANT HEAT SOAK-BACK TO EQUIPMENT COMPARTMENT AFTER MOTOR FIRING. KAPTON REQUIRED TO PREVENT DEGRADATION OF INSULATION THERMAL PROPERTIES DUE TO HEAT/SHOCK FROM MOTOR CASE	-	-	0.69	-	-	0.05
4-MIL ALUMINIZED KAPTON SANDWICHED BETWEEN TWO 2-MIL KAPTON COVER SHEETS (ALUMINIZED SURFACES FACE FORWARD); 8.7-4	MINIMIZE UNCONTROLLED HEAT LEAKS FROM SOLID MOTOR TO MAINTAIN MOTOR WITHIN ACCEPTABLE TEMPERATURE LIMITS PRIOR TO FIRING. NOZZLE CAP IS JETISONED WHEN MOTOR FIRES	-	-	0.05	0.45	0.50	0.69
4-MIL ALUMINIZED MYLAR SANDWICHED BETWEEN ONE OUTER 2-MIL KAPTON AND ONE INNER 2-MIL ALUMINIZED MYLAR COVER SHEETS (ALUMINIZED SURFACES FACE INWARD); 8.7-4	MINIMIZE SOLAR AND ALBEDO HEAT LEAK INTO AND UNCONTROLLED HEAT LEAKS OUT OF THE SENSOR ASSEMBLY. STABLE ALUMINIZED KAPTON MINIMIZES EXTERNAL SURFACE PROPERTY DEGRADATION	-	-	-	0.45	0.50	0.69
13G WHITE PAINT ON EXTERNAL SURFACES OF OMNI	MINIMIZE ABSORBED SOLAR AND ALBEDO HEAT INPUT TO REDUCE VARIATION IN TEMPERATURE DURING MISSION. LOCATION ENSURES SOLAR HEATING THROUGH MOST OF MISSION TO LIMIT MINIMUM TEMPERATURES DURING NORMAL OPERATION	-	-	-	0.24	0.39	0.88

THE ORBITER USES THERMAL CONTROL HARDWARE COMMON TO THE PROBE BUS SPACECRAFT. LOCATIONS OF HARDWARE ARE KEYED TO THE ADJACENT TABLE FOR DETAILED DESCRIPTION.

Figure 8.7-12. Thor/Delta Orbiter Spacecraft Thermal Control Description

A COMPONENT TEMPERATURE CONTROL CAPABILITY VERSUS TEMPERATURE REQUIREMENTS

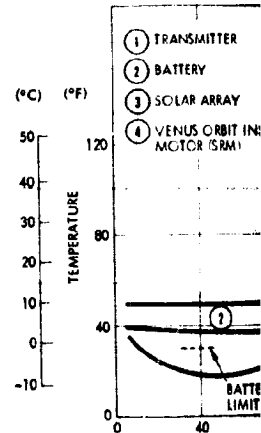
THE THERMAL CONTROL SYSTEM WILL MAINTAIN ALL COMPONENTS EXCEPT THE IR RADIOMETER WITHIN THEIR SPECIFIED ACCEPTANCE LIMITS DURING ALL MISSION PHASES. THE IR RADIOMETER TEMPERATURE WILL REACH 28°C (82°F), 16°C (28°F) ABOVE THE 12°C (54°F) SPECIFICATION LIMIT.

SUBSYSTEM AND SCIENCE COMPONENTS	PREDICTED TEMPERATURES		ACCEPTANCE OPERATING TEMPERATURE LIMITS	
	MINIMUM	MAXIMUM	MINIMUM	MAXIMUM
	C °F	C °F	C °F	C °F
COMMUNICATIONS				
OMNI ANTENNAS	-127 (-196)	24.75	-145 (-230)	93.200
FANBEAM ANTENNA	-131 (-204)	71.160	-206 (-340)	171.340
REFLECTOR FEED	-115 (-175)	24.75	-18 (-300)	38.100
S-BAND TRANSMITTERS	10.49	57.135	4.40	57.125*
POWER AMPLIFIER	10.49	57.135	4.40	57.125*
S-BAND RECEIVERS	10.49	47.108	-4.25	43.110
DATA HANDLING				
DTU	9.47	21.69	-7.20	41.105
DSU	6.43	19.67	-7.20	41.105
DDL	9.48	20.68	-7.20	41.105
ELECTRICAL POWER				
BATTERY	9.47	24.75	-1.30	29.85
DCU	10.49	38.100	-20.4	65.149
DC-DC CONVERTER	8.46	28.83	-18.0	49.120
SHUNT RADIATOR	-102 (-153)	132.270	-157 (-250)	132.270
SOLAR ARRAY	-125 (-194)	102.215	102.225	102.215
CDU	10.49	21.70	-7.20	41.105
ACS PROPULSION				
DMA	-4.25	54.130	-22.58	75.167
DEA	10.49	23.74	-12.10	43.110
CEA	9.48	20.68	-7.20	41.105
SUN SENSOR	4.39	52.125	-15.5	60.140
THRUSTER VALVE BODYS	13.55	82.180	13.55	93.200
HYDRAZINE TANKS	7.44	21.70	4.40	43.110
HYDRAZINE LINES	4.40	82.180	4.40	82.180
SOLID ROCKET MOTOR	3.37	16.62	-7.20	38.100
SCIENCE				
MAGNETOMETER ELECTRONICS	7.45	21.69	0.32	60.140
RADAP ALTIMETER ELECTRONICS	5.42	24.75	-30.22	60.140
ELECTRON TEMPERATURE PROBE ELECTRONICS	5.42	26.79	4.40	43.110
UV SPECTROMETER	10.49	38.100	0.32	40.104
ION MASS SPECTROMETER	8.46	18.65	-30.22	60.140
IR RADIOMETER	8.46	27.81	-30.22	12.34
NEUTRAL MASS SPECTROMETER	8.46	22.72	-30.22	60.140

* ALLOWED TO OPERATE AT 27°C (81°F) FOR MAXIMUM OF 0.5-HOUR PER ORBIT.

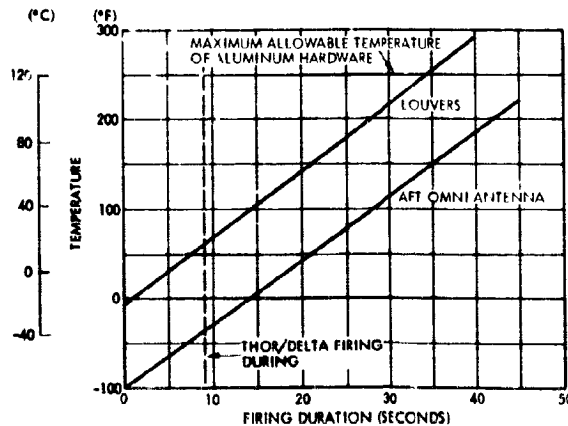
B TEMPERATURE HISTORY OF CRITICAL COMPONENTS DURING EARTH/VENUS TRANSIT

SPACECRAFT TEMPERATURES INITIALLY RISE DURING EARTH TRANSIT. SPACECRAFT GOES OUT TO 1.07 AU DURING VENUS TRANSIT. SOLAR HEATING MORE THAN DOUBLES.



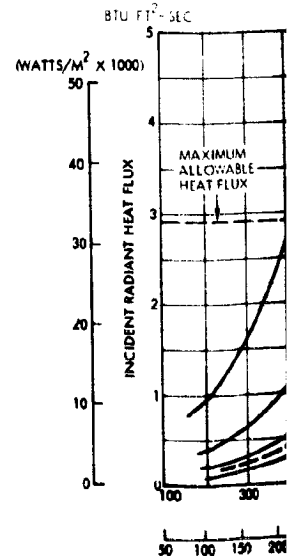
D TEMPERATURE RISE OF AFT-MOUNTED COMPONENTS DURING VENUS INSERTION MOTOR FIRING

AFT-LOCATED HARDWARE SUCH AS THE LOUVERS AND OMNI ANTENNA HEAT UP DURING MOTOR FIRING. THE RATE OF TEMPERATURE RISE IS DEPENDENT UPON THE VIEW TO THE PLUME AND THE THERMAL CAPACITANCE OF THE EQUIPMENT. EXCESSIVE HEATING WILL NOT OCCUR DURING FIRING.



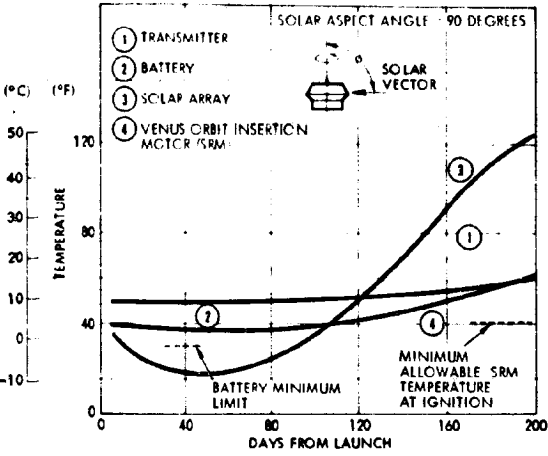
E EQUILIBRIUM TEMPERATURES OF LOW CAPACITANCE SURFACES DURING VENUS INSERTION MOTOR FIRING

LOW CAPACITANCE SURFACES SUCH AS THE TRANSMITTER AND BATTERY INSTANTANEOUSLY HEAT UP WHEN EXPOSED TO THE PLUME INCIDENT HEAT FLUX DURING VENUS INSERTION MOTOR FIRING. EQUILIBRIUM TEMPERATURES ARE DETERMINED BY THE PLUME RADIATION TO WHICH THEY ARE EXPOSED.



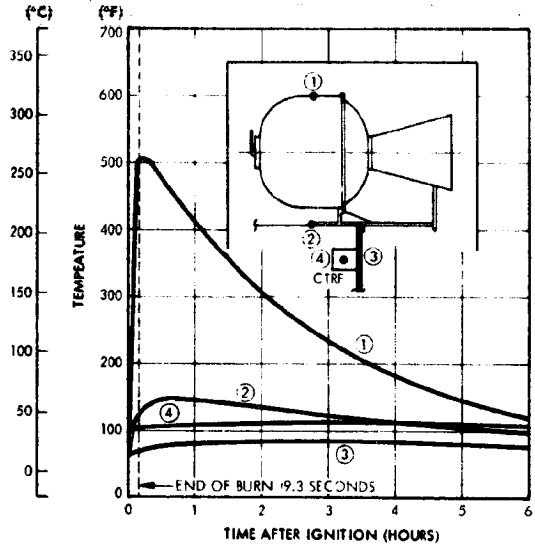
E TEMPERATURE HISTORY OF CRITICAL COMPONENTS DURING VENUS TRANSIT

SPACECRAFT TEMPERATURES INITIALLY DECREASE WITH MISSION TIME AS THE SPACECRAFT GOES OUT TO 1.07 AU AND THEN INCREASE AS THE INCIDENT SOLAR HEATING MORE THAN DOUBLES FROM ITS MINIMUM VALUE.



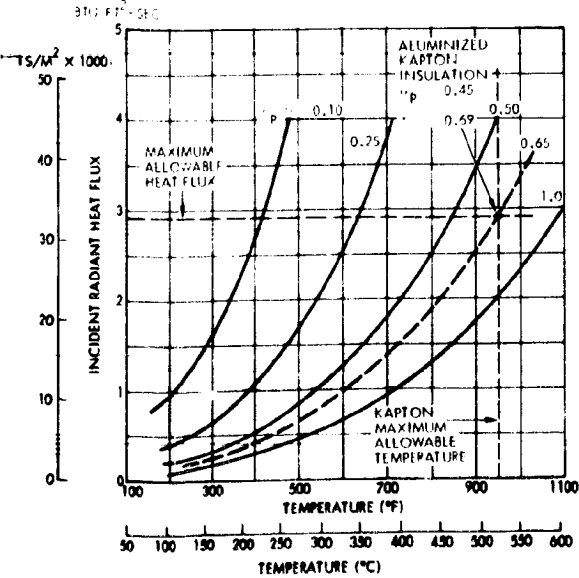
C VENUS ORBIT INSERTION SPACECRAFT TEMPERATURES FOLLOWING MOTOR IGNITION

COMPONENT AND STRUCTURE HEATING BY THE ENGINE WILL NOT BE EXCESSIVE DURING ORBIT INJECTION FIRING. PLATFORM MOUNTED ELECTRONIC COMPONENTS WILL EXHIBIT ONLY A SLIGHT TEMPERATURE RISE AND REMAIN WITHIN ACCEPTANCE LIMITS.



A TEMPERATURES OF LOW CAPACITANCE SURFACES DURING VENUS ORBIT INSERTION MOTOR FIRING

LOW CAPACITANCE SURFACES SUCH AS INSULATION WILL HEAT UP ALMOST INSTANTANEOUSLY WHEN EXPOSED TO PLUME RADIATION DURING VENUS ORBIT INJECTION MOTOR FIRING. THE EQUILIBRIUM TEMPERATURE DEPENDS UPON THE PLUME INCIDENT HEAT FLUX AND RATIO OF SURFACE ABSORPTANCE TO PLUME RADIATION; TO EMITTANCE.



F TEMPERATURE HISTORY OF CRITICAL COMPONENTS NEAR PERIAPSIS IN VENUS ORBIT

SPACECRAFT TEMPERATURES REACH MAXIMUM ORBIT VALUES AT DAY 168 AFTER INSERTION WHEN VENUS ALBEDO, EMISSION, AND FREE MOLECULAR HEATING RATES ARE AT PEAK VALUES. TEMPERATURES ALSO REACH MINIMUM ORBIT VALUES DURING THE SAME ORBIT WHEN AN 1.42-HOUR SOLAR ECLIPSE OCCURS.

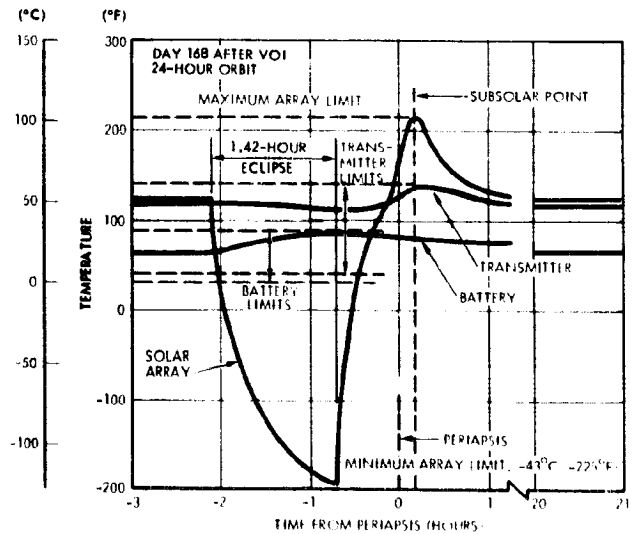
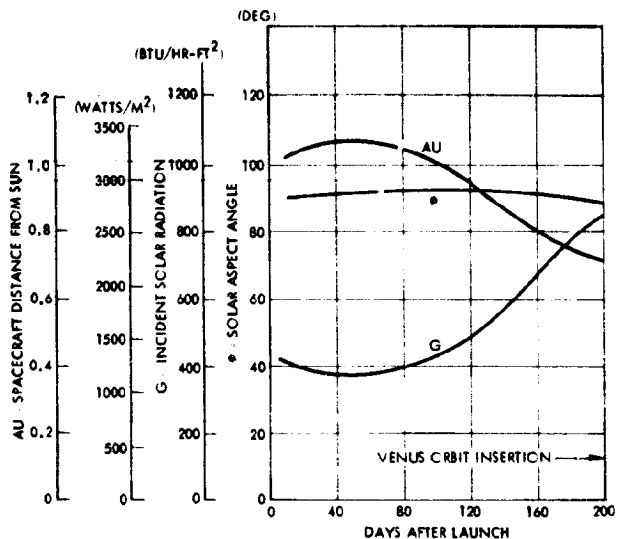


Figure 8.7-13. Thor/Delta Orbiter Spacecraft Thermal Performance

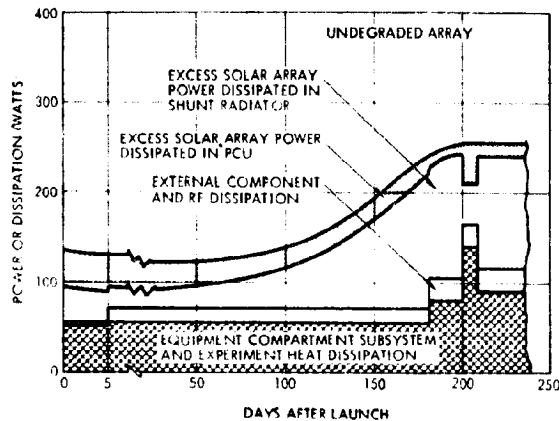
A ORBITER SPACECRAFT TRANSIT THERMAL PARAMETERS

THE SPACECRAFT SOLAR ASPECT ANGLE, INCIDENT SOLAR RADIATION INPUT, AND DISTANCE FROM THE SUN IMPACT THE THERMAL SYSTEM DESIGN. THE SPACECRAFT ELEMENT TEMPERATURES HAVE TO BE MAINTAINED WITHIN ACCEPTANCE LIMITS WITH A MISSION SOLAR HEAT FLUX VARIATION OF 1160 TO 2660 WATTS/METER² (380 TO 840 BTU/HR)



B ORBITER MISSION HEAT DISSIPATION PROFILE

A TYPICAL HEAT DISSIPATION HISTORY FOR VARIOUS ORBITER SPACECRAFT AREAS INDICATES THAT THE OVERALL MISSION HEAT DISSIPATION INCREASES NEAR VENUS AS MORE SOLAR ARRAY POWER BECOMES AVAILABLE. THIS HEAT DISSIPATION INCREASE IS ACCOMMODATED BY THE LOUVERS, WHICH VARY THE HEAT REJECTION CAPABILITY OF THE EQUIPMENT COMPARTMENT



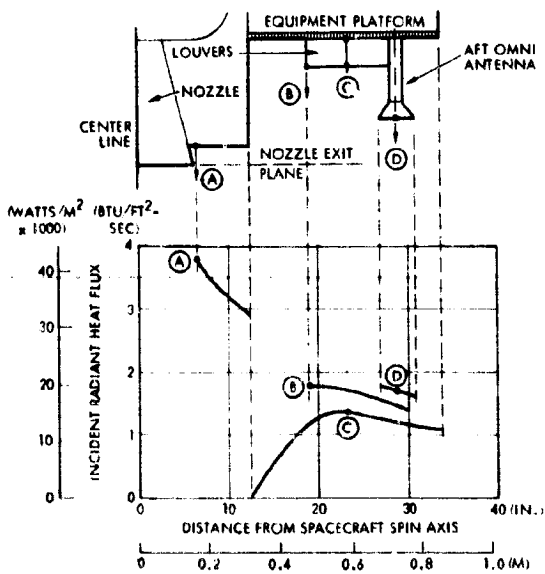
C COMPONENT H

SUBSYSTEM AND IS DISTRIBUTED IN DISSIPATION

- COMPONENT
- SCIENCE
- MAGNETOMETER
- ELECTRON TEMPERATURE
- NEUTRAL MASS SPECTROMETER
- ION MASS SPECTROMETER
- UV SPECTROMETER
- IR RADIOMETER
- RADAR ALTIMETER
- DATA HANDLING
- DIGITAL TELEMETRY
- DATA STORAGE UNIT
- DIGITAL DECODE
- COMMUNICATIONS
- S-BAND RECEIVER
- S-BAND TRANSMITTER
- S-BAND POWER AMPLIFIER
- ACS PROPELLANT
- CONTROL ELECTRONICS
- SUN SENSOR
- PRESSURE TRANSDUCER
- ELECTRICAL POWER
- PCU ELECTRONICS
- COMMAND DISTRIBUTION
- CONVERTER
- BATTERY

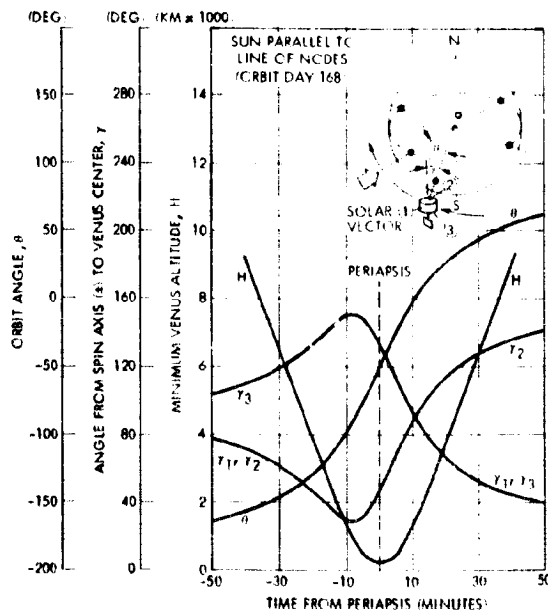
E ORBITER SPACECRAFT SOLID MOTOR PLUME INCIDENT RADIANT HEAT FLUX

THE AFT SURFACES OF THE ORBITER SPACECRAFT RECEIVE RADIANT HEATING FROM THE SOLID MOTOR PLUME FOR THE 23 SECONDS THAT THE ATLAS/CENTAUR MOTOR FIRES AT VENUS ORBIT INSERTION. CRITICAL SPACECRAFT SURFACES ARE POSITIONED TO REMOVE THE INCIDENT HEAT RATE TO ACCEPTABLE LEVELS CONSIDERING THE HEAT CAPACITY AND SURFACE ABSORPTANCE TO THE SURFACE

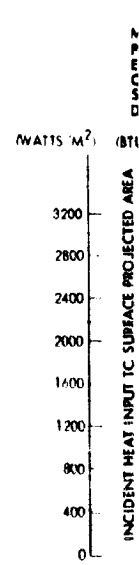


F VENUS ORBIT ANGLE AND ALTITUDE PARAMETERS NEAR PERIAPSIS

ORBITER SPACECRAFT VENUS ANGULAR AND ALTITUDE PARAMETERS NEAR PERIAPSIS WHEN THE SUN IS PARALLEL TO THE LINE OF NODES (ORBIT DAY 168) ESTABLISH THE MOST SEVERE VENUS ALBEDO HEAT INPUTS



G SOLAR AND V



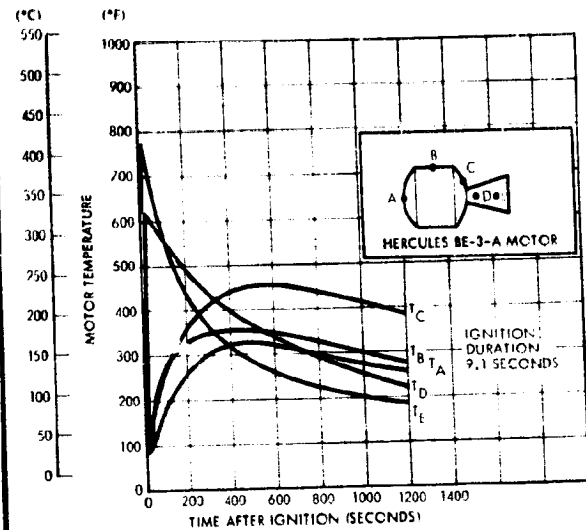
C COMPONENT HEAT DISSIPATIONS

SUBSYSTEM AND EXPERIMENT COMPONENTS ARE LOCATED SUCH THAT HEAT DISSIPATION IS DISTRIBUTED THROUGHOUT THE PLATFORM AREA. LOUVERS ACCOMMODATE VARIATIONS IN DISSIPATION AND ARE LOCATED TO FURTHER EQUALIZE PLATFORM TEMPERATURES.

COMPONENT	HEAT DISSIPATION (WATT)				
	LAUNCH	TRANSIT	ECLIPSE	PERIAPSIS	POST ECLIPSE
SCIENCE					
MAGNETOMETER	0.0	1.0	3.0	1.0	3.0
ELECTRIC TEMPERATURE PROBE	0.0	0.0	0.0	2.0	2.0
NEUTRAL MASS SPECTROMETER	0.0	0.0	12.0	12.0	12.0
ION MASS SPECTROMETER	0.0	0.0	1.0	1.0	1.0
UV SPECTROMETER	0.0	0.0	8.0	8.0	8.0
IR RADIOMETER	0.0	0.0	0.0	6.0	6.0
RADAR ALTIMETER	0.0	0.0	6.0	6.0	0.0
DATA HANDLING					
DIGITAL TELEMETRY UNIT	3.4	3.5	3.4	3.4	3.6
DATA STORAGE UNIT	0.0	0.0	0.0	4.5	0.0
DIGITAL DECODER UNIT	0.3	0.3	0.3	0.3	0.3
COMMUNICATIONS					
S-BAND RECEIVERS	4.0	4.0	4.0	4.0	4.0
S-BAND TRANSMITTER DRIVER	3.5	3.5	3.5	3.5	3.5
S-BAND POWER AMPLIFIER	12.5	18.5	44.5	44.5	44.5
ACS PROPULSION					
CONTROL ELECTRONICS ASSEMBLY AND SUN SENSORS	1.7	1.7	1.7	1.7	1.7
PRESSURE TRANSDUCER	0.4	0.4	0.4	0.4	0.4
ELECTRICAL POWER AND CONTROL					
PCU ELECTRONICS	4.0	4.0	4.0	4.0	4.0
COMMAND DISTRIBUTION UNIT	2.1	2.1	2.1	2.1	2.1
TELETYPE	3.2	3.2	3.1	1.1	3.2
BATTERY	0.0	4.2	22.0	0.0	6.5

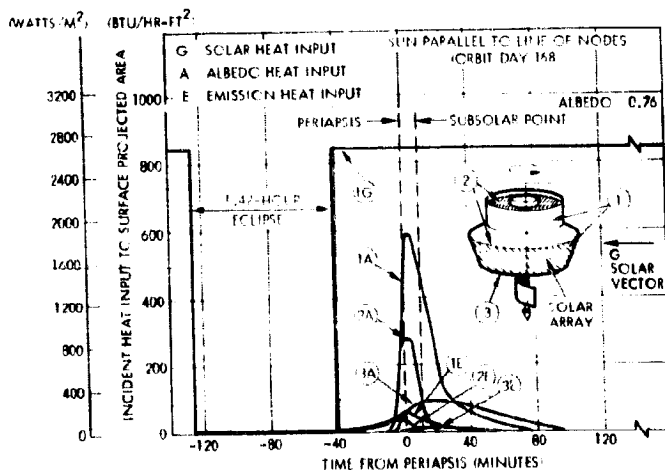
D SOLID MOTOR CASE TEMPERATURE HISTORY AFTER IGNITION

MOTOR CASING TEMPERATURE RISE DURING VENUS ORBIT INSERTION CAN HEAT THE ADJACENT ORBITER STRUCTURE. MOTOR MOUNTING IS DESIGNED TO MINIMIZE THE EFFECTS OF MOTOR HEATING TO SENSITIVE SPACECRAFT ELEMENTS. INDICATED TEMPERATURES REFLECT THE THOR/Delta DESIGN, BUT APPROXIMATE THE ATLAS/CENTAUR CONFIGURATION ALSO.



G SOLAR AND VENUS HEAT INPUTS DURING ORBIT

MAXIMUM ORBITER SPACECRAFT TEMPERATURES OCCUR NEAR VENUS PERIAPSIS, WHILE MINIMUM TEMPERATURES FOR OTHER SPACECRAFT ELEMENTS EXCEPT COMPONENTS IN THE EQUIPMENT COMPARTMENT OCCUR AT THE END OF THE 1.42-HOUR MAXIMUM ECLIPSE. THE SPACECRAFT ANTENNA IS POSITIONED IN THE SOUTHERNLY DIRECTION DURING ORBIT.



H VENUS ORBIT PERIAPSIS ALTITUDE, SOLAR ASPECT ANGLE AND SUN OCCULTATION

DAY 168 REPRESENTS THE MOST SEVERE THERMAL DESIGN CONDITION DURING VENUS ORBIT. ON THIS DAY THE ORBITER SPACECRAFT IS EXPOSED TO THE MAXIMUM ECLIPSE (1.42 HOURS) AND THEN SUBJECTED WITHIN THE HOUR TO THE WORST ALBEDO HEATING CONDITION.

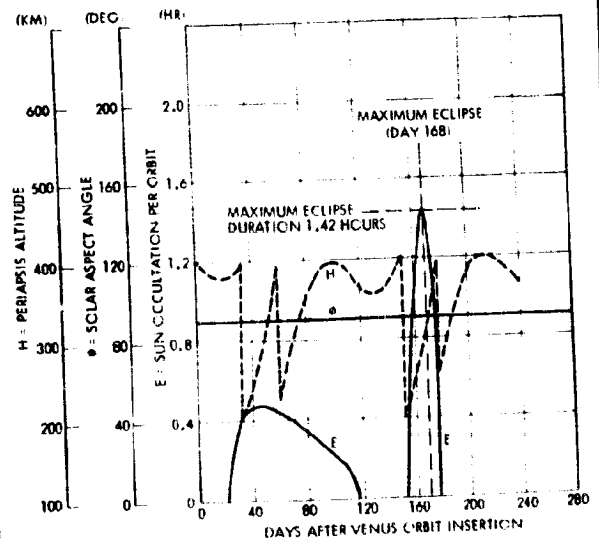


Figure 8.7-14. Recommended Thor/Delta Orbiter Spacecraft Thermal Environment

Thermal Analysis Techniques

A computer model similar to that described in Section 8.7.2.2 was used to calculate Thor/Delta orbiter temperatures. Thruster requirements and heater requirements are identical to the other configurations.

8.7.4 Optional Spacecraft Configurations

A number of other alternate configurations were investigated during the study. These included various large probe thermal control techniques and several orbiter spacecraft designs. The most significant alternate configurations are discussed below.

8.7.4.1 Probe Bus Spacecraft

Seven thermal control system techniques were reviewed before selecting the final Atlas/Centaur and Thor/Delta probe bus thermal control system designs. The advantages and disadvantages of each technique were reviewed as described in Section 8.7.5.2 before deciding on the earth-pointer design.

8.7.4.2 Orbiter Spacecraft

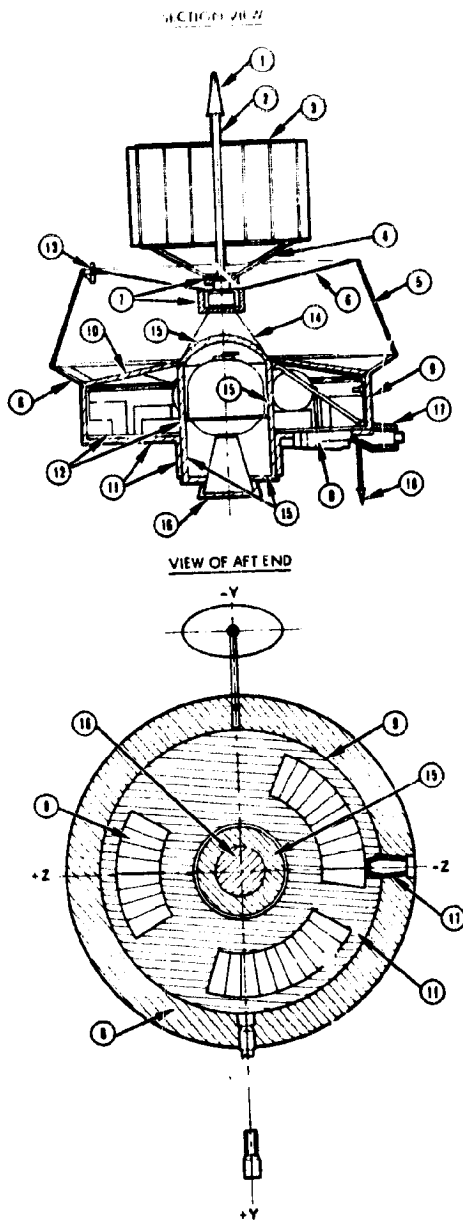
Two alternate normal-to-the-Venus-orbit-plane orbiter configurations were studied.

Despun Reflector Option A/C IV T/D III

This orbiter spacecraft was equipped with a despun reflector assembly and a 12-watt transmitter. The selected thermal control system design for this configuration is shown in Figure 8.7-15. The thermal system is similar to the other orbiter configurations and will maintain all components and experiments, except the infrared radiometer, within acceptance limits. The despun reflector element temperatures, shown in Figure 8.7-16, are considered in the antenna design to limit structural deformation to tolerable limits. Curves 5 and 6 of this figure are also applicable to the configurations shown below.

Fanbeam, Fanscan Options ^(31 W) A/C III ^(31 W) T/D III

A simplified orbiter configuration was studied that used a fanbeam antenna with a 31-watt transmitter. The design and thermal performance of this option was very similar to the Section 8.7.3 Thor/Delta and Atlas/



THE ORBITER USES RELIABLE AND FLIGHT PROVEN THERMAL CONTROL HARDWARE. LOCATIONS OF HARDWARE ARE KEYED TO THE ADJACENT TABLE FOR DETAILED DESCRIPTIONS.

I.D. NO.	NAME OF ITEM	DESCRIPTION OF HARDWARE
1	FORWARD OMNI ANTENNA THERMAL COATING	3-MIL COAT OF 5-13G WHITE PAINT ON EXTERNAL SURFACE OF OMNI ANTENNA
2	HIGH-GAIN ANTENNA THERMAL COATING	3-MIL COAT OF 5-13G WHITE PAINT ON EXTERNAL SURFACE OF HIGH-GAIN ANTENNA
3	HIGH-GAIN ANTENNA DISPERSE REFLECTOR THERMAL COATING	3-MIL COAT OF 5-13G WHITE PAINT ON EXTERNAL SURFACE OF DISPERSE REFLECTOR FRAME WIRE MESH UNCOATED
4	DISPERSE REFLECTOR SUPPORT THERMAL COATING	3-MIL COAT OF 5-13G WHITE PAINT ON EXTERNAL SURFACE OF DISPERSE REFLECTOR SUPPORT
5	SOLAR ARRAY SUBSTRATE THERMAL COATING	3-MIL COAT OF 3M BLACK VELVET PAINT ON BACK SURFACE OF SOLAR ARRAY SUBSTRATE
6	FORWARD AND MIDSHELD	ONE OUTER LAYER OF 2-MIL ALUMINIZED TEFLON (ALUMINIZED INWARD) LAMINATED TO ONE 2-MIL INNER LAYER OF CLEAR MYLAR
7	DMA COMPARTMENT INSULATION AND RADIATOR SURFACE	22 LAYERS OF 1/4-MIL ALUMINIZED MYLAR SANDWICHED BETWEEN 2 LAYERS OF ALUMINIZED KAPTON AND ONE INNER 2-MIL ALUMINIZED MYLAR (ALUMINIZED SURFACES FACE COMPARTMENT) K/X SEE FIGURE 8.7-4 3-MIL COAT OF 5-13G WHITE PAINT ON DMA COMPARTMENT RADIATOR SURFACE EXPOSED TO SPACE
8	BIMETAL ACTUATED LOUVERS	0.50 M ² (5.4 FT ²) TOTAL BLADE AREA CLOSED EFFECTIVE EMITTANCE = 0.20 FULL CLOSED AT 4°C (40°F) OPEN EFFECTIVE EMITTANCE = 0.74 FULL OPEN AT 29°C (85°F) 3-MIL COAT OF 2-93 WHITE PAINT ON PLATFORM UNDER LOUVERS
9	EQUIPMENT COMPARTMENT SIDE INSULATION	22 LAYERS OF 1/4-MIL ALUMINIZED MYLAR SANDWICHED BETWEEN 2 LAYERS OF ALUMINIZED KAPTON AND ONE INNER 2-MIL ALUMINIZED MYLAR (ALUMINIZED SURFACES FACE COMPARTMENT) K/X SEE FIGURE 8.7-4
10	EQUIPMENT COMPARTMENT TOP INSULATION	22 LAYERS OF 1/4-MIL ALUMINIZED MYLAR SANDWICHED BETWEEN 2 LAYERS OF ALUMINIZED MYLAR COVER SHEETS (ALL ALUMINIZED SURFACES FACE COMPARTMENT) K/X SEE FIGURE 8.7-4
11	EQUIPMENT COMPARTMENT AFT INSULATION	22 LAYERS OF 1/4-MIL ALUMINIZED MYLAR SANDWICHED BETWEEN 2 LAYERS OF ALUMINIZED KAPTON AND ONE INNER 2-MIL ALUMINIZED MYLAR (ALUMINIZED SURFACES FACE FORWARD) K/X SEE FIGURE 8.7-4
12	EQUIPMENT COMPARTMENT RADIATIVE AND CONDUCTIVE THERMAL COUPLING REQUIREMENTS	3-MIL COATING OF 3M BLACK VELVET PAINT ON EQUIPMENT COMPARTMENT RADIATING SURFACES BARE METAL SURFACE ON CENTRAL COLUMN AND HYDRAZINE TANKS CONDUCTIVELY COUPLED TO MOUNTING PLATFORM AND ISOLATED FROM PLATFORM PROVIDE GOOD CONDUCTION THERMAL COUPLING BETWEEN EQUIPMENT COMPONENTS (I.E., TRANSMITTER) AND PLATFORM WITH RTV MATERIAL H ≥ 142 WATTS/M ² -°C (25 BTU/HR-FT ² -°F)
13	RCS THRUSTER VALVE BODY AND SUPPLY LINE INSULATION, VALVE AND CATALYST BED HEATERS, AND THRUSTER ISOLATION PROVISIONS	LOWER ΔV THRUSTER INSULATED COMPLETELY WITH HIGH TEMPERATURE MOLYBDENUM FOIL ALL FUEL LINES ARE COPPER PLATED. LINES EXTERNAL TO THE EQUIPMENT COMPARTMENT INSULATED WITH 10 LAYERS OF NRC-1 INSULATION K/X = 0.036 WATTS/M ² -°C (0.01 BTU/HR-FT ² -°F) DUAL-RANGE THERMOSTATICALLY CONTROLLED HEATERS ON THRUSTER VALVE BODY WITH GROUND CONTROL BACKUP. PRIMARY HEATER COUPLING TO 18°C (65°F). BACKUP RANGE 7°C (45°F) TO 13°C (55°F). HEATER ELEMENT 5.2 WATTS THRUSTERS MOUNTED TO STRUCTURE WITH TITANIUM STANDOFFS
14	SUPPORT CONE THERMAL COATING	COLORLESS CHEM FILM SURFACE
15	SOLID MOTOR INSULATION	22 LAYERS OF 1/4-MIL ALUMINIZED KAPTON SANDWICHED BETWEEN 2 LAYERS OF ALUMINIZED KAPTON COVER SHEETS (ALUMINIZED SURFACES FACE FORWARD) K/X SEE FIGURE 8.7-4
16	MOTOR NOZZLE CAP INSULATION	22 LAYERS OF 1/4-MIL ALUMINIZED KAPTON SANDWICHED BETWEEN 2 LAYERS OF ALUMINIZED KAPTON COVER SHEETS (ALUMINIZED SURFACES FACE FORWARD) K/X SEE FIGURE 8.7-4
17	SUN SENSOR INSULATION	22 LAYERS OF 1/4-MIL ALUMINIZED MYLAR SANDWICHED BETWEEN 2 LAYERS OF ALUMINIZED KAPTON AND ONE INNER 2-MIL ALUMINIZED MYLAR (ALUMINIZED SURFACES FACE INWARD) K/X SEE FIGURE 8.7-4
18	AFT OMNI ANTENNA THERMAL COATING	3-MIL COAT OF 5-13G WHITE PAINT ON EXTERNAL SURFACE OF AFT OMNI ANTENNA



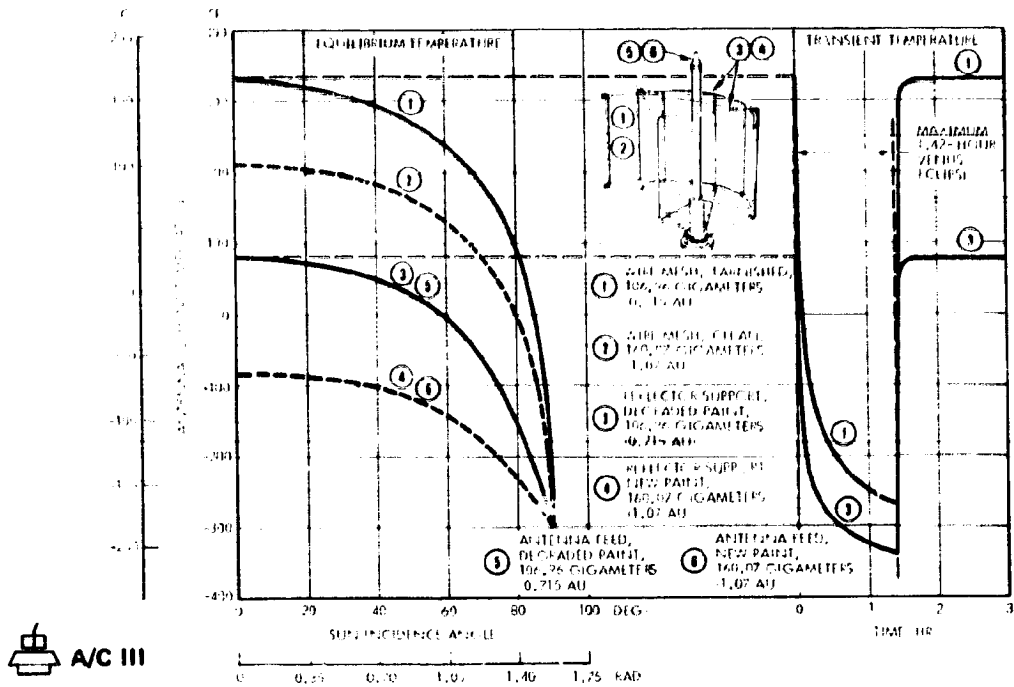
A/C III





T/D III

DESCRIPTION	PURPOSE	SURFACE THERMAL PROPERTIES				
		INSIDE		OUTSIDE		
		NEW	DEG	NEW	DEG	
13G WHITE PAINT ON EXTERNAL SURFACES OF REFLECTOR	MINIMIZE ABSORBED SOLAR AND ALBEDO HEAT INPUT TO REDUCE VARIATION IN TEMPERATURE DURING MISSION. LOCATION ENSURES SOLAR HEATING THROUGHOUT MISSION TO MAINTAIN TEMPERATURES ABOVE SURROUNDINGS			0.24	0.39	0.88
13G WHITE PAINT ON EXTERNAL SURFACES OF REFLECTOR	MINIMIZE ABSORBED SOLAR AND ALBEDO HEAT INPUT TO REDUCE VARIATION IN TEMPERATURE DURING MISSION. LOCATION ENSURES SOLAR HEATING THROUGHOUT MISSION TO MAINTAIN TEMPERATURES ABOVE SURROUNDINGS			0.24	0.39	0.88
13G WHITE PAINT ON EXTERNAL SURFACE OF REFLECTOR	MINIMIZE ABSORBED SOLAR AND ALBEDO HEAT INPUT TO REDUCE VARIATION IN TEMPERATURE AND REFLECTOR DISTORTION DURING MISSION			0.24	0.39	0.88
13G WHITE PAINT ON EXTERNAL SURFACE OF REFLECTOR	MINIMIZE ABSORBED SOLAR AND ALBEDO HEAT INPUT TO REDUCE VARIATION IN TEMPERATURE AND REFLECTOR DISTORTION DURING MISSION			0.24	0.39	0.88
13G WHITE PAINT ON EXTERNAL SURFACE OF REFLECTOR	MINIMIZE ABSORBED SOLAR AND ALBEDO HEAT INPUT TO REDUCE VARIATION IN TEMPERATURE AND REFLECTOR DISTORTION DURING MISSION			0.24	0.39	0.88
BLACK VELVET PAINT ON BACK SURFACE OF SUBSTRATE	MAXIMIZE RADIANT HEAT TRANSFER FROM BACK SURFACE OF SOLAR ARRAY		0.90	0.86	0.80	0.80
2-MIL ALUMINIZED TEFLON (ALUMINIZED SIDE FACING) STYED TO ONE 2-MIL INNER LAYER OF CLEAR MYLAR	SHIELD BACK SIDE OF SOLAR ARRAY FROM DIRECT SOLAR AND ALBEDO IMPINGEMENT. PROVIDE LOW TEMPERATURE BOUNDARY (LOW ϵ) TO MAXIMIZE HEAT TRANSFER FROM BACK SURFACE OF SOLAR ARRAY		0.66	0.10	0.15	0.66
2-MIL ALUMINIZED MYLAR SANDWICHED BETWEEN ONE OUTER 2-MIL TEFLON AND ONE INNER 2-MIL ALUMINIZED MYLAR COVER SHEET (ALL FACES FAC. COMPARTMENT)	MINIMIZE SOLAR AND ALBEDO HEAT LEAK INTO AND UNCONTROLLED HEAT LEAKS OUT OF THE DMA COMPARTMENT			0.45	0.50	0.69
13G WHITE PAINT ON DMA COMPARTMENT RADIATOR SURFACE	MAINTAINS DMA WITHIN ACCEPTANCE TEMPERATURE LIMITS			0.24	0.39	0.88
TOTAL BLADE AREA EMITTANCE = 0.20 FULL CLOSED AT 4°C (40°F) EMITTANCE = 0.74 FULL OPEN AT 29°C (85°F) 13G WHITE PAINT ON PLATFORM UNDER LOUVERS	CONTROL EQUIPMENT COMPARTMENT HEAT LEAKS TO OFFSET THE VARIATION IN EQUIPMENT AND ENVIRONMENTAL HEAT INPUT EXPERIENCED DURING THE MISSION TO MAINTAIN COMPONENT TEMPERATURES WITHIN ACCEPTABLE LIMITS			0.50	0.50	0.20 CLOSED 0.74 OPEN
2-MIL ALUMINIZED MYLAR SANDWICHED BETWEEN ONE OUTER 2-MIL TEFLON AND ONE INNER 2-MIL ALUMINIZED MYLAR COVER SHEET (ALL FACES EXCEPT INSIDE COVER SHEET FACE INWARD)	MINIMIZE SOLAR AND ALBEDO HEAT LEAK INTO AND UNCONTROLLED HEAT LEAKS OUT OF THE EQUIPMENT COMPARTMENT. STABLE ALUMINIZED KAPTON MINIMIZES EXTERNAL SURFACE PROPERTY DEGRADATION		0.69	0.45	0.50	0.69
2-MIL ALUMINIZED MYLAR SANDWICHED BETWEEN TWO 2-MIL TEFLON COVER SHEETS (ALL ALUMINIZED SURFACES EXCEPT AFT COVER SHEET)	MINIMIZE UNCONTROLLED HEAT LEAKS INTO AND OUT OF THE EQUIPMENT COMPARTMENT AND THERMALLY DECOUPLE COMPARTMENT FROM SOLAR ARRAY		0.69			0.69
2-MIL ALUMINIZED MYLAR SANDWICHED BETWEEN ONE OUTER 2-MIL TEFLON AND ONE INNER 2-MIL ALUMINIZED MYLAR COVER SHEETS (ALL FACES FACE FORWARD)	MINIMIZE UNCONTROLLED HEAT LEAKS OUT OF THE EQUIPMENT COMPARTMENT. MINIMIZE SOLID MOTOR PLUME RADIANT HEAT INPUT TO EQUIPMENT COMPARTMENT. STABLE ALUMINIZED KAPTON MINIMIZES EXTERNAL SURFACE PROPERTY DEGRADATION			0.45	0.50	0.69
13G BLACK VELVET PAINT ON EQUIPMENT PLATFORM AND HEAT SHIELD	EQUALIZE TEMPERATURE GRADIENTS WITHIN EQUIPMENT COMPARTMENT BY MAXIMIZING RADIATIVE THERMAL COUPLING BETWEEN STRUCTURE AND HEAT DISSIPATING COMPONENTS					0.90
13G BLACK VELVET PAINT ON EQUIPMENT PLATFORM AND HEAT SHIELD	MINIMIZE UNCONTROLLED HEAT LEAKS INTO AND UNCONTROLLED HEAT LEAKS OUT OF THE EQUIPMENT COMPARTMENT. THERMALLY DECOUPLE ZERO HEAT DISSIPATING COMPONENTS FROM SURROUNDING TO MINIMIZE TEMPERATURE VARIATIONS DURING TRANSIENT ENVIRONMENTAL CONDITIONS					0.10
13G BLACK VELVET PAINT ON EQUIPMENT PLATFORM AND HEAT SHIELD	MINIMIZE COMPONENT TO EQUIPMENT PLATFORM TEMPERATURE GRADIENTS TO MINIMIZE MAXIMUM COMPONENT TEMPERATURE ABOVE SURROUNDINGS					0.10
13G BLACK VELVET PAINT ON EQUIPMENT PLATFORM AND HEAT SHIELD	MINIMIZE UNCONTROLLED THRUSTER HEAT LEAK TO SPACE			0.12	0.12	0.05
13G BLACK VELVET PAINT ON EQUIPMENT PLATFORM AND HEAT SHIELD	MINIMIZE TEMPERATURE GRADIENTS IN SUPPLY LINES AND HEAT LEAKS INTO OR OUT OF THRUSTER AND LINES					0.05
13G BLACK VELVET PAINT ON EQUIPMENT PLATFORM AND HEAT SHIELD	MAINTAINS THRUSTER AND SUPPLY LINE TEMPERATURES ABOVE MINIMUM TEMPERATURE LIMITS					0.05
13G BLACK VELVET PAINT ON EQUIPMENT PLATFORM AND HEAT SHIELD	ISOLATES THRUSTER FROM STRUCTURE TO MINIMIZE HEATER POWER REQUIREMENT					0.05
13G BLACK VELVET PAINT ON EQUIPMENT PLATFORM AND HEAT SHIELD	RADIATIVELY DECOUPLE CONE FROM SOLAR ARRAY AND FORWARD SHIELD		0.05			0.05
2-MIL ALUMINIZED KAPTON SANDWICHED BETWEEN TWO 2-MIL ALUMINIZED MYLAR COVER SHEETS (ALUMINIZED SURFACES FACE INWARD)	MINIMIZE UNCONTROLLED HEAT LEAKS FROM SOLID MOTOR TO MAINTAIN MOTOR WITHIN ACCEPTABLE TEMPERATURE LIMITS PRIOR TO FIRING. MINIMIZE UNCONTROLLED HEAT LEAKS FROM THE EQUIPMENT COMPARTMENT. MINIMIZE SOLID MOTOR RADIANT HEAT/BACK TO EQUIPMENT COMPARTMENT AFTER MOTOR FIRING. KAPTON REQUIRED TO PREVENT DEGRADATION OF INSULATION THERMAL PROPERTIES DUE TO HEAT/BACK FROM MOTOR CASE		0.69			0.05
2-MIL ALUMINIZED KAPTON SANDWICHED BETWEEN TWO 2-MIL ALUMINIZED MYLAR COVER SHEETS (ALUMINIZED SURFACES FACE FORWARD)	MINIMIZE UNCONTROLLED HEAT LEAKS FROM SOLID MOTOR TO MAINTAIN MOTOR WITHIN ACCEPTABLE TEMPERATURE LIMITS PRIOR TO FIRING. NOZZLE CAP IS JETISONED WHEN MOTOR FIRES		0.05	0.45	0.50	0.69
2-MIL ALUMINIZED MYLAR SANDWICHED BETWEEN ONE OUTER 2-MIL TEFLON AND ONE INNER 2-MIL ALUMINIZED MYLAR COVER SHEETS (ALL FACES FACE INWARD)	MINIMIZE SOLAR AND ALBEDO HEAT LEAK INTO AND UNCONTROLLED HEAT LEAKS OUT OF THE SENSOR ASSEMBLY. STABLE ALUMINIZED KAPTON MINIMIZES EXTERNAL SURFACE PROPERTY DEGRADATION			0.45	0.50	0.69
13G WHITE PAINT ON EXTERNAL SURFACES OF OMNI ANTENNA	MINIMIZE ABSORBED SOLAR AND ALBEDO HEAT INPUT TO REDUCE VARIATION IN TEMPERATURE DURING MISSION. LOCATION ENSURES SOLAR HEATING THROUGHOUT MISSION TO MAINTAIN TEMPERATURES ABOVE SURROUNDINGS			0.24	0.39	0.88

Figure 8.7-15. Optional Despin Reflector Orbiter Spacecraft Thermal Control System Description



 A/C III
 T/D III

ELEMENTS OF THE REFLECTOR ASSEMBLY CAN HAVE SIGNIFICANT TEMPERATURE DIFFERENCES THAT COULD DISTURB THE REFLECTION. THE STRUCTURE WILL BE DESIGNED TO LIMIT THESE TEMPERATURE-INDUCED DISTORTIONS TO ACCEPTABLE LEVELS.

Figure 8.7-16. Optional Orbiter Despun Reflector Spacecraft Thermal Performance

Centaur configurations except for the transmitter temperature. When the higher power transmitter units are mounted to the standard honeycomb equipment platform, excessively high temperatures will result. Therefore, it is necessary in this design to provide a thermal fin insert to the platform as described in Section 8.7.5.3 to reduce the transmitter upper operating temperature to acceptable levels.

8.7.5 Tradeoffs ALL PROBE CONFIGURATIONS

Three basic tradeoff studies were performed to select the most economical and reliable thermal control system design. These studies are described in the following sections.

8.7.5.1 Methods of Accommodating Power Variations

Table 8.7-1 compares the advantages and disadvantages of three control methods that can be used to accommodate component and environmentally-induced power variations within the spacecraft equipment compartment. The louvers, heat pipes, and heaters will maintain acceptable

Table 8.7-1. Comparison of Three Thermal Control Methods to Accommodate Component and Environmentally Induced Power Variations

SYSTEM	ADVANTAGES	DISADVANTAGES
LOUVERS (HELIOS TYPE)	<ul style="list-style-type: none"> • FLIGHT PROVEN • OPERATING TEMPERATURE RANGE SELECTABLE • INHERENT REDUNDANCY 	<ul style="list-style-type: none"> • WIDE ACTIVATION TEMPERATURE RANGE
HEAT PIPES (VARIABLE CONDUCTANCE TYPE)	<ul style="list-style-type: none"> • CLOSE CONTROL OF EQUIPMENT TEMPERATURE DURING THE MISSION • POSSIBLE REDUCTION OF UNIT AND SPACECRAFT ACCEPTANCE TESTING • OPERATING TEMPERATURE RANGE SELECTABLE (PRIOR TO INTEGRATION) 	<ul style="list-style-type: none"> • REQUIRES REDUNDANCY • MIGHT AFFECT SPACECRAFT DYNAMIC BALANCE AT HIGH SPIN RATES • CONSTRAINS SPACECRAFT SOLAR SIMULATION THERMAL VACUUM TESTS
ELECTRIC HEATERS (PROPORTIONAL TYPE)	<ul style="list-style-type: none"> • CLOSE CONTROL OF EQUIPMENT TEMPERATURE DURING THE MISSION • POSSIBLE REDUCTION OF UNIT AND SPACECRAFT ACCEPTANCE TESTING • OPERATING TEMPERATURE RANGE SELECTABLE (PRIOR TO INTEGRATION) • SHUNT SIZE MIGHT BE REDUCED 	<ul style="list-style-type: none"> • REQUIRES LARGER BATTERY FOR ECLIPSE OPERATION • MIGHT REQUIRE SLIGHTLY LARGER ARRAY • REQUIRES ADDITIONAL SWITCHING CAPABILITY • REQUIRES REDUNDANCY

component temperatures throughout the mission, with the heat pipe system providing the best control. The electric heaters offer the most versatile system since they can be controlled by ground command. However, both the heat pipe and heater systems are less adaptable to design changes during the spacecraft development phase. This is because heat pipes have to be integrated into the mounting platform during its fabrication early in the program, and the heater wire routing affects the spacecraft harness design. Slight modifications can be made in both systems at a later date, but with much more program impact than needed for a louver change. Louver assemblies can be repositioned easily by bonding new screw inserts into the platform.

The program costs of all three systems are substantially the same. This is due to the fact that the heater system requires a larger array and additional command capability, and the heat pipe system complicates the performance and evaluation of thermal/vacuum tests. In addition, since most spacecraft black boxes have been previously qualified to a much

wider temperature range the potential component unit cost savings derived from the heat pipe or electric heater systems are not realized. Therefore the louver system was selected because it is flight proven, adaptable to late modifications in both temperature actuation range and platform location, by design has inherent redundancy, and does not constrain spacecraft solar simulation and thermal vacuum testing.

8.7.5.2 Influence of Large Probe on Thermal Control System Design

The thermal control system design for the probe bus spacecraft is largely dependent upon large probe temperature control since the equipment compartment and small probes are isolated from the solar environment. Table 8.7-2 lists the primary advantages, disadvantages, and characteristics of seven thermal control methods that were considered to maintain acceptable large probe temperatures.

Systems 1 through 5 were considered first at the time this tradeoff was performed to maintain similarity of the spin axis with the Thor/Delta orbiter spacecraft. The first two systems were the most simple, but did not meet the design requirements. Initially, System 2 required a heater power output of 27 watts near earth. Subsequent probe insulation tests reduced this value to 15 watts, a dissipation still too great for the current Thor/Delta configuration. The Atlas/Centaur design could support this requirement and this system is considered an alternate for that configuration.

A multilayer or high absorptance/emittance ratio cover that is jettisoned prior to large probe release is utilized in Systems 3 and 4. These systems will maintain acceptable temperatures, but add weight and complexity to the design. In System 5 the large probe is raised above the array so that it is fully exposed to the sun. This system is considered unacceptable because it strongly influences the probe thermal surfaces and produces a dynamic instability of the spacecraft.

Systems 6 and 7 use variable solar aspect angle control to maintain acceptable large probe temperatures. These systems were the most attractive from overall spacecraft design considerations, particularly the Thor/Delta configuration. A summary of the system characteristics is presented in Table 8.7-3.

Table 8.7-2. Thermal Control Method Characteristics

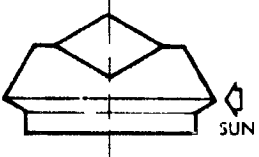
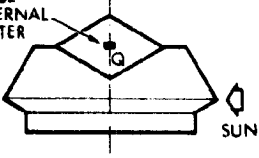
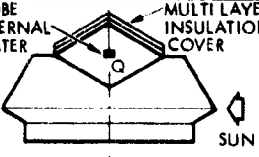
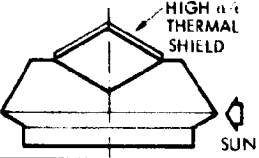
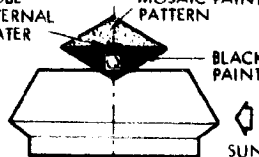
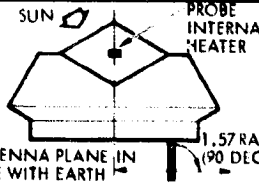
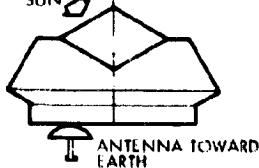
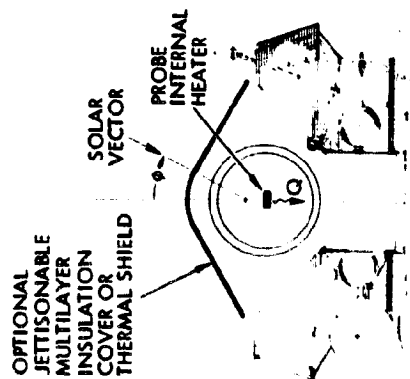


SYSTEM	DESCRIPTION	SOLAR ASPECT ANGLE (FROM SPIN AXIS)	ADVANTAGES	DISADVANTAGES
1. UNHEATED LARGE PROBE		1.57 RAD (90 DEG)	<ul style="list-style-type: none"> • LARGE PROBE HEATER NOT REQUIRED • OPERATES NORMAL TO VOP • MINOR PROBE THERMAL INTERFACE 	<ul style="list-style-type: none"> • EXCESSIVELY LOW LARGE PROBE TEMPERATURE LEVEL (-65°C (-85°F))
2. HEATED LARGE PROBE	PROBE INTERNAL HEATER 	1.57 RAD (90 DEG)	<ul style="list-style-type: none"> • SIMPLE SYSTEM • MINOR PROBE THERMAL INTERFACE • OPERATES NORMAL TO VOP 	<ul style="list-style-type: none"> • REQUIRES LARGE PROBE HEATER (15 WATTS NEAR EARTH) • REQUIRES HEATER CONTROL
3. INSULATED LARGE PROBE	PROBE INTERNAL HEATER MULTI LAYER INSULATION COVER 	1.57 RAD (90 DEG)	<ul style="list-style-type: none"> • ACCEPTABLE POWER LEVEL • OPERATES NORMAL TO VOP • MINOR PROBE THERMAL INTERFACE 	<ul style="list-style-type: none"> • REQUIRES LARGE PROBE HEATER • REQUIRES JETTISONABLE COVER • ADDED WEIGHT AND COMPLEXITY • REQUIRES HEATER CONTROL
4. THERMAL SHIELD OVER LARGE PROBE	HIGH THERMAL SHIELD 	1.57 RAD (90 DEG)	<ul style="list-style-type: none"> • LARGE PROBE HEATER NOT REQUIRED • OPERATES NORMAL TO VOP • NO PROBE THERMAL INTERFACE 	<ul style="list-style-type: none"> • REQUIRES JETTISONABLE COVER • ADDED WEIGHT AND COMPLEXITY
5. EXPOSED LARGE PROBE	PROBE INTERNAL HEATER MOSAIC PAINT PATTERN BLACK PAINT 	1.57 RAD (90 DEG)	<ul style="list-style-type: none"> • OPERATES NORMAL TO VOP 	<ul style="list-style-type: none"> • REQUIRES LARGE PROBE HEATER (9 WATTS NEAR EARTH) • REQUIRES HEATER CONTROL • MAJOR DYNAMICS IMPACT • MAJOR PROBE INTERFACE
6. SPIN AXIS ⊥ TO EARTH LINE	SUN PROBE INTERNAL HEATER ANTENNA PLANE IN LINE WITH EARTH 1.57 RAD (90 DEG) 	VARIABLE SUN ANGLE	<ul style="list-style-type: none"> • ACCEPTABLE HEATER POWER LEVEL • MINOR PROBE THERMAL INTERFACE 	<ul style="list-style-type: none"> • REQUIRES LARGE PROBE HEATER • REQUIRES HEATER CONTROL • REQUIRES ASPECT CONTROL BY GROUND COMMAND
7. MODIFIED EARTH POINTER RECOMMENDED SYSTEM	SUN ANTENNA TOWARD EARTH 	VARIABLE SUN ANGLE	<ul style="list-style-type: none"> • LARGE PROBE HEATER NOT REQUIRED • MINOR PROBE THERMAL INTERFACE 	<ul style="list-style-type: none"> • REQUIRES ASPECT CONTROL BY GROUND COMMAND

Table 8.7-3 Large Probe Thermal Control Systems for Transit Phase

SYSTEM	SOLAR ASPECT ANGLE PHASE [RAD (DEG)]	HEATER REQUIRED	DEPLOYABLE SHIELD	SYSTEM PERFORMANCE		REMARKS
				ACCEPTABLE	UNACCEPTABLE	
1. UNHEATED PROBE	1.57 (90)				X	TOO COLD [-60°C (-85°F)]
2. HEATED PROBE	1.57 (90)	X		X ^A	X ^B	REQUIRES HEATER (15 WATTS NEAR EARTH)
3. INSULATION COVER	1.57 (90)	X	X	X		ADDED WEIGHT AND COMPLEXITY
4. THERMAL SHIELD	1.57 (90)		X	X		ADDED WEIGHT AND COMPLEXITY
5. EXPOSED PROBE	1.57 (90)	X			X	LARGE OPERATING TEMPERATURE RANGE
6. MODIFIED EARTH POINTER		X		X		HEATER POWER REQUIRED BETWEEN 50 AND 100 DAYS
7. EARTH POINTER	VARIABLE			X		RECOMMENDED DESIGN

A. FOR ATLAS/CENTAUR CONFIGURATION
 B. FOR THOR/DELTA CONFIGURATION



8.7.5.3 Transmitter Heat Distribution System  

The fanbean and fanscan antenna system for the optional 31-watt Thor/Delta orbiter mission spacecraft would increase the transmitter power density to a point where a special heat distribution thermal fin would be required for transmitter mounting. This fin could be fabricated of a solid piece of aluminum or designed to use heat pipes to distribute the energy. The heat pipe system is less than half the weight of the solid metal plate, but compromises spacecraft solar simulation tests. Valid tests can be performed only when the heat pipes, bonded in the equipment mounting platform, are kept horizontal throughout the test. The weight of an aluminum thermal fin appears to be acceptable for the optional Thor/Delta configuration. If weight reduction is required at a later date the heat pipe fin could be used with the resultant test constraints.

8.8 Structure and Mechanisms

8.8 STRUCTURE AND MECHANISMS

The structure and mechanisms subsystem includes the spacecraft primary and secondary structure as well as its mechanisms. These include: 1) large and small probe retention and separation systems; 2) the magnetometer boom; 3) the nutation damper; and 4) miscellaneous deployment springs and initiators for deploying the radar altimeter, electron temperature probe, and ultraviolet fluorescence grating.

Figure 8.8-1 summarizes the key features of the subsystem. It includes information on both the probe bus and the orbiter.

The remainder of the section provides further detail on the design.

8.8.1 Structural Subsystem

Various spacecraft configurations studied were identified in Section 5.2. Since there is great structural commonality between all the configurations, only one is shown in this section. Further, since the structural configurations for the probe bus and orbiter are fundamentally identical, the probe bus design is discussed primarily, because it is much heavier and represents the more critical of the two vehicles. Where differences exist between the structures for the various configurations and the two launch vehicles, they are described.

8.8.1.1 Design Requirements

The design loads and flight environments of Section 5.2 provide the basic structural design requirements for the spacecraft. From a structural viewpoint, there are two basic differences in the design conditions between the probe bus and the orbiter:

- 1) The probe bus is approximately 30 percent heavier than the orbiter.
- 2) The orbiter is subjected to a deboost into Venus orbit; the probe bus is not.

8.8.1.2 Structural Description

The spacecraft structure consists of four primary elements: 1) the central cylinder, 2) the equipment platform, 3) the truss support system, and 4) the solar array substrate and ring supports. The structure uses conventional aluminum alloys and attachment techniques. (A beryllium

central cylinder is required for the two Thor/Delta spacecraft structures.) Each of the primary structural elements is described in the following paragraphs. Figure 8.8-1E shows the structural elements and illustrates the commonality between probe bus and orbiter. The figure is for Atlas/Centaur; Thor/Delta is similar.

Central Cylinder

The central cylinder is the basic building block for the spacecraft structure. The booster interface ring is attached to the aft end of the cylinder.

There are subtle changes in the size and function of the central cylinder related to its use as part of the probe bus or the orbiter:

- Probe Bus

Shorter than on orbiter

Forward end supports large probe, providing direct load path to booster interface for this large mass item

- Orbiter

Larger than on probe bus

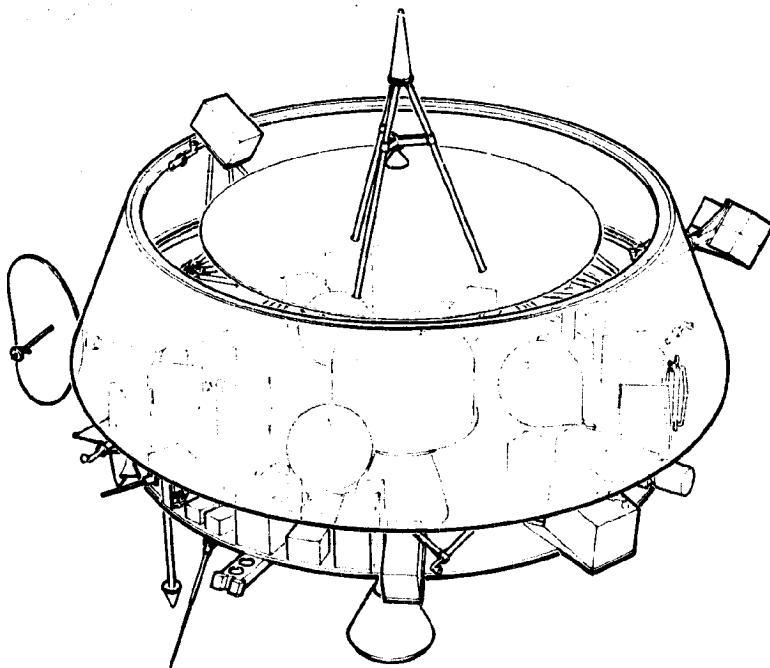
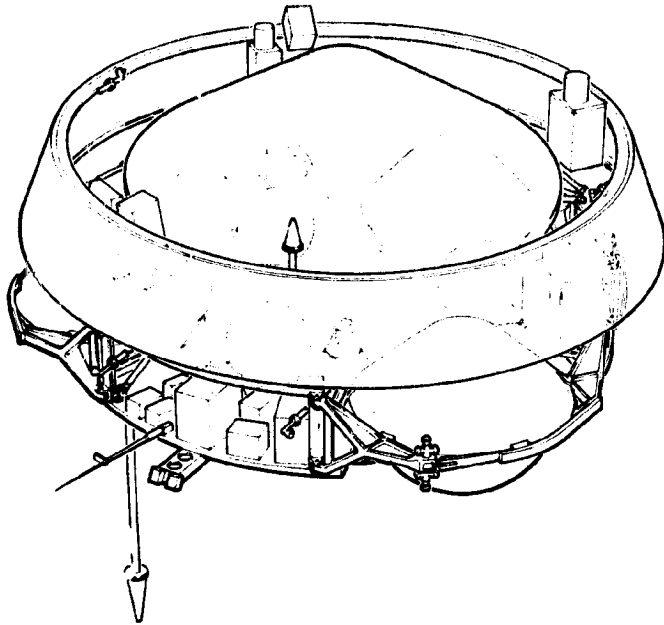
Conical forward adapter for DMA mounting for Option 3 spacecraft; extended length for preferred and Option 1 spacecraft

Internal ring to mount Venus orbit injection motor.

During the design study, various materials were evaluated for fabricating the central cylinder. Table 8.8-1 shows the gauges and weight differences for aluminum. For Atlas/Centaur, aluminum was selected. Based on weight, beryllium was chosen for Thor/Delta.

Equipment Platform

This sandwich annular panel provides the mounting surface for the majority of the spacecraft systems equipment and the science instrument components. The panel is sized to provide both adequate strength and stiffness to withstand the launch and flight loads and environments. It is 1.9 cm thick with 0.03-cm 2024-T81 aluminum alloy facesheets and 3.1-1/8-7P(5052) honeycomb core.



KEY DESIGN FEATURES

MAJOR STRUCTURE COMMONALITY BETWEEN PROBE BUS AND ORBITER
CONVENTIONAL MATERIALS AND FULLY PROVEN MANUFACTURING
TECHNIQUES USED THROUGHOUT

STRUCTURE IS DESIGNED TO FACILITATE INTEGRATION AND ACCESS
DURING TEST PHASES

TRUSS TUBES AND FITTINGS ARE DESIGNED TO MINIMIZE FABRICATION
COST WHILE MAINTAINING ABILITY TO HOLD OVERALL ALIGNMENT
AND TOLERANCES REQUIRED FOR INDIVIDUAL PARTS OF THE SPACECRAFT

STRUCTURE IS ARRANGED TO PROVIDE DIRECT LOAD PATHS FOR ALL
PRIMARY PAYLOADS (LARGE AND SMALL PROBES ON THE PROBE BUS
AND HIGH-GAIN ANTENNA AND ORBIT INSERTION MOTOR ON THE
ORBITER)

STRUCTURE IS CONFIGURED TO FACILITATE ACHIEVEMENT OF MASS
BALANCE AND FAVORABLE MOMENTS OF INERTIA RATIO

STRUCTURE IS ALSO CONFIGURED TO MAINTAIN AN ACCEPTABLE
CENTER-OF-GRAVITY SHIFT ON THE PROBE BUS DURING THE TOTAL
PROBE DEPLOYMENT SEQUENCE

PROBE RETENTION AND DEPLOYMENT SYSTEMS USE PROVEN TECH-
NIQUES AND PYROTECHNIC DEVICES

FULLY COMPATIBLE WITH THE ATLAS-CENTAUR BOOSTER SYSTEM

PRINCIPAL PHYSICAL CHARACTERISTICS

MASS ESTIMATES	PROBE BUS		ORBITER	
	KG	(LB)	KG	(LB)
PRIMARY SPACECRAFT (DRY)*	161.0	(355.0)	195.4	(430.9)
LARGE PROBE	263.6	(581.2)		
SMALL PROBES (3)	210.1	(463.2)		
SCIENCE	13.8	(30.3)	45.4	(100.1)
SOLAR ARRAY	8.2	(18.0)	14.2	(31.3)
HIGH-GAIN ANTENNA			3.3	(7.3)
ORBIT INSERTION MOTOR			163.2	(359.6)
DIMENSIONS	PROBE BUS		ORBITER	
	MM	(IN.)	MM	(IN.)
OVERALL HEIGHT	1575	62	2108	83
MAXIMUM DIAMETER	2616	103	2616	103

* LESS PROBES, SCIENCE AND/OR INSERTION MOTOR

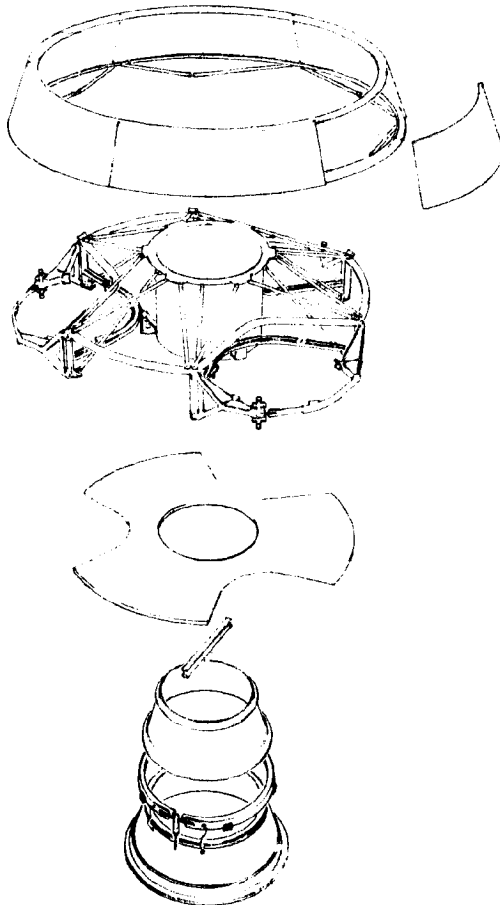
BASIS OF STRUCTURAL DESIGN

COMPONENT	PROPOSED MATERIALS AND FABRICATION TECHNIQUES	
	PROBE BUS	ORBITER
CENTRAL CYLINDER	ALUMINUM SHELL AND RINGS	SAME
TRUSS SYSTEM	ALUMINUM TUBES AND MACHINED ALUMINUM FITTINGS	SAME
EQUIPMENT PLATFORM	ALUMINUM HONEY- COMB SANDWICH (WITH CUTOUTS)	SAME
SOLAR ARRAY SUBSTRATES	ALUMINUM HONEY- COMB AND FACESHEETS	SAME (LARGER)
SMALL PROBE CONSTRAINT AND DEPLOYMENT SYSTEM	ALUMINUM MACHINED PLATE	--
HIGH-GAIN ANTENNA	--	FIBERGLASS FACESHELL/ ALUMINUM HONEYCOMB SANDWICH WITH FIBER- GLASS FELD STRUTS

RELIABILITY

OVERALL SUBSYSTEM RELIABILITY > 0.999

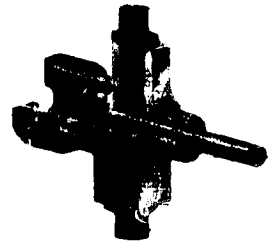
SUBSYSTEM DESIGN



MECHANISMS



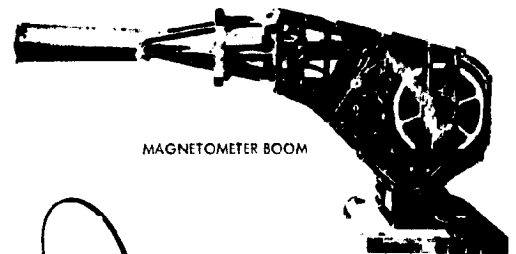
BALL LOCK



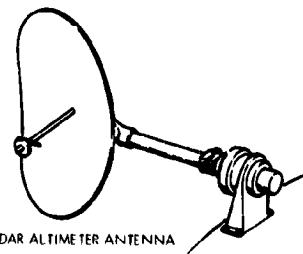
PIN PULLER



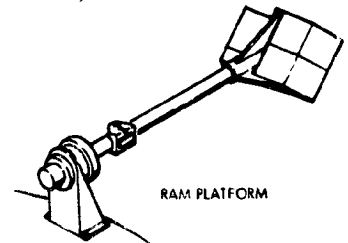
CABLE CUTTER



MAGNETOMETER BOOM



RADAR ALTIMETER ANTENNA



RAM PLATFORM

- ✓ BUS AND ORBITER
- ✓ MANUFACTURING
- ✓ COMMAND AND ACCESS
- ✓ PANEL FABRICATION
- ✓ ALL ALIGNMENT
- ✓ OF THE RADIOFREQ
- ✓ PATHS FOR ALL
- ✓ OF THE PROCBUS
- ✓ MOTOR ON THE
- ✓ ELEMENT OF MASS
- ✓ MATIC
- ✓ ACCEPTABLE
- ✓ TING THE TOTAL
- ✓ PROVEN TECH-
- ✓ SYSTEM

BUS	ORBITER
(LBS.)	(LBS.)
1355.0	195.4
1581.2	420.9
1463.2	
130.3	40.4
118.0	14.2
	3.2
	163.2
101.1	101.1
52	1103
103	1635

MATERIALS AND TECHNIQUES

ORBITER

SAME

SAME

SAME

SAME

(LARGER)

- ✓ GLASS FACESHIELD
- ✓ ALUMINUM HONEYCOMB
- ✓ SANDWICH WITH FIBER-
- ✓ GLASS FIBER STRUTS

Figure 8.8-1. Structure and Mechanisms Subsystem Summary

Table 8.8-1. Thor/Delta Central Cylinder
Material Tradeoff

MATERIAL	ρ (KG/M ³)	E (KG/M ²)	t (CM)	WEIGHT (KG)	Δ WEIGHT RELATIVE TO ALUMINUM (KG)
ALUMINUM	2768	703×10^7	0.102	2.62	0
MAGNESIUM	1771.5	457×10^7	0.127	2.10	-0.53
BERYLLIUM	1854.6	2988×10^7	0.051	0.853	-1.77
TITANIUM	4428.8	1153×10^7	0.076	3.266	+0.64

For the orbiter, the platform is essentially complete. On the probe bus, cutouts are required to accommodate the three small probes which penetrate below the level of the platform.

Truss Support System

The truss support system consists of tubes, rings, and vertical tee members.

The smaller diameter center ring forms the top closure to the central cylinder; the outer ring provides a frame for tying together the upper solar array support struts.

Diagonal struts from the lower end of the outboard verticals to the forward central cylinder ring support the outer edge of the equipment platform.

The vertical tee section members at the outer periphery of the equipment panel react the axial loads from the solar array and support the small probe support yokes. They also mount the pivoting frames for retention and release of the small probes and their thermal covers.

The nearly horizontal tubular truss members joining the inner and outer rings shown in Figure 8.8-1E react the torsional and lateral shear loads from the solar array. In addition, they provide a forward equipment compartment thermal closure support system.

Solar Array Substrate and Ring Supports

The solar array substrate is honeycomb sandwich (0.95-cm-thick core with 0.020-cm-thick aluminum facesheets) formed into conical frustum sections as shown. These panels will attach to end rings, as shown, to tie them physically together.

8.8.2 Structural and Dynamic Analyses

8.8.2.1 Structural Analysis

An analytical model of the Thor/Delta probe bus configuration was defined for use with the Structural Static Analysis Program (SSAP).

Figure 8.8-2 shows the plane, side, and isometric views of this model.

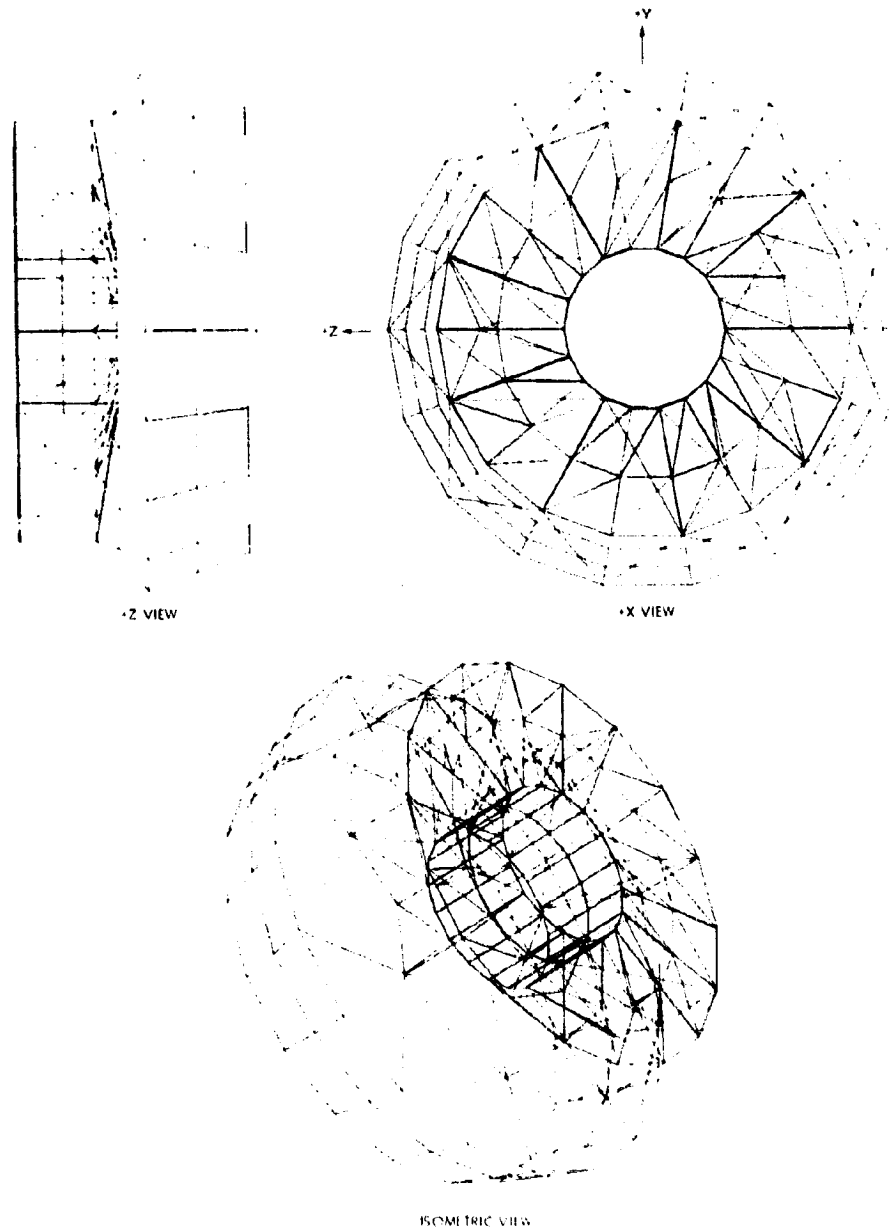


Figure 8.8-2. Computer Printout, Pioneer Venus Probe Bus

This model and program are used to determine the internal member loads within the structure when subjected to various static or pseudo-static design loading conditions.

With the internal member loads identified, the structural integrity of the spacecraft is confirmed by detailed stress analysis. Table 8.8-2 is a weight breakdown used to distribute the masses on the structure, and Table 8.8-3 presents the summary of minimum margins of safety for the critical members within the structure.

Table 8.8-2. Weight Breakdown for Analytical Model

MAJOR ASSEMBLY	COMPONENT	WEIGHT		SUBTOTAL WEIGHT	
		(KG)	(LB)	(KG)	(LB)
SOLAR ARRAY	UPPER RING	1.27	(2.80)		
	LOWER RING	1.36	(3.00)		
	BALANCE WEIGHTS	1.81	(4.00)		
	THRUSTERS	0.54	(1.20)		
	SOLAR ARRAY	6.21	(13.70)		
	STRUTS (1/2)	0.52	(1.15)		
	FORWARD OMNI AND SUPPORT	0.27	(0.60)	12.0	(26.45)
LARGE PROBE RING (STATION 119.75)	LARGE PROBE	158.98	(350.50)		
	RING WEIGHT	2.31	(5.10)		
	ATTACHMENT HARDWARE	0.14	(0.30)		
	TOP STRUTS (1/2)	0.59	(1.30)		
	DIAGONAL STRUTS (1/2)	0.41	(0.90)		
	PROBE SUPPORT AND RELEASE (LARGE)	3.63	(8.00)	166.06	(366.10)
RING (STATION 116.00)	RING	1.68	(3.70)		
	ATTACHMENT HARDWARE	0.09	(0.20)		
	VERTICALS (1/2)	0.70	(1.55)		
	SOLAR STRUTS (1/2)	0.52	(1.15)		
	THRUSTERS	1.09	(2.40)		
	TOP STRUTS (1/2)	0.59	(1.30)	4.67	(10.30)
PLATFORM OUTER RING (STATION 103.625)	FITTINGS AND ATTACHMENT HARDWARE	0.36	(0.80)		
	VERTICALS (1/2)	0.70	(1.55)		
	THRUSTERS	0.55	(1.20)		
	DIAGONAL STRUTS (1/2)	0.41	(0.90)	2.02	(4.45)
EQUIPMENT PLATFORM	PLATFORM	7.85	(17.30)		
	ATTACHMENT HARDWARE	0.14	(0.30)		
	EQUIPMENT TIEDOWN	1.36	(3.00)		
	SCIENCE	5.90	(13.00)		
	MAGNETOMETER BOOM ASSEMBLY	2.04	(4.50)		
	SCIENCE SUPPORT BRACKETS	2.27	(5.00)		
	MISCELLANEOUS BRACKETS	0.91	(2.00)		
	WOBBLE DAMPER	1.81	(4.00)		
	ANTENNA AND SUPPORT	1.13	(2.50)		
	PLATFORM-MOUNTED EQUIPMENT	51.25	(113.00)	74.66	(164.60)
				0.64	(1.40)
PROPULSION AND PROBES	OMNI ANTENNA	0.41	(0.90)		
	OMNI SUPPORT	0.23	(0.50)		
	SMALL PROBES (3)	77.70	(171.30)		
	SMALL PROBE SUPPORTS (3)	1.72	(3.80)		
	TANKS (3)	2.54	(5.60)		
CENTRAL CYLINDER	PROPELLANT (3)	25.85	(57.00)		
	PROPELLANT SUPPORT ASSEMBLIES (3)	2.27	(5.00)	110.08	(242.70)
CENTRAL CYLINDER	CENTRAL CYLINDER	2.22	(4.90)		
	SEPARATION RING	3.36	(7.40)		
	MEDIUM-GAIN ANTENNA	0.45	(1.00)		
	MEDIUM-GAIN ANTENNA SUPPORT	0.23	(0.50)	6.26	(13.80)
TOTAL	(DISTRIBUTE - MOSTLY LOUVERS)	8.71	(19.20)	8.71	(19.20)
TOTAL				385.1	(849.00)

Table 8.8-3. Minimum Margins of Safety
(Thor/Delta Probe Bus)

STRUCTURAL COMPONENT	CRITICAL LOAD CONDITION	FAILURE MODE	MARGIN OF SAFETY*	REMARKS
CENTRAL CYLINDER	THIRD-STAGE BURNOUT	SHELL BUCKLING	0.15	BERYLLIUM
EQUIPMENT PLATFORM	THIRD-STAGE BURNOUT	FACESHEET WRINKLING	0.34	$F_N = 34$ HZ
VERTICAL TEE STRUTS	9.42 RAD/S (90 RPM) SPIN	BUCKLING	0.58	
TRUSS TUBES (PLATFORM)	AXIAL VIBRATION	STIFFNESS	LARGE	MINIMUM GAUGE AND SIZE TO KEEP $F_N > 35$ HZ
SOLAR ARRAY SUPPORT TRUSS	THIRD-STAGE BURNOUT	COLUMN	LARGE	MINIMUM GAUGE AND DIAMETER
SOLAR ARRAY LOWER RING	THIRD-STAGE BURNOUT	CRIPPLING	0.16	
LARGE PROBE SUPPORT	THIRD-STAGE BURNOUT	CRIPPLING	0.07	
SMALL PROBE SUPPORT YOKE	PROBE PRELOAD (LATERAL VIBRATION)	CRIPPLING	0.35	
OMNI ANTENNA MAST	LATERAL VIBRATION	STIFFNESS	LARGE	KEEP $F_{N,LAT} > 20$ HZ

*SEE MIL HDBK-5A

8.8.2.2 Dynamic Analysis

The structural analysis model of the Thor/Delta probe bus configuration described in Section 8.8.2.1 was modified and used to compute cantilevered natural frequencies and mode shapes. The modes were then used to compute response levels to the specified sinusoidal excitation at the spacecraft/booster interface (Section 5.2) over the frequency range 20 to 100 Hz. Modes and frequencies were computed for a 216-node model incorporating an 18-node mass and stiffness model of the large probe. The small probes were considered as rigid masses.

Results are presented in the form of a summary of frequencies and mode descriptions (Table 8.8-4), and peak response levels for selected nodes (Table 8.8-5).

The fundamental frequencies of 33 Hz lateral, 50 Hz axial are sufficiently high compared to the minimum frequencies specified (20 Hz lateral, 35 Hz axial) to preclude a strong dynamic interaction between the spacecraft and booster. As a result, the accuracy of the specified launch loads for primary structure will not be significantly affected by spacecraft flexibility. The natural frequencies of the large probe are high in comparison to the spacecraft and have a minimal effect on the overall spacecraft response characteristics.

Table 8.8-4. Summary of Thor/Delta Probe Bus Configuration Modes

MODE	FREQUENCY (HZ)	PREDOMINANT MOTION
1	39	LATERAL BENDING, ROCKING
2	40	LATERAL BENDING, ROCKING
3	50	AXIAL
4	56	LATERAL BENDING, ROCKING
5	61	LATERAL TORSION
6	63	LATERAL
7	66	LATERAL
8	69	LATERAL
9	77	PLATFORM BENDING
10	82	HIGHER MODES
11	82	HIGHER MODES
12	101	HIGHER MODES
13	103	HIGHER MODES
14	105	HIGHER MODES
15	106	LARGE PROBE AXIAL

Table 8.8-5. Summary of Predicted Response Levels for Sinusoidal Input at Booster Interface



LOCATION	DIRECTION	FREQUENCY (HZ)	INPUT LEVEL* (G)	PEAK RESPONSE (G, G PEAK)
SMALL PROBE, INBOARD ATTACH POINT	AXIAL	50	2.3	42
EDGE OF EQUIPMENT PLATFORM	AXIAL	50	2.3	22
LARGE PROBE, EQUIPMENT SHELF	AXIAL	105	2.3	22
LARGE PROBE, CONE/SKIRT INTERFACE	AXIAL	105	2.3	9
SMALL PROBE, INBOARD ATTACH POINT	LATERAL	82	1.5	10
LARGE PROBE	LATERAL	33	1.5	5-8

*NOTCHING TO BE APPLIED AT FUNDAMENTAL FREQUENCIES TO MORE REALISTICALLY SIMULATE FLIGHT LOADING

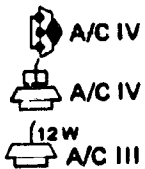
Thor/Delta Orbiter Configuration T/D III

The analysis was performed for the Thor/Delta probe bus configuration because it is the most critical from a structural weight and frequency standpoint. Because of the similarities in the structure and the weight distribution and because of the lower overall weight, the fundamental frequencies of the Thor/Delta orbiter configuration will be slightly higher than the probe bus, and peak response levels will be approximately the same.

The most significant difference will be the fanbeam antenna on the orbiter, which itself will have a fundamental frequency of approximately 10 Hz.

Atlas/Centaur Probe Bus and Orbiter Configuration

Fundamental frequencies for the Atlas/Centaur probe bus and orbiter configurations will be similar to the corresponding Thor/Delta configurations. This is due to the similarities in the structural configuration and the increased structural weight allocation, which compensates for the increased spacecraft weight and dimensions. Response levels will be approximately the same, since the spacecraft/booster input levels specified for Atlas/Centaur and Thor/Delta boosters are identical over the frequency range which contains the important modes.



8.8.3 Mechanisms

There are five primary mechanisms required on the probe bus:

- Large probe release system
- Small probe release system
- Probe electrical disconnects
- Magnetometer boom
- Nutation damper.



8.8.3.i Large Probe Release Mechanism

The single large centrally mounted probe is attached to the forward ring of the central cylinder by three equally spaced ball locks (Figure 8.8-3A). Each ball-lock mechanism uses a set of four spherical balls protruding from the shaft to engage a self-aligning notched bushing in the mating part. The drawing shows a cross section through the mating surfaces and the ball-lock assembly. The shaft reacts only tension loads at the probe-spacecraft interface. Shear loads are reacted by a recess in the spacecraft ring engaging a boss on the probe side of the interface. Compression loads are reacted directly from the probe inner shell to the support strut in bearing at the interface. Release is initiated by dual squibs generating pressure to drive the piston inside the ball-lock pin.

Outboard of each ball-lock is a separation spring housed in a retainer cup. A retaining pin in the cup which holds the spring in the compressed condition will permit ease of assembly to the underside of the support strut. The retaining pin is then removed after installation to allow the spring to bear against the probe push plate. The lower end of the spring will be permanently attached to the cup to prevent casting off as debris. The springs are designed for a 0.3 m/s (1 ft/s) separation velocity.

Table 8.8-6 shows the tradeoff study of different release schemes: three ball-lock configurations and one using bolt cutters. Design No. 2 was selected because of its light weight; it is pictured in Figure 8.8-3A.

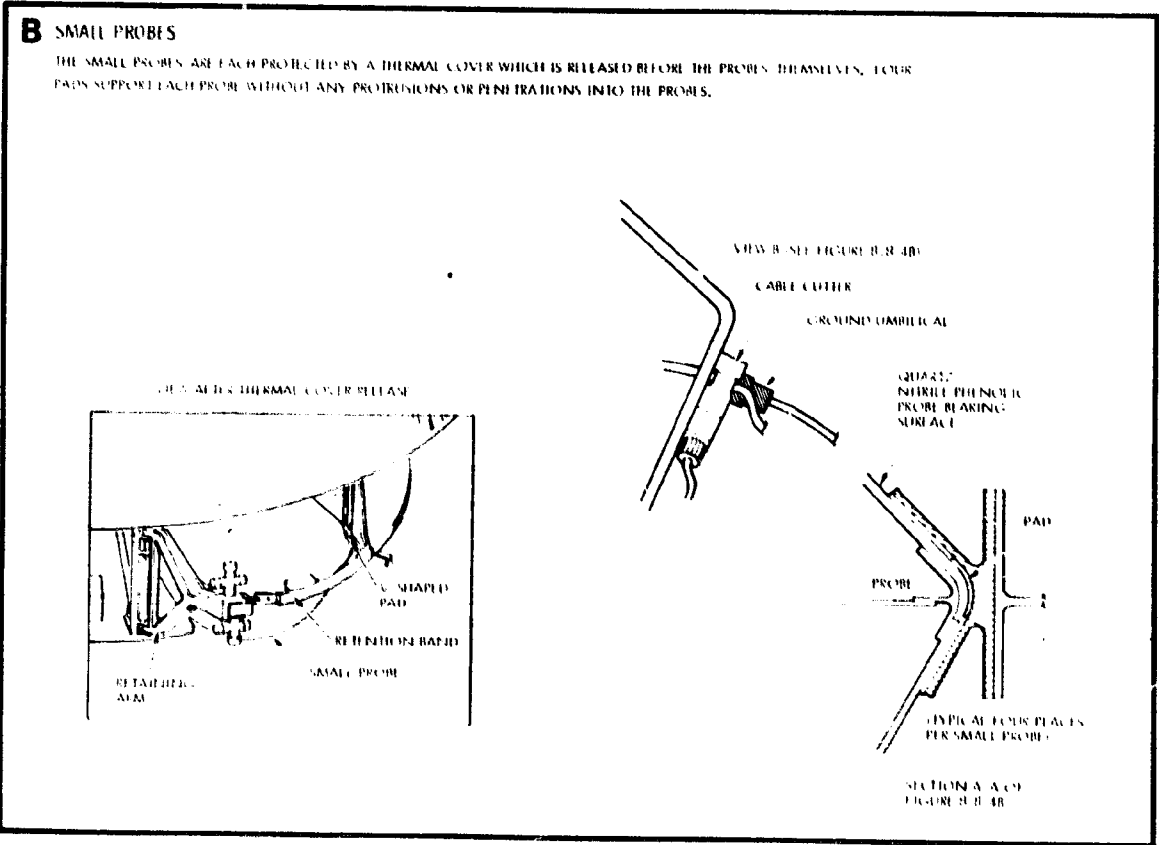
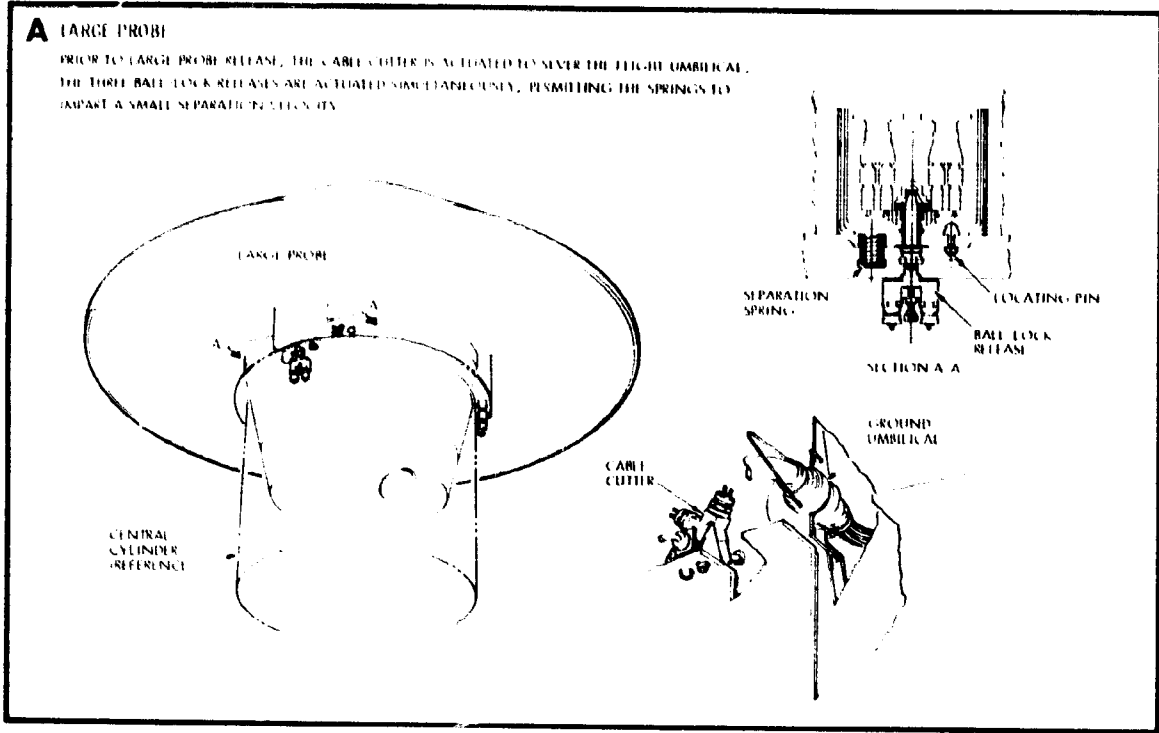


Figure 8.8.3. Probe/Bus Mechanical Interfaces

Table 8.8-6. Evaluation of Release Systems for Large Probe

DESIGN NO.	COMPONENTS	QUANTITY	UNIT WEIGHT (KG)	SUBSYSTEM WEIGHT (KG)	SYSTEM WEIGHT (KG)	REMARKS
1 (MANIFOLD SYSTEM)	BALL LOCKS	3	0.303	0.912	2.24	TUBE IS SINGLE-POINT FAILURE
	GAS GENERATIONS	2	0.240	0.481		
	ELECTROEXPLOSIVE DEVICE	4	0.009	0.036		
	PNEUMATIC LINE	(4 M)	0.240	0.240		
	ELECTRICAL DISCONNECT (G&H TECHNOLOGY, INC.)	1	0.572	0.572		
2 (INDEPENDENT SYSTEM)	BALL LOCKS	3	0.804	0.912	1.54	
	ELECTROEXPLOSIVE DEVICE	6	0.009	0.054		
	ELECTRICAL DISCONNECT (G&H TECHNOLOGY, INC.)	1	0.572	0.572		
3 (MILD DETONATING FUSE)	BALL LOCKS	3	0.304	0.912	2.68	
	MILD DETONATING FUSE (DUAL)	2	0.340	0.680		
	SHIELD CABLE	2	0	0.481		
	ELECTROEXPLOSIVE DEVICE	4	0.009	0.036		
	ELECTRICAL DISCONNECT (G&H TECHNOLOGY, INC.)	1	0.572	0.572		
4 (BOLT CUTTERS)	BOLT CUTTER	6	0.075	0.454	1.50	MAY REQUIRE 12 ELECTROEXPLOSIVE DEVICES
	RETAINER CAGE	6	0.002	0.014		
	ELECTROEXPLOSIVE DEVICE	6	0.009	0.054		
	ELECTRICAL DISCONNECT (G&H TECHNOLOGY, INC.)	1	0.572	0.572		
	SUPPORT BRACKET AND BOLT	3	0.136	0.408		

8.8.3.2 Small Probe Retention and Release Mechanism

The small probes are each supported on the probe bus with a mechanism to protect them during launch and transit environments, and to provide unperturbed initial conditions for their controlled release under pure centrifugal force (Figure 8.8-3B).

A thermal cover provides an acceptable thermal environment for the probes until shortly before probe release. The unperturbed initial conditions are attained by a two-step release process: first, the thermal cover is ejected, and at the same time the preload in the probe retention device is relieved. Then, after any spacecraft perturbations due to the first step settle down, the unpreloaded probes are released by the second step. Without any preload or other initial indeterminate forces, the initial release conditions are well known for use in accurate targeting computations.

Each small probe is held by four V-shaped pads positioned around the probe major diameter as shown in Figure 8.8-4B. The pads provide both vertical and lateral support for the probe during flight and before release. The two inboard pads are fixed to a rigid part of the spacecraft structure. Each of the two outboard pads is an integral part of a pivoting triangular frame member which is hinge-mounted at the longitudinal spacecraft tee members on each side of the probe. Torsion springs at their hinge lines force the free position of the pivoting frames to be away from the probe.

The two pivoting frames are joined around the outer major diameter of the probe by a band which effectively clamps the probe back against the two fixed inboard pads. A preload is applied to the band to prevent probe chatter during launch vibrations. This band is retained by two pin pullers which function in sequence to produce the two-step separation. The first of these pins also engages a lug which holds the thermal cover and its light framework in position around the probe and against the vertical tee members. Overlapping channels on the thermal cover and on the band provide vertical alignment of the cover, and also provide a push-off surface for leaf springs to effect cover separation at release.

The probe as retained in the spacecraft is depicted in Figure 8.8-3B, with the thermal cover removed for clarity. Also pictured is a view of the retention system pin pullers as they are engaged in the locked position (Figure 8.8-4A). A portion of the retention lug for the thermal cover is shown in the cutaway view. This lug is attached to the cover and is ejected with the cover as indicated in subsequent illustrations of the sequence of events.

The stowed position and deployment sequence is illustrated in Figures 8.8-4B and C. The stowed position is shown in Figure 8.8-4C, and the position of the lock pins with respect to the retention band for this condition is shown in Figure 8.8-4A.

The first sequence of deployment is shown in Figure 8.8-4A2, where pin puller No. 1 is actuated. The pin puller is actuated by dual (redundant) squibs which drive the piston of the pin puller assembly. The thermal closure lug is released, allowing the forces from the leaf springs as

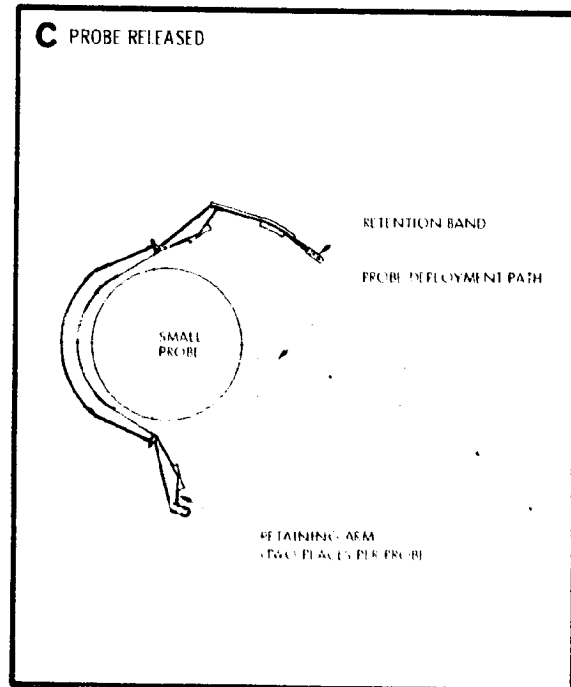
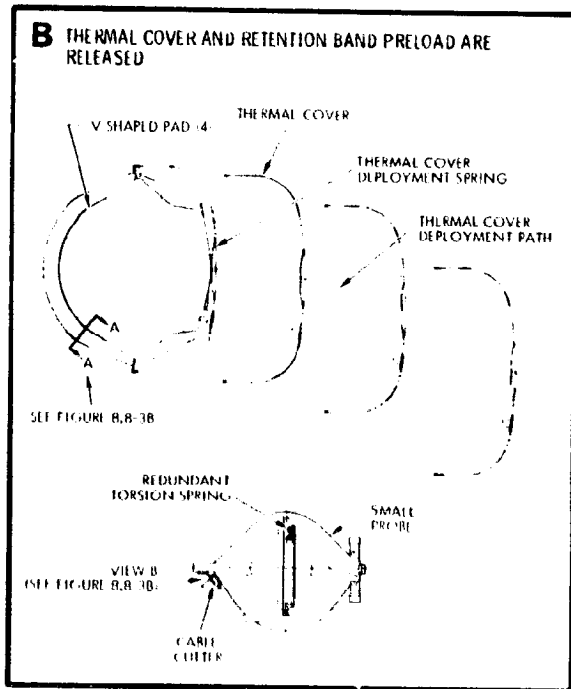
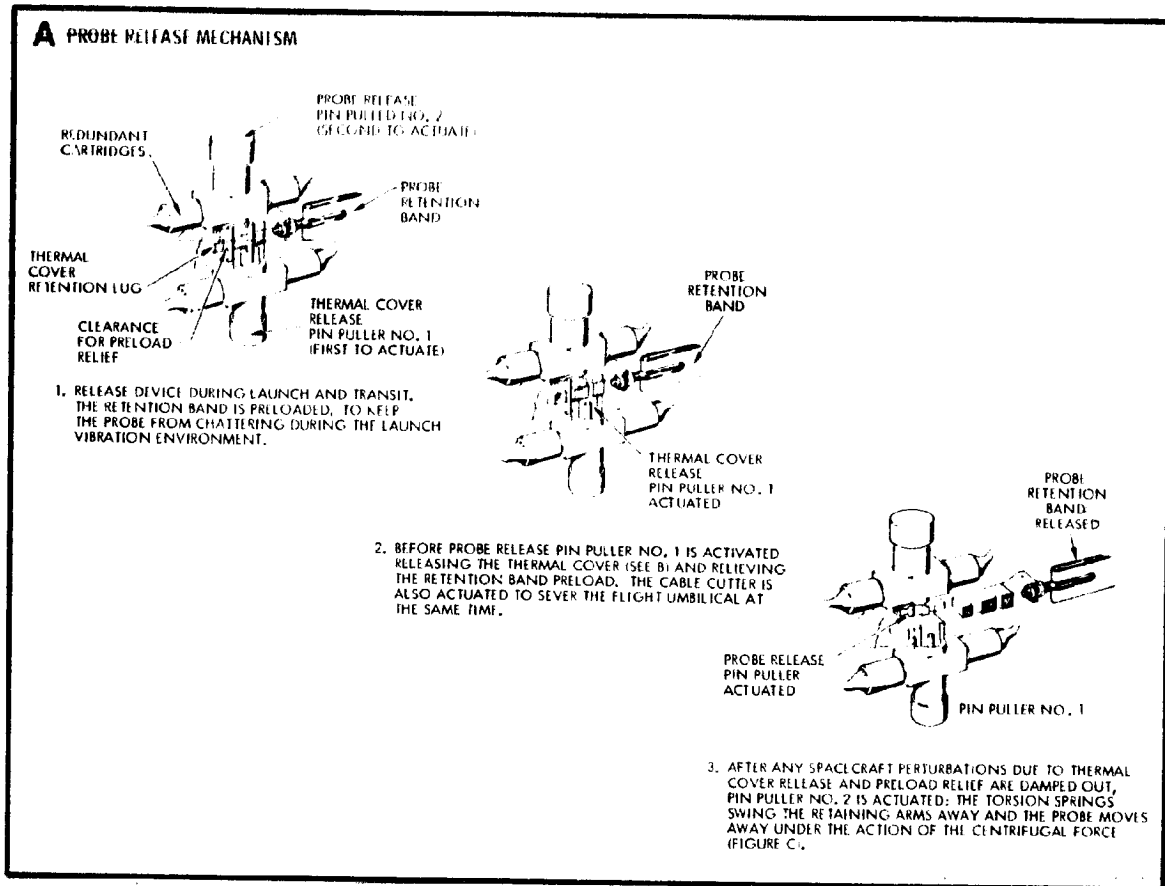


Figure 8.8-4. Small Probe Retention and Release Mechanism

A/C IV well as centrifugal force to eject the thermal cover. Figure 8.8-4B shows the initial path of the released cover. When pin No. 1 is pulled, a slotted hole in the retention band fitting permits the band to relax approximately 0.5 mm (0.020 in.), which is more than sufficient to relieve the initial preload plus any thermal expansion of the band. This allows the probe to be free from any clamping load; it is retained only by the band at the outboard pads. Also at this time the electrical cable connecting the probe to the spacecraft is severed by a redundant set of cable cutters. The cutter is actuated by the same signal which actuated pin puller No. 1. The cable is severed at this time in the sequence to ensure that there is no disturbance when the probe is finally separated from the spacecraft.

T/D III

The second step of the deployment sequence is illustrated in Figure 8.8-4A3. Pin puller No. 2 is actuated, allowing the two pivoting frames of the clamp to swing outward under the force of the torsion springs. These springs are strong enough to move the retaining frames away well before the probe begins to move under the centrifugal body force. The probe is then free to begin its independent trajectory solely under the outward acting centrifugal acceleration without any indeterminate forces. The separation mechanism and the retention band are arranged to maximize the probe-to-spacecraft clearance as the separation takes place.

8.8.3.3 Probe Electrical Disconnects

Table 8.8-7 shows the connectors that were examined between probes and spacecraft. The zero entry connectors use stiff springs to ensure contact, and would induce indeterminate initial impulses to the small probes as they separated; they would not allow unperturbed probe release, and are therefore unacceptable. The cable cutter was selected as being the lightest acceptable design. Short circuit isolation is not considered a serious drawback to its application.

8.8.3.4 Magnetometer Boom ALL ORBITER CONFIGURATIONS

Summary Specification

The magnetometer boom will be capable of mounting a two-pound mass approximately the size of a 4-inch cube on the end of a deployable element. In the retracted or stowed position it will be capable of reacting

Table 8.8-7. Electrical Disconnects

A/C IV	T/D III	TYPE	COMPONENT	UNIT WEIGHT (KG)	SUBSYSTEM WEIGHT (KG)	QUANTITY PER SPACECRAFT	TOTAL WEIGHT (KG)	REMARKS
		G&H TECHNOLOGY, INC. MODEL 704E	PLUG	0.399	0.572	4	2.288	ISOLATE AGAINST SHORTS
			RECEPTACLE	0.172				
		CABLE CUTTER*	CUTTER	0.077	0.304	4	1.216	
			BRACKET	0.136				
			CONNECTORS (1 EACH SIDE)	0.091				
		ZERO-ENTRY CONNECTORS	PLUG	0.091	0.318	4	1.272	
			RECEPTACLE	0.091				
			BRACKET	0.136				

*MARTIN MARIETTA AEROSPACE PD5000010-003

ALL ORBITER CONFIGURATIONS

a 20 G axial (thrust axis) acceleration, while at the same time reacting a 3 G lateral acceleration in any lateral axis. The temperature at the boom to magnetometer interface may range from -101.12 to +65.56°C (-150 to +150°F) and the boom will be capable of functioning over this temperature range.

The boom deployment will be in a radial direction to a maximum length of 4.8 meters from the stowed position and will be accomplished at a rate not to exceed 1 m/min. An electrical cable attached to the magnetometer will be deployed in coordination with the boom deployment and the capability to retract both at approximately the same rate will be accommodated in the boom design.

The angular position of a datum line on the outboard end of the boom will be known to within 0.017 radian (1 degree) with respect to a corresponding line on the boom extension mechanism, after repeated extension/retraction cycles and after exposure to a specified solar heating condition.

In the extended position, the boom will be capable of reacting a 0.1 G acceleration in any direction without yielding the boom or mechanism. Also, the minimum natural frequency of the boom in this extended position will be not less than 1.2 Hz.

A minimum of 20 extension-retraction cycles will be required in the design.

The boom mechanism and mechanical and electrical interface hardware will be included such that the complete mechanism can be mounted on the spacecraft equipment platform with bolts, and power leads for the motor will terminate at a connector for attachment to the spacecraft power system. Magnetometer mechanical and electrical interfaces are to be determined.

Tradeoffs and Description

This mechanism must both deploy and retract the magnetometer to an extended length of approximately 4.8 meters for Atlas/Centaur and 3 meters for Thor/Delta.

Three mechanisms have been surveyed: Astromast, Bi-Stem, and Celesco reel-type booms. The Astromast is an open section deployable truss with multiple hinges and joints. Deployment is controlled by unwinding cables from spools and letting springs in the hinges move the boom into the extended position. Retraction is accomplished by reversing the spools and pulling the mast back in via the cables. Reliability of the retraction plus indefinite accommodation for cabling makes this an undesirable choice. The Celesco and Astromast booms are shown in Figure 8.8-5.

The Bi-Stem device has not been completely evaluated for this application, but as an open boom section it is not as torsionally rigid as the Celesco closed section boom, and therefore the position of the magnetometer with respect to the spacecraft would not be known to an acceptable degree of accuracy.

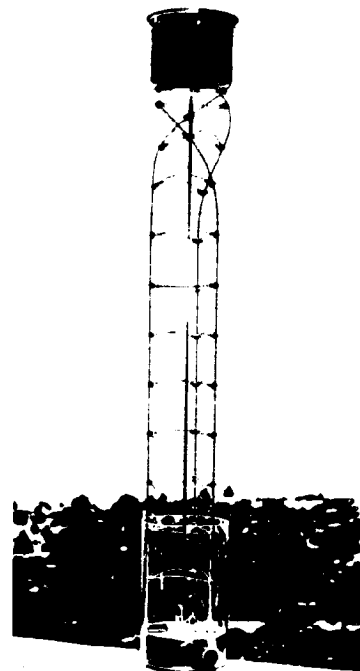
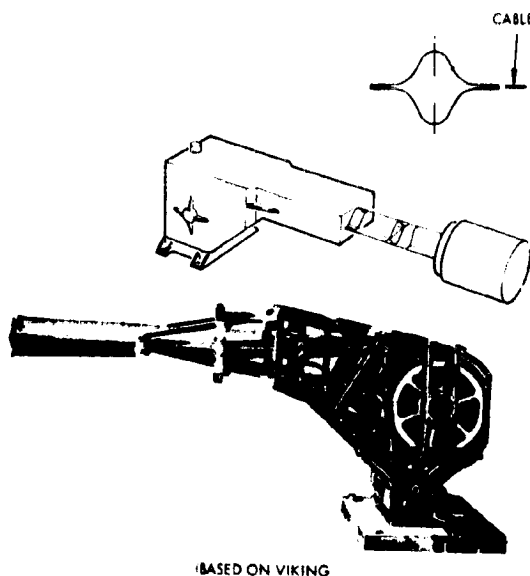
The Celesco boom is preferred for the following reasons:

- It deploys and retracts with equal facility. The boom elements are wound directly on and off a spool similar to a fishing reel.
- Cabling is accommodated (up to 20 leads) external to the boom and permits electrical attachment to the magnetometer without slip rings or brushes. Cabling is a flat strip and winds up on its own reel driven from a common shaft with the boom as it is deployed or retracted.
- It is torsionally rigid, with predictable deformations under solar heating.

ALL ORBITER CONFIGURATIONS

CELESCO BOOM

PARTIALLY DEPLOYED ASTROMAST



FLIGHT-DEMONSTRATED ON CLASSIFIED PROGRAM

EITHER DESIGN CAN MEET REQUIREMENTS; RFP FOR BOOM BEING PREPARED

Figure 8.8-5. Existing Boom Design Recommended for Magnetometer Deployment

On the probe bus the boom must be retracted before the release of small probe No. 3, which would impact it if not retracted. After probe release it is deployed again. On the orbiter spacecraft it must be retracted before the orbit insertion burn, and then subsequently redeployed. While deployed, the maximum loads on the boom normal to its axis are <0.01 and <0.10 G along its axis. Capabilities exceed 0.1 and 10 G in the two directions, respectively.

If the magnetic field at the magnetometer is less than 5γ , it may be necessary to use a longer length boom. It appears that both CeleSCO and Astromast booms can meet the specified requirements at lengths as long as 10 meters.

8.8.3.5 Nutation Damper

Description

The nutation damper recommended for use on Pioneer Venus is similar to one developed for Meteosat by CNES (France). It consists of a mercury-filled U-tube which has expanded end chambers to enable its natural frequency to be tuned to the spacecraft nutation frequency. Since natural frequency of the damper and nutation frequency are both proportional to the spin rate, the damper is self-tuning, i.e., the frequency ratio is independent of spin rate. The range of frequency ratios over which the damper is required to operate depends on the range of spacecraft nutation to spin frequency ratios (i.e., inertia ratios) encountered. The natural frequency (Table 8.8-8) is a function of the radial distance from the spin axis, length of tube, and area ratio of the tube to its expanded ends. Amplification of the relative motion between the fluid and tube is a function of the natural frequency and damping inherent in the damper design, as well as the inertia ratio of the spacecraft. The damper is mounted to the edge of the platform to achieve maximum excitation.

Table 8.8-8. Summary of Damper Design Parameters

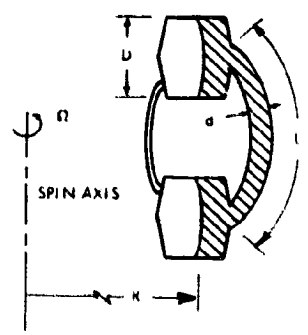
CONFIGURATION	λ	$\frac{\omega_n}{\Omega}$	R [CM (IN.)]	L [CM (IN.)]	d [CM (IN.)]	D [CM (IN.)]	WEIGHT [KG (LB)]	T _{MAX} (MIN)
THOR DELTA PROBE BUS	0.21-0.24	0.23	85.1 (33.5)	21.6 (8.5)	0.64 (0.25)	7.75 (3.05)	1.82 (4.0)	10
	0.70-0.82	0.80	85.1 (33.5)	25.4 (10)	1.02 (0.40)	3.28 (1.29)		60
THOR DELTA ORBITER	0.36-0.41	0.39	85.1 (33.5)	25.4 (10)	0.64 (0.25)	4.22 (1.66)	1.14 (2.5)	20
ATLAS CENTAUR PROBE BUS	0.22-0.24	0.23	106.7 (42)	26.7 (10.5)	0.64 (0.25)	7.80 (3.07)	2.5 (5.5)	15
	0.73-0.84	0.82	106.7 (42)	30.5 (12)	1.52 (0.60)	4.98 (1.96)		40
ATLAS CENTAUR ORBITER	0.52-0.57	0.54	106.7 (42)	30.5 (12)	1.02 (0.40)	4.93 (1.94)	1.82 (4.0)	10

$$\sqrt{\left(\frac{I_x - I_y}{I_y}\right) \left(\frac{I_x - I_z}{I_z}\right)}$$

ω_n = NATURAL FREQUENCY $\omega_n = \frac{d}{L} \cdot \frac{2R}{L}$

$\frac{\omega_n}{\Omega}$ = DAMPER TO SPIN FREQUENCY RATIO

T_{MAX} = MAXIMUM THEORETICAL TIME CONSTANT AT 0.52 RAD/S (5 RPM)



Mercury is used to minimize the damper case weight for a given weight of fluid. The original concept included the use of a damping fluid in the inboard manifold tube to provide the desired amount of energy dissipation. For the particular damper configurations that have evolved for Pioneer Venus, however, the mercury alone provides sufficient damping. Damping can be enhanced, where required, by using a cluster of smaller diameter tubes within the U-tube. Air is evacuated from the damper. The inboard connecting tube between the two end chambers is retained to prevent mercury vapor differential pressure from influencing the natural frequency.

The damper designs preferred for the various Pioneer Venus configurations are described in Table 8.8-8. Two dampers, tuned to different frequencies, are used on the probe bus because the performance of a single damper is significantly degraded by a wide range of inertia ratios encountered. The damper design for the Thor/Delta probe bus configuration that is tuned to the nutation frequencies encountered after separation of the large probe is illustrated in Figure 8.8-6.

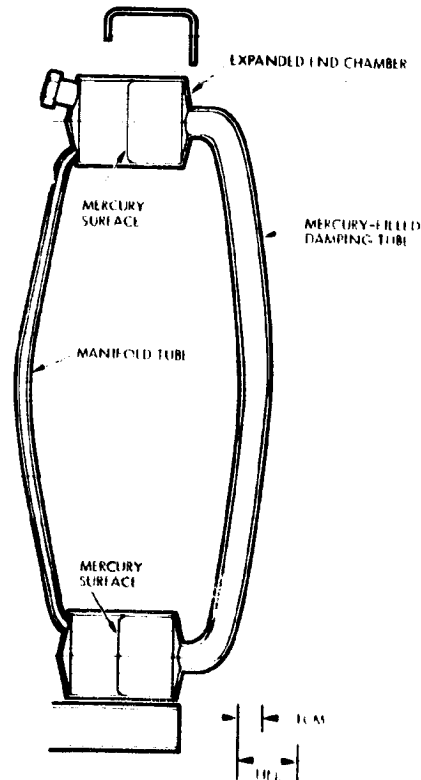


Figure 8.8-6. Nutation Damper Configuration for Thor/Delta Probe Bus ($\omega_n/\omega = 0.80$)

Basis of Recommendation and Performance Comparison to Other Dampers

The self-tuning U-tube mercury damper is preferred over other types of dampers based on performance versus weight and simplicity of design. A tuned damper is used to achieve the desired performance with a minimum weight. (An alternate method for achieving comparable performance versus weight is to use a damper, similar to that used on Pioneers 10 and 11, which operates off the motion of the magnetometer boom, taking advantage of its large inertia. This was rejected, however, because of the complication to the boom and its retraction mechanism, and because the damper is inoperable with the boom retracted.) A damper that is self-tuning, i. e., the natural frequency is proportional to the spin rate, is used to achieve the desired performance at low spin rate and to accommodate changes in spin rate without unacceptable loss of performance. Other self-tuning damper types (i. e., pendulum dampers) were rejected because of the difficulty in achieving the self-tuning aspect at low spin rates. An outward-pointing pendulum damper cannot be tuned to the nutation frequency unless the pivot is on the opposite side of the spin axis from the damper mass. In addition, the stiffness of a flexural pivot has a detuning effect at low spin rates. An inward-pointing pendulum damper and a pendulum damper oriented along the spin axis can be tuned to the nutation frequency for a particular spin rate but becomes detuned and loses performance as spin rate is varied.

The theoretical performances of a 1.8 kg (4 lb) viscous ring damper and a bellows-type damper used on Pioneers 10 and 11 have been computed as a basis of comparison and are presented in Table 8.8-9.

Performance

The theoretical time constant is plotted as a function of spacecraft inertia ratio in Figures 8.8-7 through 8.8-11 for the various configurations.

Variation with Inertia Ratio

The time constant is strongly influenced by the inertia parameter λ , through the effective excitation force acting on the fluid. As λ increases, the relative motion between the fluid, resulting from inertial forces acting on it, and the tube, decreases, resulting in a degradation of the time constant. When $\lambda = 1$, i. e., inertia ratio = 2, the fluid is in equilibrium with the tube and no relative motion occurs.

Table 8.8-9. Damper Tradeoff Comparison

TYPE	WEIGHT (KG)	WEIGHT (LB)	TIME CONSTANT (MIN)	OTHER
U-TUBE	1.8	(4.0)	- 10 (ORBITER) - 50 (PROBE)	DEVELOPMENT PROGRAM REQUIRED, TWO DAMPERS REQUIRED FOR PROBE BUS
VISCOUS RING	1.8	(4.0)	60 TO 280	PERFORMANCE NOT ACCEPTABLE
BELLOWS (PIONEERS 10 AND 11)	0.9	(2.0)	- 20	COMPLICATES MAGNETOMETER BOOM DESIGN, INOPERABLE WITH BOOM RETRACTED

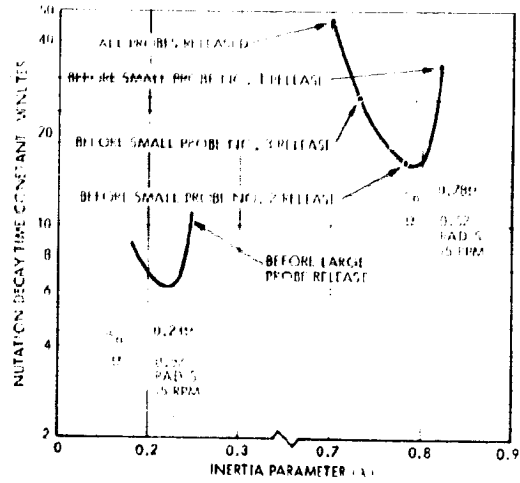


Figure 8.8-7. Thor/Delta Probe Bus Nutation Damper Theoretical Performance

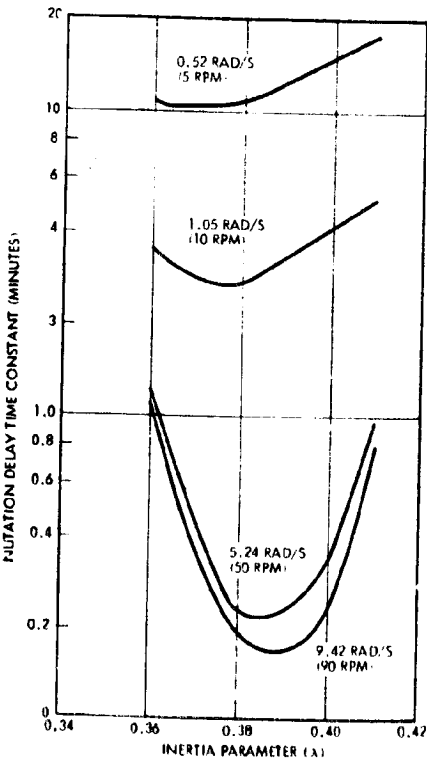


Figure 8.8-9. Thor/Delta Orbiter Theoretical Damper Performance for Various Spin Rates

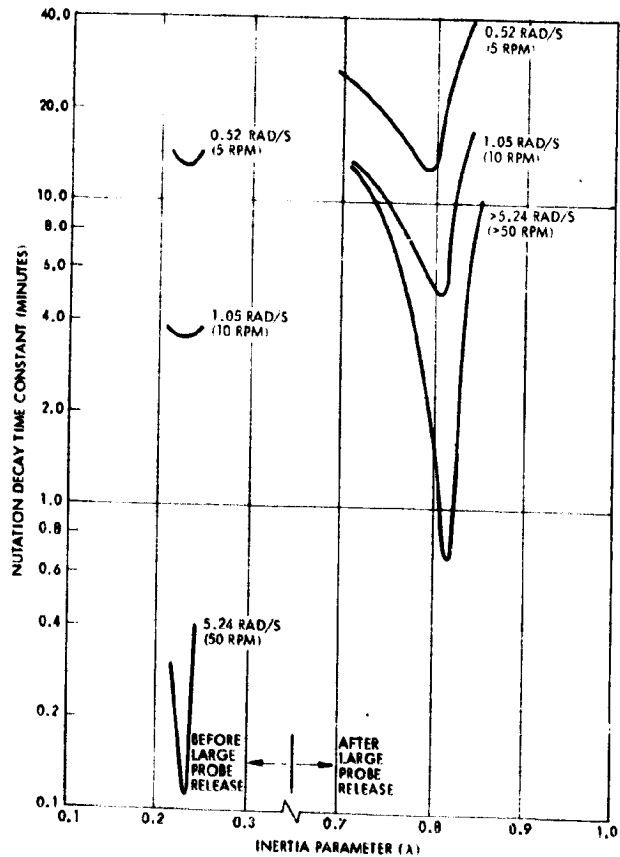


Figure 8.8-10. Atlas/Centaur Theoretical Damper Performance for Various Spin Rates

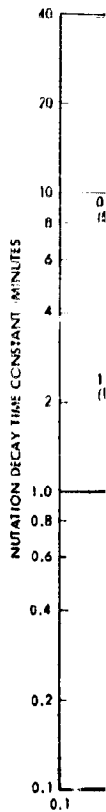


Figure 8.8-8.

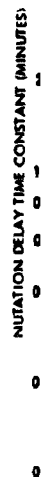


Figure 8.8-11.

FOLDOUT FRAME

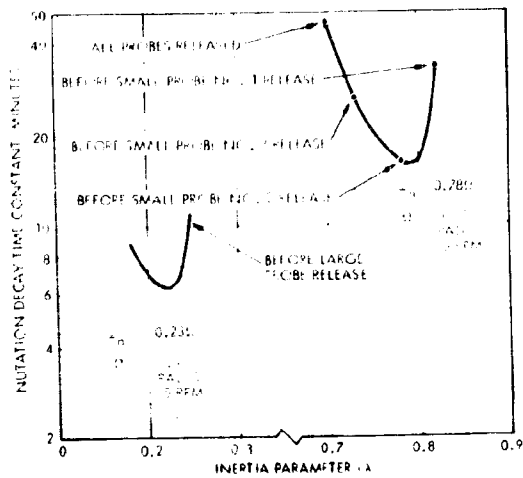


Figure 8.8-7. Thor/Delta Probe Bus Nutation Damper Theoretical Performance

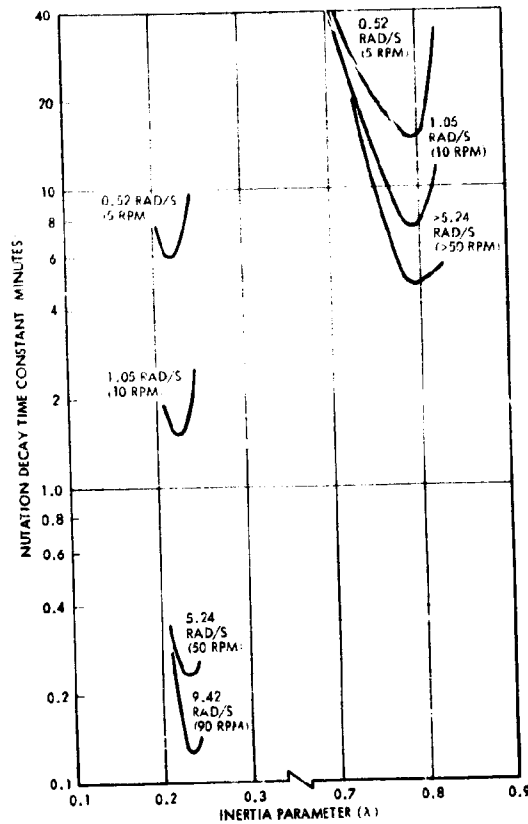


Figure 8.8-8. Thor/Delta Probe Bus Damper Theoretical Performance for Various Spin Rates

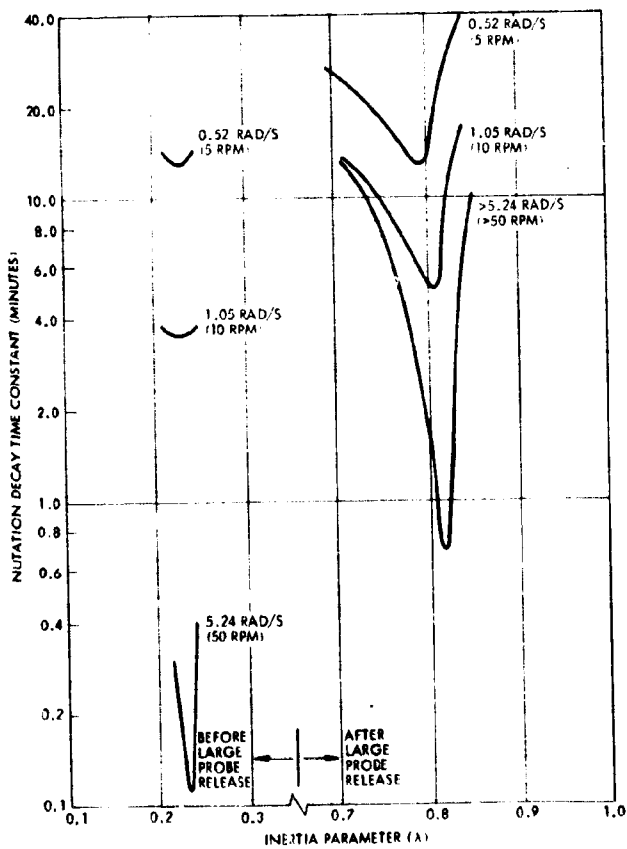


Figure 8.8-10. Atlas/Centaur Theoretical Damper Performance for Various Spin Rates

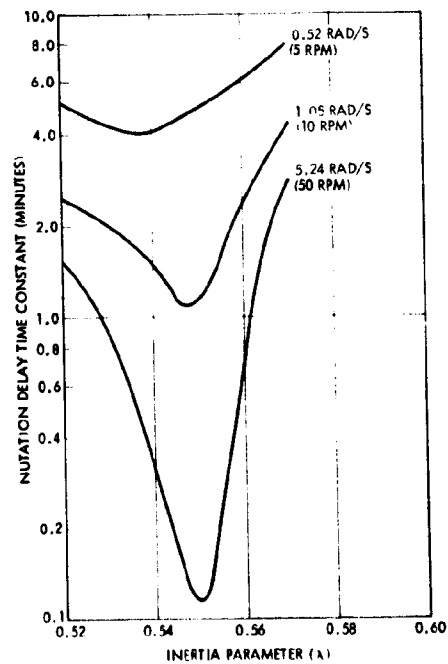


Figure 8.8-11. Atlas/Centaur Orbiter Nutation Damper Theoretical Performance for Various Spin Rates

The implication is that it becomes increasingly difficult to achieve a good time constant for high inertia ratios and the damper must be sharply tuned to achieve a high magnification factor to compensate for the excitation force reduction.

Variation with Spin Rate

The time constant variation with spin rate is shown in Figures 8.8-8 through 8.8-11. The time constant always improves with increasing spin rate; however, the amount of improvement depends on the frequency ratio and damping factor. At resonance, the time constant decreases with the square of the spin rate increase. The variation decreases toward zero as the frequency ratio moves away from resonance.

Variation with Temperature

Time constant varies with temperature through viscosity changes. The percentage variation in time constant is always less than or equal to the percentage variation in viscosity. For mercury, the variation of viscosity is approximately 15 percent over the anticipated temperature range of -6.67 to $+37.78^{\circ}\text{C}$ (20 to 100°F). The percentage variation in time constant due to temperature changes, therefore, will be between 0 and 15 percent.

Divergence Time Constant in Thor/Delta Third-Stage Injection Mode

The nutation frequencies during the Thor/Delta third-stage injection are sufficiently separated from the damper natural frequencies, resulting in a long divergence time constant (50 to 700 minutes for the orbiter and 70 to 180 minutes for the probe bus). Consequently, the wobble buildup while the spacecraft is in this spin-stabilized, unfavorable inertia ratio mode (less than four minutes) will be insignificant and no valve nor diaphragm is needed to constrain the fluid.

Damper Design Parameters

Table 8.8-8 summarizes the recommended design parameters for each configuration. Damper geometry is determined by performance and weight requirements. Tube length and diameter and end-chamber diameter are selected to provide the values of natural frequency, damping, and

mass of fluid in the tube that is required to achieve the desired time constant. The amount of fluid in the end chambers is determined by the range of amplitudes over which it is desired to maintain linear performance.

Surface Tension Effects

At low spin rates, surface tension has a significant effect on the shape of the liquid/vapor interface and could, as a result, affect the natural frequency. Damper tuning has a significant effect on performance, especially for high inertia ratio configurations for which a sharply tuned damper is required to achieve satisfactory performance. Therefore, the effect of surface tension on natural frequency must be properly assessed to ensure a minimal effect on performance. Minimization of the effect of surface tension can be achieved by using a plating material on the end-chamber surfaces that mercury will wet with a contact angle close to but less than 1.57 radians (90 degrees), thereby minimizing the surface curvature. Further analysis and scale-model testing should be performed to more accurately assess this effect.

Testing

Tests to verify damper performance should be conducted with a damper model mounted horizontally to the end of a torsional oscillator such that the motion provides excitation along the damper tube. Experimental determination of the variation of performance with excitation to natural frequency ratio, damper geometry, and damping factor should be attained. In addition, the effects of surface tension on damper natural frequency and performance should be determined through scale-model tests which simulate low Bond numbers (ratio of gravitational to surface tension forces).

8.8.4 Probe Separation Analysis A/C IV T/D III

8.8.4.1 Large Probe—Atlas/Centaur and Thor/Delta

The large probe is separated from the bus by unlocking the three ball-lock bolts, thereby allowing the three separation springs to impart an axial relative velocity of approximately 0.3 m/s (1 ft/s) between the large probe and the bus.

The relative separation velocity between the probe and the bus for the Atlas/Centaur and Thor/Delta configurations are

$$\begin{aligned} \Delta V_{\text{rel}} &= \sqrt{n k \delta^2 \frac{(M_1 + M_2)}{M_1 M_2}} \\ &= 0.31 \text{ m/s (1.02 ft/s) (Atlas/Centaur)} \\ &= 0.32 \text{ m/s (1.06 ft/s) (Thor/Delta)} \end{aligned}$$

where

n = number of separation springs = 3

k = spring rate of each spring = 23 N/cm (13.3 lb/in.)
(Atlas/Centaur)
= 11.6 N/cm (6.7 lb/in.)
(Thor/Delta)

δ = stroke of each spring = 5 cm (2 in.)

M_1 = mass of probe = 300 kg (21 slug) (Atlas/Centaur)
= 143 kg (9.8 slug) (Thor/Delta)

M_2 = mass of bus = 470 kg (32 slug) (Atlas/Centaur)
= 218 kg (15 slug) (Thor/Delta)

The inertial velocity changes of the probe and bus are determined as follows.

$$\begin{aligned} \Delta V_{\text{probe}} &= \frac{M_2}{M_1 + M_2} \Delta V_{\text{rel}} = 0.187 \text{ m/s (0.61 ft/s)} \\ &\quad \text{(Atlas/Centaur)} \\ &= 0.196 \text{ m/s (0.65 ft/s)} \\ &\quad \text{(Thor/Delta)} \end{aligned}$$

$$\begin{aligned} \Delta V_{\text{bus}} &= -\frac{M_1}{M_1 + M_2} \Delta V_{\text{rel}} = -0.123 \text{ m/s (-0.41 ft/s)} \\ &\quad \text{(Atlas/Centaur)} \\ &= -0.124 \text{ m/s (0.41 ft/s)} \\ &\quad \text{(Thor/Delta)} \end{aligned}$$

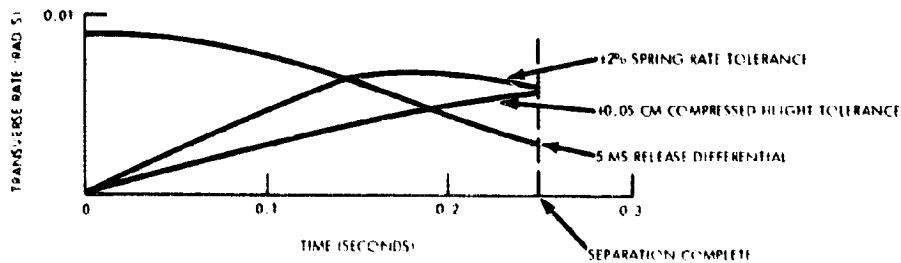
Uncertainties in these values can be limited to less than ± 5 percent by calibration of the separation springs.

The separation event will also produce disturbances which will precess the probe momentum vector and induce nutation. A summary of the primary disturbances is shown in Table 8.8-10.

Table 8.8-10. Large Probe Separation Tipoff Errors

DISTURBANCE	TRANSVERSE ANGULAR RATE (RAD/S)		MOMENTUM VECTOR SHIFT AND NUTATION ANGLE (DEG)		
	ATLAS-CENTAUR	THOR DELTA	ATLAS-CENTAUR		THOR DELTA
			10 RPM	20 RPM	
NET LATERAL SPRING FORCE 2 NEWTONS (0.44 LB) (ATLAS-CENTAUR) 1 NEWTON (0.22 LB) (THOR DELTA)	0.004	0.005	0.2	0.1	0.5
AXIAL SPRING RATE DIFFERENTIAL ±2 PERCENT	0.005	0.006	0.25	0.125	0.6
COMPRESSED HEIGHT OF EACH SPRING ±0.05 CM (±0.02 IN.)	0.003	0.005	0.15	0.08	0.5
SPRING RADIAL LOCATION ±0.15 CM (±0.06 IN.)	0.001	0.001	0.05	0.025	0.1
BALL LOCK RELEASE DIFFERENTIAL 5 MS	0.003	0.002	0.15	0.08	0.3
RSS TOTAL	0.008	0.01	0.4	0.2	1.0

The transverse rates were computed using a digital computer program. Examples of the transverse rate induced during the separation event are shown below.



The magnitudes of the momentum vector shift and nutation angle are determined as follows.

$$\theta = \alpha = \frac{A \omega_t}{C \omega_s} \times 57.3$$

where

θ = nutation angle

α = momentum vector shift

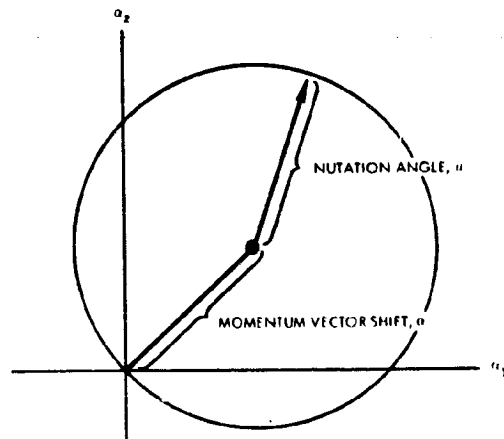
A = probe transverse moment of inertia

C = probe spin axis moment of inertia

ω_t = transverse rate after separation

ω_s = spin rate

The instantaneous attitude error after separation will be due to a combination of the momentum vector shift and nutation describing a circular path as shown below.

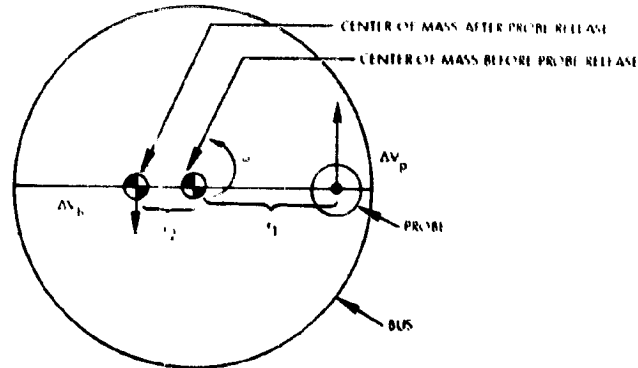


The vector representing the nutation angle will rotate at the inertial precession frequency and will tend to diminish in magnitude if the probe contains any nutation damping sources.

8.8.4.2 Small Probe Separation Analysis, Atlas/Centaur and Thor/Delta

The small probes are released sequentially from the bus with no impulse imparted to the probe during a nominal separation. As a

result, the probe travels in an inertial direction which is perpendicular to a radial line connecting the spacecraft center of mass and the probe center of mass at the instant of probe release as shown below.



No change of spin rate of either the probe or bus occurs as a result of probe release.

A velocity change will be imparted to the probe and bus as follows.

$$\Delta V_{\text{probe}} = \omega r_1$$

$$\Delta V_{\text{bus}} = \omega r_2$$

where

ω = spacecraft spin rate

r_1 = distance from probe center of mass to composite center of mass before release

Nominal values for these velocity increments are shown below, assuming a spin rate of 1.408 rad/s (10 rpm) for the Atlas/Centaur, and 0.524 rad/s (5 rpm) for the Thor/Delta.

	First Small Probe Release	Second Small Probe Release [†]	Third Small Probe Release
r_1 (meters)			
Atlas/Centaur	0.87	0.81	0.67
Thor/Delta	0.83	0.77	0.68
r_2 (meters)			
Atlas/Centaur	0.18	0.22	0.25
Thor/Delta	0.13	0.145	0.15
ΔV_{probe} (m/s)			
Atlas/Centaur	0.91	0.85	0.70
Thor/Delta	0.43	0.40	0.35
ΔV_{bus} (m/s)			
Atlas/Centaur	-0.19	-0.23	-0.26
Thor/Delta	-0.069	-0.076	-0.078

The trajectories of the small probes relative to the bus are described by the equations for an involute, i.e.,

$$\Delta R = R_0 (\cos \phi + \phi \sin \phi)$$

$$\Delta T = -R_0 (\sin \phi - \phi \cos \phi)$$

where

ΔR = radial displacement between probe and bus

ΔT = tangential displacement between probe and bus

R_0 = distance between probe center of mass and bus plus remaining probe center of mass at time of separation

ϕ = angle of rotation after time of separation

[†]The ΔV 's imparted during the second probe release will be in a direction approximately 0.16 radian (9 degrees) off perpendicular to the radial line connected to the center of the probe and the center of the spacecraft due to the center-of-mass location before second probe release.

The relative trajectories in Figure 8.8-12 show that only one probe interferes with the deployed magnetometer boom, thereby requiring retraction of the boom for only one probe release. The relative trajectories of the first and third probes released begin in a direction along a radial line passing through the spacecraft centerline; however, the relative trajectory of the second probe released begins in a direction approximately 0.16 radian (9 degrees) off a radial line because of center-of-mass offset of the bus and last remaining probe at that time.

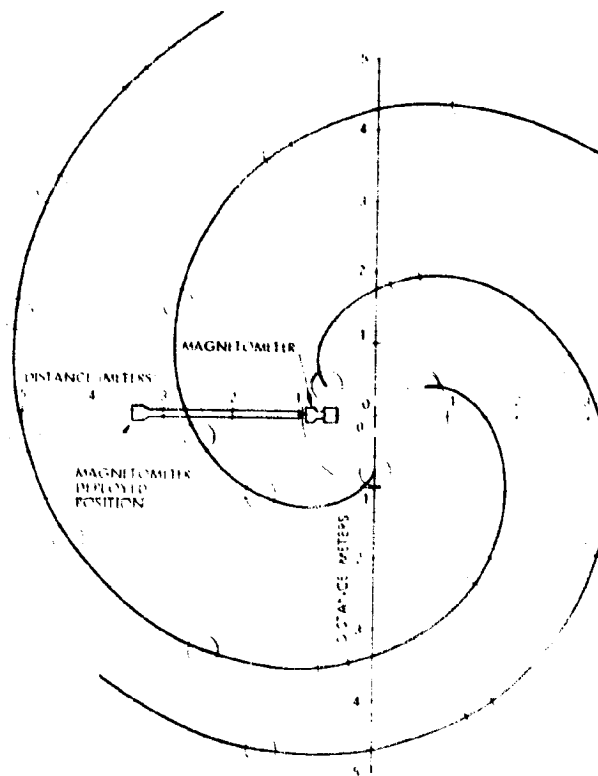
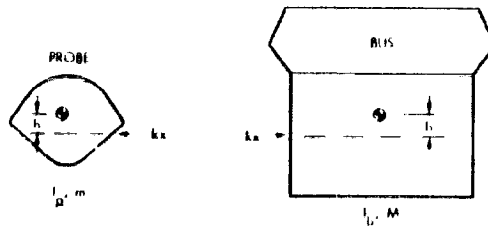


Figure 8.8-12. Small Probe Trajectories Relative to Bus (Thor/Delta Configuration)

During the small probe release, disturbances can induce transverse rates which will cause precession of the momentum vector and nutation of the spin axis after probe release.

One source of disturbance torques is the preload energy in the release mechanism. This energy can produce a force misaligned with the center of mass of the probe as shown below.



The transverse rate of the small probe induced by this disturbance is determined as follows.

$$\omega_t = \sqrt{\frac{F^2 k}{I_p \left[1 + \frac{I_p}{Mh^2} + \frac{I_p}{I_b} + \frac{I_p}{mh^2} \right]}}$$

The resulting momentum vector shift and nutation resulting from this disturbance, assuming a spin rate of 0.52 rad/s (5 rpm), is

$$\theta = \alpha = \frac{I_t \omega_t}{I_x \omega_x} \times 57.3 \approx 100 \omega_t$$

where

I_t = transverse MOI of probe

I_x = spin axis MOI of probe

m = mass of probe

I_b = transverse MOI of bus

M = mass of bus

h = offset between center of mass and impulsive force vector

$F = kx$ = disturbance force

k = spring rate of preload system

x = deflection of preload system

θ = nutation angle

α = momentum vector shift

ω_t = transverse angular rate of probe

ω_x = spin rate of probe

The curves in Figure 8.8-13 indicate the magnitude of the attitude errors as a function of the relevant parameters. Since the center of mass is approximately 2 cm above the plane of the release mechanism, the preload force at the time of release must be limited to approximately 25 to 100 newtons to limit the tipoff errors to 0.017 radian (1 degree), using representative stiffnesses for the Thor/Delta configuration. Correspondingly, the preload force must be limited to 100 to 400 newtons for the Atlas/Centaur configuration. Therefore, a design was conceived which releases the probe in two stages. The first stage releases the preload, which is necessary to hold the probe firmly during boost. After this preload is released, the probe is restrained in the release mechanism with only insignificant loads due to centrifugal force acting on the structure, thereby eliminating this source of tipoff errors.

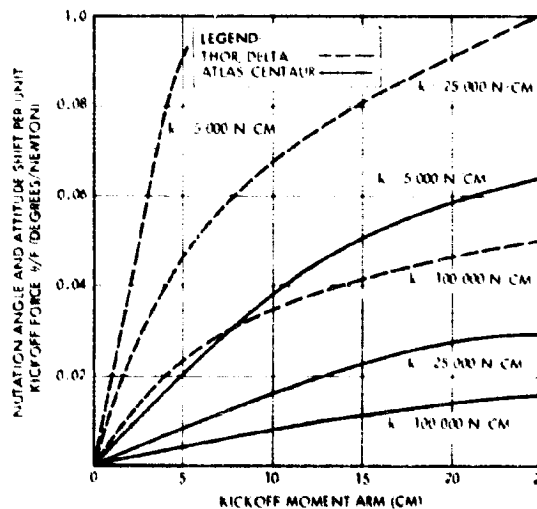


Figure 8.8-13. Small Probe Tipoff Errors for a Preloaded Release System

9. NASA/ESRO ORBITER INTERFACE

This section presents results of a technical and cost tradeoff to determine the most effective method of performing the orbiter mission as a cooperative venture with the European Space Research Organization (ESRO). It is based on variations of NASA planning which assumed that the bus portion of the spacecraft would be provided to ESRO for integration of orbiter mission-peculiar subsystems and scientific instruments, and that ESRO would perform the system test program for this mission and deliver the spacecraft to CKAFS for NASA launch and flight mission operations control.

The results presented in this section are based on the work done up through midterm, as directed by ASD:244-9/32-042, dated 13 April 1973; they do not reflect the subsequent shift to Atlas/Centaur, the addition of the X-band occultation experiment, nor the schedule impact of delaying the probe mission from 1977 to 1978.

The technical versus cost factors analyzed during the study were based on the following criteria:

- Maximum use of probe mission hardware and design
- Assignment of hardware to the original NASA contractor to sustain the experience developed on the probe mission
- Use of the probe mission design, manufacturing, and test planning and control documentation.

To fulfill these criteria, probe and orbiter commonality has to be maximized. This line of analysis points to orbit mission-peculiar hardware and other program factors as the logical assignment for ESRO participation.

It has been determined that the anticipated ESRO deboost propulsion system is adequate for the Atlas/Centaur orbiter mission and that the anticipated use of the Helios despun reflector antenna is suitable, except that incorporation of an X-band link is difficult.

Figure 9-1 illustrates the key orbiter mission-peculiar equipment incorporated into a configuration compatible with the probe bus.

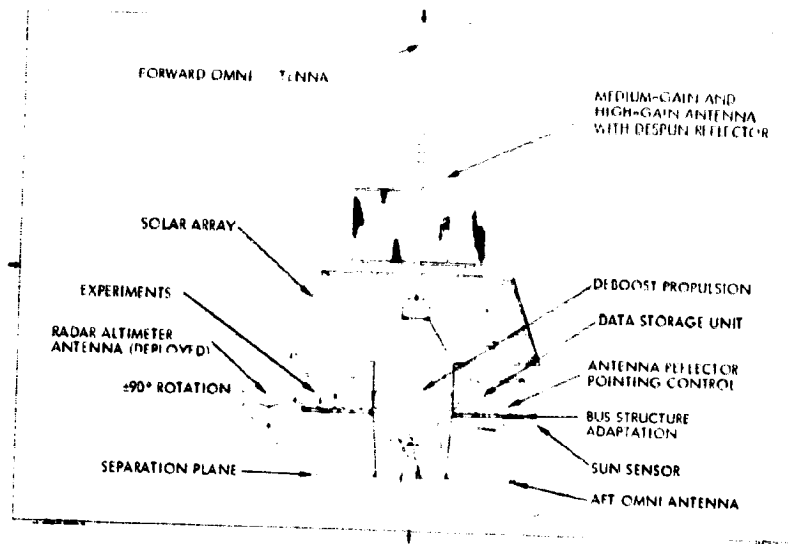


Figure 9-1. ESRO Hardware Participation

Table 9-1 expands on the mission-peculiar items. The main question is the extent of ESRO participation, and options can best be presented in terms of integration and test activities.

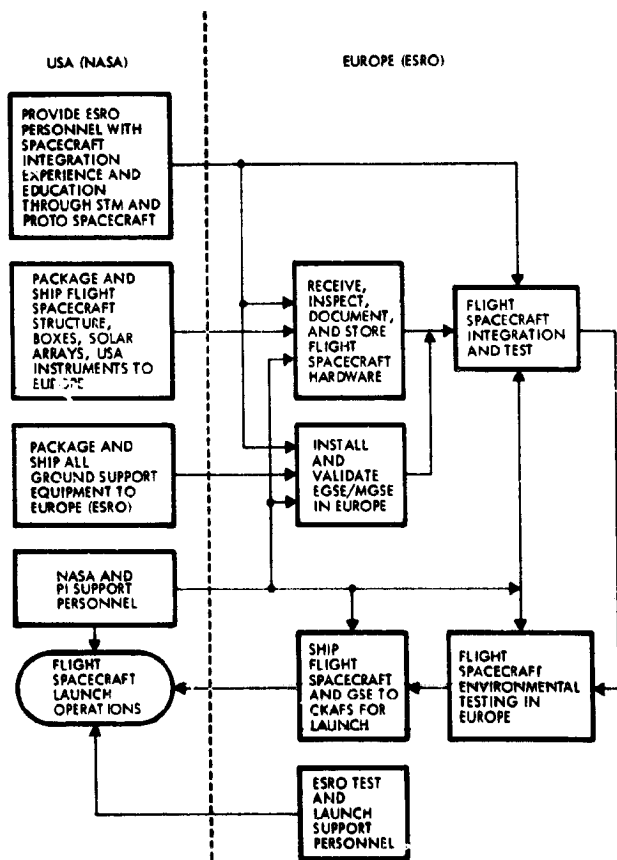
Table 9-1. ESRO Participation Definition

ORBITER MISSION-PECULIAR ITEMS	FURTHER WORK REQUIRED
1. EXPERIMENTS	INTERFACE DEFINITION AND CONTROL
2. SCIENCE DATA REDUCTION AND ANALYSIS	MISSION REQUIREMENTS INPUTS DEFINITION
3. DEBOOST PROPULSION	DEFINITION FOR DESIGN INTEGRATION
4. HIGH-GAIN ANTENNA	DEFINITION FOR DESIGN INTEGRATION
5. ADAPTATION OF PROBE BUS STRUCTURE	DEVELOPMENT STATUS AND APPLICATION
6. INTEGRATION AND TEST	THREE OPTIONS DISCUSSED (SEE FOLLOWING TEXT AND CHARTS)

Three NASA/ESRO integration participation options were reviewed; the related tasks and interface flow diagrams for the respective options are shown in Figure 9-2.

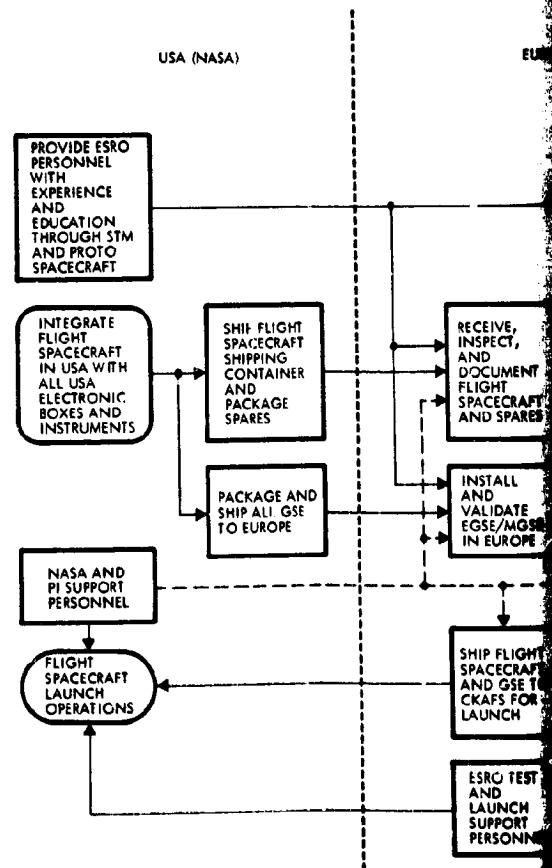
OPTION 1

- PROVIDE EDUCATION AND ORIENTATION TO ESRO PERSONNEL FOR INTEGRATION AND TEST OF WHOLE SPACECRAFT.
- PROVIDE NASA TECHNICAL SUPPORT AND TEST AUDITING AND REVIEW REPRESENTATIVES THROUGHOUT INTEGRATION AND TEST.
- PACKAGE AND SHIP ALL INDIVIDUAL FLIGHT SPACECRAFT HARDWARE AND DOCUMENTATION TO ESRO.
- PACKAGE AND SHIP ALL GROUND SUPPORT EQUIPMENT TO ESRO.
- INSTALL AND VALIDATE EGSE AND MGSE FIXTURES.
- PERFORM COMPLETE FLIGHT SPACECRAFT INTEGRATION AND TEST USING ESRO FACILITIES.
- RETURN SHIPMENT OF FLIGHT SPACECRAFT AND GSE TO CKAFS.
- JOINT ESRO/NASA LAUNCH SUPPORT TEAM AT CKAFS.



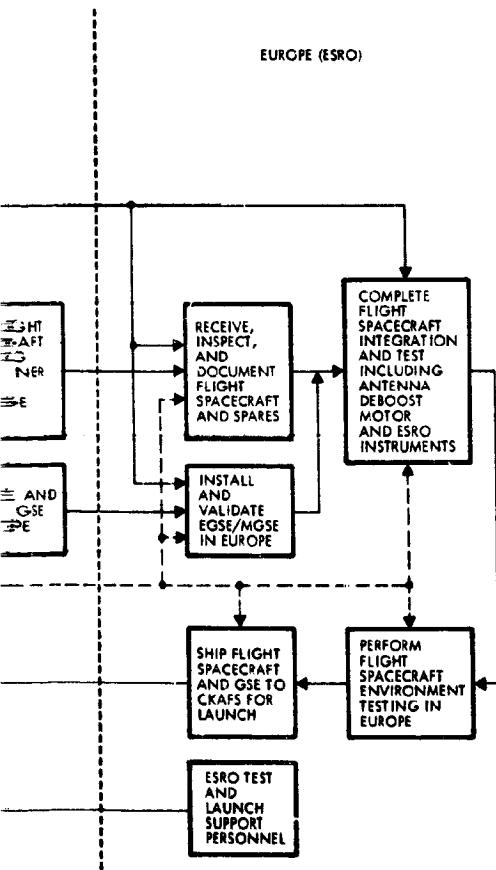
OPTION 2

- PROVIDE EDUCATION AND ORIENTATION TO ESRO PERSONNEL DURING COMPLETION OF INTEGRATION AND ENVIRONMENTAL TEST.
- PROVIDE NASA TECHNICAL SUPPORT AND TEST AUDITING AND REVIEW REPRESENTATIVE DURING COMPLETION OF INTEGRATION AND ENVIRONMENTAL TEST.
- SHIP PARTIALLY INTEGRATED FLIGHT SPACECRAFT TO EUROPE IN SHIPPING CONTAINER. SHIP AND PACKAGE BACKUP SPARE PARTS, AND DOCUMENTS.
- PACKAGE AND SHIP ALL GROUND SUPPORT EQUIPMENT TO EUROPE.
- INSTALL AND VALIDATE EGSE AND MGSE FIXTURES.
- COMPLETE FLIGHT SPACECRAFT INTEGRATION AND PERFORM ENVIRONMENTAL TESTS USING ESTEC FACILITIES.
- RETURN SHIPMENT OF FLIGHT SPACECRAFT AND GSE TO USA AND SUPPORT LAUNCH OPERATIONS.



OPTION 2

- PROVIDE PERSONNEL AND ORIENTATION TO ESRO PERSONNEL FOR SPACECRAFT INTEGRATION AND ENVIRONMENTAL TEST.
- PROVIDE TECHNICAL SUPPORT AND TEST AUDITING AND TEST FACILITY DURING COMPLETION OF INTEGRATION AND ENVIRONMENTAL TEST.
- PROVIDE INTEGRATED FLIGHT SPACECRAFT TO EUROPE IN AIRCRAFT CARRIER, SHIP AND PACKAGE BACKUP SPARES, AND SUPPORT DOCUMENTS.
- PROVIDE SHIP ALL GROUND SUPPORT EQUIPMENT TO EUROPE.
- PROVIDE VALIDATE EGSE AND MGSE FIXTURES.
- PROVIDE FLIGHT SPACECRAFT INTEGRATION AND PERFORM ENVIRONMENTAL TESTS USING ESTEC FACILITIES.
- PROVIDE SUPPORT OF FLIGHT SPACECRAFT AND GSE TO CKAFS FOR LAUNCH OPERATIONS.



OPTION 3

- PROVIDE DESIGN INTERFACE SPECIFICATIONS AND COORDINATE ESRO HARDWARE DESIGN AND DEVELOPMENT.
- PROVIDE ESRO PERSONNEL SUPPORT FOR INTEGRATION OF EUROPEAN PARTS-TEST AUDITING AND REVIEWS IN USA.
- PERFORM ALL FLIGHT SPACECRAFT INTEGRATION AND TEST IN USA USING USA ENVIRONMENTAL TEST FACILITIES.
- ESRO PROVIDES MINIMAL LAUNCH OPERATIONS SUPPORT.

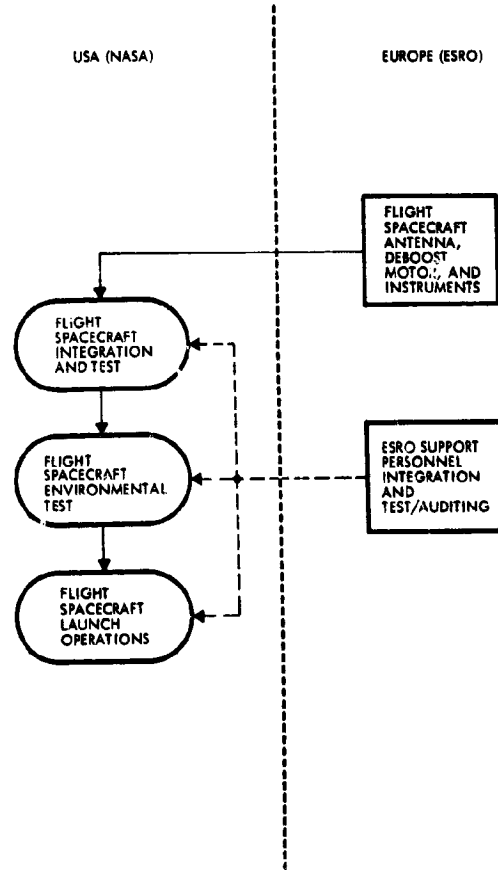


Figure 9-2. NASA/ESRO Participation Options

Each option is analyzed and summarized in terms of key points in Table 9-2. The second option is recommended on the basis of lowest total cost to NASA. However, this option also presents the most difficult management interface between NASA and ESRO because of the split in spacecraft operations between Europe and the United States.

Table 9-2. NASA/ESRO Integration and Test Operations

OPTION 1	OPTION 2	OPTION 3
INDIVIDUAL FLIGHT SPACECRAFT ELECTRICAL BLACK BOXES, APPENDAGES, THERMAL CONTROL, AND PROPULSION SHIPPED TO ESRO	INTEGRATE FLIGHT SPACECRAFT ELECTRICAL BLACK BOXES, APPENDAGES, PARTIAL THERMAL CONTROL, AND PROPULSION IN USA	INTEGRATE FLIGHT SPACECRAFT IN USA WITH ESRO SUPPORT
STRUCTURE SHIPPED TO EUROPE OR MANUFACTURED IN EUROPE	INTEGRATE USA SCIENTIFIC INSTRUMENTS IN USA	SHIP EUROPEAN SCIENTIFIC INSTRUMENTS, ANTENNA, STRUCTURE, AND DEBOOST PROPULSION TO USA FOR FLIGHT SPACECRAFT INTEGRATION AND TEST
USA SCIENTIFIC INSTRUMENTS SHIPPED TO ESRO	SHIP FLIGHT SPACECRAFT TO ESRO FOR FINAL INTEGRATION OF ANTENNA, DEBOOST PROPULSION, AND EUROPEAN INSTRUMENTS	FINAL INTEGRATION AND ENVIRONMENTAL TEST COMPLETED IN USA WITH ESRO SUPPORT
ALL INTEGRATION AND ENVIRONMENTAL TEST PERFORMED IN EUROPE	PERFORM ALL FLIGHT SPACECRAFT ENVIRONMENTAL TESTS AT ESTEC FACILITIES	
MAXIMUM OVERLAP OF ORBITER AND PROBE SCHEDULE TO MEET ORBITER LAUNCH DATE	MINIMUM SCHEDULE OVERLAP	NO SCHEDULE OVERLAP
NO USE OF APPLICABLE PROBE MISSION GSE	USE OF APPLICABLE EGSE FROM PROBE MISSION	USE OF ALL APPLICABLE PROBE MISSION GSE
PROGRAM COST HIGHER THAN OPTION 2	LOWEST PROGRAM COST TO NASA	HIGHEST PROGRAM COSTS TO NASA
EASIER INTERFACE BETWEEN NASA AND ESRO THAN OPTION 2	HARDEST INTERFACE BETWEEN NASA AND ESRO	EASIEST INTERFACE BETWEEN NASA AND ESRO

10. MISSION OPERATIONS AND FLIGHT SUPPORT

10.1 INTRODUCTION

This section describes mission operations and events to show how the baseline design performs its intended functions. The baseline sequence of events for the orbiter and probe missions are described for the preferred Atlas/Centaur configuration.

10.1.1 Orbiter Mission Operations

The preferred orbiter spacecraft is characterized by the conical solar array and is maintained in an earth-pointing attitude. The sun aspect angle at launch is about 1.48 radians (85 degrees), with the spin axis pointing about 0.33 radian (19 degrees) below the ecliptic plane. The spacecraft can remain in this attitude until the first midcourse maneuver on day 5. Prior to the midcourse, the spacecraft is precessed to earth-pointing. This maneuver also serves to calibrate the thrusters for precession. Once earth-pointing, the thrusters are fired for about 30 seconds to calibrate for the ΔV . The midcourse maneuvers are performed open loop, identically to Pioneers 10 and 11, with the calibrations performed to attain direction accuracies of about 0.02 radian (1 degree) and amplitude accuracies of a few centimeters per second.

After midcourse execution, the nominal cruise orientation would be assumed where the positive spin axis (aligned with the high-gain dish axis of symmetry) is aligned with earth. The earth-pointing attitude need not be maintained for the first 60 days since omni communication at 16 bits/s can be sustained via the 26-meter DSN.

The second and third midcourse maneuvers are performed 25 days after launch and 15 days prior to Venus orbit insertion (VOI), respectively. A flip of the spacecraft is performed at about day 110 such that the aft horn is earth pointing to maintain the sun in the forward hemisphere. This attitude is also used for the occultation experiment. The 0.44-radian (25-degree) beamwidth of the aft horn permits a two-point spin axis location strategy to replace the exact earth tracking strategy normally associated with an earth-pointing spacecraft. Orbit insertion is performed by a solid rocket motor with the spacecraft spin stabilized at

6.28 rad/s (60 rpm). After orbit insertion 200 days after launch, the spacecraft continues with the aft end earth pointing until 37 days after VOI. Once again, the spacecraft is flipped to maintain the sun in the forward hemisphere and to point the high-gain dish toward earth.

During Venus orbit operation, periapsis is maintained within 200 to 400 kilometers of the surface using four ΔV maneuvers performed on days 30, 60, 145, and 184 after insertion. About 13.7 kilograms (30 pounds) of fuel are required for three midcourse corrections (99 percent correction capability) and the four orbit trim maneuvers. Excess fuel left over from midcourse maneuvers can be used for additional orbit trims to tighten the periapsis altitude control band, or can be used for extended mission life. On-orbit operation of science is enhanced by an expanded and improved (from Pioneers 10 and 11) stored command programmer having 16 commands with ± 2 -second quantization. This command programmer can be set to perform all science commands for days or even weeks at a time with only an occasional trim of the programmer time and daily data readout from the data storage unit.

10.1.2 Probe Mission Operations


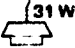
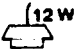

The probe spacecraft is launched with a sun aspect angle of 0.38 radian (22 degrees) at about 0.35 radian (20 degrees) above the ecliptic. This attitude is also desirable for cruise since it provides a good thermal environment for the large probe, which would otherwise require heaters. The spacecraft remains in the launch orientation until the execution of the first midcourse ΔV after which the orientation is set about 0.31 radian (18 degrees) from the launch attitude, 0.35 radian (20 degrees) above the ecliptic. This new orientation is used until day 50, or the time for the second midcourse. By day 50 the aft omni communication bit rate is down to 64 bits/s. The spacecraft now becomes an earth pointer with the aft medium-gain horn used for primary communications. The earth pointing configuration is maintained until the third midcourse, 30 days prior to entry. Alternating probe deployments and ΔV retargeting maneuvers (sequential deployment) occur every 2 days starting 25 days from entry, and ending 11 days before entry with all four probes deployed. The bus is also retargeted for entry. About 16.1 kilograms (35 pounds) of fuel is carried on the probe bus for midcourse and retargeting maneuvers.

Retargeting and probe deployments can be executed either for sequential entry or simultaneous entry (or any combination thereof) with only slight changes in fuel requirements for the retargeting.

10.1.3 Commonality of Configurations

The orbiter and probe mission have operational commonality for most maneuvers and procedures, including midcourse maneuvers, attitude determination, and attitude corrections. Probe deployment is performed very much like the midcourse ΔV except that the probe release replaces the thruster ΔV firing. The major equipment differences between orbiter and probe missions include conscan in the orbiter only, and the small probes are replaced by science and the large probe is replaced by the high-gain dish antenna. There are other slight differences (such as omni antenna complement), but most electronics and functional elements are common.

We examined four primary configuration options of the orbiter which could meet the assumed science requirements. These configurations all have a conical solar array band above the equipment compartment to maximize clear fields of view for experiments. The conical array permits operation with the sun anywhere in the forward "hemisphere" [within 1.92 radians (110 degrees) of the forward spin axis] for indefinite periods without performance degradation. The differences in these four versions are mainly in the antenna complement and the nominal flight orientation:

- 1) Spin axis aligned with earth using high-gain dish for primary communications as for Pioneers 10 and 11. 
- 2) Spin axis normal to ecliptic, using 31-watt fanbeam (pancake pattern) antenna for primary communication. 
- 3) Spin axis normal to ecliptic, using 12-watt fanbeam antenna. This option depends on the 64-meter DSN for primary science data. 
- 4) Spin axis normal to ecliptic. Despun reflector used for primary communications. 

Mission operations are similar for versions 2), 3), and 4), to that of the preferred configuration 1). Only the preferred (baseline) version is discussed in detail in this section. The major differences between the missions are discussed in Sections 1 and 8.5.

The following paragraphs discuss the procedures and rationale for midcourse maneuvers (probe bus and orbiter), probe deployment and data recovery, orbit insertion, orbit trim, attitude determination, attitude maintenance, and science operations.

10.2 ΔV MANEUVER PROCEDURES

10.2.1 First Midcourse

ALL CONFIGURATIONS

Midcourse ΔV maneuvers are performed identically on the orbiter and probe missions. The first midcourse is performed on day 5 with communication maintained via complete coverage of the omni antenna. Fuel is budgeted for 99.9 percentile injection errors which are about 7.0 m/s for the Atlas/Centaur. Two primary methods of ΔV execution can be performed by the system without ground intervention. The first primary method of ΔV execution uses thrusters which are aligned with the spin axis. This method is described in detail in this section, with the second primary method and the backup modes covered in later paragraphs.

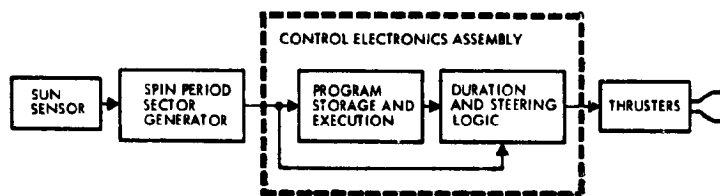


Figure 10-1. Functional Elements for Midcourse Maneuvers

Precession and ΔV maneuvers involve operation of elements in the digital telemetry unit (DTU), the propulsion subsystem, and the control electronics assembly (CEA). The functional operation of these elements is identical to that of Pioneers 10 and 11. All elements used for precession and ΔV maneuvers shown in Figure 10-1 are redundant except for the program storage and execution assembly (PSE). All functions of the PSE can also be performed by ground commands into the duration and steering logic (which is redundant) so that any single failure can be tolerated. The spin period sector generator (SPSPG) and the PSE are by far the most complex elements and are off the shelf (unmodified designs) from Pioneers 10 and 11. The duration and steering logic (DSL) and thrusters are slightly modified in that: 1) new thruster selection logic is required because of the

increased number of thrusters, and 2) the thrusters need to be separated from the cluster assemblies used for Pioneers 10 and 11. The declustered thrusters are being developed for FLTSATCOM.

A ΔV maneuver sequence is normally performed by precessing the spin axis to the direction of the desired ΔV , firing the thrusters that are aligned with the spin axis to execute the ΔV , then precessing back to the desired final orientation. The sequence is depicted in Figure 10-2. The precession is performed by firing short (1/8-second) torque pulses once per revolution at a fixed angle to the sun. This continues for the time necessary to obtain the proper orientation. The ΔV is obtained by firing two thrusters on opposite sides of the spacecraft that are aligned with the spin axis. These fire continuously until the ΔV is complete. The entire sequence is controlled by the PSE. Data loaded from the ground into the PSE is generated from known initial position and the desired final state of the spacecraft. Since the hardware elements for the ΔV are identical to Pioneers 10 and 11, the existing NASA/ARC program generation software (for data to be loaded into PSE) can be used off the shelf, without modification. A brief explanation of this flight-proven software is given in Appendix 10A.

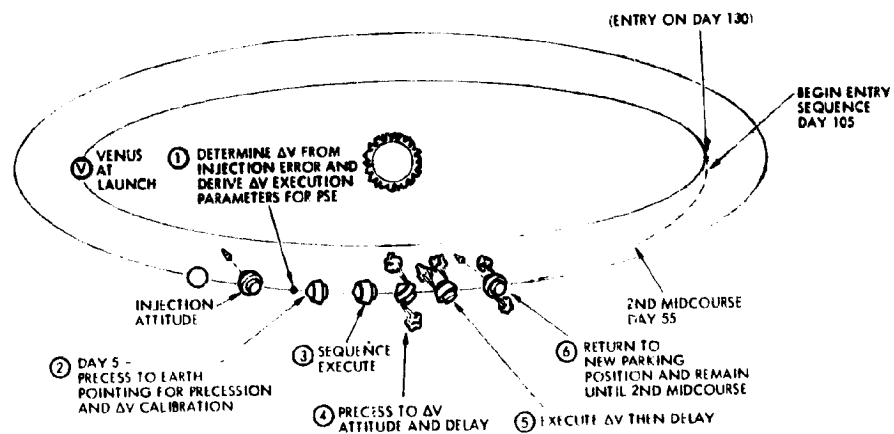


Figure 10-2. Probe Mission First Midcourse

Precessions are performed open-loop using thrusters that have been calibrated by ground test. The ground calibration is supported and refined by in-flight calibrations. The precession maneuver accuracies for open-loop maneuvers are dominated by thruster calibration error. This error

is approximately 6 percent on the ground; however, after in-flight calibration, precession maneuver accuracies on the order of 1 to 3 percent have been demonstrated for Pioneers 10 and 11, which use the identical equipment used for Pioneer Venus.

Using the stored program data as described in Appendix 10A, the ΔV sequence can be loaded and executed. A typical command sequence is shown in Table 10-1. All commands and functions are identical to those of Pioneers 10 and 11 except for the thruster selection command. This change is required because the increased number of thrusters requires a slight modification of the selection logic. The existing command software can remain unchanged for the entire command sequence except for this one item.

Table 10-1. Primary Commands for ΔV Execution

EXISTING ARC COMMAND DESIGNATOR	COMMAND FUNCTION
RIP 1-2	SELECT 0/3.14 RAD(0/180 DEG) REFERENCE FROM SP5G
RIP 5	SELECT ACS MODE OF SP5G
FMC 5	USE FORMAT C FOR TELEMETRY
SEN 1-2	SUN SENSOR IS SELECTABLE FOR REDUNDANCY
PSE 9	POWER ON TO PSE
SLA 9	POWER ON TO DSL
ACS 1	ARM REGISTER 1 AND LOAD ANGLE (α) AND MAGNITUDE OF FIRST PRECESSION (TIME)
ACS 2	ARM REGISTER 2 AND LOAD MAGNITUDE OF DELAY AND ΔV (TIME)
ACS 3	ARM REGISTER 3 AND LOAD ANGLE (α) AND MAGNITUDE OF RETURN PRECESSION (TIME)
PRE 1-2*	SELECT PRECESSION THRUSTERS
PUL 2	SELECT 1/8-SECOND PULSE LENGTH FOR PRECESSION THRUSTERS
VEL 1-2	SELECT ΔV THRUSTERS FOR FORE OR AFT THRUSTER FIRING
ACX 4	RESET PSE TO GET TELEMETRY READING OF REGISTERS AND INITIALIZE FOR MANEUVER
ACX 1	EXECUTE STORED SEQUENCE - PRECESS TO DESIRED POSITION, EXECUTE ΔV AND RETURN PRECESS TO DESIRED FINAL ORIENTATION

*MODIFIED FROM PIONEERS 10 AND 11.

Upon sequence initiation, the contents of the storage registers are transferred into their respective counters (angle counter, delay counter, primary magnitude counter) in accordance with the occurrence of the following PSE program sequence states. All stored programs cycle

through all sequence states unless interrupted by ground command. The ground commands can be used to inhibit the sequence, override the inhibit condition to continue the sequence from the point inhibited, or "stepped" to jump into the next state. Sequence "Step" is normally used to shorten a delay period.

<u>Sequence State</u>	<u>Function</u>	<u>Command</u>
S0	Reset	ACX4
S1	Delay	ACX1
S2	No. 1 Precession	
S3	Delay	
S4	Midcourse ΔV	
S5	Delay	
S6	No. 2 Precession (return)	
S7	Program Complete	

The above described sequence assumes that the axial thrusters are fired continually for the ΔV execution. Other alternatives exist as described in the following sections.

10.2.2 Second and Third Midcourse

The accuracy of the proposed method of ΔV execution has been demonstrated by Pioneers 10 and 11. For both of these spacecraft, the first midcourse maneuver ΔV was executed within 0.02 radian (1 degree) of the desired pointing direction. Precessions of 0.79 and 0.61 radians (45 and 35 degrees) were performed open-loop to obtain the pointing direction. ΔV execution magnitudes for the first midcourse of Pioneers 10 and 11 were executed to accuracies of about 3 and 1.5 percent; however, the ΔV magnitudes were trimmed in each case to negligible magnitude error by inhibiting the stored program and firing individual thruster pulses. Magnitude was checked using the doppler shift measurement capability of the DSN in real time. Since the equipment employed for Pioneer Venus is identical to that of Pioneers 10 and 11, similar accuracies are expected.

Pointing errors during midcourse ΔV maneuvers are most significant if a large first midcourse maneuver is required. In that case pointing (and other execution) errors add to the tracking errors in determining the resultant second midcourse requirements. As a figure of merit, second midcourse ΔV requirements have been shown in Figure 10-3 as a function

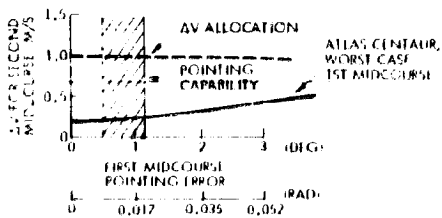


Figure 10-3. Effect of First Midcourse Pointing Error on Second Midcourse Requirements

of pointing error during the first midcourse. Pointing errors of the baseline system contribute only slightly to overall midcourse requirements. For a worst-case (99 percent) ΔV , pointing error of 0.017 radian (1 degree) would contribute about 0.12 m/s for Atlas/Centaur. This error is dominated

by ephemeris and tracking errors, with uncertainty in the solar force model also contributing. With a 1 m/s ΔV allocation for the second midcourse execution errors are negligible for the Pioneer Venus capability, as demonstrated by Pioneers 10 and 11.

Second and third midcourse maneuvers are nominally performed identically with that of the first midcourse. However, the second primary ΔV method which employs all four transverse thrusters fired in pairs can also be used. This method is discussed in the next section.

Alternatives for second and third midcourse also include leaving residuals from the first (or second) midcourse as an attempt to control the direction of the next. With the probe mission as an earth pointer, a small third midcourse could be pre-biased in the direction of the earth to eliminate reorientation for the third midcourse ΔV .

10.2.3 Maneuver Options

A major feature of the Pioneers 10 and 11 system adopted for Pioneer Venus is the design flexibility. If a ΔV is to be executed, the following options are available:

- 1) Continuous ΔV , using a stored program and either of two axial thruster pairs (axial thrusters are aligned with spin axis)
- 2) Pulsed ΔV , using a stored program and all of the transverse (spin) thruster pairs. All four spin thrusters are fired each revolution in the inertial direction of the ΔV .
- 3) Pulsed, by real-time ground command of axial thrusters
- 4) Pulsed, by real-time ground command of transverse thrusters
- 5) Pulsed or continuous as in the previous four options but using only single thruster(s) as an added backup mode.

Methods 1) and 2) are both autonomously controlled by the PSE, an unmodified part of the CEA, and are designated as primary. Methods 3), 4) and 5) are backup. To control the direction of the ΔV , another set of options are available:

- 1) Rhumb line precession to the desired attitude for execution of the ΔV by one of the above options (single maneuver to any attitude)
- 2) Execution of the ΔV by components without reorientation of the spacecraft
- 3) Precession by ground command via the so-called Type I, Type II precession (for Type I precession the spin axis remains in the plane defined by the spin axis and the sun, Type II precession is about the sun line)
- 4) Real-time pulses timed from the ground and executed at the instant received. In the event of sun sensor loss, phase control can be obtained from downlink doppler modulation. Round trip light time must be taken into consideration. This mode is the ultimate backup.

Redundancy considerations were of primary concern in the development of the design approach to maneuver execution equipment. The two sun sensors, two spin period sector generators, two duration and steering logic assemblies, the program storage and execution assembly, and the thrusters are cross-strapped so that the complete failure of one each of all of the above control elements (Figure 10-1) would not be critical to mission success. In the case of the eight thrusters, a complete mission can be obtained using as few as three thrusters: one for spinup, one for spindown, and one axial precession-velocity thruster.

A ΔV can be executed using the spin control thrusters pulsed radially where all four spin thrusters are fired each revolution (Option 2). The spin axis is precessed normal to the desired ΔV such that the plane containing the spin thrusters contains the ΔV vector. When two transverse thrusters are aligned with the ΔV , they are fired. The opposite two thrusters are fired after a 3.14 radian (180 degrees) rotation. Although this method is identical in operation to that on Pioneers 10 and 11, with the spin thrusters located in the plane containing the center of mass, this mode is greatly improved over the equivalent mode for Pioneers 10 and 11 where only two spin thrusters are used. The additional thrusters reduce

the execution time and center of mass offsets are such that precession coupling is negligible. Redundancy of transverse thrusters also permits spinup for execution of many maneuvers if desired. Dispersion errors can be reduced (by a factor inversely proportional to the square of the spin speed) by increasing spin speed for ΔV execution using a single thruster.

Spin coupling is a concern in all large ΔV maneuvers since a significant spin speed reduction causes greater ΔV dispersion and can even cause loss of spin stabilization. Spin coupling results from thruster misalignment for a ΔV obtained via the axial thrusters and from unbalanced thrusters for a ΔV produced via transverse thrusters. The worst case magnitudes of the spin coupling for the expected maneuvers are given in Figure 10-4. Significant spin changes for the Thor/Delta spacecraft version occur not only because of the higher mass-inertia ratio than for Atlas/Centaur, but also because of the large first midcourse.

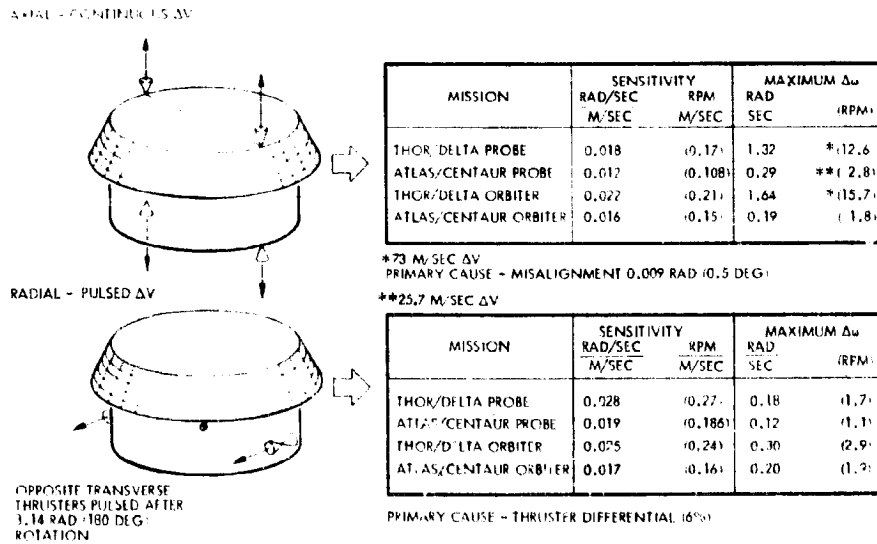


Figure 10-4. Spin Coupling Effects for Worst Case ΔV

The design of the PSE also provides the benefit of independence of spin rate for all precession maneuvers. This is achieved by precessing for a predetermined time rather than for a predetermined number of thruster pulse counts. If, for example, the spin rate doubles during the ΔV (because of spin coupling), then on the return precession each thruster

impulse will cause only one-half the angular step change; however, pulses will occur twice as often. Thus a constant rate of precession occurs with the Pioneer Venus system which is independent of spin speed. If pulse counting were used, very large precession errors could occur in the event of spin changes.

10.3 Attitude Determination Procedures

10.3.1 Introduction

For Pioneer Venus, the sun and earth have been selected as celestial references since existing off-the-shelf hardware can be used which has sufficient accuracies for all mission objectives. The sun sensor provides a pulse which, combined with the spin period sector generator, provides an exceptionally accurate roll reference. In addition, the sun sensor provides the spin axis-sun aspect angle measurement with an accuracy of 0.004 radian (0.25 degree). Earth aspect measurement is provided by the conscan signal processor adopted unmodified from Pioneers 10 and 11. Conscan provides the earth aspect with accuracy of about 0.002 to 0.003 radians (0.1 to 0.2 degrees). These two independent measurements determine essentially the same angle. As a coplanar condition is approached, the geometry causes a steady degradation in the system accuracy for fixed measurement accuracies of sun aspect and earth aspect. The effect of geometry on attitude accuracy is illustrated in Figure 10-5.

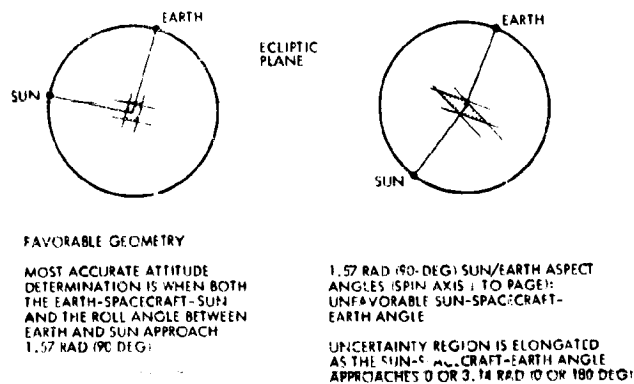


Figure 10-5. Geometry Effect on Attitude Determination Accuracy

Fortunately, unfavorable geometry occurs only for short intervals during interplanetary cruise for the orbiter and probe missions, and at the end of the orbiter mission. These short periods in no way jeopardize

or reduce mission objectives or effectiveness. The primary advantage of the selected sensors is that the measurements are direct and instantaneous, and very simple software is used that has already been developed for Pioneers 10 and 11. Although a sun aspect measurement was not used on Pioneers 10 and 11, the software needs only a single calibration curve, thus unique attitude can easily be read directly from the displayed telemetry.

10.3.2 Open-Loop Attitude Accuracy

Attitude accuracy is maintained by periodic attitude measurement and precession correction. This process continues as long as the spacecraft is in an earth-pointing configuration where attitude is maintained within the conscan range [0.17 radian (10 degrees)] for the orbiter forward end, or within the medium-gain horn beamwidth [0.21 radian (12 degrees)] on the probe bus and orbiter aft end. Offpointing occurs during mid-course maneuvers, probe deployment and retargeting, Venus orbit injection, and periapsis maintenance ΔV . Offpointing also occurs for the first 50 days of the probe mission with the spin axis pointing about 0.44 radian (25 degrees) from the sun. Attitude corrections are unnecessary during this period. After day 50, the probe mission becomes an earth pointer, tail toward earth, with doppler modulation and the sun sensor used for attitude determination. For the orbiter mission, the tail to earth attitude is maintained during the 108 to 237 day period using doppler modulation for attitude determination. The wide beamwidth of the aft horn permits a two-point spin axis pointing strategy between days 108 and 200 (VOI), with attitude corrections also unnecessary during this time. Before day 108 and after day 237, the orbiter is earth pointing, using the high-gain dish for communication and using conscan for attitude determination.

The analyses presented in detail in Section 8.5 and the orbital experience of Pioneers 10 and 11 have demonstrated that the open-loop Pioneer control concept used for these maneuvers is well within the required accuracy to meet all mission objectives. However, the Pioneer capability has been improved by the addition of sun aspect measurement which provides a check on system accuracy. The open loop accuracy will be about 0.035 radian (2.0 degrees) (3 σ) for all ΔV maneuvers even without the other attitude reference checks.

10.3.3 Precession Calibration

Precession calibration can be performed with greater accuracy for Pioneer Venus than for Pioneers 10 and 11. The calibration is performed using the sun aspect measurement capability by performing the precession calibration maneuver directly toward or away from the sun. An angular maneuver of precomputed magnitude is executed. The aspect angle change is then compared with the precomputed value to determine the correction to be applied to all future precessions.

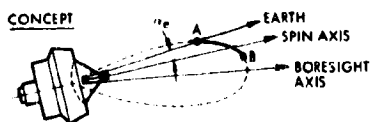
10.3.4 Earth Aspect Measurement



Earth aspect is determined by three separate methods: conscan, doppler modulation, and doppler shift. Conscan is the primary earth aspect determination method for the orbiter when the high-gain dish is pointed within 0.17 radian (10 degrees) of the earth. This is the case except during midcourse maneuvers, Venus orbit insertion, and during the time between days 108 and 237 when the aft end medium-gain horn is earth pointing. The probe bus uses omni communication for the first 50 days, thereafter operating as an earth pointer on the aft medium gain horn. Both the orbiter and the probe bus use doppler modulation for primary attitude determination when the aft end is toward earth, when offset omni antenna can be viewed. Doppler shift is used for attitude determination only once, for Venus orbit insertion.

Antenna pattern search is used only as a backup mode where conscan has failed and other methods cannot be used.

The conscan concept used on Pioneers 10 and 11 is based on the modulation of RF signals produced by pointing errors when the spacecraft antenna boresight is offset from the spin axis direction. The curve



FUNCTIONS

- DETERMINE AMPLITUDE AND PHASE (RELATIVE TO SUN PULSES) OF EARTH POINTING ERROR.
- AUTOMATICALLY CONTROL THRUSTERS TO PRECESS SPIN AXIS TOWARDS EARTH.

Figure 10-6. Conscan Concept

between points A and B in Figure 10-6 represents the ranges of antenna gain swept through during a spin cycle as a consequence of the pointing error, α_e . The modulation amplitude and phase of the fundamental are detected to produce the attitude measurement. The main advantages of the conscan approach are its good attitude determination accuracy, low cost,

and operational simplicity. Although conscan is primarily for attitude determination, it can also be used for automatic precession control to maintain earth pointing.

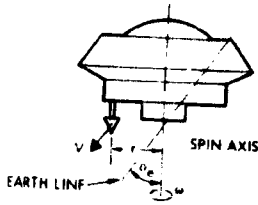


Figure 10-7. Doppler Modulation Earth Aspect Attitude Determination

The earth aspect angle can be determined from changes produced by the spin on the frequency of RF signals from an offset antenna, as in Figure 10-7. If the spin axis is misaligned from the earth (by angle α_e), the downlink signal is frequency modulated at the spin frequency, with the modulation amplitude a function of α_e .

With the spin axis near the earth line, doppler modulation can provide attitude information within 0.009 radian (0.5 degree) but accuracy degrades ranging for angles greater than 0.05 radian (60 degrees), as shown in Figure 10-8.

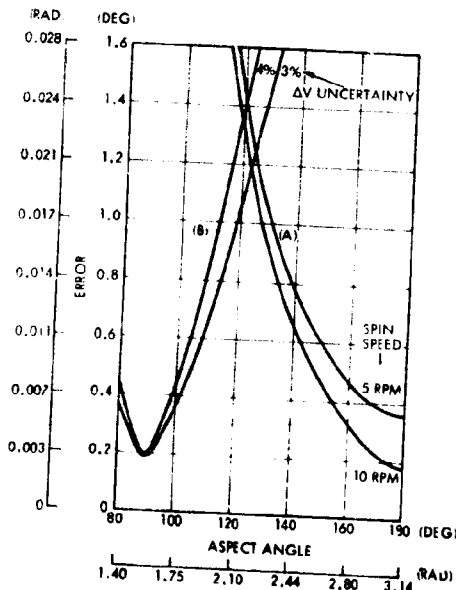


Figure 10-8. Doppler Attitude Measurement Accuracy

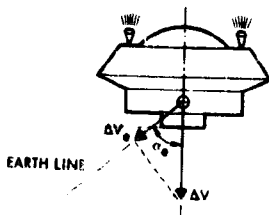


Figure 10-9. Doppler Shift Earth Aspect Attitude Determination

Doppler shifts can also be used for attitude determination with angles near 1.57 radians (90 degrees), but a ΔV maneuver is required. The component of velocity change along the earth line is obtained by doppler measurement, and the ratio of this component to the predicted value of the ΔV maneuver executed gives the cosine of the angle between the spin axis and the spacecraft-earth line (Figure 10-9). This attitude determination technique is most sensitive at spin aspect angles normal to the earth line, as shown in Figure 10-8. It is preferable to use doppler shift only in those instances where a ΔV is to be executed (midcourse, periapsis maintenance, or prone retarget) in order to minimize propellant allocations.

Doppler shift attitude determination is required for Venus orbit insertion with

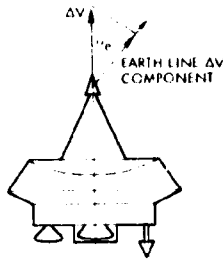


Figure 10-10. Doppler Shift for Orbit Insertion

doppler measurements made via the forward omni. This omni is on the spin axis, as shown in Figure 10-10, such that doppler modulation cannot be used. Since the earth aspect is 1.09 radians (62 degrees), doppler shift is slightly more accurate than doppler modulation, therefore no requirement for an offset omni can be justified for this one maneuver. During the 2.13 radians (122 degrees) precession maneuver from earth pointing to the Venus orbit insertion attitude, the spacecraft attains an earth aspect angle of 1.57 radians (90 degrees). At this point in the maneuver a switch must be commanded to change the communication link from the aft omni to the forward omni. Since doppler shift is most accurate at 1.57 radians (90 degrees) attitude, it is convenient to stop at this position, switch the omni, and execute the 1.0 m/s ΔV for attitude determination. The precession maneuver can then be continued open-loop to the VOI attitude with confidence in the accuracy which assures the proper attitude for insertion.

Both doppler modulation and doppler shift have been used on Pioneers 10 and 11 for attitude determination verification. No new ground capability or software is required.

10.4 ATTITUDE CORRECTIONS

Pointing requirements for science and communications, when combined with solar torque spin axis drift and earth motion, determine the frequency and magnitude of attitude correction. In the case of the probe mission, essentially no attitude correction is required until day 50 when the spacecraft becomes an earth pointer. Tracking of the earth then becomes the governing factor, since drift rates are generally less than 0.0014 radian (0.08 degree) per day. Orbiter drift rate near launch is about 0.009 radian (0.05 degree) per day, increasing to 0.0019 radian (0.11 degree) per day at Venus orbit insertion for the Atlas/Centaur, as shown in Figure 10-11.

Science pointing is not a constraint on absolute pointing accuracy since attitude determination accuracy meets the science requirements.

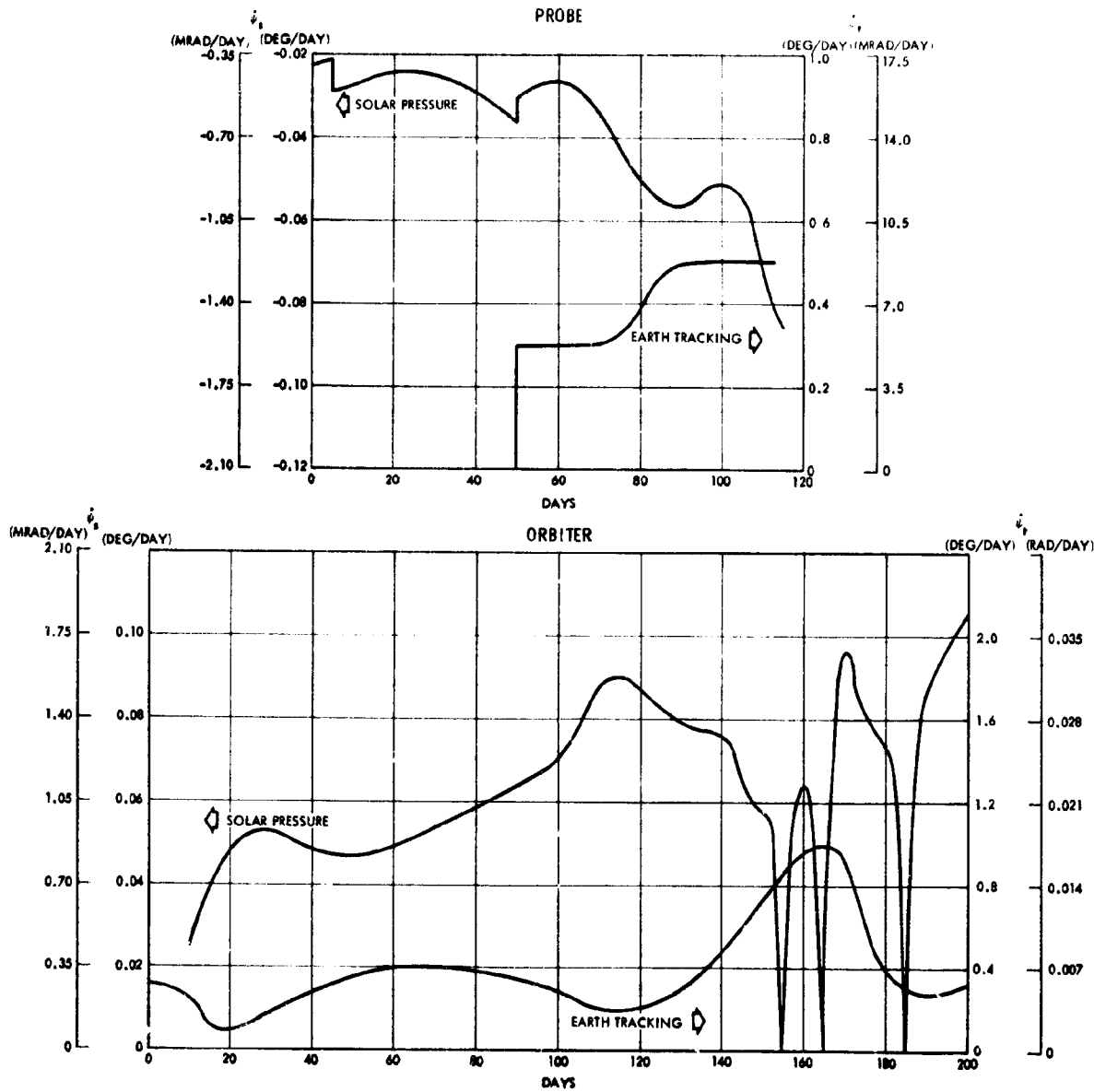


Figure 10-11. Precession Rates Due to Solar Pressure and Earth Tracking

The attitude accuracy is easily determined if earth aspect angles are small [0.70 radian (40 degrees)] for doppler modulation or within the 0.17-radian (10-degree) conscan range. Thus, absolute pointing is constrained by communications, since beamwidths are in the ± 0.21 radian (± 12 degrees) range for the medium-gain horn (probe mission and orbiter aft pointing) and ± 0.06 radian (± 3.5 degrees) for the high-gain dish (orbiter forward pointing). Earth motion ranges from 0.005 to 0.009

radians (0.3 to 0.5 degrees) per day for the probe mission. For communication on the medium-gain horn, the earth-pointing attitude need only be corrected weekly, since the beamwidth is large compared to the earth motion. For the orbiter, earth motion varies from about 0.007 radian (0.4 degree) per day near earth to a peak of 0.023 radian (1.3 degrees) per day early in the orbit phase. Communication can be maintained within the 0.12 radian (7 degrees) high-gain beamwidth by correcting earth pointing at 5-day intervals. Corrections for solar torque drift are nearly an order of magnitude less than correction for earth pointing. However, the motion caused by the solar torque describes a cone about the instantaneous sun line. For the small drift magnitudes between attitude corrections, this motion is observed as motion perpendicular to the ecliptic plane and the earth motion.

Attitude corrections for both earth motion and solar torques are readily made either by a stored program in the program storage and execution assembly (PSE) or by using the fixed angle precession logic and the stored command capability. Daily corrections can be made automatically via the stored command capability by having the stored commands recycle each 24 hours. Closed loop (conscan) can be selected in place of open loop precession to maintain earth pointing of the high-gain antenna of the orbiter. Conscan is primarily used for attitude determination, but can be used for closed-loop control to maintain the antenna pointing on the earth if desired.

10.5 GROUND STATION SUPPORT REQUIREMENT

10.5.1 DSN Support ALL CONFIGURATIONS

DSN support requirements are determined by spacecraft bit rate capability and the times of mission critical events. These include midcourse maneuvers, probe deployment and entry, Venus orbit insertion and periapsis maintenance ΔV . Figures 10-12 and 10-13 show the bit rate capabilities. For the probe mission, operations are performed using only the 26-meter DSN until the third midcourse and the probe deployment sequence. For the orbiter, the 64-meter DSN is optional for data acquisition while on orbit, but is necessary for communication during the flip maneuvers, Venus orbit insertion, and the third midcourse.

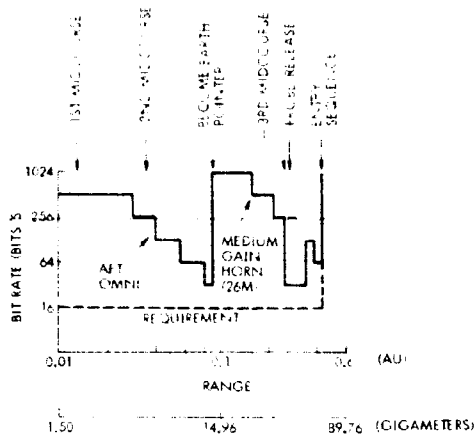


Figure 10-12. Bit Rate Capability Profile for Probe Mission

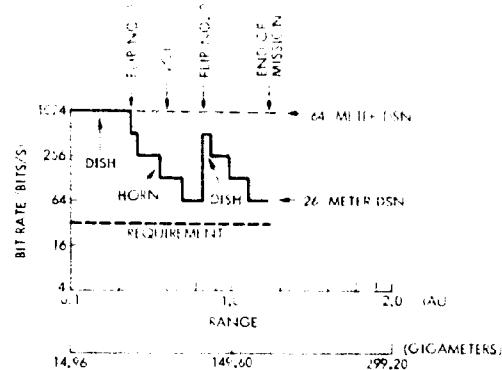
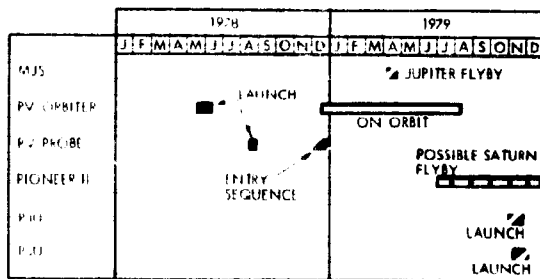


Figure 10-13. Bit Rate Capability Profile for Orbiter Mission

10.5.2 Interference with Other Missions

The DSN must be shared with other interplanetary spacecraft. Those presently known or possible for on-orbit operation in the late 1970's include Mariner-Jupiter-Saturn (MJS), Pioneer 11, Pioneer Saturn-Uranus (PSU), Pioneer Jupiter-Uranus (PJU), and Viking 1975. Of these, the Viking 1975 and Mariner Mars missions will have been essentially completed prior to Pioneer Venus launch and will no longer be requiring extensive coverage. Other surviving spacecraft using the DSN might include Pioneers 6 through 10 and Helios. Possible PSU and PJU launch windows occur in late 1979; however, these follow the nominal Pioneer Venus end-of-mission by about 3 months. A Mariner Mars might also be launched in the late 1979 window.



Those interplanetary missions which significantly overlap with Pioneer Venus are shown in Figure 10-14. The Jupiter flyby would coincide with the middle of a 1978 orbiter mission, and the Saturn flyby of Pioneer 11 might interfere with the end of the orbiter mission.

The relatively short duration of a planetary flyby (about 48 hours) would not significantly perturb orbiter operation. One orbit of data can be stored on board and dumped in 3 to 4 hours using only 26-meter stations;

therefore even if the 64-meter stations are dedicated to Mariner or Pioneer 11, no major operational difficulties are envisioned from interference with these missions.

10.5.3 Support Software Modifications

Because of the great similarity between Pioneers 10 and 11 equipment and that selected for Pioneer Venus, a quantitative measure is desired of the usable portion of the software.

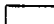

One possible measure of the required modification in the Pioneers 10 and 11 software to adapt it to the Pioneer Venus spacecraft was obtained by examination of the Pioneers 10 and 11 CRT telemetry displays from the Space Flight Operations Facility (SFOF). Each item was examined on 11 of the display formats to determine which items would be totally unchanged, modified, deleted, or added. By definition, modifications were limited to scale changes (e.g., temperatures) or name changes (e.g., experiment acronyms). All other changes were considered as deletions and additions. Deletions were caused primarily by RTG's, star logic, command memory changes, and sequencer deletion. Modifications were caused primarily by experiments and temperature ranges, and probe/orbiter only related telemetry. Additions were caused by the solar array power source, additional thrusters, and the new stored command programmer.

The study results tabulated in Table 10-2 showed 51 percent of the engineering telemetry was completely unchanged, with 25 percent deletion, 12 percent minor modification, and 12 percent addition.

An example of the display modification is shown in Figure 10-15. This subsystem display (attitude control) is typical of the displays to be modified in that about 50 percent of the items are unchanged, however, there are a somewhat higher number of additions and deletions than average. Only engineering telemetry was examined. All science telemetry was assumed as new, but was not included in the totals shown. An independent study was performed to determine the usability of the Sigma 5 EGSE software of Pioneers 10 and 11. This study showed that about 60 percent of the engineering software was directly usable.

Table 10-2. Telemetry CRT Display Modifications

	OK	DELETION	MINOR MODIFICATION	ADDITION
LAUNCH SEQUENCE	--	22	--	--
RC/CDU/DATA	35	2	15	5
CDU/DATA	27	13	--	12
POWER NO. 3	19	16	15	9
ACS/PROPULSION	42	20	5	22
ACS REGISTER STATUS	22	--	--	--
SPACECRAFT STATUS	41	6	11	2
CONSCAN	17	1	--	--
THERMAL	17	12	8	4
RTG	--	25	--	--
GROUND DATA	17	--	--	--
	237	117	54	53
PERCENT OF TOTAL	51.4	25.4	11.7	11.5

 MINOR MODIFICATION
 DELETED

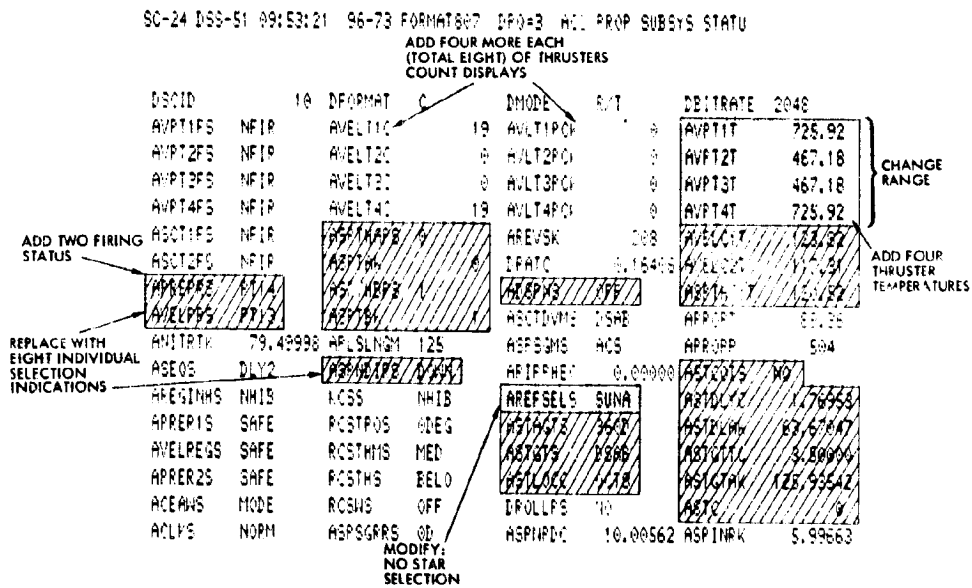


Figure 10-15. Example of Crt Telemetry Display

10.6 PROBE DEPLOYMENT SEQUENCES

10.6.1 Probe Target Selection and Release Strategy

To obtain a cost-effective and reliable system design, constraints compatible with the science requirements have been defined on entry site selection. These constraints define a crescent on the planet surface as shown in Figure 10-16. The upper edge excludes entry sites having communication angles greater than 0.96 radian (55 degrees). The lower edge eliminates sites having entry angles steeper than 0.79 radian (45 degrees). The communication angle constraint implicitly requires that entry angles shallower than 0.44 radian (25 degrees) are excluded.

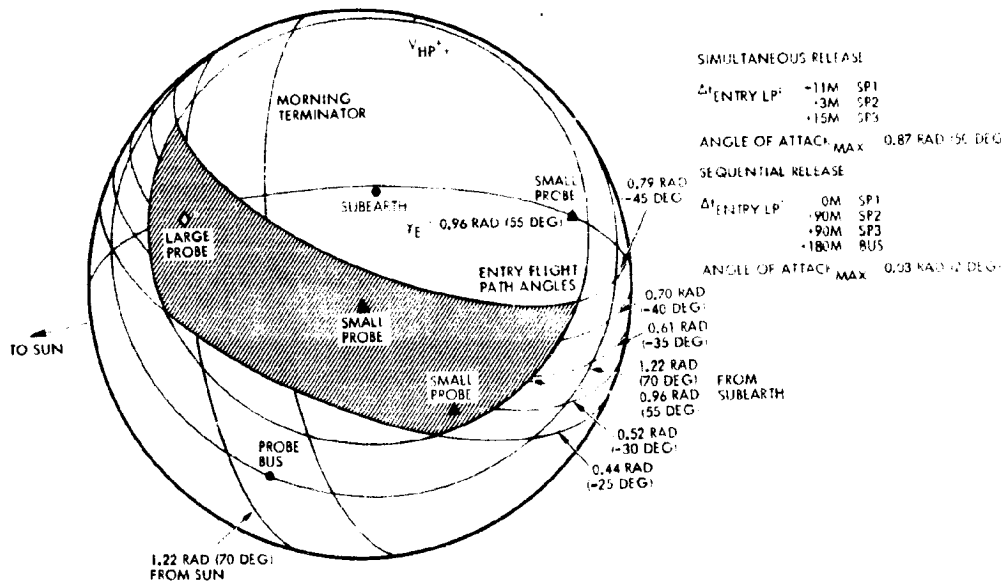


Figure 10-16. Probe Entry Locations for Simultaneous or Sequential Release

Probe deployment can be performed with either simultaneous or sequential release. Sequential release requires that the center of mass of each probe lie in the same plane as the bus center of mass in order to maintain alignment of the principal (spin) axis between deployment. Other alternatives can also be selected, including

- Probe entry site selection
- Spin rate increase prior to deployment to minimize deployment tipoff or solar torque induced error
- Retargeting to control individual probe entry times.

Sequential release is an extremely flexible deployment mode which permits the acquisition of any set of target sites within the crescent while obtaining zero angle of attack for each probe. The probes enter with solar aspect angles varying from 0.52 to 1.22 radians (30 to 70 degrees), but this variation may be accommodated with identical thermal controls on each probe. The probes may be released at any desired spin rate. Finally, the bus retargets may be designed so that all small probes enter either simultaneously with the large probe, sequentially two at a time, or at individual separate times.

The simultaneous release characteristics are also indicated on Figure 10-16. To obtain a reasonable system the probes must be released at essentially the same attitude. This causes non-zero angles of attack (α) to obtain a spread of entry sites. If released 21 days from Venus, the $\alpha = 0.87$ radian (50 degrees) pattern required a spin rate of 2.04 rad/sec (19.5 rpm). The times of arrival are different, as indicated, if maximum coverage is desired. The solar aspect angles are identical, which simplifies the thermal control problem.

Sequential release with entry two at a time appears to be the most desirable deployment mode because of its characteristics of flexibility, low spin rates, zero angle of attack, and entry time separation. This method combines the science benefits of simultaneous entry with operational ease and multiple ground station coverage. Retargeting and deployments can be performed to control the times between each probe entry to simplify the ground communications lockup.

10.6.2 Probe Release Timeline

The operational timelines of sequential and simultaneous release are essentially the same, with sequential release requiring a repetition of several events. The ground system operational timelines must cover the following functions:

- Orbit determination: conservatively a 4-hour task for both the orbit determination task and propagation of the best estimate state vector.
- Bus targeting analysis: conservatively a 1-hour task to derive the timing, ΔV 's, and attitudes if tracking data is available.

- Detail sequence and command generation: conservatively a 6-hour task to generate detailed command sequences, validate the sequences against system performance capabilities, validate actual command structure, and hold command conferences, as required. This will normally be done the day before the event.
- Release and validate commands: conservatively 1 hour to release commands, validate, transmit, and verify, and retransmit if required.
- Spacecraft implementation: conservatively 6 hours to process, verify attitude, correct attitude, execute ΔV (or probe release), and unwind to cruise attitude. Four hours from start of precession to execution is assumed.

The baseline design provides retargeting and probe deployment maneuvers to be performed alternately every 2 days, as shown in Figure 10-17.

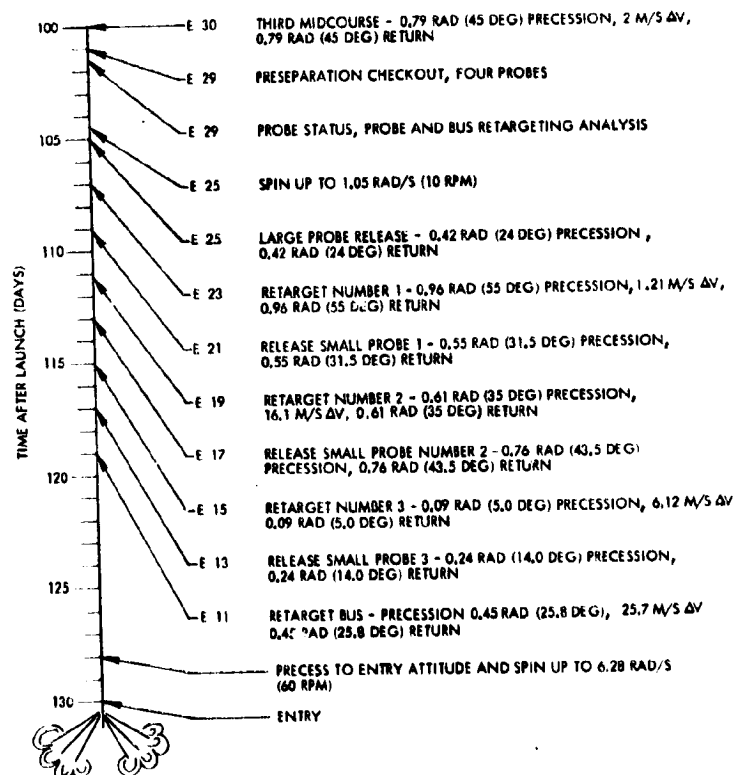


Figure 10-17. Propulsion Events Timeline

Typical precession and ΔV sequences are given, although the system flexibility permits many options. The sequence shown provides simultaneous entry of the large probe and one small probe, followed 1.5 hours later by the other two small probes, with bus entry 1.5 hours later. Slight

modification of the second retargeting in this sequence (decrease in ΔV to 0.8 m/s) would permit simultaneous entry of all probes followed by the probe bus in an additional 1.5 hours. Entry sequence data recovery is presented in Section 10.7. The level of ground support depends on whether all four probes are checked out at: 1) a single bus maintenance, or 2) sequentially just prior to each probe release. Method 1) is desired in that it provides status for all four probes at one time, thereby providing more flexibility to reassign retargets for the probes in the event of anomalies.

A mini-timeline for a probe deployment and retarget is given in Figure 10-18.

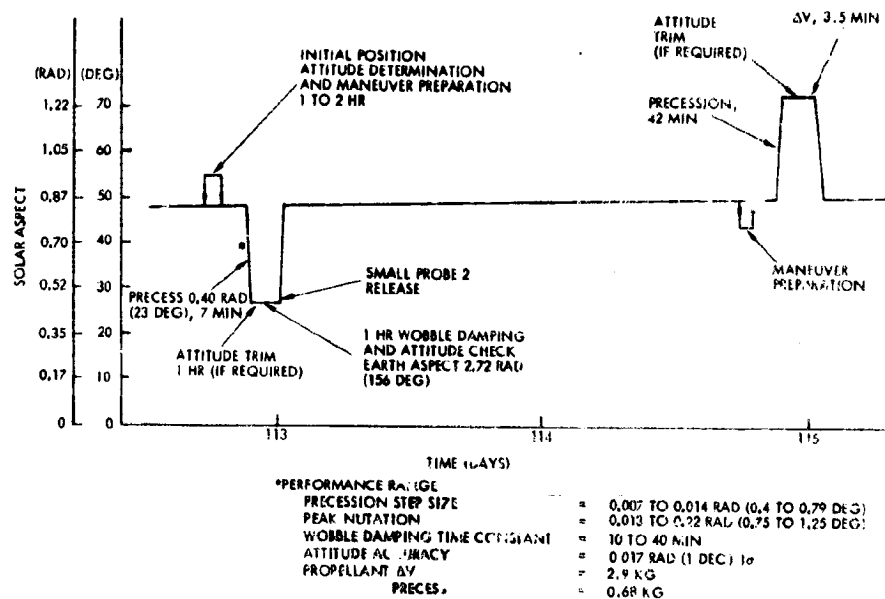


Figure 10-18. Probe Deployment Timeline

The probe release sequence time allocations are based on Pioneers 10 and 11 first midcourse maneuvers. The probe release and retargeting is performed identically to the Pioneers 10 and 11 midcourse, which allows complete ground control and monitoring of all phases of the maneuver. However, the open loop approach is a very conservative method which provides the backup of continuing to execute the preprogrammed maneuver automatically even without ground intervention or contact. Continuous monitoring permits the operator to interrupt the maneuver, determine attitude, and make changes or corrections in either pointing

direction or ΔV magnitude to improve accuracy if desired. In a contingency situation, release (or ΔV) times can be delayed. ΔV trim can be done in an arbitrary direction while in the release attitude if desired.

Maneuvers are performed every other day, and can be performed during a reasonable working day. Considerable time (2 hours) is allocated for delay prior to the ΔV and each precession in order to minimize wobble. As will be shown, all probe release maneuvers and most retarget maneuvers are on the order of 0.52 radian (30 degrees) and can be performed with high accuracy [0.02 radian (1 degree)] with only open-loop maneuvers and on-orbit calibration, which will have been supported by the midcourse maneuvers.

The timeline shown is for a nominal probe release sequence, and the worst case retarget maneuver. The sun aspect angles lie generally between 0.44 and 1.05 radians (25 and 60 degrees) for the entire deployment and retarget sequence. The conical array power capability and thermal design concepts are totally in concert with the leisurely deployment and retarget times for these events.

Figure 10-19 shows the locations of the spin axis during the entire probe deployment and retarget sequence projected onto a unit sphere about the spacecraft. Using the probe bus as an earth pointer during this period permits maximum communications utilization prior to maneuvers, and is an excellent starting point for maneuvers because the precession magnitudes required are reasonably small. Two options for mission operations are apparent. First, maneuvers can be minimized by orientation to a position (say the large probe release), executing, and staying there until the next maneuver two days later. The next maneuver is the first retarget, which is only an 0.14-radian (8-degree) precession. The spacecraft can now remain in this position until time to maneuver for the first small probe release, again a short maneuver. This process can be continued for the entire sequence, since the baseline design permits the resultant sun angles for indefinite periods. Power and thermal designs are ideal for this process. However, if high bit rate communication using only the 26-meter DSN is desired, the second option can be used; that is, the spacecraft can be precessed back to earth pointing at any time (aft of spacecraft to earth).

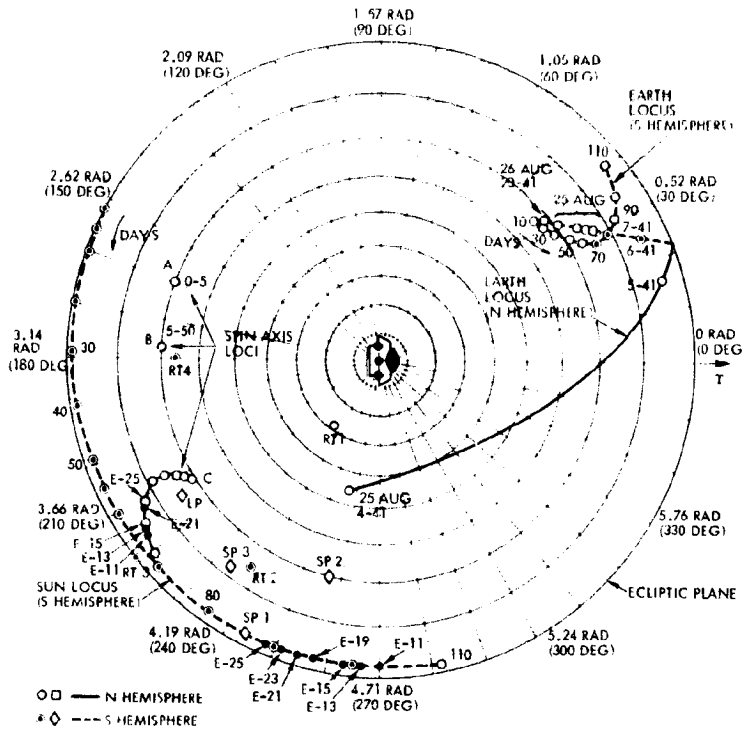


Figure 10-19. Stereographic Projection Showing Angular Geometry During Probe Bus Cruise and Probe Deployment and Retargeting Maneuvers

As part of the overall study, bus configurations which cruise with the spin axis normal to the sun line (nominally normal to the Venus orbit plane) have been considered. With the baseline modified earth-pointing approach, all probe release maneuvers are shortened considerably compared to a spacecraft with spin axis normal to the Venus orbit plane during cruise.

10.7 BUS AND PROBE ENTRY DSN COVERAGE

For the multiprobe and orbiter missions, the bus and probe entry phase imposes the most severe requirements on the utilization of the DSN, receivers, recorders, and personnel. This section discusses the entry phase impact on the DSN and recommends a bus/probe/DSN configuration that utilizes the DSN capabilities to its fullest with maximum probability of mission success.

One of the early study constraints for probe entry had been a doubly-differenced very long baseline interferometry (DDVLBI) experiment that

desired near-simultaneous entry for all four probes, with the bus entry delayed about 1 hour. With the initial requirement for a 1977 multiprobe mission the 64-meter DSN coverage consisted of Goldstone and Madrid. Additional non-DSN coverage was possible with the Arecibo and Haystack antennas, one of which was required for the DDVLBI experiment. With the simultaneous probe entry sequence, there were not enough receivers at each 64-meter site to track each of the probes and the bus in real time and provide a predetection recording capability, which requires another receiver operated in an open-loop mode. A recommended DSN configuration for this simultaneous probe entry phase was defined and is discussed in Appendix 10B. The Version IV science payload definition, which delayed the multiprobe mission to 1978, changed the optimum DSN entry coverage to Goldstone and Tidbinbilla, eliminated Arecibo, and weakened the requirement for a VLBI experiment. Figure 10-20 shows the DSN station coverage for the 1978 entry. These changes, along with a desire to improve on the redundancy of the DSN probe entry tracking capabilities, opened the door for consideration of a sequential probe entry sequence.

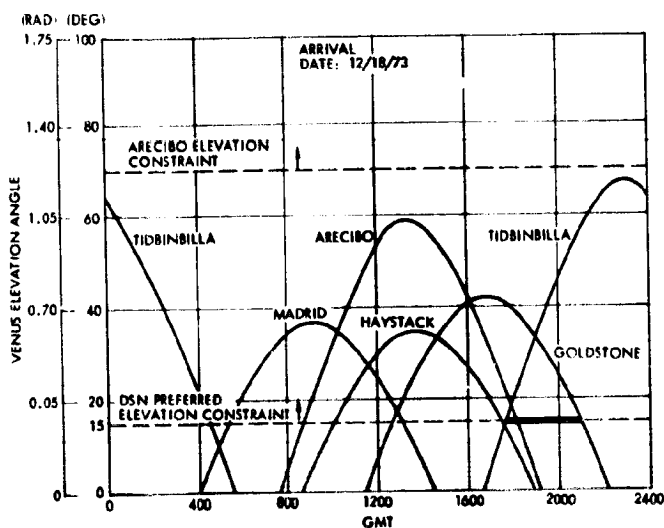


Figure 10-20. Tracking Station Coverage for 1978 Probe Mission

With sequential probe entry more than one receiver at each station could be used to track each probe. The preferred configuration discussed here recommends two-probes-at-a-time entry; first the large probe (LP)

and small probe one (SP1), then 90 minutes later small probes two and three (SP2 and SP3), and finally another 90 minutes later—bus entry (nominal end-of-mission, EOM). The entry timeline for the bus and probes is shown in Figure 10-21. The transmission periods and station receiver utilization show that two receivers (Blocks III and IV) per probe at each 64-meter station are used to insure redundant tracking. A 20-minute interval is allocated between LP/SP1 impact and SP2/SP3 entry to account for any arrival time uncertainties and possible post-impact transmissions. At approximately 30 minutes into the SP2/SP3 descent (1 hour before bus entry) a Block IV receiver at each 64-meter station should be switched to the bus as the bus entry high data rate mode is activated (1024 bits/s), requiring the 64-meter antenna. Also, the Block IV receiver is desired to use its programmable oscillator capability to track the bus through the high doppler buildup during entry.

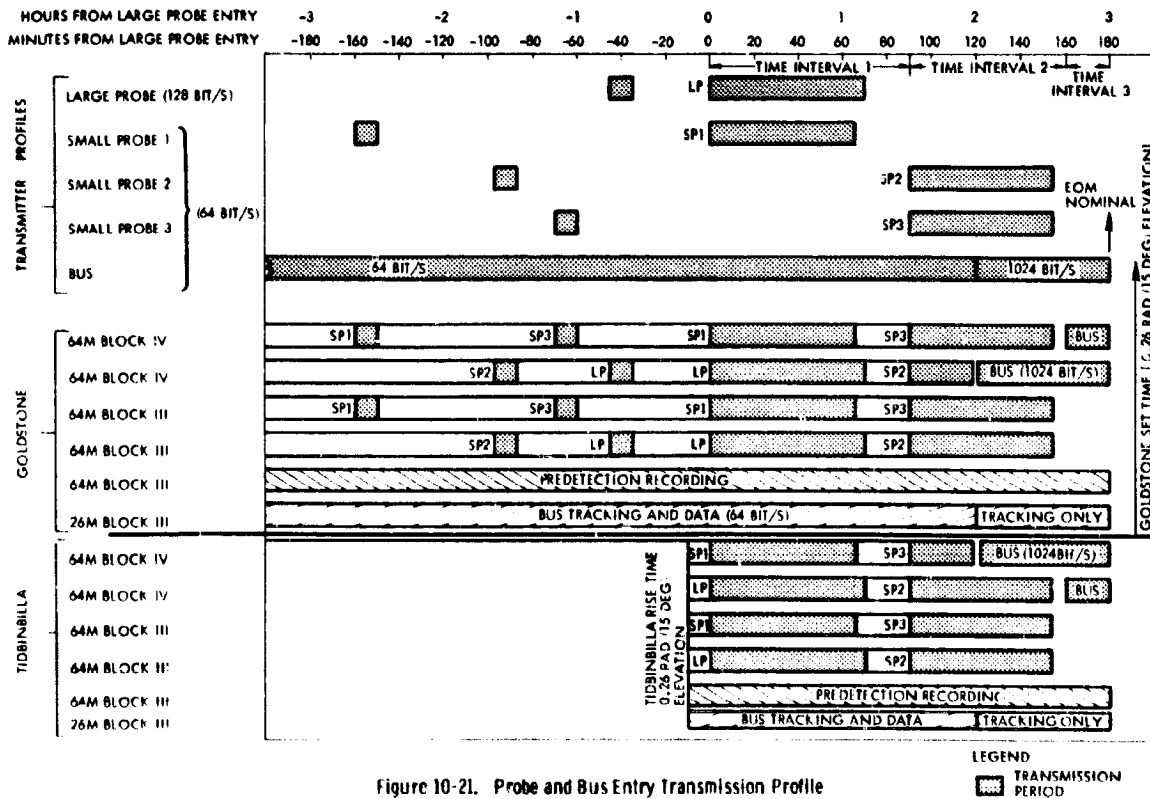


Figure 10-21. Probe and Bus Entry Transmission Profile

The link configurations for the different phases of the entry sequence are illustrated in Figure 10-22. Uplink to the bus for coherent two-way (and

NOTE: T_0 - LARGE PROBE ENTRY 250 KM

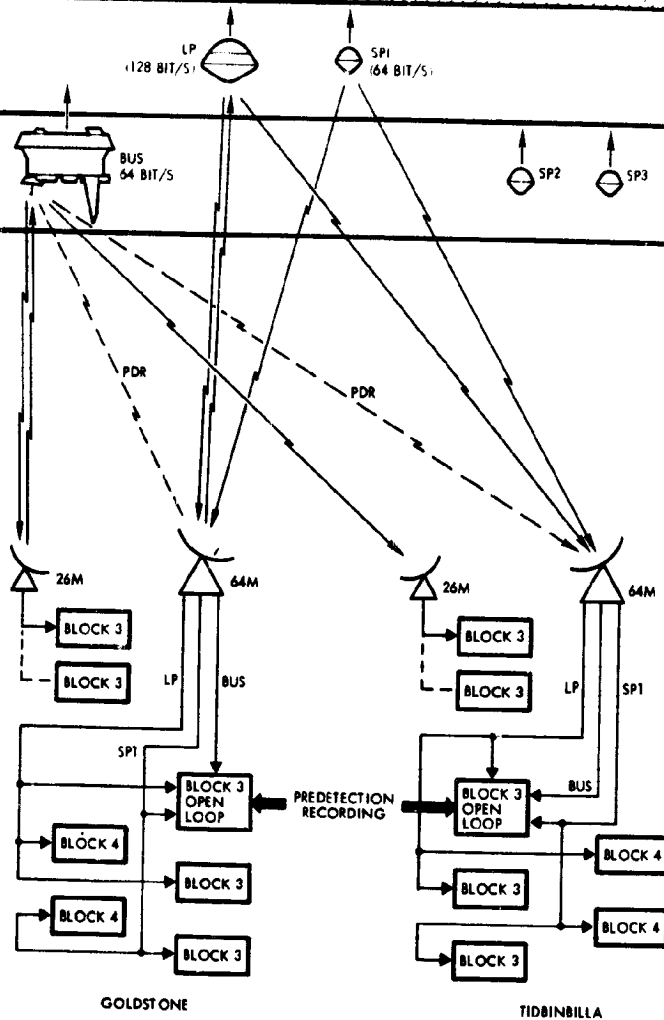
TIME INTERVAL 1
($T_0 + 90$ to $T_0 + 90$ MINUTES)

TIME INTERVAL 2
($T_0 + 90$ to $T_0 + 160$)

POST-IMPACT PHASE

ENTRY/DESCENT PHASE

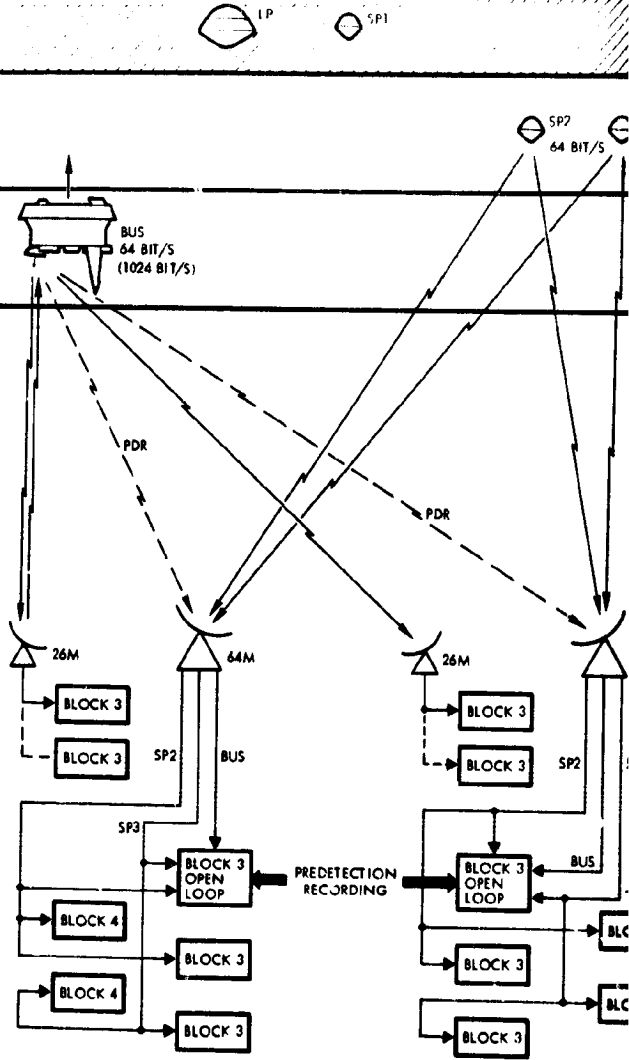
PRE-ENTRY PHASE



GOLDSTONE

TIDBINBILLA

- THE LARGE PROBE (LP) AND SMALL PROBE NO. 1 (SP1) ARE TRANSMITTING DURING THE ENTRY AND DESCENT PHASE.
- UPLINK TO THE LARGE PROBE IS MAINTAINED BY THE GOLDSTONE 64-METER DISH.
- TWO-WAY COMMUNICATION WITH THE PROBE BUS IS MAINTAINED WITH THE GOLDSTONE 26-METER DISH AND A BLOCK III RECEIVER.
- PREDETECTION RECORDING (PDR) OF PROBE AND BUS SIGNALS IS ACHIEVED WITH THE THRU-DISH 26-METER BLOCK III RECEIVER AT EACH STATION.
- DOUBLE REDUNDANT DEMODULATION OF EACH PROBE SIGNAL IS THUS ACHIEVED BY USING A BLOCK III AND IV RECEIVER AT EACH 64-METER STATION.

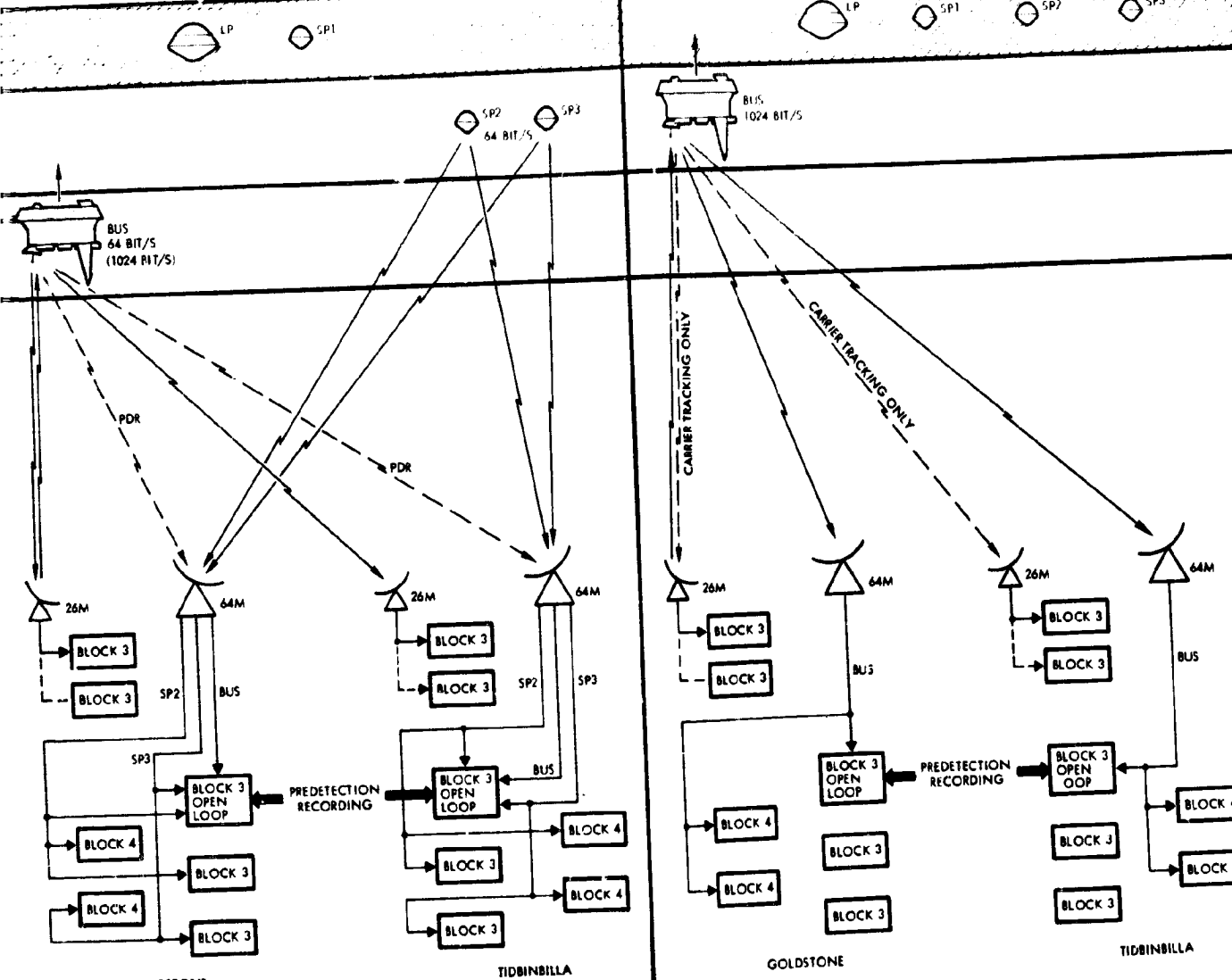
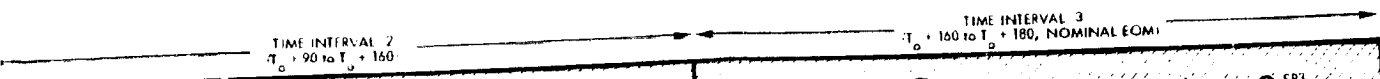


GOLDSTONE

TIDBINBILLA

- THE LARGE PROBE AND SMALL PROBE NO. 1 HAVE IMPACTED AND SUPPOSEDLY CEASED TRANSMITTING.
- SMALL PROBES 2 AND 3 (SP2 AND SP3) ARE NOW IN THE ENTRY AND DESCENT PHASE.
- TWO-WAY DATA COMMUNICATION AT 64 BIT/S WITH THE PROBE BUS IS STILL MAINTAINED BY THE GOLDSTONE 26-METER DISH UNTIL 1 HOUR BEFORE BUS ENTRY, $T_0 + 120$.
- PREDETECTION RECORDING OF BUS AND PROBE SIGNALS IS CONTINUED.
- DOUBLE REDUNDANT DEMODULATION OF EACH PROBE SIGNAL IS MAINTAINED UNTIL 1 HOUR BEFORE BUS ENTRY.
- AT 1 HOUR BEFORE BUS ENTRY ($T_0 + 120$) A BLOCK IV RECEIVER AT THE GOLDSTONE 64 METER DISH IS SWITCHED FROM SP2 TO THE BUS. AT TIDBINBILLA A BLOCK IV RECEIVER IS SWITCHED FROM SP3 TO THE BUS AT THE SAME TIME. (THIS IS DONE TO ACCOMMODATE 1024 BIT/S AND TO TRACK THE HIGH PRE-ENTRY DOPPLER OF THE BUS. CARRIER TRACKING MIGHT STILL BE MAINTAINED AT THE 26 METER STATION WITH CAREFUL MANUAL RECEIVER TUNING DURING THE HIGH DOPPLER BUILDUP.)
- THREE RECEIVER REDUNDANCY IS THEREBY MAINTAINED ON ALL PROBES.

FOLDOUT FRAME



- THE LARGE PROBE AND SMALL PROBE NO. 1 HAVE IMPACTED AND SUPPOSEDLY CEASED TRANSMITTING.
- SMALL PROBES 2 AND 3 (SP2 AND SP3) ARE NOW IN THE ENTRY AND DESCENT PHASE.
- TWO-WAY DATA COMMUNICATION AT 64 BIT/S WITH THE PROBE BUS IS STILL MAINTAINED BY THE GOLDSTONE 26-METER DISH UNTIL 1 HOUR BEFORE BUS ENTRY, $T_0 + 120$.
- PREDETECTION RECORDING OF BUS AND PROBE SIGNALS IS CONTINUED.
- DOUBLE REDUNDANT DEMODULATION OF EACH PROBE SIGNAL IS MAINTAINED UNTIL 1 HOUR BEFORE BUS ENTRY.
- AT 1 HOUR BEFORE BUS ENTRY ($T_0 + 120$) A BLOCK IV RECEIVER AT THE GOLDSTONE 64 METER DISH IS SWITCHED FROM SP2 TO THE BUS. AT TIDBINBILLA A BLOCK IV RECEIVER IS SWITCHED FROM SP3 TO THE BUS AT THE SAME TIME. (THIS IS DONE TO ACCOMMODATE 1024 BIT/S AND TO TRACK THE HIGH PRE ENTRY DOPPLER OF THE BUS. CARRIER TRACKING MIGHT STILL BE MAINTAINED AT THE 26 METER STATION WITH CAREFUL MANUAL RECEIVER TUNING DURING THE HIGH DOPPLER BUILDUP.)
- THREE RECEIVER REDUNDANCY IS THEREBY MAINTAINED ON ALL PROBES.

- ALL PROBES HAVE LANDED AND THE PROBE BUS IS MONITORED BY THE 64-METER DISHES AT TIDBINBILLA AND GOLDSTONE
- THE UPLINK SIGNAL COULD BE SWITCHED TO THE 64-METER DISH BUT OPERATIONAL CONSIDERATIONS PRECLUDE THIS RECOMMENDATION AT THIS TIME.
- REDUNDANT DEMODULATION OF THE BUS DOWNLINK IS DONE USING THE TWO BLOCK IV RECEIVERS AT EACH 64-METER STATION.
- PREDETECTION RECORDING IS CONTINUED THROUGH BUS ENTRY

Figure 10-22. Probe and Bus Data Recovery Sequential Entry

three-way) tracking is maintained from the 26-meter station. All real time downlink tracking and data recovery is fully compatible with the existing DSN receivers, subcarrier demodulators, symbol synchronizers, and data decoders. Only predetection recording for off-line processing may require the implementation of nonstandard hardware (see Appendix 10C).

10.8 ORBIT OPERATIONS

10.8.1 Venus Orbit Insertion (VOI)

Venus orbit parameters depend primarily on arrival velocity and position error, arrival weight, orientation error, timing of the insertion burn start, and dynamic performance. In addition to controlling these errors, the VOI should be independent of ground station operations. This latter requirement is necessary first because the insertion firing occurs while the spacecraft is in earth occultation, and second because this mission-critical event occurs at a predetermined time and should not depend on uplink capability. On-orbit operations for the VOI insertion, depicted in Figures 10-23 and 10-24, include precession to the proper attitude, spinup to minimize execution errors, and commanding of the ΔV start. The operations are performed to minimize the above execution errors while maintaining independence of ground station time critical commands. Attitude execution errors in the injection ΔV have an almost negligible effect compared to arrival velocity, position, and weight errors. Orbit period is the parameter most strongly affected, and this is easily corrected with the onboard ΔV capability.

10.8.2 Precession to VOI Attitude

The approximate attitude for the insertion burn is about 1.08 radians (62 degrees) from the normal position such that the +X axis (spin axis along the high gain antenna) is down 0.49 radian (28 degrees) from the ecliptic plane with 1.12-radian (67-degree) sun aspect and 1.06-radian (61-degree) earth aspect angles. Precession to this attitude and execution with as much as 0.05 to 0.07 radians (3 to 4 degrees) of pointing error would result in satisfactory orbit insertion so that errors would be well within the spacecraft correction capabilities.

ALL ORBITER CONFIGURATIONS

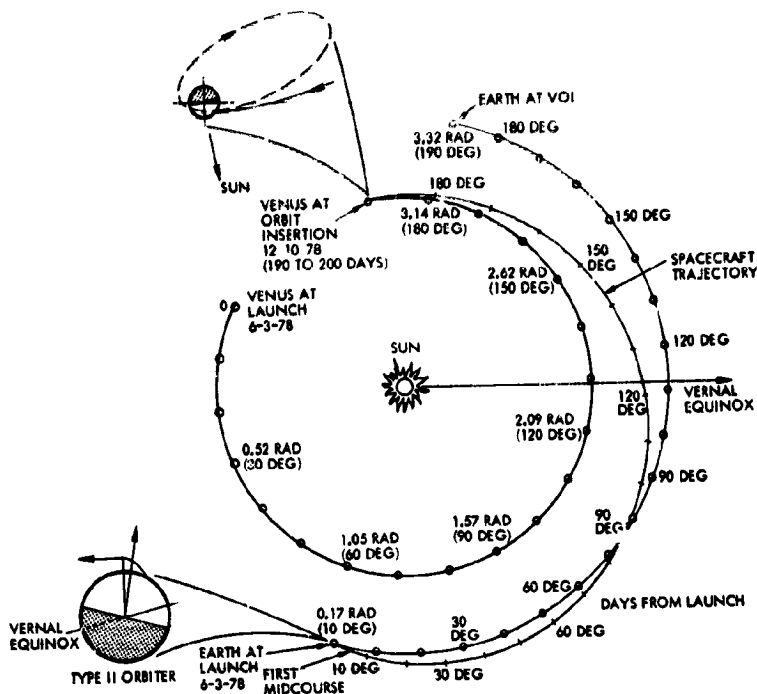


Figure 10-23a. Orbiter Mission Trajectory Characteristics

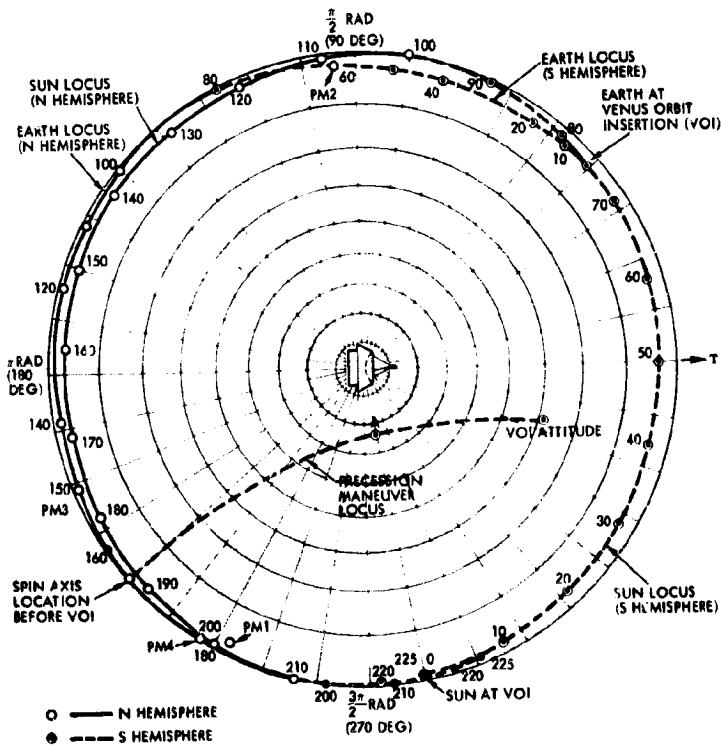


Figure 10-23b. Venus Orbit Insertion and Orbit Phase Geometry

ALL ORBITER CONFIGURATIONS

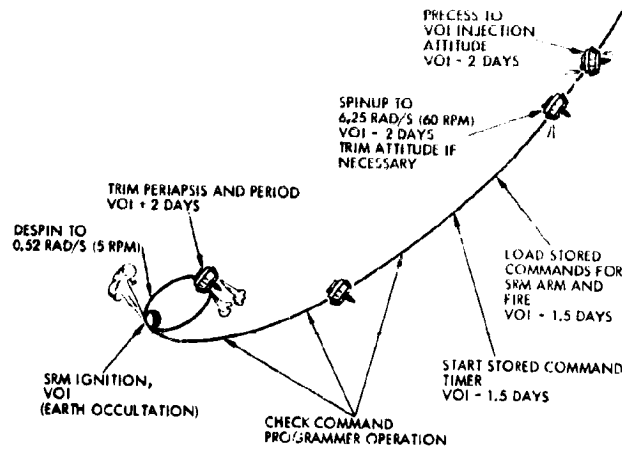


Figure 10-24. Venus Orbiter Insertion Sequence

Prior to Venus orbit insertion, the spacecraft nominal attitude is such that the tail of the spacecraft is earth pointing. A 2.13-radian (122-degree) maneuver is performed to attain the proper attitude for orbit insertion. Precession to the VOI attitude is performed using the open-loop precession capability of the PSE assembly described previously. To insure proper pointing for VOI, there are two options: 1) precess open loop from the known initial position and depend on the open loop accuracy and sun aspect measurement, or 2) perform attitude determination at an intermediate point using doppler shift. Either option will yield sufficient accuracy for insertion. For the second option, the attitude at 1.57 radians (90 degrees) to earth in the maneuver is used as a stopping point to switch the omni antenna, and execute a 1 m/s ΔV to determine attitude via the doppler shift method. The precession to VOI is then continued using the corrected attitude.

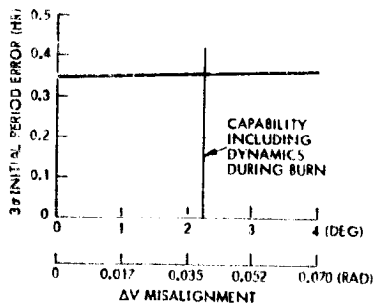


Figure 10-25. Orbit Period Error as a Function of Pointing Error

Execution errors in the burn result in three primary orbital errors: 1) deviation from nominal 24-hour period, 2) periapsis altitude error, and 3) deviation of argument of periapsis. The ΔV misalignment results primarily in an error in orbital period; however, the effect is small compared to other system errors. In Figure 10-25, the zero misalignment intercept

shows the result of all other system errors, with the curve slope showing the additional period error introduced by attitude error at injection.

For option 1) above a capability has been demonstrated by Pioneers 10 and 11 experience for precession magnitude accuracy of 3 percent of the maneuver length. For the VOI maneuver, the direction of precession is known within 0.013 radian (0.72 degree) (3σ), while the magnitude error is 0.06 radian (3.6 degrees) [3 percent of 2.12 radians (122 degrees)]. The sun aspect sensor permits measurement of the sun aspect angle within 0.003 radian (0.2 degree) and this measurement provides an excellent check of the open loop precession accuracy. Error detected in the final sun aspect should be attributed to rhumb line magnitude and corrected accordingly. Option 2) for precession attitude determination is to perform a small ΔV maneuver (1 m/s) at an intermediate [1.57 radians (90 degrees) earth aspect] position and determine the earth aspect angle by doppler shift measurement. At the VOI attitude, this method provides attitude within 0.036 radian (2.04 degrees).

For either option, the effects of the relatively large attitude errors permitted during the injection burn have an almost negligible effect on orbit parameters.

10.8.3 Stabilization Spin

To stabilize the spacecraft during the VOI burn and to overcome disturbance effects caused by the injection engine, it is necessary to spin up to approximately 6.28 rad/s (60 rpm). The dynamic analyses of Section 8.5 show that the ΔV dispersion will be less than 0.021 radian (1.2 degrees) worst case. Again, this error has a negligible effect on the resulting orbit parameters compared with arrival errors. Spinup of the spacecraft is performed by ground command. Since the spinup and precession orientation commands cannot be time critical, it is necessary to have the capability of orientation and spin up for days prior to the insertion burn. The conical solar array spacecraft design provides the capability of remaining at the insertion orientation for an indefinite time. At 6.28 rad/s (60 rpm) solar drift would be less than 0.0018 radian (0.1 degree)/day for Atlas/Centaur, such that orientation to VOI attitude and spinup can be performed as much as 1 week prior to VOI.

10.8.4 VOI Solid Rocket Motor Ignition Command Control

The solid rocket motor (SRM) ignition command must not depend on ground station timing for its execution. Furthermore, no single failure should prevent proper command timing and execution. Timing sensitivity studies (Section 4.3.3) indicate that it would be desirable to execute this mission-critical command with an accuracy of about 15 seconds.

To obtain the desired accuracy without dependence on ground station commands, an onboard programmer is required. To meet the failure mode criteria, redundant commands are also required. The onboard stored command programmer has been designed using dual independent command channels each containing an eight-command capability. No single-point failure can cause premature firing of the solid rocket motor. The ordnance arm and fire commands are separate, with both required for engine ignition. The design is equivalent to quad redundancy (see Section 8.4).

The stored command programmer design permits the load of commands at ground station leisure, with start of countdown for command execution as much as 1.52 days prior to VOI. Longer storage can easily be provided, but the 1.52-day capability was assumed adequate in view of likelihood of multiple (three) ground station coverage, although only one is required. Of the 16 command capability provided, only four are used for SRM ignition.

10.8.5 Periapsis Maintenance

The baseline orbiter trim strategy is to keep periapsis altitude within a band from 200 to 400 kilometers. Parametric analyses show that the total ΔV time does not increase significantly when the periapsis altitude control band is reduced to 25 kilometers. The number of maneuvers required to keep periapsis within the control band does increase as the control band is tightened. In fact, there is a significant increase in the number of apoapsis maneuvers when the control band is decreased from ± 100 to ± 25 kilometers. This effect is shown in Figure 10-26. Consequently, an adaptive strategy would be to control periapsis altitude from 200 to 300 kilometers or even lower, provided the additional fuel required is available. Although the baseline fuel loading does not include the extra

ALL ORBITER CONFIGURATIONS

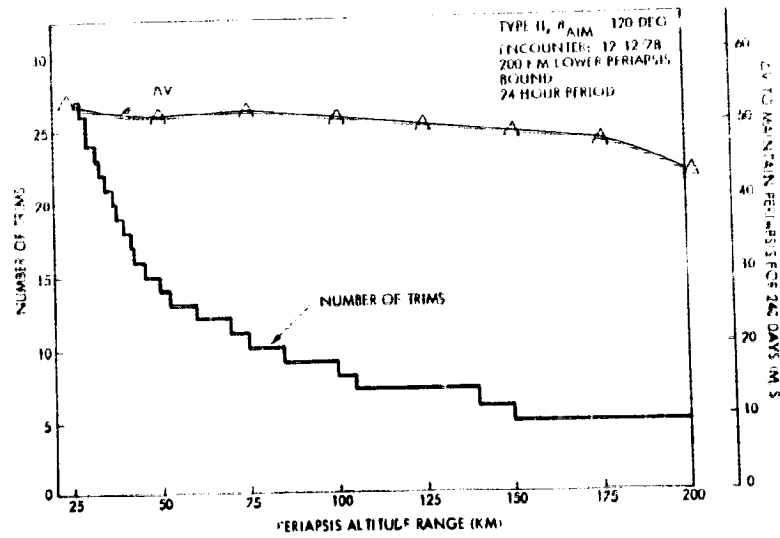


Figure 10-26. Periapsis Maintenance Altitude Variation Effects

fuel to provide this option, there is a very good chance that all the midcourse maneuvers will not require the ΔV load for each maneuver. Thus, the additional trim maneuver fuel could come from the excess. Furthermore, the fuel tanks have been purposely oversized so that weight margins at launch can be used to provide extra ΔV capability. The baseline trim strategy includes four ΔV maneuvers which occur on days 0, 60, 145 and 180 after Venus orbit insertion, as shown in Figure 10-27. These maneuvers are nominally performed at apoapsis with the ΔV direction along the velocity vector. There are a number of options for performing the first

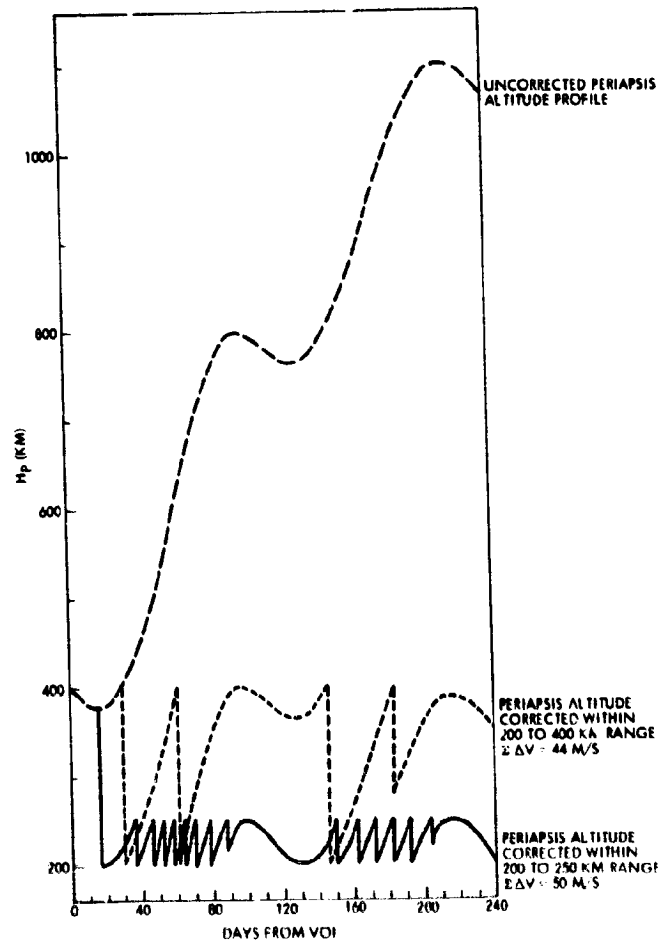


Figure 10-27. Periapsis Altitude Maintenance

periapsis ΔV maneuver including all the options discussed in Section 10.2.3. These include:

- Precess spin axis to apoapsis velocity direction, execute ΔV with axial thrusters
- Precess normal to apoapsis velocity vector and perform ΔV with radial (spin) thrusters
- Perform ΔV using components.

The latter option is most desirable for all periapsis trim maneuvers other than the first (day 30) since the downlink omni communication capability runs out after day 37. An additional alternative exists for the third periapsis maintenance ΔV when the spin axis is nearly in the orbit plane (142 ± 3 days). The ΔV can be imparted using only axial thrusters along the velocity vector at a true anomaly of 3.02 radians (173 degrees); however, the ΔV magnitude is increased from 12 m/s to about 20 m/s by this strategy.

The selected approach for periapsis maintenance is to maintain earth pointing orientation and execute the ΔV by components, using the pulsed, radial thruster ΔV ($\Delta V/SCT$) for the lateral component, and the axial thrusters for the earth line component. This method is completely discussed in Section 10.2.3.

10.8.6 Attitude Corrections



Attitude corrections to maintain earth pointing are dominated by earth motion. Small corrections are also required to correct for solar torque drift which is an order of magnitude less than the earth motion. The earth motion and solar torque drift are shown in Figure 10-28. Corrections can be made using the PSE, the fixed angle pulses, or con-scan as described in Section 10.2.3. Corrections need only maintain attitude within the antenna beamwidth, which varies from about ± 0.27 radians (± 12 degrees) early in the orbit phase (medium-gain horn), to about ± 0.017 radian (± 1 degree) at the end of the nominal mission. The frequency of attitude correction varies from alternate weeks at the start of the orbit phase to every 1.5 days at peak correction times, while communicating via the high-gain dish.

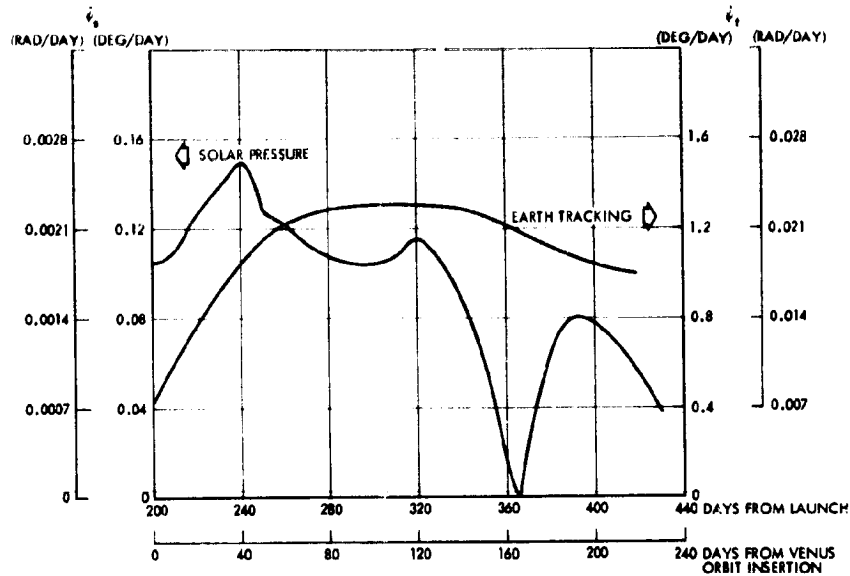


Figure 10-28. Attitude Drift Rates in Orbit Due to Solar Pressure and Earth Motion

10.8.7 Orbiter Science Operations and Options



10.8.7.1 Introduction

Flexibility in orbiter science operations is provided by equipment that is normally required for other purposes. The units which provide this additional system flexibility for science operation include the data storage unit, the command memory, the ram platform, and the earth-pointing configuration. The flexibility provided is incidental to their existence, not the cause. The most significant contributor to the operational flexibility is provided by the command memory. A 1.52-day maximum time lag is provided for 16 independent commands with 2-second quantization. One of these commands can be used to reset the command memory clock such that the command memory recycles without ground interruption. A 24-hour recycle period would permit all science operation commands that are periodic to be autonomously operated by the command memory. This system capability and its interaction with the ground stations, the data storage unit, and certain experiments is described in the following paragraphs.

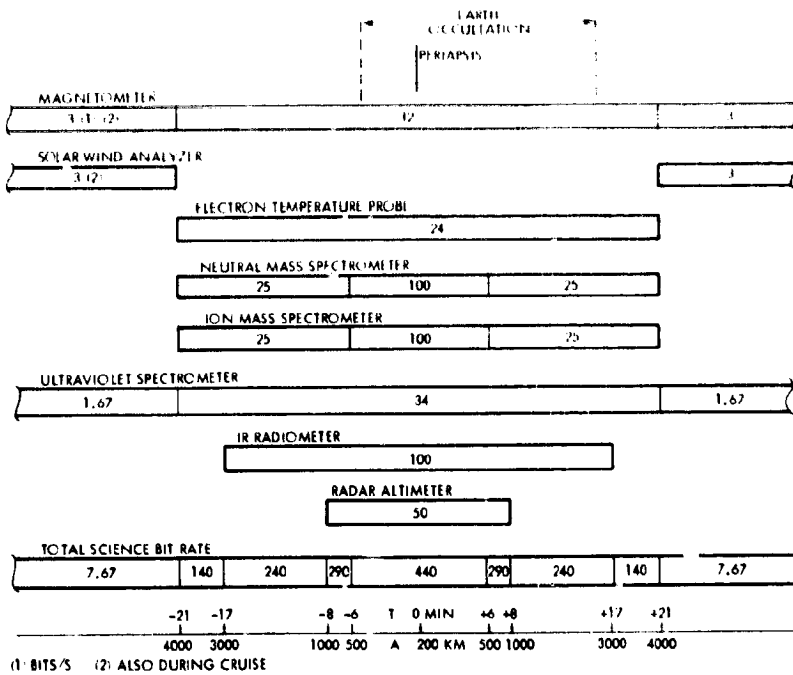


Figure 10-29. Orbiter Version IV Science Payload Data Rate Profile

10.8.7.2 Use of the Data Storage Unit and the Command Memory

Experiment operations are performed with major emphasis on high data rate near periapsis. Most experiments require higher data rates within a few minutes of periapsis with much smaller data rates (if any) at the higher altitudes shown in Figure 10-29 for the baseline instrument complement. Switching of experiment data to higher rates begins at an altitude of 4000 kilometers (21 minutes before periapsis at 200 kilometers) with commands to the electron temperature probe, neutral mass spectrometer, and ion mass spectrometer. At 3000 kilometers or 17 minutes before periapsis, the infrared radiometer is switched to the high data rate mode. The next switch is a power switching to the transmitter driver of the radar altimeter at 1000 kilometers (8 minutes before periapsis). This is the only switch of experiment power that must occur during the 24-hour orbit. The last switch before periapsis occurs to provide a second, higher bit rate for the ion and neutral mass spectrometers. As shown in Figure 10-29, the entire high bit rate switching operation is reversed after periapsis. Since a number of the bit rate switch commands are desired

simultaneously, the entire switching sequence can be performed with only eight commands. On the first command, the magnetometer, electron temperature probe, ultraviolet spectrometer and the neutral and ion mass spectrometers are switched. The second command is used for the infrared radiometer, the third for the radar altimeter transmitter driver power and high bit rate, and the fourth (which can also be a memory flag) produces the higher bit rate for the ion and neutral mass spectrometers. Commands five through eight are used to reverse the above bit rate switching after periapsis. A ninth command can be used to reset the stored command program clock after 24 hours to have the stored program repeat itself each orbit. Science operations would thereby be completely automated to run for days or even weeks with perhaps only an occasional trim of the clock reset time to account for clock drift or orbit changes.

The data storage unit becomes a key operational feature for two specific situations; earth occultation of periapsis events, and low bit rates for real-time telemetry which occur near mission end on the 26-meter ground stations. In the event of earth occultation, real-time telemetry is impossible, requiring stored commands to route data into the DSU for temporary storage. As shown in Figure 10-29, the maximum bit rate is 440 bits/s with all experiments in the highest bit rate mode. If the telemetry bit rate is above 512 bits/s, then real-time telemetry can be used and the DSU bypassed. However, the first 70 days on orbit include earth occultations within 5 minutes of periapsis, thus data storage is necessary. After day 47, the bit rate using the 26-meter DSN dish drops below 512 bits/s; however, the 1024 bits/s capability remains throughout the mission with the 64-meter DSN dish.

There are several options for data readout once the data has been stored. These include operation with the 64-meter DSN to reduce readout times, and readout in real time of some data while storing of other experiment outputs. The memory dump times for the various formats depend on the available DSN dish as shown below.

	64-Meter DSN (min)	26-Meter DSN (min)
Low altitude data	21	342
High altitude data	12	151

The data handling options include two science format structures referred to as the low altitude and high altitude formats, which are slight modifications of the A format and are in addition to the other normal formats (such as the C engineering formats). These are used with DSU operation options as follows:

- Low altitude format can be used for real-time data readout during the entire orbit if the bit rate is at least 512 bits/s. All data from experiments operating at high bit rate at periapsis is formatted and transmitted in real time.
- Low altitude "partial" format is used at low bit rates (64 bits/s). The magnetometer, electron temperature probe and the ultraviolet spectrometer data (plus housekeeping) is formatted and telemetered in real time. The remaining science data is stored unformatted in the DSU.
- The high altitude format presents real-time data from the magnetometer, solar wind analyzer and ultraviolet spectrometer, all at their lowest bit rates. This format is similar to the A/D interleaved format of Pioneers 10 and 11 with all data in the "A" section of the format. Large blank spaces (D section) will appear in the telemetry.
- High altitude format with real-time data as in the item above. The blank sections described above are filled with the memory dump data which is the unformatted (raw) data stored previously.

To summarize the capabilities, a normal sequence of operation is next described for a 26-meter DSN for an end-of-mission bit rate of 64 bits/s. The first of the eight stored commands occurs at the 4000 kilometers altitude before periapsis to change experiment bit rates. The magnetometer, electron temperature probe, and ultraviolet spectrometer are formatted and stored in the DSU memory. (If the bit rate is at least 128 bits/s, this data can also be sent real time.) The data from the ion and neutral mass spectrometers is also stored, but as unformatted raw data. The second command for bit rate change of the infrared radiometer also adds this data to the memory storage. The third and fourth stored commands perform similar functions. The eighth command not only reduces the bit rates for experiments, but also switches to the high altitude format, with only magnetometers, solar wind, and ultraviolet data presented in real time. A ground command must be used to dump the memory contents.

10.8.7.3 Occultation Experiment Operation

Earth occultation occurs during two periods, the first 70 days in orbit plus a short period from day 121 to day 146. The first occultation is centered approximately at the time about periapsis, with a maximum occultation of 20 minutes duration. The second occultation is centered at about 75 minutes before periapsis with a maximum duration of about 96 minutes. Figure 10-30 shows the duration and altitudes of the

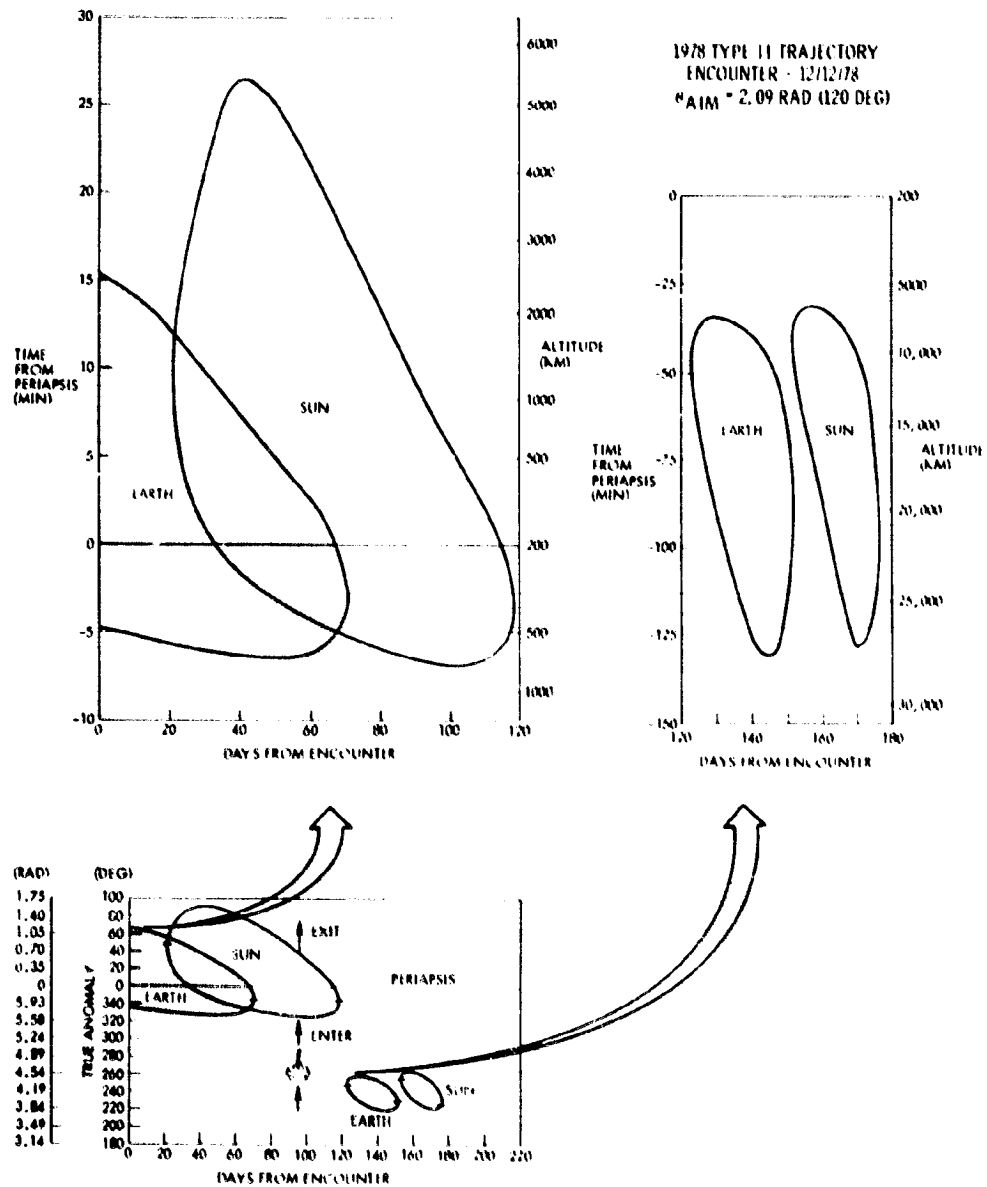


Figure 10-30. Orbiter Version III Science Payload Occultation Profiles

The earth-pointing orientation of the spacecraft is limited in sun aspect angles that can be maintained. The limiting factor is thermal control, which prohibits sun aspect angles greater than about 1.75 radians (100 degrees) to prevent direct sunlight into the louvers. A 1.52 radian (90-degree) aspect angle occurs 37 days after VOI. Although this day is nominally designated for a spacecraft flip maneuver (move from aft toward earth to front facing), the flip can be delayed as much as 18 days and remain within the 1.75-radian (100-degree) aspect angle constraint, giving a 55-day occultation experiment capability.

The aft medium-gain horn is used for both the X- and S-band occultation experiments. The baseline method for operation is to off-point the spin axis about 0.21 radian (12 degrees) to optimize both S- and X-band gain over the occultation time; however, the capability exists to precess the spacecraft during this time at a fixed rate. Fixed-rate precession can give a linear approximation within about 0.05 radian (3 degrees) of the optimum pointing direction for the entire pointing history. This is achieved by selecting the closest precession rate and the precession start time to minimize the error between the linear precession curve and the ideal pointing history. The stored program would be used to return the spacecraft to earth pointing.

During the occultation off-pointing, platform mounted experiments (ion and mass spectrometers) can be maintained pointing in the ram direction during periapsis by computing the new direction caused by the off-earth attitude, and commanding the platform to this new angle.

10.8.7.4 Experiment Platform Updating

The experiment platform can be commanded to point within 0.004 radian (0.25 degree) of the desired pointing direction relative to the spacecraft. Each ground command is used to step the platform direction by 0.009 radian (0.5 degree) in the direction determined by a polarity select command. The nominal pointing direction of the experiment platform is shown in Figure 10-31 which shows a worst-case pointing direction change of 0.031 radian (1.75 degrees) per day. This pointing profile can easily be maintained within an order of magnitude better than the estimated experiment tolerance of about 0.17 radian (10 degrees). About three and one-half

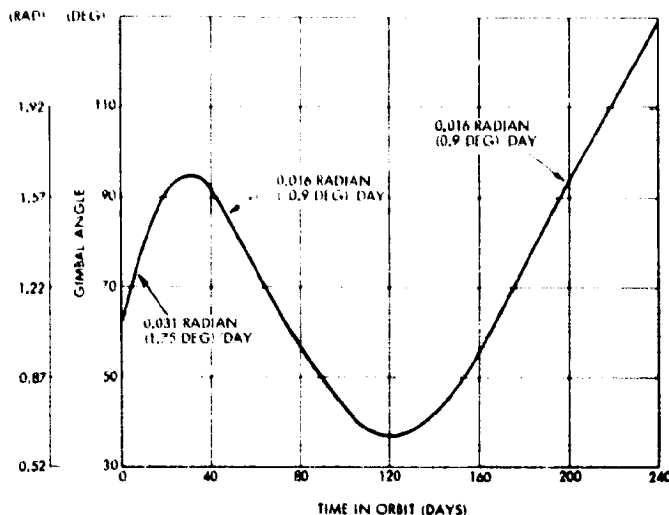


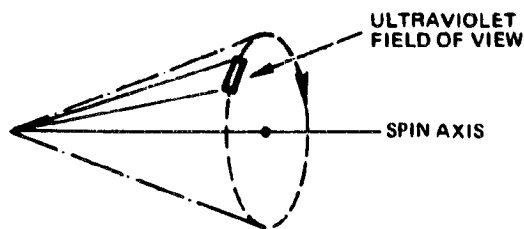
Figure 10-31. Experiment Platform Gimballing

commands per day would be used. The commanding can be performed automatically by the stored command programmer, with three commands per day for the first 4 days and four per day during the next week. Three to four commands per day would then be alternated for the next 4 weeks with only the weekly program update necessary from ground operations.

Two major experiment advantages of the experiment platform include the ability to: 1) maintain experiment pointing in the ram direction even for off-earth pointing maneuvers, and 2) point the experiment platform in the ram direction at altitudes other than periapsis if desired and at the discretion of the ground operator.

10.8.7.5 Ultraviolet Spectrometer Dayglow Maneuver

The ultraviolet (UV) spectrometer experiment capability can be extended to obtain dayglow measurements by performing an additional spacecraft maneuver. The nominal UV experiment field of view is a 0.017 by 0.0000 radian (1 by 0.17 degree) slit which scans a cone 0.14 radian (8 degrees) from the spin axis, as shown below. For optimum conditions,



the dayglow measurements should be taken with Venus just filling the 0.017-radian (1-degree) field of view. To exactly meet these conditions, the spacecraft would perform a precession maneuver of about 0.70 radian

(40 degrees) such that the cone of the FOV is just in front of the path of Venus at the time Venus is 600,000 kilometers from the spacecraft. There are two difficulties involved in this maneuver: 1) the 0.017-radian (1-degree) Venus disc (at 693,000 kilometers from Venus) occurs 1.5 days prior to entry; 2) a 0.70-radian (40-degree) precession maneuver is required to properly point the experiment. The inertial rate of Venus motion relative to the spacecraft spin axis is about 0.07 deg/hour at 1.5 days before entry, as shown in Figure 10-32. If the spacecraft is pointed within 0.017 radian (1 degree) of the desired pointing for this experiment, then 10 to 15 hours would be required before the planet passes into full experiment view. This time would not permit sufficient margin for spacecraft reorientation and spinup for entry. As a compromise, a 0.005-radian (0.34-degree) planet view of the experiment is proposed which would occur at 180,000 kilometers, 4 days before entry. Now, if the spacecraft is pointed 0.017 radian (1 degree) ahead of Venus (pointing error worst case) then Venus would pass through the FOV of the experiment 3 days out at about a 0.009-radian (0.50-degree) view diameter (see Figure 10-33). After one full day of planet viewing, the spacecraft can be oriented and spun to 6.28 rad/s (60 rpm) with sufficient time margins for entry.

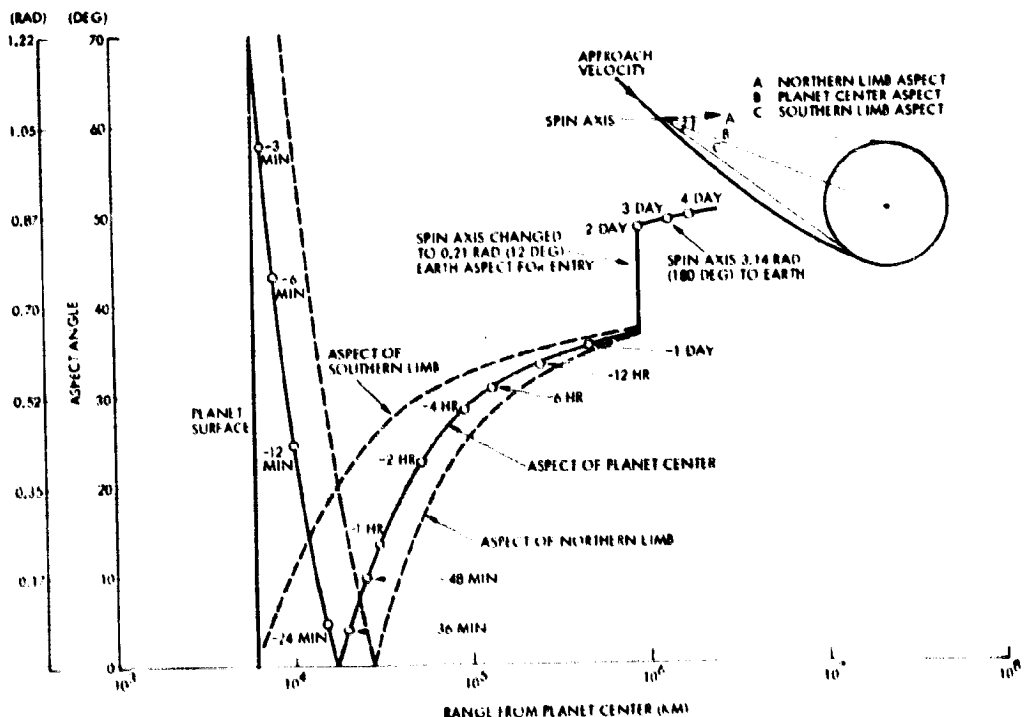


Figure 10-32. Planet Aspect to Probe Bus Spin Axis

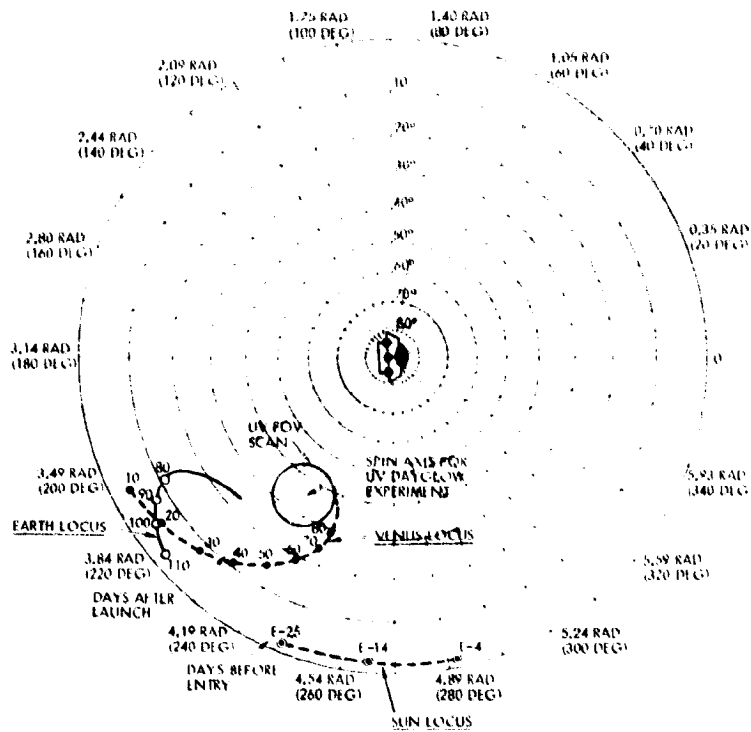


Figure 10-33. Stereographic Projection of Relative Location of Earth, Venus, Sun, and the Ultraviolet Field of View for the Dayglow Experiment

11. Launch Vehicle-Related Cost Reductions:

--

11. LAUNCH VEHICLE-RELATED COST REDUCTIONS

11.1 INTRODUCTION

A brief survey of the factors contributing most significantly to the cost of any high-technology endeavor, such as spacecraft development, shows convincingly that hardware cost reduction requires:

- Use of existing designs to reduce the design and development cost of reinventing each element of a system
- Commonality of design between elements of the system to reduce parallel effort and realize efficiencies in design, manufacture, and testing
- Generous margins in critical parameters (such as weight, volume, and power) to simplify new designs and to provide greater flexibility in application of existing designs.

The launch vehicle tradeoff studies focused on the degree to which relaxation of weight and volume constraints (consistent with Atlas/Centaur capability) could reduce overall program cost. The following sections examine the effects of weight and volume relief on costs both qualitatively and quantitatively, discuss cost/weight allocations, and summarize the Thor/Delta-Atlas/Centaur cost tradeoffs leading to the recommended mission system.

11.2 QUALITATIVE EFFECTS OF WEIGHT/VOLUME RELIEF

Thor/Delta baseline designs for the probe bus and orbiter, even with fairly tight weight constraints, are able to make extensive use of existing unit designs based largely on Pioneer 10 and 11 subsystems. The Thor/Delta probes, on the other hand, are severely weight/volume constrained and require significantly higher proportions of new and major modification design effort.

Consideration of relative influence of the development cost factors on the probe bus/orbiter and the probes is summarized in Table 11-1. This comparison shows clearly that the probes have greater potential benefit from weight/volume relaxation than do the probe bus/orbiter. Atlas/Centaur provides twice the capability of Thor/Delta for the probe missions, increasing the injection weight from 385 kg (849 lb) to 771 kg (1170 lb). Initial allocation of this capability increase between probes and

Table 11-1. Qualitative Effects of Weight/Volume Relief on Costs

COST INFLUENCE FACTOR	EFFECT ON	
	PROBE BUS ORBITER	PROBES
USE OF EXISTING DESIGNS/HARDWARE	SMALL	LARGE
IMPROVED COMMONALITY	SMALL	VERY LARGE
NEW DESIGN SIMPLIFICATION		
• HIGH MARGINS, LESS ANALYSIS/TEST	MODERATE	LARGE
• LOWER FABRICATION COSTS	SMALL	MODERATE
• PACKAGING DENSITY	SMALL	LARGE
OTHER FACTORS		
• BETTER ACCESS EFFICIENCY	SMALL	SMALL
• REDUCED WEIGHT CONTROL	MODERATE	MODERATE
• MAGNETIC CLEANLINESS	NEGLECTIBLE	LARGE
• IMPROVED SCHEDULE CONFIDENCE	SMALL	LARGE

probe bus, shown in Table 11-2, reflected the anticipated benefit to the probe design by assigning approximately three-fourths of the increase to probes and one-fourth to the probe bus. For purposes of establishing the most cost-effective weight allocation, however, both probe and probe bus design analyses explored the full range of potential cost savings, up to the full amount of increased capability availability. This aspect is treated in detail in the next section.

Table 11-2. Initial Allocation of Increased Atlas/Centaur Capability

	WEIGHT			
	THOR/DELTA (KG (LB))		ATLAS/CENTAUR (KG (LB))	
SMALL PROBE				
LARGE PROBE	237	(522)	522	(1150)
PROBE BUS	148	(327)	249	(550)
TOTAL	385	(849)	771	(1700)

11.3 COST/WEIGHT ALLOCATION

11.3.1 Optimum Use of Increased Capability

Cost, as well as several other parameters, is a major factor in selecting subsystem and system configurations. Comparisons between various configurations, or comparisons of variations within a given configuration, are best made on the basis of cost differences. They are simpler to identify and define than absolute costs since the differing

aspects between various choices can be refined without great concern about the cost of the (usually large) portion which is common.

A major tradeoff, which must always be considered in any system definition, is that between cost and weight. The significance of this factor was recognized by the addition of the Atlas/Centaur consideration to the Phase B study, with the explicit ground rule that the study "shall emphasize the low cost and not use the increased capabilities of the Atlas/Centaur launch vehicle to enhance or modify the mission." The approach described in the preceding paragraph, that of considering the cost change effects of weight changes, was also applied to the major elements of the spacecraft, the probe bus/orbiter, and the probes.

A general treatment of optimum weight allocation for minimum cost is presented in Appendix 11A. Appendix 11B treats the more general case of weight and reliability allocation for minimum cost, where cost can be expressed as a function of these factors. Application of the general n-variable cost/weight optimization criteria requires data to define total cost curves for each of the n elements comprising the system. These data are difficult to obtain even for the elements of the system that are part of the spacecraft (namely, the probe bus/orbiter and probes) and virtually impossible to obtain for the elements such as the scientific experiments, which are not yet fully defined. Correct application of the allocation technique should consider all contributing elements. Still, much useful insight into the interaction between the probe bus and probes can be obtained from a limited, two-variable treatment. This is the approach adopted for consideration of cost/weight allocation and sensitivity in this study.

In applying the general concepts to a two-variable case, the question to be answered is whether the total available capability is allocated to the two elements in the way which results in minimum cost. Further, for the increased Atlas/Centaur capability, the analysis need only consider the best allocation of the weight increase relative to the Thor/Delta baseline configuration. Establishment of the Thor/Delta probe and bus configurations as baseline cost and weight points permits treatment of Atlas/Centaur variations as incremental changes from these baseline

points. As will be shown in the following discussion of cost/weight sensitivity, the Thor/Delta baseline is very close to the optimum allocation, and thus the incremental treatment of Atlas/Centaur is valid.

In dealing with incremental changes, we may also examine cost savings (relative to the baseline), associated with weight variations, rather than absolute costs. Maximum cost savings and minimum total cost both coincide with the point at which the rate of change of cost (or savings) with weight is the same for the two elements of the system. This criterion is developed in detail in Appendix 11A.

Figure 11-1A shows, in a generalized way, how cost savings might vary with weight increase, both measured from the Thor/Delta baseline. Probe data are plotted from the left origin, and bus data from the right. The distance between the two origins (probe and bus) represents the total increase in injection capability of Atlas/Centaur over Thor/Delta, which in principle can be allocated in any proportion to the probes and bus. By plotting probe and bus weight changes from opposite boundaries of the capability limits, any vertical line defines a "possible" pair of weight allocations. Algebraic summation of the savings curves yields the total

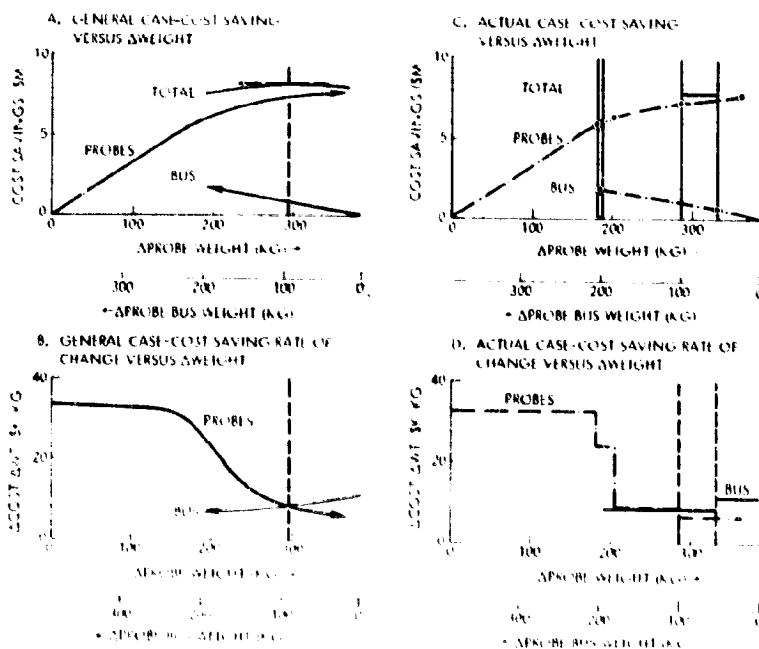


Figure 11-1. Atlas/Centaur Cost-Weight Allocation, Total Capability Increase: 386 kg (851 lb)

cost savings curve, with the maximum indicated by the vertical dashed line. Figure 11-1B is a plot of the cost/weight slopes for this general example, showing the coincidence of the equal values with the point of maximum cost savings (minimum cost) above. When plotted in this fashion (probes and bus in opposite directions), the "balance" of the equal and opposite slopes with the maximum (zero slope) point on the total savings curve is made clearly evident. This condition corresponds exactly with the criterion for the general n-variable case described in Appendix 11A.

Figures 11-1C and 11-1D illustrate the application of these concepts to practically realizable hardware cases. The data are not continuous since each point represents a distinct design with different sets of equipment and configurations. These points are shown by the circles on the probe and bus curves. The most nearly optimum pair of points shows roughly equal cost/weight change values, and further displays a significant additional margin (35 to 40 kg) over the predicted contingency requirements. These points represent the selected Atlas/Centaur probe and probe bus configurations.

The other possible pair of points, representing the lightest Atlas/Centaur probe configuration and a bus with cold gas attitude control, is nonoptimum for two reasons. The weight margin is very small and the savings curve slope (\$K/kg) for the probes is much higher than for the bus, indicating an imbalance in sensitivity to weight changes. The selected configurations are the optimum pair.

11.3.2 Cost/Weight Sensitivity - Thor/Delta

Weight allocation to achieve minimum cost depends on finding the point where the slopes of the cost versus weight curves are the same. This process does not depend on the absolute values of the slopes, only the coincidence between them. Examination of sensitivity to changes reveals some interesting related aspects of this subject.

Since we are interested in examining the effects of changes away from a nominally defined combination (presumed optimum, or near-optimum), it is convenient to establish the nominal weight allocation point as the origin. Figure 11-2 displays the cost/weight effects of

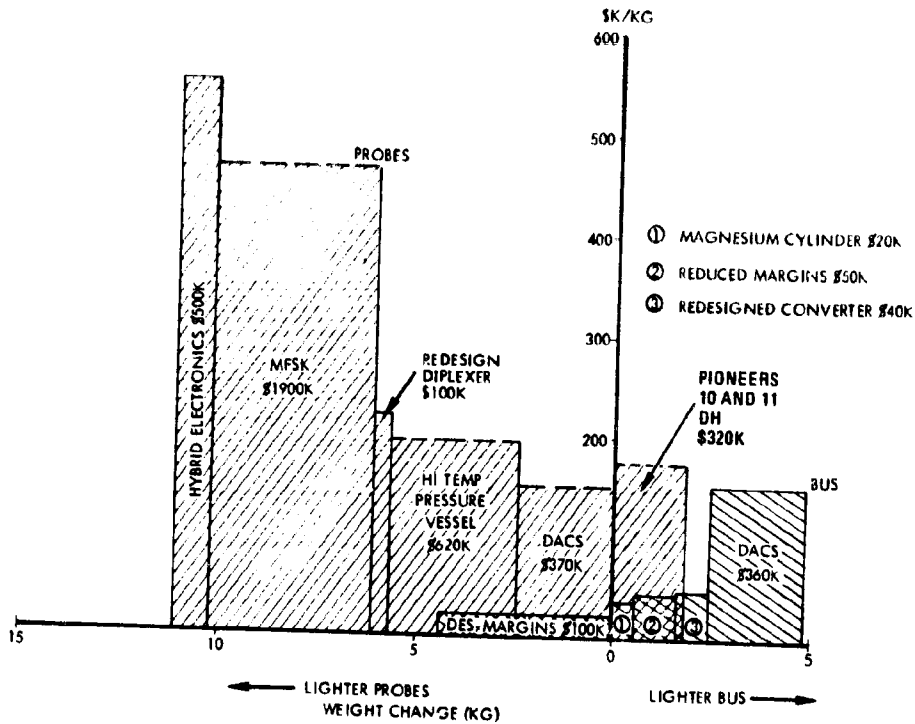


Figure 11-2. Thor/Delta Cost/Weight Tradeoffs

various combinations of design variations around the baseline configuration. Changes in one direction (say to the right) then represent simultaneous increase in probe weight and a corresponding decrease in bus weight. The reverse is true for changes in the other direction.

Considering the Thor/Delta case shown, a range of possible design changes has been identified. Most of these represent weight decreases, with corresponding cost increases, for both probes and bus. For the probes, these changes are in the range of 150-500 \$K/kg (70-230 \$K/lb). While for the bus, they are in the lower range of 20-150 \$K/kg (10-70 \$K/lb). This disparity indicates that the nominal design point should be shifted to more nearly equalize these rates of change. Weight changes of 5 kg or less represent cost changes on the order of \$500K, indicating a relatively high sensitivity to change. This observation is significant in light of the marginally small weight contingency associated with the Thor/Delta design.

11.3.3 Cost/Weight Sensitivity - Atlas/Centaur

Data for the Atlas/Centaur cost/weight tradeoffs, plotted in the same manner as the previous Thor/Delta case, are shown in Figure 11-3. In this case, the weight axis is compressed by a factor of 20 and the cost change axis expanded by a factor of 20. These changes preserve the equivalent cost per unit area, and also maintain a visual similarity between the two curves.

Cost/weight changes for both probes and bus are in the range of 7-12 \$K/kg (3-5 \$K/lb). Comparison of these rates of change, and the range of weight changes involved, indicates that Atlas/Centaur is roughly one-twentieth as sensitive as Thor/Delta. Further, the low cost change per unit weight change indicates proximity to the region of diminishing returns.

The very large areas associated with the various probe configuration changes are indicative of the large savings attained by providing sufficient weight and volume to use existing designs and high commonality in the probes.

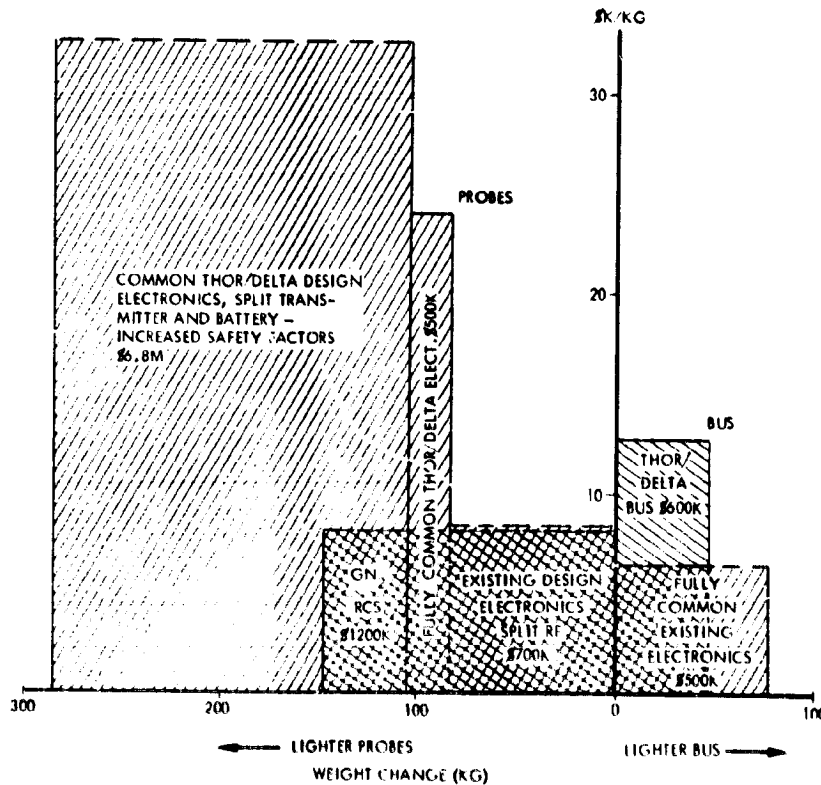


Figure 11-3. Atlas/Centaur Cost/Weight Tradeoffs

11.4 HARDWARE IMPACT

Having considered the general effects of cost/weight variations and shown (in Figures 11-1C and 11-1D) that an optimum Atlas/Centaur probe bus combination exists, we can now examine the quantitative benefits of the added Atlas/Centaur capability. The hardware categories outlined in Table 11-1 will be discussed in the following sections, with the nonhardware-related factors covered in Section 11.5.

11.4.1 Increased Utilization of Existing Designs

Design selection for the probe bus and orbiter spacecraft, based largely on Pioneer 10 and 11 subsystems results in high utilization of existing designs for both Thor/Delta and Atlas/Centaur. As can be seen from Table 11-3 for Thor/Delta, and Table 11-4 for Atlas/Centaur, more than half the units are useable without change or require modifications so minor that requalification will not be required. All of the new designs are low-risk applications of current technology.

Probe design selection, while able to draw extensively on existing designs and technology, requires significantly more new design effort for Thor/Delta (Table 11-5) than for Atlas/Centaur (Table 11-6).

Table 11-3. Use of Existing Designs - Thor/Delta

SUBSYSTEM	PROBE BUS					ORBITER				
	1*	2	3	4	TOTAL	1	2	3	4	TOTAL
ELECTRICAL POWER	0	0	1	4	5	0	0	1	4	5
COMMUNICATIONS	5	2	1	1	9	8	4	2	1	15
ELECTRICAL INTEGRATION	0	1	0	1	2	0	1	0	1	2
DATA HANDLING	1	0	1	0	2	1	0	1	1	3
ATTITUDE CONTROL	0	0	2	0	2	1	0	2	0	3
PROPULSION	4	3	0	1	8	5	3	0	1	9
THERMAL CONTROL	0	1	0	1	2	0	2	0	1	3
STRUCTURE/MECHANISMS	0	0	0	3	3	0	0	1	3	4
TOTAL	10	7	5	11	33	15	10	7	12	44
PERCENT	31	21	15	33	100	34	23	16	27	100

*1 - USE AS-IS

2 - MODIFY EXISTING DESIGN - NO REQUALIFICATION

3 - MODIFY EXISTING DESIGN - REQUALIFICATION

4 - NEW DESIGN

Table 11-4. Use of Existing Designs - Atlas/Centaur

	PROBE BUS					ORBITER				
	1*	2	3	4	TOTAL	1	2	3	4	TOTAL
ELECTRICAL POWER	0	2	1	3	6	1	2	1	3	7
COMMUNICATIONS	7	0	1	1	9	10	4	2	1	15
ELECTRICAL INTEGRATION	0	1	0	1	2	0	1	0	1	2
DATA HANDLING	1	0	1	0	2	1	0	1	1	3
ATTITUDE CONTROL	0	0	2	0	2	1	0	2	0	3
PROPULSION	4	3	0	1	8	5	3	0	1	9
THERMAL CONTROL	0	1	0	1	2	0	1	0	1	2
STRUCTURE/MECHANISMS	0	0	0	3	3	0	0	1	3	4
TOTAL	12	7	5	10	34	18	11	7	11	47
PERCENT	35	21	15	29	100	39	23	15	23	100

- *1 - USE AS-IS
- 2 - MODIFY EXISTING DESIGN - NO REQUALIFICATION
- 3 - MODIFY EXISTING DESIGN - REQUALIFICATION
- 4 - NEW DESIGN

Table 11-5. Thor/Delta Probe Design

SUBSYSTEM	SMALL PROBE					LARGE PROBE				
	1*	2	3	4	TOTAL	1	2	3	4	TOTAL
ELECTRICAL POWER	0	0	0	2	2	0	0	0	2	2
COMMUNICATIONS	0	0	3	0	3	0	1	3	0	4
DATA HANDLING AND COMMAND	0	0	0	1	1	0	0	1	0	1
HEATSHIELD/THERMAL	2	0	0	0	2	2	0	0	0	2
STRUCTURES/MECHANISMS	0	1	0	2	3	0	1	0	2	3
AEROSHELL	0	0	0	2	2	0	0	0	2	2
DECCELERATOR	--	--	--	--	--	0	0	0	1	1
TOTAL	2	1	3	7	13	2	2	4	7	15
PERCENT	15	8	23	54	100	13	13	27	47	100

- *1 - USE AS-IS
- 2 - USE AS-IS, 400-G AND HIGH-TEMPERATURE QUALIFICATION
- 3 - MODIFY EXISTING DESIGN - REQUALIFICATION
- 4 - NEW DESIGN

Table 11-6. Atlas/Centaur Probe Design

SUBSYSTEM	SMALL PROBE					LARGE PROBE				
	1*	2	3	4	TOTAL	1	2	3	4	TOTAL
ELECTRICAL POWER	0	1	0	1	2	0	1	0	1	2
COMMUNICATIONS	0	1	2	0	3	0	1	3	0	4
DATA HANDLING AND COMMAND	0	0	1	0	1	0	0	1	0	1
HEATSHIELD/THERMAL	2	0	0	0	2	2	0	0	0	2
STRUCTURES/MECHANISMS	0	1	0	2	3	0	1	0	2	3
AEROSHELL	0	1	0	1	2	0	1	0	1	2
DECCELERATOR	--	--	--	--	--	0	0	0	1	1
TOTAL	2	4	3	4	13	2	4	4	5	15
PERCENT	15	31	23	31	100	13	27	27	33	100

- *1 - USE AS-IS
- 2 - USE AS-IS, 400-G AND HIGH-TEMPERATURE QUALIFICATION
- 3 - MODIFY EXISTING DESIGN - REQUALIFICATION
- 4 - NEW DESIGN

These results are shown graphically in Figure 11-4, where bus/orbiter data are combined on the left half of the figure and probe data are on the right. The small effects of increased capability on the bus/orbiter can be summarized by the minor reduction in new designs from 30 to 27 percent. The benefits of Atlas/Centaur to the probes show clearly in the reduction of new designs from 50 to 32 percent, with corresponding increases in the use of existing designs. This improvement in utilization of existing designs results in bus/orbiter savings of \$0.3M and probe savings of \$1.5M.

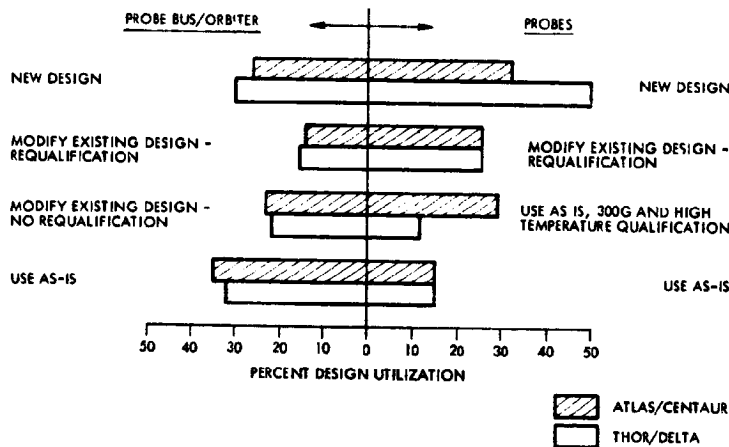


Figure 11-4. Use of Existing Designs Lowers Development Cost

11.4.2 Increased Design Commonality

Commonality between probe bus and orbiter, shown by Table 11-7, is relatively high and not launch vehicle sensitive. Considering subelements of the designs, such as structure components, commonality is improved still further. Excluding items that do not have like functions on both probe and orbiter missions (e.g., X-band equipment, probe ejection mechanism, etc.), approximately two-thirds of the units are common. These results are not surprising since bus/orbiter commonality is a prime design objective.

Similar tabulations for the small and large probes, shown in Table 11-8, illustrate the dramatic effect of Atlas/Centaur capability increase on probe commonality. The significance of these factors on cost reduction is the avoidance of much new (separate) design and development for both the small and large probes.

Table 11-7. Probe Bus/Orbiter Design Commonality

	COMMON	PROBE BUS UNIQUE	ORBITER UNIQUE	TOTAL
<u>THOR DELTA</u>				
USE AS-IS	10	0	5	15
MODIFY EXISTING DESIGN -- NO REQUALIFICATION	6	1	4	11
MODIFY EXISTING DESIGN -- REQUALIFICATION	4	1	3	8
NEW DESIGN	2	9	10	21
TOTAL DESIGNS	22	11	22	55
PERCENT OF TOTAL	40	20	40	100
<u>ATLAS CENTAUR</u>				
USE AS-IS	12	0	6	18
MODIFY EXISTING DESIGN -- NO REQUALIFICATION	6	1	5	12
MODIFY EXISTING DESIGN -- REQUALIFICATION	4	1	3	8
NEW DESIGN	1	9	10	20
TOTAL DESIGNS	23	11	24	58
PERCENT OF TOTAL	40	19	41	100

Table 11-8. Probe Design Commonality

	COMMON	SMALL PROBE UNIQUE	LARGE PROBE UNIQUE	TOTAL
<u>THOR DELTA</u>				
USE AS-IS	2	0	0	2
USE AS-IS, 400-G AND HIGH TEMPERATURE QUALIFICATION	0	1	2	3
MODIFY EXISTING DESIGN -- REQUALIFICATION	1	2	2	5
NEW DESIGN	0	7	8	15
TOTAL DESIGNS	3	10	12	25
PERCENT OF TOTAL	12	40	48	100
<u>ATLAS CENTAUR</u>				
USE AS-IS	2	0	0	2
USE AS-IS, 400-G AND HIGH TEMPERATURE QUALIFICATION	1	2	3	6
MODIFY EXISTING DESIGN -- REQUALIFICATION	4	0	0	4
NEW DESIGN	1	3	4	8
TOTAL DESIGNS	8	5	7	20
PERCENT OF TOTAL	40	25	35	100

Commonality between the probe bus and probes also improves significantly with Atlas/Centaur since Pioneer 10 and 11 data handling units can be used in the bus and both probes. In addition to the use of an existing design rather than a new one in the probes, this approach results in the savings related to common use of the same assemblies in several system elements.

The results are shown graphically in Figure 11-5, in a manner similar to that used in Figure 11-4 for design utilization. The major improvement in probe commonality results in cost savings of \$3.6M.

11.4.3 Design Simplification

Increased weight and volume margins, in addition to the major benefit of permitting a wider choice of existing designs, provides the opportunity to simplify the remaining new design effort through use of greater design margins and safety factors. This has further benefit in reducing the analysis and test effort required to verify design adequacy.

For the probe bus/orbiter, these effects are apparent primarily in structures and mechanisms since these areas have the highest concentration of new design effort. Use of standard shapes, simple fittings, and conventional fastening techniques contribute to less costly design, tooling, detail fabrication and assembly, at a relatively modest increase in weight. This approach is expected to result in at least a 10-percent lower cost in these elements. Similar effects are expected in the new electronic assemblies, although the potential is less significant in these limited cases.

The probes realize substantial cost savings from design simplification. Use of larger design margins in the pressure vessels, aeroshell, heatshield and thermal control areas permits significant reductions in development testing and analysis. In addition, the increased factors of safety permit deletion of structural model testing. The combined cost avoidance of these probe factors is \$1.4M.

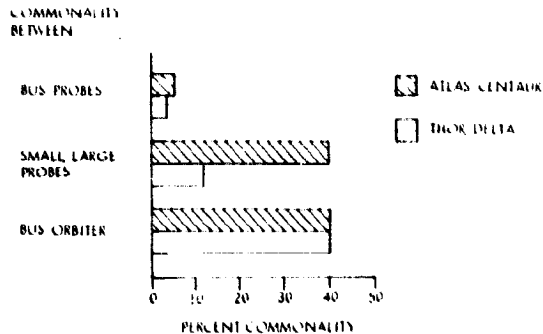


Figure 11-5. Design Commonality Lowers Development Cost

Simplification of the system level design integration and analysis tasks, due to improved commonality and more nearly optimum equipment layout, is expected to permit cost avoidance of about \$0.1M. The total result of the greater flexibility on the new design activity will be at least \$1.9M.

11.5 OTHER LAUNCH VEHICLE-RELATED FACTORS

Several other factors reflect the benefits of relaxed size and weight constraints, either directly or indirectly. Typically, spacecraft are tightly weight constrained and, to a lesser extent, size constrained. While the principal benefit from relaxing these constraints is shown in the lower hardware costs described above, there are collectively significant lesser items that deserve recognition.

The costs of "weight control," i. e., the direct action to avoid weight growth and/or effect weight reduction if overweight conditions exist, can be sizable. Comparison with recent spacecraft and planetary lander programs indicates that approximately \$0.2M can be saved in the probe bus/orbiter and at least \$0.4M in the probes for this factor. Possible additional "hidden" costs, such as retest where weight reduction redesign has invalidated previous testing, are not considered in this assessment.

The larger size of the probe bus/orbiter and probes improves access in several important aspects. Basic assembly, test, and checkout are simplified and speeded up. Perhaps more importantly, fault isolation or troubleshooting during system testing, when serial downtime is very costly in both direct manpower and diminished schedule confidence, can be significantly improved through better access to individual boxes and connectors. While very difficult to assess in an accurate quantitative fashion, this factor contributes at least \$0.1M each for both the probe bus/orbiter and probes.

Another benefit of the relative "roominess" of the probes in the Atlas/Centaur design is the marked easing of the science integration and magnetic cleanliness requirements, for the case where the payload includes the small probe magnetometer. The very tight packaging of the Thor/Delta probes poses some very stringent and demanding problems in these areas. Relaxation, due to size, is estimated to result in approximately \$0.3M savings.

11.6 THOR/DELTA-ATLAS/CENTAUR COST TRADEOFFS

Summarizing the preceding spacecraft hardware and other cost savings factors, Table 11-9 shows clearly the major impact of the Atlas/Centaur capability increase over Thor/Delta, especially on probe cost. This summary also highlights the basic findings of the study cost reduction analysis:

- To reduce cost, reduce new hardware development
- If an existing design will do the job, use it
- If a unit can be used in more than one application, do it.

Greater weight and volume allowances increase the probability of applying one or more of the above maxims.

Table 11-9. Weight/Volume Effect Cost Summary

	APPROXIMATE SAVINGS (\$M)	
	BUS/ ORBITER	PROBES
GREATER UTILIZATION OF EXISTING DESIGNS	0.3	1.5
IMPROVED COMMONALITY	---	3.6
SIMPLIFICATION OF NEW DESIGNS	0.5	1.4
OTHER FACTORS THAT LOWER COST	0.3	1.5
TOTALS	1.1	8.0

Offsetting the savings tabulated above for Atlas/Centaur is the significant increase in launch vehicle and related support costs, \$9.0M for each launch.

It may readily be seen that launch vehicle-related cost reductions, primarily for the probes, are adequate to offset the cost increment of one Atlas/Centaur, but not two. With this in mind, the concept of a "split launch" evolved, using Atlas/Centaur for the probe mission and Thor/Delta for the orbiter mission. The major probe savings are unaffected, while the loss of commonality between the probe bus and orbiter results in increased costs of about \$1.5M for these elements.

Table 11-10 summarizes these considerations, in the upper portion of the table, and provides a limited assessment of some other related costs not directly within the scope of the study. From these figures, the "split mission" concept presents a favorable cost tradeoff, even allowing for wide variations in the assessment of the related costs. For example, the intangible costs, which include such factors as schedule confidence, are likely to be affected by the use of different launch vehicles, and may even be positive (extra cost) for the "split mission." The essential result is unchanged, however. Probe savings are greatly dependent on the greater capability of Atlas/Centaur, while the probe bus/orbiter is only slightly affected by launch vehicle.

Table 11-10. Split Mission Cost Summary

COST ELEMENT	MISSION DEFINITION	ALL THOR/DELTA	ALL ATLAS/CENTAUR	ATLAS/CENTAUR PROBE THOR/DELTA ORBITER
<u>SPACECRAFT</u>				
PROBE BUS	BASELINE ↓		- 0.6	- 0.6
PROBES			- 8.0	- 8.0
ORBITER			- 0.5	+ 1.0
SUBTOTAL			- 9.1	- 7.6
LAUNCH VEHICLE			+18.0	+ 9.0
<u>TOTAL HARDWARE COST</u>				
			+ 8.9	+ 1.4
<u>RELATED COSTS</u>				
GROUND DATA HANDLING			- 0.5	- 0.5
SCIENCE DEVELOPMENT			- 2.4*	- 2.4*
INTANGIBLE			- 2.0	- 1.5
SUBTOTAL			- 4.9	- 4.4
<u>TOTAL COST DIFFERENCE</u>				
			+ 4.0	- 3.0

*BASED ON ASSESSMENT OF PROBE SCIENCE ONLY

11.7 RECOMMENDED MISSION SYSTEM

The basic cost of the Pioneer Venus multiprobe and orbiter mission spacecraft can be kept reasonably low by extensive use of existing designs, from Pioneers 10 and 11, Viking, and other programs. Use of the greater capability of Atlas/Centaur provides major cost savings in the probes, largely through greater use of existing designs and improved commonality. Improvements in the probe bus/orbiter are not sufficient to justify the use of Atlas/Centaur for both missions, within the scope of the study guidelines and data.

On the basis of these considerations, the recommended mission system uses Atlas/Centaur for the probe mission and Thor/Delta for the orbiter mission. This combination is cost effective and greatly reduces the risk inherent in the demanding multiprobe mission.

The program redirection of 13 April 1973, which delayed the probe mission launch from January 1977 to August 1978, injected several other factors into the consideration of launch vehicle selection. The close proximity of the probe mission launch to the May 1978 orbiter mission launch understandably raises concern regarding use of different launch vehicles. It is also recognized that the Thor/Delta orbiter mission, while entirely feasible for the payload defined by the study ground rules, has virtually no potential for growth or flexibility. Accordingly, the NASA decision to utilize Atlas/Centaur for both missions, considered in the total program environment (including lower spacecraft and science costs) is a fundamentally sound one. The entire program will benefit from the opportunity to demonstrate the very real benefits of reasonable relaxation in weight and volume constraints.

12. Long Lead Items and Critical Areas

12. LONG LEAD ITEMS AND CRITICAL AREAS

A study was conducted to define any high-risk, high-cost, or long lead items and areas where performance, cost, or schedule are critical. This work also included a review of all probe elements to identify any possible research and technology required to support implementation of the overall program contained in Volume II and shown in summary form in Figure 12-1.

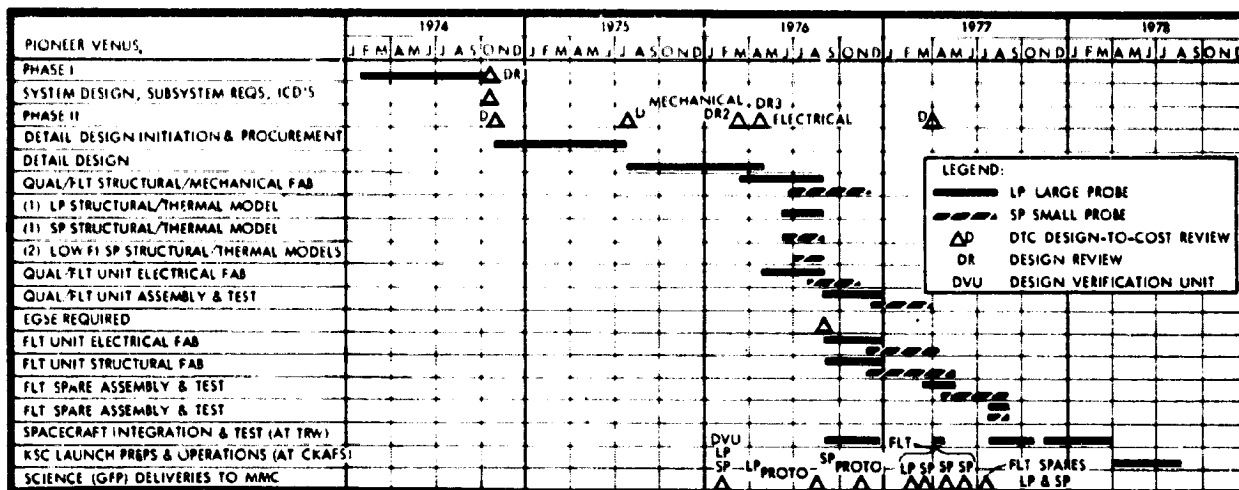


Figure 12-1. Schedule Summary

12.1 LONG LEAD

Probe program elements were examined to define any long lead items, i. e., any design activity that must start early in the program because of the technical risk involved. We concluded that no such items exist; in fact, the use of existing designs and proven technology is one of the key features of our proposed design. Therefore, we do not propose any long lead technology or hardware design activities.

12.2 CRITICAL AREAS

Examination of critical areas associated with the proposed probe program revealed that several critical performance and engineering activities exist, due primarily to hardware development, build, and delivery schedule

imposed on the probes. These schedule-related critical activities, shown in Figure 12-2, fall into three categories:

- 1) System performance (aero tests and science window development)
- 2) Interface definition
- 3) Preliminary procurement activities.

The necessity for these activities is rather obvious in supporting the center loaded program discussed in Volume III. For this program approach, it is essential that all hardware design requirements and specifications must be defined at the time "hard start" is indicated; in other words hardware must be designed, fabricated, and procured in a quick, direct fashion in order to support the schedule. No time is allowed to finalize or fine tune the aero shape, negotiate interfaces, or develop procurement paperwork after the hard start. Therefore, we have designated the activities shown in Figure 12-2 as critical areas for support of the proposed center loaded schedule.

	1974		1975						
	NOV	DEC	JAN	FEB	MAR	APR	MAY	JUN	JUL
I. SCIENCE:									
A) PROBE SCIENCE ICD MAINTENANCE & ARC/PI COORDINATION									
B) SCIENCE WINDOW DEVELOPMENT									
II. MISSION ANALYSIS									
A) PROBE DSM INTERFACE SPEC AND ICD MAINTENANCE									
III. SYSTEM DESIGN:									
A) APPROVED PARTS LIST (MMC SUBCONTRACTORS)									
B) APPROVED SYSTEM LEVEL TEST PLAN									
C) SUBSYSTEM INTERFACE AND ICD PREPARATION									
IV. MECHANICAL SUBSYSTEMS									
A) AERO CONFIGURATION TESTING									
B) DEFINITIVE PD PREPARATION									
C) SUBCONTRACTOR LIAISON (SUPPORT)									
V. ELECTRICAL SUBSYSTEMS									
A) DEFINITIVE PD PREPARATION									
B) SUBCONTRACTOR LIAISON (SUPPORT)									
C) ICD MAINTENANCE									

Figure 12-2. Critical Activities